12.12.90

BJR

THE BRITISH JOURNAL OF RADIOLOGY

Volume 62 Number 736 April 1989

CVK-H06097-15-P25853

15

X-ray Diagnosis • Ultrasound • Interventional Radiology
Radiotherapy • Oncology • Hyperthermia
Nuclear Medicine • Nuclear Magnetic Resonance
Radiation Physics • Radiobiology • Radiation Protection

BJR is published by The British Institute of Radiology BIR

AT LAST!

An Isotope Calibrator **Designed** for Brachytherapy

It's Accurate...
It's Reliable...
It's Economical

- Digital electrometer with well-type ionization chamber.
- Can be calibrated for 6 isotopes: ^{137}Cs, ^{125}I, ^{192}Ir, ^{198}Au, ^{226}Ra, and one user-selected position.
- Repeatable to within ± 2% or .01mCi, whichever is greater.

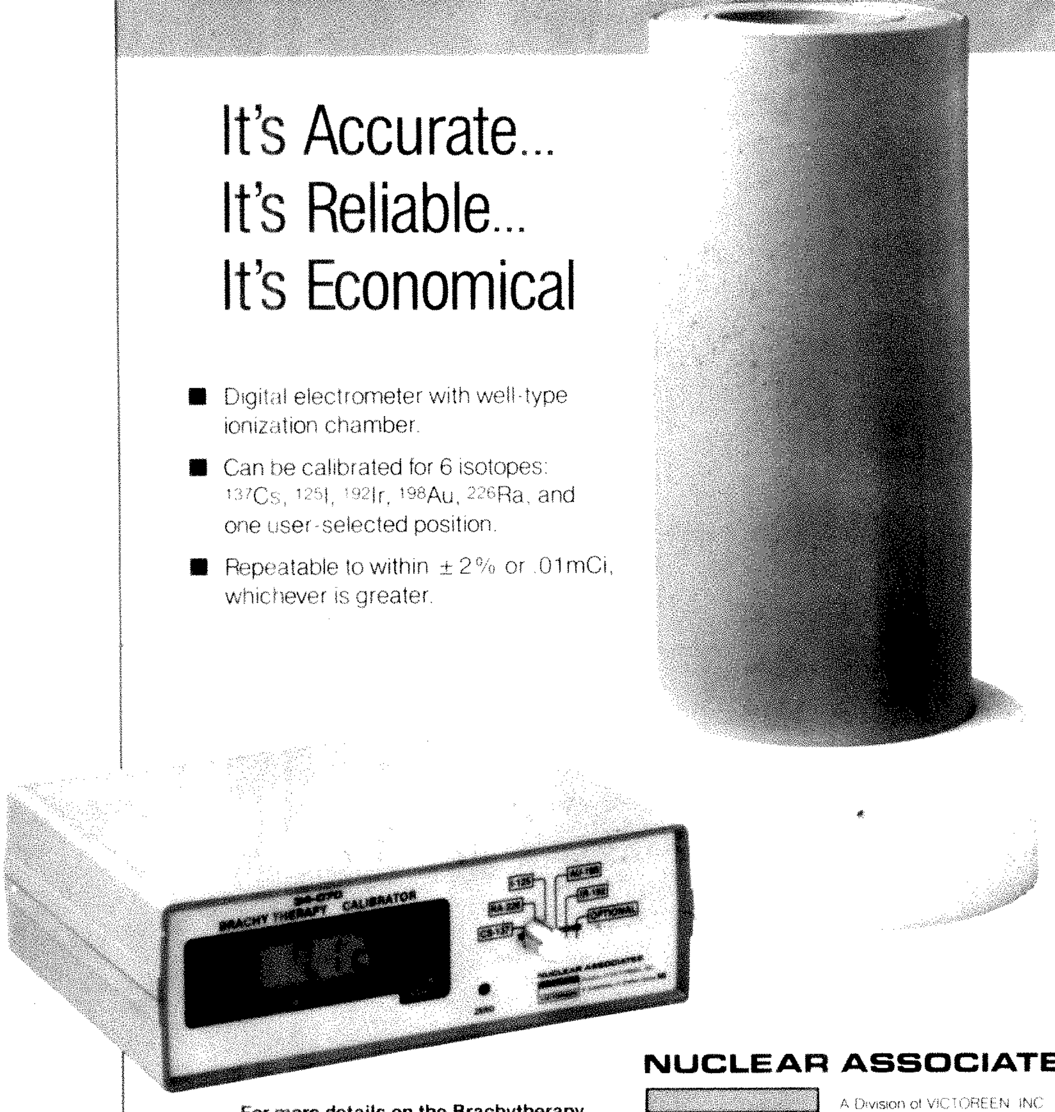

For more details on the Brachytherapy Calibrator, request Bulletin 397-14.

NUCLEAR ASSOCIATES

VICTOREEN

A Division of VICTOREEN INC
100 VOICE ROAD
CARLE PLACE NY 11514-1593 U S A
(516) 741-6360

Your Radiation Therapy Department Deserves Its OWN Isotope Calibrator!

P25853

BJR THE BRITISH JOURNAL OF RADIOLOGY

Established 1896

The Editorial Committee

Honorary Editors
J. T. Patton, FRCP, FRCR
N. J. McNally, BSc, MSc, PhD

Deputy Editors
D. G. Shaw, FRCP, FRCR
C. K. Bomford, BSc, MPhil, FInstP

Associate Editors
P. R. Blake, MD, MB, BS, BSc, FRCR
J. A. Bullimore, MB, BS, MRCS, LRCP, DMRT, FRCR
R. G. Dale, MSc, PhD, CPhys, FInstP
P. Dawson, BSc, PhD, MB, BS, MRCP, MInstP, FRCR
S. Dische, MD, FRCR
F. A. Duck, PhD, MIEEE
A. H. Freeman, MB, BS, FRCR
R. M. Harrison, BSc, MSc, PhD, FInstP
J. W. Hopewell, BSc, PhD
W. D. Jeans, MB, BS, FRCR
D. M. King, MB, BS, FRCR, DMRD
H. W. C. Loose, DMRD, FRCR
A. M. Peters, BSc, MSc, MB, ChB, MD, MRCPath
D. W. Pilling, MB, ChB, DCH, DMRD, FRCR
J. F. Reidy, MB, BS, FRCR, DMRD
J. R. K. Savage, DSc
R. A. Shields, PhD
D. M. Tait, MB, ChB, MRCP, FRCR
J. Tudor, MB, BS, FRCR
A. R. Valentine, MB, BS, MRCS, LRCP, FRCR, DMRD
G. H. Whitehouse, MB, BS, FRCP, FRCR, DMRD
A. G. Wilson, FRCP, FRCR
E. P. Wraight, MB, BChir, PhD, DMRT

Associate Editors Overseas
P. Armstrong, MB, BS, FRCR, DMRD (North America)
H. K. Baddeley, MB, BS, DMRD, FRCR, MRACR (Australasia)
S. G. A. Chenery, PhD, FCCPM (North America)
B. J. Cremin, MD, FRCR, FRACR (South Africa)
R. Fox, DPhil (Australia)
M. Takahashi, MD (Japan)
D. M. Taylor, DSc, CChem, FRSC (Continental Europe)

Managing Editor: Roderick Smith, BSc

The British Journal of Radiology is published monthly by the British Institute of Radiology, 36 Portland Place, London W1N 4AT. Telephone 01-580 4189 (editorial). Editorial communications should be addressed to the Honorary Editors in accordance with the Instructions to Authors published in the January issue each year, and copies of which may be obtained from the Managing Editor upon request.

Advertisements. Communications should be addressed to the Advertising Manager at the above address. Tel. 01-631 1168.

Subscriptions. The monthly fulfilment and distribution are carried out by Butterworth Scientific Ltd, PO Box 63, Westbury House, Bury Street, Guildford, Surrey GU2 5BH, UK. Telephone 0483 300966.

UK and Overseas subscription orders should be sent to: Westbury Subscription Services, PO Box 101, Sevenoaks, Kent TN15 8PL, UK. Telephone 0732 885833. Telex 95678. Facsimile 0732 884079. Cable Westbury, Sevenoaks, Kent. North American orders should be sent to: Journals Fulfilment Department, Butterworths, 80 Montvale Avenue, Stoneham, MA 02180, USA. Telex 880052. Telephone (617) 438 8464.

The annual subscription to *The British Journal of Radiology* (12 issues) for UK readers is £115.00. Overseas rates are £125.00. These prices include delivery by sea mail; airmail rates are available on request. Copies of this journal sent to subscribers in Bangladesh, Canada, India, Japan, Pakistan, Sri Lanka and USA are air-speeded for quicker delivery at no extra cost. Subscriptions are on a calendar year basis only.

All claims for unfulfilled subscriptions should be sent to Westbury Subscription Services at the above address.

Back issues prior to the current volume are available from Wm Dawson & Sons Ltd, Cannon House, Folkestone, Kent, England CT19 5EE. Telephone 0303 57421.

US mailing agents: Mercury Airfreight International Ltd Inc. Second class postage paid at Rahway, NJ, USA. Postmaster: send address corrections to The British Journal of Radiology, c/o Mercury Airfreight International Ltd Inc., 10B Englehard Avenue, Avenel, NJ 07001, USA.

THE BRITISH INSTITUTE OF RADIOLOGY

BIR

Founded 1897
Incorporated by Royal Charter
Patron: Her Majesty The Queen

The British Institute of Radiology is an association of persons interested in radiology and allied subjects. Meetings are held monthly from October until May. Particulars of membership and other information may be obtained on application to the General Secretary at the Institute, 36 Portland Place, London W1N 4AT.
Telephone: 01-580 4085 and 01-580 4189.
Cable Address: Britology, London W1.

President
B. S. Worthington, BSc, LIMA, MB, BS, LRCP, MRCS, DMRD, FRCR

Honorary Secretaries
M. Gowland, MB, ChB, FRCR, MRCP(Hon)
M. J. Harvey, TDCR, DMS

Honorary Treasurer
D. S. McIntosh, BSc, PhD, ARIC, MPS

General Secretary
Susan M. Johnstone, BA

Ultra-
comfortable
contrast
medium

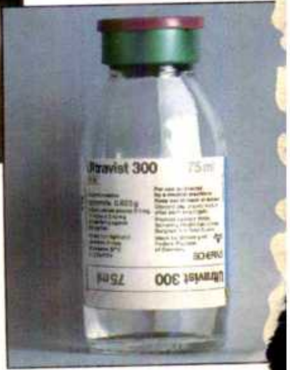

ULTRAVIST
iopromide

▼ **Prescribing Information: Presentation** Intravascular injections of non-ionic iopromide in strengths of 240mg, 300mg and 370mg of iodine/ml. **Uses** Delineation of the vascular and renal systems. **Dosage and Administration** Intravenous urography: Adult mi
doses: Ultravist 370: 0.8ml/kg body weight; Ultravist 300: 1ml/kg body weight; Ultravist 240: 1.3ml/kg body weight. Computed Tomography: Cranial CT: Ultravist 240: 1.5-2.5ml/kg body weight; Ultravist 300: 1-2ml/kg body weight; Ultravist 370: 1-1.5ml/k
weight. Whole-body CT: Dosage depends on investigation and scanner. Angiography: Dosage (6-80ml) depends on age, weight, cardiac output, general condition, and investigation. **Contra-indications, Warnings, etc** Contra-indications: Possible hypersensi
contrast media; thyrotoxicosis; cardiac decompensation; hysterosalpingography during pregnancy; acute pelvic inflammation. Warnings, etc: Caution if there is: severe hepatic or renal impairment; cardiac or circulatory insufficiency; cerebral arterioso
cerebral spasmodic conditions; epilepsy; juvenile-onset or long-standing diabetes; pulmonary emphysema; poor general health; hyperthyroidism; multiple myeloma; a history of allergy, especially if patient has received a contrast medium before. Us
preganancy only if essential. Do not mix contrast media and anti-allergic agents. With multiple myeloma, juvenile-onset or long-standing diabetes, polyuria, oliguria, gout or marasmus, do not restrict fluids. First correct disturbances of water and elect
With phaeochromocytoma, premedicate with an alpha-blocker. Administer Ultravist to recumbent patients and closely observe for at least 30 minutes. The capacity of the thyroid to take up iodine is reduced. If marked side-effects or suspected allergic re
occur during injection, and do not disappear when it is interrupted, stop the investigation. Even minor side-effects may be signs of severe reaction. Life-threatening side-effects include hypotensive collapse, circulatory failure, ventricular fibrillation, cardiac
pulmonary oedema, anaphylactic shock or other allergic manifestations and convulsions or other cerebral symptoms. **List Price:** Ultravist 370 1x100ml £43.39. **Product Licence No:** 0053/0173 Ultravist 240; 0053/0174 Ultravist 300; 0053/0175 Ultrav
Product Licence Holder: Schering Health Care Limited, The Brow, Burgess Hill, West Sussex RH15 9NE. Further information is available on request from: Schering Health Care Limited, Hospital Diagnostics and Pharmaceuticals, The Brow, Bu
SHCL UV

VOL 62 NO 736 APRIL 1989

The British Journal of Radiology

Contents

Papers

Page

The localization of myocardial ischaemia with technetium-99m methoxy isobutyl isonitrile and single photon emission computed tomography 303
D. J. West, Y. C. Najm, R. Mistry, S. E. Clarke, I. Fogelman and M. N. Maisey

The relation of radionuclide uptake by bone to the rate of calcium mineralization. I: Experimental studies using ^{45}Ca, ^{32}P and ^{99}Tc^{m}-MDP 314
R. S. Budd, G. S. Hodgson and W. S. C. Hare

The relation of radionuclide uptake by bone to the rate of calcium mineralization. II: Patient studies using ^{99}Tc^{m}-MDP 318
R. S. Budd, G. S. Hodgson and W. S. C. Hare

Phalangeal osteoid osteoma 321
Q. Meng and I. Watt

Acute rhabdomyolysis: evaluation with magnetic resonance imaging compared with computed tomography and ultrasonography 326
A. E. Lamminen, P. E. Hekali, E. Tiula, I. Suramo and O. A. Korhola

The effects of angiotensin II on Doppler signals from a soft-tissue tumour 331
P. M. Taylor, B. Moreman, S. Rimmer and I. Isherwood

The prevalence and characterization of simple hepatic cysts by ultrasound examination 335
P. A. Gaines and M. A. Sampson

Radiation-induced cell death by chromatin loss 338
I. R. Campell and H. M. Warenius

Changes in biological effectiveness of the neutron beam at Clatterbridge (62 MeV p on Be) measured with cells *in vitro* 344
D. K. Bewley, B. M. Cullen, M. Astor, E. J. Hall, S. W. Blake, D. E. Bonnett and M. Zaider

Structure–function analysis of angiotensin-converting enzyme inhibitors as modifiers of radiation-induced pulmonary endothelial dysfunction in rats 348
W. F. Ward, A. Molteni, Y. T. Kim and C. Ts'ao

Treatment of persistent and recurrent nasopharyngeal carcinoma by brachytherapy 355
J. S. T. Sham, W. I. Wei, D. Choy, C. M. Ho, P. T. H. Tai and P. H. K. Choi

The ICRU recommendations for reporting intracavity therapy in gynaecology and the Manchester method of treating cancer of the cervix uteri 362
J. M. Wilkinson and T. P. Ramachandran

Technical notes

Radiotherapy simulators and independent field wire movement 366
G. Robertson

Magnetic resonance imaging of the infant heart at 1.5 T 367
M. A. Smith, E. J. Baker, V. T. Ayton, J. M. Parsons, E. J. Ladusans and M. N. Maisey

Case reports

Balloon embolization of a congenital arterio-venous fistula between the internal mammary artery and a portal vein radicle 371
M. J. D. Cobby, W. Culling, S. C. Jordan and G. G. Hartnell

Magnetic resonance imaging of ruptured aneurysm of the ascending aorta 373
R. P. Spielmann, E. E. Küng, G. Witte and M. Heller

Dysplastic cortical hyperostosis: a new form of lethal neonatal dwarfism 376
K. Kozlowski and T. Tsuruta

Case of the month

Haemoptysis in a laundry worker 379
J. E. Jackson and D. J. Allison

Short communications

Tetrachlorodecaoxygen anion complex treatment after localized X irradiation of the rat colon 381
N. Breiter, T. Sassy and K.-R. Trott

Iotrolan in selective bronchography via the fibreoptic bronchoscope 383
S. K. Morcos, S. V. Baudouin, P. B. Anderson, R. Beedie and R. W. Bury

Correspondence

Stem-cell depletion and grid therapy 386
Y. Maruyama, R. J. Yaes, M. Urano, P. Patel and J. C. Hernandez

Effect of cirrhosis on accuracy of ^{99}Tc^{m}-tin colloid scintigraphy and ultrasound scanning in diagnosis of hepatocellular carcinoma 387
C. R. Goldfarb, F. Ongseng and H. Finestone

Reply 387
P. R. Powell-Jackson

Secretion of radioactivity in breast milk following administration of ^{123}I hippuran 388
P. J. Mountford and A. J. Coakley

Proceedings

Proceedings of The British Institute of Radiology
Imaging in stroke: how, why and when, 13 October, 1988 390

Book reviews

Sectional fetal anatomy in ultrasound. *A. Staudach* 393
Bioeffect literature reviews 1980–1987. *H.-D. Rott* 393
Computed tomography in trauma. *B. D. Toombs and C. M. Sandler* 393
Computed tomography of the temporal bone and orbit. Technique of direct multiplanar, high-resolution CT and correlative cryosectional anatomy. *F. W. Zonneveld* 394
Computed cranial and spinal imaging. A practical introduction. *J. M. Stevens, A. R. Valentine and B. E. Kendall* 394
Atlas of endourology. *K. Amplatz and P. H. Lange* 395
Ultrasound teaching cases, Vol. 1, 2nd edn. *H. B. Meire, K. C. Dewbury and D. O. Cosgrove* 395
Atlas of fetal sectional anatomy. With ultrasound and magnetic resonance imaging. *G. Isaacson, M. C. Mintz and E. S. Crelin* 395
Diagnostic imaging in paediatrics. *I. Gordon* (Ed.) 396
Congenital dysplasia and dislocation of the hip in children and adults. *D. Tonnis* 396
The dread disease: cancer and modern American culture. *J. T. Patterson* 396
Diagnostic imaging, 2nd edn. *P. Armstrong and M. L. Wastie* 397
Clinical imaging. An atlas of differential diagnosis. *R. L. Eisenberg* 397
Diagnostic imaging: an algorithmic approach. *R. L. Eisenberg* (Ed.) 398

BIR Bulletin *facing page* 398

Featured in the next issue

Doppler ultrasound in medical diagnosis (Review)
P. N. T. Wells

Nuclear medicine in the 1990s: a quantitative physiological approach (1988 BIR Mayneord Lecture)
R. J. Ott

© 1989 The British Institute of Radiology. This publication is copyright under the Berne Convention and the Universal Copyright Convention. All rights reserved, apart from any relaxations permitted under national copyright laws, no part of this publication may be reproduced, stored in a retrieval system or transmitted in any form or by any means without the prior permission of the copyright owners. Permission is not, however, required to copy abstracts of papers or of articles on condition that a full reference to the source is shown. Multiple copying of the contents of the publication without permission is always illegal.

Published by The British Institute of Radiology, 36 Portland Place, London W1N 4AT. Printed in Great Britain by The Whitefriars Press Ltd., Tonbridge. ISSN 0007 1285

VOL 62 NO 737 MAY 1989

The British Journal of Radiology

Contents

Review

Page

Doppler ultrasound in medical diagnosis 399
P. N. T. Wells

Papers

Nuclear medicine in the 1990s: a quantitative physiological approach (1988 Mayneord Lecture) 421
R. J. Ott

Relative proton density and relaxation times in liver metastases during interferon treatment 433
T. Andersson, A. Ericsson, B. Eriksson, A. Hemmingsson, E. Lindh, R. Nyman and K. Öberg

Chromium-51 EDTA/technetium-99m MDP ratio: a simple non-invasive method for assessing renal osteodystrophy 438
A. P. Nisbet, P. Shaw, D. Taube, S. Edwards, M. N. Maisey and G. Mashiter

Endoscopic correction of vesico-ureteric reflux by subureteric Teflon injection: follow-up ultrasound and voiding cystography 443
N. S. Blake and E. O'Connell

The influence of type of tube and experience of the operator on performance of small bowel enema 447
D. A. Nicholson, I. Zammit-Maempel, M. Hughes, E. Nanda Kumar and D. F. Martin

First interim progress report on the second British Institute of Radiology Fractionation study: Short *versus* long overall treatment times for radiotherapy of carcinoma of the laryngo-pharynx 450
G. Wiernik, C. J. Alcock, T. D. Bates, R. J. Berry, J. M. Brindle, J. E. Dalby, J. F. Fowler, W. R. Gajek, S. Goodman, J. L. Haybittle, J. M. Henk, J. W. Hopewell, N. Howard, R. Lindup, D. L. Phillips, R. S. Pointon, M. Rezvani and J. S. Tobias

Platinum chemotherapy, radiotherapy and the inner ear: implications for "standard" radiation portals 457
P. Kirkbride and P. N. Plowman

In vivo viability of ^{111}In-labelled granulocytes demonstrated in a sham-dialysis model 463
W. Becker, R. M. Schaefer and W. Börner

Radiation toxicity of indium-111-2-mercaptopyridine-N-oxide on HeLa S-3 cells 468
S. S. Hong, E. H. Ford and B. Greenspan

The quality of high-energy X-ray beams 473
P. D. LaRiviere

Memorandum from the British Committee on Radiation Units and Measurements. Quantities for environmental monitoring 482

Technical note

An alignment test jig for measuring the effective focal-spot size of mammographic X-ray tubes 484
M. L. Ramsdale, P. A. Hiles and C. P. Lawinski

Case reports

An isolated capitate fracture in a nine-year-old boy 487
W. W. Gibbon and A. Jackson

Distal bowel infarction following angioplasty of the internal iliac artery 489
I. C. Bennett, M. O. Downes and R. E. C. Collins

Atypical radiological features of β-glucuronidase deficiency (mucopolysaccharidosis VII) occurring in an elderly patient from an inbred kindred 491
S. Chapman, R. G. F. Gray, T. J. Constable and S. Bundey

Case of the month

The warm and tender hip 495
S. H. Lee

Correspondence

Splenic accumulation of ^{99}Tc^{m}-methylene diphosphonate 497
C. Alevizaki, E. Georgiou, E. Nikiforakis and C. Proukakis

A pressure valve for pneumatic reduction of intussusception 497
I. J. Kenney and J. E. Lutkin

"Out-of-hours radiography" 498
H-J. Maurer

The cost of imaging procedures 498
M. J. Day

Proceedings

Proceedings of the British Institute of Radiology
Paediatric Nuclear Medicine, November 23, 1988 499

Book reviews

Atlas of hysterosalpingography. *S. Karasick and D. Karasick* 504
International strategies for the eradication of carcinoma of the cervix in developing areas: proceedings of the International Working Party meeting in India 1987. *R. F. Mould and A. Rose* (Eds) 504
A textbook of radiological diagnosis, Vol. 4. The alimentary tract: the hollow organs and salivary glands. *K. C. Simpkins* (Ed.) 504
Gamuts in nuclear medicine, 2nd edn. *F. L. Datz* 504
Clinical radioimmunoimaging. *Z. D. Grossman and S. F. Rosebrough* 505
Microneurosurgery, Vol. IIIA. *M. G. Yasargil, P. J. Teddy and A. Valavanis* 505
Neuroradiology, 2nd edn. *R. G. Ramsey* 506
Radiology for anaesthesia and critical care. *C. H. Murphy and M. R. Murphy* (Eds) 506

BIR Bulletin facing page 506

Featured in the next issue

The production of chromosome structural changes by radiation: an update of Lea, 1946, Chapter VI (Review)
J. R. K. Savage

Spontaneous abrupt changes in the distribution of ventilation: a cause for apparent mismatching on ventilation/perfusion scintigraphy
A. M. Peters, I. Gordon, A. M. Kaiser, R. N. Arnot and J. P. Lavender

X-ray protection considerations for mammography screening centres (Technical note)
A. Walker and A. R. Hounsell

Upper-half body irradiation for oat cell carcinoma of the bronchus (Short communication)
A. D. Stockdale and A. Y. Rostom

© 1989 The British Institute of Radiology. This publication is copyright under the Berne Convention and the Universal Copyright Convention. All rights reserved, apart from any relaxations permitted under national copyright laws, no part of this publication may be reproduced, stored in a retrieval system or transmitted in any form or by any means without the prior permission of the copyright owners. Permission is not, however, required to copy abstracts of papers or of articles on condition that a full reference to the source is shown. Multiple copying of the contents of the publication without permission is always illegal. Published by The British Institute of Radiology, 36 Portland Place, London W1N 4AT. Printed in Great Britain by The Whitefriars Press Ltd., Member of BPCC Ltd., Tonbridge. ISSN 0007 1285

1989, *The British Journal of Radiology*, 62, 303–313

VOLUME 62 NUMBER 736 APRIL 1989

The British Journal of Radiology

The localization of myocardial ischaemia with technetium-99m methoxy isobutyl isonitrile and single photon emission computed tomography

By D. J. West, FRCR, Y. C. Najm, R. Mistry, S. E. Clarke, MRCP, I. Fogelman, BSc, MD, MRCP and M. N. Maisey, BSc, MD, FRCP, FRCR

Departments of Nuclear Medicine and Radiological Sciences, United Medical and Dental Schools of Guy's and St Thomas' Hospitals, London SE1 9RT

(Received August 1988 and in revised form November 1988)

Abstract. Thirty-two patients with suspected coronary artery disease were studied by single photon emission computed tomography (SPECT) imaging with oblique reconstructions of the myocardium following the intravenous administration of technetium-99m methoxy isobutyl isonitrile at peak exercise. All patients also underwent three-vessel coronary angiography. The SPECT technique produced very detailed images allowing easy delineation of localized myocardial defects. Segmental myocardial uptake defects were compared with diseased vessels as shown at angiography. A good correlation was shown between right coronary artery (RCA) disease and mid and proximal inferior segments and between left circumflex (LCx) artery disease and mid and proximal lateral segments, allowing accurate localization of a defect to one of these two vessels' territories. Sensitivity and specificity of detection of disease of the RCA and LCx artery were high. Defects associated with a lesion of the left anterior descending vessel were more variable.

Thallium-201 scintigraphy is an accepted method for assessing patients who have suspected or proven coronary artery disease (Lebowitz et al, 1975; Strauss & Pitt, 1978; Pierson et al, 1979). In spite of this, thallium 201 has properties that limit its usefulness for imaging: a low photon energy of 70–80 keV, low photon yield, long half-life ($T_{\frac{1}{2}}$) and expense. Once extracted it does not remain in the myocardium, but is in dynamic equilibrium with the bloodstream, which may lead to early redistribution to areas of ischaemia before the initial imaging has been completed. A technetium-99m labelled agent with myocardial uptake proportional to regional blood flow with low lung and liver uptake or rapid clearance from these organs would be a preferable myocardial perfusion agent.

Recently, several technetium-99m labelled isonitrile compounds (Deutsch et al, 1981; Jones et al, 1982; Holman et al, 1984) have been developed for myocardial imaging. Initial animal experiments were often encouraging, but human studies revealed drawbacks including slow clearance from the blood, necessitating delayed imaging (Gerson et al, 1983), high relative accumulation in the liver (Gerson et al, 1983; Gerudini et al, 1986), low myocardial uptake (Thakur et al, 1984) and high lung uptake (Gerudini et al, 1986). Clinical studies with technetium-99m methoxy isobutyl isonitrile (MIBI) have been encouraging (Khalil et al, 1987; Najm et al, 1987).

Technetium-99m MIBI is a lipophilic complex that accumulates in viable myocardial tissue proportional to the regional myocardial blood flow. Myocardial distribution has been shown by comparison with microspheres and thallium to correlate well with regional myocardial perfusion. In animal and human studies it has shown properties that make it suitable for myocardial imaging: the extraction fraction is adequate (estimated at 30%), clearance from the myocardium is delayed ($T\frac{1}{2}$ 5.5 h), there is very little lung uptake, and the initial high liver uptake clears rapidly. The agent is supplied in a kit form which can easily be labelled.

Planar myocardial imaging has disadvantages inherent in its two-dimensional basis; false positive perfusion defects can be produced by overlying soft-tissue attenuation and false negative defects may result from activity in overlying normally-perfused myocardium. Tomographic imaging methods have been applied to thallium imaging with reported improvements in both sensitivity and specificity (Holman et al, 1979; Vogel et al, 1979; Berman et al, 1980; Ritchie et al, 1982; Nohara et al, 1984). Because of its low photon energy, low photon yield and early redistribution, thallium is not ideal for single photon emission computed tomography (SPECT) studies. During a multicentre clinical evaluation of technetium-99m MIBI, we have studied 32 patients with coronary artery disease using SPECT. Uptake defects during exercise studies were compared

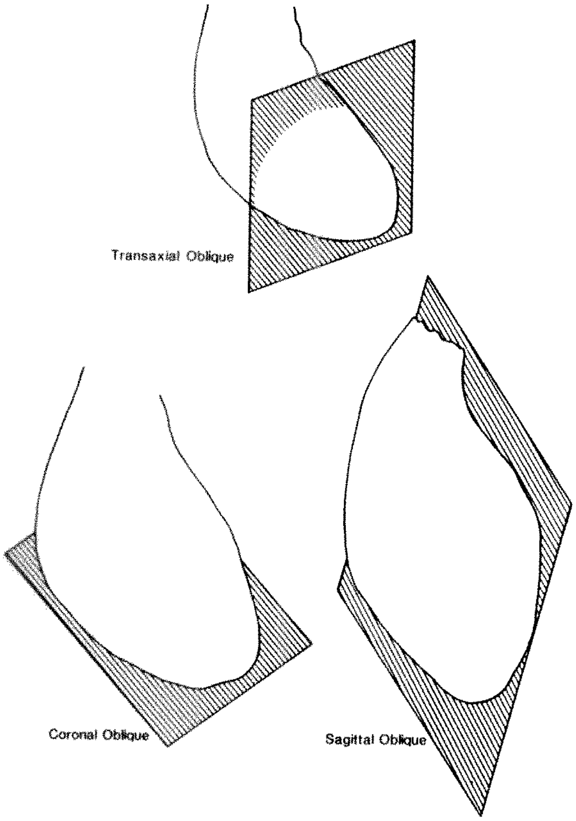

Figure 1. Orientation of the three standard scan planes used in this study.

with disease of specific coronary arteries as shown on coronary angiography.

Materials and methods

Patients

Thirty-two patients with angina pectoris who had recently undergone coronary arteriography were studied. Twenty-six patients were male and six were female, with an age range of 26 to 62 years.

Coronary arteriography

All patients underwent coronary arteriography in multiple projections. Narrowings of the right coronary artery (RCA), left anterior descending (LAD) and circumflex (LCx) arteries were graded visually according to the lumen diameter. Significant disease was defined as a stenosis of greater than 50%. The arteriograms were reported by one of us (Y.C.N.) independently of the radionuclide images.

Equipment

A Scintronix Digi camera 404 with SPECT tomographic facility and a high-resolution collimator was used. The camera was interfaced to a Data General Nova 4X computer.

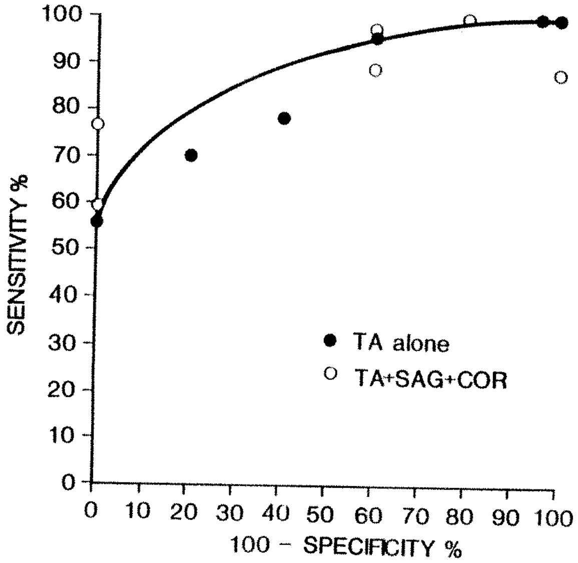

Figure 2. The ROC curve for detection of stenosis of any vessel.

Radiopharmaceutical

Technetium-99m MIBI was prepared from a kit supplied by Du Pont according to the manufacturer's instructions.

Imaging protocol

The patients were prepared by fasting for 4 h prior to the study. Beta blockers were withdrawn for 48 h. Resting 12-lead electrocardiogram (ECG) traces were obtained and a physical examination undertaken. An intravenous cannula was inserted into the right basilic vein and heparinized. Standard bicycle ergometry was performed and 500 MBq of technetium-99m MIBI was injected through the cannula at peak exercise. Exercise was continued for 30 s after injection. Imaging was performed 1–2 h later in the supine position; SPECT images were acquired in 64 steps over 360° of rotation. A 20% window was centred on the 140 KeV peak of technetium 99m. Each projection took 20 s with a total imaging time of about 25 min.

Reconstruction

Oblique angle reconstruction was used to enable tomographic slices to be obtained relative to the long axis of the heart, the lie of which was determined from transverse and coronal images. Slices parallel to three orthogonal planes were produced, as illustrated in Fig. 1. This technique provided between 10 and 20 6 mm-thick slices through the heart in orientations that are easier to analyse and compare than standard tomographic planes. The digital images were displayed on a TV monitor in 16 grades of colour linearly related to image intensity.

Image interpretation

Image interpretation was carried out by two observers without knowledge of the angiogram findings. The left

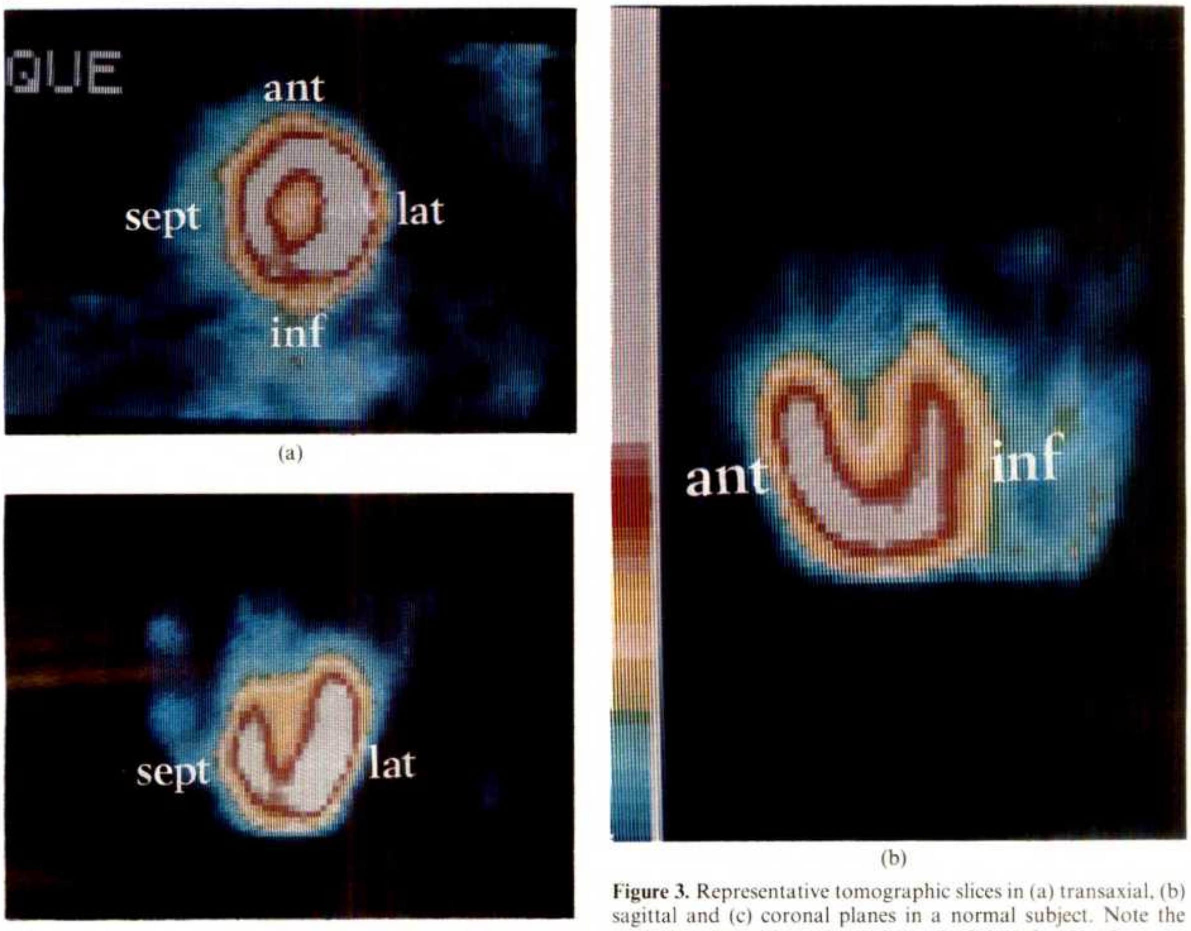

(a)

(c)

(b)

Figure 3. Representative tomographic slices in (a) transaxial, (b) sagittal and (c) coronal planes in a normal subject. Note the uniform activity throughout the wall of the left ventricle.

ventricular myocardium was divided into 12 segments, which were all easily defined by the SPECT slices. These comprised the proximal, mid and distal lateral wall, proximal, mid and distal anterior wall, proximal, mid and distal septum and the proximal, mid and distal inferior wall. Uptake defects, if detected, were ascribed to one or more segments and described in one of four categories according to our confidence level, *i.e.* normal (0), possibly abnormal (1), probably abnormal (2) and definitely abnormal (3).

The images were analysed twice, once using the transaxial (short axis) views alone and again using the additional information provided by the sagittal and coronal slices. The correlation between uptake defects present on the SPECT images and significant disease of individual coronary arteries as shown on coronary angiography was measured using the χ^2 test separately for all three levels of confidence and for both imaging techniques (transaxial alone and all three projections).

We used the results from previous studies of the localization of myocardial ischaemia, which used SPECT and thallium 201 as the basis for which segmental uptake defects should be specific for each artery. We then calculated the sensitivity and specificity of the SPECT imaging with technetium-99m MIBI for detecting coronary artery disease in general and stenosis of individual coronary arteries in particular.

Results

Coronary arteriography demonstrated all 96 major coronary arteries in the 32 patients (Table I). There was a total of 55 significantly stenosed vessels, 22 of which were occluded. Five subjects had normal coronary arteries, six had one-vessel disease, 14 had two-vessel disease and seven had three-vessel disease. Of the six

Table I. Findings at coronary angiography of the 32 patients

	RCA	LCx	LAD	Total
No significant stenosis ($\leqslant 50\%$)	17	16	8	41
Significant stenosis ($> 50\%$)	15	16	24	55
Total vessels	32	32	32	96

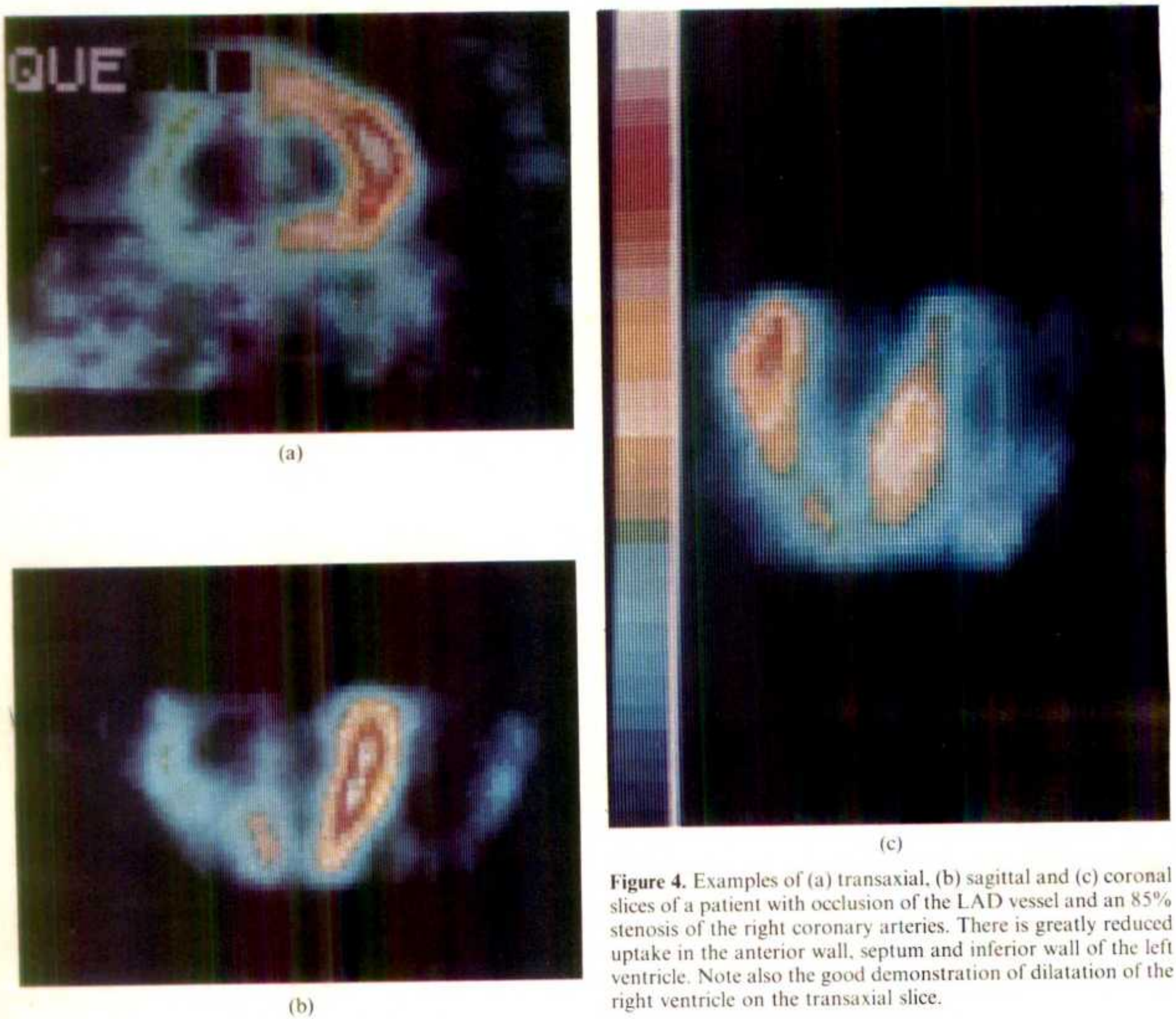

Figure 4. Examples of (a) transaxial, (b) sagittal and (c) coronal slices of a patient with occlusion of the LAD vessel and an 85% stenosis of the right coronary arteries. There is greatly reduced uptake in the anterior wall, septum and inferior wall of the left ventricle. Note also the good demonstration of dilatation of the right ventricle on the transaxial slice.

patients with single-vessel disease, the LAD artery was affected in four, the LCx artery in one and the RCA in one. There was a total of 24 diseased LAD vessels, 19 of which were associated with other vessel disease. There was a total of 16 diseased LCx vessels, 15 of which were associated with other vessel disease. There was a total of 15 diseased RCA vessels, 14 of which were associated with other vessel disease. The raw data of the number of true positives, false positives, true negatives and false negatives for each vessel at each confidence level is shown in Table II.

Detection of coronary artery disease

We assessed the ability of the test to detect any coronary artery disease by taking a true positive result as being a patient with stenosis of any one or more coronary arteries that had a segmental uptake defect. Sensitivities, specificities, positive and negative predictive values of the test for detection of disease were calculated and are presented in Table III. A sensitivity of 78% and a specificity of 100% at confidence level 3 (definitely abnormal) using all three projections was obtained. It may be that a better result could be achieved at a confidence level between 2 and 3 (probably abnormal and definitely abnormal).

The ability of the test to detect any coronary artery disease was also assessed by taking a true positive result as being a patient with disease of any of the coronary arteries who has a segmental uptake defect in at least one of the segments which corresponds to one of the diseased vessels. The results are shown in Table IV.

As expected, the sensitivities are not as good as when any defect is taken as a positive result. The best was a sensitivity of 78% at a specificity of 60%, but again, when the figures are examined more closely, it is possible that better results could be achieved using all three views and a confidence level between probable and definite, *i.e.* sensitivity between 59 and 89% and specificity between 40 and 100%.

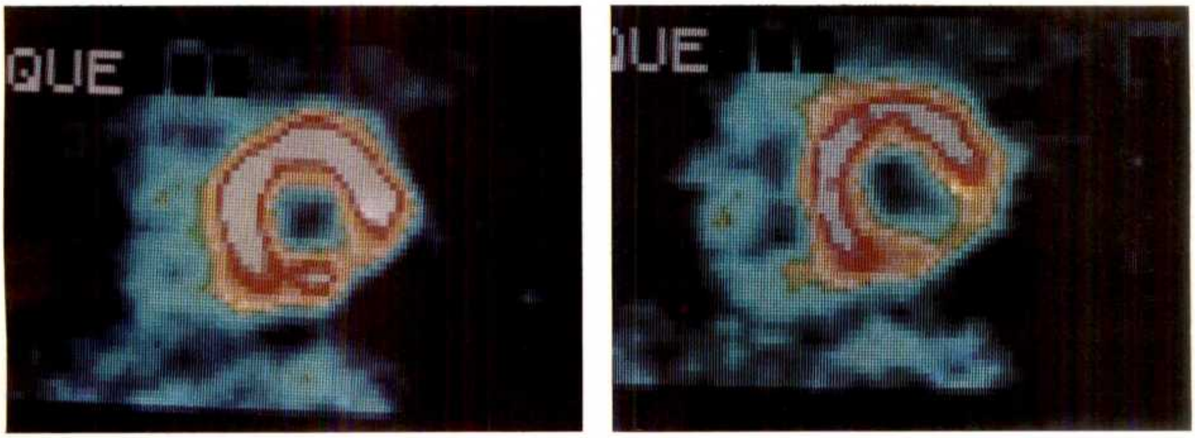

(a)

(b)

Figure 5 (a, b). Two transaxial slices of a patient with a left circumflex artery defect. Note the very sharp delineation of the defect in the low lateral wall.

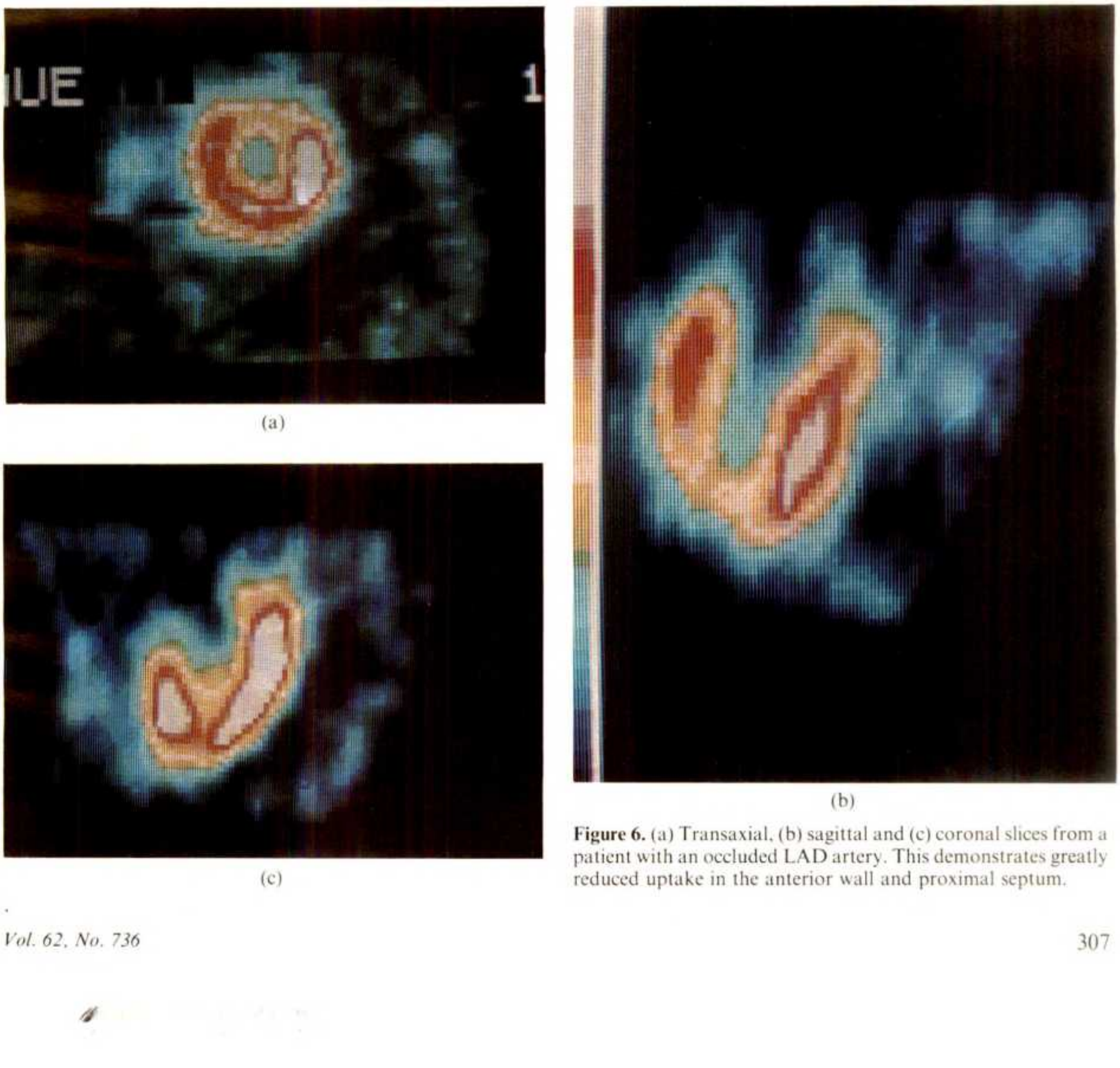

(a)

(c)

(b)

Figure 6. (a) Transaxial, (b) sagittal and (c) coronal slices from a patient with an occluded LAD artery. This demonstrates greatly reduced uptake in the anterior wall and proximal septum.

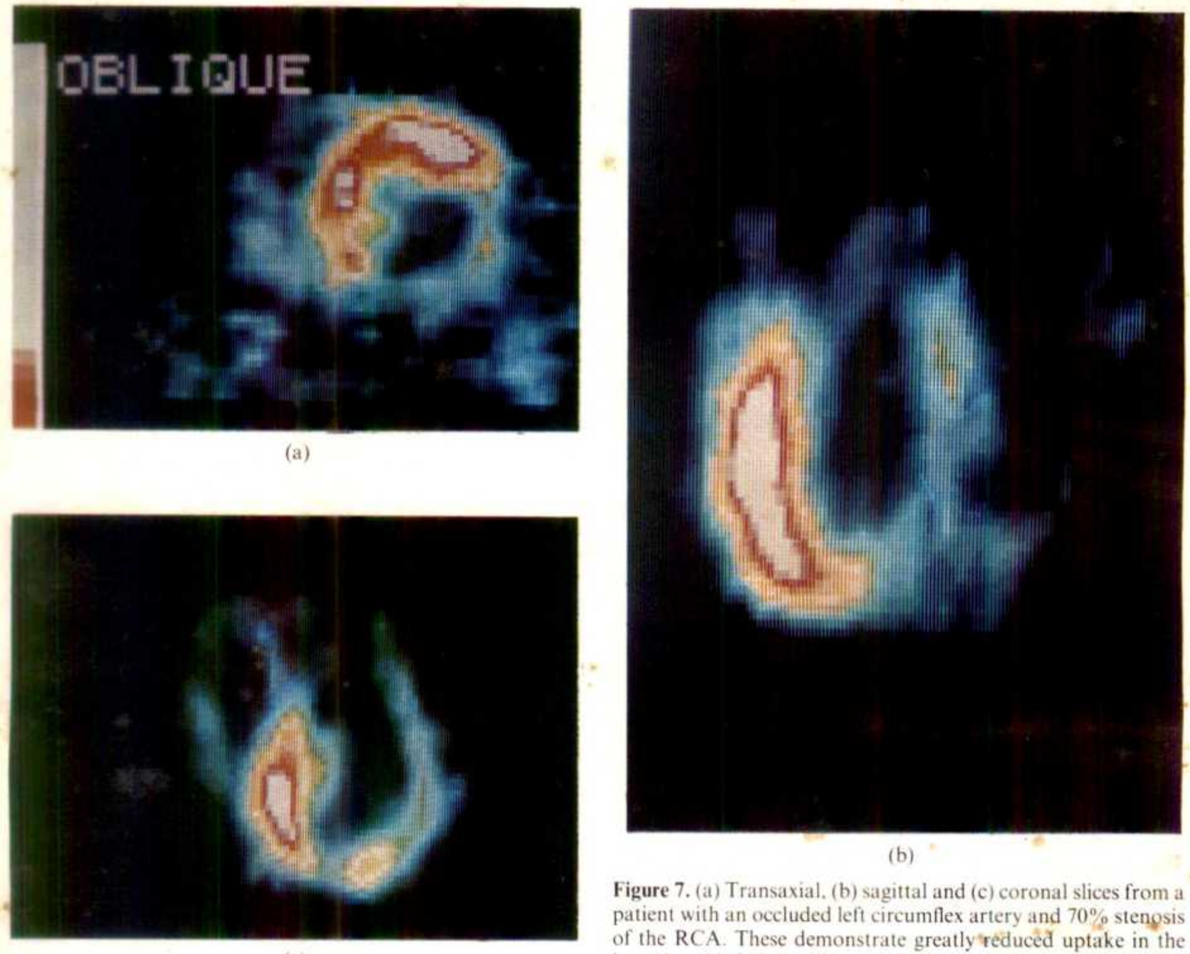

(a)

(c)

(b)

Figure 7. (a) Transaxial, (b) sagittal and (c) coronal slices from a patient with an occluded left circumflex artery and 70% stenosis of the RCA. These demonstrate greatly reduced uptake in the lateral and inferior walls.

Table II. The raw data from which the sensitivities, specificities, positive and negative predictive values were calculated

		Transaxial projection alone						Transaxial, coronal and sagittal projections					
		Possible		Probable		Definite		Possible		Probable		Definite	
		T	F	T	F	T	F	T	F	T	F	T	F
RCA	P	15	14	12	11	10	1	15	16	15	11	11	3
	N	3	0	6	3	16	5	1	0	6	0	14	4
LCx	P	15	5	11	1	5	0	14	5	12	2	7	1
	N	11	1	15	5	16	11	11	2	14	4	15	9
LAD	P	21	8	12	1	4	0	15	7	12	0	4	0
	N	0	3	7	12	8	20	1	9	8	12	8	20
Any vessel, any defect	P	27	5	26	3	19	1	27	5	26	3	21	0
	N	0	0	2	1	4	8	0	0	2	1	5	6
Any vessel, corresponding defect	P	26	5	21	2	15	0	24	5	24	3	16	0
	N	0	1	3	6	5	12	0	3	2	3	5	11

In each box of four the top left is the number of true positives, the top right the number of false positives, the bottom left the number of true negatives and the bottom right the number of false negatives. The confidence levels of reporting segmental defects are defined as possible, probable and definite.

Table III. Sensitivity, specificity, positive and negative predictive values for detection of coronary artery disease

	Transaxial projection alone			Transaxial, coronal and sagittal projections		
	Confidence level of reporting segmental defects					
	Possible	Probable	Definite	Possible	Probable	Definite
Sensitivity	100	96	70	100	96	78
Specificity	0	40	80	0	40	100
PPV	84	90	95	84	90	100
NPV	0	67	33	0	67	45

PPV = positive predictive value; NPV = negative predictive value.
A true positive result is a patient in whom any one of the coronary arteries is shown to be stenosed (> 50%) on the angiogram and who has an uptake defect as shown on the SPECT images.

Localization of disease to a vessel

When the uptake defects found were compared with the vessels known to be involved and correlated by use of a χ^2 test, we found the best correlations between RCA disease and distal, mid and proximal inferior segments ($0.001 < p < 0.01$) and the proximal septum ($p < 0.001$) and between LCx artery disease and mid ($0.001 < p < 0.01$) and proximal ($p < 0.001$) lateral segments (see Table V). Disease of the LAD artery on the other hand showed significant correlation with the distal anterior segment at only one level of confidence (possibly abnormal) using only the transaxial projection ($0.001 < p < 0.01$).

Previous SPECT studies using thallium 201 (Lenaers et al, 1977; Tamaki et al, 1984) have shown that the segmental defects corresponding most closely with disease of the major arteries are: RCA with the mid and proximal inferior segment, LCx artery with the proximal and mid lateral segments and LAD artery with the mid anterior and mid septal segments. We used defects in these segments in an attempt to predict disease in the corresponding vessels. A true positive result was taken as a patient with a stenosis on arteriography of a particular coronary artery whose SPECT images show an uptake defect in the segment corresponding to that vessel. These results are shown in Table VI.

The best results were obtained for the RCA of 73% sensitivity, 82% specificity, LCx artery 94% sensitivity, 69% specificity and LAD artery 50% sensitivity, 100% specificity, although as before there was a suggestion that more accurate results could be achieved, *i.e.* RCA specificity improved dramatically between probable and definite with less marked loss of sensitivity. The results for LAD vessel detection were significantly poorer than for the RCA and LCx vessels.

Basic characteristics of the test

As the defects were reported at three different levels of confidence and using two different image sets (transaxial and repeated with the addition of the sagittal and coronal planes), we obtained widely differing sensitivities and specificities. In order to illustrate these results and the basic characteristics of the test over a wide range of operating points, we constructed a receiver operating characteristic (ROC) curve. (Fig. 2). A very high sensitivity can be achieved at the expense of lower specificity, but a moderately high sensitivity can still be achieved while retaining high specificity levels. Receiver operating characteristic curves are of much greater value when making comparisons between different tests than are isolated figures of sensitivity and specificity at any one operating point.

Qualitative assessment

Apart from the very encouraging objective results using this new agent, we were particularly impressed by the overall clarity of the images, resulting in ease of interpretation, rapid learning and consensus. Studies on normal subjects showed generally very uniform uptake in all segments apart from some reduction in the region of the membranous septum. Defects here were therefore disregarded when reporting. The very high quality of the

Table IV. Sensitivity and specificity for detection of any coronary artery disease taking a true positive result as being a patient in whom any one of the coronary arteries was shown to be stenosed (> 50%) on the angiogram and who has an uptake defect in any of the corresponding myocardial segments

	Transaxial projection alone			Transaxial, coronal and sagittal projections		
	Confidence level of reporting segmental defects					
	Possible	Probable	Definite	Possible	Probable	Definite
Sensitivity	96	78	56	89	89	59
Specificity	0	60	100	0	40	100

Table V. Probability of correlation between myocardial uptake segmental defect and specific coronary artery stenosis

	Transaxial projection alone								
	1			2			3		
	RCA	LCx	LAD	RCA	LCx	LAD	RCA	LCx	LAD
Proximal septal	>0.5	>0.5	>0.5	0.1–0.5	>0.5	>0.5	<0.001	>0.5	0.1–0.5
Mid septal	>0.5	>0.5	>0.5	0.1–0.5	0.1–0.5	0.05–0.1	>0.5	>0.5	>0.5
Distal septal	0.1–0.5	>0.5	>0.5	>0.5	>0.5	>0.5	>0.5	>0.5	>0.5
Proximal lateral	>0.5	<0.001	>0.5	>0.5	0.001–0.01	>0.5	>0.5	0.1–0.5	>0.5
Mid lateral	0.1–0.5	0.001–0.01	0.1–0.5	>0.5	0.02–0.05	>0.5	>0.5	>0.5	>0.5
Distal lateral	0.1–0.5	0.02–0.05	>0.5	>0.5	0.1–0.5	0.1–0.5	>0.5	>0.5	>0.5
Proximal anterior	>0.5	0.1–0.5	>0.5	>0.5	>0.5	>0.5	>0.5	>0.5	>0.5
Mid anterior	>0.5	0.1–0.5	>0.5	>0.5	0.1–0.5	>0.5	>0.5	>0.5	>0.5
Distal anterior	0.1–0.5	>0.5	0.001–0.01	>0.5	>0.5	>0.5	>0.5	>0.5	>0.5
Proximal inferior	>0.5	0.1–0.5	>0.5	0.1–0.5	0.1–0.5	>0.5	0.001–0.01	0.1–0.5	>0.5
Mid inferior	>0.5	>0.5	>0.5	0.1–0.5	0.1–0.5	0.02–0.05	0.001–0.01	0.1–0.5	>0.5
Distal inferior	0.1–0.5	0.2–0.5	0.1–0.5	0.01–0.02	0.02–0.05	>0.5	0.001–0.01	0.1–0.5	>0.5
	Transaxial, sagittal and coronal projections								
	1			2			3		
	RCA	LCx	LAD	RCA	LCx	LAD	RCA	LCx	LAD
Proximal septal	0.1–0.5	>0.5	>0.5	0.02–0.05	0.1–0.5	0.05–0.1	0.05–0.1	>0.5	0.1–0.5
Mid septal	0.1–0.5	0.1–0.5	>0.5	>0.5	0.1–0.5	0.1–0.5	0.1–0.5	>0.5	>0.5
Distal septal	0.1–0.5	>0.5	>0.5	>0.5	0.05–0.1	>0.5	>0.5	0.1–0.5	>0.5
Proximal lateral	>0.5	0.001–0.01	>0.5	0.1–0.5	0.001–0.01	<0.5	>0.6	0.05–0.1	>0.5
Mid lateral	0.1–0.5	0.01–0.02	>0.5	0.05–0.1	0.02–0.05	0.1–0.5	0.1–0.5	0.05–0.1	>0.5
Distal lateral	0.02–0.05	0.05–0.1	>0.5	0.1–0.5	0.1–0.5	>0.5	>0.5	>0.5	>0.5
Proximal anterior	>0.5	0.1–0.5	>0.5	>0.5	>0.5	>0.5	>0.5	>0.5	>0.5
Mid anterior	>0.5	>0.5	>0.5	>0.5	>0.5	0.1–0.5	>0.5	0.1–0.5	>0.5
Distal anterior	>0.5	>0.5	>0.1–0.5	>0.5	>0.5	>0.5	>0.5	>0.5	>0.5
Proximal inferior	>0.5	>0.5	>0.5	0.1–0.5	0.1–0.5	>0.5	0.01–0.02	0.1–0.5	>0.5
Mid inferior	0.1–0.5	0.1–0.5	>0.5	0.05–0.1	0.01–0.02	>0.5	0.01–0.02	0.1–0.5	0.1–0.5
Distal inferior	0.02–0.05	0.1–0.5	>0.5	0.001–0.01	0.1–0.5	0.1–0.5	0.05–0.1	>0.5	>0.5

Table VI. Sensitivity and specificity of detection of stenosis of individual coronary arteries at the three different confidence levels using either transaxial slices only or all three slices for the interpretations

	Transaxial projection alone			Transaxial, coronal and sagittal projections		
	Possible	Probable	Definite	Possible	Probable	Definite
RCA sensitivity	100	80	67	100	100	73
RCA specificity	18	35	94	6	35	82
LCx sensitivity	94	69	31	87	75	44
LCx specificity	69	94	100	69	88	94
LAD sensitivity	88	50	17	63	50	17
LAD specificity	0	88	100	12.5	100	100

A true positive result is a patient in whom a particular vessel has been shown to be stenosed at angiography (>50%) and has an uptake defect in the expected segment on SPECT imaging.

images results in a feeling of confidence in the test result, which is enhanced by the ability to support initial findings by using additional image sets obtained in orthogonal planes. The borders of uptake defects were usually very sharply defined and even small islands of perfused tissue and small isolated defects could be well demonstrated. Examples of some of the examinations in this study are shown in Figs 3 to 7.

The quality of the images and the very clear demarcation of the non-perfused segments is immediately obvious and is in contrast with those from SPECT studies using thallium 201. These images are only representative 6 mm tomographic slices from each examination, in which there are between 30 and 60 slices. To appreciate the full potential in demonstrating uptake defects, together with their extent and spatial localization, requires the interpreter to view each slice sequentially on the TV monitor. Viewing of all slices can be achieved with practice in about 5 min.

Discussion

The development of new technetium-99m labelled isonitrile compounds has provided myocardial imaging agents that avoid many of the shortcomings of thallium 201. The particular properties of high energy (140 KeV), high photon yield, delayed clearance from the myocardium and low lung uptake of technetium-99m MIBI make it much better suited to SPECT imaging than thallium 201. Single photon emission computed tomography has been shown to increase both sensitivity and specificity of thallium studies and its particular advantages have been summarized by Tamaki et al (1984) as giving more accurate segmental analysis, better visualization of deeper segments, high-contrast images allowing minor degrees of ischaemia to be detected, reduced interference by lung and abdominal uptake and ability to perform quantitative analysis.

Since SPECT imaging was first applied to thallium studies there has been much discussion about the relative merits of using a full 360° or limited 180° rotation. The 180° rotation technique has a much shorter acquisition time and improved image contrast. The first of these two factors is of little importance with technetium-99m MIBI scanning because this agent does not redistribute, and the second factor is much less marked because the photon energy of technetium is higher than thallium. The 180° technique shows, however, a higher incidence of artefacts, leading to false positive perfusion abnormalities and image distortion. Taking these factors into consideration we have used the full 360° data acquisition.

Myocardial scintigraphy with both thallium and MIBI aims to detect areas of reduced perfusion. Deductions can be made from these findings about the patency of individual coronary arteries, which may be moderately accurate. However, even if the test could detect perfectly the perfusion to each myocardial segment, there are several factors that prevent completely accurate coronary artery disease prediction.

First, collateral vessels have been shown to provide adequate protection from ischaemia in the distribution of a dominant right coronary artery (Wainwright et al, 1980). It is not clear how important collateral vessels are but there is little doubt that they do play a protective role in at least some patients. Scintigraphy in such patients would result in false negative results. Secondly, the coronary artery anatomy varies from patient to patient. Consequently, although the majority conform to a standard pattern, it is not possible to predict accurately individual coronary artery disease from a knowledge of segmental perfusion. For example, in a right dominant type of circulation, the inferior and proximal lateral segments are supplied by the RCA and in a left dominant type by the left coronary artery. Thirdly, the blood flow to normal myocardium is non-homogeneous. There are areas, *e.g.* apex and membranous septum, of reduced perfusion. Generally, these are fairly constant from one patient to the next, so do not cause significant difficulties, but one must be aware of them to avoid too much importance being attached to such defects. Fourthly, the significance of individual coronary artery lesions is affected by factors which complicate comparison with the angiogram, *e.g.* the presence of left main-stem disease can modify the significance of lesions in distal vessels. Fifthly, increased metabolic demands, *e.g.* aortic stenosis, can lead to defects despite angiographically non-significant lesions.

The results of clinical trials of new diagnostic tests usually produce point figures for sensitivity and specificity. It is not surprising that widely varying figures are produced from different studies, but such figures can be confusing. This difficulty arises because different workers are often using different criteria for deciding when to call a test positive or negative. The relationship of sensitivity to specificity over the whole range of operating points (the dividing lines between test normal and test abnormal) can be displayed graphically as the ROC curve. This is a characteristic of the test, which is independent of prevalence, operating point and position. The ROC curve is more useful in describing the performance of a test than a point estimate of sensitivity and specificity.

As we reported the abnormal scans at three levels of confidence, using two different image sets, we produced six different sensitivity pairs for each vessel, which we were able to plot as an ROC curve. This technique not only gives a better impression of the basic characteristics of the test but will help to decide which operating point to choose for routine work and determine the optimum sensitivity/specificity values for particular uses of the test. The choice of operating point will depend on the purpose to which the test is put. If, for example, it were to be used as a screening tool we would need to pick up a large proportion of those with the disease but avoid exposing normal subjects to invasive and potentially dangerous confirmatory investigations. In these circumstances, it would be necessary to sacrifice some sensitivity to reduce the numbers of false positives. The ROC curve can help to choose the ideal operating point on this basis.

Our results for detection of coronary artery disease showed a sensitivity range from 100 to 70% and a specificity range from 100 to 0%. The figures were slightly better when using all three image sets rather than just the transaxial. The best result was a sensitivity of 78% and a specificity of 100%. However, it is possible, by learning, that the optimum operating point may be chosen so that a better result could be achieved in between a probable and definite confidence level with all three projections, *i.e.* sensitivity between 96 and 78% and specificity between 40 and 100%. Two aspects need to be considered here, however. First, there is no one most favourable result in a non-ideal test. Gains in sensitivity will always be made at the expense of specificity. The purpose to which this test is to be put will need to be known to determine the best result. Secondly, our figures for specificity are unlikely to be reliable. Specificity is calculated solely on the disease-negative subjects of which we had only five. The assessment of the accuracy of the test in detecting any coronary artery disease will necessitate studying large numbers of normal subjects. The results for detection of any coronary artery disease using only myocardial segments corresponding to the diseased vessels show, as would be expected, a slight reduction in sensitivity and a slight increase in specificity. The same comments as above apply to the specificity figures and thus it is not possible to draw conclusions about which of the two methods is more satisfactory.

In assessing the ability of the test to detect specific vessel disease we first had to decide what would constitute a true positive result for each vessel. Other workers undertaking similar studies with thallium 201 used a χ^2 test to determine which segment showed a significant correlation with each vessel (Lenaers et al, 1977; Tamaki et al, 1984). There is no reason to suspect that using MIBI rather than thallium would change such correlations, but we did perform our own χ^2 testing, which confirmed their findings for the RCA and LCx vessels but showed that the LAD vessel only correlated significantly with one segment (distal anterior), which did not concur with these previous studies. Justifiable criticism could be levelled at studies that calculate sensitivities and specificities of a test having decided what is a positive test from their own results. Bias is avoided by deciding what is a positive test from accepted wisdom or findings from previous studies. We chose the latter and came up with best figures for the RCA of sensitivity 73%, specificity 82%, for the LCx artery of sensitivity 94%, specificity 69% and for the LAD artery of sensitivity 50% and specificity 100%.

The results for RCA and LCx artery disease detection are thus very acceptable, but disappointing for the LAD artery. The specificity figures here are likely to be more accurate than for any vessel disease because there were significant numbers of disease-negative patients (*i.e.* those who had at least one vessel that was not diseased). The reasons for the poor pick-up of the LAD vessel lesions are not clear. The LAD territory is closest to the surface of the body and would thus logically be more easily demonstrated. One possible explanation relates to the paucity of single-vessel disease in our patients. It is well known that multiple-vessel disease reduces the sensitivity of detection of individual coronary artery disease. Nineteen of the 24 patients with diseased LAD vessels also had disease of at least one other vessel. Therefore, it would be possible, for example, for a diseased RCA vessel to dominate the myocardial perfusion pattern or to limit exercise so that perfusion to the LAD territory was not reduced at the time of scanning. It is interesting to note that in 13 of the 19 patients who had multiple-vessel disease, including an LAD lesion, the LAD lesion was less severe than one of the other lesions. It would be necessary to study a large number of patients with single-vessel disease to ascertain the true sensitivity and specificity values of the test.

Conclusions

The subjective quality of the images is superb. Defects, even small ones, stand out so clearly that it is likely that less experience and expertise will be required to interpret the images compared with standard planar thallium studies. Confidence in the findings by the referring clinicians is thus likely to be that much greater. These points are particularly important in those departments undertaking relatively few cardiac studies.

Our figures for sensitivity and specificity are, with the exception of LAD disease detection, very acceptable. It is likely that, with more experience of the test, results could be improved further. We believe that good quality tomography with this agent will enable us to approach the limit of accuracy of any isotopic technique for determining myocardial perfusion. Detection of coronary artery disease by this means will never be completely accurate because of the limits imposed by collateral flow, anatomical variation and the need for normal myocardium with which to compare.

References

Berman, D., Staniloff, H. Freeman, M., Garcia, E., Pantaleo, N., Maddahi, J., Waxman, A., Forrester, J. & Swan, H. J. C., 1980. Thallium-201 stress myocardial scintigraphy: comparison of multiple pin hole tomography with planar imaging in the assessment of patients undergoing coronary arteriography. *American Journal of Cardiology, 45,* 481 (Abstr.).

Deutsch, E., Glavan, K. A., Sodd, V. J., Nishiyama, H., Ferguson, D. L. & Lukes, S. J. 1981. Cationic Technetium 99m complexes as potential myocardial imaging agents. *Journal of Nuclear Medicine, 22,* 897–907.

Gerson, M. C., Deutsch, E. A., Nishiyama, H., Libson, K. F., Adolph, R. J., Grossman, L. W., Sodd, V. J., Fortman, D. L., Vanderheyden, J. L., Williamson, C. C. & Saenger, E. L. 1983. Myocardial perfusion imaging with Technetium 99m DMPE in man. *European Journal of Nuclear Medicine, 8,* 371–374.

Gerudini, P., Savi, A., Gilardi, M. C., Margonato, A., Vicedomini, G., Zecca, L., Hirth, W., Libson, K., Bhtia, J. C., Fazio, F. & Deutsch, E., 1986. Evaluation in dogs and humans of three potential Technetium 99m myocardial perfusion agents. *Journal of Nuclear Medicine, 27,* 409–416.

Holman, B. L., Hill, T. C., Wynne, J., Lovett, R. D., Zimmerman, R. E. & Smith, E. M., 1979. Single photon transaxial emission computed tomography of the heart in normal subjects and in patients with infarction. *Journal of Nuclear Medicine, 20,* 736–740.

Holman, B. L., Jones, A. G., Lister-James, J., Davison, A., Abrams, M. J., Kirshenbaum, J. M., Tumeh, S. S. & English, R. J. 1984. A new technetium 99m labelled myocardial imaging agent, hexakis (T-butylisonitrile)-technetium (I) [technetium 99m MTBI]: initial experience in the human. *Journal of Nuclear Medicine, 25,* 1350–1355.

Jones, A. G., Davison, A., Abrams, M. J., Brodack, J. W., Kassis, A. I., Goldhaber, S. Z., Holman, B. L., Stemp, L., Manning, T. & Hechtman, H. B., 1982. Investigations on a new class of Technetium cations. *Journal of Nuclear Medicine, 23,* 16.

Khalil, M. N., Williams, H., Heard, T. J., Shephard, A., Hartley, G., Early, M. Y., Berry, J. M. & Hubner, P. J., 1987. Technetium 99m methoxy isobutyl isonitrile (M.I.B.I.) for myocardial imaging. *Nuclear Medicine Communications, 8,* 233.

Lebowitz, E., Greene, M. W., Fairchild, R., Bradley-Moore, P. R., Atkins, H. L., Ansari, A. N., Richards, P. & Belgrave, E., 1975. Thallium-201 for medical use. *Journal of Nuclear Medicine, 16,* 151–155.

Lenaers, A., Block, P., Vanthiel, E., Lebedelle, M., Becquevort, P., Erbsmann, F. & Ermans, A., 1977. Segmental analysis of Thallium-201 stress myocardial scintigraphy. *Journal of Nuclear Medicine, 18,* 509–516.

Najm, Y. C., Maisey, M. N., Fogelman, I., Clarke, S., Curry, P. V. L. & Sowton, E., 1987. Exercise scintigraphy for coronary artery disease detection using new Technetium 99m labelled myocardial imaging agent: comparison with Thallium-201. *Nuclear Medicine Communications, 8,* 235.

Nohara, R., Kambara, H., Suzuki, Y., Tamaki, S., Kadota, K., Kawai, C., Tamaki, M. & Torizuba, K., 1984. Stress scintigraphy using single photon emission computed tomography in the evaluation of coronary artery disease. *American Journal of Cardiology, 53,* 1250–1254.

Pierson, R. N., Friedman, M. I., Tansey, W. A., Castellana, G. S., Enlander, D. & Huang, P. J., 1979. Cardiovascular nuclear medicine: an overview. *Seminars in Nuclear Medicine, 9,* 224–240.

Ritchie, J. L., Williams, D. L., Harp, G., Stratton, J. L. & Caldwell, J. H., 1982. Transaxial tomography with Thallium-201 for detecting remote myocardial infarction. Comparison with planar imaging. *American Journal of Cardiology, 50,* 1236–1241.

Strauss, H. W. & Pitt, B., 1978. Evaluation of cardiac function and structure with radioactive tracer techniques. *Circulation, 57,* 645–654.

Tamaki, N., Yonekura, Y., Mukai, T., Kodama, S., Kadota, K., Kambara, H., Kawai, C. & Torizuka, K., 1984. Stress Thallium-201 transaxial emission computed tomography: quantitative versus qualitative analysis for evaluation of coronary artery disease. *Journal of the American College of Cardiology, 4,* 1213–1221.

Thakur, M. L., Park, C. H., Fazio, F., Gerudini, P., Margonato, A., Vicedomini, G., Colombo, R., Colombo, F., Gilardi, M. & Fregoso, F., 1984. Preparation and use of Technetium 99m DEPE as a cardiac perfusion agent. *International Journal of Applied Radiation and Isotopes, 35,* 507–515.

Vogel, R., Kirch, D., Le Free, M. T., Rainwater, J. O., Jensen, D. P. & Steele, P. P., 1979. Thallium-201 myocardial perfusion scintigraphy. Results of standard and multi pinhole tomographic technique. *American Journal of Cardiology, 43,* 787–793.

Wainwright, R. J., Maisey, M. N., Edwards, A. C. & Sowton, E., 1980. Functional significance of coronary collateral circulation during dynamic exercises evaluated by Thallium-201 myocardial scintigraphy. *British Heart Journal, 43,* 47–55.

1989, *The British Journal of Radiology*, *62*, 314–317

The relation of radionuclide uptake by bone to the rate of calcium mineralization

I: Experimental studies using ^{45}Ca, ^{32}P and ^{99}Tc^{m}-MDP

By R. S. Budd, PhD, *G. S. Hodgson, MD and †W. S. C. Hare, MD, FRCR, FRACR

Physical Sciences Unit and *Peter MacCallum Research Laboratories, Peter MacCallum Cancer Institute, and †Department of Radiology, University of Melbourne, Royal Melbourne Hospital, Australia

(*Received June 1988*)

Abstract. The study of the uptake of radionuclides by bone has been undertaken in a mouse tail graft model using ^{45}Ca, ^{32}P and a routine bone scanning agent ^{99}Tc^{m}-MDP, together with serial calcium determinations. The model provided an experimental system in which the calcium mineral content and the rate of mineralization both changed progressively throughout its development. A significant linear correlation was found between ^{45}Ca and ^{32}P uptake and the rate of calcium mineralization, which held for all stages of the graft's growth. Both radiotracers therefore accurately reflected the calcium mineral deposition. In the case of ^{99}Tc^{m}-MDP, the correlation with mineralization rate only applied for the most active growth period of the graft when the rate was increasing. For all radiotracers, the peak in bone uptake corresponded to the maximum in mineralization rate.

Although the concept of the dependence of radiotracer uptake by bone on the rate of calcium mineralization has been accepted for many years (Charkes, 1970), there has been an absence of direct experimental evidence in support of the relation, due in part to a shortage of animal models suitable for investigation.

In this paper, the uptake of ^{45}Ca (calcium chloride), ^{32}P (sodium phosphate) and ^{99}Tc^{m}-MDP (technetium-99m methylene diphosphonate) has been studied in a mouse tail graft model in which the calcium mineral content and the rate of mineralization both changed progressively throughout its development.

Materials and methods

The experimental system was adapted from a model originally reported in the rat (Huggins & Anderson, 1970). The tails of 0.5–1.5-day-old BCF-1 mice (C57BL × BALB/c-F1) were amputated at their junction with the torso. Under a microscope, the skin was carefully removed exposing the tail bud, which consisted of avascular cartilage with intervertebral discs at periodic intervals along the cartilage rod. This was weighed and measured. Recipient mice were 26–30-day-old BCF-1 males which, under light ether anaesthetic, had a 3–4 mm incision in their lower abdomen and a small subcutaneous pocket formed by blunt dissection. With forceps, the graft was carefully inserted inside the pocket which was then closed with a metallic clip. In this environment, some 95% of the grafts were accepted and grew rapidly, differentiating into bone complete with bone marrow and forming a firm structure containing many vertebrae.

Using this technique, the grafts have been studied for periods up to 12 weeks. Prior to harvest, the recipient mice received a tail vein injection of ^{45}Ca (2.0 MBq), ^{32}P (1.0 MBq) or ^{99}Tc^{m}-MDP (2.0 MBq). Three hours later the animals were killed and immediately dissected. The grafts were then placed in pre-weighed counting tubes and their weight determined. For both ^{99}Tc^{m}-MDP and ^{32}P, the activity was counted in a well-type counter (Teledyne Isotopes, Model SW-88-I). In the case of studies involving ^{45}Ca, samples were dissolved in 5.0 ml of 0.5M HCl. From this volume, 0.5 ml was removed and added to 4.5 ml of scintillant and 0.1 ml of glacial acetic acid. Counting was performed in an automatic liquid scintillation counter (Packard Tri-carb, Model 3385). In all investigations, a reference source of 1% of the injected dose was prepared and at each point at least six animals were investigated, the results being expressed as mean and one standard deviation.

The calcium content of the grafts was determined by atomic absorption spectrophotometry from the calcium leached out after decalcification (Huggins & Anderson, 1970).

Results

The growth of the graft was found to follow an S-shaped curve as shown in Fig. 1. This summarizes the general knowledge that after a period of active growth the size of any particular multicellular organism approaches a limiting value. Initially, the graft was approximately 0.5 cm in length with a mean weight just over 5 mg. Within the first 6 weeks, there was a rapid eight-fold increase in weight and after 10–12 weeks, the graft reached a maximum weight of almost 50 mg and a length between 3 and 4 cm. The growth of the graft was much less than that of the normal intact tail, which reached a weight of 60 mg in the first week and a maximum weight in excess of 600 mg after 12 weeks. The effect of grafting, therefore, was to delay the growth rate of the tail such that the development and mineralization normally occurring within the first week could be studied

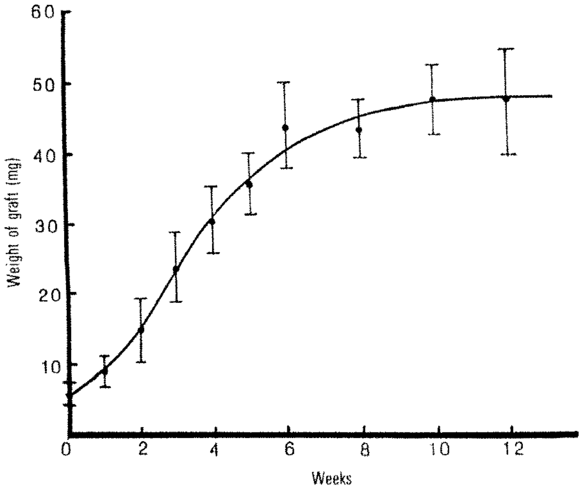

Figure 1. Growth of the mouse tail graft.

in detail at weekly intervals over a period of 10 to 12 weeks. This model minimized the normal animal-to-animal variations in growth and mineral deposition that would have been present had an attempt been made to study the intact tail at daily intervals during the first week. Also, it eliminated the variability and uncertainty of radiotracer uptake associated with intraperitoneal injection that would have been necessary.

The calcium content expressed as a fraction of the graft weight (mg Ca^{2+}/mg graft) is shown in Fig. 2 where it can be seen that the Ca^{2+} concentration approached a maximum value of 10% after about 12 weeks. The rate of mineralization at weekly intervals (expressed as mg Ca^{2+}/mg graft/week) is given by the gradient or the derivative of the curve at that time and this is also depicted in Fig. 2. The rate increased to a maximum between 3 and 4 weeks and then became progressively less, diminishing more and more slowly as mineralization proceeded. Radiotracer uptake by bone could therefore be studied under conditions in which both the absolute calcium content and the rate of mineralization progressively changed.

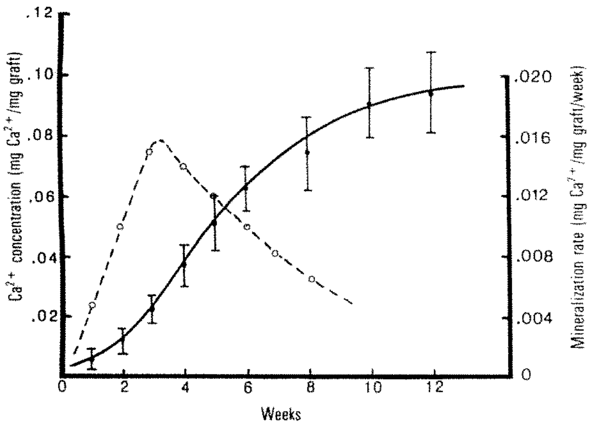

Figure 2. Ca^{2+} concentration (———) and rate of mineralization (– – –) of the mouse tail graft.

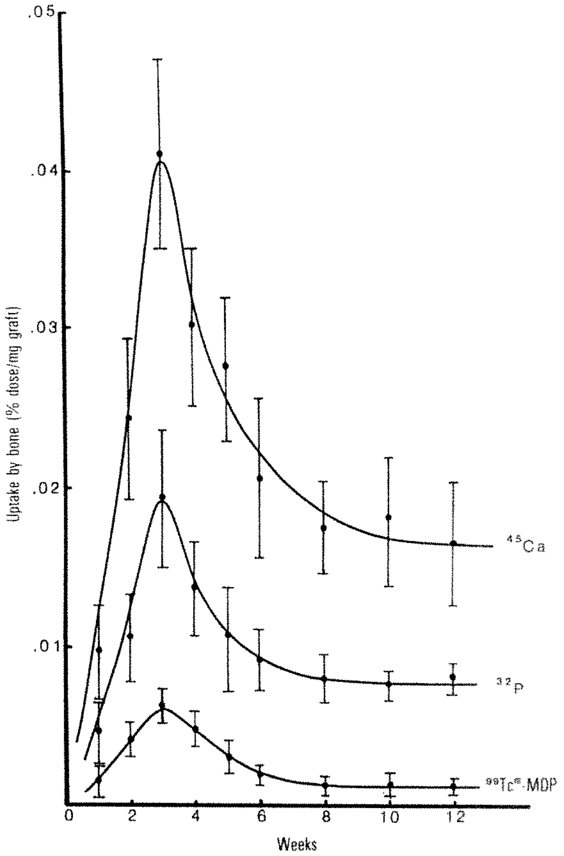

Figure 3. Uptake by the tail graft of ^{45}Ca, ^{32}P and $^{99}Tc^{m}$-MDP at 3 h.

The uptake (% dose/mg) of ^{45}Ca, ^{32}P and $^{99}Tc^{m}$-MDP in the graft at weekly intervals, determined 3 h after injection, is shown in Fig. 3. All three radiotracers demonstrated a rapid rise in bone uptake with a well defined peak at 3 weeks. This was followed by a gradual reduction in tracer accumulation at a somewhat slower rate relative to the initial uptake. These results suggested a clear correlation between the radiotracer uptake by bone and the rate of calcium mineralization (Fig. 2). This relationship is well documented in Fig. 4 where solid symbols refer to the upswing of the results (Weeks 1, 2 and 3) and open symbols to the downswing (Weeks 4, 5, 6 and 8).

It can be seen that for ^{45}Ca and ^{32}P there was a significant linear correlation between radiotracer uptake and the rate of mineralization during both the upswing and downswing phases (see Table I). With regard to $^{99}Tc^{m}$-MDP, however, the correlation held true for only the most active growth period of the graft, that is, during the upswing phase of the first 3 weeks. After this time, other factors in determining $^{99}Tc^{m}$-MDP uptake such as

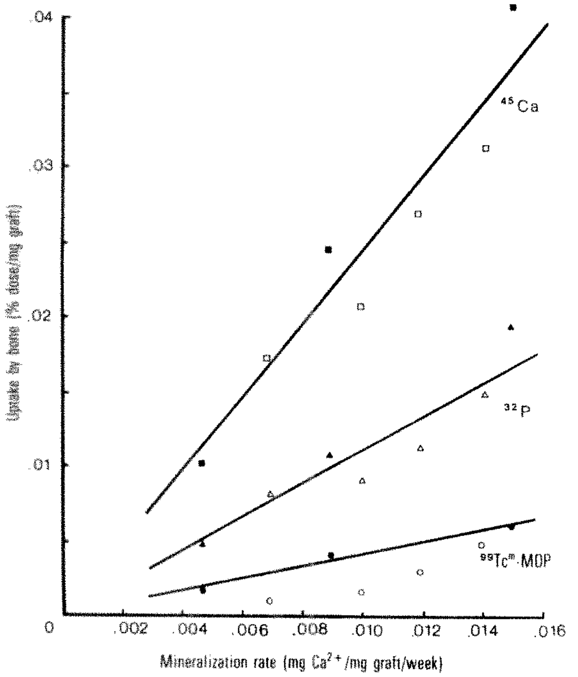

Figure 4. Correlation of the 3-h uptake of radiotracers by the graft with the rate of mineralization. Solid symbols refer to the upswing of the results (Weeks 1, 2, 3) and open symbols refer to the downswing (Weeks 4, 5, 6, 8).

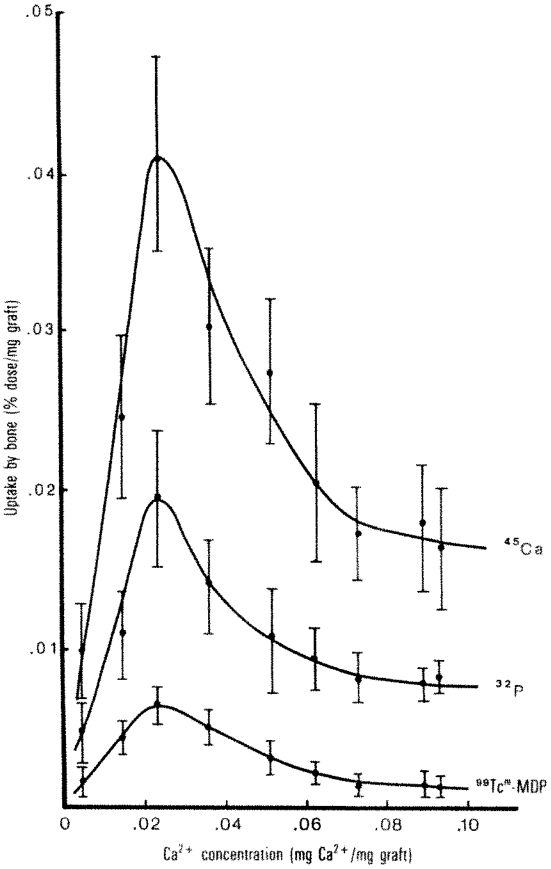

Figure 5. Relation of radiotracer uptake at 3 h with calcium concentration.

available bone surface area became important (Budd, 1986). Beyond Week 4, the ^{99}Tc^{m}-MDP uptake was less than that anticipated on the basis of the upswing results.

The relation between radiotracer uptake and the calcium concentration in the graft is shown in Fig. 5. For all radiotracers, the uptake and the calcium concentration increased in parallel initially until a clearly defined stage of the graft's development was reached at which time further mineralization was accompanied by a reduction in radiotracer uptake. The peak in tracer uptake corresponded to the maximum in mineralization rate and occurred when the calcium concentration was approximately 0.025 mg Ca^{2+}/mg graft.

Table I. Linear regression analysis for the correlation of radiotracer uptake with rate of mineralization

			95% confidence limits	
^{45}Ca	k	2.643	1.837	3.450
$r = 0.93$	c	−0.002	−0.018	0.006
^{32}P	k	1.272	0.788	1.755
$r = 0.91$	c	−0.002	−0.007	0.003
^{99}Tc^{m}-MDP	k	0.405	0.231	0.578
$r = 0.92$	c	−0.001	−0.002	0.002

$$Y = kX + c$$

where Y is the radiotracer uptake; X is the rate of mineralization; k is the proportionality constant; c is the intercept; and r is the correlation coefficient.

The correlations for ^{45}Ca and ^{32}P were determined during both the upswing and downswing phases whereas the correlation for ^{99}Tc^{m}-MDP was determined for only the first 3 weeks of graft growth.

Discussion

The importance of the rate of mineralization on radionuclide uptake by bone has received little attention in the literature. In one report, comparative studies of several bone-seeking radiotracers were undertaken in normal and rachitic rats induced by vitamin D deficiency (Genant et al, 1974). The choice of this model was based on earlier findings that had shown that all phases of osteogenesis including matrix formation, osteoid formation and mineralization rate were decreased in rachitic rats compared with controls (Baylink et al, 1970). However, Genant and co-workers found that the radiotracer uptake, rather than being decreased as anticipated, was in fact slightly greater in the rachitic rats than in the controls. Consequently, they concluded that the uptake of the bone-seeking agents was independent of the rate of mineralization even though no attempt was made to measure this in their animals.

However, it has been reported that true rickets in rats can only be obtained by means of a high calcium–low phosphorus, vitamin D-deficient diet (Cousins & Deluca, 1972). The authors claimed that if the diet contained adequate calcium and phosphorus, bone lesions did occur but morphologically they were not true rickets and in fact the work of Baylink and others (1970) was cited as an example of this. The conclusion drawn by Genant and co-workers, that the rate of mineralization was not an important factor in determining radiotracer uptake by bone, could therefore be questioned.

In contrast to this, the mouse tail graft model reported here provided a system in which the calcium content and the rate of calcium mineralization both underwent considerable change during the development of the graft. The studies involving ^{45}Ca, ^{32}P and the routine scanning agent ^{99}Tc^{m}-MDP confirmed that there was a significant linear correlation between radionuclide uptake and the rate of mineralization.

In addition, the relation between radiotracer uptake and the calcium concentration (Fig. 5) showed that the developmental status of the graft could not be accurately predicted at any time on the basis of the radiotracer uptake alone, since the same level of uptake could be obtained on either side of the biphasic relationship. A knowledge of the calcium concentration would be required, therefore, in order to decide whether a given level of radiotracer uptake was associated with the early development of the graft or its near completion.

It is also clear from the results that ^{45}Ca and ^{32}P both have a greater affinity for bone than the scanning agent ^{99}Tc^{m}-MDP. This is not surprising as calcium and phosphorus are the principal constituents of the skeleton in the form of hydroxyapatite $Ca_{10}(PO_4)_6(OH)_2$ (Spiers, 1968), which contains over 99% and 90% of the total body content of each, respectively (Mitchell et al, 1945). Additionally, they both reflected the calcium mineral deposition in bone more accurately than did ^{99}Tc^{m}-MDP. Unfortunately, neither calcium nor phosphorus exists in a radionuclide form with suitable physical characteristics for routine clinical nuclear imaging.

While the results obtained with ^{99}Tc^{m}-MDP have been less predictable, they have still proved to be of considerable value. In particular, the relation of its uptake with calcium concentration (Fig. 5) has improved the understanding of the pathophysiological mechanisms reflected in the radionuclide images of bone metastases and this subject is considered in a companion paper (Budd et al, 1989).

References

Baylink, D., Stauffer, M., Wergedal, J. & Rich, C., 1970. Formation, mineralization and resorption of bone in vitamin D-deficient rats. *Journal of Clinical Investigation*, *49*, 1122–1134.

Budd, R. S., 1986. *The Study of the Uptake of Radionuclides by Bone and its Application to the Detection of Metastases*, PhD Thesis (University of Melbourne).

Budd, R. S., Hodgson, G. S. & Hare, W. S. C., 1989. The relation of radionuclide uptake by bone to the rate of calcium mineralization. II: Patient studies using ^{99}Tc^{m}-MDP. *British Journal of Radiology*, *62*, 318–320.

Charkes, N. D., 1970. Bone scanning: principles, technique and interpretation. *Radiologic Clinics of North America*, *VIII*, 259–270.

Cousins, R. & Deluca, H. F., 1972. Vitamin D and bone. In *The Biochemistry and Physiology of Bone*, 2nd edn, ed. by G. H. Bourne (Academic Press, New York), Vol. II, pp. 281–335.

Genant, H. K., Bautovich, G. J., Singh, M., Lathrop, K. A. & Harper, P. V., 1974. Bone-seeking radionuclides: an *in vivo* study of factors affecting skeletal uptake. *Radiology*, *113*, 373–382.

Huggins, C. B. & Anderson, K. P., 1976. Growth of transplanted tails of infant rats in adolescent allogeneic recipients. *Proceedings of the National Academy of Science*, *73*, 3283–3287.

Mitchell, H. H., Hamilton, T. S., Steggerda, F. R. & Bean, H. W., 1945. The chemical composition of the adult human body and its bearing on the biochemistry of growth. *Journal of Biological Chemistry*, *158*, 625–637.

Spiers, F. W., 1968. The macroscopic and microscopic structure of bone. In *Radioisotopes in the Human Body: Physical and Biological Aspects* (Academic Press, New York), pp. 119–154.

P9 5077

1989, *The British Journal of Radiology*, 62, 318–320

The relation of radionuclide uptake by bone to the rate of calcium mineralization

II: Patient studies using ^{99}Tc^{m}-MDP

By R. S. Budd, PhD, *G. S. Hodgson, MD and †W. S. C. Hare, MD, FRCR, FRACR

Physical Sciences Unit and *Peter MacCallum Research Laboratories, Peter MacCallum Cancer Institute, and †Department of Radiology, University of Melbourne, Royal Melbourne Hospital, Australia

(Received June 1988)

Abstract. The relation of radionuclide uptake by bone and rate of calcification has been studied in normal vertebrae and in vertebral metastases from cancer of the prostate. Specifically, the determination of ^{99}Tc^{m}-MDP uptake by radionuclide scanning and the estimation of calcium concentration of trabecular bone by dual-energy computed tomography have provided the means of obtaining a relation between these parameters which was similar to that found in an animal model, in which the dependence of radionuclide uptake on the rate of mineralization was established. This relationship has enabled the experimental findings to be extrapolated to those in patient studies and has shown that in sclerotic bone lesions, the increase in ^{99}Tc^{m}-MDP uptake accompanying the progression of the metastases was proportional to the rate of calcification.

In an animal model, it has been shown that uptake by bone of the radiotracers ^{45}Ca, ^{32}P and ^{99}Tc^{m}-MDP (technetium-99m methylene diphosphonate) were all related to the rate of calcium mineralization (Budd et al, 1989). In the present study, this relationship has been investigated in patients with cancer of the prostate by the comparison of ^{99}Tc^{m}-MDP uptake by, and calcium concentration of, normal vertebrae and vertebral bone metastases.

Patients and methods

Investigations were undertaken in 43 male patients with cancer of the prostate who attended the Peter MacCallum Cancer Institute. Baseline bone scans and computed tomography (CT) were performed prior to radiotherapy or hormone therapy. Since the most common sites for bone metastases have been shown to be the dorsal and lumbar vertebrae (Jaffe, 1958), the study has been initially confined to these areas.

Radionuclide imaging

Between 3 and 5 h after the intravenous injection of 700 MBq of ^{99}Tc^{m}-MDP, the bone scan was performed using a scanning detector gamma camera (Technicare Sigma 438). In addition to the routine anterior and posterior views of the entire skeleton, a static posterior view of the spine was stored on computer (ADAC Clinical Data System or GE Star II) so that a quantitative index of the radionuclide uptake could be estimated. Regions of interest (ROI) were assigned over vertebrae from T7 to L4 together with a similar region between the iliac crest and the kidney as shown in Fig. 1. The radionuclide uptake in each vertebra could then be expressed as a bone to soft-tissue ratio similar to that described for T12 by Constable and Cranage (1981). Preliminary results obtained in five patients (three with normal scans and two with spinal metastases) had indicated that in the absence of obstructive uropathy, the bone to soft-tissue ratio remained steady within the time interval of 3 and 5 h post-injection. Consequently, only patients with normal renal function were included.

Computed tomographic imaging

With a Siemens DR3 CT scanner, 4 mm thick scans were obtained through sites chosen on the basis of the radionuclide bone scan. Using the 125 kV and 96 kV energy modes, between one and four vertebrae (average two) were scanned through the midplane (Fig. 2) in an investigation that was completed in under 10 min. On each CT image, the trabecular cavity was sampled using

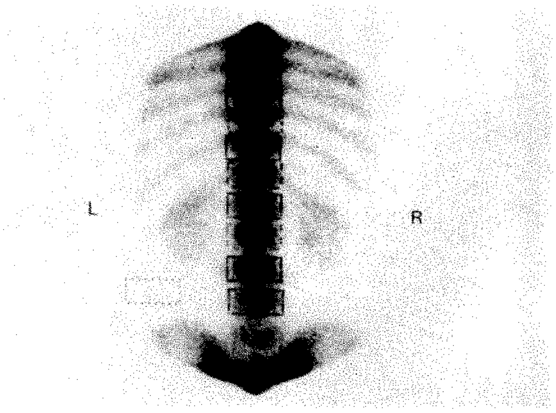

Figure 1. ^{99}Tc^{m}-MDP static image of the spine showing positions of the regions of interest.

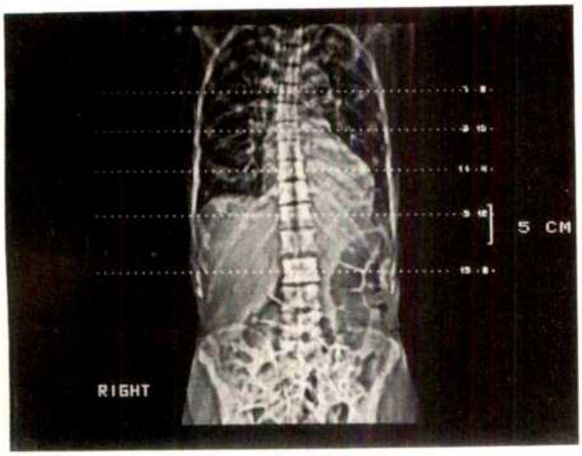

Figure 2. Computed tomographic topogram showing typical scan sites through the midplane of the vertebrae.

an irregular ROI as illustrated in Fig. 3, the same region being applied to the 125 kV and 96 kV images of each section. Average CT numbers were recorded and the difference in these values was proportional to the mineral content (Genant & Boyd, 1977), which could be expressed in terms of equivalent levels of K_2HPO_4 (mg/ml) by calibration with suitable reference phantoms (Sephton, 1985). K_2HPO_4 has almost the same effective atomic number as hydroxyapatite and is a common reference material for bone mineral determination.

Results

At presentation, six patients were found to have no bone metastases. Of the remaining 37 patients, seven had minimal bone disease involving at most two vertebrae, the other 30 patients having widespread metastases throughout the spine and pelvis.

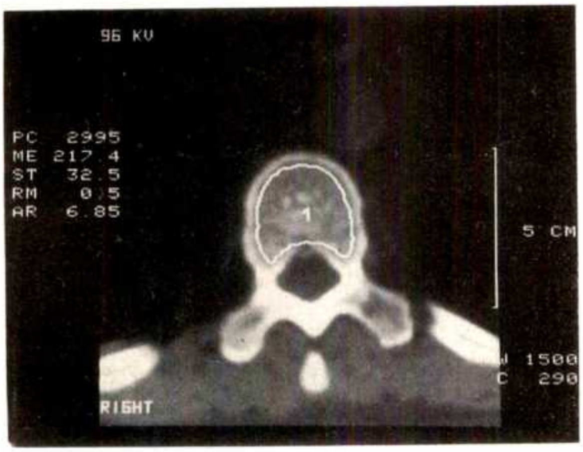

Figure 3. Illustration of the use of an irregular region of interest to determine the equivalent mineral content of trabecular bone.

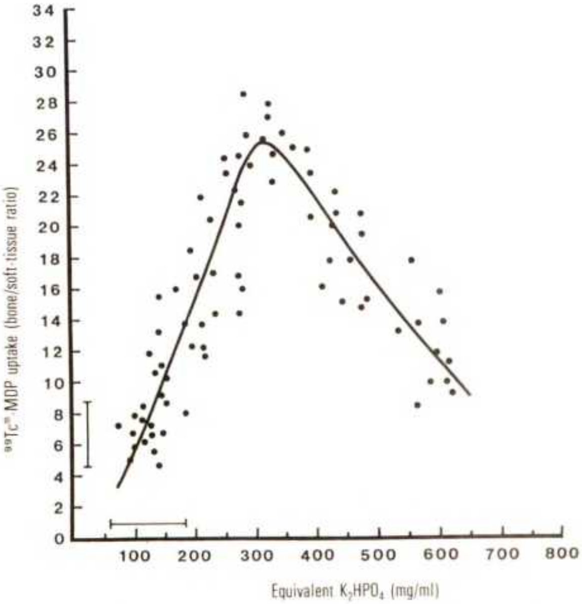

Figure 4. Relation of ^{99}Tc^{m}-MDP uptake by, with the equivalent mineral content of, individual vertebrae. Data are shown for normal vertebrae and for sclerotic bone metastases. The normal range for both parameters is shown thus (⊢⊣).

With regard to the CT investigation, quantitation was critically dependent upon the scanning technique and required both the 125 kV and 96 kV images to be perfectly aligned and for neither to include any breathing or movement artefacts. Consequently, a number of CT scans had to be rejected on technical grounds leaving a total of 78 data points from the 43 patients.

Figure 4 shows the relation of ^{99}Tc^{m}-MDP uptake data with the equivalent K_2HPO_4 mineral content for individual vertebrae from the patients studied. The normal range for both parameters is shown along each axis. The patients were males with ages from 55 to 75 years and the normal bone mineral range for this age group (60–180 mg/ml equivalent K_2HPO_4) was taken from published data (Genant et al, 1983).

All the data were obtained during the baseline studies performed before the patients commenced therapy. The data from patients with no bone involvement fell within the normal range for both parameters. In the patients with metastases, as the calcium mineral of the marrow cavity increased, there was first an increase in ^{99}Tc^{m}-MDP uptake. This relationship continued until a clearly defined level of calcification was reached at which time further calcification was accompanied by a reduction in radiotracer uptake. As the calcium content increased even higher, ^{99}Tc^{m}-MDP uptake in the normal range was observed. At the peak of ^{99}Tc^{m}-MDP uptake, the mineral content was approximately 300 mg/ml equivalent K_2HPO_4. This corresponded to a calcium concentration of approximately 0.077 mg Ca^{2+}/mg bone (Budd, 1986).

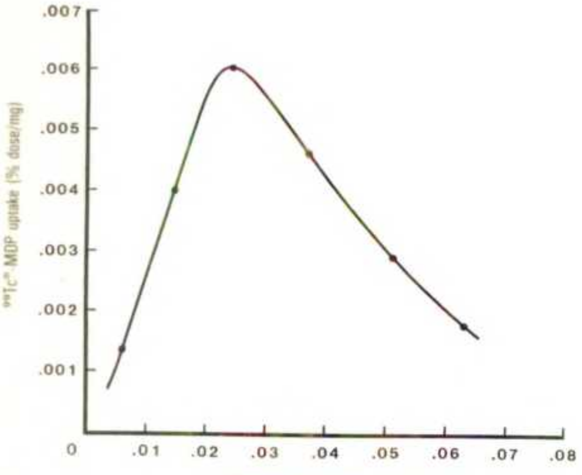

Figure 5. Relation of ^{99}Tc^{m}-MDP uptake by, with calcium concentration of, vertebrae of the grafted mouse tail (from Budd et al, 1989).

Discussion

In the companion study using the mouse tail graft model (Budd et al, 1989), the relationship between ^{99}Tc^{m}-MDP uptake and Ca^{2+} concentration as reproduced in Fig. 5 was obtained. During the early stages of the graft's development, a linear correlation was shown to exist between ^{99}Tc^{m}-MDP uptake and the rate of Ca^{2+} mineralization, with the peak at 3 weeks corresponding to the maximum rate of mineralization. In the present study of patients with bone metastases, rates of mineralization *in situ* could not be obtained but the relationship of ^{99}Tc^{m}-MDP uptake with calcium concentration (Fig. 4) is entirely consistent with the pattern in the animal model.

This observation implies that in the development and progression of sclerotic bone metastases, the relationship between ^{99}Tc^{m}-MDP uptake and rate of calcification is similar to that found in the growth of the mouse tail graft. In particular, this means that ^{99}Tc^{m}-MDP uptake in bone-forming lesions is proportional to the rate of calcification during the period in which uptake is increasing and that the peak corresponds to the maximum rate of calcification. Furthermore, the biphasic nature of Fig. 4 gives some insight into the reported observations that a decline in radionuclide uptake can be associated with either progression or remission of disease (Galasko & Doyle, 1972; Castronovo et al, 1973; Shearer et al, 1974; Condon et al, 1981).

Many advanced stages of metastases involve almost the entire vertebral cavity and in such cases the rigid structure of the cortical bone would limit any further progression. This in turn would be accompanied by a reduction in the ^{99}Tc^{m}-MDP uptake as seen on the radionuclide scan. Obviously, the degree of progression of a metastasis could not be accurately predicted at any time on the basis of the ^{99}Tc^{m}-MDP uptake data alone, since the same level could be obtained on either side of the biphasic relationship. A knowledge of the equivalent K_2HPO_4 concentration therefore would be required for a complete understanding of its status.

References

BUDD, R. S., 1986. *The Study of the Uptake of Radionuclides by Bone and its Application to the Detection of Metastases*. PhD Thesis (University of Melbourne).

BUDD, R. S., HODGSON, G. S. & HARE, W. S. C., 1989. The relation of radionuclide uptake by bone to the rate of calcium mineralization. I: Experimental studies using ^{45}Ca, ^{32}P and ^{99}Tc^{m}-MDP. *British Journal of Radiology, 62*, 314–317.

CASTRONOVO, F. P., POTSAID, M. S. & PENDERGRASS, H. P., 1973. Effects of radiation therapy on bone lesions as measured by ^{99m}Tc diphosphonate. *Journal of Nuclear Medicine, 14*, 604–605.

CONDON, B. R., BUCHANAN, R., GARVIE, N. W., ACKERY, D. M., FLEMING, J., TAYLOR, D., HAWKES, D. & GODDARD, B. A., 1981. Assessment of progression of secondary bone lesions following cancer of the breast or prostate using serial radionuclide imaging. *British Journal of Radiology, 54*, 18–23.

CONSTABLE, A. R. & CRANAGE, R. W., 1981. Recognition of the superscan in prostatic bone scintigraphy. *British Journal of Radiology, 54*, 122–125.

GALASKO, C. S. B. & DOYLE, F. H., 1972. The response to therapy of skeletal metastases from mammary cancer; assessment by scintigraphy. *British Journal of Surgery, 59*, 85–88.

GENANT, H. K. & BOYD, D., 1977. Quantitative bone mineral analysis using dual-energy computed tomography. *Investigative Radiology, 12*, 545–551.

GENANT, H. K., CANN, C. E., POZZI-MUCELLI, R. S. & KANTER, A. S., 1983. Vertebral mineral determination by quantitative CT: clinical feasibility and normative data. *Journal of Computer Assisted Tomography, 7*, 554.

JAFFE, H. L., 1958. Tumors metastastic to the spine. In *Tumors and Tumorous Conditions of the Bones and Joints* (Lea and Febiger, Philadelphia), pp. 589–618.

SEPHTON, R. G., 1985. Evaluation of two CT scanners for dual energy applications. *Australasian Physical and Engineering Sciences in Medicine, 8*, 11–16.

SHEARER, R. J., CONSTABLE, A. R., GIRLING, M., HENDRY, W. F. & FERGUSON, J. D., 1974. Radioisotope bone scintigraphy with gamma camera in the investigation of prostate cancer. *British Medical Journal, ii*, 362–365.

1989, *The British Journal of Radiology*, *62*, 321–325

Phalangeal osteoid osteoma

By *Quanfei Meng and †Iain Watt

Department of Radiology, Bristol Royal Infirmary, Bristol BS2 8HW

(*Received July 1988 and in revised form November 1988*)

Abstract. Although the typical features of osteoid osteomas are well known, those arising in phalanges are frequently misdiagnosed. This is partly because of their rarity (9% of osteoid osteomas in the Bristol Bone Tumour Registry occur in phalanges), and also because of atypical radiological features. The most common appearance is of an eccentric lesion with soft-tissue swelling and a relative absence of sclerosis, suggesting osteomyelitis.

An osteoid osteoma is a benign, bone-forming tumour, initially described in 1932 by Jaffe and Mayer, with a further re-definition in 1935 by Jaffe. Usually, the radiological features are not in doubt, but difficulty may arise when the lesion arises at an atypical site. Osteoid osteomas usually occur in long bones, especially the femur and tibia, and are characterized by pain and tenderness, especially at night, and relieved by salicylate. Radiographs typically reveal an extensive zone of sclerosis surrounding a small central translucent area, within which stippled calcification (nidus) may be visualized (Wilner 1982; Murray & Watt 1987).

Tumours arising in phalanges of the hand and foot are rare (Jackson et al, 1977). Whilst the basic symptoms, signs and radiological appearances share most characteristics of those arising in the more common sites, they are frequently misdiagnosed. The clinical and radiological features of phalangeal osteoid osteoma have been reviewed from the files of the Bristol Bone Tumour Registry, with a view to identifying the atypical features that may cause diagnostic difficulty.

Clinical material

Between 1946 and 1987, 93 cases of osteoid osteoma were classified by the Bristol Bone Tumour Registry. Eight lesions were localized in the phalanges of the hand or foot. Full documentation was available in all patients, including clinical follow-up averaging 42 months (range 7 months to 8 years) from initial evaluation.

All but one patient was less than 30 years old (range 13 to 42 years), and there were more males than females, the age and sex distribution being similar to that in osteoid osteoma overall (Jackson et al, 1977; Dahlin, 1979; Wilner, 1982) save for a slightly higher male dominance (3:1 as opposed to 2:1). Five lesions were located in the fingers (three terminal phalanges, two proximal). The three toe lesions were in terminal phalanges. Seven lesions were on the right side. All patients complained of local pain in the involved digit, particularly at night in four and on movement in two. The effect of salicylate or other analgesic had not been recorded. All described local swelling, constant in seven but intermittent in one. Duration of symptoms, prior to diagnosis, varied from 4 months to 3 years. Three patients gave a history of trauma before the onset of symptoms. No history of antecedent infection was elicited. On examination, swelling was found in all affected digits, with focal tenderness in seven, and obvious redness or discoloration in two. Reduced range of movement at the nearest joint was present in two cases. Nail hypertrophy was noted in three, involving thumbs or little toes. All patients were misdiagnosed prior to excision biopsy.

Radiological appearances

Terminal phalanges

All lesions were peripherally situated; those in the fingers (three) were close to the base of the terminal tufts and subcortical (Figs 1, 2), whereas those in the toes (three) were at the tips of the phalanges (Figs 3, 4). All had a circular or oval translucency with ill defined margins, the lucency being of the order of 4 mm × 6 mm in size. Adjacent sclerosis was minimal (Figs 1, 3). Slight cortical thinning and expansion was observed in three cases (two fingers, one toe) (Figs 1, 3). A nidus was shown in five cases (83%); in one this was markedly eccentric (Fig. 4) and in another, two nidi were present, one eccentrically located, the other central within the radiolucency. The density of the nidus was not increased in most cases, such that in two it could not be located on lateral radiographs (Fig. 1). Periosteal new-bone formation did not occur.

All three toe lesions exhibited remarkable soft-tissue swelling disproportionate to the bony abnormalities (Fig. 4). In one case the central radiolucency increased in size from 8 to 12 mm in diameter during a 7-month delay of diagnosis (Fig. 3a,b). Premature epiphyseal fusion occurred in the radial half of a thumb phalanx in a 15-year-old boy (Fig. 1).

Proximal phalanges

Both lesions were located proximally in finger digits, close to the palmar cortex and associated with obvious soft-tissue swelling (Fig. 5). Well defined bone

---

* Present address: Department of Radiology, The First Affiliated Hospital, Sun Yat-Sen University of Medical Sciences, Guangzhou, Guangdong, People's Republic of China.

† Author for correspondence.

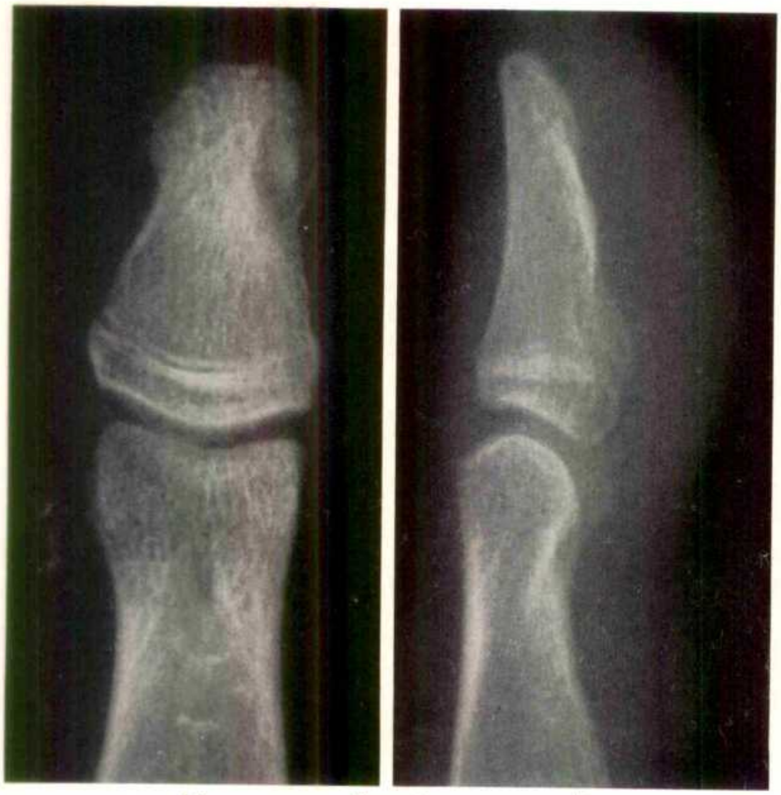

(a) **Figure 1** (b)

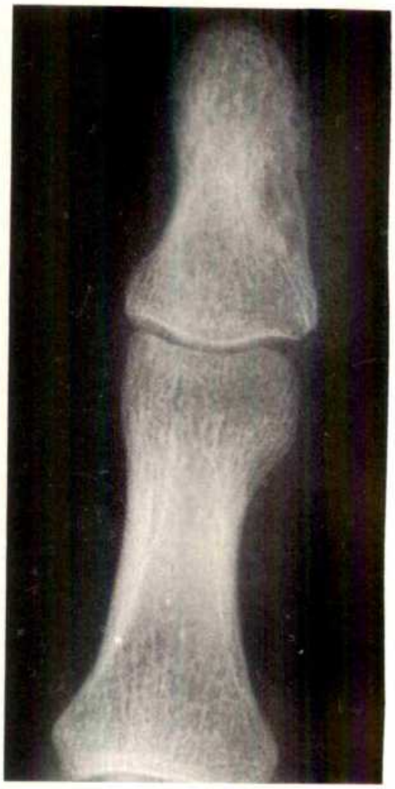

Figure 2

Figure 1. Terminal phalanx, right thumb of a 15-year-old boy. (a) Antero-posterior radiograph showing a subcortical lesion with a central nidus close to the base of the terminal tuft. Note the ill defined margins, slight cortical expansion, minimal sclerosis and that the radial half of the epiphyseal plate has fused. (b) Lateral radiograph; the nidus cannot be located.

Figure 2. Antero-posterior radiograph of the terminal phalanx, right thumb, revealing a small, subcortical, oval translucency with ill defined margins and minimal surrounding sclerosis, located close to the base of the terminal tuft. Slight cortical expansion is also shown.

destruction in one was surrounded by sclerosis and cortical thickening. A 2 mm × 2 mm nidus was contained within the lesion. The other lesion differed insofar as an area of ill defined bone destruction was associated with a little sclerosis and shell-like periosteal new-bone formation.

The only further investigations available comprised technetium-99m hydroxymethylene diphosphonate (HMDP) bone scintigraphy in two patients. In each, an area of increased activity was observed on the early, blood-pool image, as well as the delayed bone phase. In one, abnormally increased radionuclide activity was located throughout the distal end of a proximal phalanx, within which a second area of increased activity was superimposed, corresponding to the lesion itself (Fig. 5).

Clinical management

All lesions were excised eventually, seven without evidence of recurrence and with remission of symptoms. One lesion recurred twice; on each occasion a new radiolucency was detected adjacent to the excision site (Fig. 5c). Symptomatic relief, without further recurrence, occurred after a third exploration.

Discussion

Phalangeal osteoid osteomas are undoubtedly rare. In one large series, only six of 158 collected cases (3.8%) arose in the phalanges of the hand and none in the foot (Dahlin, 1979). Another report records about 5% of osteoid osteomas arising in fingers and 2% in toe phalanges (Jackson et al, 1977). The incidence in the Bristol Bone Tumour Registry is very similar at 5.4% in the fingers and 3.2% in toes. No evidence exists to suggest that these incidences reflect any known bias of case referral. Osteoid osteoma arising in terminal phalanges would seem very rare.

Twenty-nine previously reported cases in fingers and 20 cases in toes have been collected from the world literature (Jaffe, 1935; Sherman, 1947; Carroll, 1953; Freiberger et al, 1959; Schajowicz et al, 1970; Bordelon et al, 1975; Nakatsuchi et al, 1984; Beauchamp et al, 1985; Szabo & Smith, 1985). The summation of these cases suggests a typical history of pain, worse at night,

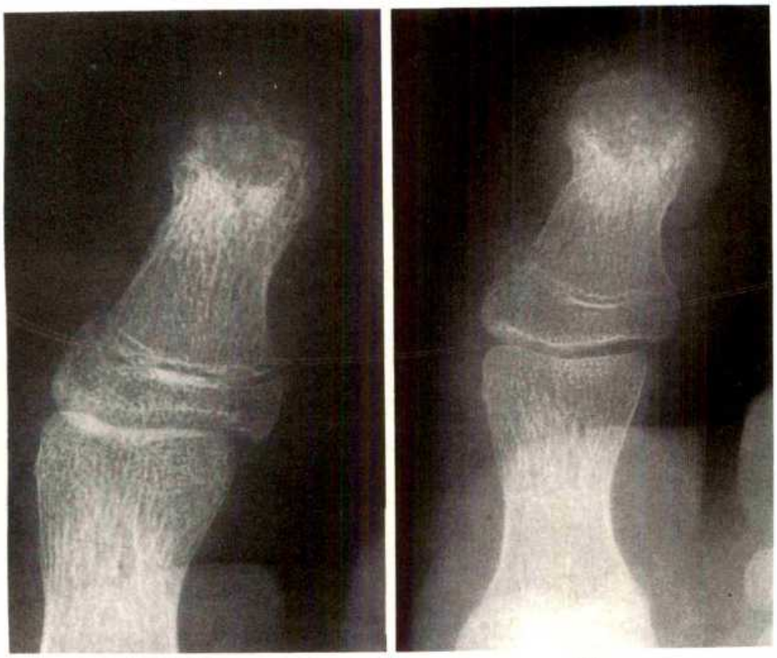
(a) (b)

Figure 3. Radiographs of the right great toe. (a) An ill defined lesion is located at the tip of the distal phalanx with minimal adjacent sclerosis. Note also the lack of cortical margin, central nidus or periosteal new-bone formation. (b) Seven months later, the lesion has increased in size with further cortical thinning and expansion.

relieved by salicylate. Local soft-tissue swelling, with point tenderness and limitation of movement at adjacent joints was also relatively common (Dahlin, 1979; Greenfield, 1986). Local erythema, heat and hyperhydrosis have also been reported. Lesions located in terminal phalanges have been associated with enlargement, both of the phalanx and adjacent soft-tissue swelling, together with nail changes, both hypertrophic and hypotrophic (Mangini, 1967; Sullivan, 1971; Grundberg, 1977; Nakatsuchi et al, 1984; Szabo & Smith, 1985).

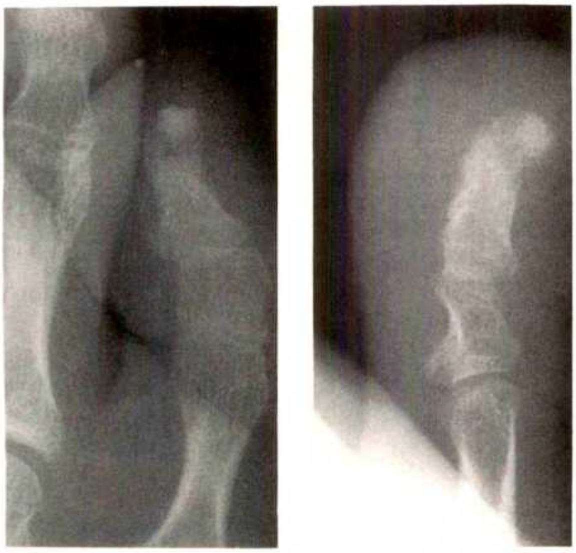
(a) (b)

Figure 4. Distal phalanx of right little toe. (a) Antero-posterior and (b) lateral radiographs demonstrate appreciable soft-tissue swelling, disproportionate to the bony abnormalities. The cortical margin is not complete and the nidus is eccentrically placed.

Classical teaching suggests that the radiological features of osteoid osteomas may be classified according to location into cortical, cancellous and subperiosteal types (Edeiken et al, 1966; Greenfield, 1986). The typical tumour is cortical, comprising a small radiolucency less than 1 cm in diameter, subcortically placed, and associated with dense adjacent bone sclerosis and periosteal reaction. The latter may be laminated. A nidus is usually detected centrally within the radiolucency. The cancellous variety is similar, insofar as a small oval or round radiolucency is present, but with little or no adjacent sclerosis. Occasionally, a discrete sclerotic rim may surround the radiolucency and in long-standing cases, an area of endosteal cortical thickening may be seen, often slightly removed from the radiolucency. The least common variety is subperiosteal, presenting as a rounded soft-tissue mass between 0.5 and 1 cm in diameter, immediately adjacent to bone. The underlying cortex demonstrates pressure defect or irregular bone resorption (Edeiken et al, 1966; Brabants & Geens, 1986). Bone response is usually minimal. A faint sclerotic margin may be seen in occasional cases (Wilner 1982; Lander et al, 1986).

The cortical variety of osteoid osteoma is the most common overall (Edeiken et al, 1966), but the cancellous and subperiosteal varieties are said to be more frequent in the small bones of the hand and foot (Swee et al, 1979;

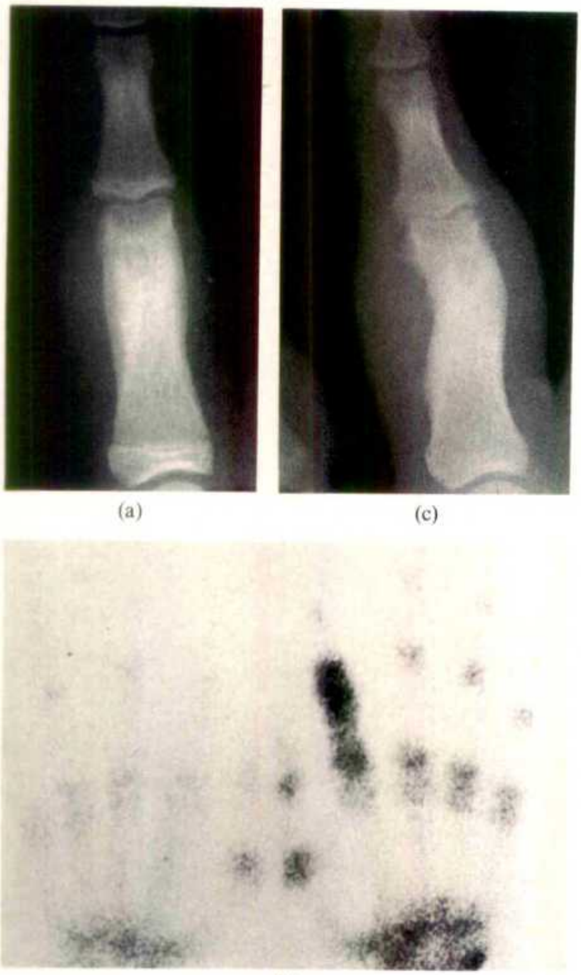

(a) (c)

(b)

Figure 5. (a) Pre-operative radiograph of the right index finger revealing an area of well defined bone destruction, containing a nidus, surrounded by marked sclerosis and cortical thickening distally in the proximal phalanx. Obvious fusiform soft-tissue swelling is present and the appearances are typical of conventional osteoid osteoma. (b) Skeletal scintigraphy shows increased radionuclide activity located throughout the distal end of the phalanx within which a second area of increased activity is superimposed. (c) A radiograph of the same finger taken before the third exploration demonstrating a new radiolucency with a nidus adjacent to the previous excision site.

Shereff et al, 1983). In the present series the lesions in proximal phalanges comprise one each of the cortical and subperiosteal varieties. These should not have caused diagnostic difficulty, the radiological features being not dissimilar to those already described in the literature. However, the six lesions located in terminal phalanges exhibited some unusual features which may have contributed to misdiagnosis. Whilst sharing the characteristics of cancellous type lesions (a radiolucency located within cancellous bone with little or no adjacent sclerosis), they were associated with the subperiosteal-type feature of cortical bulging (Figs 1, 2). Furthermore, although all the lesions were subcortical, periosteal new-bone formation and cortical thickening did not occur. Indeed, two cases in which considerable expansion of bone and associated soft-tissue swelling were present showed deficiency of the overlying cortical margin (Fig. 4). In both, the radiolucent nidus was situated eccentrically and a diagnosis of sepsis was considered because of these features. Skeletal scintigraphy served to confirm the highly active nature of the lesion but was not helpful in distinguishing an osteoid osteoma from focal infection.

This diagnostic difficulty has been previously emphasized (Shereff et al, 1983; Beauchamp et al, 1985). The probable explanation for the relative absence of periosteal new-bone formation and cortical thickening in terminal phalangeal lesions is the relative deficiency of periosteum on these bones, due to a large proportion of the surface being covered by tendon insertions. In addition, cancellous bone is more abundant and the cortices thinner compared with a typical tubular bone such as a femur (Williams & Warwick, 1980). This is the likely cause of a similar absence of periosteal new-bone formation in osteoid osteomas involving carpal bones (Rosenfeld et al, 1973; Herndon et al, 1974; Jensen, 1979; Alcalay et al, 1982).

The radiological differential diagnosis of osteoid osteoma arising in a terminal phalanx includes chronic infection, epidermoid inclusion cyst, glomus tumour, chondroma and thorn-induced pseudotumour. Clinical distinction between chronic pyogenic infection and osteoid osteoma may be difficult, since soft-tissue swelling, local heat and redness occur in both. Furthermore, as indicated, the margin of the radiolucent area of the osteoid osteoma may be incomplete, with an eccentrically located nidus suggesting a sequestrum. Whilst this may make differential diagnosis difficult, the presence of an essentially oval radiolucency containing a small area of calcification should weigh the balance in favour of osteoid osteoma. Disuse osteoporosis is also less likely to occur in osteoid osteoma.

An epidermoid inclusion cyst may cause confusion, since a radiolucency is seen involving the terminal phalanx. However, the lack of a history of previous trauma and a dense, central area of calcification should militate against the diagnosis, and furthermore, that the tumour is frequently pain-free and not tender to touch.

Chondroma in a short tubular bone is usually asymptomatic. It is frequently expanded, well demarcated and without periosteal new bone or a soft-tissue mass. No central area of dense focal calcification occurs, although there may be scattered zones of amorphous or ring-like calcification.

Plant thorns are capable of producing a pathological response within bone. Evidence of bone change and symptoms, which include pain and swelling, become manifest 4 to 16 weeks after the initial puncture. Thorn-induced bone changes are usually demonstrated by an area of ill defined cortical bone destruction, with associated periosteal new-bone formation. The area of bone resorption may be relatively well defined, but without expansion or calcification within the lytic area (Gerle, 1971).

Acknowledgments

We are grateful for the receipt of a Sino-British Friendship Scholarship to study in the UK (Q.M.) and to Miss Louise Byrne for her secretarial assistance.

References

ALCALAY, M., CLARAC, J. & BONTOUX, D., 1982. Double osteoid osteoma in adjacent carpal bones. *Journal of Bone and Joint Surgery, 64A*, 779–780.

BEAUCHAMP, C. P., MORTON, K. S., DUNCAN, C. P. & BEAUCHAMP, R. D., 1985. Osteoid osteoma; a 30 year experience with 76 cases at the University of British Columbia. *Journal of Bone and Joint Surgery, 67B*, 328

BORDELON, R. L., CRACCO, A. & BOOK, M. K., 1975. Osteoid osteoma producing premature fusion of the epiphysis of the distal phalanx of the big toe. *Journal of Bone and Joint Surgery, 57A*, 120–121.

BRABANTS, K. & GEENS, S., 1986. Subperiosteal juxtaarticular osteoid osteoma. *Journal of Bone and Joint Surgery, 68B*, 320–324.

CARROLL, R. E., 1953. Osteoid osteoma in the hand. *Journal of Bone and Joint Surgery, 35A*, 888–893.

DAHLIN, D. C., 1979. *Bone Tumours: General Aspects and Data on 6,221 cases*, 3rd edn (Charles C. Thomas, Springfield, Illinois), pp. 75–85.

EDEIKEN, J., DEPALMA, A. F. & HODES, P. J., 1966. Osteoid osteoma. *Clinical Orthopaedics and Related Research, 49*, 201–206.

FREIBERGER, R. H., LOITMAN, B. S., HELPERN, M. & THOMPSON, T. C., 1959. Osteoid osteoma: a report on 80 cases. *American Journal of Roentgenology, 82*, 194–205.

GERLE, R. D., 1971. Thorn-induced pseudotumours of bone. *British Journal of Radiology, 44*, 642–645.

GREENFIELD, G. B., 1986. *Radiology of Bone Diseases*, 4th edn (J. B. Lippincott, Philadelphia), pp. 618–625.

GRUNDBERG, A. B., 1977. Osteoid osteoma of the thumb: report of a case. *Journal of Hand Surgery, 2*, 226.

HERNDON, J. H., EATON, R. G. & LITTLER, J. W., 1974. Carpal tunnel syndrome. *Journal of Bone and Joint Surgery, 56A*, 1715–1718.

JACKSON, R. P., RECKLING, F. W. & MANTZ, F. A., 1977. Osteoid osteoma and osteoblastoma. *Clinical Orthopaedics and Related Research, 120*, 303–313.

JAFFE, H. L., 1935. Osteoid osteoma: a benign osteoblastic tumor composed of osteoid and atypical bone. *Archives of Surgery, 31*, 709–728.

JAFFE, H. L. & MAYER, L., 1932. An osteoblastic osteoid tissue forming tumor of metacarpal bone. *Archives of Surgery, 24*, 550–564.

JENSEN, E. G., 1979. Osteoid osteoma of the capitate bone. *The Hand, 11*, 102–105.

LANDER, P. H., AZOUZ, E. M. & MARTON, D., 1986. Subperiosteal osteoid osteoma of the talus. *Clinical Radiology, 37*, 491–493.

MANGINI, U., 1967. Tumors of the skeleton of the hand. *Bulletin of the Hospital for Joint Diseases, 28*, 61–103.

MURRAY, R. & WATT, I., 1987. Osteoid osteoma. In *A Textbook of Radiology and Imaging*, ed. by D. Sutton, 4th edn (Churchill Livingstone, Edinburgh), pp. 145–148.

NAKATSUCHI, Y., SUGIMOTO, Y. & NAKANO, M., 1984. Osteoid osteoma of the terminal phalanx. *Journal of Hand Surgery, 9B*, 201–203.

ROSENFELD, K., BORA, F. W. & LANE, J. M., 1973. Osteoid osteoma of the hamate. *Journal of Bone and Joint Surgery, 55A*, 1085–1087.

SCHAJOWICZ, F., AIELLO, C. L. & SLULLITEL, I. 1970. Cystic and pseudocystic lesions of the terminal phalanx with special reference to epidermoid cysts. *Clinical Orthopaedics and Related Research, 68*, 84–92.

SHEREFF, M. J., CULLIVAN, W. T. & JOHNSON, K. A., 1983. Osteoid osteoma of the foot. *Journal of Bone and Joint Surgery, 65A*, 638–641.

SHERMAN, M. S., 1947. Osteoid osteoma. Review of the literature and report of thirty cases. *Journal of Bone and Joint Surgery, 29*, 918–930.

SULLIVAN, M., 1971. Osteoid osteoma of the fingers. *The Hand, 3*, 175–178.

SWEE, R. G., MCLEOD, R. A. & BEABOUT, J. W., 1979. Osteoid osteoma: detection, diagnosis and localization. *Radiology, 130*, 117–123.

SZABO, R. M. & SMITH, B., 1985. Possible congenital osteoid osteoma of a phalanx. *Journal of Bone and Joint Surgery, 67A*, 815–816.

WILLIAMS, P. L. & WARWICK, R. (Eds), 1980. *Gray's Anatomy*, 36th edn (Churchill Livingstone, Edinburgh), pp. 371–375.

WILNER, D., 1982. *Radiology of Bone Tumours and Allied Disorders* (W. B. Saunders, Philadelphia), pp. 144–216.

1989, *The British Journal of Radiology*, 62, 326–331

Acute rhabdomyolysis: evaluation with magnetic resonance imaging compared with computed tomography and ultrasonography

By Antti E. Lamminen, MD, Pauli E. Hekali, MD, *Eero Tiula, MD, Ilkka Suramo, MD and Ossi A. Korhola, MD

Department of Diagnostic Radiology and *First Department of Internal Medicine, Meilahti Hospital, University Central Hospital, Helsinki, Finland

(Received October 1988 and in revised form November 1988)

Abstract. Fifteen patients with acute rhabdomyolysis were evaluated with low field magnetic resonance (MR) imaging and the results compared with those obtained using computed tomography (CT) and ultrasonography (US). With MR imaging, abnormal muscles with areas of increased signal intensity were seen in every patient, which probably reflects increased water content or increased mobility of water molecules caused by inflammatory reaction and oedema in the injured and necrotic muscles. Computed tomography without intravenous contrast medium demonstrated abnormal muscles in most patients examined with this modality. The CT findings consisted of areas of focal hypodensity in muscles. With US, abnormal muscles were seen in less than half of the patients studied. The normal structure of striated muscle was focally disturbed and areas of both decreased and increased echogenicity were found. Magnetic resonance imaging had a higher sensitivity in the detection of abnormal muscles than CT or US (100%, 62% and 42%, respectively). The findings of all these modalities are non-specific, but together with the clinical and laboratory data they confirm the diagnosis of rhabdomyolysis. The information gained from imaging studies is useful in the assessment of the extent and distribution of rhabdomyolysis. The precise identification of affected muscle compartments by MR imaging is valuable when surgical fasciotomy is considered for treatment; the procedure can then be appropriately directed to the compartments with clearly abnormal muscles.

The usefulness of magnetic resonance (MR) imaging in the evaluation of skeletal muscle pathology has been demonstrated (Fisher et al, 1986; Murphy et al, 1986). Acute intramuscular haemorrhage, infection and post-operative changes display high-signal-intensity areas on spin–echo (SE) imaging with T_2-weighted sequences (Dooms et al, 1985; Fisher et al, 1986). A previous experimental study showed that MR imaging was a sensitive method for detecting muscle infarction (Herfkens et al, 1983), and so MR may also be useful for the identification and localization of acute rhabdomyolysis and associated compartment syndrome. Only a few MR imaging case reports of this disorder have been published to date (Zagoria et al, 1986), and no comparative studies between MR imaging and other modalities have been made. There are very few reports on the application of low-field MR in the evaluation of skeletal muscle disorders although a low magnetic field may have benefits with regard to better T_1 contrast resolution (Sepponen et al, 1985).

In this study, we evaluated the MR findings in acute rhabdomyolysis at low field strength and compared the results with those of computed tomography (CT) and ultrasonography (US).

Materials and methods

Between December 1985 and July 1988, 15 consecutive patients with acute rhabdomyolysis underwent MR imaging in the acute phase of the disease, *i.e.* the first week in hospital.

One or more follow-up examinations were performed for every case. Thirteen of the patients also had CT and 12 had US examinations during the acute phase.

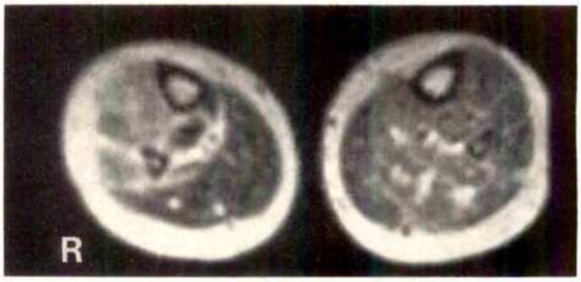

Figure 1. *Case 8.* Acute rhabdomyolysis due to drug overdose in a 43-year-old woman. Transaxial PS 1000/60 ms image of legs showing diffusely increased signal intensity in the anterior and peroneal muscle compartments of the right leg and in all muscle compartments of the left leg. In the left superficial posterior compartment, the medial head of gastrocnemius muscle is less affected than the other muscles. The lesions were confirmed at surgery.

Address for correspondence: Antti E. Lamminen, MD, Department of Diagnostic Radiology, Meilahti Hospital, University Central Hospital, Haart maninkatu 4, 00290 Helsinki, Finland.

Table I. Results of MR, CT and US imaging in the evaluation of acute rhabdomyolysis

Case no./ age (years)/ sex	Peak value of creatine kinase (i.u.)	Results of imaging studies[a]			Surgical confirmation
		MR	CT	US	
1/39/M	18400	+	+	−	No
2/55/M	322800	+++	++	−	Yes
3/73/F	135300	++	−	+	No
4/32/M	294000	+++	++	−	Yes
5/52/F	1516	++	++	−	Yes
6/63/M	28677	++	+	ND	Yes
7/26/F	67500	++	ND	ND	Yes
8/43/F	74820	+++	ND	ND	Yes
9/46/M	57560	++	−	−	No
10/36/M	62000	+++	−	+	No
11/64/M	3295	+++	++	−	Yes
12/44/M	42600	+++	−	+	No
13/32/M	154480	+	−	+	No
14/32/F	889000	+++	+	−	Yes
15/28/M	67500	+++	+++	++	Yes

[a] +, pathological finding in one muscle compartment; ++, pathological finding in two muscle compartments; +++, pathological finding in three or more muscle compartments; −, no pathological findings; ND, not done.

Magnetic resonance examinations were performed before CT and US scans. The imaging studies were routinely directed to the gluteal and lower limb muscles; additional images of the thoracic and upper limb musculature were obtained when there was a clinical suspicion of lesions in these areas. The diagnosis was confirmed clinically and by laboratory methods; a serum creatine kinase (CK) concentration >540 i.u. l^{-1} was required for diagnosis (normal, $\leqslant 270$ i.u. l^{-1}). Surgical confirmation (muscle biopsy or fasciotomy) was available in nine cases. There were 10 men and five women, ranging in age from 26 to 73 years. In 10 patients (Cases 1, 4, 6, 7, 8, 9, 10, 12, 14, and 15, Table I), the aetiology of rhabdomyolysis was drug or alcohol intoxication. In two cases (Cases 2 and 13), the syndrome resulted from excessive muscular activity, and in one case (Case 3), it resulted from prolonged immobilization and external compression. In one patient (Case 5), rhabdomyolysis was produced by ischaemic muscle injury caused by excessive use of ergot alkaloids, and in another (Case 11), by ischaemic complications after reconstructive arterial surgery.

Magnetic resonance imaging was performed with a low-field resistive magnet operating at a field strength of 0.02 T, which corresponds to a proton resonance frequency of 0.8 MHz (Acutscan, Instrumentarium Corporation). Images were obtained in transaxial and coronal planes using partial saturation (PS) sequences with a repetition time (TR) of 1000 ms and an echo time (TE) of 60 or 80 ms. The term PS sequence is used

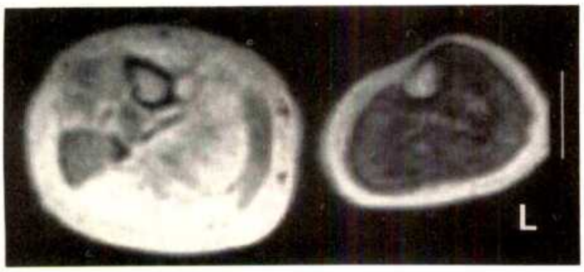

(a)

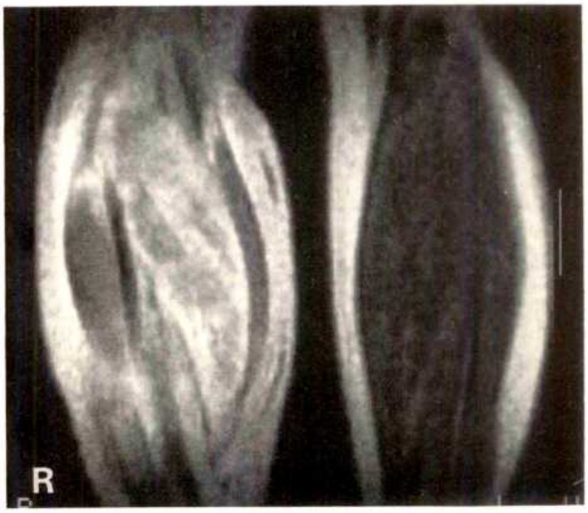

(b)

Figure 2. *Case 7.* Clearly increased muscle signal intensity in the right leg of a 26-year-old woman with drug overdose. Rhabdomyolysis was surgically proved in the anterior and deep posterior muscle compartments, and also in the lateral head of gastrocnemius muscle in the superficial posterior compartment. Transaxial (a) and coronal (b) PS 1000/60 ms images.

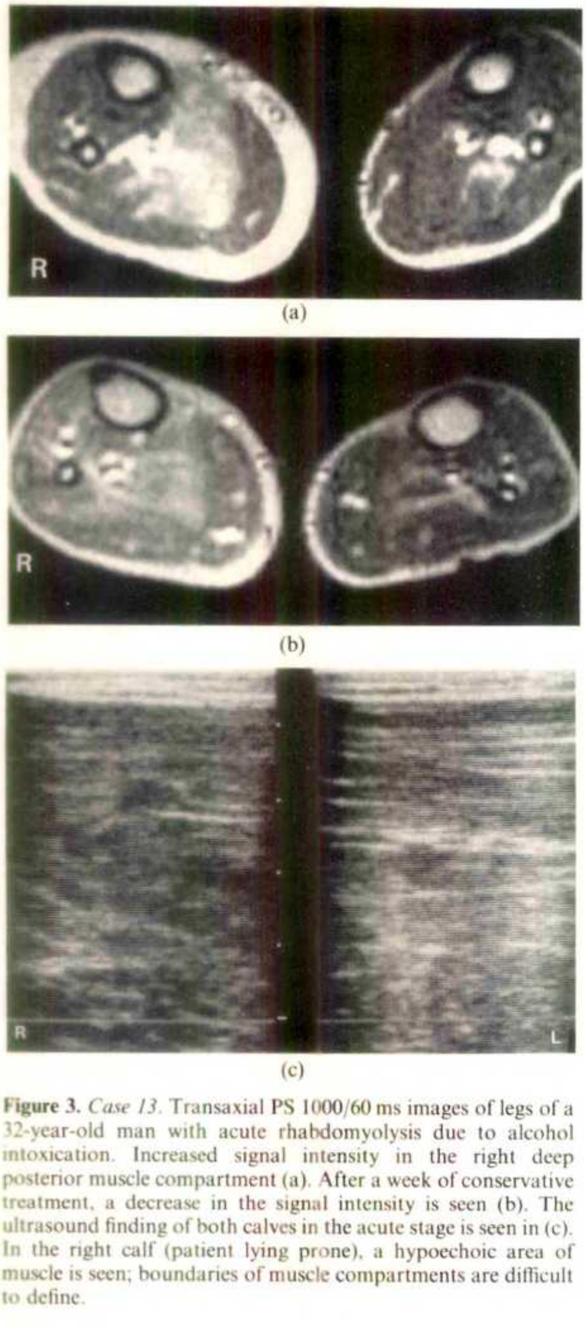

(a)

(b)

(c)

Figure 3. *Case 13.* Transaxial PS 1000/60 ms images of legs of a 32-year-old man with acute rhabdomyolysis due to alcohol intoxication. Increased signal intensity in the right deep posterior muscle compartment (a). After a week of conservative treatment, a decrease in the signal intensity is seen (b). The ultrasound finding of both calves in the acute stage is seen in (c). In the right calf (patient lying prone), a hypoechoic area of muscle is seen; boundaries of muscle compartments are difficult to define.

according to the definition by Bydder and Young (1985). In four patients, images were also obtained with short TI inversion–recovery (STIR) sequences (Bydder et al, 1985) of TR/TI/TE = 1500/50/40 ms and 1500/100/40 ms (TI = inversion time). The acquisition of PS images was repeated four times for signal averaging, and the acquisition of STIR images was repeated twice. The section thickness was 10 mm. Matrix size was 128 × 256. Surface coils were used for all but one patient. The evaluation of signal intensities was based on visual analysis of the grey-scale image, with the intensity of subcutaneous fat used as a reference (Dooms et al, 1986). The CT examinations were performed with a Somatom DR 2 scanner (Siemens AG) with a section thickness of 8 mm. The US studies were performed with real-time equipment (RT 3000, General Electric) using a 5.0 MHz linear transducer.

Results

In every patient with acute rhabdomyolysis proved by clinical and laboratory methods, increased signal intensity of muscles was seen in the partial saturation MR images (Table I). The distribution and intensity of pathological muscle signals varied, the intensity ranging from a slight and diffuse contrast difference (Fig. 1) to very intense, clearly demarcated lesions (Fig. 2). In the extremities, abnormal signal intensity in the acute stage was usually associated with an increase in the cross-sectional diameter of the affected muscle or muscular compartment.

In follow-up examinations, a decrease in abnormal signal was seen in association with clinical improvement and a decrease in serum CK values (Fig. 3 a, b). The diameter of the affected limb also returned towards normal. In two patients, fasciotomies were complicated by wound infection, which spread deeply into the necrotic muscle tissue of the legs. In these cases, the follow-up MR examination revealed increasing and more widely spreading abnormal signal areas.

The STIR sequences showed good contrast between normal and abnormal muscles, but at this field strength suffered from a low signal-to-noise ratio. The advantage of STIR images compared with PS images was the better differentiation of the damaged muscle from adjacent fat, due to partial suppression of the fat signal (Fig. 4a, b, c).

Computed tomography without intravenous contrast medium was able to demonstrate abnormal muscles in eight of the 13 cases examined with this modality. The CT findings consisted of areas of focal hypodensity in muscles and fascial thickening due to oedema (Fig. 4d).

In five of the 12 patients studied with US, abnormal changes in muscular structure and echogenicity were seen. These findings consisted of foci of decreased echogenicity in muscles and a locally disorganized fascicular architecture (Fig. 3c); in two patients, regions of slightly increased muscular echogenicity were also found.

The sensitivity of MR imaging in the detection of abnormal muscles in this patient population with an established clinical diagnosis of rhabdomyolysis was 100% (15 of 15), whereas the sensitivity of CT was 62% (eight of 13), and that of US 42% (five of 12).

Discussion

Rhabdomyolysis is defined as a syndrome resulting from skeletal muscle injury with release of muscle cell contents into the extracellular fluid and plasma. The most important clinical marker of rhabdomyolysis is an

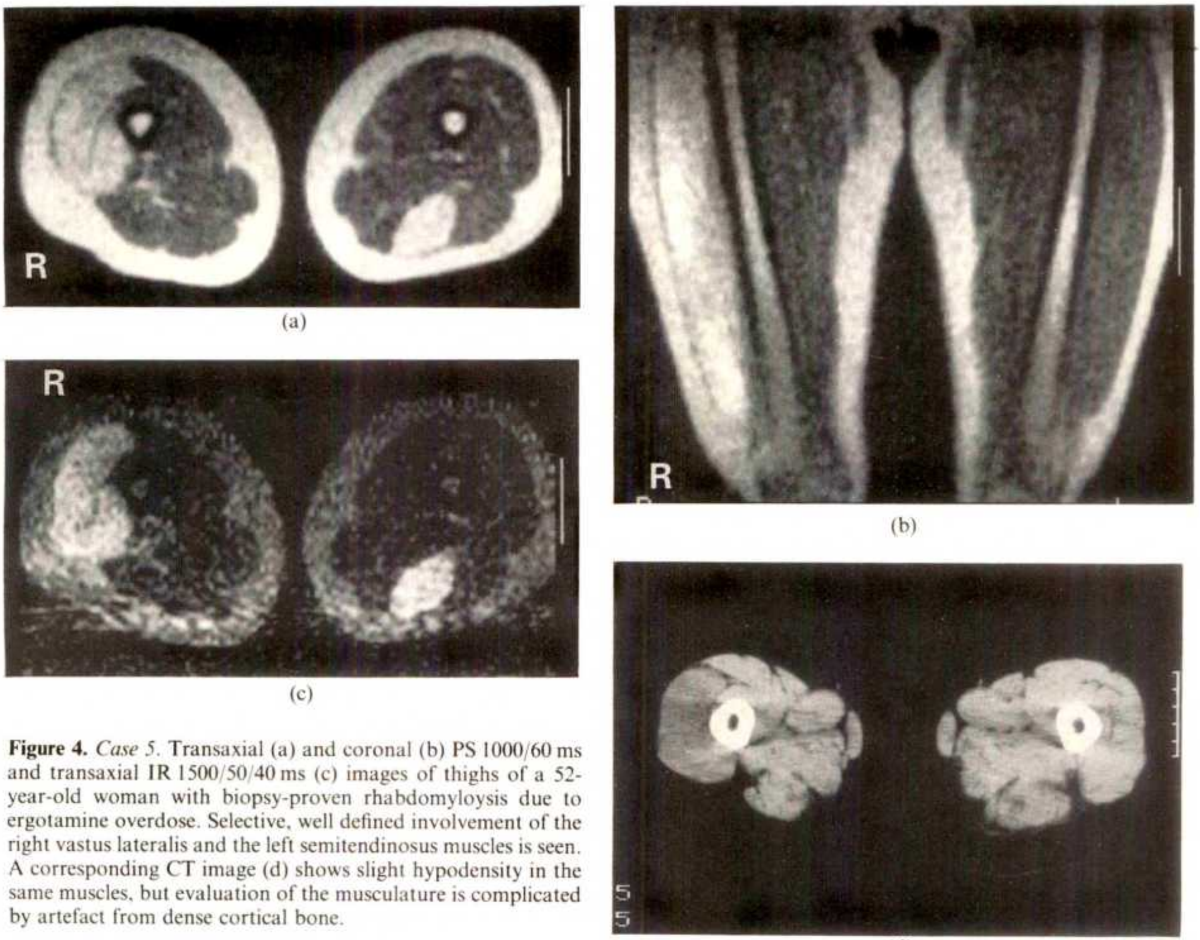

(a)

(b)

(c)

(d)

Figure 4. *Case 5.* Transaxial (a) and coronal (b) PS 1000/60 ms and transaxial IR 1500/50/40 ms (c) images of thighs of a 52-year-old woman with biopsy-proven rhabdomyloysis due to ergotamine overdose. Selective, well defined involvement of the right vastus lateralis and the left semitendinosus muscles is seen. A corresponding CT image (d) shows slight hypodensity in the same muscles, but evaluation of the musculature is complicated by artefact from dense cortical bone.

elevated serum creatine kinase level. The causes of the syndrome include drug or alcohol overdose, prolonged muscular compression, ischaemic muscle injury, thermal muscle injury, direct trauma, excessive muscular activity, polymyositis, and various metabolic disorders (Gabow et al, 1982). The syndrome was first described among trauma casualties during the London Blitz in World War II (Bywaters & Beall, 1941). Particularly in dehydrated subjects, marked rhabdomyolysis with myoglobinuria can lead to acute renal failure, often requiring temporary dialysis treatment. Renal damage may be prevented by adequate hydration of the patient and by alkalinization of the urine. Often, however, localized oedema of limb muscles is a prominent feature of rhabdomyolysis, leading to acute muscle compartment syndrome. Early fasciotomy is then necessary in order to relieve ischaemia within the compartment (Schreiber et al, 1972; Rorabeck & Clarke, 1978).

In studies on the rat with 0.35 T MR imaging, infarcted muscles had significantly longer T_1 and T_2 values at 24 h after vascular occlusion than the control muscles. These changes corresponded to a significant increase in the water content of infarcted muscles (Herfkens et al, 1983). The pathophysiological phenomena in compartment syndrome include muscle necrosis, increased intramuscular pressure and tissue oedema (Rorabeck & Clarke, 1978; Owen et al, 1979); it has been postulated that oedema and inflammation account for some of the signal changes seen in MR imaging of rhabdomyolysis (Zagoria et al, 1986). The contribution of intrinsic macromolecular changes in damaged muscle is difficult to evaluate. It is probable that the areas of high signal intensity seen in our patients reflect increased water content or increased mobility of water molecules due to inflammatory reaction in the injured and necrotic muscles.

In a small subgroup of patients, we applied STIR pulse sequences, advocated for body imaging by Bydder et al (1985). Our preliminary results show that these sequences seem to have promising characteristics in muscle lesion imaging due to high lesion-to-muscle contrast and suppression of the signal from subcutaneous fat. In this comparative study, MR imaging was the best modality in visualizing the affected muscles and muscle compartments; increased signal intensity was proven by fasciotomy to represent necrotic and/or oedematous muscle tissue. The optimal field strength in clinical MR imaging remains a controversial issue, in particular with regard to contrast differentiation. In spite of its inherent low signal-to-noise ratio, low-field imaging may offer some advantages (Margulis & Crooks, 1988; Smith, 1988). The spin-lattice relaxation processes of biological tissues, characterized by T_1, depend on the magnetic field strength (Koenig et al, 1984). In low fields the T_1 relaxation times are shorter and the relative differences in T_1 between different tissues are larger. This may provide more information about the biological processes at the macromolecular level, thus leading to better contrast resolution (Sepponen et al, 1985).

The CT findings of this study were in agreement with those previously described (Vukanovic et al, 1980); focal intramuscular lesions with a low attenuation coefficient were seen in most, but not all, patients examined with CT. These lesions were not as conspicuous as they were in the corresponding MR images. Computed tomography was not as sensitive as MR imaging in the detection of rhabdomyolytic muscles. The sensitivity of CT would probably be greater with intravenous contrast enhancement, but contrast medium must be avoided in rhabdomyolysis because it may cause further deterioration in renal function (Winearls et al, 1980).

Ultrasonography was the least sensitive modality in the evaluation of muscle necrosis. Most abnormal US findings seen were consistent with the findings reported previously (Fornage & Nerot, 1986); however, in addition to hypoechoic foci, areas of increased echogenicity were also found in two patients.

In patients with a clinical and laboratory diagnosis of acute rhabdomyolysis, low-field MR imaging sensitively clarified the distribution of muscle lesions. Magnetic resonance was more sensitive than US or CT. The findings of all these modalities are non-specific, but together with the clinical and laboratory data they confirm the diagnosis of rhabdomyolysis. The precise identification of affected muscle compartments is especially valuable when fasciotomy is considered; the procedure can be directed to the compartments with clearly abnormal muscles, thus relieving oedema and pressure-related ischaemia in the appropriate areas.

Acknowledgment

This study was supported by a grant from the Pehr Oscar Klingendahl Foundation, Helsinki, Finland.

References

Bydder, G. M., Pennock, J. M., Steiner, R. E., Khenia, S., Payne, J. A. & Young, I. R., 1985. The short TI inversion recovery sequence—an approach to MR imaging of the abdomen. *Magnetic Resonance Imaging, 3*, 251–254.

Bydder, G. M. & Young, I. R., 1985. Clinical use of the partial saturation and saturation recovery sequences in MR imaging. *Journal of Computer Assisted Tomography, 9*, 1020–1032.

Bywaters, E. G. L. & Beall, D., 1941. Crush injuries with impairment of renal function. *British Medical Journal, i*, 427–432.

Dooms, C. G., Fisher, M. R., Hricak, H & Higgins, C. B., 1985. MR imaging of intramuscular hemorrhage. *Journal of Computer Assisted Tomography, 9*, 908–913.

Dooms, G. C., Hricak, H., Margulis, A. R. & de Greer, G., 1986. MR imaging of fat. *Radiology, 158*, 51–54.

Fisher, M. R., Dooms, G. C., Hricak, H., Reinhold, C. & Higgins, C. B., 1986. Magnetic resonance imaging of the normal and pathologic muscular system. *Magnetic Resonance Imaging, 4*, 491–496.

Fornage, B. D. & Nerot, C., 1986. Sonographic diagnosis of rhabdomyolysis. *Journal of Clinical Ultrasound, 14*, 389–392.

Gabow, P. A., Kaehny, W. D. & Kelleher, S. P., 1982. The spectrum of rhabdomyolysis. *Medicine, 61*, 141–152.

Herfkens, R. J., Sievers, R., Kaufman, L., Sheldon, P. E., Ortendahl, D. A., Lipton, M. J., Crooks, L. E. & Higgins, C. B., 1983. Nuclear magnetic resonance imaging of the infarcted muscle: a rat model. *Radiology, 147*, 761–764.

Koenig, S. H., Brown, R. D. III, Adams, D., Emerson, D. & Harrison, C. G., 1984. Magnetic field dependence of 1/T1 of protons in tissue. *Investigative Radiology, 19*, 76–81.

Margulis, A. R. & Crooks, L. E., 1988. Present and future status of MR imaging. *American Journal of Roentgenology, 150*, 487–492.

Murphy, W. A., Totty, W. G. & Carroll, J. E., 1986. MRI of normal and pathologic skeletal muscle. *American Journal of Roentgenology, 146*, 565–574.

Owen, C. A., Mubarak, S. J., Hargens, A. R., Rutherford, L., Garetto, L. P. & Akeson, W. A., 1979. Intramuscular pressures with limb compression: clarification of the pathogenesis of the drug-induced muscle compartment syndrome. *New England Journal of Medicine, 300*, 1169–1172.

Rorabeck, C. H. & Clarke, K. M., 1978. The pathophysiology of the anterior tibial compartment syndrome: an experimental investigation. *Journal of Trauma, 18*, 299–304.

Schreiber, S. N., Liebowitz, M. R. & Bernstein, L. H., 1972. Limb compression and renal impairment (Crush syndrome) following narcotic and sedative overdose. *Journal of Bone and Joint Surgery, 54A*, 1683–1692.

Sepponen, R. E., Sipponen, J. T. & Sivula, A., 1985. Low field (0.02 T) nuclear magnetic resonance imaging of the brain. *Journal of Computer Assisted Tomography, 9*, 237–241.

Smith, F. W., 1988. Musculo-skeletal magnetic resonance imaging using inversion recovery pulse sequences at 0.08 T. *Clinical Radiology, 39*, 412–417.

Vukanovic, S., Hauser, H. & Wettstein, P., 1980. CT localization of myonecrosis for surgical decompression. *American Journal of Roentgenology, 135*, 1298–1299.

Winearls, C. G., Ledingham, J. G. G. & Dixon, A. J., 1980. Acute renal failure precipitated by radiographic contrast medium in a patient with rhabdomyolysis. *British Medical Journal, 281*, 1603.

Zagoria, R. J., Karstaedt, N. & Koubek, T. D., 1986. MR imaging of rhabdomyolysis. *Journal of Computer Assisted Tomography, 10*, 268–270.

1989, *The British Journal of Radiology*, 62, 331–334

The effects of angiotensin II on Doppler signals from a soft-tissue tumour

By P. M. Taylor, MRCP, FRCR, *B. Moreman, BSc, MSc, S. Rimmer, DMRD, FRCR and I. Isherwood, MD, FRCP, FRCR

Department of Diagnostic Radiology, University of Manchester, Manchester M13 9PT and *Regional Department of Medical Physics, Christie Hospital and Holt Radium Institute, Manchester M20 9BX

(*Received June 1988 and in revised form September 1988*)

Abstract. A 10 mHz continuous-wave Doppler system has been used to detect blood flow within a sarcoma implanted in a rabbit's ear. The effects of vasoconstriction produced by intravenous angiotensin II were studied. Criteria are described that enabled differentiation of the Doppler signals from the tumour from those of the adjacent central artery. The effect of vasoconstriction upon these criteria is also described.

Doppler ultrasound has been used to study neoplastic circulation in humans and a number of tumours of the lymphatic system, breast and kidneys have been investigated (Mountford & Atkinson, 1979; Jellins et al, 1983; Dubbins & Wells, 1986). It has been postulated that Doppler ultrasound may enable early detection of superficial tumours (Burns et al, 1982). Signals have been identified arising both from the arteries supplying tumour and from the tumour itself. The aims of this study were to establish, with an animal model, criteria that might permit consistent differentiation of those signals arising in tumour from those arising in the supplying artery and to determine whether induced changes in vessel calibre would affect the discriminatory value of these criteria.

Materials and methods

Instrumentation

A 10 mHz continuous-wave Doppler system employing a dual-element transducer with a 3 mm diameter face focused 6 mm from the face was used (Fig. 1).

The system was modified to give two outputs in phase quadrature. These outputs were fed into a heterodyne processor, which separated the forward and reverse flow signals. These directional signals were recorded on one channel of a reel-to-reel magnetic tape recorder (Teac, Tascam 22) and the non-directional signals into the other channel. Both channels were fed into stereo headphones worn by the investigator, the directional signals being heard by one ear and the non-directional by the other.

For analysis, the non-directional signals were fed into an Angioscan I spectrum analyser (Unigon Inc.), which uses fast Fourier transformation to produce frequency spectra. These are displayed on a monitor with frequency as ordinate, time as abscissa and grey-scale intensity representing amplitude. Each spectrum has 128 frequency points and 256 sequential spectra can be displayed simultaneously with a time resolution of 6.5 ms. The spectra scroll from right to left across the screen.

A 300 Hz high-pass filter was used to filter out any low frequency wall "thump". Five hundred and twelve sequential spectra were fed into an Apple II microcomputer for which a software program had previously been written to determine the maximum frequency in each spectrum and to provide a plot of the maximum frequency shift against time. The plot contained a varying number of cardiac cycles, depending on the pulse rate. From this information the means of several measurements of maximum frequency during

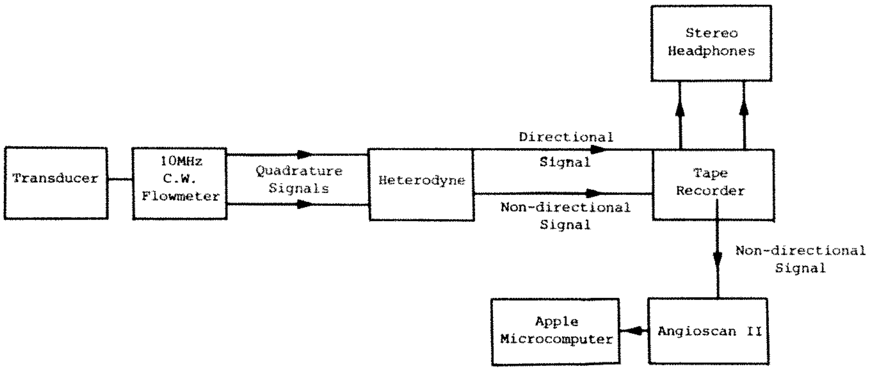

Figure 1. Equipment used for acquiring, storing and processing Doppler signals.

systole (MAX), of minimum frequency during diastole (MIN) and of the time-averaged, mean frequency (TAM) were calculated for each site insonated. The mean pulse rate before and during infusion of angiotensin was recorded.

Tumour and insonation

A VX2 sarcoma was propagated in the thigh of a donor rabbit and 0.1 ml of tumour suspension was injected subcutaneously into the pinna of each of 12 female New Zealand white half lop cross rabbits. The location in the pinna was chosen to ensure that tumour growth did not involve the central vascular bundle. Between 7 and 14 days the rabbits were sedated with 0.6 ml of Hypnorm (fentanyl citrate 0.315 mg and fluansone 10 mg/ml) intramuscularly. The diameter of the tumour was measured along its smallest dimension using calipers. The tumour and the central artery of the pinna were isonated and ultrasound recordings were made at four sites at 90° intervals around the circumference of the tumour and from the central artery proximal and distal to the tumour site. A vein on the contralateral pinna was then cannulated and angiotensin II infused at 500 ng/kg body weight/min. Ten minutes after the start of infusion, the recordings were repeated. All studies were performed in the same air conditioned room with an ambient air temperature of 16–18°C.

For each tumour, the ratios MAX/TAM and MIN/TAM were calculated as:

$$\mathrm{MAX} = \frac{\mathrm{MAX}_a + \mathrm{MAX}_b + \mathrm{MAX}_c + \mathrm{MAX}_d}{4}$$

$$\mathrm{TAM} = \frac{\mathrm{TAM}_a + \mathrm{TAM}_b + \mathrm{TAM}_c + \mathrm{TAM}_d}{4}$$

$$\mathrm{MIN} = \frac{\mathrm{MIN}_a + \mathrm{MIN}_b + \mathrm{MIN}_c + \mathrm{MIN}_d}{4}$$

where a, b, c and d are the four sites of insonation of the tumour. The same ratios were calculated for the proximal artery and the distal artery. The results before and after vasoconstruction were then compared using Student's *t*-test.

Results

The results are shown in Table I and Figs 2 and 3. Tumours varied in their growth rate. Rapidly growing tumours were therefore examined early before skin ulceration developed. Investigation of slower growing tumours was delayed until satisfactory vascularity developed to generate Doppler signals. One rabbit developed a cardiac arrhythmia during infusion and was therefore excluded from the results. All animals experienced a decrease in heart rate during vasoconstriction except one which showed the greatest change in the MAX/TAM ratio of the tumour. A fall in the MIN/TAM ratio was observed in nine tumours, eight proximal and nine distal arteries. In three arteries the ratio remained constant whilst a rise was observed only in two proximal arteries. Changes in the MAX/TAM ratio showed considerable variation over the tumour and no significant change could be detected. Eighteen of the 22 arterial sites insonated showed a decrease in the MAX/TAM ratio. The range of values of the arterial MAX/TAM ratio was markedly reduced following pharmacologically induced vasoconstriction.

Discussion

It has been shown that Doppler blood flow signals can be detected arising from malignant tumours (Mountford & Atkinson, 1979; Burns et al, 1982) and their supplying vessels (Dubbins & Wells, 1986). Signals from a tumour originate from new vessels formed by the neoplasm. A tumoral angiogenesis factor has been identified which is responsible for neovascularization (Feneslau et al, 1981). Tumour vessels are immature and lack contractile elements (Lagergen et al, 1960), but are demonstrable by contrast angiography. Pharmaco-angiography has been used to provide better visualization of malignant circulations (Ekelund et al, 1978). Tumour vessels fail to constrict when an exogenous vasoconstrictor is injected, resulting in preferential blood flow through them and

Table I. The age and size of tumours and the calculated MAX/TAM and MIN/TAM ratios for the tumour and arterial sites

Rabbit	Tumour age (days)	Size (mm)	MAX/TAM						MIN/TAM					
			Tumour		Proximal artery		Distal artery		Tumour		Proximal artery		Distal artery	
			Basal	+Angio	Basal	+Angio	Basal	+Angio	Basal	+Angio	Basal	+Angio	Basal	+Angio
1	13	7	4.86	3.24	4.90	2.75	3.56	2.64	1.88	1.83	1.32	1.73	1.55	1.75
2	8	14	3.76	3.18	3.21	2.55	2.98	2.72	1.74	2.04	1.56	1.59	1.58	1.58
3	9	14	3.68	4.43	3.03	2.48	3.70	2.48	2.30	2.51	1.48	1.68	1.71	1.77
4	8	12	3.56	3.80	3.73	2.82	3.51	2.65	2.10	2.27	1.48	1.64	1.63	1.72
5	12	12	3.78	3.63	2.61	2.76	2.66	2.78	2.04	2.14	1.66	1.68	1.60	1.79
6	14	7	3.62	3.49	3.08	2.62	3.41	2.72	1.88	2.04	1.44	1.77	1.47	1.67
7	12	10	4.01	3.82	3.17	2.89	3.24	2.82	2.12	2.08	1.51	1.77	1.54	1.68
8	7	9	3.29	3.60	3.44	2.82	3.49	2.93	2.02	2.22	1.60	1.60	1.60	1.73
9	5	10	3.55	3.30	2.66	2.58	2.88	2.80	1.83	1.91	1.62	1.60	1.57	1.65
10	17	7	3.83	3.41	2.69	2.72	2.93	2.83	1.89	1.92	1.49	1.52	1.56	1.64
11	10	7	4.42	3.60	3.52	2.72	3.28	2.94	2.05	2.13	1.76	1.66	1.64	1.65

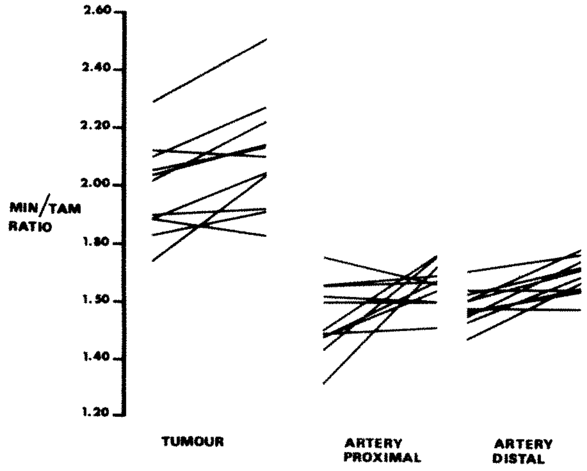

Figure 2. MIN/TAM ratio before and after vasoconstriction in the tumour and the central artery proximal and distal to the tumour ($p < 0.02$ in all sites.)

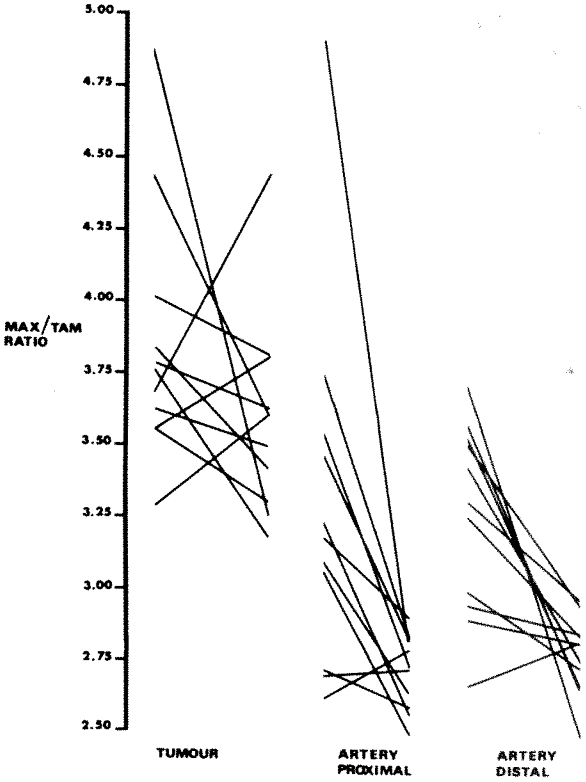

Figure 3. MAX/TAM ratio before and after vasoconstriction in the tumour (not significant) and central artery proximal ($p < 0.02$) and distal ($p < 0.02$) to the tumour.

therefore better opacification during angiography. Pharmaco-angiographic studies of experimental hepatic and renal tumours have shown that angiotensin II is a most effective vasoconstrictor (Ekelund et al, 1976), acting on arteries, arterioles and, to a lesser extent, on the venous circulation (Bowman & Rand, 1980). The presence of abnormal Doppler signals from a rabbit VX2 sarcoma has been previously documented (Burns et al, 1983). We sought to establish whether a Doppler correlate of pharmaco-angiography existed.

It was initially intended to infuse Angiotensin directly into the central artery of the pinna following transfemoral catheterization. Preliminary experiments, however, demonstrated that marked changes in flow occurred when the catheter was positioned in the common carotid artery before infusion of vasoactive agents. These changes were presumed to be due to physical reduction in the vessel lumen. The mechanism for similar changes observed in the central artery of the contralateral pinna is at present unexplained, although it is possible that it is a reflex phenomenon mediated by baroreceptors within the carotid vessels. On the basis of these experiments, however, it was decided to administer angiotensin systemically in order to exclude local mechanical alterations to flow.

Angiotensin produces a pressor effect by its general vasoconstrictor and positive inotropic action, resulting in a reflex bradycardia. This would be expected to increase mean flow velocity in both tumour and normal vessels. Maximum blood flow velocity in non-constricted tumour vessels should be increased, whilst that in the constricted artery should be decreased. It is difficult to predict the effect on minimum blood flow velocities. The measurement of absolute flow velocity within tumour vessels is not possible as the angle of insonation is unknown. Since the angle may vary between measurements, comparison of relative flow velocities before and after vasoconstriction is also unreliable. To overcome this the ratios MAX/TAM and MIN/TAM were calculated.

During vasoconstriction, the rise in mean flow velocity should produce a fall in the MAX/TAM ratio in the artery, whilst the response in tumour should be dependent on the relative rise in maximum flow velocity with respect to mean flow. The results support the predictions and demonstrate a fall in the arterial MAX/TAM ratio but an inconsistent change in the tumour ratio. The MIN/TAM ratio showed a significant rise during vasoconstriction in both artery and tumour. The changes in the ratios, although significant, were small. If a rise in mean velocity is assumed, then it seems likely that these observations are due to a smaller rise in the minimum velocity.

With respect to the differentiation of tumour from arterial signals, it is apparent that measurement of the MIN/TAM ratio before vasoconstriction could differentiate the two sources. A ratio greater than 1.8 was not observed from any arterial source and 10 of the 11 tumours showed larger ratios. Following vasoconstriction, despite the rise in arterial MIN/TAM ratios, a value greater than 1.8 was observed only from tumour.

In the basal state there was considerable overlap of tumour and arterial MAX/TAM ratios. Following vasoconstriction the marked fall in arterial MAX/TAM ratios ensured that a ratio of greater than 3 only arose from the tumour. The use of vasoconstriction therefore enhances the value of the MAX/TAM ratio in the differentiation of tumour and arterial signals.

The significance of these observations lies in their application to human studies. Parameters that correlate with the presence of a malignant circulation in breast carcinoma have been described (Minasian & Bamber, 1982). The possibility of an automated system to detect malignancy using Doppler ultrasound has been discussed (Burns et al, 1982). If such a system were to be developed then variation of Doppler flow signals by vaso-active drugs should be considered. Several drugs, in particular those used in the treatment of hypertension, angina and cardiac failure, can produce alterations in systemic vascular resistance. We have shown that vasoconstrictors facilitate the differentiation of malignant and abnormal circulations. The detection of tumours in humans may be aided by the use of drugs with a vasoconstrictor action, such as β-blockers. Further human studies are indicated and we also propose to undertake further animal studies exploring the action of vasodilators on the Doppler signals.

References

BOWMAN, W. C. & RAND, M. J., 1980. In *Textbook of Pharmacology* (Blackwell, Oxford).

BURNS, P. N., GOWLAND, M. R. & RIMMER, S., 1983. The use of Doppler ultrasound in the detection of changes in blood flow in tumour circulation. *Journal of Physiology, 342,* 12–13.

BURNS, P. N., HALLIWELL, M., WELLS, P. N. T. & WEBB, A. J., 1982. Ultrasonic Doppler studies of the breast. *Ultrasound in Medicine and Biology, 8,* 127–143.

DUBBINS, P. A. & WELLS, I., 1986. Renal carcinoma: duplex Doppler evaluation. *British Journal of Radiology, 59,* 231–236.

EKLUND, L., GERLOCK, J. & GONCHARENKO, V., 1978. The ephedrine effect in renal angiography revisited. *Clinical Radiology, 29,* 387–392.

EKLUND, L., GOTHLIN, J., JONSSON, N. & SJOGREN, H. O., 1976. Pharmacoangiography in experimental tumours. Evaluation of vasoactive drugs. *Acta Radiologica, 17,* 329–342.

FENESLAU, A., WATT, S. & MELLO, R. T., 1981. Tumour angiogenic factor: purification from a Walker 256 rat tumour. *Journal of Biological Chemistry, 256,* 9605–9611.

JELLINS, J., KOSSOFF, G., BOYD, J. & REEVE, T. S., 1983. The complimentary role of Doppler to the B-mode examination of the breast. *Journal of Ultrasound in Medicine, 10,* 29.

LAGERGREN, L., LINDBONN, A. & SONDERBERG, G., 1960. Vascularisation of fibromatous and fibrosarcomatous tumours; histopathologic microangiographic and angiographic studies. *Acta Radiologica, 53,* 1–16.

MINASIAN, M. & BAMBER, J. C., 1982. A preliminary assessment of an ultrasonic Doppler method for the study of blood flow in human breast cancer. *Ultrasound in Medicine and Biology, 8,* 357–364.

MOUNTFORD, R. A. & ATKINSON, P., 1979. Doppler ultrasound examination of pathologically enlarged lymph nodes. *British Journal of Radiology, 52,* 464–467.

1989, *The British Journal of Radiology*, *62*, 335–337

The prevalence and characterization of simple hepatic cysts by ultrasound examination

By P. A. Gaines, MRCP, FRCR and M. A. Sampson, MRCP, FRCR

Department of Radiology, Royal Hallamshire Hospital and Northern General Hospital, Sheffield

(*Received September 1988*)

Abstract. To help assess the significance of liver cysts we have prospectively documented their prevalence and characteristics within a general population being referred for ultrasound. Simple hepatic cysts occur in 2.5% of the population, becoming increasingly common with age. They show a preference for women, the right lobe of the liver and are occasionally multiple. The differential diagnosis is discussed.

Modern imaging techniques have led to the recognition of some incidental lesions that usually have no clinical relevance, *e.g.* simple renal cysts, liver capillary haemangiomas. Simple hepatic cysts are a congenital abnormality that are usually asymptomatic, but, as with all lesions that may have either no clinical importance or may be part of a defined condition or syndrome (*e.g.* polycystic kidneys, von Hippel-Lindau disease), the prevalence and characteristics of these lesions within the population should be known. We have documented these features within a general population being referred for an ultrasound examination of the abdomen, and we discuss their differential diagnosis.

Patients and methods

One thousand six hundred and ninety-five consecutive patients referred for abdominal or pelvic ultrasound examinations were examined by departmental radiologists for the presence of hepatic cysts using a 3.5 or 5 mHz sector probe. All positive examinations and the patients' notes were reviewed by the authors. Only lesions fulfilling strict criteria for a cystic lesion were accepted (Fig. 1). These features are: (i) an anechoic structure (occasional thin septa were accepted), (ii) a smooth internal margin without a discernible wall and (iii) posterior acoustic enhancement.

Address correspondence to: Dr P. A. Gaines, Department of Radiology, C Floor, Royal Hallamshire Hospital, Glossop Road, Sheffield S10 2JF.

Table I. Age-related prevalence of hepatic cysts

Age (years)	Number of subjects	Number with cysts	%
<20	44	0	0
20–29	120	1	0.83
30–39	160	2	1.25
40–49	222	1	0.45
50–59	280	1	0.36
60–69	360	11	3.05
70–79	369	17	4.6
80+	140	10	7

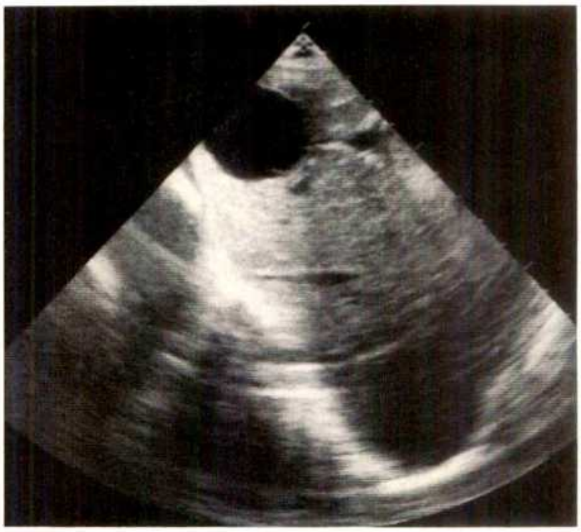

Figure 1. A simple cyst in the right lobe of the liver with marked posterior acoustic enhancement.

Patients with polycystic disease of the liver and kidneys, and those with typical evidence of metastases, were excluded. The population examined was not expected to harbour hydatid disease. The age and sex distribution of the subjects are shown in Tables I and II.

Results

Forty-three patients out of 1695 examined were found to have a total of 57 hepatic cysts, a prevalence of 2.5%,

Table II. Sex-related prevalence of hepatic cysts

	Number of subjects	Number with cysts	%
Male	771	15	1.95
Female	924	28	3.03
Total	1695	43	2.54

Table III. Relationship of the size of hepatic cysts to age of patient

Age (yrs)	No. of patients	No. of cysts	Size of hepatic cysts						
			≤1 cm	1.1–2 cm	2.1–3 cm	3.1–4 cm	4.1–5 cm	5.1–6 cm	6.1–7 cm
20–29	1	2	2						
30–39	2	2		1					1
40–49	1	1				1			
50–59	1	2			1	1			
60–69	11	13		5	2	4	2		
70–79	17	22	4	10	4	1	2	1	
80–89	8	13	1	8	2		1		1
90+	2	2			1			1	
Total	43	57	7	24	10	7	5	2	2

and distributed as shown in Tables I and II. Eleven patients (26%) had multiple lesions up to a maximum of three cysts; the remainder had solitary lesions.

An increasing prevalence with age is demonstrated (Fig. 2), ranging from none below the age of 20 years up to 7% of patients over 80 years old. Although cysts become more common with age, their distribution of size remains approximately constant (Table III), the most frequent diameter being 1.1–2 cm.

Five cysts were multilocular and in each case were divided by only thin septa. Cysts were most common in the right lobe of the liver (R = 46, L = 11) and in female patients (1.7:1).

Discussion

Simple hepatic cysts are considered to result from obstruction of congenitally derived aberrant bile ducts, leading to stasis and retention (Moschowitz, 1906). Why such lesions should not appear until middle age is unclear, but they seem to enlarge to a diameter of usually between 1 and 5 cm and then remain stable. Although occasionally they present as an abdominal mass, hepatomegaly, abdominal pain or obstructive jaundice, most are discovered as an incidental finding (Sanfelippo et al, 1974). They contain colourless or yellow fluid. Most lesions are solitary, some are septate and, as demonstrated in other reports, there is a preference for women and the right lobe of the liver (Jones et al, 1974).

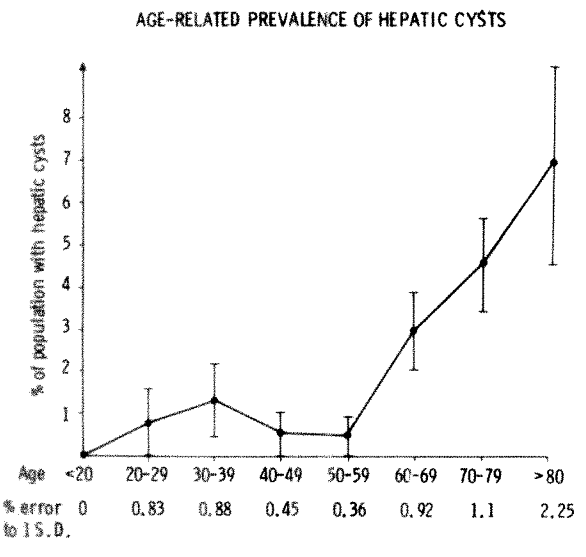

Figure 2. Graphical representation of the age-related prevalence of hepatic cysts.

A prevalence of between 1 in 200–600 cases has been previously reported during laparotomy or autopsy examination (Sanfelippo et al, 1974). Our study using ultrasound examination has shown that they are considerably more common, occurring in 2.5% of the general population and increasing to 7% in patients older than 80 years.

Although simple hepatic cysts are a frequent finding in the older population, they are uncommon in the young. Cysts may then be significant if they represent a disease marker. For example, in von Hippel-Lindau disease the presence of a hepatic cyst may be the only manifestation of the disease (Jennings & Gaines, 1988). A cystic lesion of the liver, especially in the younger age group, should raise the possibility of an alternative diagnosis when not fulfilling strict criteria for cysts or when the dividing septa are thick. Intrahepatic gallbladders, echinococcal cysts (King, 1973) and sarcomatous metastases may produce thin-walled masses with no internal echoes. Non-sarcomatous necrotic metastases are usually multiple (66%), have a thick, irregular wall and there are often more typical lesions present (Wooten et al, 1978). Abscesses have irregular walls and some low-level internal echoes. Injury may produce a cystic biloma or a haematoma which can appear cystic within a few days; a history of trauma will be apparent. Mesenchymal hamartomas occur in infants when simple liver cysts are rare, and biliary cystadenomas or cystadenocarcinomas are very unusual lesions, often showing thick septation and papillary projections (Hill & Sanders, 1985).

Acknowledgments

We would like to thank all the departmental radiologists who co-operated with this work and Mrs Y. Steel for typing the manuscript.

References

HILL, M. C. & SANDERS, R. C., 1985. *Ultrasound Annual* (Raven Press, New York), pp. 142–154.

JENNINGS, C. M. & GAINES, P. A., 1988. The abdominal manifestations of von Hippel-Landau disease and a radiological screening protocol for an affected family. *Clinical Radiology, 39*, 363–367.

JONES, W. J., MOUNTAIN, J. C. & WARREN, K. W., 1974. Symptomatic non-parasitic cysts of the liver. *British Journal of Surgery, 61*, 118–123.

KING, D. L., 1973. Ultrasonography of echinococcal cysts. *Journal of Clinical Ultrasound, 1*, 64–67.

MOSCHOWITZ, E., 1906. Nonparasitic cysts (congenital) of the liver, with a study of aberrant bile ducts. *American Journal of Medical Science, 131*, 674–699.

SANFELIPPO, P. M., BEAHRS, O. H. & WEILAND, L. H., 1974. Cystic disease of the liver. *Annals of Surgery, 179*, 922–925.

WOOTEN, W. B., GREEN, B. & GOLDSTEIN, H. M., 1978. Ultrasonography of necrotic hepatic metastases. *Radiology, 128*, 447–450.

1989, *The British Journal of Radiology*, 62, 338–343

Radiation-induced cell death by chromatin loss

A model to explain the shape of low-linear-energy-transfer cell survival curves

*Ian R. Campbell, FRCS, MRCR and Hilmar M. Warenius, PhD, FRCP, FRCR

University of Liverpool CRC Department of Radiation Oncology, Mersey Regional Centre for Radiotherapy and Oncology, Clatterbridge Hospital, Merseyside L63 4LA

(*Received August 1987 and in revised form November 1988*)

Abstract. A model is proposed which relates reproductive death of cells caused by radiation to loss of chromatin at cell division. This loss of chromatin can occur through chromosomal deletions or through the formation of asymmetrical chromosomal exchanges. It is proposed that smaller doses of radiation produce fewer chromatin breaks, which are more likely to be accurately repaired, compared with larger doses. Consequently, smaller doses of radiation are less efficient in causing cell death, leading to a shoulder on the cell survival curve. Experimental evidence supports this model, and the fit between the derived formula and experimental cell survival curves is good. The derived formula approximates to the linear-quadratic equation at low doses of radiation.

Many models have been proposed to explain the relationship between doses of low-linear-energy-transfer (LET) radiation, such as X rays, and loss of the reproductive capability of cells (loosely referred to as "cell death"). For many experimental systems, both *in vitro* and *in vivo*, the shape of the relationship when cell survival is plotted against radiation dose on semilogarithmic axes is an initial shoulder region followed by a straight line portion (Puck & Marcus, 1956). Many of the models that have been proposed in the past have fitted the experimental cell survival data closely but have used hypothetical concepts such as specific intracellular targets, for which there is no biological basis. Examples are the single-target, multihit model and the multitarget, single-hit model (Elkind & Whitmore, 1967).

More recently, the model of Chadwick and Leenhouts (1973) has gained some acceptance. This does have a biological basis in that cell death is taken to be due to breakage, either separately or simultaneously, of the two strands of DNA. The Chadwick–Leenhouts model gives rise to a formula (the linear-quadratic equation) which provides a good fit to experimental data at low doses of radiation. However, the model frequently fails at high doses of radiation when the surviving proportion of cells is $< 10^{-2}$, since the linear-quadratic equation remains a continuously curving function whereas experimental data usually follow a linear relation. Furthermore, a central feature of the Chadwick–Leenhouts model is that double-strand DNA breaks occur with a frequency bearing a linear-quadratic relation to the dose of radiation whereas there is considerable experimental evidence that the frequency of double-strand DNA breaks is linearly related to radiation dose (Sawada & Okada, 1972; Blöcher, 1982). Currently, popularity is growing for "repair" models based on the ideas of repair and misrepair of radiation-induced lesions (Calkins, 1971; Goodhead, 1980; Tobias et al, 1980), but these models again rely heavily on hypothetical concepts.

This paper presents a mathematical model that is based on the large body of biological data available and also accurately fits cell survival data over a wide range of doses and experimental conditions. It is based on the idea that reproductive cell death by radiation occurs as a consequence of loss of chromatin from the cell. The idea is not new [it was put forward by Lea (1946) in the early days of radiobiology] but the mathematical implications of it have not previously been explored. The basis is that radiation causes breaks in the chromatin that may not rejoin or may rejoin incorrectly, leading to chromatin fragments which are lost during cell division and to consequent cell death. The model will be explained by a series of assumptions, justifications of those assumptions, and conclusions. It will be explained in terms of "chromatin breaks" and "loss of chromatin" rather than "DNA double-strand breaks" and "loss of DNA", although it is likely that chromatin breaks are directly related to double-strand DNA breaks. The term "chromatin" is used to include both DNA and its supporting molecular structure.

The model

Assumption 1: A break in the chromatin of a cell by low-LET radiation occurs with a frequency proportional to the dose

Evidence in favour of Assumption 1 comes from studies of the relationship between chromosomal aberrations and the dose of low-LET radiation. Some aberrations require a single chromatin break (terminal deletions), while others require two chromatin breaks (*e.g.* centric rings, reciprocal translocations and chromosome dicentrics) (Savage, 1975). For aberrations requiring a single break, aberration frequency is proportional to dose, while for aberrations requiring two breaks, aberration frequency is very nearly proportional to dose squared (Chu et al, 1961). For tricentric chromosome aberrations, aberration frequency is proportional to dose cubed (Revell, 1966), although exactly how these are formed is unclear. All of these relationships would be expected if breaks occur with a frequency proportional to dose. Furthermore, DNA double-strand breaks occur at a frequency proportional to dose (Sawada & Okada, 1972; Blöcher, 1982), although the exact relation of DNA double-strand breaks to chromatin breaks is not clear.

---

*Author for correspondence.

The only explanation for this is that a chromatin break occurs through the interaction of the chromatin with the ionizations produced by a single photon. This raises the question as to how a single photon with low average LET (*i.e.* high average separation between ionizations) can cause a chromatin break, since a chromatin break might be expected to require the energy from several ionizations within a small volume in order to break both DNA strands and the supporting structure. The explanation could be through the localized areas of dense ionization that occur along the tracks of low average LET radiation (Elkind, 1967). These high-LET regions occur both at the end of the track of a secondary electron and also through δ rays. Thus in low-LET radiation there are scattered regions of high LET, whereas in high-LET radiation there is a continuous column of high LET.

Assumption 2: There are repair mechanisms in the cell that are capable of rejoining chromatin breaks

It is through these repair mechanisms that the many varieties of chromosomal aberrations are formed (with the exception of terminal deletions). Chromatin breaks may or may not be repaired (Bender et al, 1974; Savage, 1975), and chromatin ends that are rejoined may or may not be rejoined appropriately (Bender et al, 1974; Savage, 1975), although the molecular processes involved are unclear. Following irradiation, DNA double-strand breaks are largely repaired within an hour (Cole et al, 1980; Blöcher & Pohlit, 1982), which is approximately the timescale of formation of chromosomal aberrations (Dewey et al, 1971a), and also the timescale of repair of "sublethal damage" (Elkind & Sutton, 1959).

Assumption 3: The probability that any individual chromatin break will be repaired (correctly or incorrectly) will be independent of the number of chromatin breaks within the nucleus

It would be expected that the value of p, *i.e.* the probability of chromatin breaks being rejoined, would vary between different cell types and, for a given cell type, between different phases of the cell cycle, but it will be assumed that it is independent of the number of chromatin breaks.

This is the most speculative of the assumptions. Chromatin repair mechanisms are not well understood at present, and it is conceivable that repair mechanisms are saturable, *i.e.* that the probability of repair decreases progressively with increasing numbers of chromatin breaks. Indeed, some models of cell survival are based on just such a hypothesis. This assumption is not in fact essential to the model since if an alternative assumption is made, that the probability of repair is constant up to a maximum number of chromatin breaks and zero thereafter, then the derived curves would not be very different in shape, unless the maximum number of repairable breaks is less than six.

Assumption 4: Those chromatin ends that rejoin will rejoin at random

If the chromatin ends rejoin correctly then the original chromosomes are reformed. If the ends rejoin incorrectly, then there will be chromosomal aberrations produced. Evidence in favour of random rejoining is the equal frequency of asymmetrical and symmetrical chromosome-type aberrations (Savage & Papworth, 1982) (symmetrical aberrations result from rejoining of chromosome fragments such that each acentric fragment joins to a fragment containing a centromere, whereas asymmetrical aberrations result from other types of rejoining). However, there are some indications that rejoining (correctly or incorrectly) is more likely to occur between fragments of the same chromosome rather than fragments of different chromosomes, possibly because of mechanical barriers within the nucleus preventing mixing of decondensed chromosome threads (Savage & Papworth, 1973). Assumption 4 is not essential to the model since if there is preferential rejoining so as to reform the original chromosomes, then the result is equivalent to a reduction in the number of chromatin breaks.

Assumption 5: Cells that lose chromatin die in attempting to divide, while if there is no chromatin loss then the cells will survive

Cells can lose chromatin either through chromosomal deletions (when some chromatin ends have not rejoined) or through asymmetrical chromosomal exchanges. Symmetrical chromosomal exchanges do not lead to chromatin loss and indeed are difficult to detect unless chromosomal banding techniques are used (Savage & Papworth, 1982). Four lines of evidence support Assumption 5. First, asymmetrical chromosomal aberrations tend to disappear after several cell divisions whilst symmetrical aberrations are much more likely to survive (Sasaki & Norman, 1967). Secondly, following irradiation, those cells in which a chromosome fragment or a micronucleus appears are either incapable of cell division or can only carry out a limited number of divisions (the micronucleus is a small separated fragment of the nucleus containing the fragment of chromatin, and is easier to visualize than the chromatin fragment itself) (Grote & Revell, 1972; Joshi et al, 1982). Thirdly, observations of cell death from radiation agree well with predictions from observed frequencies of asymmetrical chromosomal exchanges and deletions and their survival (Carrano, 1973a,b). Fourthly, the correlation between the number of cells with asymmetrical chromosomal aberrations and the number of cells killed is seen over a range of doses and different radiation qualities (Roberts & Holt, 1985), and also when radiosensitivity is made to vary by treatment with colcemid or 5-bromodeoxyuridine or by irradiation in different parts of the cell cycle (Dewey et al, 1971b). These experimental findings refer mainly to chromosome-type aberrations. In situations where there is a large proportion of chromatid-type aberrations, *e.g.* where the cell cycle time is very short, Assumption 5 may depart significantly from reality.

It is clear that chromosomal deletions do not inevitably result in cell death as chromosomal studies have shown their long-term persistence in living cells (Couzin, 1979). However, these surviving deletions may represent only a tiny proportion of the deletions that have occurred, which is certainly the case after irradiation in two studies (Grote & Revell, 1972; Joshi et al, 1982).

How chromosomal deletions in a diploid cell result in cell death is not immediately apparent, as there should be a corresponding intact chromosome containing equivalent genetic material. Possibly the cell detects chromatin loss and there are mechanisms that prevent the cell surviving, or possibly recessive lethal genetic abnormalities in the intact equivalent chromosome are revealed.

Assumption 6: The number of chromatin breaks per cell produced by low-LET radiation is distributed randomly according to the Poisson distribution

If the mean number of chromatin breaks per cell is m, then the probability of N breaks in a cell is given by the general term of the Poisson distribution, *i.e.*

$$\frac{m^N \exp(-m)}{N!} \qquad (1)$$

Evidence for random distribution of chromatin breaks is the finding that the relative frequency of chromosome breakpoints is approximately proportional to chromosome length (Couzin, 1979). Under Assumption 1, considerable evidence was put forward for chromatin breaks occurring at a frequency proportional to the radiation dose. Hence the mean number of chromatin breaks per cell (m) is proportional to dose D, *i.e.* $m = D/D_{CB}$ where D_{CB} is the dose necessary to cause an average of one chromatin break per cell.

Hence the probability of N breaks is

$$\frac{(D/D_{CB})^N \exp(-D/D_{CB})}{N!}$$

Derived survival after N *chromatin breaks*

The consequences of these six assumptions will now be considered. First, as examples, particular numbers of chromatin breaks will be considered, followed by the general case of N breaks.

No breaks. Clearly all cells will survive.

One break. There will be two chromatin ends. The chance of the break being repaired is p (from Assumption 3). If the chromatin ends do rejoin, this will necessarily be correctly, reforming the original chromosome, and hence the survival will be p.

Two breaks. This will result in four chromatin ends. As the chance of a pair of chromatin ends rejoining is p, the chance of all four ends rejoining is p^2. There will be three possible ways of equal likelihood in which these four ends can be rejoined. One way will result in restitution of the original chromosomes, the second will result in a symmetrical chromosomal exchange and so no chromatin loss, and the third arrangement will result in an asymmetrical chromosomal exchange and so cell death. In the first and second cases, the cell will survive, while in the third case the cell will lose chromatin and will be assumed to die. The expected survival will therefore be $\frac{2}{3}p^2$.

N breaks. As N increases, the expected survival will decrease through two factors. First, the chance of all the chromatin ends rejoining will progressively fall, and secondly, the chance of an asymmetrical chromosomal exchange during rejoining will progressively increase. The number of different arrangements of the $2N$ chromatin ends taken in pairs is ${}_{2N}C_2 = (2N)!/(N!\ 2^N)$. Each break will be assumed to result in a chromatin fragment containing a centromere and a chromatin fragment without a centromere (the more complicated situation of more than one break on a chromosome arm will not be considered here and does not make a significant difference). There will be no asymmetrical exchanges if each chromatin end containing a centromere rejoins with a chromatin end that does not contain a centromere. This will occur in $N!$ of the $(2N)!/(N!\ 2^N)$ possible rearrangements, *i.e.* with a probability of $N!\ N!\ 2^N/(2N)!$. Since the probability of all the chromatin ends rejoining is p^N, the expected survival is

$$\frac{N!\ N!\ 2^N\ p^N}{(2N)!} \qquad (2)$$

Derived overall survival

The contribution to total survival from cells in which N chromatin breaks have occurred is the chance of N breaks occurring multiplied by the chance of survival after N breaks, and the total expected survival in all cells is the sum of these products, summing for all values of N, *i.e.* expected survival is

$$\sum_{N=0}^{\infty} \frac{(D/D_{CB})^N \exp(-D/D_{CB})}{N!} \times \frac{N!\ N!\ 2^N\ p^N}{(2N)!}$$

i.e.

$$\text{Survival} = \exp(-D/D_{CB}) \sum_{N=0}^{\infty} (2p\ D/D_{CB})^N\ N!/(2N)! \qquad (3)$$

where D is the dose given, D_{CB} is the dose necessary to cause an average of one chromatin break per cell, and p is the probability that a chromatin break will be repaired.

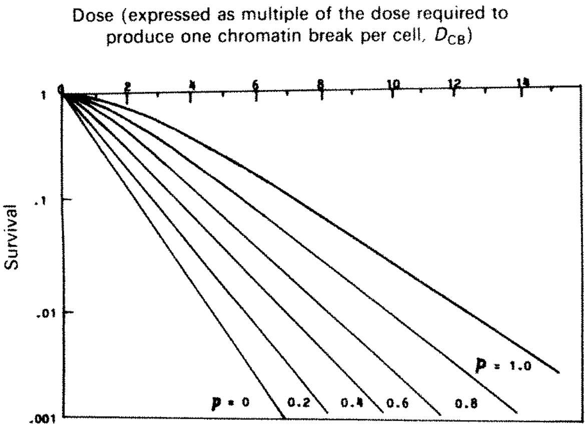

Figure 1. Cell survival curves derived from the proposed model [Equation (3)] for different values of p (the probability of repair of a chromatin break).

Derived cell survival curves

Figure 1 shows Equation (3) for different values of p on a semilogarithmic plot of survival against dose, with dose expressed as multiples of the dose required to cause one chromatin break per cell. Each line has a shoulder and exponential portion with the size of the shoulder varying, larger shoulders occurring with larger values of p, *i.e.* with greater probability of repair of chromatin breaks. Cell survival curves are commonly characterized by the parameters n (the intercept on the survival axis of the exponential portion of the curve) and D_0 [the slope of the exponential portion expressed as the dose required to reduce survival to a fraction of 1/e (Elkind & Whitmore, 1967)]. By these definitions, the curves shown have values of n lying between 1 and 6, and values of D_0 lying between 1.0 and 2.0 times the dose needed for an average of one chromatin break per cell. These values of n correspond approximately to the range of those found experimentally (Elkind & Whitmore, 1967), and the range of values of D_0 (*i.e.* within a factor of 2) corresponds approximately to the range of values of D_0 at different phases of the cell cycle (Terasima & Tolmach, 1963; Sinclair, 1968). Values of D_0 from experimental systems generally lie in the range 100–200 cGy (Elkind & Whitmore, 1967), suggesting that doses of the order of 100 cGy are needed to produce an average of one chromatin break per cell.

Relationship to the linear-quadratic equation

The derived formula for cell survival, *i.e.* Equation (3), can be expanded and expressed as a polynomial of the form

$$\text{Survival} = \exp-(\alpha D + \beta D^2 + \gamma D^3 + \text{higher powers of } D)$$

When this is done, the values taken by α, β and γ are $\alpha = (1-p)/D_{CB}$, $\beta = p^2/6D_{CB}^2$, and $\gamma = 2p^3/5D_{CB}^3$. Hence, at low doses of radiation, Equation (3) approximates to $\exp-(\alpha D + \beta D^2)$, *i.e.* to the linear-quadratic equation. The α/β ratio, in terms of the proposed model, would then be equal to $6(1-p)\ D_{CB}/p^2$.

Discussion

The model described gives a satisfactory fit to the experimental shape of cell survival curves, with curvature down to a surviving proportion of about 0.3 and then an approximately linear relation, and predicts extrapolation numbers that approximate to those found experimentally. The model is particularly successful in predicting that cell survival will follow not one curve but a family of curves with shoulders of different sizes, with the size of the shoulder increasing and the slope of the exponential portion decreasing with increasing ability of the cell to repair breaks in the chromatin. Hence cells at different stages in the cell cycle might be expected to show differences in the size of the shoulder and of the gradient of the exponential portion of the cell survival curve, as has been reported (Terasima & Tolmach, 1963; Sinclair, 1968). Cells in mitosis and G_2 might be expected to be relatively poor at repairing chromatin breaks, being committed to the process of cell division, and this would fit with their survival curves having relatively small shoulders (Terasima & Tolmach, 1963; Sinclair, 1968), although repair of double-strand breaks has been reported as independent of stage in the cell cycle (Blöcher et al, 1983). This flexibility of the model contrasts with the single curve of fixed shape that is predicted by many other models of cell survival.

The proposed model implies that what is called "sublethal damage" may be those chromatin breaks that have been induced and which will be accurately repaired if further chromatin breakage is not immediately sustained, and "lethal damage" is damage that will never be repaired or whose repair is not sufficient to prevent cell death. This is supported by two observations. First, the timescale of repair of chromatin breaks is similar to the timescale of repair of sublethal damage, with both processes mainly complete within 1 h (Elkind & Sutton, 1959; Dewey et al, 1971a); the timescale of repair of potentially lethal damage is also similar (Dewey et al, 1971a). Secondly, the oxygen concentration has a similar effect on the extents of both chromosomal aberrations and sublethal damage, with oxygen enhancement ratios of around 2.5 and K values of 3–10 μmol l^{-1} in each case (Gray, 1957; Alper, 1960).

The model has been described in terms of "loss of chromatin" rather than "loss of double-strand DNA", although these are probably closely related. In irradiated *E. coli*, there are approximately the same number of lethal events as DNA double-strand breaks (Bonura et al, 1975). By contrast, in mammalian cells, it is clear that a double-strand DNA break does not inevitably result in cell death through a chromatin break since of the order of 20 double-strand breaks per cell are produced at a dose equivalent to D_0 (Veatch &

Okada, 1969; Cole et al, 1980). However, there is a parallel between DNA double-strand breaks and chromatin breaks in that the timescale for repair is similar (Dewey et al, 1971a; Cole et al, 1980; Blöcher & Pohlit, 1982).

The case for acceptance of the model would be strengthened if predictions made from the model were to be confirmed experimentally. Five predictions can be made. First, at low doses of radiation ($<D_0$), when the mean number of chromatin breaks per cell predicted by the model is less than one or two, the ratio of terminal deletions to exchange aberrations would be expected to be higher than at high doses of radiation. This first prediction is perhaps superfluous since it follows directly from some of the experimental evidence that forms the basis of Assumption 1 of the model (deletions are linearly related to dose whilst exchanges occur at a rate proportional to the square of the dose).

Secondly, a similar finding of a relatively high ratio of deletions to exchange aberrations would be predicted at low-dose-rate irradiation, *i.e.* when the dose-rate is low enough to allow significant rejoining of chromatin breaks during the irradiation, so that there is a reduced opportunity for interaction between two or more separate chromatin breaks within a nucleus.

Thirdly, in those situations where the shoulder on the cell survival curve is small, *i.e.* certain cell lines, certain phases of the cell cycle and certain experimental conditions, then p in the terms of the model should be small and chromosomal aberrations should be mainly terminal deletions rather than dicentrics or centric rings. In those situations where the shoulder on the cell survival curve is large, then p should be large and dicentrics and centric rings should be relatively more numerous.

Fourthly, since chromatin lost from the chromosomes appears as a micronucleus in the cytoplasm of the cell (Streffer et al, 1982), the proportion of cells containing micronuclei should correspond with the number of cells killed, and this correspondence should hold over all experimental conditions. There is some experimental evidence for this both *in vitro* (Midander & Revesz, 1980; Streffer et al, 1982), and also *in vivo* after irradiation of human tumours (Streffer et al, 1982).

Fifthly, prematurely condensed chromosome (PCC) breaks are not equivalent to complete chromatin breaks, since of the order of 10 PCC breaks occur per D_0 dose (Cornforth & Bedford, 1983) compared with a prediction of between one and two chromatin breaks by the model.

The approximation of the derived formula to the linear-quadratic equation at low doses of radiation is convenient since much work has been done on the importance of α/β ratios and their relation to early and late radiation damage, and the model described is therefore compatible with these advances. This approximation to the linear-quadratic equation at low doses of radiation is not unique to the model described but is generally true of many models, since any smooth curve can be represented as a polynomial series, which will approximate to the linear-quadratic equation at low doses.

The formula derived from the model described is applicable to low-LET radiation only. With high-LET radiation, Assumption 6 does not apply, *i.e.* chromatin breaks are not distributed randomly between cells according to the Poisson distribution, but instead there is an excess of cells with multiple hits (Streffer et al, 1982).

Numerous models have been proposed in the past to account for the shape of cell survival curves and merely to add one more would be of little value. Furthermore, there are many indications that the process of reproductive cell death from radiation is very complex, and a model as simple as the one proposed could not be more than a first approximation. However, we believe that the proposed model is important not only in explaining cell survival data, but also in concentrating attention on what is the critical sequence of radiation-induced lesions that leads to cell death. There is much evidence for this being DNA double-strand breaks, leading to chromatin breaks, chromosomal aberrations and chromatin loss, and finally reproductive cell death.

Acknowledgments

We thank Dr P. Bryant and Dr P. D. Holt for helpful comments during preparation of the manuscript.

References

ALPER, T., 1960. Cellular radiobiology. *Annual Review of Nuclear Science, 10,* 489–530.

BENDER, M. A., GRIGGS, H. G. & BEDFORD, J. S., 1974. Mechanisms of chromosomal aberration production. III. Chemicals and ionizing radiation. *Mutation Research, 23,* 197–212.

BLÖCHER, D., 1982. DNA double-strand breaks in Ehrlich ascites tumour cells at low doses of X rays. I. Determination of induced breaks by centrifugation at reduced speed. *International Journal of Radiation Oncology, Biology, Physics, 42,* 317–328.

BLÖCHER, D., NÜSSE, M. & BRYANT, P. E., 1983. Kinetics of double-strand break repair in the DNA of X irradiated synchronized mammalian cells. *International Journal of Radiation Oncology, Biology, Physics, 43,* 579–584.

BLÖCHER, D. & POHLIT, W., 1982. DNA double-strand breaks in Ehrlich ascites tumour cells at low doses of X-rays. II. Can cell death be attributed to double-strand breaks? *International Journal of Radiation Oncology, Biology, Physics, 42,* 329–338.

BONURA, T., TOWN, C. D., SMITH, K. C. & KAPLAN, H. S., 1975. The influence of oxygen on the yield of DNA double-strand breaks in X-irradiated *Escherichia coli* K-12. *Radiation Research, 63,* 567–577.

CALKINS, J., 1971. A method of analysis of radiation response based on enzyme kinetics. *Radiation Research, 45,* 50–62.

CARRANO, A. V., 1973a. Chromosome aberrations and radiation-induced cell death, I. Transmission and survival parameters of aberrations. *Mutation Research, 17,* 341–353.

—— 1973b. Chromosome aberrations and radiation-induced cell death, II. Predicted and observed cell survival. *Mutation Research, 17,* 355–366.

CHADWICK, K. H. & LEENHOUTS, H. P., 1973. A molecular theory of cell survival. *Physics in Medicine and Biology, 18*, 78–87.

CHU, E. H. Y., GILES, N. H. & PASSANO, K., 1961. Types and frequencies of human chromosome aberrations induced by X rays. *Proceedings of the National Academy of Sciences, 47*, 830–839.

COLE, A., MEYN, R. E., CHEN, R., CORRY, P. M. & HITTELMAN, W., 1980. Mechanisms of cell injury. In *Radiation Biology in Cancer Research*, ed. by R. E. Meyn & H. R. Withers (Raven Press, New York), pp. 33–58.

CORNFORTH, M. N. & BEDFORD, J. S., 1983. X-ray-induced breakage and rejoining of human interphase chromosomes. *Science, 222*, 1141–1143.

COUZIN, D., 1979. Frequency changes with time *in vivo* of radiation-induced chromosomal aberrations in skin fibroblasts. *Mutation Research, 60*, 367–380.

DEWEY, W. C., MILLER, H. H. & LEEPER, D. B., 1971a. Chromosomal aberrations and mortality of X-irradiated mammalian cells: emphasis on repair. *Proceedings of the National Academy of Sciences, 68*, 667–671.

DEWEY, W. C., STONE, L. E., MILLER, H. H. & GIBLAK, R. E., 1971b. Radiosensitization with 5-bromodeoxyuridine of Chinese hamster cells X-irradiated during different phases of the cell cycle. *Radiation Research, 47*, 672–688.

ELKIND, M. M. & SUTTON, H., 1959. X-ray damage and recovery in mammalian cells in culture. *Nature, 184*, 1293–1295.

ELKIND, M. M. & WHITMORE, G. F., 1967. *The Radiobiology of Cultured Mammalian Cells* (Gordon & Breach, New York).

GOODHEAD, D. T., 1980. Models of radiation inactivation and mutagenesis. In *Radiation Biology in Cancer Research*, ed. by R. E. Meyn & H. R. Withers (Raven Press, New York), pp. 231–247.

GRAY, L. H., 1957–8. The influence of oxygen on the response of cells and tissues to ionizing radiation. *Lectures on the Scientific Basis of Medicine, 7*, 314–347.

GROTE, S. J. & REVELL, S. H., 1972. Correlation of chromosome damage and colony-forming ability in Syrian hamster cells in culture irradiated in G_1. *Current Topics in Radiation Research Quarterly, 7*, 303–309.

JOSHI, G. P., NELSON, W. J., REVELL, S. H. & SHAW, C. A., 1982. X-ray-induced chromosome damage in live mammalian cells, and improved measurements of its effects on their colony-forming ability. *International Journal of Radiation Oncology, Biology, Physics, 41*, 161–181.

LEA, D. E., 1946. *Actions of Radiations on Living Cells* (Cambridge University Press, Cambridge).

MIDANDER, J. & REVESZ, L., 1980. The micronucleus (MN) in irradiated cells as a measure of survival. *British Journal of Cancer, 41*, Supplement IV, 204.

PUCK, T. T. & MARCUS, P. I., 1956. Action of X-rays on mammalian cells. *Journal of Experimental Medicine, 103*, 653–666.

REVELL, S. H., 1966. Evidence for a dose-squared term in the dose–response curve for real chromatid discontinuities induced by X-rays, and some theoretical consequences thereof. *Mutation Research, 3*, 34–53.

ROBERTS, C. J. & HOLT, P. D., 1985. Induction of chromosome aberrations and cell killing in Syrian hamster fibroblasts by γ rays, X rays and fast neutrons. *International Journal of Radiation Biology, 48*, 927–939.

SASAKI, M. S. & NORMAN, A., 1967. Selection against chromosome aberrations in human lymphocytes. *Nature, 214*, 502–503.

SAVAGE, J. R. K., 1975. Classification and relationships of induced chromosomal structural changes. *Journal of Medical Genetics, 12*, 103–122.

SAVAGE, J. R. K. & PAPWORTH, D. G., 1973. The relationship of radiation-induced dicentric yield to chromosome arm number. *Mutation Research, 19*, 139–143.

—— 1982. Frequency and distribution studies of asymmetrical versus symmetrical chromosome aberrations. *Mutation Research, 95*, 7–18.

SAWADA, S. & OKADA, S., 1972. Effects of BUdR-labelling on radiation-induced DNA breakage and subsequent rejoining in cultured mammalian cells. *International Journal of Radiation Oncology, Biology, Physics, 21*, 599–602.

SINCLAIR, W. K., 1968. Cyclic X-ray responses in mammalian cells *in vitro*. *Radiation Research, 33*, 620–643.

STREFFER, C., VAN BEUNINGEN, D. & MOLLS, M., 1982. Possibilities of the micronucleus test as an assay in radiotherapy. In *Progress in Radio-Oncology II*, ed. by K. H. Kärcher, H. D. Kogelnik & G. Reinartz (Raven Press, New York), pp. 243–251.

TERASIMA, T. & TOLMACH, L. J., 1963. Variations in several responses of HeLa cells to X-irradiation during the division cycle. *Biophysical Journal, 3*, 11–33.

TOBIAS, C. A., BLAKELY, E. A., NGO, F. Q. H. & YANG, T. C. H., 1980. The repair–misrepair model of cell survival. In *Radiation Biology in Cancer Research*, ed. by R. E. Meyn & H. R. Withers (Raven Press, New York), pp. 195–230.

VEATCH, W. & OKADA, S., 1969. Radiation-induced breaks of DNA in cultured mammalian cells. *Biophysical Journal, 9*, 330–346.

1989, *The British Journal of Radiology*, 62, 344–347

Changes in biological effectiveness of the neutron beam at Clatterbridge (62 MeV p on Be) measured with cells *in vitro*

By D. K. Bewley, DSc, B. M. Cullen, PhD, *M. Astor, MA, *E. J. Hall, DSc, †S. W. Blake, MSc, †D. E. Bonnett, PhD and *M. Zaider, PhD

MRC Cyclotron Unit, Hammersmith Hospital, Du Cane Road, London W12 0HS, *College of Physicians and Surgeons of Columbia University, New York, USA and †MRC Cyclotron Unit, Clatterbridge Hospital, Bebington, Wirral, Merseyside

(*Received July 1988 and in revised form October 1988*)

Abstract. Chinese hamster V79 cells have been used to assess changes in RBE of the p(62)Be neutron beam at the Clatterbridge Hospital with depth in a phantom and with use of a hydrogenous filter. The cells were exposed at depths of 2 and 12 cm and at a depth of 2 cm with a hydrogenous filter. Two groups of experimenters each conducted two experiments. The ratios of relative biological effectiveness (RBE) at a depth of 12 cm to that at 2 cm were found by the two groups to be 0.99 ± 0.04 and 0.96 ± 0.02 (standard errors). The effect of a polythene filter 4.5 cm thick was measured at a depth of 2 cm and the ratio of RBE with and without the filter was found by both groups to be 0.99 ± 0.02. All the experiments suggest that there may be small effects of beam hardening by depth and filtration but these results are in marked contrast with those obtained using an *in vivo* system.

The Clatterbridge neutron therapy facility consists of a single-particle, fixed-energy cyclotron which can accelerate protons to 62 MeV, together with an isocentric treatment gantry capable of 360° rotation. Neutrons are generated by protons incident on a beryllium target located in the gantry. The protons deposit 36 MeV within the beryllium and are stopped in the copper backing of the target. The profile of the neutron beam is then flattened by an iron filter before final collimation. A more detailed description of the facility, beam production and collimation has been given elsewhere (Bonnett et al, 1988).

Before the beam was used for the treatment of malignant disease, radiobiological tests of the quality of the neutron beam were made by several workers using a number of biological systems. This paper is concerned with the use of aerobic Chinese hamster V79 cells to study changes of relative biological effectiveness (RBE) with filtration and depth in a phantom and is presented as a companion to the paper by Hornsey et al (1988) on the same subject. The possibility of a changing RBE with depth arose from previous studies with neutron beams generated by protons on beryllium at the Cleveland NASA cyclotron (Hall et al, 1982, 1983).

Materials and methods

Two separate sets of experiments were performed, one by Hall and Astor and the other by Cullen. Hall and Astor used a line of V79 cells that was obtained from Dr M. Elkind in 1970 and has been continuously cultured in the laboratory ever since. For these experiments the cells were plated into rectangular Corning flasks in New York and allowed to attach by incubation overnight at 37°C. The flasks were then cooled to room temperature, filled with medium and transported by air to the site of the neutron beam. After irradiation at room temperature, the flasks were incubated at 37°C for 8 days, after which the colonies were fixed and stained for counting. Details of the technique have been given previously by Hall (1977). During irradiation, the cells were attached to the back surface of the flask so that the neutrons passed through 2 cm of medium before reaching the cells, assuring full secondary-proton equilibrium.

In Cullen's experiments, known numbers of cells (V79-171B) were irradiated in suspension in plastic pots. The cells and medium filled a volume 15 mm diameter and 40 mm high. The pots were sunk into holes in Perspex blocks to achieve secondary-proton equilibrium. The cells settled gradually during each irradiation. They were then plated, incubated for 8 days and the colonies were counted.

In both experiments the neutron beam was horizontal. The surface of the phantom was 150 cm from the target with a field size of 20 cm × 20 cm. In Cullen's experiments the centres of the pots were at depths of 2 or 12 cm and in Hall's and Astor's experiments the layers of cells were also at depths of 2 or 12 cm. The phantom was made of Perspex and measured 30 cm × 30 cm × 25 cm thick. Additional experiments were performed at a depth of 2 cm with a polythene filter 4.5 cm thick in place of the iron flattening filter.

Both sets of investigators performed two experiments at Clatterbridge during the period September 1984 to February 1986. Hall and Astor and their colleagues carried out irradiations at Hammersmith and Clatterbridge on the same day in 1984. In 1985 they made simultaneous experiments on the neutron beams at Houston (Texas) and Clatterbridge. These more extensive intercomparison experiments between different neutron facilities will be reported elsewhere.

Dosimetry was based on A-150 chambers containing tissue-equivalent gas and the doses quoted here

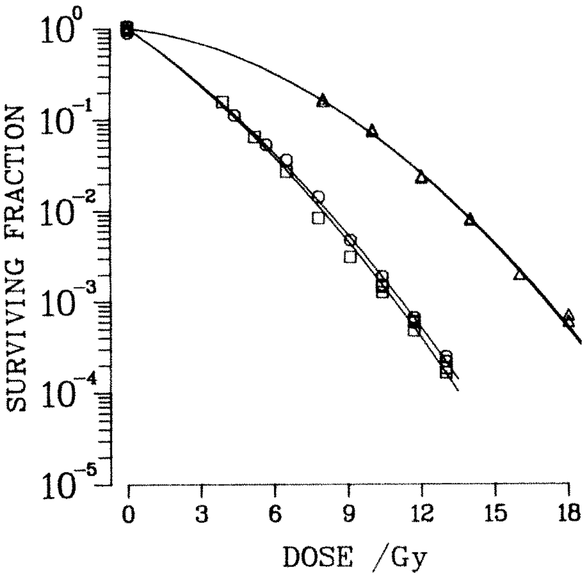

Figure 1. Survival data measured by Cullen for cells irradiated by Clatterbridge neutrons at a depth of 2 cm with (○) and without (□) a filter. Also shown are the 250 kV X-ray data (△). Error bars (not shown, for clarity) are generally smaller than the size of the symbol used to represent the data. The curves represent best fits to the data using a linear-quadratic dose–effect relationship (see text).

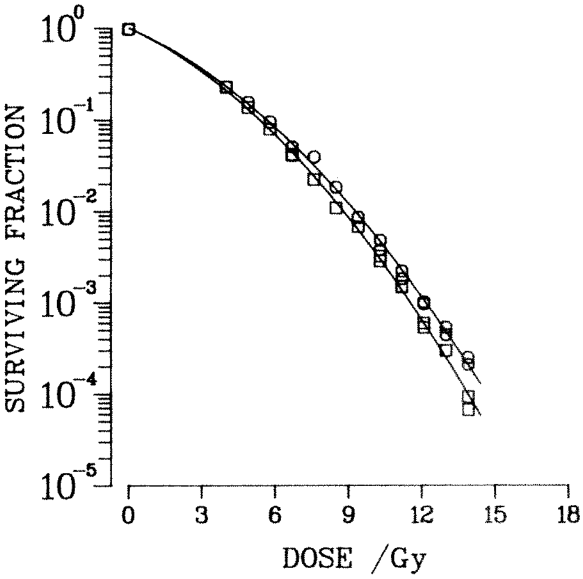

Figure 2. As Fig. 1 at depths of 2 (□) and 12 cm (○).

represent total dose (N+γ) derived according to the European protocol (Broerse et al, 1981). The chambers were placed in the phantom close to the position of the cells. The flasks and pots containing the cells covered a considerable area. The relationship between the dose at the position of the chamber and the mean dose received by the cells varied with depth and filtration, raising the question as to whether a dosimetric correction is needed. This subject is discussed in the Results section.

Data analysis

At each dose, either four replicate flasks were irradiated (Hall and Astor) or cells were irradiated in one pot and diluted onto four replicate Petri dishes (Cullen). Control experiments were typically performed twice for each radiation type, each experiment consisting of eight replicates. Estimates of the variance of the mean surviving fraction were calculated either directly from the replicate results or by applying Poisson statistics to the pooled data. The larger of these two values was used in the analysis.

In the analysis we used a linear-quadratic dose–effect relationship of the form:

$$S(D) = \exp[-\gamma - \alpha(rD) - \beta(rD)^2] \qquad (1)$$

where $S(D)$ is the expected fraction of cells surviving a dose D, and α, β and γ are adjustable parameters. The parameter γ accounts for the fact that control results ($D=0$) were treated here as regular data points. Because of the small variation in cellular response to the three different neutron fields, we found it justifiable (and also convenient) to analyse the neutron data collectively with a common set of parameters (α, β) and assess changes in the beams only through a dose-modifying factor r [see Equation (1)]. It can be shown on statistical grounds that the present data cannot be used to reject this approach against the usual procedure of using independent parameters (α, β) for each field. If we assign, arbitrarily, the value $r=1$ to the data for the surface (2 cm), unfiltered neutrons, r for the other two beams represents the RBE of these neutrons relative to the former condition.

Results

Equation (1) was fitted to the data in the maximum likelihood sense (as γ is related to the plating efficiency it is different for each experiment). The solid curves in Figs 1 and 2 show the results of this procedure applied to the measurements of Cullen. Hall's and Astor's results were similar. Data points shown in these figures

Table I. Survival curve parameters

Condition	α(Gy^{-1})	β(Gy^{-2})	RBE
Cullen			
depth 2 cm	0.43±0.03	0.018±0.002	1
2 cm, filtered	0.43±0.03	0.018±0.002	0.97±0.02
2 cm	0.28±0.03	0.027±0.002	1
12 cm	0.28±0.03	0.027±0.002	0.95±0.015
X rays	0.076±0.030	0.019±0.002	
Hall and Astor			
depth 2 cm	0.21±0.03	0.053±0.004	1
depth 12 cm	0.21±0.03	0.053±0.004	0.98±0.04
2 cm, filtered	0.21±0.03	0.053±0.004	0.97±0.02

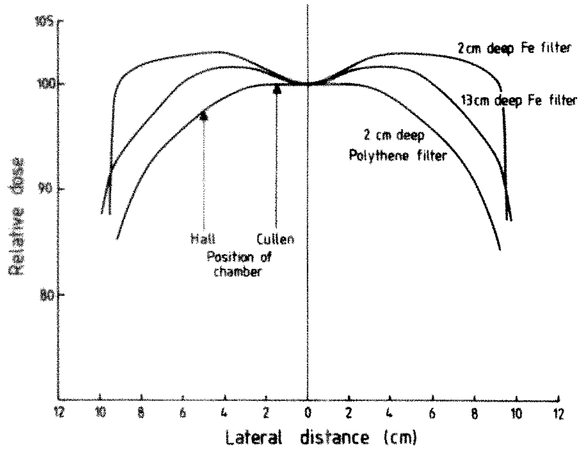

Figure 3. Profiles of the Clatterbridge neutron beam at depths of 2 and 13 cm in water with the normal iron flattening filter and at a depth of 2 cm with a 4.5 cm thick polythene filter instead of the flattening filter. The profiles were measured along the principal axes of a 20 cm × 20 cm field.

are normalized to $\exp(-\gamma)$, *i.e.* to our estimate of the plating efficiency in each experiment. Table I contains the parameters thus obtained (errors correspond to one standard deviation).

In Hall's and Astor's experiments the cells were spread over an area 11 cm × 16.5 cm and the chamber was 5 cm from the beam axis. In Cullen's experiments the cells were included in an area 8 cm × 6.5 cm and the chamber was 1.5 cm from the axis. Figure 3 shows profiles of the neutron beam at Clatterbridge measured at depths of 2 and 13 cm in water with the normal iron flattening filter and at a depth of 2 cm with the polythene filter. Profiles along the diagonals were also measured but are not shown. A depth of 13 cm was chosen as Awschalom et al (1983) have shown that 12 cm of Perspex is nearly equivalent to 13 cm of water. Isodose distributions in the plane of the cells were constructed from this information in order to calculate the ratio of the mean cell dose to the dose at the chamber.

The results of these calculations are given in Table II. In Table III the RBE values given in Table I have been corrected for the ratios of mean cell dose to chamber dose given in Table II. No additions to the uncertainties have been made as the dosimetric measurements were more precise than the biological ones.

Table II. Ratio of mean cell dose to chamber dose at Clatterbridge

Condition		Hall & Astor	Cullen
Iron flattening filter	depth 2 cm	0.996	1.006
	depth 13 cm	0.982	0.999
4.5 cm polythene filter	depth 2 cm	0.977	0.989

Discussion

The changes in RBE given in Table III are small (1–4%) and similar to the uncertainties of the observations. On the other hand, all four results are in the expected direction, suggesting that there may be slight hardening of the beam at depth and with addition of a polythene filter.

The principal conclusion to be drawn is that these changes in RBE are much smaller than those seen by Hornsey et al (1988). These authors used the crypt cell survival assay and found changes in RBE of 11%. It is not clear why the two systems have given such different results. In the work of Hornsey et al the variation in dose received by the mice was smaller than in the experiments reported here and no correction was needed for non-uniformity of dose. Hall et al (1979) have reported the use of a number of biological systems to measure differences in RBE between neutron generators. Survival of V79 cells seemed just as sensitive to changes in neutron energy as was the crypt cell assay. The present results show the importance of using several biological systems.

The dosimetric correction, involving the ratio of mean cell dose to chamber dose, would be the correct procedure if cell survival was linearly related to dose. In fact, however, it is log survival which is nearly proportional to dose. A more accurate method would be to calculate isosurvival distributions in the plane of the cells rather than isodose distributions. As the survival curves are continuously bending this would have to be done at each survival level.

To see if this approach would produce a noticeably different result, an isosurvival distribution was calculated for the condition where the isodose distribution shows the greatest variation, namely with the polythene filter at a depth of 2 cm. The isosurvival distribution was calculated over the area occupied by the cells of Hall and Astor, at a dose of 7 Gy corresponding to a survival of about 10^{-2}. The mean survival relative to survival at the position of the chamber was found to be 1.142. The mean effective dose received by the cells relative to the dose at the chamber would be 0.979. The ratio of physical doses was 0.977 (Table II). This method therefore gives a correction only 0.2% different from that obtained directly from the isodose distribution. A similar calculation for Cullen's cells gave an even smaller correction. In these circumstances the direct calculation was considered adequate.

A change in depth or filtration alters the intensity profile across the neutron beam. The importance of this effect depends on the area covered by the cells or other

Table III. Biological effectiveness relative to a depth of 2 cm, normal iron flattening filter, corrected for dose distributions

	Hall & Astor	Cullen
Depth 12 cm	0.99 ± 0.04	0.96 ± 0.02
Polythene filter	0.99 ± 0.02	0.99 ± 0.02

test material and on the location of the dose-measuring device. In the particular cases discussed here the effects were small, ±2% (Table II), but the corrections were valuable in showing that the small changes in RBE presented in Table I are partly due to a dosimetric artefact.

Biological studies of this kind are slow and labour intensive. To assess changes in radiation quality on a finer scale, for example as a function of field size and thickness of filter, it is more practical to rely on microdosimetry or neutron spectroscopy, reserving biological observations to validate these faster physical measurements.

Acknowledgment

The participation of M. Astor, E. J. Hall and M. Zaider in this project is based on grant CA18506 awarded to the Radiological Research Laboratory of Columbia University.

References

AWSCHALOM, M., ROSENBERG, I. & TEN HAKEN, R. K., 1983. Scaling neutron absorbed dose distributions from one medium to another. *Medical Physics, 10*, 436–443.

BONNETT, D. E., BLAKE, S. W., SHAW, J. E. & BEWLEY, D. K., 1988. The Clatterbridge high-energy neutron therapy facility: specification and performance. *British Journal of Radiology, 61*, 38–46.

BROERSE, J. J., MIJNHEER, B. J. & WILLIAMS, J. R., 1981. European protocol for neutron dosimetry for external beam therapy. *British Journal of Radiology, 54*, 882–898.

HALL, E. J., 1977. Radiobiological intercomparison *in vivo* and *in vitro*. *International Journal of Radiation Oncology, Biology, Physics, 3*, 195–201.

HALL, E. J., WITHERS, H. R., GERACI, J. P., MEYN, R. E., RASEY, J., TODD, P. & SHELINE, G. E., 1979. Radiobiological intercomparisons of fast neutron beams used for therapy in Japan and the United States. *International Journal of Radiation Oncology, Biology, Physics, 5*, 227–233.

HALL, E. J., ZAIDER, M., BIRD, R. & ASTOR, M., 1982. Radiobiological studies with therapeutic neutron beams generated by $p^+ \rightarrow Be$ or $d^+ \rightarrow Be$. *British Journal of Radiology, 55*, 640–644.

HALL, E. J., ZAIDER, M., BIRD, R. & ROBERTS, W., 1983. Radiobiological studies with therapeutic neutron beams generated by $p^+ \rightarrow Be$ or $d^+ \rightarrow Be$. *British Journal of Radiology, 56*, 349–350.

HORNSEY, S., MYERS, R., PARNELL, C. J., BONNETT, D. E., BLAKE, S. W. & BEWLEY, D. K., 1988. Changes in relative biological effectiveness with depth of the Clatterbridge neutron therapy beam. *British Journal of Radiology, 61*, 1058–1062.

1989, *The British Journal of Radiology*, 62, 348–354

Structure–function analysis of angiotensin-converting enzyme inhibitors as modifiers of radiation-induced pulmonary endothelial dysfunction in rats

By *W. F. Ward, PhD, †A. Molteni, MD, PhD, *‡Y. T. Kim, MD and †C. Ts'ao, PhD

Departments of *Radiology and †Pathology, Northwestern University Medical School, Chicago, Illinois 60611, and ‡Resurrection Hospital, Chicago, Illinois 60631, USA

(*Received August 1988 and in revised form November 1988*)

Abstract. We have previously demonstrated that thiol-containing collagen antagonists (penicillamine) and angiotensin-converting enzyme (ACE) inhibitors (Captopril and CL242817) ameliorate endothelial dysfunction in irradiated rat lung. The purpose of the present study was to determine whether the non-thiol ACE inhibitor CGS13945 also modifies radiation-induced pulmonary endothelial dysfunction in rats sacrificed 2 months after a single dose (0–30 Gy) of ^{60}Co γ rays to the right hemithorax. The CGS13945 was administered in the feed continuously after irradiation at a regimen of 30 mg (kg body weight)$^{-1}$ day^{-1}. Four markers of lung endothelial function were monitored: ACE activity, plasminogen activator (PLA) activity, and prostacyclin (PGI_2) and thromboxane (TXA_2) production. Right lung ACE and PLA activities decreased with increasing radiation dose, and CGS13945 significantly ameliorated both responses. Dose-reduction factors (DRF) for the inhibitor were 1.80 for ACE activity and 1.41 for PLA activity ($p < 0.05$). In contrast, lung PGI_2 and TXA_2 production increased with increasing radiation dose, and CGS13945 did not influence either response significantly. Thus the ACE inhibitor CGS13945 modifies radiation-induced pulmonary endothelial dysfunction in rats, indicating that the presence of a thiol group is not essential for therapeutic efficacy in this class of compounds. On the other hand, CGS13945 exhibits a differential sparing of radiation-induced pulmonary endothelial dysfunction, as does penicillamine. A structure–function analysis of the present and previous data indicates that all of the ACE inhibitors tested (Captopril, CL242817 and CGS13945) spare the radiation-induced suppression in lung ACE and PLA activity; all of the thiol compounds tested (penicillamine, Captopril and CL242817) spare the radiation-induced elevation in lung PGI_2 and TXA_2 production; and the thiol ACE inhibitors (Captopril and CL242817) spare all four endothelial responses. These data confirm a novel and potentially important application for ACE inhibitors as modifiers of radiation-induced lung injury, and suggest that there are at least two components to their mechanism of therapeutic action in this model.

Lung tolerance imposes dose and volume limitations on thoracic radiotherapy treatment plans, since the pulmonary reactions induced by ionizing radiation are refractive to management. Therefore new approaches allowing intervention in the pathogenesis of radiation lung damage might be of clinical interest, provided these do not spare tumour response equivalently. One way to circumvent untoward modification of tumour response would be to manipulate pulmonary radiation reactions pharmacologically after completion of the irradiation. This therapeutic strategy would influence the pathophysiology rather than cell kill in the radiation treatment volume, and might complement modifiers of cellular lethality such as WR-2721 or hypoxic cell radiosensitizers.

Inhibitors of angiotensin-converting enzyme (ACE) are interesting candidates in this regard. They were initially developed as antihypertensive agents (Gavras & Gavras, 1987), and were then found to be effective in the treatment of congestive heart failure (Franciosa, 1987). The prototype ACE inhibitor Captopril also has been reported to improve kidney function in patients with diabetic nephropathy (Hommel et al, 1986), to improve cardiopulmonary status in patients with pulmonary hypertension (Stumpe et al, 1986), and to alleviate rheumatoid arthritis (Martin et al, 1984). In experimental studies, ACE inhibitors suppress granulomatous reactions in mice (Weinstock et al, 1981; Schrier et al, 1982), reduce histamine- and serotonin-induced vascular permeability in rat skin (Fantone et al, 1982), and ameliorate pulmonary hypertension induced by either chronic hypoxia (Zakheim et al, 1975; Rabinovitch et al, 1980) or the pyrrolizidine alkaloid monocrotaline (Molteni et al, 1985, 1986, 1987, 1988) in rats.

We have reported recently that the ACE inhibitors Captopril and CL242817 ameliorate radiation-induced pulmonary endothelial dysfunction in rats (Ward & Hinz, 1987; Ward et al, 1988; Ward et al, 1989). Captopril also appears to delay the onset of radiation-induced pulmonary arterial perfusion defects in rats (Graham et al, 1988). It should be noted that the collagen antagonist D-penicillamine similarly spares endothelial dysfunction and hypoperfusion in irradiated rat lung (Ward, 1981; Ward et al, 1987). The mechanism of therapeutic action of ACE inhibitors in irradiated lung is not clear at present, but these data suggest a novel and potentially important application for this class of

---

Address for correspondence: William F. Ward, PhD, Department of Radiology, Northwestern University Medical School, 303 East Chicago Avenue, Chicago, Illinois 60611, USA.

compounds as modifiers of radiation-induced tissue injury. The therapeutic efficacy of Captopril is not restricted to lung reactions, since Robbins and Hopewell (1986) have demonstrated that the drug improves the glomerular filtration rate in irradiated pig kidney.

It is perhaps only coincidental that the first three radiation-modifying agents studied by our laboratory (penicillamine, Captopril and CL242817) are all thiol or thioacetate compounds. Thus it is possible that their common therapeutic efficacy in irradiated rat lung reflects a non-specific thiol effect, independent of their primary mechanisms of action. This hypothesis can be tested by evaluating the radiation-modifying action of a non-thiol ACE inhibitor under similar experimental conditions. The distinction between thiol and non-thiol ACE inhibitors also appears to be important in the treatment of rheumatoid arthritis, since Captopril is effective in rheumatoid patients (Martin et al, 1984), whereas Enalapril, a non-thiol ACE inhibitor, is not (Jaffe, 1984).

The compound CGS13945 (1-[4-(ethoxycarbonyl)-2,4-dimethyl-2*R*,4*R*-butyryl]-2,3-dihydro-2*S*-indole-2-carboxylic acid) is an orally active non-thiol ACE inhibitor whose antihypertensive activity is approximately equivalent to that of Captopril and CL242817 on an equimolar basis (Miller et al, 1984). It is de-esterified in serum to the biologically-active free dicarboxylic acid CGS13934, a conversion which occurs in rats and humans but apparently not in dogs (Miller et al, 1984). It was decided to use CGS13945 as a representative of non-thiol ACE inhibitors for the present study because it partially prevents cardiopulmonary damage induced by monocrotaline (Molteni et al, 1988), as do penicillamine, Captopril and CL242817 (Molteni et al, 1985, 1986). In this study we determined whether CGS13945 can ameliorate radiation-induced pulmonary endothelial dysfunction in rats, using the experimental design and end-points employed in previous evaluations of the other ACE inhibitors as radiation modifiers (Ward et al, 1988, 1989). It was tested at a concentration (30 mg kg^{-1} day^{-1}, continuously in the feed) known to provide significant protection against monocrotaline pneumotoxicity (Molteni et al, 1988).

Materials and methods

Adult male Sprague-Dawley rats (Harlan Industries) were housed at 23 ± 1°C in the Northwestern University Center for Experimental Animal Resources, a central housing facility approved by the American Association for the Accreditation of Laboratory Animal Care. This experiment was conducted in accord with PHS policy on humane care and use of live vertebrate animals in research. The animals had *ad libitum* access to powdered chow (Ralston-Purina) and drinking water containing 500 mg of oxytetracycline per litre.

Animals weighing 350–400 g were anaesthetized with sodium pentobarbital (35 mg kg^{-1}, i.p.) and exposed to a single dose of $^{60}Co\ \gamma$ rays (10–30 Gy) to a 3.5 cm^2 right hemithorax port as described previously (Ward et al, 1988). The dose-rate was approximately 2.3 Gy min^{-1} from a Phillips 6000 Rhm teletherapy unit. Control animals were anaesthetized and sham-irradiated. Half of each dose group consumed standard powdered feed continuously after irradiation, and half received feed containing 0.06% (w/w) CGS13945 (Ciba-Geigy). Daily food consumption averaged 20 g per rat in all treatment groups throughout the study, resulting in a CGS13945 regimen of approximately 30 mg kg^{-1} day^{-1}.

Two months after irradiation, all animals were killed by pentobarbital overdose (70 mg kg^{-1}, i.p.) and exsanguination from the abdominal aorta. The medial lobe of the right lung was weighed and stored at −20°C. Within 2 weeks after autopsy, the lung samples were thawed and homogenized, and ACE activity in the homogenate was determined by the method of Cushman and Cheung (1971). Protein concentration in the homogenate was determined by the biuret reaction, using bovine serum albumin as a standard. Angiotensin-converting enzyme activity was expressed as mU per right medial lobe (RML) and U(g $protein)^{-1}$ as described previously (Ward et al, 1983).

The superior lobe of the right lung was stored at −20°C until assayed for plasminogen activator (PLA) activity by the fibrin plate lysis method (Astrup & Albrechtsen, 1957) as described previously (Ts'ao et al, 1983). Data were expressed as area of the fibrin plate lysed under standard *in vitro* conditions.

The inferior lobe of the right lung was minced, weighed and incubated at 37°C in 3.0 ml of Dulbecco's phosphate buffered saline (pH = 7.4) containing glucose (1 mg ml^{-1}). After a 10-min incubation, prostaglandin production was stopped by adding 0.1 ml aliquots of the culture medium to an equal volume of 2 mM acetylsalicyclic acid. The samples were then left at room temperature for 1 h, frozen in liquid N_2 and stored at −70°C. Prostacyclin (PGI_2) and thromboxane (TXA_2) concentration in the samples was determined by radioimmunoassay of their stable metabolites, 6-keto-$PGF_{1\alpha}$ and TXB_2, respectively (New England Nuclear, Boston, MA). Data were expressed as ng of prostanoid produced per mg of lung mince during the 10-min incubation.

All data were plotted as dose–response curves and subjected to linear regression analysis. The modifying action of CGS13945 was quantified as the ratio of isoeffective doses at a common intermediate response in the drug-treated and control animals (DRF), and as the ratio of response curve slopes in the control and CGS13945-treated animals (SR). The significance of the two controlled variables (radiation dose and drug treatment) was determined by multiple analysis of variance (Zar, 1974). All values represent the mean ± SEM.

Results

Pulmonary endothelial function

Angiotensin-converting enzyme activity. Right lung ACE activity in untreated rats decreased with increasing radiation dose, from a value of 848 ± 32 mU RML^{-1} in sham-irradiated animals to 317 ± 26 mU RML^{-1} in the group exposed to 30 Gy (Fig. 1). It was found that CGS13945 had no effect on lung ACE activity in sham-irradiated animals (Table I), but significantly ($p = 0.01$) ameliorated the radiation-induced suppression in ACE activity. Calculated at a response level of 500 mU RML^{-1}, the isoeffective doses for CGS13945-treated and untreated rats, 29.8 and 16.6 Gy, respectively, indicated a DRF of 1.80 (Fig. 1, Table II). This DRF value was largely independent of radiation dose, since the response curve slope ratio (0.85) did not differ significantly from unity (Table I). Comparable CGS13945 dose modification was observed when ACE activity was expressed as U(g protein)$^{-1}$ (Table I).

Plasminogen activator activity. Right lung PLA activity also decreased with increasing radiation dose to approximately half the normal activity in untreated animals exposed to 30 Gy (Fig. 1, Table I). It was found that CGS13945 displaced the response curve to the right by a significant ($p = 0.03$), dose-independent increment of 1.41 (Fig. 1), while having no effect on PLA activity in sham-irradiated rats (Table I).

Prostacyclin and thromboxane production. Right lung PGI_2 and TXA_2 production increased with increasing radiation dose in both untreated and CGS13945-treated animals (Fig. 1). Although the slope of the former response curves was slightly greater, analysis of variance demonstrated that the effect of CGS13945 treatment was not significant for either response (Table II). The DRF values were not independent of radiation dose, but were < 1.20 for both responses over the entire dose range. Neither did CGS13945 influence the production of the two prostanoids in the lungs of sham-irradiated animals (Table I).

Side-effects. It was found that CGS13945 had no effect on pulmonary endothelial function in sham-irradiated rats (Table I). Likewise, the ACE inhibitor had no

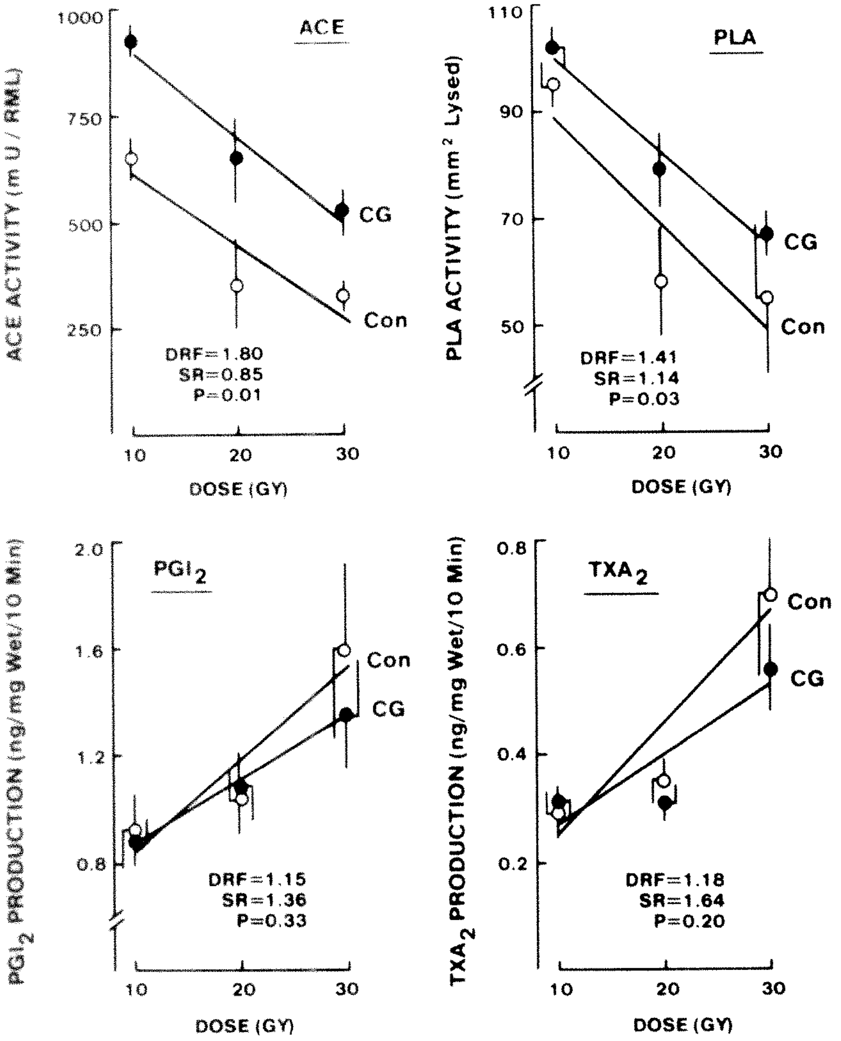

Figure 1. Plots of endothelial function in the right lung against radiation dose in untreated control rats (○) and CGS13945-treated rats (●) sacrificed 2 months after a single dose of ^{60}Co γ rays to the right hemithorax. Mean ± SEM; $n = 6$. Lines were fitted by linear regression analysis. The modifying effect of CGS13945 was calculated as the ratio of isoeffective doses in the drug-treated and untreated animals (DRF), and as the ratio of response curve slopes in the untreated and CGS13945-treated animals (SR). The p value indicates the significance of the CGS13945 effect as determined by analysis of variance. Upper left: angiotensin-converting enzyme activity. Upper right: plasminogen activator activity. Lower left: prostacyclin production. Lower right: thromboxane production.

Table I. Effect of CGS13945 on radiation-induced pulmonary endothelial dysfunction[a]

Response	Diet	Right hemithorax dose (Gy)			
		0	10	20	30
Lung protein (mg RML^{-1})	Control CGS13945	12.1 ± 0.7[b] 11.9 ± 0.6	11.8 ± 0.9 11.3 ± 0.4	15.5 ± 1.1 14.0 ± 1.2	24.3 ± 2.5 21.5 ± 2.0
ACE activity (mU RML^{-1})	Control CGS13945	848 ± 32 870 ± 40	658 ± 46 923 ± 38	350 ± 94 652 ± 111	317 ± 26 520 ± 66
ACE activity [U (g protein)$^{-1}$]	Control CGS13945	74.3 ± 8.2 76.8 ± 7.3	60.7 ± 7.5 82.6 ± 5.2	24.4 ± 6.6 52.3 ± 6.2	13.7 ± 1.3 26.4 ± 3.3
PLA activity (mm^2 lysed)	Control CGS13945	110 ± 9 106 ± 7	95 ± 4 102 ± 4	58 ± 10 79 ± 7	55 ± 6 67 ± 4
PGI_2 production [ng (mg wet)$^{-1}$ (10 min)$^{-1}$]	Control CGS13945	0.85 ± 0.10 0.83 ± 0.08	0.91 ± 0.13 0.87 ± 0.07	1.03 ± 0.11 1.09 ± 0.12	1.60 ± 0.33 1.37 ± 0.22
TXA_2 production [ng (mg wet)$^{-1}$ (10 min)$^{-1}$]	Control CGS13945	0.24 ± 0.02 0.26 ± 0.02	0.28 ± 0.04 0.31 ± 0.03	0.35 ± 0.04 0.31 ± 0.03	0.70 ± 0.16 0.56 ± 0.08

[a] Rats were sacrificed 2 months after exposure to a single dose of ^{60}Co γ rays to the right hemithorax. [b] Mean ± SEM; $n = 6$.

Table II. Linear regression parameters for radiation dose–response curves[a]

Response	Diet	*r*	Slope	ED		DRF	SR	*p*
				(Level)	Gy			
ACE activity (mU RML^{-1})	Control CGS13945	0.91 0.98	−17.05 −20.15	(500) (500)	16.6 29.8	1.80	0.85	0.01
PLA activity (mm^2 lysed)	Control CGS13945	0.90 0.98	−2.000 −1.750	(70) (70)	19.5 27.4	1.41	1.14	0.03
PGI_2 production [ng (mg wet)$^{-1}$ (10 min)$^{-1}$]	Control CGS13945	0.93 1.00	0.0340 0.0250	(1.2) (1.2)	20.6 23.6	1.15	1.36	0.33
TXA_2 production [ng (mg wet)$^{-1}$ (10 min)$^{-1}$]	Control CGS13945	0.93 0.87	0.0205 0.0125	(0.4) (0.4)	17.7 20.8	1.18	1.64	0.20

[a] Rats were sacrificed 2 months after exposure to a single dose of ^{60}Co γ rays to the right hemithorax.

significant effect on body weight gain, on heart weight, or on the weights of the cardiac right ventricle or the left ventricle plus septum (data not shown). In gross appearance and behaviour, CGS13945-treated rats were indistinguishable from the untreated control animals.

Discussion

These data demonstrate that the non-thiol ACE inhibitor CGS13945 administered continuously after hemithoracic irradiation ameliorates endothelial dysfunction in the ipsilateral lung of rats sacrificed 2 months post-irradiation. Thus the presence of a thiol group is not essential for therapeutic efficacy in this class of radiation modifiers. In its ability to spare the radiation-induced suppression in lung ACE and PLA activity, CGS13945 resembles the thiol ACE inhibitors Captopril (Ward et al, 1988) and CL242817 (Ward et al, 1989). Unlike the other ACE inhibitors, however, CGS13945 has no significant effect on the radiation-induced elevation in lung PGI_2 and TXA_2 production. Thus CGS13945 differentially modifies pulmonary endothelial radioresponsiveness, as does penicillamine (Ward et al, 1987). Like penicillamine (Ward et al, 1987), CGS13945 (30 mg kg^{-1} day^{-1}) provides therapy without evidence of side-effects for at least 2 months of continuous administration in rats. In this respect CGS13945 is superior to Captopril and CL242817, since both of the latter cause reductions in body weight gain, in heart weight, and in cardiac left ventricle plus septum weight (Ward et al, 1988, 1989).

This study completes an initial structure–function analysis of modifiers of radiation-induced pulmonary endothelial dysfunction in rats. As noted in Table III, the series now includes a compound which is a thiol but not an ACE inhibitor (penicillamine), one which is an ACE inhibitor but not a thiol (CGS13945), and two compounds which are both thiols and ACE inhibitors (Captopril and CL242817). The chemical structures of the four modifiers are shown in Fig. 2. A summary of the modifying efficacy of the four agents in irradiated rat

Table III. Modifiers of radiation-induced pulmonary endothelial dysfunction in rats[a]

Modifier	Thiol	ACE inhibitor
Penicillamine[b]	Yes	No
Captopril[c]	Yes	Yes
CL242817[d]	Yes	Yes
CGS13945	No	Yes

[a] Rats were sacrificed 2 months after exposure to a single dose of ^{60}Co γ rays to the right hemithorax. [b] Ward et al (1987). [c] Ward et al (1988). [d] Ward et al (1989).

Table IV. Modifier sparing of pulmonary endothelial radiation response[a]

Modifier	Pulmonary endothelial response			
	↓ACE	↓PLA	↑PGI$_2$	↑TXA$_2$
Penicillamine[b]	No	No	Yes	Yes
Captopril[c]	Yes	Yes	Yes	Yes
CL242817[d]	Yes	Yes	Yes	Yes
CGS13945	Yes	Yes	No	No

[a] Rats were sacrificed 2 months after exposure to a single dose of ^{60}Co γ rays to the right hemithorax. [b] Ward et al (1987). [c] Ward et al (1988). [d] Ward et al (1989).

lung reveals that all of the ACE inhibitors (Captopril, CL242817 and CGS13945) spare the radiation-induced suppression in ACE and PLA activity, all of the thiols (penicillamine, Captopril and CL242817) spare the radiation-induced increase in PGI$_2$ and TXA$_2$ production, and the thiol ACE inhibitors (Captopril and CL242817) spare all four endothelial responses (Table IV). Thus the mechanism of action of ACE inhibitors as radiation modifiers appears to be influenced partly but not entirely by the presence of a thiol group. This may represent a non-specific action shared by other thiols such as penicillamine, resulting in a reduction in the hyperproduction of prostacyclin and thromboxane by the irradiated endothelium. There is evidence in this model that the rate of eicosanoid production is substrate rather than enzyme limited (Ward & Hinz, 1987). In this case, the effect of thiol compounds may be to reduce the release of arachidonic acid from the plasma membrane of irradiated endothelial cells. This hypothesis can be tested more conveniently *in vitro*. However, ACE inhibitors exhibit additional radiation-modifying activity independent of thiol chemistry in that they spare the reduction in endothelial ACE and PLA activities. It is not clear at present whether this therapeutic effect is the result of ACE inhibition *per se*, or is the result of some action independent of angiotensin and bradykinin metabolism. It should be noted that the three ACE inhibitors are proline derivatives and share a common core structure (Fig. 2). Non-proline ACE inhibitors can be tested in this model, in order to distinguish between these alternatives.

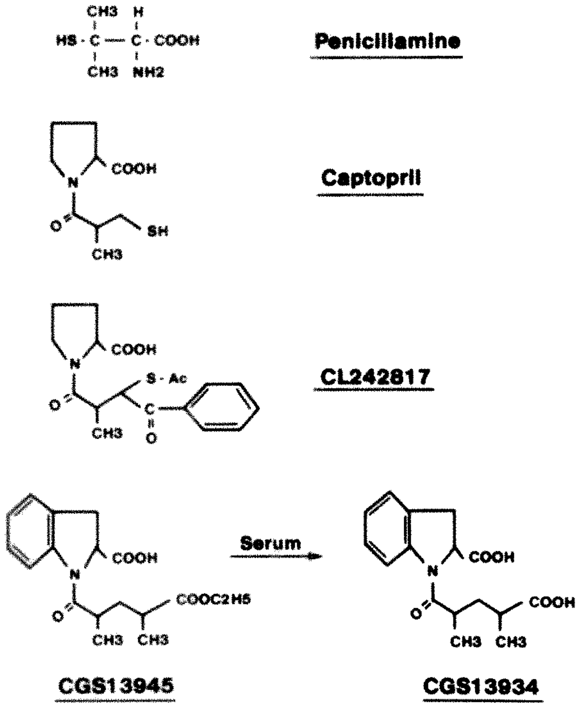

Figure 2. Chemical structures of penicillamine and the ACE inhibitors Captopril, CL242817 and CGS13945.

It is a curious but consistent observation that not all ACE inhibitors suppress lung ACE activity in rats. Of the six ACE inhibitors studied by our group, CL242817, MK421, CGS16617 and RO31-2848 significantly reduce lung ACE activity, whereas Captopril and CGS13945 do not (Molteni et al, 1987). In the present series of radiation studies, we intentionally selected those ACE inhibitors with the lowest intrinsic suppressive effect on lung ACE activity, in order to be able to evaluate their efficacy against the radiation-induced reduction in lung ACE.

At present, this comparison of modifier efficacy must be considered qualitative rather than quantitative. It was not clear *a priori* on what basis the modifier regimens should be selected for comparison. The three ACE inhibitors were evaluated on the basis of equivalent antihypertensive action, but this is not a relevant criterion for penicillamine. Thus it will be necessary to test the four modifiers at equimolar concentrations before they can be compared quantitatively. Likewise it will be necessary to test the ACE inhibitors at times other than 2 months post-irradiation, in order to determine whether their modifying action represents simply a delay in onset of endothelial dysfunction or a sustained reduction in the severity of damage. Penicillamine is the only modifier to be evaluated at longer times after irradiation, and its primary actions are to delay the onset and accelerate the recovery of radiation-induced lung damage (Ward, 1981; Port & Ward, 1982; Ward et al, 1984).

The observation that pharmacological intervention initiated after completion of radiation can attenuate the pulmonary endothelial response is not easily reconciled with the hypothesis that radiation-induced organ dysfunction is attributable largely if not solely to cell kill (Withers et al, 1980; Michalowski, 1981). The observation that CGS13945 (Fig. 1) and penicillamine (Ward et al, 1987) differentially modulate endothelial radioresponsiveness argues even more strongly against that hypothesis, at least in lung.

In conclusion, these data confirm a novel and potentially important application for ACE inhibitors as modifiers of radiation reactions in normal tissue, and suggest that there are at least two components to their mechanism of therapeutic action. The observation that Captopril ameliorates perturbations in the glomerular filtration rate in irradiated pig kidney (Robbins & Hopewell, 1986) also suggests that this therapeutic action of ACE inhibitors is neither species nor organ specific. This class of compounds is sufficiently diverse in chemical structure (De Felice & Kostis, 1987) that inhibitors with additional mechanisms of action, greater effectiveness and fewer side-effects than Captopril, CL242817 and CGS13945 may emerge.

Acknowledgments

This study was supported in part by PHS grant HL25106 from the National Heart, Lung and Blood Institute, DHHS, and by the Park Ridge Health Foundation. The excellent technical assistance provided by Joann Hinz and Ivy Weiss is gratefully acknowledged, as is the generous donation of CGS13945 by the Ciba-Geigy Corp., Summit, NJ.

References

ASTRUP, T. & ALBRECHTSEN, O. K., 1957. Estimation of the plasminogen activator and the trypsin inhibitor in animal and human tissues. *Scandinavian Journal of Clinical and Laboratory Investigation, 9*, 233–243.

CUSHMAN, D. W. & CHEUNG, H. S., 1971. Spectrophotometric assay and properties of the angiotensin converting enzyme of rabbit lung. *Biochemical Pharmacology, 20*, 1637–1648.

DEFELICE, E. A. & KOSTIS, J. B., 1987. New ACE inhibitors. In *Angiotensin Converting Enzyme Inhibitors*, ed. by J. B. Kostis & E. A. DeFelice (Liss, New York), pp. 213–261.

FANTONE, J. C., SCHRIER, D. & WEINGARTEN, B., 1982. Inhibition of vascular permeability changes in rats by Captopril. *Journal of Clinical Investigation, 69*, 1207–1211.

FRANCIOSA, J. A., 1987. The use of ACE inhibitors in congestive heart failure. In *Angiotensin Converting Enzyme Inhibitors*, ed. by J. B. Kostis & E. A. DeFelice (Liss, New York), pp. 123–148.

GAVRAS, I. & GAVRAS, H., 1987. The use of ACE inhibitors in hypertension. In *Angiotensin Converting Enzyme Inhibitors*, ed. by J. B. Kostis & E. A. DeFelice (Liss, New York), pp. 93–122.

GRAHAM, M. M., EVANS, M. L., DAHLEN, D. D., MAHLER, P. A. & RASEY, J. S., 1988. Drug suppression of late radiation injury in the rat lung. Presented at the 36th Annual Meeting of the Radiation Research Society, Philadelphia, 16–21 April, 1988.

HOMMEL, E., PARVING, H., MATHIESEN, E., EDSBERG, B., NIELSEN, M. D. & GIESE, J., 1986. Effect of Captopril on kidney function in insulin-dependent diabetic patients with nephropathy. *British Medical Journal, 293*, 479–480.

JAFFE, I., 1984. Angiotensin converting enzyme inhibitors in rheumatoid arthritis. *Arthritis and Rheumatism, 27*, 840.

MARTIN, M. F. R., MCKENNA, F., BIRD, H. A., SURRALL, K. E., DIXON, J. S. & WRIGHT, V., 1984. Captopril: a new treatment for rheumatoid arthritis? *The Lancet, i*, 1325–1328.

MICHALOWSKI, A., 1981. Effects of radiation on normal tissues; hypothetical mechanisms and limitations of *in situ* assays of clonogenicity. *Radiation and Environmental Biophysics, 19*, 157–172.

MILLER, D., WATKINS, B. E., HOPKINS, M. F., TONNESEN, S. T. & ORSDELL, D. V., 1984. Antihypertensive assessment of two new angiotensin-converting enzyme (ACE) inhibitors; CGS13945 and CGS13934. *Drug Development Research, 4*, 179–189.

MOLTENI, A., WARD, W. F., TS'AO, C., SOLLIDAY, N. H. & DUNNE, M., 1985. Monocrotaline-induced pulmonary fibrosis in rats; amelioration by Captopril and penicillamine. *Proceedings of the Society for Experimental Biology and Medicine, 180*, 112–120.

MOLTENI, A., WARD, W. F., TS'AO, C. & SOLLIDAY, N. H., 1986. Monocrotaline-induced cardiopulmonary damage in rats: amelioration by the angiotensin converting enzyme inhibitor CL242817. *Proceedings of the Society for Experimental Biology and Medicine, 182*, 483–493.

MOLTENI, A., WARD, W. F., TS'AO, C. & SOLLIDAY, N. H., 1987. Monocrotaline-induced cardiopulmonary injury in rats: modification by thiol and non-thiol ACE inhibitors. *Clinical and Experimental Hypertension, 9A*, 381–385.

MOLTENI, A., WARD, W. F., TS'AO, C. &SOLLIDAY, N. H., 1988. Monocrotaline-induced cardiopulmonary injury in rats: modification by the nonthiol ACE inhibitors CGS13945 and CGS16617. *Archives Internationales de Pharmacodynamie et de Thérapie, 291*, 21–40.

PORT, C. D. & WARD, W. F., 1982. The ultrastructure of radiation injury in rat lung: modification by D-penicillamine. *Radiation Research, 92*, 61–82.

RABINOVITCH, M., GAMBLE, W. J., WILLIAMS, G. & REID, L., 1980. SQ14225 converting enzyme inhibitor diminishes pulmonary artery hypertension secondary to chronic hypoxia in rats. *Federation Proceedings, 39*, 765.

ROBBINS, M. E. C. & HOPEWELL, J. W., 1986. Physiological factors effecting renal radiation tolerance: a guide to the treatment of late effects. *British Journal of Cancer, 53*, Supplement VII, 265–267.

SCHRIER, D. J., RIPANI, L. M., KATZENSTEIN, A. L. & MOORE, V. L., 1982. Role of angiotensin converting enzyme in bacilli Calmette Guerin-induced granulomatous inflammation. *Journal of Clinical Investigation, 69*, 651–657.

STUMPE, K. O., SCHMENGLER, K., BETTE, L., OVERLACK, A. & KOLLOCH, R., 1986. Persistent hemodynamic and clinical improvement after Captopril in patients with pulmonary hypertension. *Herz, 11*, 217–225.

TS'AO, C., WARD, W. F. & PORT, C. D., 1983. Radiation injury in rat lung. III. Plasminogen activator and fibrinolytic inhibitor activities. *Radiation Research, 96*, 301–308.

WARD, W. F., 1981. Radiation-induced pulmonary arterial perfusion defects: modification by D-penicillamine. *Radiology, 139*, 201–204.

WARD, W. F., SOLLIDAY, N. H., MOLTENI, A. & PORT, C. D., 1983. Radiation injury in rat lung. II. Angiotensin-converting enzyme activity. *Radiation Research, 96*, 294–300.

WARD, W. F., MOLTENI, A., TS'AO, C. & SOLLIDAY, N. H., 1984. Radiation injury in rat lung. IV. Modification by D-penicillamine. *Radiation Research, 98*, 397–406.

WARD, W. F. & HINZ, J. M., 1987. Prostacyclin and thromboxane production by irradiated rat lung. In *Prostaglandin and Lipid Metabolism in Radiation Injury*, ed.

by T. L. Walden Jr & H. N. Hughes (Plenum Press, New York), pp. 147–158.

Ward, W. F., Molteni, A., Ts'ao, C. & Solliday, N. H., 1987. Functional responses of the pulmonary endothelium to thoracic irradiation in rats: differential modification by D-penicillamine. *International Journal of Radiation Oncology, Biology, Physics*, *13*, 1505–1513.

Ward, W. F., Kim, Y. T., Molteni, A. & Solliday, N. H., 1988. Radiation-induced pulmonary endothelial dysfunction in rats: modification by an inhibitor of angiotensin converting enzyme. *International Journal of Radiation Oncology, Biology, Physics*, *15*, 135–140.

Ward, W. F., Molteni, A. & Ts'ao, C., 1989. Radiation-induced endothelial dysfunction and fibrosis in rat lung: modification by the angiotensin converting enzyme inhibitor CL242817. *Radiation Research*, in press.

Weinstock, J. V., Ehrinpreis, M. M., Boros, D. L., & Gee, J. G., 1981. Effect of SQ14225, an inhibitor of angiotensin-I-converting enzyme, on the granulomatous response to *Schistosoma mansoni* eggs in mice. *Journal of Clinical Investigation*, *67*, 931–936.

Withers, H. R., Peters, L. J. & Kogelnick, H. D., 1980. The pathobiology of late effects of irradiation. In *Radiation Biology in Cancer Research*, ed. by R. E. Meyn & H. R. Withers (Raven Press, New York), pp. 439–448.

Zakheim, R. M., Mattioli, L., Molteni, A., Mullis, K. B. & Bartley, J., 1975. Prevention of pulmonary vascular changes of chronic alveolar hypoxia by inhibition of angiotensin-I-converting enzyme in the rat. *Laboratory Investigation*, *33*, 57–61.

Zar, J. R., 1974. *Biostatistical Analysis* (Prentice-Hall, Englewood Cliffs, New Jersey), pp. 121–181.

1989, *The British Journal of Radiology*, *62*, 355–361

Treatment of persistent and recurrent nasopharyngeal carcinoma by brachytherapy*

By †J. S. T. Sham, MB, BS, DMRT, FRCR, ‡W. I. Wei, MB, BS, DLO, FRCS(Edin), D. Choy, MB, BS, DMRT, FRCR, ‡C. M. Ho, MB, BS, FRCS(Edin), P. T. H. Tai, MB, BS and P. H. K. Choi, MB, BS, DMRT, FRCR

Department of Radiotherapy and Oncology and ‡Department of Surgery, University of Hong Kong, Queen Mary Hospital, Pokfulam, Hong Kong

(*Received August 1988 and in revised form November 1988*)

Abstract. The early results of brachytherapy for persistent and recurrent nasopharyngeal carcinoma in 30 patients is presented. Fifteen patients were treated by intracavitary caesium, 12 patients were treated by interstitial gold grain implant using the split-palate approach and three patients were treated by both intracavitary caesium and interstitial gold grain implant for the first and second relapse in the nasopharynx, respectively. The overall tumour control rate for intracavitary caesium was 5/18 (28%) with median follow-up of 25.2 months, and for interstitial gold grain implant it was 9/14 (64%) with median follow-up of 16.5 months. Interstitial gold grain implantation appears to be effective in the treatment of persistent and recurrent nasopharyngeal carcinoma.

Nasopharyngeal carcinoma is a radiosensitive tumour, yet recurrence in the nasopharynx after radical radiotherapy is a common cause of treatment failure (Mesic et al, 1981). It has also been shown that high-dose re-irradiation of recurrent nasopharyngeal carcinoma can result in 50% survival, and a radiation dose less than 60 Gy is inadequate (Wang, 1987). The neuro-endocrine and soft-tissue damage after a single course of radical external radiotherapy for nasopharyngeal carcinoma is not insignificant (Lam et al, 1987; Lee et al, 1988), and the side-effects of a second course of radical external radiotherapy for recurrent disease will be more pronounced.

Brachytherapy has the advantage of giving a high radiation dose to the tumour with a much lower dose to the adjacent normal tissue (Hilaris, 1968). Brachytherapy has been used with various degrees of success in the treatment of other head and neck cancers (Goffinet et al, 1985) and tumours of the base of the skull (Bernstein & Gutin, 1985). The earlier experience of brachytherapy of nasopharyngeal carcinoma was mainly limited to intracavitary therapy (van Herik & Erich, 1955; Suit et al, 1960; Rudd et al, 1966; Deitsch et al, 1973; Wang et al, 1975). More recently, interstitial implants were employed in the management of recurrent nasopharyngeal carcinoma to circumvent the problems encountered by intracavitary brachytherapy, such as the relatively slow fall-off of dose and irregular contour of the nasopharynx (Vikram & Hilaris, 1984; Harrison & Weissberg, 1987).

In our centre we have used brachytherapy to re-irradiate recurrent nasopharyngeal carcinoma. We have extended the use of brachytherapy to boost the dose to tumours that persist after completion of the first course of radical external radiotherapy. Here we report our experience on the use of intracavitary caesium intubation and of interstitial gold grain implant with the split-palate approach.

Patients and methods

From August 1985 to July 1987, 346 patients with nasopharyngeal carcinoma were treated by radiotherapy at the Department of Radiotherapy and Oncology, Queen Mary Hospital. Two hundred and ninety-three of them were new cases treated with primary radical external radiotherapy. Twelve patients were treated for persistent disease by brachytherapy. Forty-one patients were treated for recurrent disease, 18 of these 41 patients being treated entirely or partly with brachytherapy. The 30 patients who had been treated with brachytherapy in the course of their illness formed the basis of this review. Between August 1985 and October 1986, caesium intubation was the type of brachytherapy employed. In August 1986 the first gold grain implantation was performed and from November 1986 all patients requiring brachytherapy were treated by this method.

All patients were initially treated by a course of radical external radiotherapy as described by Ho (1982). They were monitored after radiotherapy every 2 weeks to monthly with indirect nasopharyngeal mirror examination for 3 months, then the interval between examinations was lengthened to monthly for the first year, and to every 2 to 3 months starting from the second year. Fibreoptic endoscopy was arranged when mirror examination was considered inadequate. Tumours identified within 4 months after the first course of radical external radiotherapy were considered persistent tumours. Recurrent tumours were those detected after 4 months. The presence of tumour was confirmed by biopsy in all cases. Computed tomography (CT) was used to determine the extent of disease in selected cases. Those patients with tumour limited to the nasopharynx were candidates for brachytherapy. A similar policy of follow-up examination was adopted after the booster radiation or re-irradiation to monitor the subsequent course of disease.

---

* The findings of this study were partly presented at the EORTC meeting, Hong Kong, September 14–16, 1987.

† Author for correspondence.

Caesium intubation

This was done under local anaesthesia on an out-patient basis. The nasal fossae and nasopharynx were anaesthetized by topical Cetacaine spray. A 2 cm long caesium tube was sealed at the tip of a latex tubing (Fig. 1). The tubing was inserted through the nasal cavity and its position checked by fluoroscopy. The tip of the latex tubing was kept in position by cotton swab-sticks soaked with ligocaine inserted through the same nasal fossa. The aim was to keep the source as close to the roof of the nasopharynx as possible (Fig. 2a). The outer end of the latex tube was fastened by tape to the patient's face.

For single-source intubation, the dose was prescribed at the points located on the plane through the centre of the source and perpendicular to it, and the points were at 1 cm from the centre of the source. For double-source (bilateral) intubation, the dose was prescribed at the two points located on the plane, through their centres and perpendicular to the long axis of the sources; the points were 1 cm from the midpoint of the line joining the centres of the sources. Ten gray were given to these points in each session, which lasted 4 to 5 h. The treatment was given weekly, giving a total dose of 20 or 30 Gy in 2 or 3 weeks.

Caesium intubation was used alone to give a booster dose to persistent tumours, and was used in combination with a course of external radiotherapy for recurrent tumours.

Gold grain implant

This was done under general anaesthesia. The soft palate was split in the midline up to the hard palate and the periosteum was elevated to expose as much of the nasopharynx as possible. Gold grains were inserted under direct vision using the gold grain gun. The accurate placement of the gold grains was achieved with the help of templates (Fig. 3). These templates have flexible handles and have different patterns for tumours of different size and shape. The rings at the end of the claws mark out the ideal position of the gold grains.

After the gold grains were inserted, a small piece of thin lead shield was inserted into the nasopharynx for radiation protection during the suturing of the palate (Fig. 3) and a piece of horseshoe-shaped lead screen was moved into the space separating the surgeon and radiotherapist from the patient. A piece of lead glass was also incorporated into the lead screen to minimize the dose to the surgeon's eyes. The palate wound was closed in one layer for the initial few cases. Subsequently, the palate wound was closed in three layers, which usually takes 45 min. Sixty gray were prescribed at the plane 0.5 cm from the plane of implant. The patients were usually discharged on the 4th day.

Gold grain implant was often used alone in the treatment of both persistent and recurrent tumours.

Results

Thirty patients, 18 male and 12 female, were treated by one or both of these brachytherapy techniques. Their age ranged from 29 to 64 years (median 43 years). The initial stage and treatment, and interval to documentation of persistent or recurrent tumours are shown in Tables I and II, respectively. Additional treatment for persistent tumour, second therapy for recurrent tumour and local tumour control are listed in Tables III and IV. The third therapy and the end result for three patients (Cases 28 to 30) treated by both techniques of brachytherapy are shown in Table V.

Treatment for persistent tumours

Seven patients were treated by caesium intubation. Information on local tumour control was incomplete because one patient was lost to follow-up. In four patients (57%) the nasopharyngeal tumour remained under control with a median follow-up of 25.2 months. Two patients relapsed in the nasopharynx at 1 and 3.9 months after caesium intubation.

Five patients were treated by gold grain implantation, which was successful in four patients. Implantation was unsuccessful in one patient, the gold grains failing to stay in position and supplementary external radiotherapy was given instead. It was noted during implantation that the tumour was too friable to hold the gold grains. Information on local tumour control was incomplete in one patient lost to follow-up. In three patients the tumour in the nasopharynx remains under control with a median follow-up of 16.5 months. No patient relapsed in the nasopharynx.

Treatment of recurrent tumours

Eleven patients were treated by caesium intubation. Information on local tumour control was incomplete due

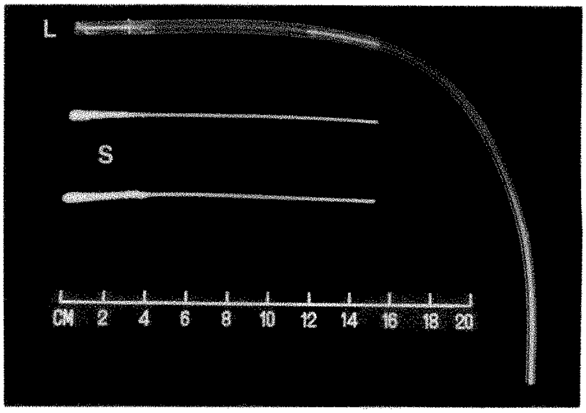

Figure 1. The latex tube (L) holding the caesium source at its tip and the swab-sticks (S) used to keep the source in position during treatment.

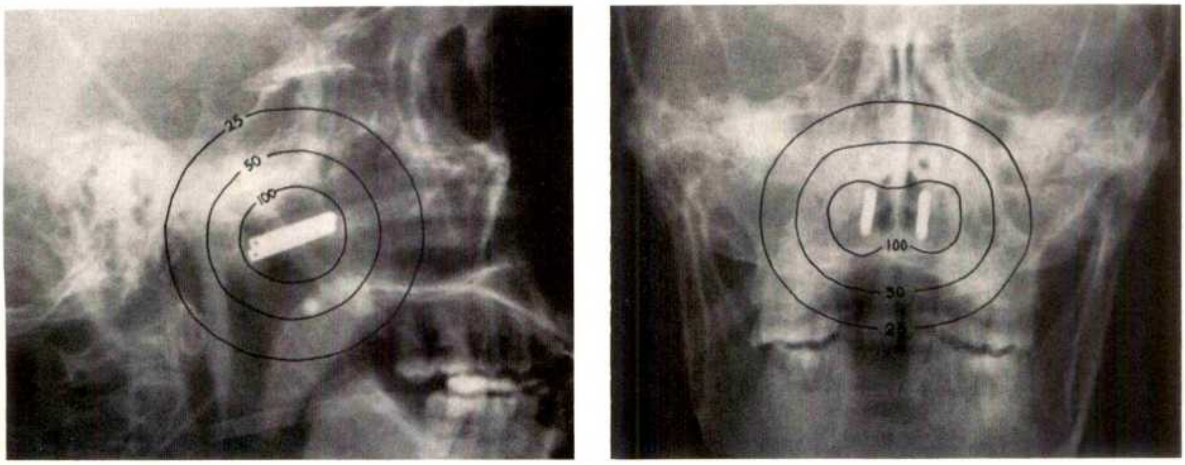

(a)

(b)

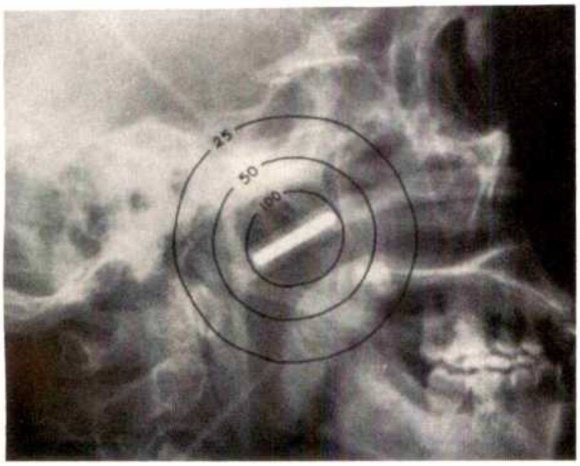

(c)

Figure 2. (a) Lateral and (b) antero-posterior skull radiographs, showing a pair of caesium tubes inserted. The sources were close to the roof of the nasopharynx, but they were kept from the posterior wall by the tips of the latex tubings. When the caesium tubes were pushed further in (c), instead of positioning themselves at the junction between the roof and the posterior wall, the elasticity of the latex tubings displaced the tubes away from the roof of the nasopharynx. The dose was prescribed at 100%.

to loss from follow-up or death from distant metastases in two patients. In one patient (9%) the tumour in the nasopharynx remained under control at 23.4 months. Eight patients relapsed in the nasopharynx at 1.5 to 19.8 months after caesium intubation (median 9 months).

Ten patients were treated by gold grain implantation. Information on local tumour control was incomplete in two patients who died from distant metastases. Two patients relapsed in the nasopharynx. In six patients (60%) the tumour in the nasopharynx remained under control with a median follow-up of 16.3 months (range 13.5–25.7 months).

Pattern of local failure

The recurrent tumours were limited to the lateral pharyngeal recess in three of the 10 patients who relapsed after caesium intubation. In the other seven patients the disease was extensive, involving the nasopharynx, sphenoid, ethmoids, and antra at the time of diagnosis. Both patients in whom gold grain implantation was unsuccessful relapsed with extensive disease in the sphenoid, ethmoid and antrum but with no evidence of disease in the nasopharynx.

Our horseshoe-shaped lead screen and the thin lead shield placed inside the nasopharynx ensures the maximal dose to the trunk of the surgeon is less than 0.015 cGy per implant of eight gold grains.

Complications

The most common complication of gold grain implantation was delay in wound healing and fistula formation at the junction between the soft and hard palate. Delayed healing occurred in the early cases when the palate wound was sutured in one layer. The problem of fistula formation improved when the palate wound was closed in three layers. Four of the five patients who

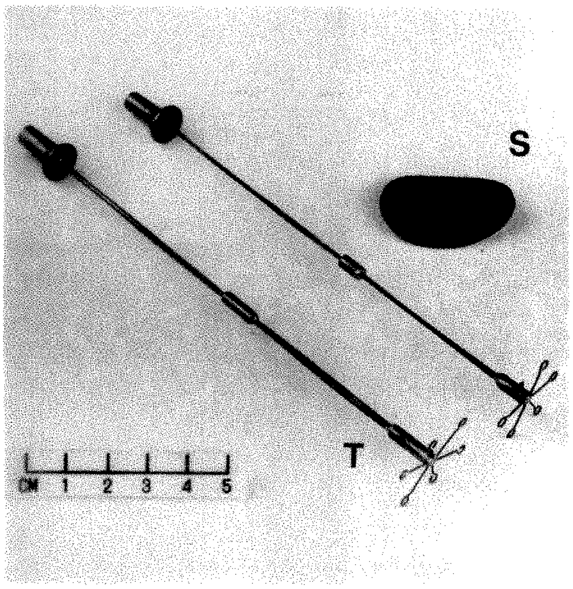

Figure 3. The templates (T) used to guide the accurate placement of gold grains and the thin lead shield (S), which is placed behind the soft palate while the palate wound is being closed.

developed fistula healed spontaneously. A small fistula of 1 mm diameter persisted in one patient, but it caused no functional impairment.

Gold grains falling out, resulting in technical failure of the treatment, was another complication. This occurred in one patient in this series. One female patient in the caesium intubation group developed amenorrhoea and secondary hypothyroidism 26 months after the initial course of radical external radiotherapy. In both groups of patients, radiation necrosis and infection of the nasopharyngeal mucosa occurred. These were managed successfully with antibiotics.

Table I. Initial stage and radiotherapy of patients treated for persistent nasopharyngeal tumour

Case	T stage	Initial radical radiotherapy	Interval to additional treatment (months)
1	1	A[a]	0.1
2	1	A	0.2
3	1	A	0.2
4	1	B[b]	0.5
5	1	A	0.5
6	1	B	0.7
7	2	B	0.9
8	3	B	1.0
9	1	A	1.5
10	1	A	2.0
11	1	A	2.0
12	2	B	3.2

[a] Technique A: split-field technique with two lateral opposing facial fields and one anterior facial field; a central tumour dose of 3.5 Gy was given three times per week to 59.5 Gy.

[b] Technique B: lateral opposing facio-cervical fields for the first part of treatment; a midplane tumour dose of 2.5 Gy was given four times per week to 40 Gy. This was changed to split-field technique with two lateral opposing facial fields and one anterior facial field; a central tumour dose of 3.5 Gy was given three times per week to another 21 Gy.

Table II. Initial radiotherapy and interval to relapse for patients treated for recurrent nasopharyngeal tumour

Case	T stage	First radical radiotherapy	Interval to local relapse (months)
13	2	A	4.1
14	3	B	6.9
15	2	B	9.4
16	2	B	12.6
17	1	B	13.5
18	1	B	14.4
19	1	B	14.7
20	1	A	16.3
21	1	B	18.3
22	1	B	24.6
23	2	B plus ERT boost 30 Gy/12 fractions/ 3 weeks	27.2
24	1	A	36.5
25	1	A	42.1
26	1	A	45.4
27	1	40 Gy/16 fractions/ 4 weeks plus 15.2 Gy/4 fractions/ 1.5 weeks	91.7
28	3	A	10.6
29	1	B	7.6
30	1	B	11.7

ERT = external radiotherapy.

Discussion

The value of high-dose re-irradiation of recurrent nasopharyngeal carcinoma has been proven and it has been shown that a dose less than 60 Gy was inadequate (Wang, 1987). As the dose that can safely be given to the nasopharynx is limited by the normal-tissue tolerance, brachytherapy, in theory, is a useful method of radiotherapy in such a situation. It has the advantage of delivering a high dose to a small localized area, with rapid fall-off of dose beyond the target volume. However, brachytherapy of nasopharyngeal carcinoma has not gained wide acceptance as the nasopharynx does not lend itself to brachytherapy easily. Irregular contours make accurate mould and intracavitary treatment difficult. Inaccessibility of the nasopharynx is a great hindrance to mould and interstitial therapy. While rapid dose fall-off is an asset for brachytherapy, it also results in marginal failure when case selection is done without the use of more sophisticated techniques like CT and fibreoptic endoscopy. The pattern of relapse after brachytherapy, with extensive disease in the adjacent

Table III. Additional treatment and end result for patients treated for persistent nasopharyngeal tumour

Case	Additional treatment	Length of local control (months)	Local tumour control
1	Cs double-source 30 Gy	34.1	+
2	Cs double-source 20 Gy	28.2	+
3	ERT 10 Gy/4 fractions/1 week Cs double-source 20 Gy	18.4	+
4	Cs double-source 20 Gy	25.2	+
5	GG (7)	16.7	+
6	Cs double-source 30 Gy	23.0	+
7	GG (4)	9.4	+
8	Cs single-source 30 Gy	1.0	–
9	Cs single-source 30 Gy	3.9	–
10	GG (6)	11.3	+
11	GG (4)	16.5	+
12	GG (10), technical failure	5.7	–

Cs = caesium intubation; GG = gold grain implant (number of gold grains implanted); ERT = external radiotherapy.

regions and little or no tumour in the nasopharynx, attests to this.

Interstitial implantation can overcome the problems of irregular contours. Hilaris et al (1968) advocated the use of palatal fenestration for interstitial implantation, but it has not been widely accepted because the patients must wear a palatal obturator for the rest of their life. More recently, a transnasal approach has been advocated for interstitial implantation of nasopharyngeal carcinoma (Vikram & Hilaris, 1984; Harrison & Weissberg, 1987).

Table IV. Second therapy and end result for patients treated for recurrent nasopharyngeal tumour

Case	Second therapy	Length of local control (months)	Local tumour control
13	GG (11)	15.6	+
14	GG (6)	10.0	–
15	GG (6)	17.0	+
16	ERT 50 Gy/20 fractions/5 weeks Cs single-source 30 Gy	3.7	–
17	ERT 40 Gy/16 fractions/4 weeks Cs double-source 20 Gy	2.3	+
18	GG (7)	14.7	+
19	ERT 50 Gy/20 fractions/5 weeks Cs double-source 30 Gy	10.8	–
20	ERT 40 Gy/16 fractions/4 weeks Cs double-source 30 Gy	19.8	–
21	ERT 66 Gy/33 fractions/6.5 weeks Cs single-source 20 Gy	20.5	+
22	ERT 55 Gy/22 fractions/5.5 weeks Cs single-source 20 Gy	10.9	–
23	Cs double-source 20 Gy	7.1	–
24	GG (3)	11.3	+
25	GG (6)	25.7	+
26	ERT 40 Gy/16 fractions/4 weeks Cs double-source 30 Gy	23.4	+
27	ERT 40 Gy/16 fractions/4 weeks GG (7)	13.5	+
28	ERT 50 Gy/25 fractions/5 weeks Cs double-source 20 Gy	1.5	–
29	ERT 50 Gy/25 fractions/5 weeks Cs double-source 30 Gy	3.9	–
30	ERT 50 Gy/25 fractions/5 weeks Cs double-source 30 Gy	13.6	–

See Table III for abbreviations.

Table V. Third therapy and end result for patients relapsed after second course of external radiotherapy and caesium intubation

Case[a]	Third therapy	Length of local control (months)	Local tumour control
28	GG (13)	8.7	–
29	GG (8)	23.0	+
30	GG (12)	13.2	+

GG = gold grain implant (number of gold grains implanted).
[a]Same case number as that in Tables II and IV.

The area of the nasopharynx accessible to the tip of an applicator introduced transnasally is limited by the anatomy of the nasal fossae. It may be difficult to implant the lateral pharyngeal recesses, which are common sites of disease.

The split-palate approach that we have adopted provides a good view of the nasopharynx, including the lateral pharyngeal recesses, and allows manoeuvring of the tip of the applicator under direct vision. With the help of the templates, the distribution of sources can match the optimal plan designed before operation. A blind spot of this technique is the posterior part of the nasal septum. Fortunately, tumours located in this spot are infrequent. Although this technique involves surgical splitting of the palate, long-term functional disability has not been encountered. It is encouraging that prolonged control could be achieved with gold grain implant in patients who relapsed again after the second course of external radiotherapy plus caesium intubation.

Additional advantages of interstitial implantation include the continuous low-dose-rate irradiation provided by gold grain implantation and its very rapid fall-off of dose (Fig. 4) compared with intracavitary therapy. The dose and the biological effect on the brain and pituitary–hypothalamic axis is minimized; this is an important parameter to consider in radical re-irradiation of nasopharyngeal carcinoma to 60 Gy or more.

Compared with interstitial implantation, intracavitary therapy, such as caesium intubation, has the advantage of being simple. However, it has many limitations. Being limited by the anatomy of the nasal fossae through which the caesium tubes are introduced, it may be difficult, if not impossible, to position the sources close to the lateral pharyngeal recesses (Fig. 2). In our caesium intubation series, three of the nine local relapses were limited to the lateral pharyngeal recess. It is also not possible to position the caesium tube close to the inflection point at the junction between roof and posterior wall of the nasopharynx (Fig. 2).

One of the important causes of the local failure after radical external radiotherapy of early nasopharyngeal carcinoma is relative underdosing of tumour because the dose is limited by the tolerance of the adjacent normal tissue. It is radiobiologically sound to treat tumours that persist after the initial course of radical radiotherapy. A smaller dose is required and less time is given for the tumour to seed metastases. With this in mind, we have extended the use of brachytherapy to treat persistent tumours after external radiotherapy. The optimal timing to give a booster dose of radiation will depend on the knowledge of the regression pattern of this tumour after radiotherapy. A study to this effect has been started in our centre.

Our early results of gold grain implantation are promising and are comparable to the reported experience of interstitial implantation of nasopharyngeal carcinoma (Vikram & Hilaris, 1984). The role of brachytherapy in treatment of persistent and recurrent nasopharyngeal carcinoma requires further study, especially in relation to the problems of access and the selection of suitable cases.

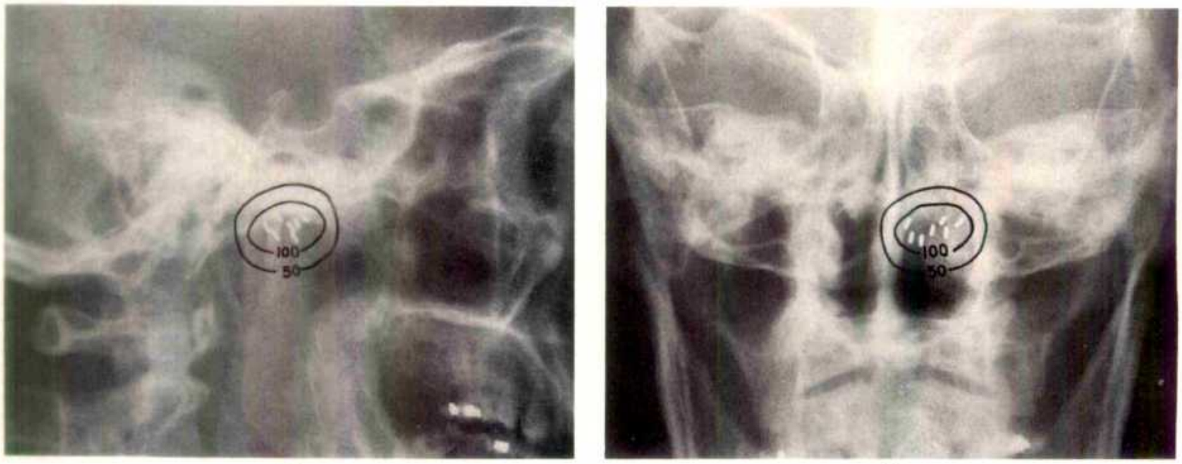

(a) (b)

Figure 4. (a) Lateral and (b) antero-posterior skull radiographs showing the gold grains inserted. Note the rapid dose fall-off compared with caesium intubation. The dose was prescribed at 100%.

Acknowledgment

This study was supported by grants from the Hong Kong Anti-Cancer Society. The authors would like to thank Mr C. K. Lau and Mr P. M. Wu for preparing the illustrations and Mr Alex Lam for photographic assistance.

References

BERNSTEIN, M. & GUTIN, P. H., 1985. Interstitial irradiation of skull base tumours. *Canadian Journal of Neurological Sciences, 12,* 366–370.

DEITSCH, M., SEGALL, B. M. & LEEN, R., 1973. Retreatment of recurrent nasopharyngeal malignancy using a radium mould. *Journal of Prosthetic Dentistry, 30,* 315–320.

GOFFINET, D. R., FEE, W. E. JR., WELLS, J., AUSTIN-SEYMOUR, M., CLARKE, D., MARISCAL, J. M. & GOODE, R. L., 1985. ^{192}Ir pharyngoepiglottic fold interstitial implants. The key to successful treatment of base tongue carcinoma by radiation therapy. *Cancer, 55,* 941–948.

HARRISON, L. B. & WEISSBERG, J. B., 1987. A technique for interstitial nasopharyngeal brachytherapy. *International Journal of Radiation Oncology, Biology, Physics, 13,* 451–453.

VAN HERIK, M. & ERICH, J. B., 1955. A radium applicator for treating carcinoma of the nasopharynx. *Archives of Otolaryngology, 62,* 189–201.

HILARIS, B. S., 1968. Techniques of interstitial and intracavitary radiation. *Cancer, 22,* 745–751.

HILARIS, B. S., LEWIS, J. S. & HENSCHKE, U. K., 1968. Therapy of recurrent cancer of the nasopharynx. Value of interstitial and intracavitary radiation. *Archives of Otolaryngology, 87,* 506–510.

HO, J. H. C., 1982. Nasopharynx. In *Treatment of Cancer,* ed. by K. E. Halnan (Chapman & Hall, London), pp. 249–268.

LAM, K. S. L., HO, J. H. C., LEE, A. W. M., TSE, V. K. C., CHAN, P. K., WANG, C., MA, J. T. C. & YEUNG, R. T. T., 1987. Symptomatic hypothalamic-pituitary dysfunction in nasopharyngeal carcinoma patients following radiation therapy: a retrospective study. *International Journal of Radiation Oncology, Biology, Physics, 13,* 1343–1350.

LEE, A. W. M., NG, S. H., HO, J. H. C., TSE, V. K. C., POON, Y. F., TSE, C. C. H., AU, G. K. H., O, S. K., LAU, W. H. & FOO, W. W. L., 1988. Clinical diagnosis of late temporal lobe necrosis following radiation therapy for nasopharyngeal carcinoma. *Cancer, 61,* 1535–1542.

MESIC, J. B., FLETCHER, G. H. & GOEPFERT, H., 1981. Megavoltage irradiation of epithelial tumours of the nasopharynx. *International Journal of Radiation Oncology, Biology, Physics, 7,* 447–453.
30, 435–437.

RUDD, K. D., GREEN, A. E., JR., MORROW, R. M. & HANCOCK, J. A., 1966. Radium source appliance for treatment of nasopharyngeal cancer. *Journal of the American Dental Association, 72,* 862–866.

SUIT, H. D., LLOYD, R. S., ANDREWS, J. R. & SNEIDER, S. E., 1960. Technique for intracavitary irradiation of the nasopharynx. *American Journal of Roentgenology, 84,* 629–631.

VIKRAM, B. & HILARIS, B., 1984. Transnasal permanent interstitial implantation for carcinoma of the nasopharynx. *International Journal of Radiation Oncology, Biology, Physics, 10,* 153–155.

WANG, C. C., 1987. Re-irradiation of recurrent nasopharyngeal carcinoma—treatment techniques and results. *International Journal of Radiation Oncology, Biology, Physics, 13,* 953–956.

WANG, C. C., BUSSE, J. & GITTERMAN, M., 1975. A simple afterloading applicator for intracavitary irradiation of carcinoma of the nasopharynx. *Radiology, 115,* 737–738.

1989, *The British Journal of Radiology*, *62*, 362–365

The ICRU recommendations for reporting intracavitary therapy in gynaecology and the Manchester method of treating cancer of the cervix uteri

By J. M. Wilkinson, MSc and T. P. Ramachandran, PhD

Christie Hospital, Manchester, UK and the Regional Cancer Centre, Trivandrum, India

(*Received September 1988 and in revised form November 1988*)

Abstract. The recommendations of the International Commission on Radiation Units and Measurements for reporting intracavitary therapy have been considered with particular regard to the Manchester method of treating cancer of the cervix uteri. The total reference air kerma is calculated and tabulated as a function of prescription for the standard Manchester applicator arrangements. Furthermore, it is shown that the volume contained within a particular isodose surface may be determined, with very acceptable accuracy, from the total reference air kerma by the use of a simple empirical expression.

The International Commission on Radiation Units and Measurements (ICRU) recommends that the record of an intracavitary application of radionuclides for the treatment of cervical carcinoma should contain, *inter alia*, the total reference air kerma, a description of the "reference volume" and the absorbed dose at reference points (ICRU, 1985). These parameters are interrelated, and particularly so when a systematic approach such as the Manchester system (Meredith, 1967) is adopted. In this paper we discuss these relationships and extend the discussion to include the much used historical quantity, milligram hours.

Milligram hours and total reference air kerma

If the geometrical arrangement of sources in a brachytherapy treatment and the relative strengths of those sources is predetermined, then the dose at any point is proportional to the product of the total source strength and the duration of the application. Historically, the source strength has been specified in terms of content, and in the case of radium sources this was usually the radium mass stated in milligrams. The duration of brachytherapy treatments has conveniently been given in hours. Hence the product of total source strength and the duration, for a radium application, was presented as milligram hours (mg h). A memorandum from the British Committee on Radiation Units and Measurements (BCRU, 1984) recommends that brachytherapy source strength should now be specified in terms of emission rather than content, and that the quantity used for such specifications should be air-kerma rate at 1 m. The total source strength in an application is thus the sum of the air-kerma rates for the individual sources, or the total reference air-kerma rate. Consequently, the product of total source strength and the duration of the application in hours becomes the total reference air kerma. For a particular radium source, the ratio of the air-kerma rate at 1 m and the radium content in milligrams is a constant that depends on the filtration thickness, and the same factor will numerically convert milligram hours to total reference air kerma. A conversion factor of 7.2 is used for radium sources of 0.5 mm platinum filtration, based on an exposure-rate constant of 0.825 R m^2 h^{-1} Ci^{-1} and an exposure-to-kerma factor of 8.73×10^{-3} Gy R^{-1} (1 $R = 2.58 \times 10^{-4}$ C kg^{-1} and 1 $W = 33.85$ J C^{-1}) (BCRU, 1984; Massey et al, 1985). Thus:

1 mg h = 7.2 μGy total reference air kerma
(for filtration = 0.5 mm Pt)

For gynaecological intracavitary therapy, radium tubes with 1 mm platinum filtration were frequently used. This reduces the emission per unit mass by a further 10%. Hence:

1 mg h = 6.5 μGy total reference air kerma
(for filtration = 1.0 mm Pt)

The 10% reduction is consistent with the tabulated data for radium line sources given by Meredith (1967) to be used for Manchester system calculations, although it is noted that ICRU Report 38 (ICRU, 1985) suggests a 7% reduction.

The revised Manchester system (Tod & Meredith, 1953) assumed radium tubes, with 1 mm platinum filtration, of 20 mm total length and 13.5 mm active length, contained in rubber applicators of specific size and shape. The treatments were prescribed in terms of exposure at Point A, and the exposure rates at Point A were determined using the line source data for 1 mm Pt filtration referred to earlier. An idealized, or reference, geometry was assumed. The relative source positions in the reference geometry and the radium content of each tube were specified such that the calculated Point A exposure rate in the reference geometry was constant, to within ±2%, for a standard insertion consisting of a central tube and two transverse ovoids. This was true irrespective of whether the central tube was long (60 mm) or medium (40 mm), or whether the ovoids were small, medium or large, or whether the ovoids were touching or separated by a 1 cm spacer. The majority of patients were treated with some combination of these applicator arrangements, for which the average Point A exposure rate was taken as 57.3 'R' h^{-1} leading to a total duration of 140 h for an 8000 'R' prescription for radical, intracavitary only, radiotherapy. The symbol 'R' acknowledges that the units are not true röntgens as, retrospectively, various systematic errors have been recognized (Gibb & Massey, 1980). It has not, in general, been the practice in Manchester to adjust the treatment times to allow for the source geometry actually achieved in the patient, which will invariably differ from the reference geometry. The milligram hours, and hence the total reference air kerma, is therefore constant for a given Point A prescription and a given applicator set. When adopting SI units for brachytherapy, care was taken not to introduce any systematic change in the actual treatment and, for example, both an 8000 'R' prescription and a 7500 cGy prescription result in the same total reference air kerma for any given combination of applicators (Gibb & Massey, 1980). Table I gives milligram hours and total reference air kerma for two common prescriptions and the various applicator combinations.

Reference volume and total reference air kerma

The ICRU (1985) defines the reference volume as the tissue volume encompassed by a reference isodose surface. It is to be expected from the work of Parker (1938) that the volume contained within any particular isodose surface will vary by only a few per cent for a given value of the milligram hours, provided that the elongation of the volume (*i.e.* the ratio of the maximum dimension to the minimum dimension) is not excessive. A spherical volume can be determined as a function of the milligram hours (or total reference air kerma) by considering the total activity concentrated into a point source at the centre. If it is assumed that, over short distances and in point source geometry, scattering compensates for attenuation, and that essentially all energy released will be locally absorbed, then the volume V of the sphere (in cubic centimetres) is given by:

$$V = \tfrac{4}{3}\pi \left[\frac{(K \times [\mu/\rho]^{m}_{\mathrm{air}} \times 10)}{D}\right]^{3/2}$$

where K is the total reference air kerma in mGy, D is the dose on the isodose surface in Gy, and $[\mu/\rho]^{m}_{\mathrm{air}}$ is the ratio of the mass energy absorption coefficients for the medium and air. Using a value of 1.102 for this ratio (*i.e.* that for muscle to air for ^{137}Cs γ radiation) the expression reduces to:

$$V = 153 \times \left[\frac{K}{D}\right]^{3/2} \ (\mathrm{cm}^3)$$

In practice, of course, the sources are distributed between the interuterine tube and vaginal ovoids, and at a few centimetres away from the applicators the volume enclosed within an isodose surface may be described as pear-shaped.

A computer program was written to determine the actual volumes contained within the 45, 60 and 75 Gy isodose surfaces for all standard Manchester system geometries, and a selection of non-standard geometries, assuming the standard duration for a prescription of 75 Gy at Point A. To simplify the calculation, a simulation of the Manchester system with ^{137}Cs pellets was used (Wilkinson et al, 1983). The non-standard geometries were chosen so as to give either unusually wide, or unusually long and narrow, isodose surfaces. For example, at one extreme, approximately 65% of the total reference air kerma was assigned to sources in the vaginal applicators which were assumed to be high in the lateral fornices, more widely separated than expected, and used in conjunction with the shorter (40 mm) interuterine tube. At the other extreme, half of the total reference air kerma was assigned to sources in the longer (60 mm) interuterine applicator, and it was assumed that this was used in conjunction with vaginal ovoids, which were displaced from their traditional transverse positions so as to lie near to the vaginal axis.

The volume integrations were performed, both with and without correction for tissue absorption, by calculating the dose at the centre of a large number of contiguous volume elements (each 1 mm × 1 mm × 1 mm), which constituted a three-dimensional array of sufficient dimensions to enclose the 45 Gy isodose surface. Those elements where the calculated dose was higher than that on the chosen isodose surface were summed separately for each of the three dose levels. Two tissue absorption correction

Table I. Milligram hours and total reference air kerma in mGy as a function of prescription for standard Manchester system applicators

Applicators (central tube + transverse ovoids)	8000 'R' (75 Gy) Duration 140 h		6500 'R' (60 Gy) Duration 114 h	
	(mg h)	Total reference air kerma (mGy)	(mg h)	Total reference air kerma (mGy)
Medium central tube + two small ovoids	8400	54.6	6840	44.5
Medium central tube + two medium ovoids	9100	59.2	7410	48.2
Medium central tube + two large ovoids	9800	63.7	7980	51.9
Long central tube + two small ovoids	9800	63.7	7980	51.9
Long central tube + two medium ovoids	10 500	68.3	8550	55.6
Long central tube + two large ovoids	11 200	72.8	9120	59.3

methods were used: the build-up factor method of Kornelson and Young (1981) and the Meisberger polynomial (Meisberger et al, 1968). The ratio of the integrated volume to that determined by the above expression for a point source was calculated in each case. Without tissue absorption, the mean ratio for all geometries and for the three isodose surfaces was 1.11 with a standard deviation of 1.5%. With a tissue absorption correction the integrated volumes were 9% less when using the Kornelsen and Young method of correction, or 4% less when using the Meisberger polynomial method. The difference in these values emphasizes the uncertainty that exists when attempting to incorporate tissue absorption corrections in brachytherapy calculations. No attempt was made to allow for shielding of each source by the others, or for absorption in the applicators, but the effects of these on the volume calculation will be small.

It is suggested, therefore, that for intracavitary therapy using a central tube and transverse ovoids, the volume V enclosed by an isodose surface may be calculated by the expression:

$$V = 160\left[\frac{K}{D}\right]^{3/2} \ (\mathrm{cm}^3)$$

where K is the total reference air kerma in mGy and D is the dose on the isodose surface in Gy. This is equivalent to using a tissue absorption correction that is a mean of the two methods investigated. Strictly, the expression applies only for caesium sources in geometries that are similar to those used in the traditional Manchester method. However, the mass absorption coefficient ratio is essentially constant over the energy range 300 keV to 2 MeV and so the only differences arising from the use of other common radionuclides are those which are due to changes in the tissue absorption and scattering effects. Based on the Meisberger polynomials, the volumes for the same total reference air kerma would be marginally less when using ^{60}Co or ^{226}Ra in place of caesium, but the build-up factor method suggests the reverse and so the above expression remains a reasonable compromise. For ^{192}Ir, the volume, based on an average of the two correction methods, will be about 6% larger than that for ^{137}Cs with the same total emission.

Table II. Volumes contained within the 60 Gy isodose surface for a Manchester system insertion, when performed strictly in accordance with the Manchester practice, for a prescribed dose of 75 Gy at Point A

Applicators (central tube + transverse ovoids)	Volume within 60 Gy isodose surface (cm^3) for prescribed dose of 75 Gy at Point A
Medium central tube + two small ovoids	135
Medium central tube + two medium ovoids	155
Medium central tube + two large ovoids	175
Long central tube + two small ovoids	175
Long central tube + two medium ovoids	190
Long central tube + two large ovoids	210

For the traditional Manchester geometries there will be a random error of ±3% (two standard deviations) depending on the distribution of the active material that is actually achieved. Major deviations from the traditional Manchester geometries may result in larger errors, but as the change from point source geometry is only 11%, these cannot be enormous. As indicated earlier, there is a significant uncertainty inherent in the tissue absorption correction and errors must be considered in this context. For ^{137}Cs sources inserted in accordance with the Manchester practice and prescribed as 75 Gy (8000 'R') at Point A, the volumes contained within the 60 Gy isodose surface, will, to a good approximation, be those given in Table II. The figures in this table have been determined from the above expression, using the data in Table I, and rounded to the nearest 5 cm^3. The 60 Gy isodose surface is chosen in accordance with the ICRU recommendations for radical intracavitary-only therapy.

Conclusions

It has been shown that the volume contained within an isodose surface can be easily calculated from the total reference air kerma, which in turn, when using the Manchester system strictly as it is practised in Manchester, is readily determined from the Point A prescription. The fact that such relationships exist may be regarded as a criticism of the ICRU advice in that any observed effect that can be correlated with volume will also be correlated with total reference air kerma, and recording both parameters is therefore superfluous. Furthermore, tolerance to intracavitary therapy is unlikely to be determined by the total volume within an isodose surface, but is more likely to be governed by, for example, the area of bladder or rectal mucosa exceeding a particular dose at a particular dose-rate. It would appear then that these particular ICRU recommendations are somewhat arbitrary and probably not useful. It is therefore to be hoped that, in future, better scientific justification will be given prior to any recommendations that require additional effort from the international radiotherapy community.

References

BCRU, 1984. Specification of brachytherapy sources. Memorandum from the British Committee on Radiation Units and Measurements. *British Journal of Radiology, 57,* 941–942.

Gibb, R. & Massey, J. B., 1980. Radium dosage: SI units and the Manchester System. *British Journal of Radiology, 53,* 1100–1101.

ICRU, 1985. *Dose Volume Specification for Reporting Intracavitary Therapy in Gynaecology,* Report 38 (International Commission on Radiation Units and Measurements, Bethesda, Maryland, USA).

Kornelson, R. O. & Young, M. E. J., 1981. Brachytherapy build-up factors. *British Journal of Radiology*, *54*, 136.

Massey, J. B., Pointon, R. S. & Wilkinson, J. M., 1985. The Manchester System and the BCRU recommendations for brachytherapy source specification. *British Journal of Radiology*, *58*, 911–913.

Meisberger, L. L., Keller, K. J. & Shalek, R. J., 1968. The effective attenuation in water of the gamma rays of gold 198, iridium 192, caesium 137, radium 226, and cobalt 60. *Radiology*, *90*, 953–957.

Meredith, W. J. (Ed.), 1967. *Radium Dosage: The Manchester System*, 2nd edn (E. & S. Livingstone, Edinburgh).

Parker, H. M., 1938. A dosage system for interstitial radium therapy. Part II: Physical aspects. *British Journal of Radiology*, *11*, 313–340.

Tod, M. C. & Meredith, W. J., 1953. Treatment of cancer of the cervix uteri—a revised "Manchester Method". *British Journal of Radiology*, *26*, 252–257.

Wilkinson, J. M., Moore, C. J., Notley, H. M. & Hunter, R. D., 1983. The use of Selectron afterloading equipment to simulate and extend the Manchester System for intracavitary therapy of the cervix uteri. *British Journal of Radiology*, *56*, 409–414.

1989, *The British Journal of Radiology*, *62*, 366–367

Technical notes

Radiotherapy simulators and independent field wire movement

By G. Robertson, BSc, MSc

West of Scotland Health Boards, Department of Clinical Physics and Bioengineering, 11 West Graham Street, Glasgow G4 9LF

(*Received October 1988*)

When using the radiotherapy treatment simulator to determine a region to be treated, it is frequently required to move one field edge without altering the remainder. It is necessary both to change the field size and to reposition the field centre. This can be time consuming, particularly if the simulator operator is inexperienced, or if all edges of the field are not simultaneously displayed by the image intensifier. With the co-operation of simulator manufacturers, it may be possible to overcome this problem using the current generation of microcomputer-controlled simulators.

Varian have incorporated in their Ximatron CX series of radiotherapy treatment simulators a microcomputer for control and display purposes. The field-defining crosswires can be moved either symmetrically or asymmetrically. In the symmetrical mode, the field-defining crosswires are symmetrical about the beam centre, *i.e.* $dx1 = dx2$ (Fig. 1), while the asymmetrical mode the four field-defining wires $x1$, $x2$, $y1$ and $y2$ can be moved independently. The jaws of the current generation of linear accelerators are capable of being set similarly. Situations exist where it is desirable to use asymmetrical fields, but in the great majority of cases it is more appropriate to use a symmetrical field arrangement.

The technique which has evolved in Glasgow using the existing features of the Varian simulator to determine the boundaries and centre of a symmetrical field is outlined below.

1. With the field wires in the symmetrical mode, an approximate field size and centre is selected. (This can be done either directly or from the remote console under fluoroscopic control.)
2. With the asymmetrical mode selected, the field wires are then moved independently to indicate the desired field edges.
3. The field size is noted and the field edges are marked on the patient's skin surface.
4. The field is then set up in the symmetrical mode and the treatment couch shifted until the field edges match with the patient marks, thus enabling correct simulation of the treatment beam and the marking of the field centre.

A problem with this technique is that simulation at Step 2 is not geometrically correct. In addition, the transfer from the asymmetrical to the symmetrical mode (Steps 3 and 4) is both cumbersome and time consuming.

These difficulties could both be overcome if, while in the symmetrical mode, crosswire and couch movement could be linked such that if a particular field edge is altered, an appropriate simultaneous couch movement is made, thereby ensuring correct beam geometry at all times. This could be quickly and easily selectable using

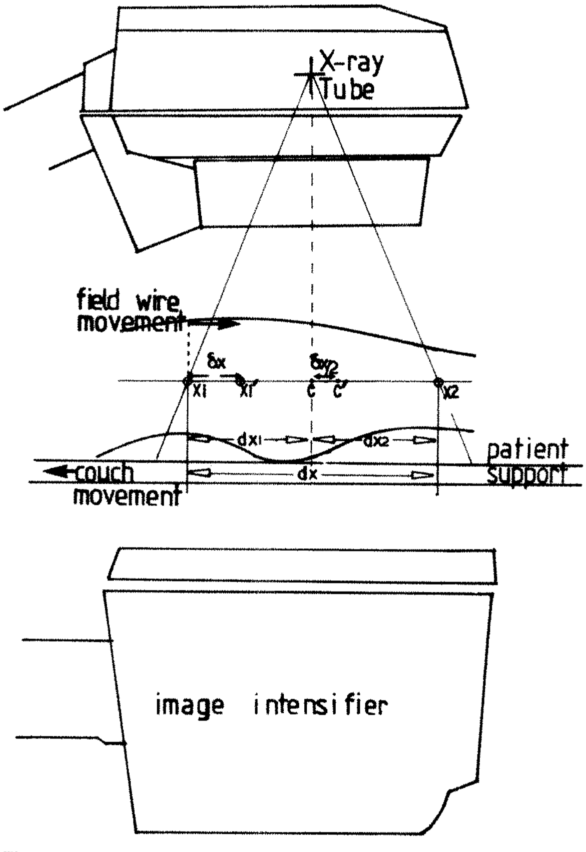

Figure 1. Schematic diagram of a simulator, where $x1$ and $x2$ are the field-defining wires and C is the central axis of the beam. Field wire $x1$ moves a negative distance δx to $x1'$. The new field size becomes $dx + \delta x$. The patient support moves a distance $-\delta x/2$ such that $x2$ remains in the same position.

1989, *The British Journal of Radiology*, *62*, 367–370

the softkeys (function keys) and would eliminate the time-consuming transfer from the asymmetrical to the symmetrical mode. If, for example, the $x1$ field wire is to be moved by a distance δx the new value for dx is d$x + \delta x$ and the couch has to be moved a distance $\delta x/2$ such that $x2$ remains constant (Fig. 1). The same would apply for the $x2$, $y1$ and $y2$ field wires.

This software modification would make it possible to alter one edge of a symmetrical field without influencing the remainder and would make a significant impact on the length of time taken to perform the simulation procedure, thereby reducing the likelihood of restlessness and subsequent patient movement.

Magnetic resonance imaging of the infant heart at 1.5 T

By M. A. Smith, BSc, MSc, PhD, *E. J. Baker, MA, MD, MRCP, V. T. Ayton, DCR(R), *J. M. Parsons, MB, BS, MRCP, *E. J. Ladusans, BSc, MRCP and M. N. Maisey, BSc, MD, FRCP, FRCR

Division of Radiological Sciences and *Department of Paediatric Cardiology, United Medical and Dental Schools of Guy's and St Thomas' Hospitals, Guy's Hospital, London Bridge, London SE1 9RT

(Received August 1988 and in revised form November 1988)

Magnetic resonance (MR) has been found to be of value in many fields of medicine but has yet to find an established place in the study of diseases of the heart. Published studies of the heart have demonstrated its ability to identify areas of acute myocardial infarction (Been et al, 1985b) and old infarcts (Higgins et al, 1984b), to recognize hypertrophic cardiomyopathies (Been et al, 1985a), pericardial effusions (Stark et al, 1984) and constrictive pericarditis (Soulen et al, 1985). It is, in addition, possible to measure ventricular volumes (Longmore et al, 1985) and images containing blood-flow-related data can be acquired (Ridgway & Smith, 1986; Underwood et al, 1987).

Magnetic resonance imaging (MRI) has been suggested to have a particularly valuable role in the study of the anatomy of the congenitally malformed heart (Higgins et al, 1984a) and imaging studies of a limited number of cases have been published (Jacobstein et al, 1985a,b; Boxer et al, 1986; Didier & Higgins, 1986; Didier et al, 1986; Fletcher & Jacobstein, 1986; von Shulthess et al, 1986). However, in these studies from a small number of research centres there is very little experience in the use of MRI in infants. Since 90% of patients with congenital heart disease present in the first year of life (Hoffman & Christianson, 1978), if MRI is to play a role in the investigation of congenital cardiovascular abnormalities it is essential to be able to image infants within the first year.

Imaging of the heart has generally been performed using low- and medium-field strength magnetic resonance systems with a field strength of 0.6 T or less (Higgins et al, 1985; Didier et al, 1986; Smith et al, 1986; Underwood et al, 1987). Cardiac triggering poses few problems at these field strengths but it has been thought that difficulties may arise with higher-field systems at 1.5 T and above. Despite this, however, the high-field MR systems have a potentially important advantage for the study of congenital heart disease in children; the signal-to-noise ratio from these systems is higher than from low- and mid-field systems resulting in improved spatial resolution or shorter imaging times. Both these advantages are particularly valuable in the study of infants.

An alternative approach for paediatric imaging is to use the echo-planar imaging technique (Rzedzian, 1983). With this method the images can be obtained in 60–120 ms, so that patient and cardiac motion are frozen. A drawback with echo-planar imaging is that, as yet, the image quality is poorer than that obtained using triggered conventional imaging techniques at the same field strength. In addition, the technique is not generally available.

The research described in this paper set out to determine the feasibility of investigating cardiovascular abnormalities in young infants making use of the improved spatial resolution that can be obtained with a high-field MR system.

Imaging technique

The subjects were imaged using a 1.5 T whole-body MR system manufactured by Philips Medical Systems (Gyroscan). To image the heart or the great vessels, the acquisition of the MR image must be synchronized with the patient's heartbeat. To achieve this with a high-field MR system, care must be taken over the positioning of the electrodes. If the three electrodes are placed in the conventional position used for triggering in other imaging modalities, or in MRI at low- and medium-field strengths, unacceptable distortion of the electrocardiogram (ECG) is produced. The R wave is sharply defined as required but the T-wave amplitude is greatly increased and may be the same size as the R wave, thus

---

Address reprint requests to Dr M. A. Smith.

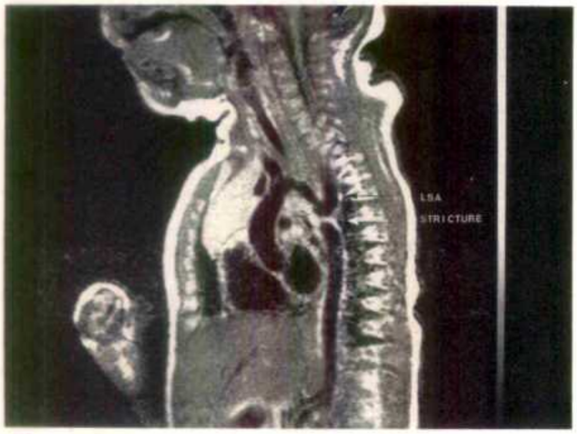

Figure 1. Aortic coarctation in a 6-week-old infant. This section shows clearly the relationship of the left subclavian artery (LSA) to the stricture.

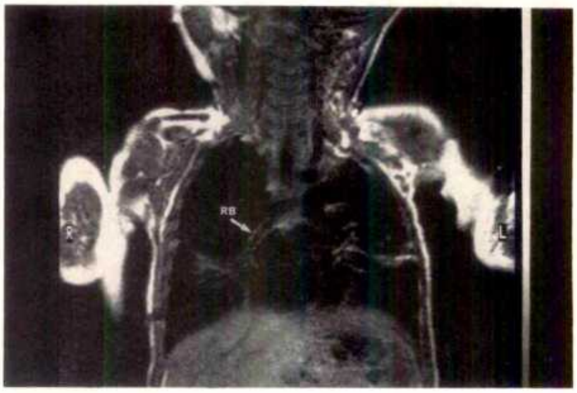

Figure 3. Infant aged 6 months with right lower lobe consolidation. This coronal image demonstrates the hyperinflated right lung with narrowing of the right main bronchus (RB), shown on subsequent images to be caused by the azygos vein and pulmonary artery.

introducing the possibility of incorrect triggering from the T wave. This distortion does not indicate a risk to the patient because it is not caused by the magnetic field disturbing the electrical conduction within the heart but by the motion of conducting material, particularly blood in the great vessels, in the high magnetic field. The distortion is reduced to an insignificant level by placing the three electrodes close together around the left nipple. Pre-gelled disposable silver/silver chloride electrodes (medicotest Q-10-A) were used and the ECG was transmitted using a telemetry system. Specialized electrodes, sometimes proposed for MRI, were not required.

The standard proton radiofrequency (RF) transmit and receive head coil was used. This is circular in cross-section with an internal diameter of 32 cm. The size and design of the coil enabled the infant to be positioned inside without difficulty and visual contact was possible if necessary throughout the investigation.

The infant was wrapped in a blanket and placed on a thin, firm mattress, which was strapped in a semicircle round the patient to restrict movement. The majority of subjects were imaged supine. The first 12 babies to be imaged were fed immediately prior to the MRI investigation and the investigation was undertaken without sedation. However, although this procedure was successful in most cases, in some, time was needed for them to settle during the investigation and this difficulty increased as infants with more severe abnormalities were studied. Consequently, most subsequent infants were given sedation of 75 mg/kg chloral.

Simultaneous 5 mm sections were acquired using a spin–echo sequence with echo time (TE) of 30 ms and a field of view of 200–250 mm. A matrix size of 256 × 256 was used but with each image being constructed from 180 signals instead of the usual 256. This resulted in a reduction in scan time with only a slight reduction in

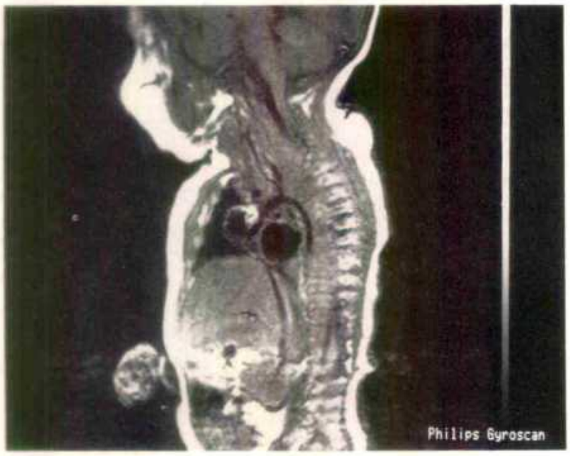

Figure 2. Aortic hypoplasia in a 12-week-old infant. The MR scan clearly demonstrates severe hypoplasia of the whole aortic arch and descending aorta without any localized narrowing. The patient's weakened medical condition and reduced lumen made her a poor candidate for X-ray angiography.

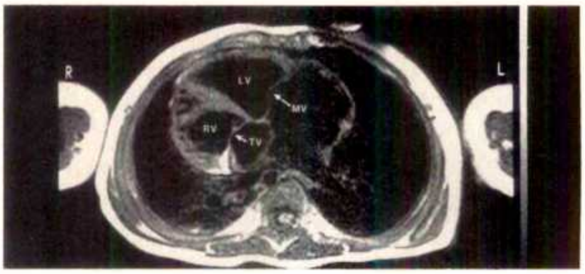

Figure 4. Congenitally corrected transposition in a 10-month-old infant. A smooth-walled anterior left ventricle (LV) and a posterior trabeculated right ventricle (RV) are shown with associated tricuspid (TV) and mitral valves (MV). Other images in the series showed the pulmonary artery arising from the left ventricle and the aorta from the right ventricle.

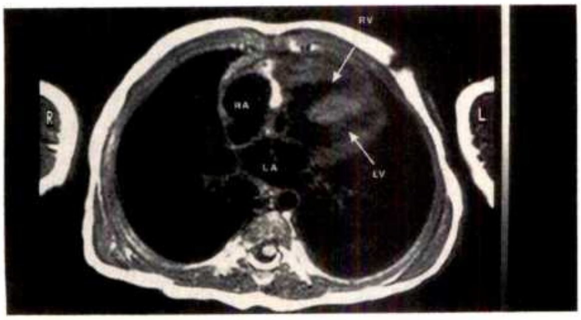

Figure 5. Tetralogy of Fallot in a 19-week-old infant. The ventricular septal defect, valve cusps of the overriding aorta and hypertrophied right ventricle are clearly seen.

spatial resolution in the phase-encoded direction. The MR system was triggered on each heartbeat, even for heart rates as high as 140 beats per minute. Once in position, a series of sections was acquired in the transverse direction from which the angles of obliquity could be obtained. Double-oblique imaging was then used to obtain the appropriate angulation, for example, through the arch and descending section of the aorta. Two signal averages were performed resulting in a typical scan time for a set of seven sections of about 6 min. The total investigation time per patient varies with the complexity of the congenital abnormality; typically, it is currently between 60 and 90 min.

Measurements were performed on a high-contrast resolution phantom and a line pair separation of 1.5 mm and 0.95 mm was obtained in the phase-encoded and frequency-encoded directions, respectively. The RF power absorption for children of different age imaged using the procedure are all below the maximum recommended specific absorption rate (SAR) with a typical value for a 6-week infant of 0.08 W/kg.

Results

The technique has been used to image over 40 infants under the age of 12 months. Electrocardiogram triggering was successfully achieved in all cases and respiratory motion artefacts were not found to be a problem. Constant observation of the patient from the end of the magnet and monitoring of the ECG ensured patient safety. In one instance, an ill, oxygen-dependent infant was imaged with the attendant clinician inside the magnet.

The technique has been successful in imaging a range of congenital disorders including coarctation of the aorta ($n = 22$), atrial and/or ventricular septal defect ($n = 14$), transposition ($n = 5$), Fallot's tetralogy ($n = 3$) and multiple cardiac defects. Images were obtained successfully from all patients and examples showing the quality of images obtained are given in Figs 1 to 5.

Discussion

The superior signal-to-noise ratio obtained with a high-field MR system enables good-quality, thin sections to be obtained in a reasonably short time period, which we feel is particularly suitable for the investigation of cardiac disease in the infant. Imaging soon after feeding can eliminate the need for any sedation, but for reliable, rapid throughput imaging, mild sedation is required. A series of diagnostic quality images can be obtained in a sufficiently short time to enable MRI to be considered as a possible routine technique for cardiac investigation in these children. Although a rigorous comparative study with ultrasound has not yet been undertaken, our experience suggests that the amount of anatomical detail is at least equal to and generally greater than that achieved using echocardiography. In a number of cases MRI eliminated the need for an X-ray angiogram.

A study is currently in progress to determine the clinical value of MRI in congenital heart disease in infants.

Acknowledgments

We would like to thank the following for financial support: the British Heart Foundation, Sir Philip and Lady Harris, Philips Medical Systems and the United Medical and Dental Schools of Guy's and St Thomas' Hospitals.

References

Been, M., Kean, D., Smith, D. A., Douglas, R. H. B., Best, J. J. & Muir, A. L., 1985a. Nuclear magnetic resonance in hypertrophic cardiomyopathy. *British Heart Journal*, *54*, 48–52.

Been, M., Smith, M. A., Ridgeway, J. P., Brydon, J., Douglas, R., Kean, D. M., Best, J. J. & Muir, A. L., 1985b. Characterisation of acute myocardial infarction by gated magnetic resonance imaging. *Lancet*, *ii*, 348–350.

Boxer, R. A., LaCorte, M. A., Singh, S., Cooper, R., Fishman, M. C., Goldman, M. & Stein, H. L., 1986. Nuclear magnetic resonance imaging in evaluation and follow-up of children treated for coarctation of the aorta. *Journal of the American College of Cardiology*, *7*, 1095–1098.

Didier, D. & Higgins, C. B., 1986. Identification and localisation of ventricular septal defects by gated magnetic resonance imaging. *American Journal of Cardiology*, *57*, 1363–1368.

Didier, D., Higgins, C. B., Fischer, M. R., Osaki, L., Silverman, N. H. & Cheitklin, M. D., 1986. Congenital heart disease: gated MR imaging in 72 patients. *Radiology*, *158*, 227–235.

Fletcher, B. D. & Jacobstein, M. D., 1986. MRI of congenital abnormalities of the great arteries. *American Journal of Roentgenology*, *146*, 941–948.

Higgins, C. B., Byrd, B. F., Farmer, D. W., Osaki, L., Silverman, N. H. & Cheitlin, M. D., 1984a. Magnetic resonance imaging in patients with congenital heart disease. *Circulation*, *70*, 851–860.

Higgins, C. B., Lanzer, P., Stark, D., Botvinck, E., Schiller, N. B., Crooks, L., Kaufman, L. & Lipton, M., 1984b. Imaging by nuclear magnetic resonance in patients with chronic ischaemic heart disease. *Circulation*, *69*, 523–531.

Higgins, C. B., Stark, D. & McNamara, M. T., 1985. Magnetic resonance imaging of the heart: a review of the experience in 172 subjects. *Radiology*, *155*, 671–679.

Hoffmann, J. I. E. & Christianson, R., 1978. Congenital heart disease in a cohort of 19 502 births with long-term follow-up. *American Journal of Cardiology*, *42*, 641–647.

Jacobstein, M. D., Fletcher, B. D., Goldstein, S. &

RIEMENSCHNEIDER, T. A., 1985a. Magnetic resonance imaging in patients with hypoplastic right heart syndrome. *American Heart Journal, 110,* 154–158.

—— 1985b. Evaluation of atrioventricular septal defect by magnetic resonance imaging. *American Journal of Cardiology, 55,* 1158–1161.

LONGMORE, D. B., KLIPSTEIN, R. H., UNDERWOOD, S. R., FIRMIN, D. N., HOUNSFIELD, G. N., WATANABE, M., BLAND, C., FOX, K., POOLE-WILSON, P. A., REES, R. S. O., DENISON, D., MCNALLY, A. M. & BURMAN, E. D., 1985. Dimensional accuracy of magnetic resonance imaging in studies of the heart. *Lancet, i,* 1360–1362.

RIDGWAY, J. P. & SMITH, M. A., 1986. A technique for velocity imaging using magnetic resonance imaging. *British Journal of Radiology, 59,* 603–607.

RZEDZIAN, R., MANSFIELD, P., DOYLE, M., GUILFOYLE, D. N., CHAPMAN, B., COUPLAND, R. E., CHRISPIN, A. & SMALL, P., 1983. Real time nuclear magnetic resonance clinical imaging in paediatrics. *Lancet, ii,* 1281–1282.

VON SCHULTHESS, G. K., HIGHASHINO, S. M., HIGGINS, S. S., DIDIER, D., FISCHER, M. R. & HIGGINS, C. B., 1986. Coarctation of the aorta: MR imaging. *Radiology, 158,* 289–296.

SMITH, M. A., RIDGWAY, J. P., BRYDON, J. W. E., BEEN, M., DOUGLAS, R. H. B., KEAN, D. M., MUIR, A. L. & BEST, J. J. K., 1986. ECG-gated T_1 images of the heart. *Physics in Medicine and Biology, 31,* 771–778.

SOULEN, R. L., STARK, D. D. & HIGGINS, C. B., 1985. Magnetic resonance imaging of constrictive pericardial disease. *American Journal of Cardiology, 55,* 480–484.

STARK, D. D., HIGGINS, C. B., LANZER, P., LIPTON, M., SCHILLER, N., CROOKS, L. E., BOTVINCK, E. B. & KAUFMAN, L., 1984. Magnetic resonance imaging of the pericardium: normal and pathological findings. *Radiology, 150,* 469–474.

UNDERWOOD, S. R., FIRMIN, D. N., KLIPSTEIN, R. H., REES, R. S. O. & LONGMORE, D. B., 1987. Magnetic resonance velocity mapping: clinical application of a new technique. *British Heart Journal, 57,* 404–412.

1989, *The British Journal of Radiology*, *62*, 371–373

Case reports

Balloon embolization of a congenital arterio-venous fistula between the internal mammary artery and a portal vein radicle

By *Mark J. D. Cobby, MRCP, †William Culling, MRCP, †Stephen C. Jordan, FRCP and George G. Hartnell, MRCP, FRCR

Departments of Radiology and †Cardiology, Bristol Royal Hospital for Sick Children, St Michael's Road, Bristol BS2 8BJ

(*Received September 1988*)

Congenital arterio-venous fistulae between a systemic artery and portal vein are extremely rare. There are only two case reports in the English language (Glass et al, 1960; Stanford et al, 1970) of a fistula between an internal mammary artery and the portal venous system. We report a case presenting at an early age, which was successfully treated by balloon embolization.

Case report

A full-term, female infant was noted to have a loud, continuous murmur over the left lower sternum when 2 days old. The pregnancy had been uneventful and feeding and growth progressed normally over the next 5 months. There were no episodes of cyanosis or other abnormality. The chest radiograph was normal. A provisional diagnosis of a coronary artery fistula was made.

Echocardiography showed no intracardiac abnormality and no evidence of a coronary artery fistula. At the age of 7 months, the child underwent cardiac catheterization, which showed normal pressures, saturations and anatomy. A dilated and hypertrophied vessel arising from the left subclavian artery in the expected position of the internal mammary artery was observed. This crossed the midline at the level of the diaphragm and became narrowed and kinked, communicating with a large anterior vessel that passed into the liver to supply the portal venous system (Fig. 1). A subsequent aortogram and selective arteriogram demonstrated normal origins and anatomy of the coeliac and superior mesenteric arteries with a patent portal vein.

In view of the risk of developing portal venous hypertension, closure of the arterio-venous fistula was advised. As the anatomy of the origin of the left subclavian and internal mammary arteries was thought to be favourable, this was performed by balloon embolization when the child was 10 months old. A balloon was chosen in preference to a coil as it was felt that it would be difficult to position a coil in a sufficiently distal site. In particular, the uninflated balloon had a larger diameter than the fistula, so preventing the possible passage of the uninflated balloon into the portal system should it become detached prematurely. From a right femoral artery approach the left internal mammary artery was selectively cannulated and the catheter tip positioned just proximal to the narrowed segment of the vessel. Embolization of the distal internal mammary artery was successfully achieved by

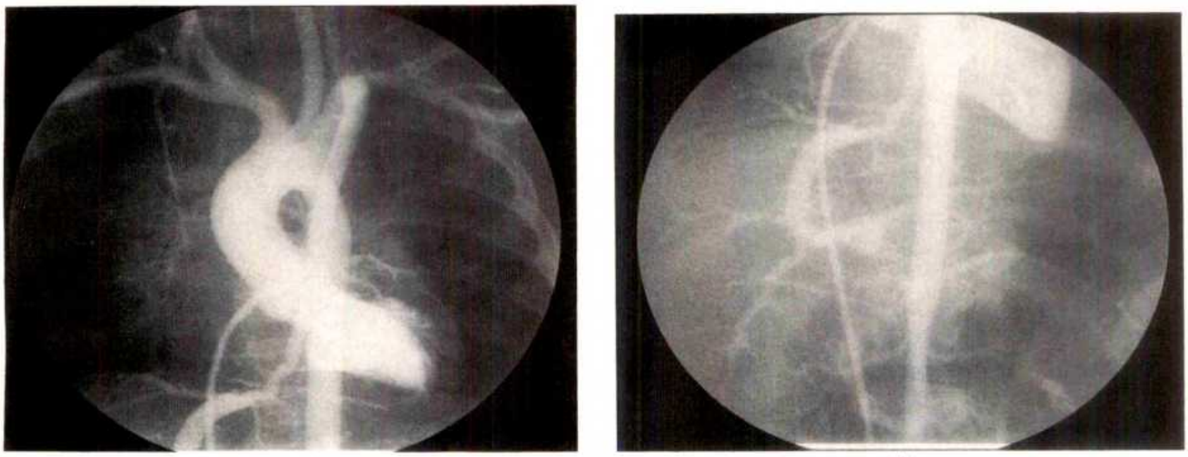
(a) (b)

Figure 1. (a, b) Cine angiogram, postero-anterior views; left ventricular injection. A dilated and hypertrophied left internal mammary artery is seen to arise from the normal position, cross the midline and descend below the diaphragm to communicate with the portal venous system.

---

*Author for correspondence.

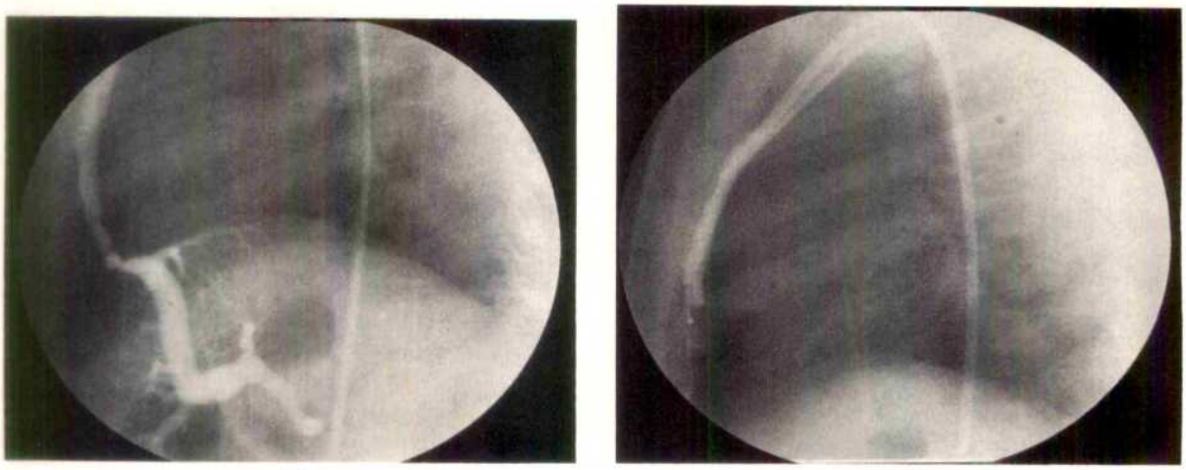

(a) (b)

Figure 2. (a) Cine angiogram, left lateral view; selective injection of left internal mammary artery prior to embolization. The hypertrophied internal mammary artery communicates with a dilated portal venous radical. The artery becomes narrowed and kinked just prior to, and as it descends through, the diaphragm. (b) Cine angiogram, left lateral view; selective injection of left internal mammary artery following balloon embolization. The artery has been successfully occluded just at the point where it started to narrow.

detaching a 6.0 mm Stoesslein-Münster Balloon (William Cook, Europe) (Fig. 2). The procedure was without complication and abolished the precordial murmur. The child was discharged home 2 days later and has remained well with no recurrence of the murmur.

Discussion

This case is very similar to that described by Glass et al (1960) who presented an infant in heart failure found to have a continuous murmur within hours of birth. An aortogram demonstrated a dilated left internal mammary artery communicating with a large portal venous radicle, which descended anteriorly to communicate with a patent ductus venosus. Because of increasing distress from the large fistula, surgical closure was performed on the 4th day but the child died. Post-mortem examination confirmed the anatomy as well as finding an unsuspected coarctation and patent ductus arteriosus.

One further case with some similarity to this has also been described, in which a congenital arterio-venous fistula originated from the right subclavian artery, descended the thoracic wall and communicated with the portal system via an aneurysmal vessel below the diaphragm (Gorlach et al, 1984).

Congenital arterio-venous fistulae are rare and usually located in the extremities, head or neck (Gomese & Bernatz, 1970). There are a number of case reports of congenital communication between the internal mammary artery and vein (Wells & Hurt, 1957; Stafford et al, 1969) and isolated reports of congenital fistulae between the internal mammary artery and pulmonary artery (Stafford et al, 1969) or thoracic wall (Maier & Stout, 1950; Ancalmo et al, 1979). They are frequently asymptomatic and may be discovered because of a continuous precordial murmur, but they may present with heart failure or some other complication of the shunt. Because of the potential complications, closure is usually recommended. In cases of systemic artery–portal venous communications, closure is particularly important to prevent the development of portal hypertension.

Embolization of these large, single-lumen fistulae provides an attractive alternative to surgery. In cases where it is difficult to manipulate the catheter tip to the most favourable position immediately proximal to the fistula, the ability to float a balloon into position may make this technique preferable to coil embolization. Balloon embolization has previously been performed in the treatment of surgical shunts and a variety of arterio-venous fistulae (Mitchell et al, 1985) but mainly in adult patients. This case illustrates the successful use of balloon embolization in a rare congenital arterio-venous fistula at an unusually young age.

Acknowledgment

We would like to thank Mr Art Hicks of William Cook, Europe, for providing the embolization balloon.

References

ANCALMO, N., OCHSNER, J. L. & KING, T. D., 1979. Congenital arterio-venous fistula of the internal thoracic artery and chest wall. *Journal of Pediatric Surgery*, *11*, 271–272.

GLASS, I. H., ROWE, R. D. & DUCKWORTH, J. W. A., 1960. Congenital arterio-venous fistula between the left internal mammary artery and ductus venosus: unusual cause of congestive heart failure in the newborn infant. *Pediatrics*, *26*, 604–610.

GOMESE, M. R. & BERNATZ, P. E., 1970. Arterio-venous fistulas. A review and 10 year experience at the Mayo Clinic. *Mayo Clinic Proceedings*, *45*, 81–102.

Gorlach, G., Hagel, K. H., Mulch, J., Scheld, H. H. & Hehrlein, F. W., 1984. Congenital arterio-venous fistula between the subclavian artery and the portal vein. *Journal of Cardiovascular Surgery*, *25*, 378–380.

Maier, H. C. & Stout, A. P., 1950. Congenital arterio-venous fistulas of the thoracic wall. *Circulation*, *1*, 809–812.

Mitchell, S. E., Kan, J. S. & White, R. I., 1985. Interventional techniques in congenital heart disease. *Seminars in Roentgenology*, *20*, 290–311.

Stafford, R. W., Kronenberg, M. W., Dunbar, J. D. & Wooley, C. F., 1969. Continuous precordial murmurs due to internal mammary artery fistulas. *American Journal of Cardiology*, *24*, 414–419.

Stanford, W., Fixler, D. E., Armstrong, R. G., Lindberg, E. F. & Johnson, H. H., 1970. Congenital arterio-venous fistula between the left internal mammary artery and ductus venosus: a case report. *Journal of Thoracic and Cardiovascular Surgery*, *60*, 248–252.

Wells, B. G. & Hurt, R., 1957. Congenital arterio-venous fistula of the internal mammary vessels. *British Heart Journal*, *19*, 135–137.

Magnetic resonance imaging of ruptured aneurysm of the ascending aorta

By R. P. Spielmann, MD, *E. E. Küng, MD, G. Witte, MD and M. Heller, MD

Department of Diagnostic Radiology and *Institute of Pathology, University Hospital Eppendorf, Hamburg, Federal Republic of Germany

(Received August 1988)

Magnetic resonance imaging (MRI) has been recognized as an excellent method to assess pathology of the thoracic aorta (Amparo et al, 1985; Geisinger et al, 1985; Glazer et al, 1985; Dinsmore et al, 1986). However, it is generally not feasible in the investigation of acute complications of aortic disease, because the strength of the magnetic field and the restricted access to the patient during the investigation preclude adequate monitoring and therapy in most instances. In this paper, the case of a ruptured aortic aneurysm is presented, which was imaged a few hours after the onset of symptoms. Although the patient was haemodynamically stable at the time of the examination, she died 2 h after the procedure, before surgery could be performed. A post-mortem examination was obtained, and the findings were compared with the magnetic resonance images.

Case report

An 80-year-old woman was admitted to our hospital within 1 h of the onset of severe chest pain. Blood pressure values were in the lower normal range, although there was a long history of arterial hypertension. Myocardial infarction was excluded by electrocardiogram (ECG) and enzyme examination. The physical examination revealed a diastolic heart murmur suggestive of incompetence of the aortic valve. A plain radiograph of the thorax showed abnormal widening of the mediastinum. On subsequent two-dimensional echocardiography, aneurysm of the ascending aorta and some pericardial fluid were recognized.

As the patient was haemodynamically stable, MRI appeared practicable to assess the extent of the aneurysm and to investigate the presence of aortic dissection. The scans were performed with a 1.5 T imager (Gyroscan, Philips) using ECG-triggered spin–echo sequences. The heart-beat interval was around 700 ms. After a first series of transverse slices through the ascending aorta and the aortic arch (time to echo (TE) = 20 ms, 10 mm slice thickness, 128 × 128 matrix, two measurements, 3 min acquisition time), coronal sections through the ascending aorta and the proximal aortic arch were obtained (TE = 30 ms, 7 mm slice thickness, 256 × 256 matrix, four measurements, 12 min acquisition time). No complications occurred during the examination.

The magnetic resonance (MR) images demonstrated a large fusiform aneurysm of the ascending aorta, which extended from the aortic root into the proximal aortic arch (Fig. 1). Expansion of the posterior mediastinum and the heterogeneous signal intensity of the mediastinal fat revealed infiltration by mediastinal haemorrhage. Widening of the pleural and pericardial cavities indicated intracavitary fluid accumulation. An increased thickness of the aortic wall was suggestive of intramural haematoma.

Two hours after the MR investigation, the patient suddenly deteriorated and died before surgery could be performed. The post-mortem examination confirmed the aneurysm of the ascending aorta (maximum diameter 8 cm). Haemothorax, haemopericardium and massive interstitial haematoma of the mediastinum were present. Section of the ascending aorta revealed a tear through both intima and media of the vessel wall (Fig. 2), which extended proximally to the ostium of the right coronary artery. Dissecting haematoma within the aortic wall was found around the site of the tear. However, a false flow channel with re-entry into the true aortic lumen was not present. The wall of the aneurysm exhibited extensive atherosclerosis. Histology produced no evidence of additional degenerative or inflammatory changes.

Discussion

Spin–echo MRI provides high-contrast images of the great mediastinal vessels because of the absence of signal from rapidly flowing blood. The extent and diameter of aneurysms of the thoracic aorta can be reliably assessed by multiplanar MRI (Glazer et al, 1985; Dinsmore et al,

---

Address correspondence to: Dr R. P. Spielmann, Department of Diagnostic Radiology, Universitätskrankenhaus Eppendorf, Martinistrasse 52, 2000 Hamburg 20, Federal Republic of Germany.

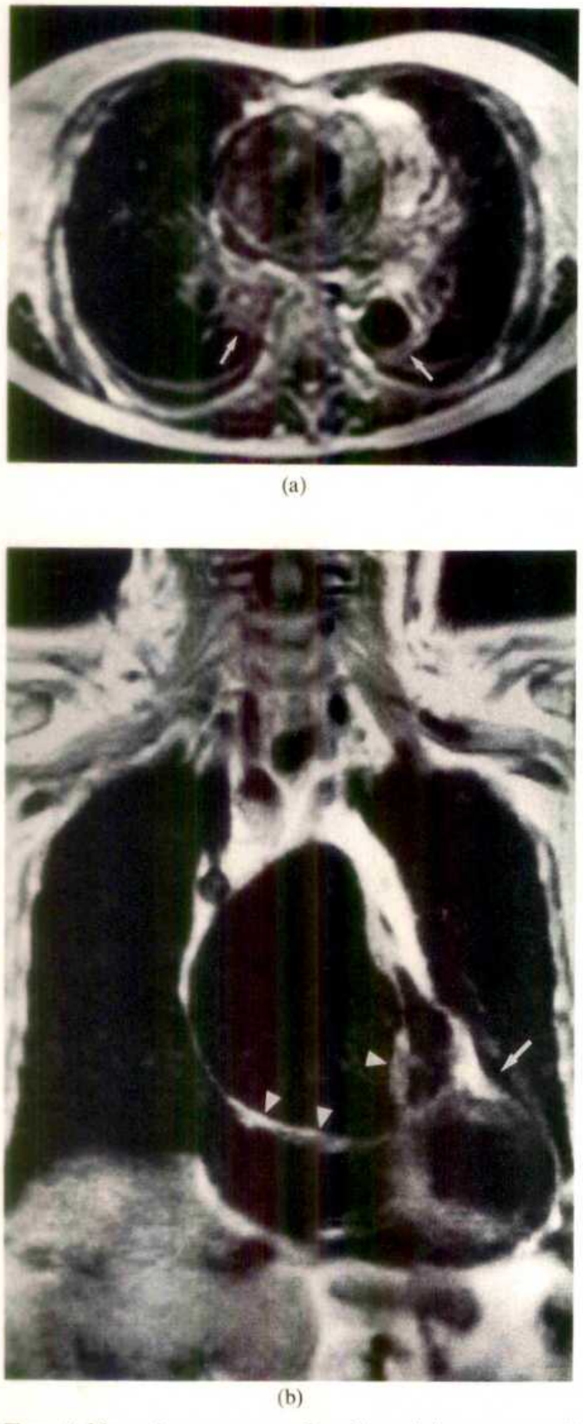

(a)

(b)

Figure 1. Magnetic resonance sections through the aneurysm of the ascending aorta. (a) Transverse section (128 × 128 matrix, two measurements, 3 min acquisition time). Note the mass expanding the posterior mediastinal compartment (arrows) and widening of the pleural space. (b) Coronal section (256 × 256 matrix, four measurements, 12 min acquisition time). Increased wall thickness (arrowheads) and widening of the pericardial cavity (arrow) is shown.

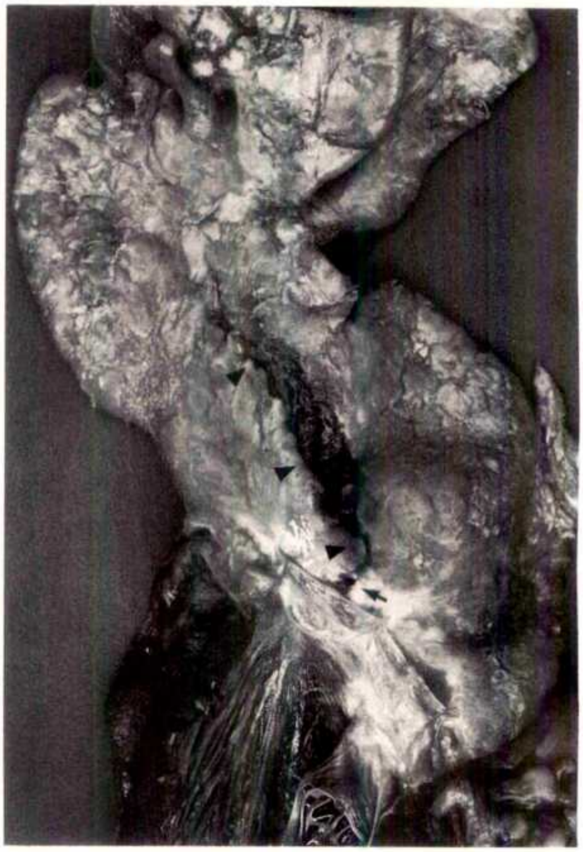

Figure 2. Pathological specimen showing a view of the inner surface of the ascending aorta. The tear in the aortic wall (arrowheads) extends proximally to the ostium of the right coronary artery (arrow) and there is extensive atherosclerosis.

1986; Schaefer et al, 1987). In the presence of aortic dissection with formation of a false flow channel, the intimal flap is clearly visualized on MRI (Amparo et al, 1985; Geisinger et al, 1985; Barentsz et al, 1987; Spielmann et al, 1988).

This report demonstrates the findings on MRI in a case of ruptured aneurysm of the ascending aorta. Although the tear in the wall of the aneurysm was not identified, the associated haematoma could be suspected from the images. The main findings were infiltration of the mediastinum, widening of the pericardial and pleural cavities and localized thickening of the aneurysmal wall. Besides intramural haematoma, differential diagnosis of the wall thickening had to consider intraluminal clot and atherosclerotic plaque. Similarly, the other findings were not specific for haematoma. Only the combination of the findings and the clinical condition of the patient led to the correct diagnosis of a leaking aneurysm with intramural and mediastinal haemorrhage.

The major obstacle to the idendification of fresh haemorrhage is its uncharacteristic signal intensity on the T_1-weighted spin–echo images (Unger et al, 1986;

Gomori & Grossman, 1987). In particular, detection of acute aortic dissection may be difficult on MRI if the dissection does not result in a false flow channel. In addition, acute mediastinal bleeding cannot be differentiated from other infiltrating disease of the mediastinum. This limitation has to be taken into account if MRI is used to assess acute complications of aortic disease.

At present, computed tomography (CT) is widely used to study the presence of aortic dissection and mediastinal haemorrhage. Acute mediastinal haemorrhage can be recognized on non-enhanced CT as an area of diffuse or localized hyperdensity relative to the surrounding tissues (Wolverson et al, 1983). Haemopericardium and haemothorax are demonstrated by accumulation of hyperdense fluid in the pericardial and pleural cavities. In some cases, the source of the bleeding may be identified by the extravasation of contrast medium (Gamsu, 1983). Dissection with formation of a false flow channel is diagnosed with high accuracy on CT if dynamic scanning with an intravenous bolus injection of contrast medium is performed (Oudkerk et al, 1983, Thorsen et al, 1983).

A major advantage of MRI over CT for the study of the thoracic aorta is the lack of a need for iodinated contrast media as well as the free choice of the orientation of the imaging plane. Magnetic resonance imaging will probably become the preferred non-invasive method for the diagnosis of aneurysm and dissection of the thoracic aorta. However, further experience is required to determine the value of MRI for the detection of acute mediastinal haemorrhage in symptomatic patients.

References

Amparo, E. G., Higgins, C. B., Hricak, H. & Sollitto, R., 1985. Aortic dissection: magnetic resonance imaging. *Radiology, 155,* 399–406.

Barentsz, J. O., Ruijs, J. H. J., Heystraten, F. M. J. & Buskens, F., 1987. Magnetic resonance imaging of the dissected thoracic aorta. *British Journal of Radiology, 60,* 499–502.

Dinsmore, R. E., Liberthson, R. R., Wismer, G. L., Miller, S. W., Liu, P., Thompson, R., McLoud, T. C., Marshall, J., Saini, S., Stratemeier, E. J., Okada, R. D. & Brady, T. J., 1986. Magnetic resonance imaging of thoracic aortic aneurysms: comparison with other imaging methods. *American Journal of Roentgenology, 146,* 309–314.

Gamsu, G., 1983. Computed tomography of the mediastinum. In *Computed Tomography of the Body,* ed. by A. A. Moss, G. Gamsu & H. K. Genant (W. B. Saunders, Philadelphia), p. 232.

Geisinger, M. A., Risius, B., O'Donell, J. A., Zelch, M. G., Moodie, D. S., Graor, R. A. & George, C. R., 1985. Thoracic aortic dissections: magnetic resonance imaging. *Radiology, 155,* 407–412.

Glazer, H. S., Guttierrez, F. R., Levitt, R. G., Lee, J. K. T. & Murphy, W. A., 1985. The thoracic aorta studied by MR imaging. *Radiology, 157,* 149–155.

Gomori, J. M. & Grossman, R. I., 1987. Head and neck hemorrhage. In *Magnetic Resonance Annual 1987,* ed. by H. Y. Kressel (Raven Press, New York), pp. 71–112.

Oudkerk, M., Overbosch, E. & Dee, P., 1983. CT recognition of acute aortic dissection. *American Journal of Roentgenology, 141,* 671–676.

Schaefer, S., Peshock, R. M., Malloy, C. R., Katz, J., Parkey, R. W. & Willerson, J. T., 1987. Nuclear magnetic resonance imaging in Marfan's syndrome. *Journal of the American College of Cardiology, 9,* 70–74.

Spielmann, R. P., Langkowski, J., Roden, K., Schuchert, A., Maas, R., Witte, G. & Heller, M., 1988. Kernspintomographie der thorakalen Aortendissektion. *Fortschritte auf dem Gebiete der Röntgenstrahlen und der Nuklearmedizin, 148,* 121–126.

Thorsen, M. K., San Dretto, M. A., Lawson, T. L., Foley, W. D., Smith, D. F. & Berland, L. L., 1983. Dissecting aortic aneurysms: accuracy of computed tomographic diagnosis. *Radiology, 148,* 773–777.

Unger, E. C., Glazer, H. S., Lee, J. K. T. & King, D., 1986. MRI of extracranial hematomas: preliminary observations. *American Journal of Roentgenology, 146,* 403–407.

Wolverson, M. K., Crepps, L. F., Sundaram, M., Heiberg, E., Vas, G. W. & Shields, J. B., 1983. Hyperdensity of recent hemorrhage at body computed tomography: incidence and morphologic variation. *Radiology, 148,* 779–784.

1989, *The British Journal of Radiology*, 62, 376–378

Dysplastic cortical hyperostosis: a new form of lethal neonatal dwarfism

By K. Kozlowski and †T. Tsuruta

Department of Radiology, Royal Alexandra Hospital for Children, Sydney, Australia and Department of Orthopaedic Surgery, Mie University School of Medicine, Mie-Ken, Japan

(Received September 1988 and in revised form October 1988)

A new form of lethal neonatal dwarfism is reported. The name of dysplastic cortical hyperostosis is proposed for this entity.

Case report

A Japanese, stillborn, male infant was delivered by a 28-year-old mother by a caesarean section after 28 weeks gestation. The pregnancy was complicated by polyhydramnios (2000 ml).

The mother was not exposed to any teratogenic agent. There was no parental consanguinity nor was there a family history of short stature or bone disease. No details of the father's age or the number of siblings were available.

At autopsy, it was found that the infant weighed 2900 g, crown-heel length was 37.7 cm and head circumference 37.4 cm. There was shortening of both the trunk and extremities and there was considerable oedema (Fig. 1).

The lungs were hypoplastic (left 2.7 g, right 3.0 g) with incomplete lobulation of the right lung. The cerebral sulci were poorly developed (? lissencephaly). There was complete renal duplication on the left and the orifice of the right coronary artery was high in position. Hepatosplenomegaly was noted.

The most striking radiographic finding was the generalized, symmetrical cortical thickening throughout the skeleton. This was most marked in the long bones and ribs, where the cortical thickening was wavy in outline. The medullary cavity was markedly narrowed. Similar sclerosis was seen in the clavicles and scapulae. The metacarpals and metatarsals had milder cortical sclerosis but in addition showed proximal tapering of the bones. The phalanges were less involved but all the tubular bones were shortened. The pelvis was less sclerotic but the acetabular angles were flat with lateral pointing of the ischia inferiorly. The vertebral bodies were poorly developed with coronal clefts and there was a club foot deformity bilaterally. The skull was small and the mandible normal (Fig. 2).

Discussion

The skeletal changes presented are unique and, to the best of our knowledge, have not been reported previously.

Shortening of stature with symmetrical cortical hyperostosis of the affected bones and hypoplastic/dysplastic short tubular bones, pelvis and vertebrae are strong evidence of a congenital bone dysplasia.

The only disease which in our experience can cause confusion is the neonatal form of Caffey's disease, infantile cortical hyperostosis. Even in the most severe form of the disease (Knitter & Kozlowski, 1964; Labrune et al, 1983) when the changes are bilateral, they are asymmetrical. In the severe, multifocal forms, the mandible almost always shows periosteal thickening, but was normal in our patient. The ribs are involved in their antero-medial parts, whereas in our case there is uniform involvement of all the ribs. Finally, another major, extraosseous sign of Caffey's disease was missing in our patient, namely, the deep, hard, soft-tissue swelling that overlies the bone changes (Beluffi et al, 1984). In this case, the tissues were soft because of generalized oedema.

I-cell disease (Lemaitre et al, 1976) and GM I gangliosidosis (Landing et al, 1964) may show superficial radiographic similarities to our patient, including

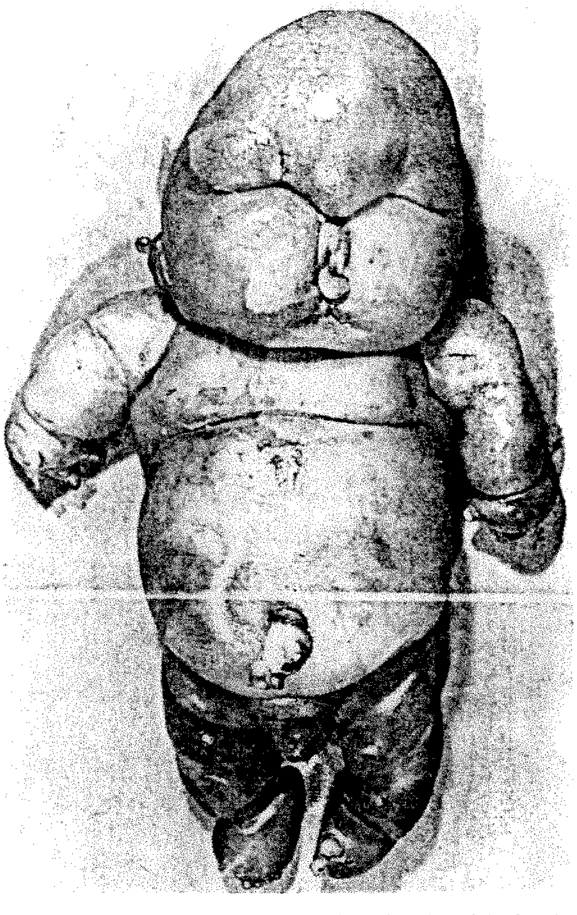

Figure 1. Photograph of the patient. The deformity of the face in this Japanese child is the result of oedema.

---

†Deceased.

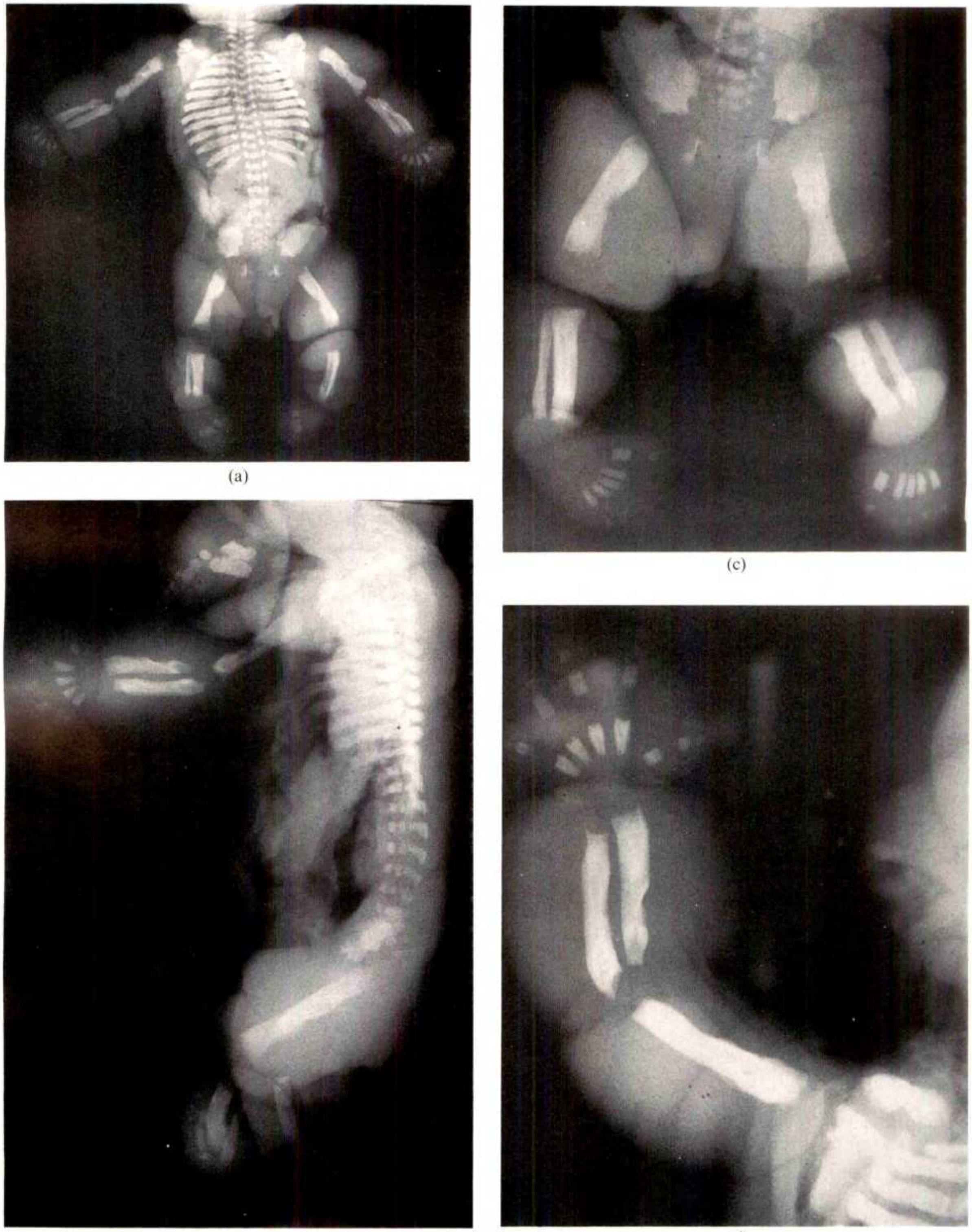

(a)

(c)

(b)

(d)

Figure 2. (a–d). Symmetrical hyperostotic changes affecting predominantly the long tubular bones, ribs, clavicles, sternum and to a lesser degree the scapulae and iliac bones. All the ribs are uniformly affected. The proximal ends of the metacarpals are pointed and there are coronal cleft vertebrae in the lumbar spine.

excessive periosteal bone formation (cloaking), which may resemble cortical hyperostosis with pointing of the proximal ends of the metacarpals. However, in both those disorders, bone mineralization is diminished. Multiple fractures, subperiosteal resorption and epiphyseal stippling are common features in the neonatal, severe form of I-cell disease but was not present in the case being reported. Finally, both these disorders show a Hurler-like phenotype.

Finally, Engelmann's disease (Bye et al, 1988), which shows sclerosis and thickening of the diaphyses of the long bones, manifests itself in the second year of life or later.

The name of dysplastic cortical hyperostosis seems to us to summarize the diagnostic radiographic features of the disease.

Acknowledgments

The authors would like to thank Professor A. Poznanski from the Children's Memorial Hospital, Chicago for reviewing the manuscript.

References

BELUFFI, G., CHIROCO, G., COLOMBO, A., CECILIANI, L., DELL'ORBO, C., FIORI, P., PAZZAGLIA, U. & QUACCI, D., 1984. Report of a new case of neonatal cortical hyperostosis. Histological and ultrastructural study. *Annales de Radiologie, 27*, 79–88.

BYE, A. M. E., HODSON, E., KEWLEY, G. & KOZLOWSKI, K., 1988. Progressive diaphyseal dysplasia and a low muscle carnitine. *Pediatric Radiology, 18*, 340.

KNITTER, T. & KOZLOWSKI, K., 1964. Przypadek wrodzonej postaci korowego przerostu kosci niemowlat (hyperostosis corticalis infantum). *Pediatria Polska, 39*, 461–462.

LANDING, B. H., SILVERMAN, F. N., CRAIG, J. M., JACOBY, M. D., LAHEY, M. D. & CHADWICK, D. L., 1964. Familial neurovisceral lipidosis. *American Journal of Diseases of Children, 108*, 503–522.

LABRUNE, M., GUEDJ, G., VIAL, M., BESSIS, R., ROSET, M. & KERBRAT, V., 1983. Maladie de Caffey à début anténatal. *Archives Françaises de Pédiatrie, 40*, 39–43.

LEMAITRE, L., REMY, J., FARRIAUX, J. P., DHONDT, J. L. & WALBAUM, R., 1978. Radiological signs of mucolipoidosis II or I-cell disease. A study of nine cases. *Pediatric Radiology, 7*, 97–105.

1989, *The British Journal of Radiology*, 62, 379–380

Case of the month

Haemoptysis in a laundry worker

By *J. E. Jackson, MRCP and D. J. Allison, BSc, MD, FRCR

Department of Diagnostic Radiology, Hammersmith Hospital, Du Cane Road, London W12 0HS

(*Received March 1988*)

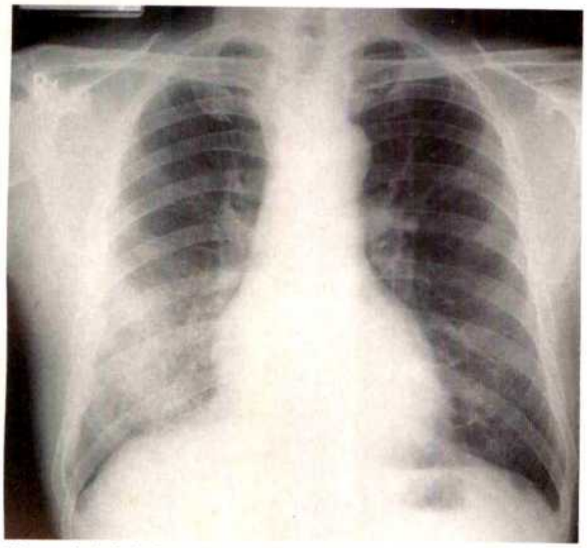

Figure 1. Admission chest radiograph.

A 39-year-old man of Philipino origin, who moved to England in April 1986, presented in January 1987 to his local hospital, as an emergency, following a massive haemoptysis. He had suffered four smaller haemoptyses during the preceding 4 months. The patient denied any history of cough, sputum, chest pain or wheezing although he had noted mild dyspnoea on exertion and had smoked until about 1 year previously. Bronchoscopy on admission revealed friable mucosa but no actual bleeding. He was subsequently referred to this hospital for further investigation.

Physical examination was unremarkable. Baseline laboratory investigations revealed only a mild microcytic anaemia and his arterial blood gases were normal. The chest radiograph on admission (Fig. 1) and a ventilation/perfusion lung scan (Fig. 2) are shown below. What abnormalities are present and what are the possible diagnoses? How would you further investigate this patient?

---

*Author for correspondence.

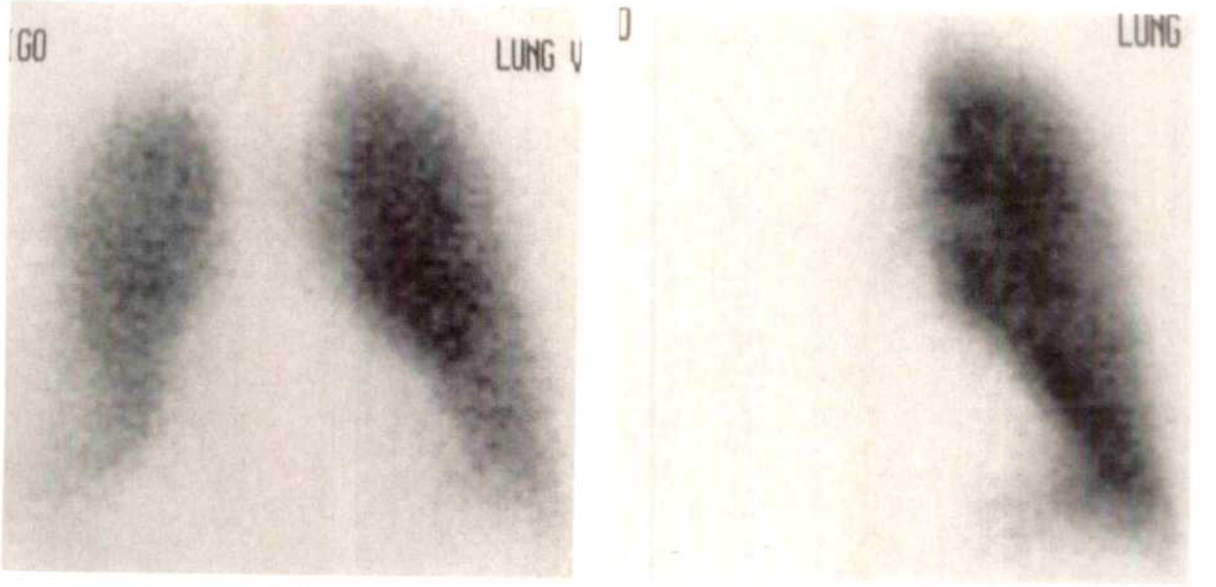

(a) (b)

Figure 2. (a) Anterior ventilation lung scan image. (b) Anterior perfusion lung scan image.

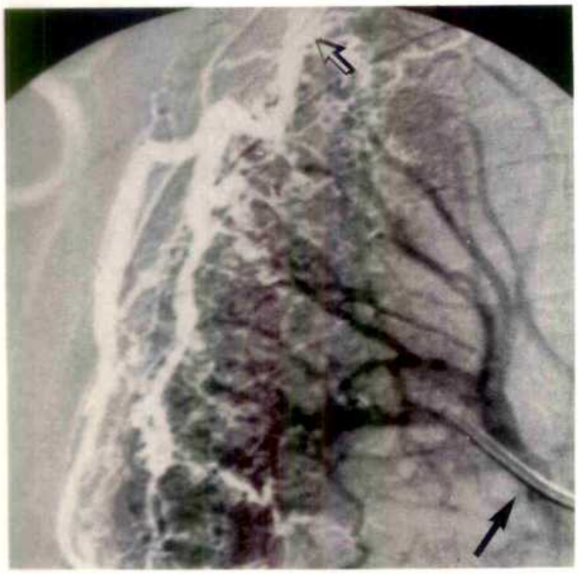

Figure 3. Digital subtraction angiogram showing both the feeding lateral thoracic artery (in white) and the draining pulmonary arterial branches (in black). The contrast medium has been injected through a selectively positioned catheter in the thoracic feeding artery (white arrow); a second catheter (black arrow) has been placed in the pulmonary artery for pressure measurements and blood gas analysis.

Table I. Causes of unilateral lung non-perfusion

Congenital
1. Severe pulmonary artery stenosis.
2. Pulmonary artery agenesis.
3. Systemic–pulmonary arterial communication.

Acquired
1. Massive thromboembolism.
2. Chronic granulomatous mediastinitis (usually because of either histoplasmosis or tuberculosis
3. Extrinsic compression, *e.g.* tumour, lymph node.
4. Systemic–pulmonary arterial communication.

The chest radiograph shows a widespread, ill defined area of increased opacity in the right lung field affecting principally the middle and lower zones. The proximal pulmonary arteries appear normal. The radionuclide lung scan shows an almost normal distribution of ventilation with minimal diminution to the right lower zone, but no evidence of any perfusion of the right lung.

The differential diagnosis of unilateral lung non-perfusion includes both congenital and acquired causes, which are listed in Table I. The relative wellbeing of the patient and the normal gases exclude the diagnosis of massive pulmonary embolism. Chronic granulomatous mediastinitis can uncommonly cause pulmonary artery occlusion and a prominent reticular pattern in the involved lung; however, the mediastinal contour is usually asymmetrically widened (Kinard et al, 1985). Severe pulmonary artery stenosis is associated with well recognized radiographic findings. Pulmonary artery agenesis may present with recurrent haemoptyses but the chest radiograph usually demonstrates a small, poorly vascularized lung, which is often associated with ipsilateral tracheal deviation, diaphragmatic elevation and a small hilum. A reticular pattern from the collateral circulation can occasionally be seen (Mehta et al, 1987).

A systemic-to-pulmonary arterio–arterial fistula causes reversal of blood flow in the affected pulmonary artery but would have to be very extensive to involve the entire lung.

Coronary arteriography showed an atrial vessel supplying pulmonary anastomotic vessels to the right hilum. A main pulmonary artery arteriogram showed non-opacification of the right pulmonary artery. The right pulmonary artery was selectively catheterized and showed reversal of flow. Subsequently, aortic, internal mammary and lateral thoracic arteriograms (Fig. 3) were performed revealing numerous systemic-to-pulmonary arterial fistulae with reversal of flow in the entire right pulmonary arterial tree. Bronchography was normal.

Discussion

Fistulous communications between the systemic arteries (excluding the coronaries) and the pulmonary artery are rare. The aetiology of reported cases includes: congenital abnormality; trauma, for example following intercostal catheter insertion, artificial pneumothorax therapy or thoracotomoy (Syme, 1975); inflammation, such as may occur following tuberculosis (Earl et al, 1972), or severe bronchiectasis; or as a complication of Hodgkin's disease (Poh et al, 1986). The lack of any previous relevant history in our patient, the extensive nature of his malformation and the presence of a coronary–pulmonary arterial anastomosis (a known congenital anomaly) all suggest a congenital aetiology for his arterio–arterial communications.

Most patients with such fistulae are asymptomatic, and the anomalies are detected because of the presence of a continuous murmur or an abnormal chest radiograph. Rib notching may be present if the intercostal arteries are involved in the afferent supply of the anomaly. The right lung has been reported as being affected twice as often as the left. Selective arteriography is the diagnostic investigation of choice as it identifies the feeding vessels and the extent of the anomaly. The disorder may be treated by either surgery or therapeutic embolization.

References

EARL, G. M., MOHR, J. A., WHITE, R. H. & STEIN, P. D., 1972. Subclavian arterial–pulmonary arterial fistula associated with healed cavitary tuberculosis. *American Review of Respiratory Disease*, *106*, 898–903.

KINARD, R. E., ORRISON, W. W. & WILLIAMS, J. E., 1985. Absent right pulmonary artery flow in a young man. *Investigative Radiology*, *20*, 785–789.

MEHTA, A. C., LIVINGSTON, D. R., KAWALEK, W., GOLISH, J. A. & O'DONNELL, J. K., 1987. Pulmonary artery agenesis presenting as massive hemoptysis: a case report. *Angiology—The Journal of Vascular Diseases*, January, 67–71.

POH, S. C., WANG, Y. T. & TAN, L. K. A., 1986. Systemic to pulmonary artery fistulas in Hodgkin's disease. *American Review of Respiratory Disease*, *134*, 1324–1326.

SYME, J., 1975. Systemic to pulmonary arterial fistula of the chest wall and lung following lobectomy. *Australasian Radiology*, *19*, 326–333.

1989, *The British Journal of Radiology*, *62*, 381–383

Short communications

Tetrachlorodecaoxygen anion complex treatment after localized X irradiation of the rat colon

By N. Breiter, MDVet, T. Sassy, MSc and K.-R. Trott, MD

Strahlenbiologisches Institut der Universität München and Institut für Strahlenbiologie der GSF, Neuherberg, Federal Republic of Germany and Department of Radiation Biology, St Bartholomew's Hospital, London

(*Received May 1988 and in revised form November 1988*)

Late radiation effects in the rat colon are assumed to be due primarily to mucosal atrophy caused by progressive damage to the vascular connective tissues of the mucosa and submucosa. The atrophic mucosa is particularly susceptible to infection, inflammation and mechanical friction exerted by the faeces (Trott et al, 1986). Experiments to control these secondary damaging factors by the application of cortisone, antibiotics and laxatives (Trott et al, 1986) resulted only in a short prolongation of the median survival time. More protection was obtained after dramatically reducing the volume of the faeces by feeding a residue-free synthetic diet, which was fully absorbable in the jejunum. However, this treatment had to be given continuously after irradiation.

Substances which stimulate tissue regeneration might be an attractive alternative to prevent progression of subclinical radiation injury to gross tissue failure. Since tetrachlorodecaoxygen anion complex (TCDO) has been described to have such properties (Hinz et al, 1984, 1986) we have investigated the effect of TCDO on the progression of chronic radiation injury after local irradiation of rat colon in a series of pilot experiments.

Table I. Observed incidences and latency times for radiation damage in the colon of treated rats

Schedule	Number of animals	Incidence of large bowel stenosis	Median latency time (days)
1 (topical)			
control	6	6	23
TCDO concentrated	7	6	30
TCDO dilute	7	7	30
2 (intravenous)			
control	8	8	26
TCDO	4	3	60
3 (intravenous)			
control	8	8	26
TCDO	8	5	32
4 (intraperitoneal)			
control	8	8	28
TCDO	5	3	29

Methods

Female Wistar/Neuherberg rats weighing 230–270 g were used for the localized irradiation of a defined part of the colon, from 26 to 50 mm proximal to the anus. The method has previously been described in detail (Kiszel et al, 1984). In all experiments a dose of 23 Gy of 300 kV X rays was given, which has been shown to produce large bowel stenosis caused by an ulcer in the colon in over 90% of animals after irradiation. The observation period was 100 days. After single doses of irradiation most ulcers occur in this period.

The animals were given TCDO after irradiation. The various doses, schedules and application techniques are shown in Table I. Topical treatment (Schedule 1) was started on Day 2 after irradiation and was given twice per week. A TCDO solution [0.5 ml Oxoferin, (OXO Chemie GmbH)] was injected with a bulb-headed cannula directly into the irradiated part of the colon. Two different concentrations of TCDO were applied: $3.1\ \mathrm{mmol\ l^{-1}}$ (concentrated) in the group of animals receiving undiluted TCDO and $0.8\ \mathrm{mmol\ l^{-1}}$ (diluted) in the group receiving TCDO diluted with saline. The local application of TCDO in these concentrations has been proven to be non-toxic (Blaszkiewitz, Oxo Chemie, oral communication, October 1988).

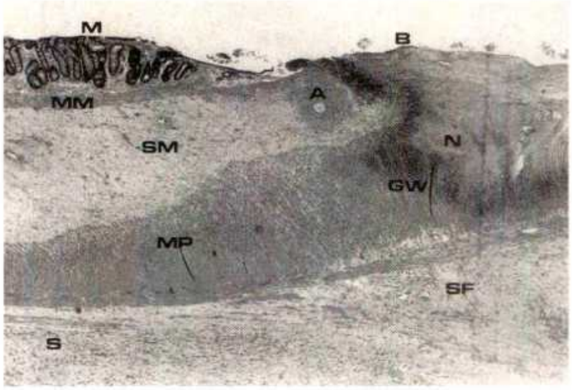

Figure 1. Radiation ulcer in the colon of the rat, 4 weeks after irradiation with a single dose of 23 Gy and after treatment with physiological saline. M = mucosa; MM = muscularis mucosae; SM = submucosa; MP = muscularis propria; S = serosa; N = necrosis; GW = wall of granulocytes; A = submucosal artery with media necrosis; B = islands of bacteria; SF = subserosal fibrosis.

Address for correspondence and reprint requests: Dr N. Breiter, Institut für Strahlenbiologie der GSF-München, Ingolstädter Landstr. 1, 8042 Neuherberg, Federal Republic of Germany.

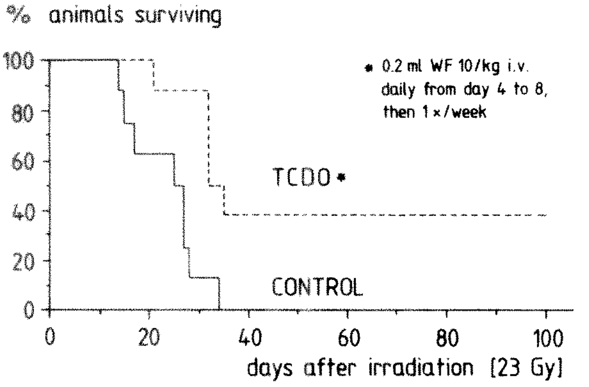

Figure 2. Survival curves for rats locally irradiated to the colon with 23 Gy and systemically treated with TCDO (Schedule 3) compared with animals treated with saline.

For the following systemic treatment schedules a more concentrated "ready to use" solution [WF 10 (OXO Chemie GmbH)] was used. This contained TCDO in a concentration of 15.5 mmol l^{-1} in an isotonic, aqueous solution. In Schedule 2, systemic treatment was given by intravenous injection at weekly intervals starting on Day 4 after irradiation. A total of 0.4 ml of WF 10 per kg body weight was injected each week. In a third experiment (Schedule 3) the number of intravenous applications was increased and the dose per injection was decreased. Thus WF 10 was given daily from Day 4 to Day 8 after irradiation and then once a week using a dose of 0.2 ml per kg body weight. In the last experiment (Schedule 4), TCDO was applied intraperitoneally twice per week, starting on Day 2 after irradiation. Since absorption after intraperitoneal application was not exactly known, the dose was increased to 0.8 ml WF 10 per kg body weight for each treatment. An acute LD_{50} for a single systemic intraperitoneal or intravenous application of WF 10 was found to be 11.3 ml per kg body weight. The daily application of 2 ml of WF 10 per kg body weight, given for a duration of 2 years, resulted in no toxicity (Blaszkiewitz, OXO Chemie, oral communication, October 1988).

Irradiated animals were given physiological saline and these acted as controls in each experiment.

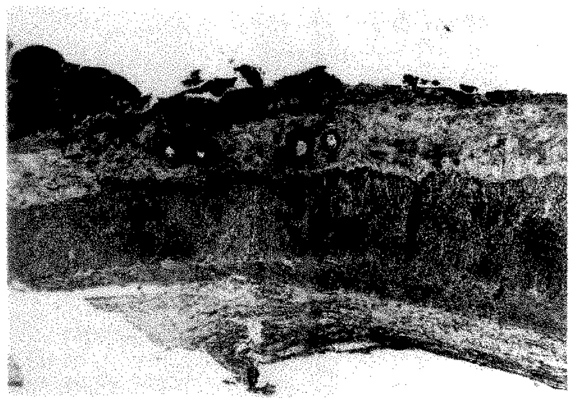

Figure 3. Radiation ulcer in the colon of the rat, 6 weeks after irradiation with a single dose of 23 Gy and treatment with TCDO. N = necrosis; MM = muscularis mucosae.

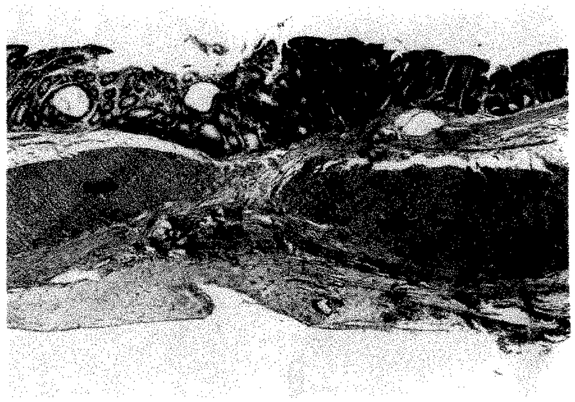

Figure 4. Healed radiation ulcer after TCDO treatment, 100 days after irradiation with a single dose of 23 Gy. MP = muscularis propria; SF = subserosal fibrosis.

Animals were palpated every other day and were sacrificed when large-bowel obstruction was diagnosed as described previously (Kiszel et al, 1984). Rectoscopy was performed every other week on all animals, starting 1 week after irradiation.

Results

The application of saline to irradiated animals had no therapeutic effect (Table I). About 2–4 weeks after irradiation "control" rats in all schedules developed an endoscopically detectable radiation-induced ulcer that extended round the whole circumference of the colon and rapidly led to rectal obstruction. Histologically (Fig. 1), mucosa, submucosa and part of the muscularis propria were necrotic, interspersed and covered with bacteria. In the periphery, the lesions were demarcated by a wall of granulocytes which invaded the adjacent circular musculature. Submucosal and subserosal tissues, including the larger vessels, were fibrotic and degenerate. The larger vessels were often occluded.

The results after TCDO treatment are shown in Table I. Schedule 2 showed a distinct increase in the median latency time and TCDO treatment also decreased the incidence of large-bowel obstruction (Table I). Schedule 3 appeared to be especially promising, and full data are given in Fig. 2. The results in the systemic application Schedules 2–4 did not appear to differ significantly. However, the incidence of large-bowel obstruction was less after systemic application (60–75%) than after local application (86–100%), although the significance of this result is difficult to ascertain. The recovery from irradiation-induced ulcers of the large bowel increased significantly ($p<0.01$) from 0/24 to 6/17 in all groups receiving systemic TCDO treatment taken together, relative to their controls.

Endoscopic observations demonstrated that all TCDO-treated animals developed ulcers, and of these 31 animals 24 subsequently developed large-bowel stenosis as shown in Table I and Fig. 2. However, these ulcers developed later and they were smaller than in the control group of rats. Histologically (Fig. 3), these ulcers appeared to be more superficial. Necrotic tissue interspersed and covered with bacteria was found only in the mucosa propria. The muscularis mucosae was not continually interrupted and often only erosions were found covered with bacteria. Granulocytes were rather diffusely distributed and did not demarcate any regions of grossly necrotic tissue. There was pronounced submucosal oedema and inflammation and a distinct subserosal fibrotic reaction. Vessel damage was much less extensive than in animals not treated with TCDO. Only moderate fibrinoid and hyalinoid degeneration of the arterial vessel walls was seen. Thrombosed vessels in the submucosa and subserosa, which is a common finding after radiation alone, was never seen.

In the seven animals that survived the observation period (100 days) after TCDO treatment, healing of radiation ulcers was seen endoscopically. Histologically (Fig. 4), a hyperplastic mucosa was found with hypertrophic crypts. These were irregular and often cystic, invading deep into the muscularis propria. The muscularis mucosae, submucosa and muscularis propria were interrupted or absent. The hyper-regenerated mucosa was abutting on to the muscularis propria. The serosa showed reactive fibrosis.

Discussion

From these experiments it can be concluded that TCDO may influence the time of onset, the severity and the healing of radiation-induced ulcers in the rat colon. Endoscopical and histological observations showed that the ulcers were smaller and more superficial after TCDO treatment and that these ulcers did not inevitably cause functional rectal obstruction but healed in a considerable proportion of the treated animals.

Before more extensive studies have been performed it is only possible to speculate on the possible underlying mechanisms. It has been shown that TCDO increases the oxygen supply in patients with poorly healing wounds (Hinz et al, 1984). Furthermore, it has been shown to activate macrophages. These macrophages have an antibacterial and mitogenic activity and can induce the production of fibroblasts, endothelial cells and vessels. These effects resulted in better wound cleaning, formation of granulation tissue and re-epithelialization (Hinz et al, 1986).

Contrary to initial expectations, the systemic intravenous or intraperitoneal application appeared superior to the local application of TCDO. If confirmed in further experiments this type of observation may help to suggest mechanisms of action and future directions of work. Futher experiments are planned using different doses and different schedules of drug and radiation in order to quantify more accurately the sparing effect observed in the pilot experiments and to establish dose-modification factors, and also to improve further the already promising initial results.

Acknowledgment

We thank OXO Chemie GmbH for subsidizing the experimental studies.

References

HINZ, J., HAUTZINGER, H. & STAHL, K. W., 1986. Rationale for, and results from, a randomised, double-blind trial of tetrachlorodecaoxygen anion complex in wound healing. *Lancet*, *i*, 825–828.

HINZ, J., KÜHNE, W. F. & STAHL, K. W., 1984. Local tetrachlorodecaoxide treatment to improve oxygen supply in non healing wounds. *Lancet*, *ii*, 630.

KISZEL, Z., SPIETHOFF, A. & TROTT, K.-R., 1984. Large bowel stenosis in rats after fractionated local irradiation. *Radiotherapy and Oncology*, *2*, 247–254.

TROTT, K-R., BREITER, N. & SPIETHOFF, A., 1986. Experimental studies on the pathogenesis of the chronic radiation ulcer of the large bowel in rats. *International Journal of Radiation Oncology, Biology, Physics*, *12*, 1637–1643.

Iotrolan in selective bronchography via the fibreoptic bronchoscope

By S. K. Morcos, FRCS, FFRRCSI, FRCR, S. V. Baudouin, MRCP, P. B. Anderson, MA, FRCP, R. Beedie, FRACR and R. W. Bury, BSc, MB, ChB

Department of Diagnostic Radiology and Thoracic Medicine, Lodge Moor Hospital, Sheffield S10 4LH

(*Received November 1988*)

The standard technique of selective bronchography via the fibreoptic bronchoscope using Dionosil aqueous suspension (Glaxo) as described by Flower and Shneerson (1984) has disadvantages. The medium is a thick suspension and is extremely difficult to inject. Direct injection into the suction channel may cause blockage if the channel is not adequately cleaned. Furthermore, Dionosil may induce chemical pneumonia, lung collapse and compromise of lung function if a large volume is used (Flower & Armstrong, 1986). It also augments the adverse effect of bronchoscopy on arterial oxygen saturation (Goldman et al, 1987).

These difficulties have prompted the idea of using a different type of contrast medium that can be injected directly into the suction channel of the bronchoscope without the attendant complications. The physicochemical properties of iotrolan, a non-ionic dimer, suggest that it could be useful in selective bronchography. It is iso-osmolar with blood at a concentration of 240 mgI ml^{-1} with a viscosity of 3.9 cP at 37°C. At a concentration of 300 mgI ml^{-1} it is slightly hyperosmolar (320 m osm kg^{-1}) and the viscosity is 8.1 cP at 37°C. Animal work and clinical evaluation have indicated that this medium is comparable in safety to the other low-osmolar media that are currently in wide clinical use, possibly with better neural tolerance (Hammer & Deisenhammer, 1985).

The aim of this study was to assess the safety and efficacy of iotrolan 240 in a group of patients requiring selective bronchography.

Materials and methods

Selective bronchography via the fibreoptic bronchoscope using iotrolan 240 was carried out in 11 patients, six men and five women with a mean age of 54 years (range 34–72 years).

The study was carried out with the approval of the Hospital Ethics Committee and under a licence from the Department of Health and Social Security. Written specific consent was obtained from all patients. The indications for the bronchograms were possible bronchiectasis in eight patients, a solitary pulmonary nodule in two patients and recurrent collapse of the left upper lobe in one patient. Patients less than

Table I. Incidence and grading of side-effects

Side-effects	Severity	No. of patients
Immediate (following the administration of iotrolan 240)		
Cough	Mild	1
	Moderate	1
Stomach ache	Moderate	1
Within 4 h of the bronchogram		
Vomiting	Mild	1
	Moderate	1
Nausea	Moderate	1
Pins and needles, pain in the ankles and feeling faint	Moderate	1
Within 24 h of the bronchogram		
Feeling weak	Mild	1
Vomiting	Moderate	1
Broken skin around the mouth	Moderate	1
Within 7 days of the bronchogram		
Sore throat	Mild	2
Hoarse voice	Mild	1

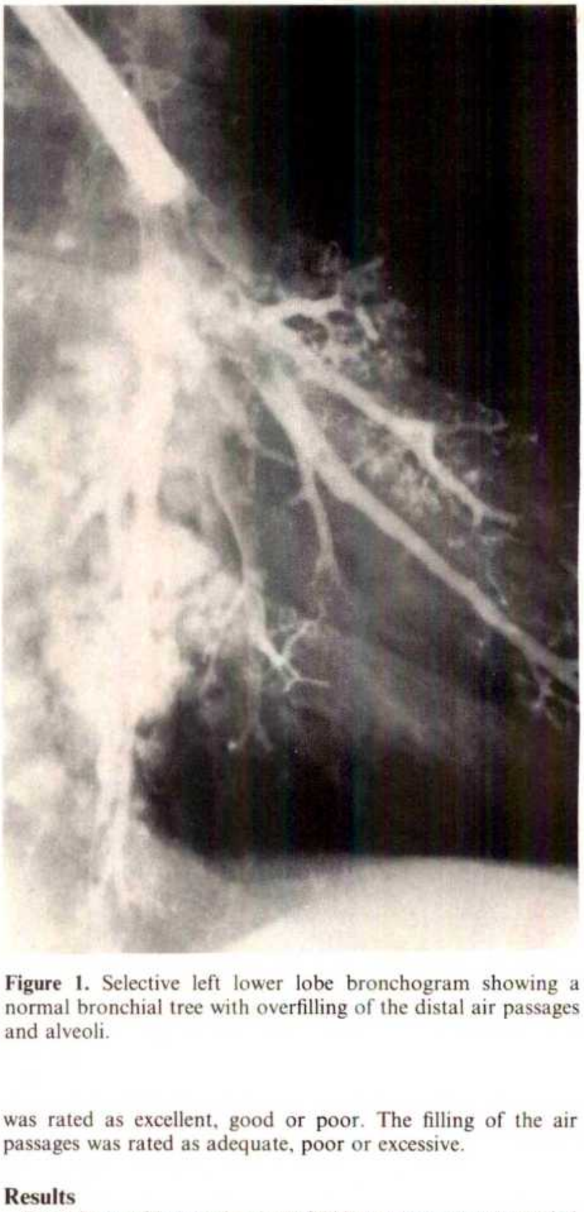

Figure 1. Selective left lower lobe bronchogram showing a normal bronchial tree with overfilling of the distal air passages and alveoli.

18 years of age, those with a strong history of allergy and those with poor respiratory function were excluded.

All patients had had a recent chest radiograph and spirometry was performed immediately prior to the examination. The bronchoscopy was performed under local anaesthesia (lignocaine, 4%) and was carried out either by P.B.A. or S.V.B. All patients received 0.6 mg atropine and 10 mg morphine as pre-medication. In addition, one patient was given 4 mg midazolam. Arterial oxygen saturation was monitored continuously by pulse oximetry (Ohmeda Biox 3700E) for 4 h from the beginning of the bronchoscopy. At the end of the bronchoscopic examination the tip of the bronchoscope was placed in the appropriate segmental or lobar bronchus and suction was carried out to clear any secretions. Iotrolan was then injected directly into the suction channel under fluoroscopic control and adequate collimation.

The amount of contrast medium used per patient was determined by the degree of filling of the bronchial tree and the number of lung segments under examination. Spot radiographs were carried out immediately at the end of the injection. The screening and the spot radiographs were supervised by S.K.M., R.B. and R.W.B. Suction via the bronchoscope was carried out at the end of the examination. A chest radiograph was taken 4 h later and only repeated at 24 h if any new abnormality was noticed. Respiratory function tests were repeated at 4 and 24 h after the examination and the patients were kept under observation in hospital for 24 h. Immediately after the examination and at the 1-week follow-up, the patients were asked a non-directive question by P.B.A. or S.V.B. to elicit the occurrence of any side-effects. Any responses were rated as mild, moderate or severe. The patients were also asked to rate their impression of the procedure on a four-point scale. All the radiographs were assessed by S.K.M. and the bronchograms were classified as diagnostic or unsatisfactory and the quality was rated as excellent, good or poor. The filling of the air passages was rated as adequate, poor or excessive.

Results

Bronchographic examination of 64 lung segments was carried out in this study (range 2–13 segments per patient). The average amount of contrast medium used per patient was 15 ml (range 8–27 ml). The incidence and severity of side-effects are given in Table I. The examination was diagnostic in nine patients (five bronchiectasis and four normal bronchial trees) and unsatisfactory in two cases. The quality of the examinations was rated good in nine patients and poor in the remaining two. Overfilling of distal air passages occurred in seven patients (Fig. 1). Underfilling was noted in one patient (Fig. 2) and adequate filling in three patients. Bronchiectasis was demonstrated in these four cases.

Complete disappearance of the contrast medium from the lungs occurred in four patients within 4 h. In seven patients a small amount of contrast medium in the alveoli and bronchial tree was noted after 4 h. This had completely resolved in the five patients who had a 24-h post-bronchogram chest radiograph.

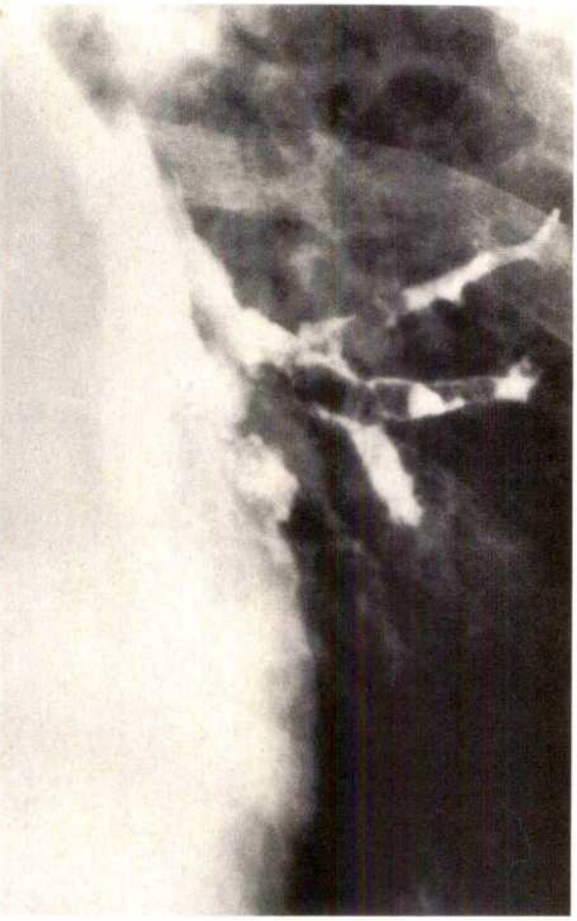

Figure 2. Selective bronchogram showing underfilling of the air passages of a bronchiectatic left lower lobe.

Four patients became significantly hypoxic (oxygen saturation <90%) during the procedure. In three cases this occurred before the administration of iotrolan.

The patients' impression of the bronchoscopic part of the examination was rated "a bit uncomfortable" by seven patients and "not unpleasant" by the remaining four. The bronchographic part was rated as "not unpleasant at all" by 10 patients and "a bit uncomfortable" by one patient.

Discussion

This pilot study demonstrates the safety of iotrolan 240 in selective bronchography in a group of 11 patients. The only significant complications were arterial desaturation, moderate nausea and vomiting. In three patients the arterial desaturation occurred before the administration of iotrolan and can be ascribed to the bronchoscopy alone. The fourth patient had bilateral extensive bronchiectasis. In all patients, oxygen saturation had returned to pre-bronchoscopic levels after 4 h. Moderate nausea and vomiting lasting for several hours occurred only in one case in which a large volume (27 ml) of contrast medium was used to examine multiple (13) lung segments.

The procedure was acceptable to the patients and was easy to perform. It was not time-consuming, with an average of 19 min for the whole examination (range 11–30 min). In contrast to Dionosil, iotrolan does not obscure bronchoscopic vision and does not interfere with further procedures following the bronchogram such as transbronchial biopsy.

The main drawback of this technique is the relatively low viscosity of the contrast medium, which can result in rapid filling of the bronchial tree and overfilling of the distal air spaces and alveoli. Therefore the timing of the spot radiographs is critical and any delay will result in inadequate demonstration of the bronchial tree. The rapid filling of the distal air spaces did not cause diagnostic difficulties in most cases. It was noted exclusively in lung segments with a normal bronchial tree, whereas in bronchiectasis slow and underfilling was observed. Thus, rapid filling can be used as an indirect sign to exclude the diagnosis of bronchiectasis. In only two cases, with a solitary pulmonary nodule, was the examination not diagnostic. In one case the bronchus of the relevant lung segment was not filled and in the other rapid filling obscured detail. The latter case was the first patient in this study. Alveolar filling did not result in any serious side-effects and the contrast medium is presumably absorbed into the circulation to be excreted by the kidneys. Complete clearance from the lungs usually occurred within 24 h of the examination.

The results of this study have encouraged us to contemplate a new trial using iotrolan 300 in a similar group of patients. It is hoped that the higher viscosity at this concentration will improve the quality of the bronchogram.

In conclusion, selective bronchography of a limited number of lung segments via the fibreoptic bronchoscope using iotrolan 240 is a safe procedure. The recommended dose is 2–3 ml per segment. Caution is necessary in those with extensive disease. It is intended to extend our observations, particularly regarding the changes in respiratory function and arterial oxygen saturation in comparison with a control group. This will be reported in a further publication. The success of this technique will revive the use of bronchography and it will become a complementary part of the bronchoscopic examination. Additional diagnostic information may be obtainable without exposing the patient to any significant extra discomfort or risk.

Acknowledgments

We are most grateful to Mr G. W. Gill, Principal Scientific Officer of the Respiratory Function Unit, and to the radiographic staff of the X-ray Department at Lodge Moor Hospital for their help and co-operation. Our thanks to Dr E. C. Carter and Mr C. Eaglen of Schering Health Care Ltd for their support and for supplying the iotrolan. Our gratitude to Mrs M. Crookes for typing the manuscript.

References

Flower, C. D. R. & Armstrong, P., 1986. *Diagnostic Radiology, Anglo-American Textbook of Imaging*, ed. by D. J. Allison & R. G. Grainger (Churchill Livingstone, Edinburgh and London), pp. 135.

Flower, C. D. R. & Shneerson, J. M., 1984. Bronchography via the fibreoptic bronchoscope. *Thorax, 39*, 260–263.

Goldman, J. M., Currie, D. C., Morgan, A. D. & Collins, J. V., 1987. Arterial oxygen saturation during bronchography via the fibreoptic bronchoscope. *Thorax, 42*, 694–695.

Hammer, B. & Deisenhammer, E., 1985. Iotrol, a new water soluble non-ionic dimeric contrast medium for intrathecal use. *Neuroradiology, 27*, 337–341.

1989, *The British Journal of Radiology*, *62*, 386–387

Correspondence

(The Editors do not hold themselves responsible for opinions expressed by correspondents)

Stem-cell depletion and grid therapy

THE EDITOR—SIR,

The stem-cell depletion hypothesis postulates that there exists for each organ a limiting critical volume, which can be repopulated by a single surviving stem cell and for which damage can be repaired by repopulation (Yaes & Kalend, 1988; Yaes et al, 1988). When the critical volume is totally depleted of stem cells, irreversible damage occurs. Certain organs such as the spinal cord yield very interesting experimental results, where the frequency of transverse myelitis has varied with the minimal critical length of cord irradiated (Hopewell et al, 1987; van der Kogel, 1987; Hopewell & van der Kogel, 1988). The critical length of spinal cord has been determined to be approximately 2–5 mm in WAG/Rij rats and <4 mm in Sprague-Dawley rats. Both sets of data indicated a critical length of spinal cord that must be irradiated to cause myelitis and that lies between 2 and 5 mm for the rat. Similar predictions have been made using a model based on functional subunits (Withers & Taylor, 1988; Withers et al, 1988).

Can there be implications of relevance to human cancer radiotherapy? Both of these sets of experimental data recall human radiotherapy observations and data where the concept of critical stem-cell volume has been tested. They suggest methods to test the concept in the practice of radiotherapy that may increase tissue tolerance specifically for late-reacting organs where tissue tolerance has limited the use of radiotherapy.

In 1909, Kohler conceived radiation-sieve therapy, and Liberson (1933) used it as a means to protect skin and normal tissues during radiation therapy. Becker (1956) used this method for supervoltage therapy, and Kaneda et al (1965) used it to show that 5-year survivals could be obtained in lung cancer patients treated by ^{60}Co sieve therapy. Urano et al (1968) studied the sieve method for tumour therapy and found that 1.23 times greater dose was required for tumour control but that skin and soft-tissue tolerance increased by a factor of 1.8. This gives an interesting grid gain factor (GGF) of about 1.5.

Furthermore, Jolles (1953) demonstrated that other indirect mechanisms could contribute to tolerance and tumour control. Grid therapy was useful for skin tumour therapy using orthovoltage radiation, and may also be useful for megavoltage radiotherapy of deep tumours lying, for example, in or adjacent to the spine or the spinal cord. The spinal cord represents the classical situation where a precision linear accelerator beam, treatment planning and beam-shaped blocks have been used to control risk of late effects.

Is it possible that grid therapy can be used for modern therapy as well? Would a grid with appropriate spacing increase cord tolerance and permit delivery of a therapeutic radiation dose more safely over the spine? It is a treatment method worthy of further study and certainly could prove useful in situations where dose has been limited because a tumour may be situated very close to the radiosensitive organ. While the spinal cord apparently represents the simplest organ responding as a linear organ with stem cells distributed in a series of "slices" (Yaes, 1988), one can also postulate other organs and sites where grid therapy may increase tolerance.

For example, the kidney, lung, brain and heart all represent late-responding organs where dose-limiting sensitivity and tolerance have restricted the dose of radiation that can be delivered. Kaneda's (1965) results suggest that grid therapy may be useful for lung cancer and large thoracic tumors. Such tumours frequently lie close to the spine, as well as to the lung and heart, and make high-dose irradiation difficult (for example, massive lung tumours, lymphoma and Hodgkin's disease). Another site is the abdomen. Bath therapy may be useful with gastrointestinal tumours but radiosensitivities limit dose and volume.

While the stem-cell depletion hypothesis and the idea of critical volume represent interesting observations for the radiobiology of the rat, there may also be implications for radiotherapists to ponder for future clinical trials. The idea of critical volume in the migration of stem cells within a limited volume from adjacent regions to prevent delayed complications is important. It is supported by experimental data not only for spinal cord but also for skin (Hopewell, 1986). Critical volume stresses the potential importance of tissue organization in many radiation effects, and the actual type and significance of those effects in long-term outcomes of therapy. Since a tumour is essentially unorganized, it also suggests a method of improving therapeutic ratios. As a means of preventing or forestalling adverse tissue reactions that presently limit our therapeutic endeavors in homogeneity of dose, critical volume may be worth investigation. The grid or sieve method may be a useful method to resurrect for many radiation therapy situations if the present reports are a guide.

Yours, etc.,

YOSH MARUYAMA
ROBERT J. YAES
MUNEYASU URANO
PUSHPA PATEL
J. CARLOS HERNANDEZ

Department of Radiation Medicine,
University of Kentucky Medical Center,
Lexington,
Kentucky 40536,
USA

(*Received November 1988*)

References

BECKER, J., WEITZEL, G. V. D. & DECKEN, C. B., 1956. Die Gittermethode bei der Strahlenbehandlung mit ultraharten Roentgenstrahlen van 15 MeV. *Strahlentherapie*, *107*, 191–196.

HOPEWELL, J. W., 1986. Mechanisms of the action of radiation on skin and underlying tissues in radiation damage to the skin. In *Radiation Damage to Skin*, ed. by H. Jammet, F. Dabwon, G. B. Gerber, J. W. Hopewell, J. L. Haybittle & L. Whitfield, *British Journal of Radiology*, Suppl. 19, (British Institute of Radiology, London), pp. 39–47.

HOPEWELL, J. W., MORRIS, A. D. & DIXON-BROWN, A., 1987. The influence of field size on the late tolerance of the rat spinal cord to single doses of X rays. *British Journal of Radiology*, *60*, 1099–1108.

HOPEWELL, J. W. & VAN DER KOGEL, A. J., 1988. Volume effects in the spinal cord. *British Journal of Radiology*, *61*, 973–975.

KOHLER, A., 1909. Zur Roentgentiefetherapie mit

Messendosen. *Münchener Medizinische Wochenschrift*, *56*, 2314–2316.

Jolles, B., 1953. *X-ray Sieve (Grid) Therapy in Cancer: A Connective Tissue Problem* (Little, Boston).

Kaneda, H., Maeda, M., Oku, T., Kobayashi, T. & Nakatsuka, J. 1965. Heilungsresultate beim Bronchialkarzionoma mittels Siebbestrahlung. *Strahlentherapie*, *126*, 27–91.

Liberson, F., 1933. Value of multi-perforated screen in deep x-ray therapy: preliminary report on new methods of delivering multiple erythema doses without permanent injury. *Radiology*, *20*, 186–195.

Maeda, M., Kobayashi, T., Nakatsuka, J., Yamada, C., Urano, M. & Imemura, T., 1964. The influence of the structure of a telecobalt sieve to inhomogeneity quotient and mean depth doses. *Nippon Acta Radiologica*, *24*, 395–403.

Urano, M., Kaneda, G., Shimazaki, S. & Hayashi, S., 1968. Radiation dose tumor-control assays for irradiation through a sieve. *American Journal of Roentgenology*, *102*, 38–42.

van der Kogel, A. J. 1987. Effect of volume and localization on rat spinal cord tolerance. In *Radiation Research: Proceedings of the 8th International Congress*, ed. by E. M. Fields, J. F. Fowler, J. H. Hendry & D. Scott (Taylor & Francis, London), p. 352.

Withers, H. R. & Taylor, J. M. G., 1988. Volume effects in spinal cord. *British Journal of Radiology*, *61*, 973.

Withers, H. R., Taylor, J. M. G. & Maciejewski, B., 1988. Treatment volume and tissue tolerance. *International Journal of Radiation Oncology, Biology, Physics*, *14*, 751–760.

Yaes, R. J., Gorman, S., Berner, B., Kalend, A. & Maruyama, Y., 1988. Comment on the recent results of Hopewell, Morris and Dixon-Brown on radiation myelitis produced by irradiation of very short segments of rat spinal cord. *British Journal of Radiology*, *61*, 967–969.

Yaes, R. J. & Kalend, A., 1988. Local stem-cell depletion model for radiation myelitis. *International Journal of Radiation Oncology, Biology, Physics*, *14*, 1247–1259.

Effect of cirrhosis on accuracy of $^{99}\mathrm{Tc}^{\mathrm{m}}$-tin colloid scintigraphy and ultrasound scanning in diagnosis of hepatocellular carcinoma

The Editor—Sir,

As diagnostic imagers for the largest alcohol detoxification institute in the United States, we were interested in the report by Dr Powell-Jackson and associates (1987), which compared the accuracy of radiocolloid scintigraphy and ultrasound in the diagnosis of hepatocellular carcinoma (HCC) in cirrhotics.

While we agree that advanced parenchymal disease of any sort reduces both the sensitivity and specificity of scintigraphy for space-occupying disease, we differ with the authors' preference for ultrasound to detect HCC in a cirrhotic patient. In our experience and that of the few who have reported their findings (Higashi et al, 1972; Langhammer et al, 1972; Manfredi et al, 1973; Silberstein, 1976; Teates et al, 1978; Cornelius & Atterbury, 1984; Gentili et al, 1985; Copper 1987), the gallium–radiocolloid dual-tracer methods is the most accurate non-invasive imaging technique (surpassing computed tomography, magnetic resonance imaging and ultrasound) for HCC diagnosis.

Apart from a significant pre-test possibility of hepatic abscess, the finding of focal or substantial gallium uptake in a region of reduced radiocolloid activity is strong evidence for HCC. Our preferred strategy is to perform the dual-tracer study first and use ultrasound to assess equivocal results or provide biopsy guidance to confirm positive cases.

Yours, etc.,

C. Richard Goldfarb
Fukiat Ongseng
Howard Finestone

Department of Radiology,
Division of Nuclear Medicine,
Beth Israel Medical Center,
New York 10003,
USA

(*Received August 1988*)

References

Cooper, J. N., 1987. Hepatic carcinoma. *Gastroenterology Clinics of North America*, *16*, 591–602.

Cornelius, E. A. & Atterbury, C. E., 1984. Problems in the imaging diagnosis of hepatoma. *Clinical Nuclear Medicine*, *9*, 30.

Gentili, A., Sfakianakis, G., Jeffers, L. J., Reddy, K., Schiff, E. & Serafini, A. N., 1985. Gallium-67 scintigraphy in the evaluation of patients with clinical or laboratory evidence of hepatoma. *Journal of Nuclear Medicine*, *26*, P109.

Higashi, T., Nakayama, Y., Murata, A., Nakamura, K., Sugiyama, M., Kawaguchi, T. & Suzuki, S., 1972. Clinical evaluation of ^{67}Ga-citrate scanning. *Journal of Nuclear Medicine*, *13*, 196–201.

Langhammer, H., Glaubitt, D. & Grebe, S. F., 1972. Gallium for tumor scanning. *Journal of Nuclear Medicine 14*, 208–214.

Manfredi, O. L., Quinones, J. D. & Bortok, S. P., 1973. In *Medical Radioisotope Scintigraphy* (International Atomic Energy Agency, Vienna), Vol. 2, pp. 583–594.

Powell-Jackson, P., Forbes, A., Michell, M. & Williams, R., 1987. Effect of cirrhosis on accuracy of $^{99}\mathrm{Tc}^{\mathrm{m}}$-tin colloid scintigraphy and ultrasound scanning in diagnosis of hepatocellular carcinoma. *British Journal of Radiology*, *60*, 1221–1222.

Silberstein, E. B., 1976. Cancer diagnosis: the role of tumor imaging radiopharmaceuticals. *American Journal of Medicine*, *60*, 226–237.

Teates, C. D., Bray, S. T. & Williamson, B. R. J., 1978. Tumor detection with the gallium citrate. *Clinical Nuclear Medicine*, *3*, 456–459.

(*Author's reply*)

The Editor—Sir,

In reply to the letter of Goldfarb, Ongseng and Finestone, we have no evidence to support or refute the contention that the gallium–radiocolloid dual-tracer method is the most accurate, non-invasive imaging technique for HCC diagnosis. We would be interested to see their detailed results.

Yours, etc.,

P. R. Powell-Jackson

The Maidstone Hospital,
Hermitage Lane,
Maidstone,
Kent ME16 9QQ

(*Received September 1988*)

1989, *The British Journal of Radiology*, 62, 388–389

Secretion of radioactivity in breast milk following administration of ^{123}I hippuran

The Editor—Sir,

Administration of a radiopharmaceutical to a lactating mother will result in the secretion of radioactivity in her milk, and her breast-fed infant will receive a radiation dose from ingested activity. For many radiopharmaceuticals, there is little data available on which to base appropriate radiation protection advice (Mountford & Coakley, 1988). The recent referral of a hypertensive lactating mother for an ^{123}I-OIH dynamic renal scan (DRS) provided an opportunity to obtain some relevant measurements.

A dehydrated DRS was performed after injection of 22 MBq of ^{123}I-OIH (Mallinckrodt Diagnostica), followed 1.5 h later by a hydrated DRS using 21 MBq of ^{123}I-OIH (Chan et al, 1988). The mother was advised not to feed her 8-week-old infant for 24 h from the end of the second DRS and to express milk at her usual feeding times. The volume, the concentration of ^{123}I and the proportion of protein associated radioactivity (after precipitation with 0.5 mol/l trichloroacetic acid) are given in Table I for each milk sample. Fitting a mono-exponential decay curve to the measured activity concentrations by the method of least squares gave an effective half-life of 3.5 h corresponding to a biological half-life of 4.8 h.

In order to make valid comparisions between different sets of secretion data, a common method of analysis has been proposed as follows (Mountford & Coakley, 1988).

The ingested activity for uninterrupted feeding was quantified by assuming an infant consumed 850 ml of milk per day with the first feed at 3 h after injection and 4 h between each subsequent feed (International Commission on Radiological Protection (ICRP), 1975). The concentration of activity in each feed was taken from the curve fitted as above. It was calculated by this method that an infant would ingest 0.43 MBq, which was equivalent to 1.2% of the administered activity when given as a single injection. The difference between this fractional ingested activity and the value of 3.9% calculated by the same method from the ^{123}I-OIH data of Rose, Prescott and Herman (1988, personal communication) may have been due to differences in the quantity of unbound ^{123}I iodide injected, and in the rates of iodide secretion and of dehalogenation *in vivo*.

Very little activity was associated with breast milk protein (Table I). If this activity was entirely in the form of free iodide, the effective dose-equivalent (EDE) to a 4 kg infant was estimated to be 0.6 mSv for a single injection of 20 MBq, using a simple body weight correction of adult EDE per unit activity and assuming a fractional thyroid uptake of 35% (ICRP, 1988). Measurements of radionuclide and radiochemical purity were not made, but the manufacturers specified that less than 5% of the iodine was not bound to hippuran, ^{124}I was absent, and the ^{125}I activity was less than 0.6% of the ^{123}I activity at the calibration time. Taking the concentration of ^{125}I in this first feed to be 0.6% of that for ^{123}I, the ^{125}I contamination was estimated to contribute a further EDE of 0.3 mSv for a single injection of 20 MBq (ICRP, 1988).

Table I. The activity concentrations of ^{123}I measured in the patient's breast milk after the double injection of ^{123}I hippuran, the volumes of milk expressed and the proportions of the protein associated activity

Time after the second injection (h)	Volume of milk (ml)	Activity concentration (kBq/ml)	Protein associated (%)
2.9	54	2.22	3.1
6.4	32	0.80	5.8
10.4	39	0.26	6.9
21.4	103	0.05	3.1

Although the 1 mSv annual EDE limit recommended by the National Radiological Protection Board (NRPB, 1986) for members of the public was not exceeded by the total (^{123}I and ^{125}I) EDE estimated from this case for a single injection, this limit was less than the EDE of 2 mSv for ^{123}I alone calculated from the data of Rose, Prescott and Herman (1988, personal communication). Acquisition of further secretion data and confirmation of the chemical forms ingested could allow a definite period of interruption to be quantified in order to reduce the dose to the infant. Because the mammary gland is known to concentrate free iodide (Mountford et al, 1986), this period will have to refer to a specified level of unbound ^{123}I iodide contamination in addition to those for ^{124}I and ^{125}I.

Much lower values of fractional ingested activities of 0.01–0.015% have been calculated for ^{99}Tc^{m}-DTPA (Ahlgren et al, 1985; Mountford et al, 1985). However, animal experiments have shown that unbound iodide and unbound pertechnetate have the same transport mechanisms in the mammary gland (Mountford et al, 1986), and the effective half-lives in human milk of ^{123}I-OIH and ^{99}Tc^{m}-DTPA are very similar. The greater activity concentrations in milk for ^{123}I-OIH may be due to the presence of a greater quantity of the unbound radionuclide and a greater ability of the breast to secrete all the radiochemical species injected. The EDE per unit activity of ^{99}Tc^{m} is less than that for ^{123}I (ICRP, 1988), there are much greater dosimetric uncertainties for radioiodine ingestion by a newborn infant because of variations in thyroidal metabolism (Hedrick & Milavickas, 1987), and ^{123}I-OIH may contain radionuclide impurities. Therefore, it was concluded that, where possible, ^{99}Tc^{m}-DTPA should be used instead of ^{123}I-OIH for renal investigations of breast-feeding mothers.

Yours, etc.,
P. J. Mountford
A. J. Coakley

Department of Nuclear Medicine,
Kent and Canterbury Hospital,
Ethelbert Road,
Canterbury,
Kent CT1 3NG

(*Received October 1988 and in revised form November 1988*)

Acknowledgments

The authors gratefully acknowledge the help and advice of Dr P. J. Blower.

References

Ahlgren, L., Ivarsson, S., Johansson, L., Mattson, S. & Nosslin, B., 1985. Excretion of radionuclides in human breast milk after the administration of radiopharmaceuticals. *Journal of Nuclear Medicine*, *26*, 1085–1090.

Chan, O., Downes, M. O., Mountford, P. J. & Coakley, A. J., 1988. Is hydration important in dynamic renal scanning in the identification of renal artery stenosis? *Nuclear Medicine Communications*, *9*, 202.

Hedrick, W. R. & Milavickas, L. R., 1987. Re-evaluation of the newborn thyroid dose from radioiodines. *Journal of Nuclear Medicine*, *28*, 1208–1209.

ICRP, 1975. *Report of the Task Group on Reference Man*, Publication 23 (Pergamon Press, Oxford).

—— 1988. *Radiation Dose to Patients from Radiopharmaceuticals*, Publication 53 (Pergamon Press, Oxford).

MOUNTFORD, P. J. & COAKLEY, A. J., 1988. A review of the secretion of radioactivity in human breast milk: data, quantitative analysis and recommendations. *Nuclear Medicine Communications*, in press.

MOUNTFORD, P. J., COAKLEY, A. J. & HALL, F. M., 1985. Excretion of radioactivity in breast milk following injection of Tc-DTPA. *Nuclear Medicine Communications*, *6*, 341–345.

MOUNTFORD, P. J., HEAP, R. B., HAMON, M., FLEET, I. R. & COAKLEY, A. J., 1986. Suppression of technetium-99m and iodine-123 secretion in milk of lactating goats. *Journal of Nuclear Medicine*, *28*, 1187–1191.

NRPB, 1986. *Dose Limits for Members of the Public*, NRPB-GS4 (Her Majesty's Stationery Office, London).

1989, *The British Journal of Radiology*, 62, 390–392

Proceedings of The British Institute of Radiology

Imaging in stroke: how, why and when

Abstracts of papers presented at a meeting of the BIR held at the British Institute of Radiology, 36 Portland Place, London W1N 4AT, on Thursday, 13 October, 1988

Chairman: Dr I. M. Holland

Stroke: recent advances, recent dilemmas, by P. A. G. Sandercock
Computed tomography in stroke, by T. T. Lewis
Angiography in patients with cerebrovascular disease, by A. Molyneux
The role of ultrasound in stroke patients, by M. D. Hourihan
Does magnetic resonance imaging have a role in vascular disease? by B. S. Worthington

Stroke: recent advances, recent dilemmas

P. A. G. Sandercock
Department of Clinical Neurosciences, Western General Hospital, Edinburgh EH4 2XU

There have been several important advances in the understanding of the epidemiology, clinical features, clinicopathological classification and management of stroke. About 100 000 patients each year in the UK suffer a first-ever stroke. Projections from the Oxfordshire Community Stroke Project suggest that this number will rise to about 133 000 a year by the year 2023, although the number of patients newly handicapped by stroke will not rise. Clinical classification has improved and now reasonably homogeneous groups of patients can be identified with similar underlying pathological mechanisms. Clinical trials have now identified effective means of secondary stroke prevention; antihypertensive agents, antiplatelet therapy, cholesterol lowering and smoking cessation are all of proven benefit. Trials are underway of anticoagulants and antiplatelet therapy in atrial fibrillation and carotid endarterectomy for carotid stenosis. Laboratory progress has identified a number of agents that hold promise in the treatment of acute stroke. However, these advances have also highlighted problems in the clinical care of patients with stroke and in research in acute stroke treatment and secondary stroke prevention. In the UK, stroke care is delivered haphazardly and unequally. There is no triage of patients to select those most likely to benefit from specialist investigations such as computed tomography or angiography. Stroke due to cerebral infarction is often clinically indistinguishable from stroke due to primary intracerebral haemorrhage. It is important that any patient who is to be started on aspirin or anticoagulants should have a CT scan before treatment is started, yet CT is only available in 40% of health districts in England and Wales. This creates dilemmas for clinicians. Improvements in clinical trial methodology and advances in the laboratory have encouraged rapidly expanding trials of treatment in acute stroke, but, unfortunately, the current organization of stroke care is not at all favourable for the advancement of clinical trials in acute stroke in the UK. In conclusion, there has been a great improvement in knowledge in all aspects of acute stroke: clinical features, epidemiology, treatment and prevention. However, progress has also created dilemmas for clinicians and researchers alike.

Computed tomography in stroke

T. T. Lewis
Department of Neuroradiology, Frenchay Hospital, Bristol BS16 1LE

Computed tomography (CT) is the most accessible technique for imaging cerebral vascular disease; 20% of all CT examinations may be for presumed stroke. In addition to the demonstration of vascular calcification, aneurysms, subarachnoid haemorrhage and intracerebral haemorrhage, it is valuable for assessment of cerebral infarction. It can exclude haemorrhage (10% of all strokes) if anticoagulant therapy is proposed. Seventy-five per cent of strokes occupy a single territory, the commonest being in the territory of the middle cerebral artery (60%). Posterior fossa infarction (10%) is not as readily shown. Fifty per cent of infarcts can be detected by CT at less than 12 h, rising to 80% at 24 h. A normal scan with an appropriate clinical history has the same prognostic significance as one showing infarction. The first abnormalities are obscuration of the grey/white interface, low density, mass effect and, occasionally, increased density of a thrombosed artery. Between 1 and 2 weeks the infarct may become partially obscured but subsequently its margins become sharply defined and its density that of cerebrospinal fluid. Contrast enhancement has been advocated but is not usually indicated. Enhancement patterns can be ring, solid or cortical and enhancement is seen in over 80% of cases at some time, maximal at the 3rd week. There is evidence to suggest that enhancement with ionic contrast media is associated with a slightly poorer prognosis. Computed tomography should be used to establish the diagnosis in cases with clinical doubt, to exclude haemorrhage, identify surgically treatable lesions and to diagnose subarachnoid haemorrhage. It is also indicated in the investigation of patients with transient ischaemic attacks and those for whom carotid artery surgery is contemplated.

Angiography in patients with cerebrovascular disease

A. Molyneux
Department of Neuroradiology, Radcliffe Infirmary, Oxford OX2 6HE

The value of angiographic examination in patients with cerebrovascular disease must be related to the potential changes in the management of the patients that follow from the findings on angiography. This depends largely on the perceived value of surgical treatment for patients with carotid artery disease as the underlying cause of their strokes or transient ischaemic attack. At present this is unproven and trials are underway to try and establish whether carotid surgery has a role. Intravenous digital subtraction angiography (DSA) has a number of attractions. It is said to be non-invasive and provides information about the carotid bifurcations. However, it is, and can only remain, a screening test as it does not give reliable exclusion of carotid artery stenosis in a proportion of patients, the percentage of unsatisfactory studies depending on the series. Both bifurcations must be visualized in two projections to exclude significant stenosis. It also does not provide adequate information for decision on surgical management as it is impossible to image the carotid syphon and the intracranial carotid adequately on intravenous studies. Intra-arterial studies are the method of choice for demonstrating carotid disease. Whether conventional radiography or DSA is used is probably immaterial. The best catheter for use in patients with arterial disease is the Simmonds 3 (sidewinder catheter) which makes catheterization of the tortuous brachiocephalic vessels quite straightforward. The catheter has two major advantages: (i) it is only possible to catheterize the common carotid artery and in most patients it is not possible to reach the bifurcation and (ii) it does not require the use of a guidewire in the brachiocephalic vessels. There are some indications for angiography in the demonstration of other forms of cerebral vascular disease, *e.g.* patients with subarachnoid haemorrhage or parenchymal haemorrhage, and patients with vasculitic illnesses in whom it is uncertain whether a cerebral vasculitis is present. Occasionally a lesion on computed tomography or magnetic resonance imaging may be the basis of cerebral vascular disease or other pathology, and sometimes in posterior fossa, ischaemia, looking for subclavian stenoses or vertebral stenoses which may be amenable to surgery or angioplasty.

The role of ultrasound in stroke patients

M. D. Hourihan
Department of Radiology, University Hospital Wales, Cardiff

The cerebrovascular symptoms comprising the stroke syndrome, including amaurosis fugax and transient ischaemic attacks, arise principally from either intracranial or extracranial vascular disease. Management of extracranial carotid disease has either been undertaken without investigation or it has depended on angiography to document carotid stenosis. The deficiency of this anatomical approach, including the limitations of angiography, its invasive nature and the absence of functional information, has aided the development of ultrasound techniques to provide both anatomical and functional information about the arteries and flow of blood within them. Barber et al (1974) reported the use of ultrasound to provide simultaneous high-resolution real-time B-mode images of arteries and functional information about blood flow by spectral analysis. This is duplex scanning. High-resolution B-mode imaging shows the vessel walls clearly contrasted against the echolucent blood-filled lumen. Images can show the wall thickness, the presence or absence of stenosis, the presence or absence of plaque and its density (fibrous or calcified), intraplaque haemorrhage and irregularities of the wall or ulceration. These anatomical details are greater than those seen on angiography (Rubin et al, 1987), and are important if we consider ulceration to be the location of mural thrombus, the source of fibrin or platelet emboli, and intraplaque haemorrhage to be the reason for cholesterol or atheromatous emboli. Spectral analysis allows assessment of the velocity of the cellular elements of the blood. Each vessel has a characteristic spectral display, which alters when the vessel is diseased. The principal changes are an increase in the peak frequency caused by a stenosis and or widening of the range of velocities in turbulent flow, especially distal to a stenosis. The degree of stenosis is assessed from the spectral analysis and its accuracy has been compared with angiography (Dreisbach et al, 1983). The role of ultrasound in stroke patients is established even though it may be neither universally acknowledged nor precisely defined. There is a defined role in screening patients with either TIAs or frank stroke and a strong case can be made for the use of duplex in monitoring the state of the carotid arteries when following the response to medical or surgical treatment. In many centres the usual management of the stroke patient has depended on the exclusion of an intracranial bleed by computed tomography and then, unless enthusiastic surgeons demand angiography, to start the patient on aspirin. The newer trend is for duplex scanning to be increasingly used to measure the degree of stenosis, to look at the morphology of the vessel wall and to monitor the progress of disease in the vessel wall (Spencer, 1987). The advantages of this cheap, non-invasive, reproducible investigation are to provide functional data and qualitative evaluation of plaque in multiple planes.

References

Barber, F. E., Baker, D. W., Nation, A. W. C., Strandness, D. E. & Reid, J. M., 1974. Ultrasonic duplex echo-Doppler scanner. *IEEE Transactions on Biomedical Engineering, 21,* 109–113.

Dreisbach, J. N., Seiberk, C. E., Smazal, S. F., Stavros, A. T. & Daigle, R. J., 1983. Duplex sonography in the evaluation of carotid artery disease. *American Journal of Neuroradiology, 4,* 678–680.

Rubin, J. R., Bondi, J. A. & Rhodes, R. S., 1987. Duplex scanning versus conventional arteriography for the evaluation of carotid artery plaque morphology. *Surgery, 102,* 749–755.

Spencer, M. P., 1987. *Ultrasonic Diagnosis of Cerebrovascular Disease* (Martinus Nijhoff, Dordrecht).

Does magnetic resonance imaging have a role in vascular disease?

B. S. Worthington
Division of Radiology, University Hospital, Nottingham

Studies of ischaemic infarction in experimental animals have shown that magnetic resonance imaging (MRI) can reliably detect tissue changes within hours as areas of high signal intensity on T_2-weighted spin-echo sequences. In ischaemic tissue the fractional change in specific gravity is less than that in water content accounting for a greater sensitivity of MRI compared with computed tomography (CT), a finding which remains to be exploited in the evaluation of proposed interventions in acute ischaemia, such as reperfusion and calcium channel blocking agents. Macroinfarcts involving areas of brain conforming to the territories of major arteries and their branches display similar patterns to those well documented on CT but with a much clearer delineation of those in the posterior fossa. The ability to map the contour of major extra- and intracranial vessels and study flow patterns within the major venous sinuses can be readily identified. the major arteries supplying a particular territory. Thrombosis within the major venous sinuses an be readily identified. Lacunar infarcts within the basal ganglia and centrum semiovale are a frequent finding in the scans of hypertensive patients. Multifocal areas of high signal intensity on T_2-weighted spin–echo images are a frequent finding in asymptomatic elderly patients. Many of these areas of abnormal signal intensity are thought to represent areas of ischaemic demyelination and as such are a marker of vascular disease, showing an increased incidence in those with multiple risk factors. The appearances on MRI of haemorrhage are complex, evolve with time and depend on the technique used for their demonstration. At least four different paramagnetic species are implicated which alter relaxation times and change tissue susceptibility. It is now clear that acute, subacute and chronic resolving haemorrhage can all be clearly characterized. Sources of haemorrhage such as angiomas are readily identified on flow sensitive sequences and MRI can be used to monitor treatment whether by embolization or surgery.

1989, *The British Journal of Radiology*, *62*, 393–398

Book reviews

Sectional Fetal Anatomy In Ultrasound. By A. Staudach, pp. x + 198, 1987 (Springer-Verlag, Berlin), DM120.
ISBN 3-540-18213-6 (Berlin)
0-387-18213-6 (New York)

One would think that with ultrasound such a well established technique in obstetrics, extending back over 20 years, a book devoted almost entirely to normal anatomy would be superfluous. This is, however, most certainly not the case with this present text, which has been most carefully and painstakingly produced and crystallizes the author's extensive experience of ultrasound over more than 20 years. The book describes the basic ultrasound techniques employed and also those required for producing the pathological sections which complement the ultrasound appearances. It is most refreshing to find an author who goes into great detail about the different techniques, including *in vitro* imaging, and explains those techniques which have failed as well as those which have succeeded. There is also a very frank discussion of missed diagnoses which will give encouragement to all those concerned with this aspect of ultrasound diagnosis. This is followed by a further general section emphasizing the scanning protocol required for comprehensive evaluation of the fetus, followed by specific sections on the examination of the head, the spine and spinal cord, the neck, the thorax, the abdomen, genito-urinary tract and the skeleton.

Whilst there are a few examples of pathological conditions, most of the text emphasizes technique, pitfalls and normal appearances. The list of references is very extensive and up-to-date. The author has not flinched from casting doubt on some well accepted measurement protocols, producing evidence, where necessary, of the shortcomings of some of these.

It is hard to criticise such a well produced book, but the separation of text from figures sometimes by two or more pages restricts easy reference. It contains more detail than would be required for candidates undertaking the Diploma in Medical Ultrasound, but will be of immense interest to all those involved in confirmation of fetal normality, and will provide most readers with further stimulation to improve their own technique. This book should find a place on the library shelves of every department undertaking obstetric ultrasound and will be of great interest to the more experienced obstetric ultrasonographer. The price (120 DM) is a reflection of the high quality and number of the illustrations and is not excessive.

D. W. Pilling

Bioeffect Literature Reviews 1980–1987. By H.-D. Rott, p. 88, 1988 (Springer-Verlag, Berlin), DM15.
ISBN 3-540-18340-X (Berlin)
0-387-18340-X (New York)

People wanting to be familiar with scientific studies of the bioeffects of ultrasound will certainly find it helpful to have critiques of more than 50 recently published papers on the subject. The "Watchdog Group" of the European Federation of Societies for Ultrasound in Medicine and Biology has met annually since 1979. One of the tasks of the nine members of the Group is continuously to assess the existing documentation, particularly in relation to any new evidence that might modify existing conclusions and recommendations.

Although this little book purports to review the literature for 1980–87, in fact it covers the period 1978–86. It is interesting — and maybe even significant — that most of the papers assessed were published in 1982 and that the literature seems now to be decreasing in volume! From the point of view of the diagnostic radiologist, however, what is important is that the various statements and letters from the watchdogs, reproduced at the end of the book, have little negative to say about the safety of ultrasound, apart from reinforcing the wisdom of minimizing the exposure. For example, they say that "Routine clinical scanning of every woman during pregnancy is not contraindicated by the evidence currently available from biological investigation, and its performance should be left to clinical judgement".

This conveniently compact and inexpensive volume should be in every portfolio of ultrasonic bioeffects publications.

P. N. T. Wells

Computed Tomography in Trauma. By Barry D. Toombs and Carl M. Sandler, pp. viii + 215, 1987 (W. B. Saunders, Philadelphia), £45.00.
ISBN 0-7216-8889-6

This compact book reviews the role of computed tomography in trauma, and is derived principally from the experience of authors from Texas. The two short opening chapters provide some useful background clinical information on the causes and consequences of trauma and a brief outline of the clinical evaluation of the traumatized patient. Subsequently the book is divided into sections covering the role of CT, and abnormalities found, in patients with chest, abdominal, pelvic, spinal and facial trauma. There are additional chapters covering the sequelae of thoracic and abdominal trauma.

The book principally concerns the role of CT in diagnosis and management of clinical problems related to trauma, but intentionally not head injury. It offers a well balanced view of the place of CT in relation to other imaging techniques and acknowledges that there are some limitations to CT, for example in the evaluation of abdominal injuries, where bowel and mesenteric abnormalities may be difficult to diagnose. All sections include useful practical details of optimum CT technical factors. There is also information as to suitable sedation for children requiring scanning, and the rationale and technique for contrast enhancement before and during scanning.

The book is profusely illustrated, and the scans are of very acceptable quality, considering that many of these patients may not have been easy to scan. The role of image planar reformations is covered in some detail, particularly in the chapters on spinal and facial trauma, and, appropriately, in these sections there is also an introduction to three-dimensional CT imaging. Useful relevant references are given at the end of each chapter, and simple but informative line diagrams are used effectively in several of the chapters, although I found my attention flagging at the rather long and detailed legends to the figures.

This small book contains much useful information, and it would make an invaluable bench book for any department with CT scanning facilities. Radiological registrars approaching the final Fellowship examination and their more senior colleagues would glean useful facts from this text, as would those working in casualty departments. It is moderately priced and would make a useful addition to any departmental library. A good buy.

J. E. Adams

Computed Tomography of the Temporal Bone and Orbit. Technique of Direct Multiplanar, High-resolution CT and Correlative Cryosectional Anatomy. By Frans W. Zonneveld, pp. xii + 202, 1987 (Urban & Schwarzenberg, Munich), £82.50. ISBN 3-541-72231-2

In the previous two decades, polytomography provided the ultimate imaging mode for fine bone detail, but as Hounsfield correctly foresaw, computed tomography with its greater disciminatory efficiency could supplant polytomography when thin sections and reduced pixel size became available. This dramatic improvement in spatial resolution took place in the early 1980s. Meantime, soft-tissue density discrimination, the original forte of CT, has now to some extent passed to magnetic resonance. Thus the challenge of spatial resolution for the demonstration of small osseous structures within the petrous temporal bone is now by CT.

As pointed out in the introduction to this book, the temporal bone and orbit make a more convincing test object than the plastic geometrical phantoms used by physicists. This goes some way to explain how this comprehensive book, including clinical applications, came to be written by a physicist working for one of the major manufacturers of X-ray equipment. Fortunately, the work is almost, but not entirely, free of any bias towards the machines of that company.

The book is superbly produced and illustrated with good clear line drawings and diagrams. However, I found the colour prints of histological sections not always helpful in understanding the anatomy, although they must account in large part for the price of £83. This is perhaps a personal niggle and it is difficult to see how the correlation between CT and histology could be improved except by labelling the latter. The English is immaculate, the text without fault and the bibliography comprehensive. The accounts of the development of CT and its application to imaging investigations of eye and ear are fascinating and must be the ultimate work in this field. I liked particularly the clear, informative discussions on improvement of spatial resolution with the problems of partial volume averaging, radiation dose and noise — difficult concepts for clinicians but recommended reading for all who wish to understand the limitations as well as the capabilities of CT.

For all its excellence, it is difficult to see a market for this book. The clinical applications cover just two aspects of temporal bone abnormality, the second of which — the vestibular aqueduct — is of dubious practical value even in specialist centres. Likewise, two clinical problems affecting the orbit are considered, namely space-occupying lesions and trauma to the bony margins of the orbit. This does not seem very logical. It might have been better to keep to the normal section anatomy of temporal bone and orbit but here there is, in the opinion of the writer, an overdose of different projections for the temporal bone. However, I would agree that direct imaging is preferable to reformatting, as long as the required patient position can be obtained and careful consideration is given to radiation dose. Gantry tilt and a swivelling table are necessary for several of these projections, which seem to have found little favour with most authorities.

Mainly in relation to these aspects, there is a very readable account of the fundamentals of CT, and the book will be a valuable reference work for specialist radiology departments. However, it hardly seems appropriate for district general hospitals and its high price seems to preclude individual purchase.

PETER PHELPS

Computed Cranial and Spinal Imaging. A Practical Introduction. By John M. Stevens, Alan R. Valentine and Brian E. Kendall, pp. xii + 248, 1987 (Heinemann Medical, London), £35.00. ISBN 0-433-00001-5

The first edition, *A Practical Introduction to Cranial CT*, by A. R. Valentine, P. Pullicino and E. Bannan, was a popular text and deservedly so, with its clear account of the basics and differential diagnosis all fitted into a handy, pocket-sized book. It was with great interest that I approached the new edition, now by J. M. Stevens, A. R. Valentine and B. E. Kendall. The authors have three challenges: (1) a comparison with the first edition; (2) choice of an introductory text, which is particularly difficult when the target readership is broadly based; and (3) where to place MRI when neuro-imaging is still evolving.

It is surprising that the introduction is a comparison between CT and MRI, when logically this should be at the end, after discussion of the various advantages and disadvantages, and I suspect the authors felt as if they were on shifting sands during the gestation period. The first chapter proper is an account of the technical aspects of CT and MRI, although there is a further chapter on the physical basis of image production in MRI. I am never quite sure of the value of this format in an introductory text; CT is so well established it is perhaps superfluous to discuss the physical basis and any description of MRI will be superficial and tend to confuse rather than clarify. The chapter on "Anatomy — functional aspects" is excellent, but statements such as "The substantia gelatinosa inhibits incoming sensory information presynaptically; it contains numerous opiate binding sites activated by endorphins, which are opiate-like polypeptide neurotransmitters abundant in the region. Cells in other layers respond preferentially to certain types of receptor, conferring some modality specificity on the cord" inhibit rather than stimulate! One has to be very keen to delve further and I fear this otherwise very good section will generally be unread. "The abnormal CT scan" is a very well organized lucid account which sets the scene for the ensuing chapters.

The pathology is divided into broad anatomical sites, with further aetiological subdivisions, though there are separate chapters on inflammatory disease and the post-operative scan. A very wide range of diseases is described, discussed and illustrated either by CT, MRI or both but it is a pity the tables, which fitted so well into the previous text, have been relegated to the appendices. Did the authors consider the novice when placing "Mass-infarct or glioma" last before the index? This is the type of problem the less experienced and skilled face frequently and I would have welcomed an earlier and more explanatory text and illustrations. There is, in general, a lack of balance and, personally, I would swap the rare conditions, detailed anatomy (there are very good anatomical texts, as the authors acknowledge) and the physics for more elaboration on everyday practical problems. Surely an introductory text should have a separate chapter with clear guidance on cerebral trauma?

The style of writing is flowing and elegant though, in comparison with the more forthright and terse approach usually found in medical texts, this prose sounds a little verbose. The occasional spelling mistake was not intrusive. The images are, by and large, of very good quality but some of the axial T_2 weighted images are rather low in contrast with further degradation by the matt paper. A disappointing number of the images are incorrectly positioned or annotated.

How have the three challenges been met? It is probably not fair to compare the two editions, as their aims are different; there is a lack of balance for the novice and another edition will be required to find the balance with MRI.

In spite of all these criticisms this is still a very good book and deserves to succeed. There is no doubt that with careful reading, the trainee in radiology or neurosciences would have a very sound base upon which to build. Every library should have a copy but individuals should have a "good read" at the booksellers before purchase. The first edition had instant appeal but now a more comprehensive and erudite approach is preferred — the thinking person's guide. It is more expensive, of course, but still good value.

C. E. L. FREER

Atlas of Endourology. By K. Amplatz and P. H. Lange, pp. xviii + 344, 1986 (Year Book Medical Publishers Inc, Chicago), £91.00.
ISBN 0–8151–0160–0

Recently there have been many advances in the interventional field, particularly in uroradiology. With the advent of new methods of dealing with urinary calculi, strictures and tumours, new techniques are being evolved and refined and this atlas is one of several publications about these techniques. The authors say that endourology, in the broadest sense, is the discipline that involves closed intervention to any part of the urinary tract for visualization and manipulation. However, they concede that endourology most often refers to procedures done through percutaneous approach to the kidney and collecting system and also to retrograde ureteroscopy.

The atlas, offering a pictorial description of the major technical manoeuvres, is aimed at beginners in endourology as well as those with some experience. The essential but often neglected subject of radiation protection is clearly and succinctly covered in the opening chapter and the succeeding 10 chapters discuss and illustrate the various aspects of percutaneous nephrostomy. There are 13 chapters on the subject of percutaneous nephrolithotomy and ureteric procedures get another five chapters. The relevant anatomy of the kidney and the ureter is adequately mentioned and there is a good description of the steps in the procedures, the choice of equipment including catheters, tubes and stents. The transplant kidney is not forgotten nor are the potential complications of the procedures and their management. Attention is drawn to the changing role of endourological procedures relating to the extracorporeal shock-wave lithotripsy, which is becoming increasingly available, even in the UK.

However exhaustive the book may seem, there are a few omissions, *e.g.* application of lasers and endoscopic treatment of tumours of the collecting system. There are numerous illustrations of radiographs, photographs and line diagrams which, in general, are of good quality, but some of the endoscopic photographs could have been better. This book exemplifies the team approach and effort of the radiologists and urologists in achieving their common goal.

In my opinion, and in that of urological colleagues, the authors have succeeded in their objective in providing a practical illustrated guide in the performance of endourological procedures. Priced at £91.00, this book is not expensive by current prices and deserves a place in the major radiology and urology departments.

L. N. S. MURTHY

Ultrasound Teaching Cases, Vol. 1, 2nd edn. By Hylton B. Meire, Keith C. Dewbury and David O. Cosgrove, pp. x + 189, 1987 (John Wiley & Sons Ltd, Chichester), £45.00.
ISBN 0–471–91486–X

When I reviewed the first edition of this book, I remarked that I was looking forward to Volume II. Perhaps my only disappointment about this second edition is that it does not represent a second volume. The presentation and format are the same as in the first edition. A selection of images of a particular pathology are displayed and the reader is encouraged to make his or her opinion on possible diagnoses. The ultrasound appearances are then discussed by the authors, differential diagnoses discussed and a final diagnosis presented. Most cases indicate that there was surgical and/or histological confirmation. A few pertinent references are provided where appropriate.

The cases are of a uniformly high standard and image quality if anything is better than in the first edition. Several new cases have been added to this second edition; some of these are replacements, others are additions. The image format remains that of static B-scans for the most part although the newer additions are extremely well documented, frozen, real-time images.

The book is fun as well as being informative and should be in every ultrasound department library if not on every trainee Registrar's bookshelf. However, if the first edition already sits there then I can think of little to recommend further expenditure unless the first edition is as well thumbed as my own. I am still waiting for Volume II!

P. A. DUBBINS

Atlas of Fetal Sectional Anatomy. With Ultrasound and Magnetic Resonance Imaging. By G. Isaacson, M. C. Mintz and E. S. Crelin, pp. xi + 184, 1986 (Springer-Verlag, Berlin), DM228.
ISBN 0–387–96248–4 (New York)
3–540–96248–4 (Berlin)

As an atlas this book is devoted almost entirely to images with little accompanying text. The format is the same throughout, anatomic cross sections with ultrasound and/or magnetic resonance (MR) images of the same section on the right-hand page and explanatory line diagrams of that section on the left-hand page. There are chapters on head and neck, thorax and abdomen, fetal limbs and special studies of brain development, ductus venosus and the fetal heart. Each area is covered comprehensively and systematically with sagittal, coronal and axial sections, the reader never being left in any doubt as to the location of a particular plane of section.

The anatomical specimens are of 20- and 30-week aborted fetuses and they are of uniformly high quality throughout. The accompanying line diagrams are also excellent, the only criticism of them being that they have so many labels it is sometimes difficult to locate the structures you are searching for. For the most part, there is very good correlation between the plane of section of the anatomical specimen and the ultrasound and MR images. Occasionally the orientation is a little confusing, for example, in the demonstration of sagittal sections of the head (the very first images in the book!) the occiput is on the left of the anatomical specimen but on the right of the accompanying images; later in the book, the same occurs with fetal limbs. However, these minor irritations are few and far between and in the majority of cases the anatomical ultrasound and MRI sections all correspond beautifully. All areas of the body are covered equally and there is no attempt to weight the book towards areas of particular clinical interest, *e.g.* the spine or the urinary tract.

Only just over half the anatomical sections have corresponding ultrasound images but unfortunately the quality is not uniformally high making the demonstration of ultrasound anatomy rather disappointing, particularly as the quality of the anatomical specimens is so high. This then is not a book one would recommend to anyone just starting to learn antenatal ultrasound although it may be a useful bench book for the more experienced practitioner wishing to clarify difficult anatomical sections; however, in these days of high-quality, real-time imaging, I doubt if it would be used very frequently even in this situation. The MRI coverage is more comprehensive and of better quality than the ultrasound, and if in the future antenatal MRI comes into clinical usage then it may well be here that the book is of most value.

M. R. GOWLAND

Diagnostic Imaging in Paediatrics. Ed. by Isky Gordon, pp. xviii + 313, 1987 (Chapman and Hall Medical, London), £57.50.
ISBN 0-412-22730-4

This book, according to the preface, was written with the aim of giving the paediatrician or the general practitioner with a significant paediatric workload, a comprehensive approach to the diagnostic imaging investigations in clinical problems. The cover also adds that it would give the radiologist a view of paediatricians' problems.

The first chapter is an introduction to imaging techniques, the second chapter covers psychological problems, and subsequent chapters cover the various systems: respiratory, cardiovascular, abdominal mass, oncology and haematology, urinary tract, hypertension, skeletal system, gastrointestinal tract, endocrine system and finally neuroradiology.

The first chapter describes the various techniques currently available but, for the general practitioner and paediatrician, although the cover is comprehensive, some of the explanations of imaging techniques are a little superficial: magnetic resonance imaging for example. There is a section on radiation dosage, using a mixture of old and new units, and although these have been extracted from various papers, they are somewhat confusing and the phrase "Exposures greater than 50 rads" taken out of context is misleading.

The psychological disorders are well dealt with for the clinician, but no reference is made to the psychological problems encountered in the actual investigations themselves.

Obviously the whole subject of paediatric radiology, covered in a relatively small volume, inevitably results in many of the paragraphs consisting largely of lists. This is particularly true of respiratory and skeletal systems. Flow charts and differential diagnosis lists are used and they are particularly good in the urinary tract and investigation of abdominal masses. In other instances the pathway is clearly defined for the clinician but I think the radiologist would require more detail to reach a definitive diagnosis. For example, the investigation of suspected bronchiectasis does not discuss the value of MRI or CT.

The section on neuroradiology discusses very well the philosophy of investigation, and covers the vast field well, highlighting the important clinical features.

The illustrations in general are adequate, although many of them would benefit from either line diagrams or "touched-up" radiographs, to demonstrate abnormalities only just visible; also, especially for the general paediatrician or general practitioner, some — particularly ultrasound — would benefit from arrows indicating the anatomy and pathology. In general the captions are correct, in reference to the text, although Fig. 716 is referred to in the text as hydronephrosis and later as a dysplastic kidney.

For the general practitioner with a paediatric interest and for the paediatrician some of the text proves a little superficial, and in the other instances information provided by the discussion of the detailed investigations may be of little value.

Because of the multiple authors, there is a variability of style which, although not too distracting, is definitely noticeable. Repetition is avoided by reference to the other chapters.

The book aims at a wide audience with different background knowledge. The subject is also vast and these render the production of a small comprehensive text difficult. However, the book does contain a tremendous amount of information and is well presented. For the paediatrician, it provides a comprehensive guide to what is available in the investigation of clinical disease; for the radiologist it gives a view of the whole field of paediatric radiology. I do not think that it is sufficiently detailed to take the place of a bench book for paediatric radiology departments, as more selective definitive texts are already available; it should however be available in reference libraries and radiology departments; it is well worth reading. Radiological books, because of their prolific illustrations are expensive to produce and at £57.50 the book is not cheap. For the individuals to whom it is mainly directed, *i.e.* general practitioners and paediatricians, it may prove a little too expensive to purchase.

ANDREW W. DUNCAN

Congenital Dysplasia and Dislocation of the Hip in Children and Adults. By Dietrich Tonnis, pp. xxiii + 536, 1987 (Springer-Verlag, Berlin), DM298.
ISBN 3-540-13015-2 (Berlin)
0-387-13015-2 (New York)

The stated aim of this book is to give a review of the present state of knowledge of congenital dislocation of the hip and it succeeds admirably. It is aimed at all those with an interest in congenital dislocation and dysplasia of the hip, but particularly orthopaedic surgeons and radiologists. It is a mine of information and beautifully illustrated. There is a wealth of detail on the anatomy of the hip and its radiology and an important chapter on ultrasound. There is also a thoughtful chapter on biomechanics, which emphasizes the inadequacy of load models and that the human hip is a biological system which only obeys mechanical laws to a certain degree. This is followed by a careful analysis of both conservative and operative treatment of congenital hip dislocation, based on extensive studies and particularly the collected statistics of the CHSD (Commission for the Study of Hip Dysplasia of the German Society of Orthopaedics in Traumatology). This is based on 30 centres in Austria, Switzerland and the Federal Republic of Germany producing a very large volume of data, which formed the basis of many interesting and definitive statements made in the book.

The book is well translated from the German and reads easily. It should be read by all who have an interest in congenital dysplasia and dislocation of the hip and I am sure will remain a standard work on this subject for many years.

Inevitably a large number of the references are in German and I personally do not like the references being grouped together at the end of the book rather than at the end of each chapter.

Apart from this minor criticism I can strongly recommend this book to anyone with an interest in the subject, particularly if they would find it difficult to read the original articles in German.

J. A. FIXSEN

The Dread Disease: Cancer and Modern American Culture. By James T. Patterson, pp. xiii + 380, 1987 (Harvard University Press, Cambridge, Mass.), £20.75; $31.25 (Europe).
ISBN 0-674-21625-3

This book is described by the author as a cultural history of cancer in the United States, starting in 1887. It is not a detailed study of cancer research, of therapy or of the experiences of patients. He concentrates on elucidating the ways that the dread disease has reflected social and personal careers during the modern industrial era of United States history.

By 1915 chronic illnesses such as heart ailments and cancer loomed as the most alarming and challenging medical problems of the age. The American medical profession gained unprecedented respectability, especially with the upper-middle professional classes. They developed an alliance against cancer started by surgeons and gynaecologists and then involving many other types of non-medical personnel. In 1937 Congress joined this alliance.

The persistence and growth of popular cancerphobia are the main themes of this book. By 1945 Americans became more driven than ever by dreams of good health, of conquering disease and of escaping early death, and a war on cancer has gone on with gradually increasing activities. There has always been a large percentage of individuals who have challenged the work undertaken by the professional workers in the treatment of cancer and much of this is also described in the book.

In 1885 America's war hero General Grant was dying of cancer of the mouth. Following this, there was increased knowledge about the frequent development of cancer. The deaths it causes and how it might be dealt with became more important matters. From 1890 to 1915 cancer was seen as a dread disease but the professional standing of doctors then rose strikingly. There were increases in the amounts and types of cancer therapy, with advances in the use of chemotherapy and therapeutic uses of X rays or radium. As other diseases were gradually cured the treatment of cancer became more important for the medical profession.

There was an increase in cancer deaths and surgery remained the most hopeful means of treatment. More people became concerned with the need for different types of treatment. The Government joined the fight and special finance was obtained. Doctors discovered how to cure some types of cancer. Also an increasing number of scientists developed knowledge about its treatment and the value of cancer research became increasingly important. It became more widely reported in newspapers and mass circulation magazines. After 1945 there was a rapid development of the work in cancer treatment and the ACS and NCI collected more money and arranged meetings with writers and publishers. Radiotherapy and chemotherapy became more popular and important.

Cigarette consumption per person is described in detail. In the early 1960s more than 50% of adult American males smoked and about 33% of women. By 1985 the male smokers had dropped to about 33% and the women to about 28%. Smoking caused many deaths from lung cancer and cancers of other parts of the body and considerable damage in pregnant women.

Considerable fears developed about the rapid increase of cancer and the deaths which it caused. A view developed that the Federal Government must be the source of action against cancer. Those in favour and those opposed to Cancer Establishment are both discussed. Immunotherapy was produced by NCI. Up to 1985 various forms of treatment were devised but no great change in achievement has appeared.

B. WINDEYER

Diagnostic Imaging, 2nd edn. By Peter Armstrong and Martin L. Wastie, pp. viii + 407, 1987 (Blackwell Scientific, Oxford), £19.80.
ISBN 0-632-01261-7

The first edition of this work was called *X-ray Diagnosis* and, in the words of the authors, "covered the subject of conventional radiology in reasonable detail but provided only a few pages on the imaging modalities". I confess that I never read it, but feel confident that this new edition fully justifies the title *Diagnostic Imaging*.

Aimed at medical students and young doctors in training, it is destined to achieve a pre-eminent position on their bookshelves. I am amazed that a hard-backed book, so lavishly illustrated, can be offered at a price of only £19.80. If the publishers can issue it in soft-back at a price close to £10.00 they will overcome the psychological price barrier firmly in the minds of impecunious medical students and have a best-seller on their hands! In fact I will also strongly recommend it to our first-year radiology trainees to keep them amused whilst they study for the Part I FRCR!

The book is beautifully presented, with text in easily read double columns. Illustrations are copious, well annotated and generally of high quality. It is a tribute to the printers' skills that I could find only five reproductions out of nearly 800 that were sub-optimal. (For future editions these are: Figs 2-55, 2-109, 5-69, 12-17, and 16-11. Additionally Fig. 11-21 is printed upside down.)

The authors are clearly experienced teachers, picking out of the firmament of knowledge the constellations and patterns of essential information in a precise but readable narrative, supplemented by compact lists, useful tables and quality line diagrams.

A short introductory chapter covers the use of an imaging department, basic physics of imaging, contrast media and radiation hazards. Then follow 14 chapters, each based on a body system, with a standard format in which relevant techniques and their normal appearances are covered, followed by highly selected and structured accounts of the abnormal. Where traditional methods have been superseded in clinical practice, this is made clear, and readers are introduced to the real world of contemporary clinical imaging.

It would be surprising if a reviewer could find nothing in a book with which he or she did not entirely agree, and this encounter was unexceptional. However, as the disagreements were mostly of a minor nature or coloured by personal prejudice they are best kept *sub judice*. They would not detract from my wholehearted recommendation of this excellent book.

PHILIP OWEN

Clinical Imaging. An Atlas of Differential Diagnosis. By Ronald L. Eisenberg, pp. xii + 901, 1988 (Heinemann Medical, London), £80.00.
ISBN 0-433-00042-2

> "Pattern recognition leading to the development of differential diagnoses is the essence of radiology . . . This book offers differential diagnoses for a broad spectrum of radiographic patterns, not only in conventional radiography but also in ultrasound and computed tomography . . . A wealth of illustrations is provided . . . extensive cross referencing . . ."
>
> from the Preface.

The author presents a well organized, thorough list of differential diagnosis of various radiological patterns, accompanied by high-quality photographs to aid him in this task. Furthermore, the typical imaging findings for each condition are listed, as well as additional comments to cover other possibilities and differential points. The text is easy to use, with chapters on the main organ systems commonly reviewed by radiologists, and further subdivision of each system into headings of radiographic patterns. For example, finding a diffuse reticulonodular pattern on a chest radiograph would lead one to the chest section to look up that title, and to 27 possible main considerations, elaborated to 40 diagnoses in all. The accompanying descriptions and illustrations then assist the reader in ranking choices into high and low probabilities, and it is this information which is intended to separate this text from a simple book of lists.

In reading such a radiograph, I understand of course that one is often presented with a paucity of clinical data, and that it is the job of radiologists to evaluate the radiograph and establish an appropriate differential diagnosis. To do so, they must not only be trained in pattern recognition, but also possess some knowledge of epidemiology and disease processes in the clinical entities involved. If the patient is a young black rather than elderly white patient, for instance, the suspicion of sarcoidosis would surely rank higher here; yet this is not mentioned once in the book's 17 listings of the disease.

My point is simply to recognize the limitations this text sets itself, with its fine illustrations and descriptions. Differential diagnosis is not synonymous with pattern recognition. The author does stress that his book is meant to complement radiology textbooks rather than to supplant them. My concern is that a pocket book of lists may achieve almost as much, whilst being a lot lighter.

ANDREW BERMAN

My comments follow those of a final-year elective medical student, using the book during a period of intensive radiological study. I have had the volume by my side in everyday work for some weeks, and referred to it often. My first reaction is to take my hat off to the author's prodigious industry and inventiveness. He has categorized and illustrated a vast gallery of radiographic appearances, to make a book that is weighty in every sense (3kg). He is also remarkable for the breadth of his knowledge, from discussions on ovarian ultrasound to cerebellar CT. This is a comprehensive volume, to keep by one at the reporting desk for handy reference.

The value of the text for daily learning will turn very much on individual radiological style. I happen to share Berman's reservations about pattern recognition as the endpoint of radiologists, and would prefer diagnostic physicians in touch with their patient's clinical problem. However, many radiologists cherish the photographer-detective role: "it's all there on the film, boy". They will enjoy this book.

THOMAS SHERWOOD

Diagnostic Imaging: An Algorithmic Approach. Ed. by Ronald L. Eisenberg, pp. xx + 713, 1987 (Lippincott, Philadelphia), £79.50.
ISBN 0–397–58300–1

This fascinating book is devoted to the consideration of the most appropriate imaging investigative pathway in 47 different clinical and radiographic problems. To aid him in this mammoth task the editor has co-opted a total of 76 contributors, but he has clearly maintained tight editorial control of the format and style of the book. Virtually all of the chapters adopt the same method of presentation and commence with a brief description of the incidence, aetiology and relevant clinical features of the subject under discussion. The range of diagnostic imaging methods available are then discussed at greater length and their relative merits are compared. Consideration is given to the sensitivity, specificity and relative cost of each imaging method as well as the relationships between varying radiological procedures and the available treatment options. Each chapter concludes with a graphic depiction or flow diagram of the recommended algorithm, which is sometimes almost too complicated to be easily assimilated!

The introduction to the book reviews the background to the problem of the sensible use of diagnostic imaging and includes some discussion of the history and development of the newer imaging techniques. It also compares the costs of radiological evaluation of similar diagnostic problems in 1975 and 1987, and in so doing demonstrates the impact of these new methods on the costs and length of hospital admission. Although these are priced in US dollars, the underlying message is still quite clear.

The chapters themselves are loosely grouped in system orientation so that the thoracic section, for example, commences with discussion of the solitary pulmonary nodule and is followed by chapters on chest pain, pulmonary embolism and aortic aneurysm. Contributions on mediastinal masses, pleural masses and pericardial disease complete this particular section. Each chapter is generously illustrated and contains an appropriate bibliography.

This is a most unusual and intriguing textbook, the content of which commends itself to radiologists and also clinicians who initiate the radiological investigations. Most of the chapters are only 15 pages or so in length, and a single subject is therefore easily absorbed at bedtime without inducing somnolence!

D. M. KING

1989, *The British Journal of Radiology*, 62, 399–420

VOLUME 62 NUMBER 737 MAY 1989

The British Journal of Radiology

Review article

Doppler ultrasound in medical diagnosis

By P. N. T. Wells, DSc, FEng

Department of Medical Physics, Bristol and Weston Health Authority and Department of Radiodiagnosis, University of Bristol, Bristol General Hospital, Bristol BS1 6SY

(*Received September 1988 and in revised form December 1988*)

Christian Andreas Doppler (often erroneously called Johann Christian) was born in Salzburg on 29 November 1803. The paper that made his name famous, "On the coloured light of the double stars and certain other stars of the heavens", was presented on 25 May 1842 and published in the following year (Doppler, 1843). At that time, Doppler was Professor of Mathematics and Practical Geometry at the Technical Institute in Prague; he subsequently held appointments in Schemnitz and Vienna, and died in Venice on 17 March 1853. A full account of these events can be found in an article by Eden (1986).

Even more intriguing than Doppler's paper is the fact that Doppler was wrong! An Englishman, James Bradley, one-time Vicar of Bridstow, near Ross-on-Wye in Monmouthshire, had earlier published an article concluding that "when the Eye is moving in different Directions, the apparent Place of the Object would be different." (Bradley, 1729). Doppler used this as the starting-point for his explanation of the effect of relative motion between a source of white light and an observer—a shift towards the blue for an approaching source, and towards the red for a receding source—but he overlooked the then already known fact that the radiation from a visible star extends on each side of the visible spectrum into the ultraviolet and the infrared. Despite its basic fallacy, Doppler's explanation does turn out serendipitously to be correct when the whole spectrum of the radiation involved is considered, and the "Doppler effect" is important in many branches of physics, applied science and engineering. In particular, Doppler radar and sonar systems are nowadays in very widespread use for the detection of movement and the measurement of velocity.

The first paper in English reporting the ultrasonic Doppler detection of moving cardiac structures was published by Shigeo Satomura in 1957. Subsequently, Ziro Kaneko (Kaneko et al, 1961) showed that the Doppler shift in the frequency of ultrasound backscattered by moving blood was also detectable and this opened up the application of the method to the solution of important clinical problems. Initially, it was in the detection of fetal heart motion that the Doppler effect proved its usefulness (Callagan et al, 1964), and subsequently it has come to be applied in cardiovascular investigations and in the study of various aspects of blood flow and associated pathology.

Basic principles and Doppler physics

An excellent review of the scientific basis of Doppler ultrasound can be found in the book by Atkinson and Woodcock (1982); only a brief summary of the essential principles is given here.

The Doppler equation

When ultrasound is reflected, the frequency of the received wave is shifted from that of the incident wave if the reflector has a component of velocity along the ultrasonic beam. The relationship is:

$$f_D = 2v(\cos\gamma)f/c \qquad (1)$$

where $f_D = f - f'$ (f is transmitted ultrasonic frequency and f' is received ultrasonic frequency), c = speed of ultrasound, v = speed of reflector, and γ = angle of attack. The angle of attack, γ, is equal to the angle between the direction of movement of the reflector and the effective direction of the ultrasonic beam. Typical values are $f = 3$ MHz, $v = 1$ m s^{-1} and $c = 1500$ m s^{-1}; the corresponding Doppler shift frequency $f_D = 4$ kHz for $\gamma = 0°$.

The choice of the ultrasonic frequency

The detection of ultrasound backscattered by blood ultimately depends on the signal-to-noise ratio. The choice of the ultrasonic frequency that gives the maximal signal-to-noise ratio is determined by the optimal

---

Offprints of this paper are available from the Publications Office, British Institute of Radiology, 36 Portland Place, London W1N 4AT, at a price of £3.00 each. Please send remittance with order.

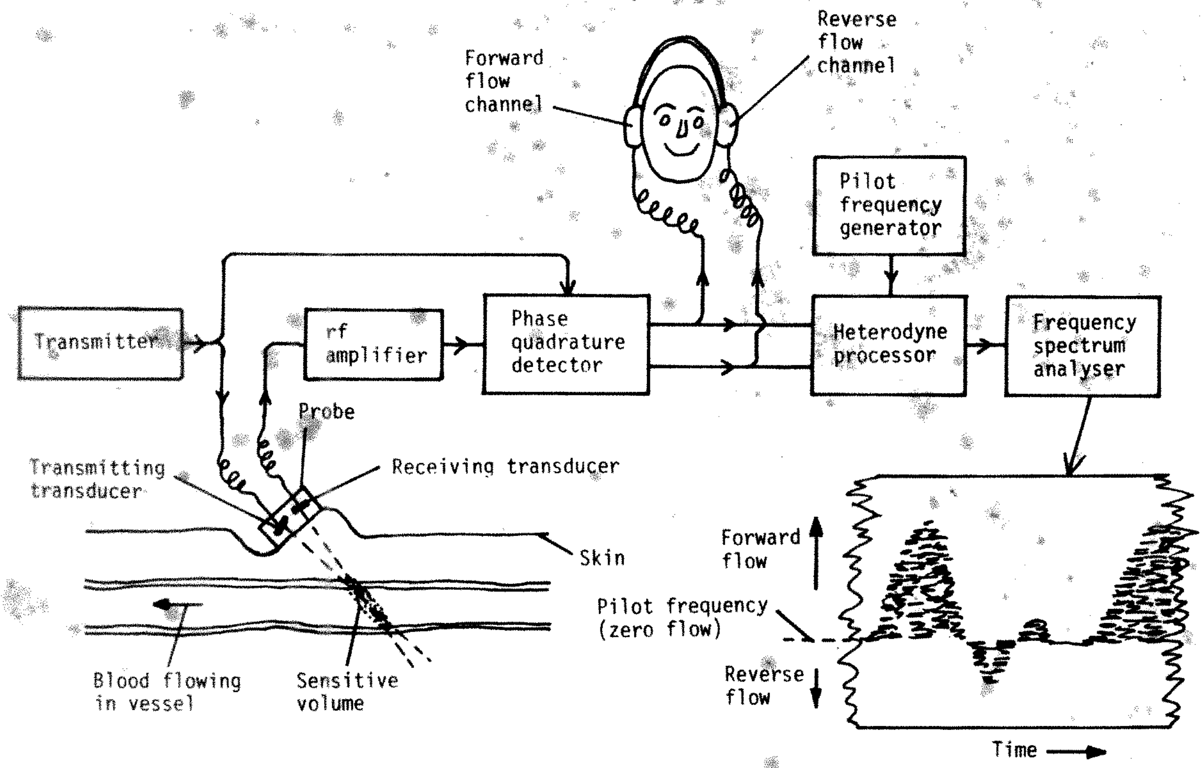

Figure 1. Basic elements of a continuous-wave Doppler system. In this system, phase quadrature detection separates the Doppler signals into forward and reverse flow components, and frequency spectrum analysis of the output from the heterodyne processor results in a recording in which the pilot frequency corresponds to zero flow.

compromise between the backscattering efficiency of the blood (which increases with the fourth power of the frequency) and the required depth of penetration (which has to decrease with the frequency). In practice, a frequency of around 3 MHz is generally used for a penetration of about 100 mm, increasing to 10 MHz at 20 mm. The choice of frequency is also affected by the desirable Doppler frequency shift range and the problem of aliasing (which are discussed later) and, often, because the same transducer is used for imaging (for which the beam is usually optimized) and for Doppler studies.

One way in which the power of the Doppler shift signals might be increased would be by the use of appropriate blood-borne contrast agents such as encapsulated microbubbles. Microbubbles are available that are small enough to cross over the lungs from the right to left side of the heart (Miszalok et al, 1986). Thus, intravenous injection of the contrast agent can enhance the echogenicity of blood in the systemic circulation.

Ultrasonic beams for Doppler applications

The ultrasonic beam shape depends on the geometry of the transducer, the focusing arrangements and the wavelength of the ultrasound. There are three fundamental differences between the considerations that apply to the design of beams for pulse–echo imaging and for Doppler applications. The fact that the same transducer often has to be used for both purposes means that compromises may have to be made. First, in continuous-wave (CW) Doppler systems, overloading of the receiver and masking of the detected ultrasonic waves would occur if the same transducer was used as transmitter and receiver and, to avoid this, separate transducers usually have to be employed, mounted close together but acoustically and electrically isolated. Secondly, in Doppler studies it is often desirable to have a wider beam than for imaging, for example because all the blood flowing in a vessel is of interest, whereas in imaging the narrowest possible beam gives the best resolution. Finally, the optimal ultrasonic frequency for Doppler studies at a given penetration is generally lower than that for imaging, and the bandwidth is less because the range resolution is not so important (with CW Doppler, there is no range resolution apart from that fixed by factors such as focusing, transmitting and receiving beam overlap and attenuation in overlying tissue).

Instrumentation

In this section, only the more recent developments in Doppler instrumentation are discussed in depth; the well established systems are mentioned briefly. For more information, see, for example, Wells (1977, 1980) and Atkinson and Woodcock (1982).

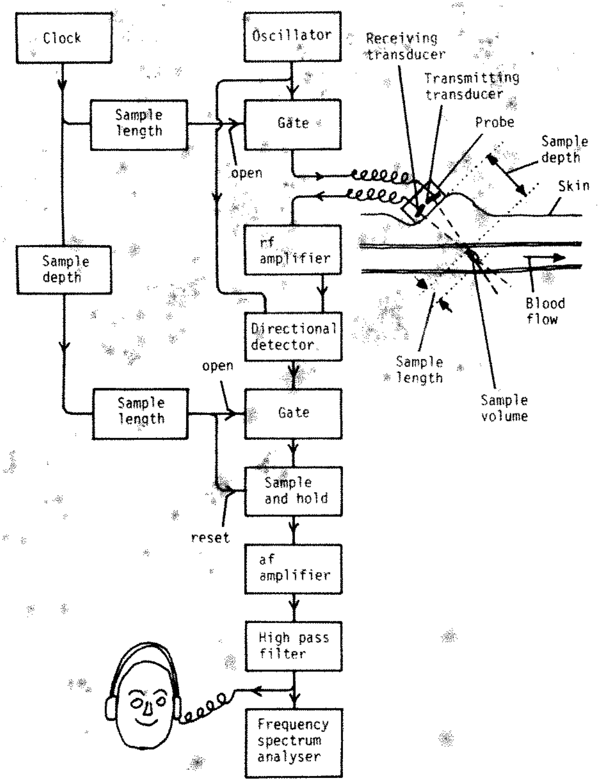

Figure 2. Block diagram of a simple pulsed Doppler system. The pulse repetition rate is determined by the clock; typically, it might be 5 kHz. Each time the clock emits a trigger pulse (in this example, once every 200 μs) the first sample length circuit produces a pulse (say 2 μs in duration). This opens the first gate to allow a 2 μs burst of the output from the oscillator (which runs continuously at the ultrasonic frequency of, say, 3 MHz) to excite the transmitting transducer in the probe to emit a 2 μs pulse (corresponding to a length of 3 mm) of ultrasound into the patient. Echoes returning to the receiving transducer (including echoes Doppler-shifted in frequency as the result of scattering from moving targets) are amplified in the radiofrequency (rf) amplifier before being mixed with a signal derived from the oscillator and subjected to directional detection. (In a practical system, provision would need to be made to deal with the forward and reverse flow signals, but, in the interest of clarity, this complication is omitted from the diagram.) The output from the directional detector thus depends on the velocities of moving targets in the ultrasonic beam, delayed in time according to their depths. The sample depth circuit is triggered by the clock at the instant that each pulse is transmitted, and it produces a trigger pulse (for example, for a delay of 20 μs, the depth is 15 mm) to enable the second sample length circuit to open the second gate (again for 2 μs) to allow the desired Doppler sample (3 mm long) to be held by the sample-and-hold circuit until the process is repeated with the next pulse. The output from the sample-and-hold circuit (*i.e.* the range-gated Doppler signal) is amplified by the audiofrequency (af) amplifier, filtered, and fed to the headphones and the frequency spectrum analyser.

Continuous-wave Doppler systems

A block diagram of a CW Doppler system is shown in Fig. 1. Uninterrupted ultrasonic waves of constant frequency and amplitude are transmitted into the patient. Echoes from stationary reflectors lying along the ultrasonic beam have the same frequency as the transmitted waves, but moving structures and flowing blood give rise to Doppler frequency shifts. Phase quadrature detection separates the signals from approaching and receding targets depending on whether they have higher or lower frequencies than that of the transmitter; in the simplest systems, non-directional detection may be used.

Pulsed Doppler systems

Pulsed Doppler systems use pulse–echo range measurement for the selection of Doppler signals from moving targets according to their distances from the ultrasonic probe. Figure 2 is a block diagram showing the essential components. Both the depth and the length of the sample volume can be controlled by the operator by appropriate selection of the time delays.

The Doppler signals obtained with a pulsed Doppler system are "sampled" in the sense that the output waveform consists of a series of discrete values at the pulse repetition rate. It is a general rule that this kind of sampling process is free from ambiguity only if the sampling frequency (the pulse repetition rate) is at least twice the maximum signal frequency. This is known as the "Nyquist criterion"—if it is not satisfied, aliasing occurs in the display of frequencies exceeding the Nyquist limit. Although this is a fundamental limitation, the very existence of aliasing may give diagnostic clues in the interpretation of Doppler signals. There are many practical situations in which frequency ambiguity can be avoided by increasing the pulse repetition rate above that dictated by the go-and-return pulse–echo time delay for the desired penetration, but at the expense of introducing the less-confusing artefact of range ambiguity. Of course, lowering the ultrasonic frequency results in a lower Doppler shift frequency for a given target velocity, and this may sometimes be a useful strategem.

Presentation and analysis of Doppler signals

Doppler signals obtained from moving structures and flowing blood are complicated, transient and rather alien to diagnostic radiologists who are familiar with the more tangible art and science of image interpretation. Some people have the ability to extract useful information by listening to Doppler signals, and those who make the effort to develop this skill can do much with the simplest of apparatus. Nevertheless, although the trained ear is good at distinguishing between useful signals and extraneous noises, and at recognizing sound patterns in fairly brief time periods, it is subjective rather than objective, qualitative rather than quantitative, and is poor at detecting long-term trends and changes.

Because of the compexity of target motion within the sensitive volume of the ultrasonic beam, the Doppler signals usually cover a continuously varying spectrum of

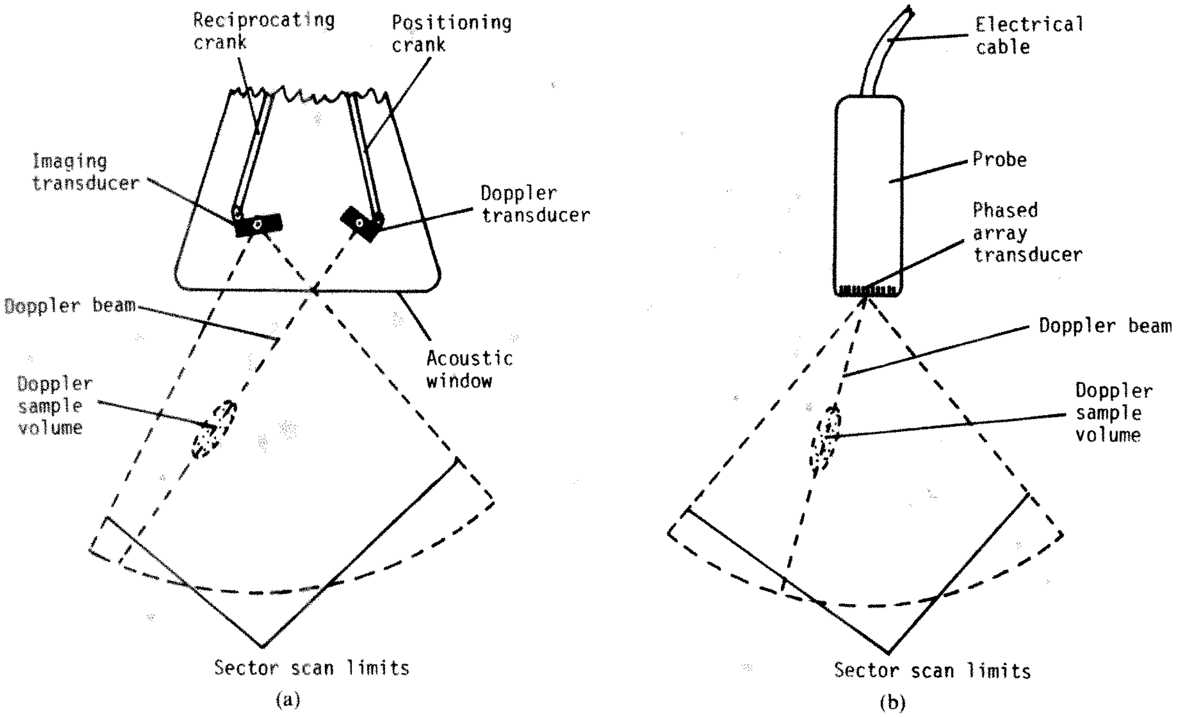

Figure 3. Typical ultrasonic duplex scanners. (a) Mechanically oscillated transducer for imaging with a separate offset Doppler transducer that can be directed (either manually or by servo control) to the desired orientation for Doppler studies. (b) Phased array producing a sector scan. The phased array is also used for Doppler signal acquisition. The Doppler beam can be steerable within the sector with pulsed operation, but, for CW operation, it is usually fixed in the direction normal to the surface of the array.

frequencies and amplitudes. Processing is necessary to display these signals visually or to extract quantitative information. Nowadays, frequency spectrum analysis is usually carried out by the fast Fourier transform (FFT) technique. This is a digital process that itself introduces statistical fluctuations in the output, but is convenient and inexpensive for the production of a display in which the variation of both amplitude and frequency is shown with respect to time. The frequency spectrum makes it possible for Doppler signals to be interpreted visually, and qualitative data, such as the mean and maximum instantaneous or time-averaged frequencies and the signal power, can be obtained by further processing. The problem of the statistics of the FFT might be avoided by employing autoregressive modelling for frequency spectrum analysis (Kaluzynski, 1987).

Duplex scanning systems

A duplex scanning system is one that enables two-dimensional ultrasonic pulse–echo imaging to guide the placement of an ultrasonic Doppler beam and thus to allow the anatomical location of the origin of the Doppler signals to be identified. Since its inception, the common usage of the term "duplex" has changed; what most people now consider to be a duplex scanner is one that has real-time imaging capability with either the imaging transducer or a separate transducer used to collect CW or pulsed Doppler signals, either simultaneously with imaging or sequentially.

Duplex scanners can be based on either mechanical or electronic array real-time imaging. Some typical arrangements are illustrated in Fig. 3. The image frame rate is limited by the depth of the scanned field and the number of lines per frame. If the depth is, say, 100 mm, the go-and-return pulse–echo delay time is about 130 μs per line. The corresponding maximum pulse repetition rate (equal to the number of image lines collected per second) is about 7700 Hz. This means that images made up of, say, 77 lines per frame can be collected at 100 frames per second, and so on.

For the collection of Doppler signals, the ultrasonic beam has effectively to be stationary and to dwell in the desired position sufficiently frequently and for a sufficiently long time during each acquisition period to allow adequate sampling of the moving targets. Inertia prevents the acceleration and deceleration of the moving parts of mechanical sector scanners that would be necessary for simultaneous collection of imaging and Doppler data, so the "frozen" image frame approach is necessary unless a separate transducer is used for Doppler signal acquisition. Movement of the beam of an array scanner can be started and stopped

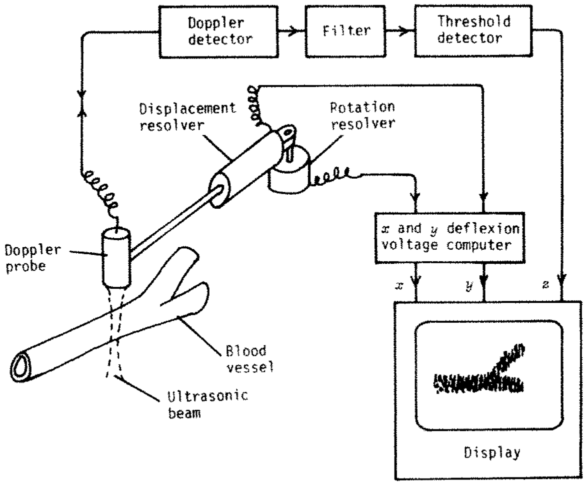

Figure 4. Continuous-wave Doppler system for two-dimensional visualization of blood vessel distribution. The position of the manually scanned probe is measured by a polar co-ordinate arrangement, the resolvers of which control the x (horizontal) and y (vertical) deflexion voltage computer driving the cathode-ray tube display. The output from the Doppler detector is fed through a filter to remove low-frequency signals resulting mainly from skin contact changes, and then passes to a threshold detector so that the z (brightness-controlling) signal is stored in the display to form a two-dimensional image. The display may be colour-coded according to Doppler shift frequency, corresponding to blood flow velocity.

instantaneously, so simultaneous operation is possible with this type of system.

Two-dimensional Doppler flow imaging

Figure 4 is a block diagram of a two-dimensional CW Doppler flow imaging system of the kind originally proposed by Reid and Spencer (1972). The Doppler probe, containing the transmitting and receiving ultrasonic transducers, is mounted on a co-ordinate measuring system that allows its position on the surface of the patient to be transferred, in terms of electrical signals, to horizontal and vertical timebase deflexion generators, so that the position of the spot on the display follows the position of the probe on the surface of the patient. When the ultrasonic beam passes only through stationary structures within the patient, there is no output from the Doppler detector and no registration appears on the display. When, during the scanning process, the Doppler probe is moved so that the beam happens to pass through a vessel in which blood is flowing, a signal appears at the output from the Doppler detector and this is arranged to increase the brightness of the display. When the scanning process has been completed so that the whole of the surface of interest has been explored, a two-dimensional image of regions within which blood is flowing appears on the display.

The simplest type of two-dimensional Doppler flow imaging system employs continuous waves. In more complicated systems, a multigated pulsed Doppler arrangement is employed and this makes it possible for depth information to be obtained and incorporated in the image (Fish, 1981). A pulsed Doppler flow imaging system may be considered to be a three-dimensional method of acquiring Doppler information, with a two-dimensional display in any desired plane.

Real-time Doppler colour flow imaging

The Doppler flow imaging system just described displays a two-dimensional map of regions in which flow is taking place, but it does not visualize stationary structures. A real-time imaging system using pulse–echo ultrasound shows the structure in grey scale but does not usually include flow information. Combining these two processes—flow imaging and real-time scanning—provides a Doppler colour flow map in which both structure and blood flow can be seen simultaneously.

In fact, the first demonstration of the feasibility of combining pulse–echo images with two-dimensional Doppler information was published by Eyers et al in 1981. Their system produced complete picture frames at the rate of four per second, and so cannot be considered truly to have been "real-time". It was not until Kasai et al published their important paper in 1985 that the feasibility of carrying out the process in real time was generally appreciated. Figure 5 is a block diagram showing the principles of this approach. A phased-array, two-dimensional, real-time scanner of the conventional type was used, combined with what was called a "Doppler autocorrelation flow detector".

The Doppler autocorrelation flow detector operates as illustrated in Fig. 6a. Doppler signals from a phase quadrature detector are split into two paths. One path leads directly to one input of a multiplier and the other path leads to the other input of the same multiplier but through a delay line, which introduces a time shift exactly equal to the interval between the transmission of successive ultrasonic pulses. As shown in Fig. 6b, if the echo wavetrains corresponding to consecutive pulses originate only from stationary structures, each wavetrain is identical and the output from the multiplier is a constant (*i.e.* non-time-varying) wavetrain. If there is movement of the reflecting structures anywhere along the ultrasonic beam, consecutive wavetrains have phase shifts due to the Doppler effect. The output from the multiplier then contains segments of wavetrain that vary in amplitude from pulse to pulse. Feeding the output from the multiplier into an integrator processes the signals so that the output from the integrator has a constant value except for those segments of time corresponding in depth to target movements along the ultrasonic beam.

In autocorrelation detection, the output from the multiplier (and integrator) is fed into parallel gates clocked in sequence, with one gate corresponding to each pixel along the ultrasonic beam. The outputs from these gates are the Doppler signals corresponding to each pixel and can be arranged to colour-code the pixels according to the corresponding Doppler shift frequencies which, in

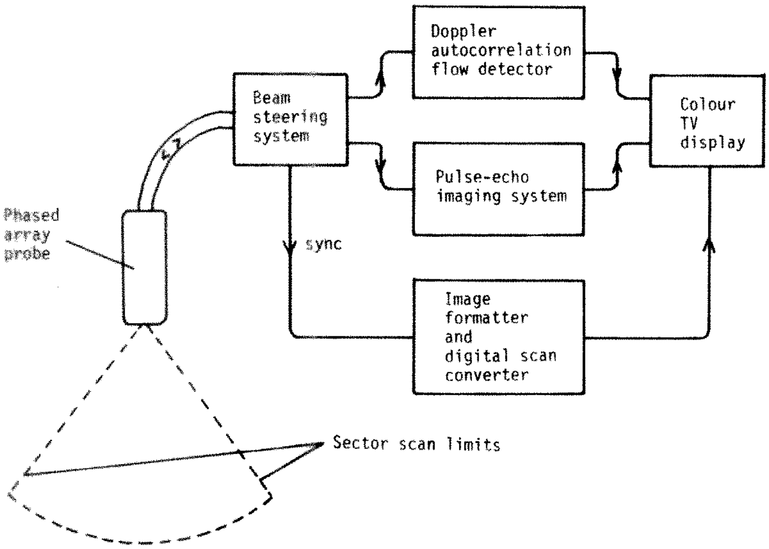
Doppler autocorrelation flow detector
Beam steering system
Colour TV display
Pulse-echo imaging system
Phased array probe
sync
Image formatter and digital scan converter
Sector scan limits

Figure 5. Block diagram of a typical Doppler colour flow imaging system. The conventional phased-array transducer produces a grey-scale, real-time, pulse–echo sector scan with electronic beam steering and digital scan conversion. Simultaneously, the Doppler autocorrelation flow detector colour-codes the two-dimensional image.

turn, correspond to the target vector velocities in each pixel in the image. It is important to notice that the autocorrelation detection technique is based on the comparison of the phase of echo wavetrains obtained with consecutive ultrasonic cycles. It does not operate by phase comparison with a fixed wave derived from the transmitting oscillator.

An alternative detection method, known as "multigate detection", does employ a phase reference derived from the transmitting oscillator. As shown in Fig. 7, the output from the Doppler receiver is mixed with a signal derived directly from the continuously running transmitter oscillator to produce a Doppler-shifted wavetrain that, just as in the autocorrelation detection scheme, is separated into its constituent pixel components by sequentially clocked gates. This detection scheme has the advantage of deriving the "true" Doppler shift frequency, rather than the "relative" Doppler shift frequency, which is what is produced by the autocorrelation method. It has the further advantage of better signal-to-noise ratio but is more demanding in terms of electronic circuit complexity. A disadvantage of the autocorrelation detection method is that dynamic range considerations require the cancellation of the strong echoes from stationary structures. As shown in Fig. 8, this can be achieved by means of a delay line canceller that operates by accepting successive echo wavetrains and subtracting consecutive wavetrains. The actual subtraction process is accomplished by inverting the wavetrain fed directly to an adding circuit, the other input to which is the previous wavetrain fed through a delay line that introduces a delay exactly equal to the interval between ultrasonic pulses. The output from the adding circuit is zero except when there is a difference between consecutive wavetrains, the difference resulting from phase changes due to the Doppler effect. The result is the cancellation of the stationary (usually large-amplitude) echoes and the retention of the Doppler information.

Dynamic range considerations require the use of a delay line canceller with the autocorrelation detection method. In the case of the multigate detection method, with its fixed phase reference, the performance can be significantly improved by the use of a delay line canceller and all commercially available systems seem to employ one.

The display of Doppler colour flow images

Various schemes of colour coding are adopted in different instruments and individual preferences vary. In general, however, flow towards the transducer is colour-coded either in red or blue, and *vice versa*, for flow away

Figure 6. Operation of the Doppler autocorrelation flow detector. (a) The beam-steering electronics permit each Doppler line in the image to be processed in sequence. For any typical Doppler beam position, the pulse period delay line allows sequential echo wavetrains to be multiplied and integrated. The output Doppler signals are segmented according to depth by the sequentially clocked gates. (b) Echo wavetrains arrive sequentially ($S_0, S_1, S_2, \ldots$) from the receiver. The multiplier accepts the wavetrains directly after being fed through the delay line, which introduces a delay exactly equal to the interval between consecutive ultrasonic pulses, so the output from the multiplier is ($S_0 \times S_1, S_1 \times S_2, \ldots$). If there is no movement of the targets along the ultrasonic beam, the wavetrains are all identical. However, if movements do occur anywhere along the beam (in this diagram, such movements are represented as occurring in the times between the pairs of vertical dotted lines drawn on the wavetrains), corresponding phase changes cause changes in the amplitudes of the multiplied pairs of wavetrains ($S_0 \times S_1, S_1 \times S_2, \ldots$). Short-term variations in these multiplied waveforms are smoothed by the integrator ($\int(S_0 \times S_1), \int(S_1 \times S_2), \ldots$). Consequently, the output to the sequential gates, when displayed on an oscilloscope with a repetitively swept timebase, is constant except where Doppler shift frequencies occur.

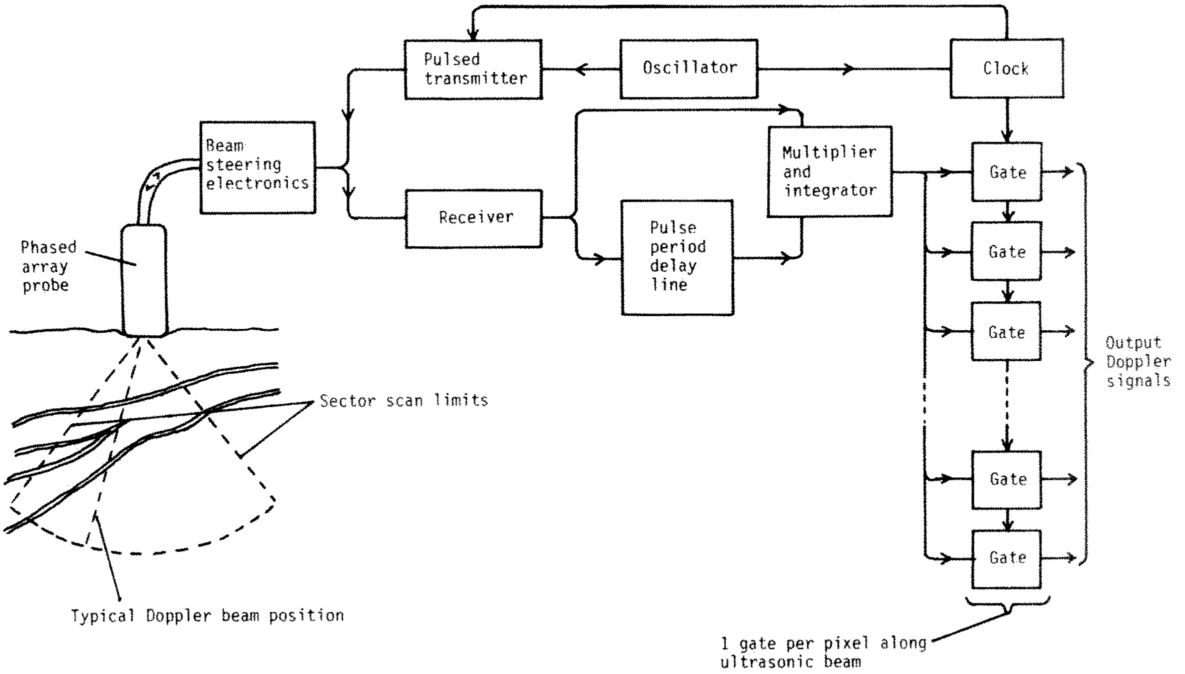
Pulsed transmitter
Oscillator
Clock
Beam steering electronics
Multiplier and integrator
Receiver
Pulse period delay line
Gate
Gate
Gate
Gate
Gate
Output Doppler signals
Phased array probe
Sector scan limits
Typical Doppler beam position
1 gate per pixel along ultrasonic beam

(a)

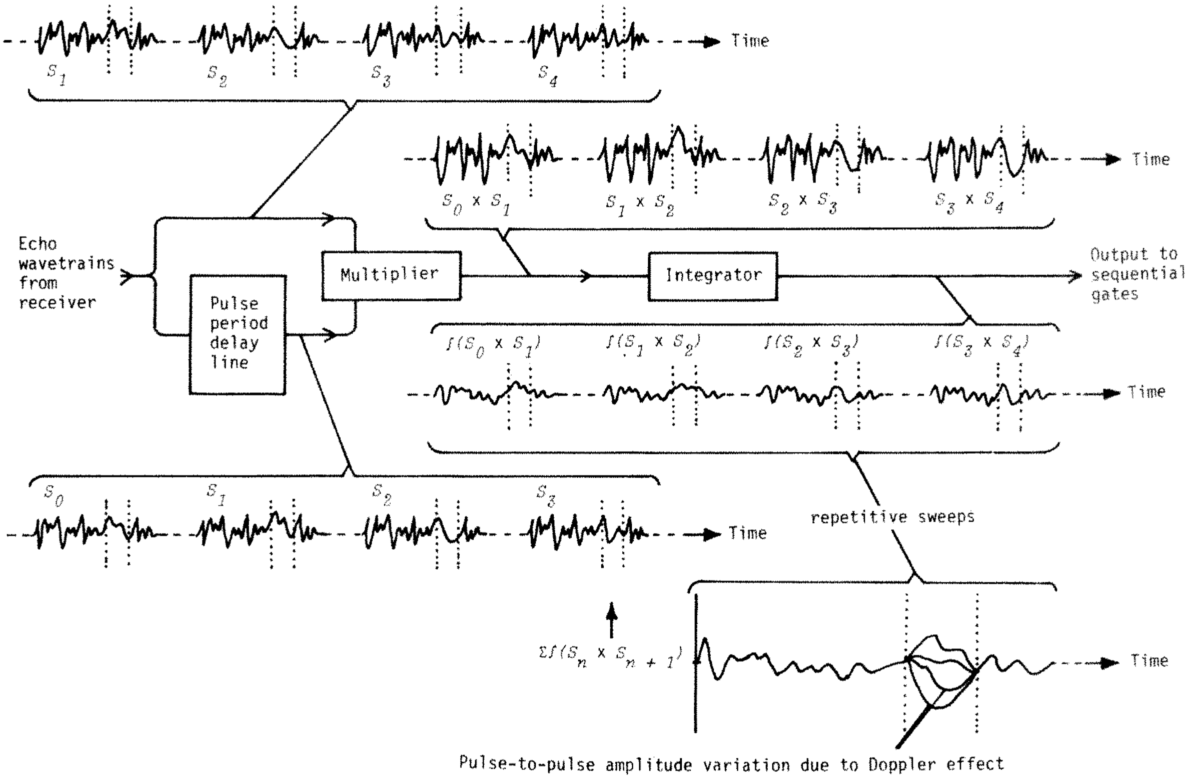
Time
S_1
S_2
S_3
S_4
Time
$S_0 \times S_1$
$S_1 \times S_2$
$S_2 \times S_3$
$S_3 \times S_4$
Echo wavetrains from receiver
Multiplier
Integrator
Output to sequential gates
Pulse period delay line
$\int(S_0 \times S_1)$
$\int(S_1 \times S_2)$
$\int(S_2 \times S_3)$
$\int(S_3 \times S_4)$
Time
S_0
S_1
S_2
S_3
Time
repetitive sweeps
$\Sigma\int(S_n \times S_{n+1})$
Time
Pulse-to-pulse amplitude variation due to Doppler effect

(b)

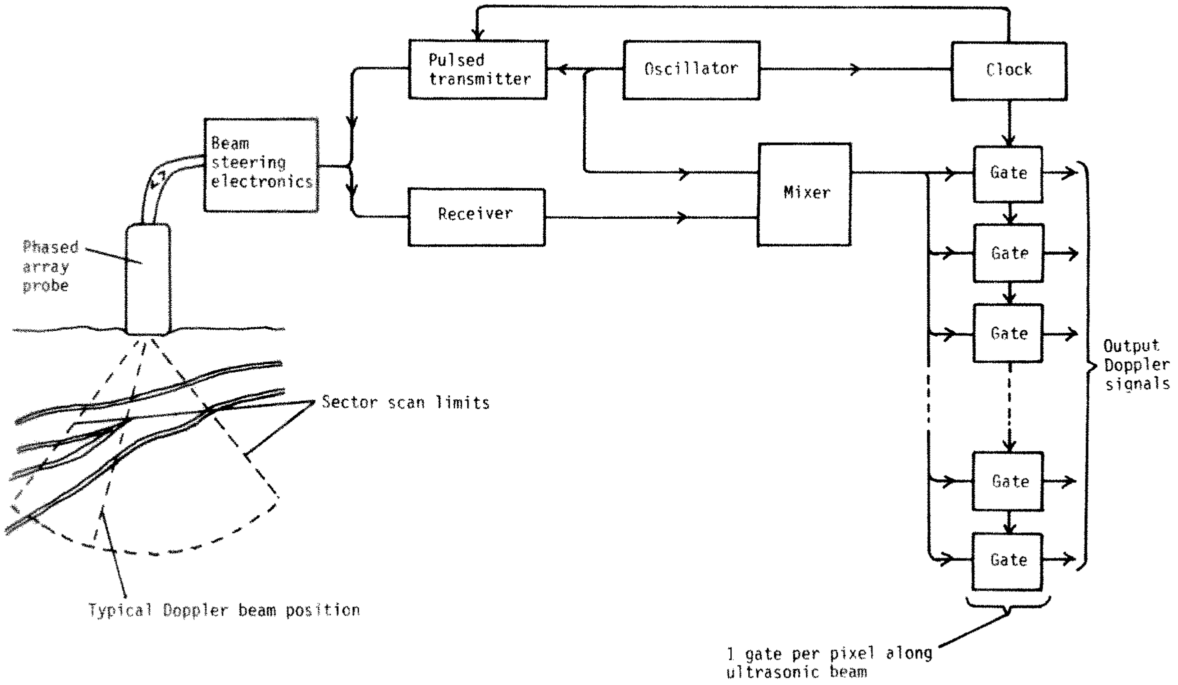

Figure 7. Operation of the Doppler multigate flow detector. The beam-steering electronics permit each Doppler line in the image to be processed in sequence. For any typical Doppler beam position, the received echo wavetrain is mixed with a signal at the transmitted frequency to produce a signal which is segmented according to depth by the sequentially clocked gates.

from the transducer. The colour scale may pass through various shades and tones according to the actual values of Doppler shift frequency.

As an alternative to colour frequency coding, the colour may be coded according to the power of the Doppler signal. With frequency coding, the colour of the image depends on the angle of attack between the flow direction and the ultrasonic beam. Power coding represents the amount of blood; the directional information is limited to the indication of whether the flow is towards or away from the probe, so that interpretation of the images is sometimes easier.

In addition to the demonstration of flow direction and volume, it is possible to derive from the Doppler frequency spectrum a signal that can be considered to be related to flow disturbance in the blood flow. Flow disturbance increases the Doppler frequency spectral variance and this is a quantity that can be derived and coded in an appropriate colour (typically, green).

In weather radar systems, the vector velocity is determined by the use of two observation stations in known positions in relation to the target volume (Doviak & Zrnic, 1984). As illustrated in Fig. 9, the same technique could be applied in medical diagnosis (provided that the ultrasonic propagation paths from two scanning points were free from obstructions such as bone and gas). The resultant of the vectors measured from each observation point corresponds to the true in-plane vector velocity.

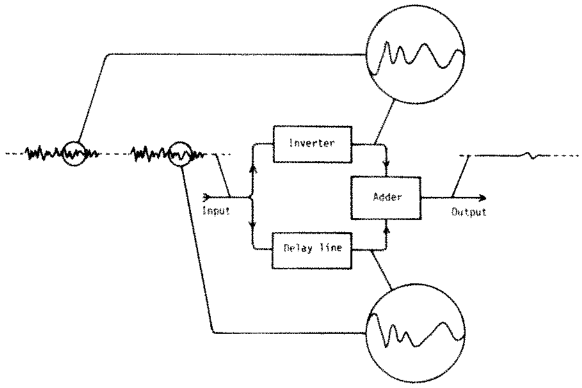

Figure 8. Operation of the delay line canceller. The delay line introduces a delay exactly equal to the interval between consecutive ultrasonic pulses, so that the output from the adder is zero except when there is a difference between wavetrains caused, for example, by the Doppler effect. In this diagram, the circles illustrate segments of wavetrains containing Doppler shifts, drawn to a large scale to clarify the process. Thus, echoes from stationary structures are eliminated but the Doppler signals are retained.

Another possible approach to the velocity vector problem depends on separating contributions made by the Doppler effect and fluctuation scattering. This technique would require the two signal contributions to

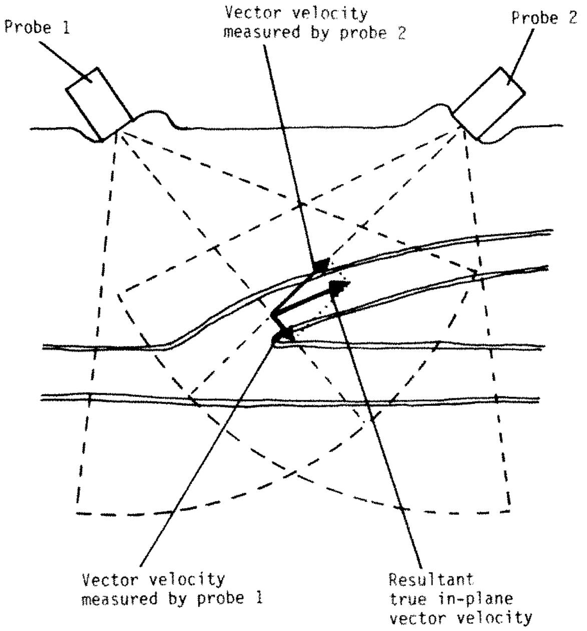
Probe 1
Vector velocity measured by probe 2
Probe 2
Vector velocity measured by probe 1
Resultant true in-plane vector velocity

Figure 9. The true in-plane vector velocity is the resultant of the vector velocities measured from two different positions in the image plane. Successful implementation of this approach would depend on having two suitable acoustic windows.

be identified and this might be possible by appropriate processing of the upper and lower frequency sidebands.

Image frame rate in colour flow imaging

The factors that limit the frame rate in pulse–echo real-time imaging are explained in this review in the earlier discussion of duplex scanning systems. In duplex scanning, it is the frame rate that is of most interest since this determines the maximum rate of change of structure or scan plane position that can be observed. In Doppler colour flow imaging, it is the time per frame for pulse–echo imaging that is of most importance, since this corresponds to the amount of time that has to be devoted to the collection of a single frame of grey-scale structural information.

In a pulsed Doppler system, the maximum frequency that can be detected unambiguously is that set by the Nyquist limit. For example, if the penetration is 100 mm, the corresponding time per line is 130 μs. If consecutive pulses are transmitted without any additional delay, the maximum pulse repetition frequency is equal to 7700 s^{-1}, since this is the number of lines that can be acquired per second. According to the Nyquist criterion, as illustrated in Fig. 10, the corresponding maximum unambiguously detectable Doppler shift frequency is half the maximum pulse repetition frequency, *i.e.* 3900 Hz. Taking this example a little further, with an ultrasonic frequency of 3 MHz and $\gamma = 0°$, this corresponds to a maximum unambiguously detectable velocity of 100 cm s^{-1}. If the velocity exceeds the Nyquist limit, the ambiguity that appears in the frequency spectral display is one in which the spectrum seems to be folded over; it is sometimes hard for this to be identified. In a colour flow imaging system in which the Nyquist limit is exceeded, the display cycles through the colour scale and it is usually the case that the artefact is easily recognizable in the image; it is, however, difficult to estimate the actual velocity from the colour display.

It is the high-frequency constraint on the frame rate that is of most practical importance in Doppler colour flow imaging systems. In a typical situation, as illustrated in Fig. 11, the following conditions might apply:

Assume acceptable lowest detectable frequency threshold $= 10$ cm s^{-1}

Corresponding lowest detectable frequency threshold $= 380$ Hz at 3 MHz and 0°

Time for one Doppler frequency shift cycle

$$= \frac{1}{380} \times 10^3 = 2.63 \text{ ms}$$

= minimum dwell time per line

Time per frame $= 2.6 \times 80 = 210$ ms

$$\text{Frame rate} = \frac{1}{210} \times 10^3$$

$$= 4.8\ s^{-1}$$

At this point, it is intellectually satisfying to realize that two different phenomena contribute to the audible signal produced by a system designed to measure the Doppler shift frequency. Figure 12a shows the true Doppler situation in which the incident frequency is shifted either upwards or downwards depending on the direction of flow. Substitution in the Doppler equation reveals that, for a typical situation with an ultrasonic transmitted frequency of 3 MHz, a flow velocity of 30 cm s^{-1}, $\gamma = 30°$ and $c = 1500$ m s^{-1}, the Doppler shift frequency is 1200 Hz. In addition to the Doppler effect, another phenomenon contributes to the output from the system, as illustrated in Fig. 12b. In the extreme situation where flow is perpendicular to the direction of the ultrasonic beam, $\gamma = 90°$ and the Doppler shift frequency is zero independent of the flow velocity. Nevertheless, flow perpendicular to the beam is accompanied by a fluctuation in the amplitude of the received ultrasonic signal, which depends on the flow velocity and the dimensions of the ultrasonic beam. The effect is known as "fluctuation scattering". If D is the diameter of the beam and v the flow velocity, the frequency f_f of amplitude fluctuation is given by (Atkinson, 1975):

$$f_f \simeq \frac{0.7v}{D} \qquad (2)$$

In a typical situation, such as might apply for the calculation of the Doppler shift frequency as just described, with a flow velocity of 30 cm s^{-1} and a beam diameter of 1 mm, substitution in this equation reveals that the fluctuation frequency is about 210 Hz. An important difference between the Doppler shift and fluctuation scattering contributions to the output signal

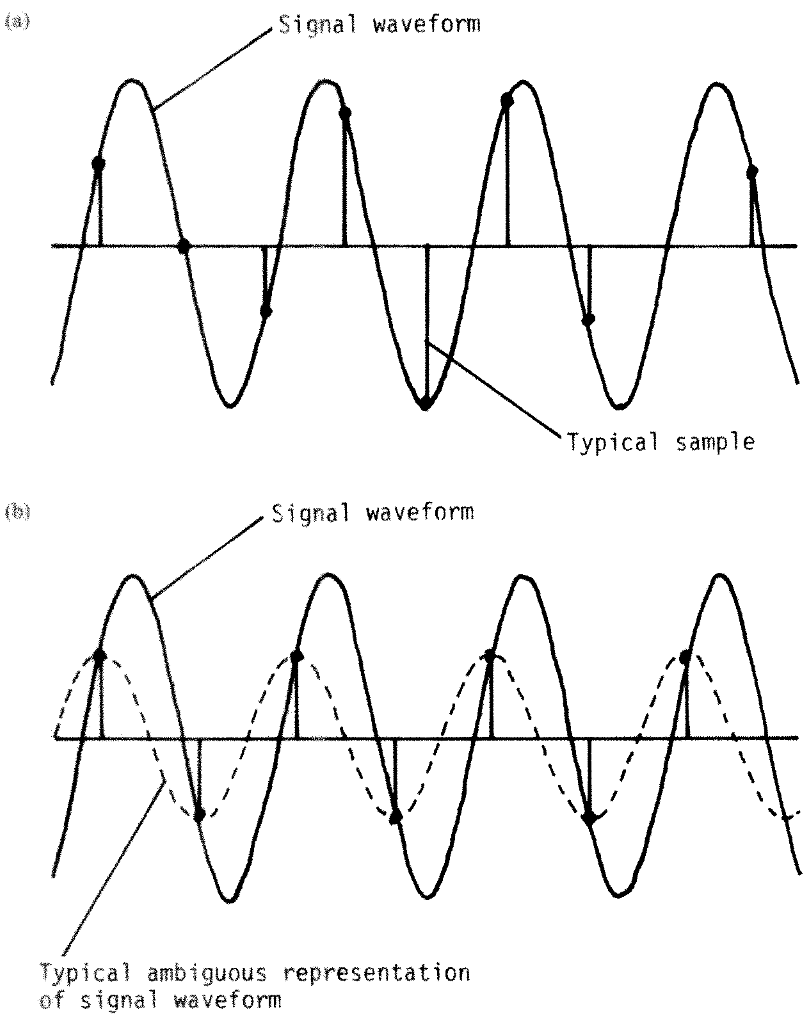

Figure 10. The Nyquist sampling criterion. (a) The signal is sampled at more than twice its own frequency; the sampling points unambiguously define the signal waveform. (b) The signal is sampled at exactly twice its own frequency; depending on the phase relationship between the signal and the samples, the sampled amplitude is incorrectly defined. At still lower sampling frequencies, frequency ambiguity also occurs in the sampled waveform.

is that the Doppler signal is single sideband, either above or below the transmitted frequency, whereas the fluctuation frequency is double sideband and distributed identically above and below the transmitted frequency. Although fluctuation scattering might at first be thought to be likely to be troublesome, it should be appreciated that, because of its double sideband characteristic, the output from a mean velocity detector corresponds only to the Doppler shift signal, since the upper and lower sidebands of the fluctuation scattering signal sum to zero.

It is possible to increase the colour Doppler image frame rate by adopting one or more of several compromise strategems. These include the colour-coding

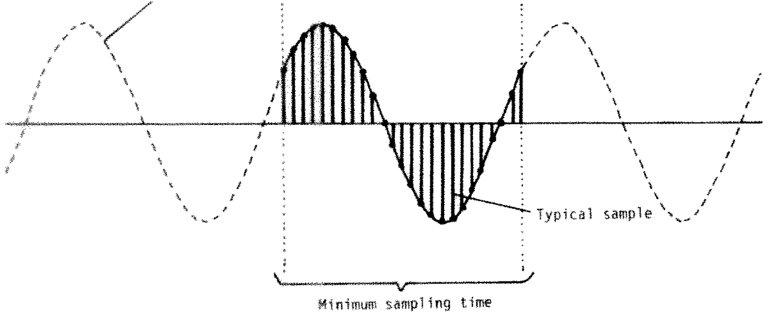

Figure 11. Minimum sampling time necessary to define any particular signal frequency. Sampling for at least one cycle of the signal waveform is the minimum requirement and this is the high-frequency constraint on the frame rate in Doppler colour flow imaging systems.

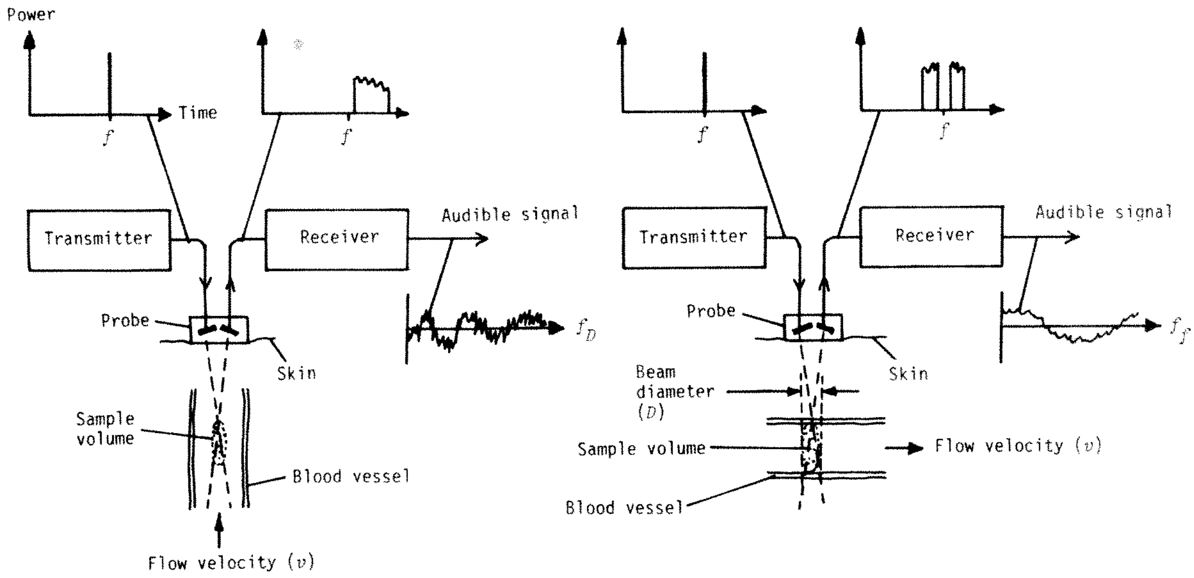

(a) (b)

Figure 12. The origins and characteristics of Doppler shift and fluctuation scattering signals. (a) The Doppler effect, in which the frequency of the received signal is shifted into a sideband depending on the direction of flow. (b) Fluctuation scattering resulting in double sideband amplitude modulation.

of only part of the image, increasing the ultrasonic frequency, raising the minimum displayed Doppler shift frequency threshold, increasing the pixel width, and collecting fewer lines, filling missing pixels by interpolation. The fact that commercially available Doppler colour flow imaging systems all operate at frame rates higher than possible without compromise needs to be remembered when clinical images are being interpreted.

As with pulse–echo imaging, the colour flow image frame rate might be increased by employing parallel (*i.e.* simultaneous) transmission and reception for different parts of the image plane (Shattock et al, 1984). Another contribution to the noise in the system arises because of speckle (which is another aspect of fluctuation scattering) and, in principle, this could be suppressed by collecting Doppler information at different ultrasonic frequencies, either serially or in parallel (Luckman et al, 1987).

Systems for blood flow volume rate measurement

Essentially there are two approaches to the measurement of blood flow volume rate by Doppler ultrasound. The first, which is obvious and traditional, depends on measuring the cross-sectional area of the vessel and the average velocity of the blood flowing through it, and multiplying these two quantities together. The second, which is ingenious and still quite new, depends on making an estimate from measurements of the average velocity of the blood and the energy of the ultrasound that it backscatters.

The traditional method is most commonly implemented with a duplex scanner. The vessel is scanned in longitudinal section and its diameter measured from the image (preferably where the beam is perpendicular to the vessel axis) or from the A-scan. The cross-sectional area of the lumen is then calculated, usually on the assumption that the vessel is cylindrical. The various sources of error have been discussed by Gill (1985). In situations where this assumption is clearly invalid, *e.g.* in the case of the larger veins, a transverse scan may be used to allow the area to be estimated by planimetry. Unfortunately, Doppler measurement of the blood flow velocity depends on knowing the relative directions of the ultrasonic beam and the flow (the angle γ in Equation 1), and so a different beam direction to the perpendicular one optimally chosen for diameter measurement needs to be selected for measuring the Doppler frequency shift. In any event, the measurement of this angle, which should ideally be less than about 60°, is a further potential source of error.

Although it is generally easy to obtain a Doppler signal from flowing blood, if the ultrasonic beam optimized for imaging is used for Doppler, the sample volume is necessarily smaller than the vessel lumen, even if the sample volume length is increased to reach from one side of the vessel to the other. Unless there is a plug flow velocity profile, only the maximum flow velocity can be determined accurately; the estimation of the average flow velocity requires the use of a correction factor to allow for the non-uniform insonation of the blood. For example, in the ideal case of a parabolic flow velocity profile, the average velocity is half the maximum velocity. Most duplex scanners embody circuits that extract the average Doppler shift frequency in the

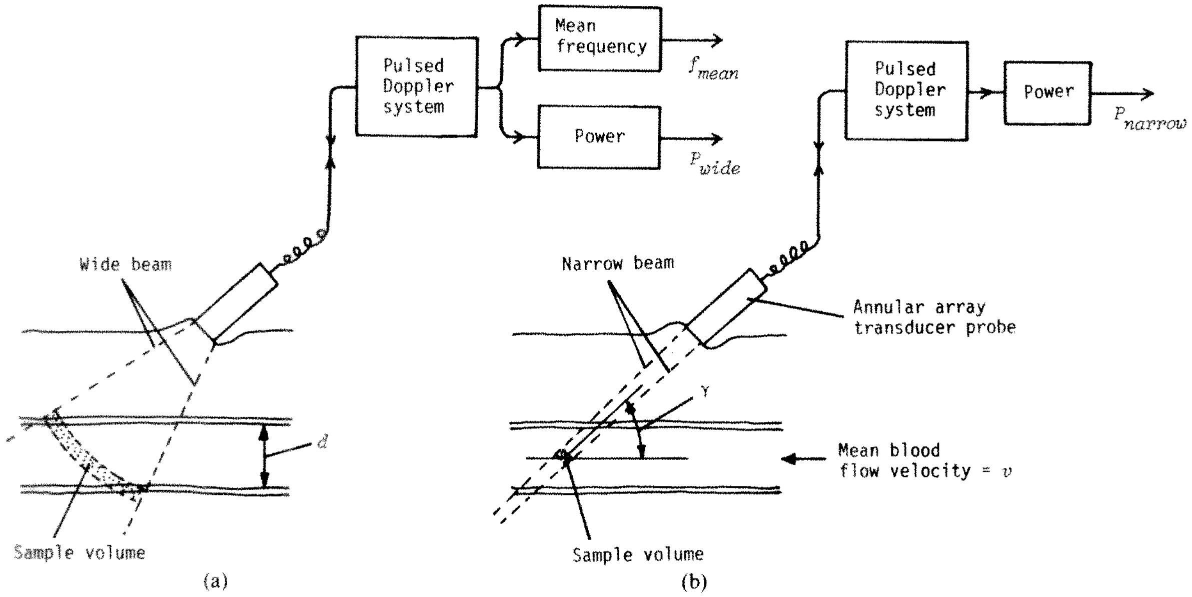

Figure 13. The attenuation-compensated blood flow volume ratemeter. Wide and narrow beams are both produced by appropriate phase and amplitude control of the signals associated with an annular array transducer. (a) With the wide beam, $f_{\text{mean}} = v \cos \gamma$ and $P_{\text{wide}} = kd^2/\cos \gamma$. (b) With the narrow beam, $P_{\text{narrow}} = k\,k'$, where k is an unknown constant (depending on the ultrasonic attenuation in the overlying tissue and the backscattering power of the blood), and k' is a calibration constant. Hence $(v \cos \gamma)(kd^2/\cos \gamma) = kQ$, where Q = volume rate, and $Q = (f_{\text{mean}})(P_{\text{wide}})(P_{\text{narrow}})k'$.

detected spectrum, and then the correction factor chosen (which can most easily be determined by simulation on a flow rig) needs to take account of the vessel diameter, the sample volume size and the actual flow conditions.

An improvement in the accuracy of the estimation of the average flow velocity can be obtained by measuring the flow velocity profile and integrating the area under this curve when it is rotated about its peak, assuming that the flow has circular symmetry. This approach can be implemented either by means of a multigated pulsed Doppler system (Fish, 1981; Hoeks et al, 1981) or by one which has an "infinite gate" (Nowicki & Reid, 1981). Account has to be taken of the angle γ, but this can be estimated from the two-dimensional Doppler scan, which can also provide an estimate of the vessel diameter.

An alternative solution to the problem of measuring the time-average velocity of blood flow is to use an ultrasonic beam wide enough uniformly to insonate the entire lumen of the blood vessel. A suitable beam can be formed by means of an annular transducer array with appropriate phase and amplitude grading of the signals associated with each transducer element (Fu & Gerzberg, 1983). In fact, such a beam does not yet seem to have been used to improve the accuracy of the traditional velocity–area method, but it is an essential feature of the attenuation-compensated blood flow volume ratemeter (Evans et al, 1986, 1989b). This is a practical realization of the second of the two different main approaches to the blood flow volume rate measurement problem. The principles are illustrated in Fig. 13. The wide beam provides the power spectrum of all the flowing blood, and the narrow beam allows this to be corrected for the attenuation in the overlying tissue so that the blood flow volume rate can be calculated. The resulting measurement is independent of the area of the cross-section of the vessel and its orientation. So far, instruments based on this principle have only been made for measuring the cardiac output with the transducer placed in the suprasternal notch; incorporation in a duplex scanning system would permit the study of many other vessels, the anatomical positions of which are not obvious without imaging guidance.

Instruments for intracavitary, endoscopic and intraoperative applications

However excellent any non-invasive ultrasound imaging or measurement method may be, it is likely that if the same technique is applied invasively it will become even better. Amongst the advantages enjoyed by invasive methods are the reduction or elimination of overlying tissues—so that higher ultrasonic frequencies can be used and less beam distortion occurs—and the possibilities for controlling the geometries of the studies. Examples of what can be done include more direct access to the ovarian vessels by a Doppler probe in the lateral fornix (Taylor et al, 1985), colour flow imaging of the heart with an oesophageal endoscope (Roelandt & Sutherland, 1988) and intraoperative measurement of blood flow volume rate in exposed arteries (Beard et al, 1986).

Clinical applications

Cardiology

Doppler techniques, including colour flow imaging, are complementary to real-time scanning and M-mode studies in cardiological investigations. Nowadays, real-time, two-dimensional scanning is the primary procedure, providing an overall view of cardiac structure and function. The importance of M-mode has declined since the 1960s, so that its remaining uses are in the measurement of distance and time and in the study of rapid events such as valve leaflet flutter.

Doppler techniques are important because they make it possible for intracardiac blood flow to be observed and for some aspects of haemodynamics to be measured (Wilde, 1989). In summary, Doppler techniques are used in cardiology for the measurement of flow in the aorta, for the assessment of congenital and acquired heart diseases and for the estimation of pressure gradients.

In 1972, Light and Cross first described the technique, which they called "transcutaneous aortovelography", by which ultrasonic Doppler signals are acquired from blood flowing in the thoracic aorta, using a transducer positioned in the suprasternal notch. In the absence of information about the cross-sectional area of the aorta, it is only possible to follow changes in cardiac function resulting from exercise, therapy and so on. Although preoccupation with the problems of the early instrumentation diminished enthusiasm for the method, there is no doubt that it can provide clinically useful data (Barker et al, 1985).

The traditional approach to the ultrasonic Doppler measurement of cardiac output depends on obtaining values for the cross-sectional area of the aorta and the average velocity of the blood flowing through it. This is fraught with problems. The cross-sectional area can be estimated by pulse–echo ultrasound, but it changes throughout the cardiac cycle. A value for the average flow velocity can be obtained by assuming a flat velocity-flow profile close to the aortic valve during systole, but the plug-shaped jet may not extend to the walls of the aortic root. Moreover, different probe positions are necessary for imaging and for Doppler. Although quite good accuracies have been reported (see, for example, Claflin et al (1988)), it is hardly surprising that the method has not become popular. The attenuation-compensated blood flow volume ratemeter has the potential to change this situation (Evans et al, 1989a). Using the combined wide- and narrow-beam approach, with the probe positioned in the suprasternal notch, and without the need for any imaging guidance, a correlation coefficient of 0.96 was obtained when compared with traditional dilution measurement of cardiac output in a series of 54 patients.

In congenital and acquired heart diseases, in patients in whom vascular stenosis cannot be confirmed by the traditional ultrasound studies, the Doppler detection of increased velocity in systole is useful additional information (Simpson et al, 1985). Similarly, in suspected regurgitation, flow reversal or turbulence in the region of the valve may be observed during diastole (Veyrat et al, 1984). It is important to remember that the Doppler shift frequency only corresponds to the maximum velocity of the jet if the beam and the jet directions are coincident, and, because the velocities are likely to be high, continuous-wave Doppler may be necessary to avoid the problem of exceeding the Nyquist limit of pulsed Doppler unless the high pulse repetition frequency facility is employed (Otto & Pearlman, 1985). The Doppler characteristics of prosthetic and bioprosthetic valves depend on their construction and function, but careful study can be rewarding (Veyrat et al, 1985). Cardiomyopathies can be assessed from the effects that they have on neighbouring valve function (Gardin et al, 1985). Intracardiac masses may likewise modify the haemodynamic situation (Panidis et al, 1986).

The particular contributions that Doppler studies can make in congenital heart disease are discussed in this review in the section concerned with paediatrics.

When a fluid flows through an orifice, its velocity increases and its pressure drops. In the heart, the purpose of the valves is to allow the free transfer of blood or the total arrest of flow, depending on the phase in the cardiac cycle; ideally, there would be no pressure drop across an open valve. The degree of valvular stenosis is usually described quantitatively in terms of the pressure gradient across the valve and traditionally this is measured directly by the invasive procedure of cardiac catheterization.

The relationship between the drop of pressure across an orifice and the velocity of flow through it is well known in hydrodynamic theory as the "Bernoulli equation", named after the Swiss mathematician who lived from 1700 to 1782. Although the full Bernoulli equation is complicated, a modified form can be used to estimate pressure gradients in cardiology from Doppler measurements of flow velocity:

$$P = 4V^2 \tag{3}$$

where P is the pressure gradient (mmHg) and V is the peak velocity (m s^{-1}) at the narrowing. This equation is valid for pressure drops of more than about 70 mmHg and for orifices with diameters greater than about 3.5 mm (Holen et al, 1977). Despite these limitations, this technique depends only on taking care that the maximum velocity of the jet is measured (and colour flow imaging can reduce the likelihood of error) and has come into quite widespread clinical use (Hatle et al, 1978; Loperfido et al, 1987; Veyrat et al, 1987).

As far as the mitral valve is concerned, it has been shown (Libanoff & Rodbard, 1968) that the most consistently useful index of the severity of stenosis is the "pressure half-time" ($T_{1/2}$). This can be measured ultrasonically as the time taken for the peak pressure gradient in early diastole (calculated from Equation 3) to drop to half its value. This is related to the mitral valve area (MVA) as follows:

$$\mathrm{MVA} = 220/T_{1/2} \tag{4}$$

where MVA is in square centimetres and $T_{1/2}$ is in milliseconds.

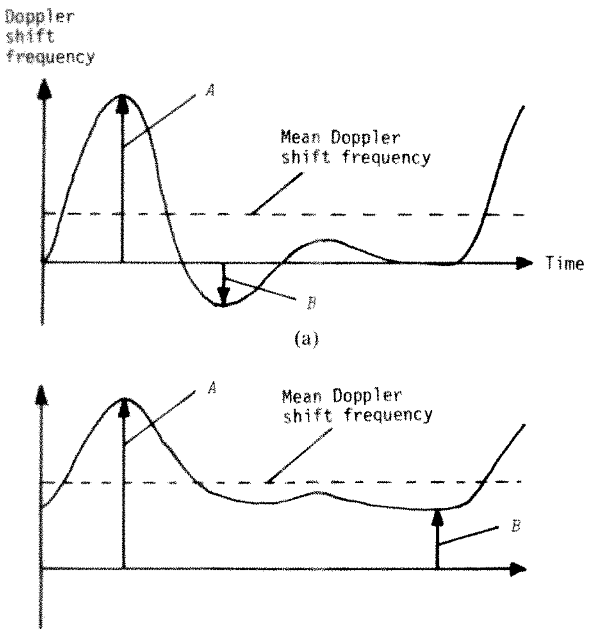

(a)

(b)

Figure 14. Examples of blood-velocity/time waveforms. (a) Waveform associated with high impedance vascular bed, characterized by reverse flow in diastole. (b) Waveform associated with low-impedance bed, with forward flow throughout the cardiac cycle.

An ingenious extrapolation may make it possible for the absolute value of the pressure in the pulmonary artery to be estimated from valve pressure gradients determined non-invasively by Doppler ultrasound. In patients with tricuspid regurgitation, the maximum velocity through the valve in systole gives the pressure difference between the right ventricle and the right atrium. The atrial pressure is likely to be 5–10 mmHg, and hence the systolic pulmonary artery pressure can be estimated. Similarly, the gradient of pulmonary regurgitation can be used to estimate the diastolic pressure since the right ventricular pressure is around 5–10 mmHg at this phase in the cardiac cycle (Currie et al, 1985; Masuyama et al, 1986). A similar approach can be used to estimate left ventricular end-diastolic pressure in the presence of aortic regurgitation (Handsoe & DeMaria, 1985).

Doppler colour flow imaging is very attractive in cardiological investigations. The images are startling in impact and graphic in the demonstration of intracardiac flow patterns, allowing the immediate detection of many abnormalities, including those which can only be diagnosed by skilled operators using duplex scanning. At present, the most promising applications in the adult are in acquired valvular diseases (Omoto et al, 1984).

Peripheral vascular circulation

The traditional ultrasonic Doppler approach to the measurement of the arterial status of the lower limb depends on measurements of the pulsatility indices of the velocity/time waveforms as the pulse propagates along the artery, and its transit times (Atkinson & Woodcock, 1982).

Blood-velocity/time waveforms (typical examples of which are shown in Fig. 14) can be characterized in terms of several different indices, the most popular of which are:

$$\text{Pulsatility index (PI)} = \frac{1}{A_0^2} \sum_{n=1}^{N} A_n^2 \qquad (5)$$

where A_n is the amplitude of the nth Fourier harmonic of the waveform and A_0 is the mean value (Woodcock, 1970). A simpler but closely equivalent derivation (Gosling & King, 1975) is now almost always used:

$$\text{PI} = \frac{A-B}{\text{mean}} \qquad (6)$$

An index that does not require the calculation of the mean is the "resistance index" (RI) introduced by Pourcelot (1974):

$$\text{RI} = \frac{A-B}{B} \qquad (7)$$

Another popular index is that of Stuart et al (1980), known as the A/B ratio.

In essence, the objective of waveform analysis is to derive a simple numerical index, or set of indices, which characterizes the physiological and pathological states of the blood vessel and the organs associated with it. For example, the pulsatility index increases with increasing distal impedance; moreover, this is explicable by means of a simple haemodynamic model. The coefficients derived by Laplace transform analysis can similarly be related to elastic modulus, distal impedance and proximal lumen radius (Skidmore & Woodcock, 1980). As an alternative, a completely empirical approach can be adopted in which the features that distinguish normal waveforms from waveforms obtained from individuals with known disease processes are arbitrarily identified by the technique known as "principal components analysis" (Martin et al, 1980; Evans, 1984).

An excellent but quite typical example of the kinds of data that can be obtained by non-invasive ultrasonic Doppler studies has been presented by Baker et al (1984). They analysed the signals from the femoral artery in 60 limbs with arterial disease and in 20 limbs in normal control subjects, using the Laplace transform damping method to assess aorto-iliac stenosis. With a damping value of 0.60 used as the cut-off point between non-occlusive lesions and iliac stenosis of greater than 50% diameter reduction, the sensitivity was 100% and the specificity 93% when the results were compared with angiography. The particular advantage of the Laplace transform analysis is that, unlike pulsatility index measurements, the accuracy is not affected by downstream disease.

In fact, it is no longer the actual method of analysis that limits the clinical information that can be obtained from single-value waveforms such as the maximum or mean velocity/time relationships derived from accessible vessels. For more information, the most promising approach is to begin quantitatively to study the frequency spectral distribution of the Doppler signal in more detail.

Because they lack natural pulsation, the Doppler assessment of peripheral veins requires more active test procedures. Manual compression of a distal site is necessary to determine vessel patency and valve function (Sumner, 1979). Doppler tests generally perform rather badly in comparison with venography (Day et al, 1976). Real-time ultrasound imaging, however, is probably now the most appropriate initial investigation for patients suspected to have deep vein thrombosis (O'Leary & Kane, 1988) and Doppler ultrasound is a useful adjunct.

Unlike arteriography and venography, which only give anatomical information, and the indirect non-invasive vascular procedures, which reflect haemodynamic status, ultrasound studies are unique in inexpensively and conveniently combining both anatomical and physiological data. The techniques that have already been developed allow precise localization and characterization of disease and are of great value in monitoring progression and the effects of treatment. The additional and complementary capability of colour flow imaging as a preliminary to more quantitative studies promises to speed up the work of the vascular laboratory and further to reduce the likelihood of error.

Cerebrovascular circulation

The widespread availability of duplex scanners and, more recently, the development of real-time colour flow imaging systems have rather obscured the solid, conscientious work that was done a decade or so ago with manually operated two-dimensional Doppler scanners. For example, White et al (1980) rather self-deprecatingly described the imaging of the vertebral artery and the demonstration of retrograde flow in "steal" syndromes. More bullishly, Lusby et al (1981) concluded that a multigated, pulsed Doppler imaging system had the capability necessary for routine screening of patients with low- or high-grade stenoses of the carotid artery bifurcation.

Duplex scanning is a reliable technique for the initial screening of patients with clinical suspicion of carotid disease (Malat et al, 1986). It is a sensible preliminary to angiography and is excellent for monitoring patients with early lesions or transient ischaemic attacks, and after endarterectomy.

The assessment of the extent of carotid artery disease from the Doppler frequency spectrum is a well established method (Spencer & Reid, 1979; Sheldon et al, 1983; Morin et al, 1988). The basis of the technique is that the blood flow is disturbed by atheromatous plaques protruding into the vessel lumen, the resulting turbulence giving rise to Doppler shift frequencies spread over a wider spectrum than that of those from normal arteries. For example, in comparison with biplanar angiography, Hames et al (1985) found that the sensitivity of duplex scanning was 93% and the specificity 98% in 85 patients with more than 50% stenosis; less accurate results were obtained with lesser degrees of stenosis. An additional clue to the severity of disease is provided by the direction of periorbital flow, which reverses as the degree of carotid artery stenosis increases above about 50% (Sillesen et al, 1987).

Although duplex scanning is similar in accuracy to angiography in the evaluation of the proximal common carotid arteries and the bifurcation, a pre-operative angiogram is still necessary to search for more distal and proximal disease and to evaluate the vertebro-basilar system, especially prior to vertebral or subclavian bypass.

One of the most significant limitations of duplex studies of the extracranial carotid arteries is that only a small volume of the vessel lumen can be evaluated at a time. Colour flow imaging has the advantage of allowing flow patterns to be studied, and the rapid identification of branches and associated anatomical variations (Zierler et al, 1987). The method does lack the quantitative capability of duplex scanning, however, and so the two approaches continue to be complementary.

Although currently the main application of ultrasound in neurology is in the evaluation of the extracranial arteries, the measurement of systolic and diastolic flow velocities in the basal cerebral arteries through the intact skull has been shown to the reliable and reproducible (Arnolds & von Reutern, 1986). Static and dynamic compression tests can be used for the positive identification of the middle, anterior and posterior cerebral arteries, and the basilar artery can be located without risk of ambiguity through the occipital foramen. The Doppler investigations add haemodynamic data to angiography and allow serial studies to be carried out in pathological conditions. For example, Padayachee et al (1986) have described the assessment of flow in the circle of Willis in patients with extracranial carotid disease and the consequent elucidation of the collateral pathways.

Obstetrics and the female pelvis

It is easy to detect Doppler signals from an active ovary (Taylor, 1988). Early in the normal menstrual cycle, both ovaries give rise to similar high-impedance signals of low amplitude and without evidence of diastolic flow. The amplitude and frequency of the signals from the ovary developing the dominant follicle then increase, having maximum values around Day 21, and with continuous flow throughout diastole. After Day 23, there is a rapid reversion to the conditions existing at the beginning of the cycle.

In women with stimulated cycles and bilateral ovulating ovaries, the flow changes occur symmetrically. If pregnancy occurs, the corpus luteum maintains its function for the first trimester and the active waveforms persist throughout this period. The presence of luteal flow is good evidence of continuing pregnancy in patients with threatened abortion, and can be definitive in the diagnosis of ectopic pregnancy.

The most satisfactory and commonly used signal for non-invasive fetal heart rate estimation is obtained by Doppler ultrasound. The fetal heart rate is a good indicator of the status of the fetus, particularly during labour (Flynn & Kelly, 1977). Imaging is seldom used to locate the heart, since the Doppler signals are characteristic enough to be self-evident (Callagan et al, 1964). Continuous monitoring is possible with the transducer strapped to the maternal abdomen.

Kurjak et al (1988) have pointed out that, until the end of the 1970s, the only aspect of fetal cardiovascular physiology that could be investigated during human pregnancy was the fetal heart rate. Although FitzGerald and Drumm (1977) described the Doppler detection of flow in the umbilical vein, it was left to Gill (1979) to be the first to estimate the blood flow volume rate in this vessel, using measurements of average velocity and cross-sectional area. To be clinically useful, it is generally better to describe the flow in terms of (ml min^{-1} kg^{-1}), but this requires an estimate also to be made of the fetal weight, which is itself subject to large errors.

Although the clinical status of the fetus has been reported to be correlated with values of blood flow volume rates in the umbilical vein and in the fetal aorta (Gill et al, 1984; Griffin et al, 1985), the technique has not been widely adopted. Apart from the skill and patience needed for the measurements, it has been suggested by Kurjak et al (1988) that this has been due to the almost simultaneous revival in interest in the much easier and faster technique of fetal Doppler waveform analysis. The reason for this growing enthusiasm was the new availability of real-time duplex scanners, which allowed pulsed Doppler signals reliably to be obtained from fetal vessels that could be confidently identified. The usual measures of pulsatility have been applied but with rather uniformly disappointing results in the prediction of fetal health. For example, pulsatility estimates in the umbilical artery lack the sensitivity and specificity necessary for use as a prospective test for intrauterine growth retardation (IUGR) (Trudinger et al, 1986), although there seems to be no doubt that there is an increase in waveform pulsatility in growth retarded fetuses, presumably because of the decrease in diastolic flow resulting from increased placental resistance. Disappearance of diastolic flow in the fetal aorta is also a bad omen (Hackett et al, 1987). Presumably because of the "brain-sparing effect", there is a decrease in pulsatility index in the internal carotid artery (and an increase in the umbilical artery and aorta) in fetuses with post-natally confirmed IUGR (Wladimiroff et al, 1986).

Doppler blood flow signals can easily be obtained from the maternal external and internal iliac arteries and, usually, from the uterine and ovarian arteries (Taylor et al, 1985). The pulsatility indices in both the uterine and ovarian arteries fall as pregnancy proceeds beyond about the 12th week. Using the external iliac artery as an anatomical landmark, Doppler signals can be obtained from the arcuate artery (Campbell et al, 1983). The waveform normally demonstrates low pulsatility and high velocity throughout diastole, but the pulsatility increases if there is a lack of trophoblast invasion. Later in pregnancy, increase in pulsatility is quite a good indicator of fetal compromise (Campbell et al, 1986; Trudinger et al, 1987). Colour flow imaging should make this investigation easier (Pearce & McParland, 1988) and might help to resolve doubts about the reliability of the method (Hanretty et al, 1988).

It has to be admitted that studies of flow in individual vessels have not resulted in the identification of a good method for detecting IUGR. Because of this, it is natural that attempts have begun to see if the desired information can be obtained by observing the relationship between flows in pairs of vessels. For example, it has been shown that from 26 weeks gestation onwards, the ratio of the flow volume rates in the umbilical vein and the descending aorta remains constant in normal pregnancies (Chen et al, 1988). It seems possible that the ratio might change if the fetus is compromised.

Using ultrasound imaging alone, it is virtually impossible to distinguish between hydatidiform mole, hydropic degeneration, degenerating fibroids or ovarian dysgerminomas and the rare but serious condition of gestational trophoblastic neoplasia. This tumour is highly vascular, however, and raised systolic and diastolic Doppler frequency shifts can be detected in the uterine artery (Taylor et al, 1987b).

The prenatal diagnosis of congenital heart disease by ultrasound imaging is already quite well established (Allan et al, 1986). Supplementary information can be obtained by duplex scanning and there is clear evidence that colour flow imaging can be helpful in the elucidation of cardiovascular anomalies (DeVore et al, 1987; Matsumura et al, 1987).

Gastroenterology

It is only recently that interest has developed in Doppler studies in the abdomen. So far, attention has been concentrated mainly on the portal vein, the blood supply to the gut and liver transplantation.

It is obvious that the mean blood flow velocity measured by a pulsed Doppler system with a sample volume that includes the blood in the centre of the lumen but not all the remaining blood must tend to overestimate the blood flow volume rate. Moriyasu et al (1986) simulated blood flow in the portal vein by means of a circulation model and, for their equipment, derived a correction factor of 0.57 to account for this. They tested the validity of this correction in the inferior vena cava of dog. In man, they estimated that the volume flow rate in the portal vein was 889 ± 284 ml min^{-1} (mean ± 1 SD) in normal fasting volunteers. Our own unpublished results compare well with this: we measured the volume flow rate to be 864 ± 188 ml min^{-1} in normal supine subjects and observed that this was reduced to 662 ± 169 ml min^{-1} in the standing position. Zoli et al (1986) have shown that flow in the portal vein is quite unaffected by cirrhosis, although the associated increase in the calibre of the vessel results in a reduction in blood flow velocity.

Portal vein patency and direction of flow are critical considerations in the pre-operative assessment of patients who are candidates for decompressive shunts or liver transplants. For example, when flow is from the liver, selective distal splenorenal shunting is inappropriate and a total shunt is necessary. Another problem is the detection of partial thrombus in the portal vein, which often cannot be seen on real-time imaging but which gives rise to flow disturbance on duplex scanning (Alpern et al, 1987) and which is likely to be clearly visible on colour flow imaging. Cavernous transformation of the portal vein is a rare condition, the diagnosis of which can be confirmed by the detection of relatively non-pulsatile, low-velocity Doppler signals (Raby & Meire, 1988).

In healthy subjects, the blood flow volume rate in the superior mesenteric artery, measured by duplex ultrasound scanning, has been found to be $517 \pm 19\,\mathrm{ml\,min^{-1}}$ (mean ± 1 SE) (Qamar et al, 1986a). (As might be expected, the pulsatility index decreases following the ingestion of a meal (Qamar et al, 1986b).) This compares with the $703 \pm 24\,\mathrm{ml\,min^{-1}}$ flow measured in the coeliac axis in fasting subjects, which increased by 38% immediately after ingestion of a liquid meal (Qamar et al, 1985). It is important to note that other methods of measuring intestinal blood flow are invasive and unsuitable for studying ill patients (Qamar & Read, 1985). The blood flow in the superior mesenteric artery has been compared in normal subjects and in patients with dumping syndrome (Aldoori et al, 1985). Following a liquid meal, the volume flow rate approximately doubled in both groups within 5 min, but remained elevated for more than 45 min in the dumping syndrome patients.

Portable duplex scanning is a useful technique for the initial evaluation of liver transplants (Taylor et al, 1986). Complications that can be identified by Doppler include hepatic artery occlusion and portal vein occlusion and stenosis. The method is complementary to ultrasound imaging, which can detect biliary obstruction, intrahepatic and extrahepatic fluid collections, and air in the portal vein due to ischaemic bowel.

Beckly (1984) has described an interesting endoscopic Doppler technique for the prediction of haemorrhage in peptic ulcers. The presence of a sharply localized arterial signal in the ulcer base is a warning sign.

Urology

One of the earliest clinical applications of the ultrasonic Doppler effect was in the assessment of the vascular supply to the transplanted kidney (Sampson, 1969). The use of duplex scanning to locate the main renal artery and its segmental branches within the renal sinus, the interlobular branches between the pyramids and the arcuate branches at the corticomedullary junction now allows the examination to be put on a rational basis so that signs of rejection due to occlusion or stenosis (with associated high-velocity jets) can be detected early (Taylor et al, 1987a). Acute vascular rejection is often associated with increased renovascular impedance, which results in increased pulsatility index. With a threshold pulsatility index of 1.5, Rigsby et al (1982) found that the sensitivity of this test was 79% and the specificity 90%; raising the threshold increases the specificity. Although biopsy is still necessary for the definitive diagnosis of acute tubular necrosis, the pulsatility index remains constant and so can be used to distinguish the condition from rejection, especially in the early post-operative period, for the selection of the appropriate treatment (Piccirillo et al, 1988).

Renal artery stenosis leads to Doppler spectral broadening and an increase in systolic velocity (Dubbins, 1986), although Rigsby et al (1988) have advised caution because of technical problems due to fat, muscle and intestinal gas. Vascular renal carcinomas tend to reduce the impedance to renal artery flow, and this results in reduction in pulsatility index and increased Doppler shift signal frequencies in diastole (Dubbins & Wells, 1986).

Anatomical and vascular causes of impotence are potentially curable. Although the penile–brachial pressure index obtained by Doppler studies has quite wide acceptance as a screening test (Abelson, 1975) the results can be equivocal. If a duplex study demonstrates dilatation of the dorsal penile artery and increased flow during papaverine-induced erection, however, arteriogenic impotence can be excluded (Hricak et al, 1986). Suspected venous leakage should be investigated by cavernosography.

Paediatrics

Doppler ultrasound can be used in the neonate to investigate congenital heart disease, left-to-right shunting through the patent ductus arteriosus, cardiac output and cerebral haemodynamics (Drayton & Skidmore, 1986). Doppler information is complementary to that obtained by traditional imaging methods. Thus, it is useful where there may be a small ventricular septal defect, coarctation of the aorta, valvular stenosis or regurgitation, unusual communications or other flow-restricting lesions (Wilde, 1988). Colour flow imaging has an important role here.

Many of the Doppler techniques used in adult cardiology are applicable in the neonate. The neonatal circulation is very labile, however, mainly because of the immaturity of the control mechanisms, and the situation may be further complicated by instability in very sick babies. Persistence of left-to-right shunting is a major cause of morbidity in pre-term infants and Doppler studies can provide quantitative data (Barron et al, 1984).

In infants, the blood vessels are small and it is difficult to determine the cross-sectional area of the aorta. By taking great care with the measurements, however, Claflin et al (1988) reported a random error of only 7% in the reproducibility of cardiac output estimates in neonates.

Ultrasound imaging of the neonatal brain is now well established as a valuable technique for the detection of intraventricular haemorrhage (Maklad, 1986). The most conveniently accessible cerebral vessels for Doppler studies in the neonate are the anterior and middle cerebral arteries and the carotid arteries in the neck. These vessels are too small for reliable ultrasound measurement of absolute blood flow volume rate, so research has so far concentrated on changes in flow rates and on the pulsatilities of the flow velocity/time waveforms. Moreover, most of the published data relate to the Pourcelot index since, unlike the pulsatility index, this does not require the estimation of the mean Doppler shift frequency but only the maximum and minimum frequencies (see Equation 7). Altered flow patterns occur in hydrocephalus (Hill & Volpe, 1982) and patent ductus arteriosus (Perlman et al, 1981). The anterior, middle and posterior cerebral arteries, the circle of Willis and its tributaries can be seen by Doppler colour flow imaging (Mitchell et al, 1988b). The clinical value of this remains fully to be demonstrated. Although the methodology is sound, Drayton and Skidmore (1986) concluded, from their review of the literature, that none of the studies of cerebral Doppler signals so far reported appears to be appropriate for routine clinical application. The same authors reported their own work on a promising approach based on volumetric measurements at three sites in the aorta, allowing estimates to be made of volume flow rates to the head, neck and arms, through the patent ductus arteriosus, and to the abdomen and legs. Unavoidable random errors occur, however, and the technique is more applicable to population studies than to the individual.

Extracorporeal membrane oxygenation is being used increasingly often, especially in the USA, in the treatment of the newborn with severe respiratory failure and who have not responded to conventional ventilation assistance. The principal hazard of the procedure is that of cerebral haemorrhage and infarction. The pulsatility normally decreases in the anterior cerebral, middle cerebral and internal carotid arteries at the outset of treatment. So far, no reliable correlation has been found to exist between the flow characteristics and the onset of damage (Taylor et al, 1988a), although results with colour flow imaging are quite encouraging (Mitchell et al, 1988a).

Oncology

The Doppler technique has great potential for the non-invasive characterization of tumours. The phenomenon originally discovered by Wells et al (1977) results from neovascularization of malignant lesions. For example, in comparison with normal breast arteries and benign lesions, malignant lesions give rise to Doppler signals of higher frequencies and higher amplitudes, and flow continues throughout diastole. Burns et al (1982) demonstrated that the high-frequency signals are due to arterio-venous shunts; the low impedance of the tumour vascular bed accounts for the other characteristics of the Doppler signals. Out of 55 patients with breast malignancy, only 4% had none of the characteristics of abnormal signals, whereas there were 84% true negatives in 349 subjects with benign lesions. Good though these results may be, the method is not good enough for screening. At present, the most important applications in breast disease are in the preliminary investigation of suspicious lumps and in the management of cancer therapy. In pre-menopausal women, Sambrook et al (1987) have shown that the most useful results are obtained at midcycle.

Taylor et al (1988b) detected abnormal Doppler signals in 44 of 47 patients with primary malignant tumours of the liver, kidney, adrenal gland or pancreas. Two different signal types were noted: a high-velocity signal ($n = 38$) with Doppler shift frequencies exceeding 3 kHz (using an ultrasonic frequency of 3 MHz) and a very low-impedance signal ($n = 9$) demonstrating little systolic–diastolic variation. In three patients, both types of signal were present. In comparison with angiography, Doppler ultrasound is generally more sensitive to arterio-venous shunting. In addition, imaging and Doppler studies may be complementary. For example, it may not be possible to distinguish between the textures in the scans of malignant and benign thyroid lesions, but the detection of a high-frequency Doppler signal from the superior thyroid artery is a reliable indicator of hyperthyroidism (Woodcock et al, 1985). Moreover, follicular carcinoma of the thyroid gives rise to Doppler signals that are different from those from adenoma.

Until the development of colour flow imaging, the application of Doppler techniques to the problem of malignancy was limited by the difficulty of exploring large volumes of tissue with single ultrasonic beams. Rubin et al (1987) have shown not only that multidirectional flow, presumably due to complex arterial patterns and arterio-venous shunts, can be demonstrated by colour flow imaging, but also that the flow patterns (in an animal model) can be modified (and enhanced) by vasoactive drugs.

Tumours that demonstrate X-radiographic enhancement with the administration of vascular contrast medium also, in general, can be identified by Doppler colour flow imaging (Shimamoto et al, 1987). The administration of ultrasound contrast agents would be likely to enhance this effect.

The safety of Doppler ultrasound

Extensive surveys of the biological effects of ultrasound have failed to reveal any evidence of hazard with the exposure conditions used in contemporary diagnostic techniques (Wells, 1987).

Taylor (1987) has cogently argued against the trend towards bureaucratic regulation of the use of Doppler ultrasound. The position taken by the US Food and Drug Administration, for example, is that the "output" of ultrasonic instruments must not exceed that of the machines that were in common clinical use before the enactment of the present legislation in 1976. Clearly this approach to the control of a technique with no known biological hazard is controversial. Although no-one should be needlessly exposed to ultrasound, it should be for the doctor to decide, preferably with the active participation of the patient, whether the likely benefit of the examination outweighs the detriment. In this context, the principal sources of detriment are the financial cost of the test and the risk of misdiagnosis; there is almost certainly no biological risk at all. Indeed, it sometimes seems that it might be better if ultrasound did carry a tiny but quantifiable biological detriment, since that might help to put all the fuss into perspective for those not perceptive enough to realize that there might conceivably be other yet undiscovered effects! The whole matter has been thoroughly explored by Wells (1986), who concluded that the use of skill and good judgement in the allocation of resources, the involvement of appropriately qualified, trained and capable staff and the provision of the right balance of suitable and properly maintained equipment is the best way to ensure prudence in the use of ultrasound.

Acknowledgments

I am grateful to my colleagues Dr H. S. Andrews, Miss H. S. Brown, Ms S. E. A. Cole, Dr J. M. Evans, Dr M. Halliwell, Dr N. P. Luckman, the late Dr M. I. Qamar, Professor A. E. Read and Dr R. Skidmore for much good advice and for permission to quote unpublished data. Mrs J. R. Fish and Mr G. P. Garland gave excellent help in the preparation of the manuscript and the illustrations. This review is based on the Toshiba Lecture that I was honoured to present to the British Medical Ultrasound Society in December 1987 and it is a pleasure to thank Dr M. R. Jones for the encouragement that she gave me.

References

Abelson, D., 1975. Diagnostic value of penile pulse and blood pressure: a Doppler study of impotence in diabetics. *Journal of Urology, 113*, 636–639.

Aldoori, M. I., Qamar, M. I., Read, A. E. & Williamson, R. C. N., 1985. Increased flow in the superior mesenteric artery in dumping syndrome. *British Journal of Surgery, 72*, 389–390.

Allan, L. D., Crawford, D. C., Chita, S. K. & Tynan, M. J., 1986. Prenatal screening for congenital heart disease. *British Medical Journal, 292*, 1717–1719.

Alpern, M. B., Rubin, J. M., Williams, D. M. & Caper, P., 1987. Porta hepatitis: duplex Doppler US with angiographic correlation. *Radiology, 172*, 53–56.

Arnolds, B. J. & von Reutern, G.-M., 1986. Transcranial Doppler sonography. Examination technique and normal reference values. *Ultrasound in Medicine and Biology, 12*, 115–123.

Atkinson, P., 1975. An ultrasonic fluctuation velocimeter. *Ultrasonics, 13*, 275–278.

Atkinson, P. & Woodcock, J. P., 1982. *Doppler Ultrasound and its Application in Clinical Measurement* (Academic Press, London).

Baker, J. D., Machleder, H. I. & Skidmore, R., 1984. Analysis of femoral artery Doppler signals by Laplace transform damping method. *Journal of Vascular Surgery, 1*, 520–524.

Barker, I., Alderson, J., Lydon, M. & Franks, C. I., 1985. Cardiovascular effects of spinal subarachnoid anesthesia. *Anesthesia, 40*, 533–536.

Barron, J. V., Sahn, D. J., Valdes-Cruz, L. M., Lima, C. O., Goldberg, S. J., Grenadier, E. & Allen, H. O., 1984. Clinical utility of two-dimensional Doppler echocardiographic techniques for estimating pulmonary to systemic blood flow ratios in children with left to right shunting atrial septal defect, ventricular septal defect or patent ductus arteriosus. *Journal of the American College of Cardiology, 3*, 169–178.

Beard, J. D., Evans, J. M., Skidmore, R. & Horrocks, M., 1986. A Doppler flowmeter for use in theatre. *Ultrasound in Medicine and Biology, 12*, 883–889.

Beckly, D. E., 1984. The use of an endoscopic Doppler device in prediction of haemorrhage. *British Journal of Radiology, 57*, 447.

Bradley, J., 1729. An account of a new discovered motion of the fix'd stars. *Philosophical Transactions of the Royal Society (London), 35*, 637–661.

Burns, P. N., Halliwell, M., Wells, P. N. T. & Webb, A. J., 1982. Ultrasonic Doppler studies of the breast. *Ultrasound in Medicine and Biology, 8*, 127–143.

Callaghan, D. A., Rowland, T. C. & Goldman, D. E., 1964. Ultrasonic Doppler observation of the fetal heart. *Obstetrics and Gynecology, 23*, 637.

Campbell, S., Diaz-Recasens, J., Griffin, D. R., Cohen-Overbeek, T., Pearce, J. M., Willson, K. & Teague, M. J., 1983. New Doppler technique for assessing uteroplacental blood flow. *Lancet, i*, 675–677.

Campbell, S., Pearce, J. M. F., Hackett, G., Cohen-Overbeek, T. & Hernandez, C., 1986. Qualitative assessment of uteroplacental blood flow: early screening test for high-risk pregnancies. *Obstetrics and Gynecology, 68*, 649–653.

Chen, H. Y., Chang, F. M., Huang, H. C., Hsieh, F. J. & Lu, C. C., 1988. Antenatal fetal blood flow in the descending aorta and in the umbilical vein and their ratio in normal pregnancy. *Ultrasound in Medicine and Biology, 14*, 263–268.

Claflin, K. S., Alverson, D. C., Pathak, D., Angelus, P., Blackstrom, C. & Werner, S., 1988. Cardiac output determinations in the newborn. *Journal of Ultrasound in Medicine, 7*, 311–315.

Currie, P. J., Seward, J. B., Chan, K. L., Fyfe, D. A., Hagler, D. J., Mair, D. D., Reeder, G. S., Nishimura, R. A. & Tajik, A. J., 1985. Continuous wave Doppler determination of right ventricular pressure: a simultaneous Doppler-catheterization study in 127 patients. *Journal of the American College of Cardiology, 6*, 750–756.

Day, T. K., Fish, P. J. & Kakkar, V. V., 1976. Detection of deep vein thrombosis by Doppler angiography. *British Medical Journal, 1*, 618–620.

Devore, G. R., Horenstein, J., Siassi, B. & Platt, L. D., 1987. Fetal echocardiography VII. Doppler color flow mapping: a new technique for the diagnosis of congenital heart disease. *American Journal of Obstetrics and Gynecology, 156*, 1054–1064.

Doppler, C., 1843. Ueber das farbige Licht der Doppelsterne und einiger anderer Gestirne des Himmels. *Abhandlungen Koniglich-bohmische Gesellschaft, Ser. 2*, 465–482.

Doviak, R. J. & Zrnic, D. S., 1984. *Doppler Radar and Weather Observations* (Academic Press, New York).

Drayton, M. R. & Skidmore, R., 1986. Doppler ultrasound in the neonate. *Ultrasound in Medicine and Biology, 12*, 761–772.

Dubbins, P. A., 1986. Renal artery stenosis: duplex Doppler evaluation. *British Journal of Radiology, 59*, 225–229.

Dubbins, P. A. & Wells, I., 1986. Renal carcinoma: duplex Doppler examination. *British Journal of Radiology, 59*, 231–236.

Eden, A., 1986. The beginnings of Doppler. In *Transcranial Doppler Sonography*, ed. by R. Aaslid (Springer, Vienna), pp. 1–9.

Evans, D. H., 1984. The interpretation of continuous wave ultrasonic Doppler blood velocity signals viewed as a problem in pattern recognition. *Journal of Biomedical Engineering, 6*, 272–280.

Evans, J. M., Skidmore, R., Baker, J. D. & Wells, P. N. T., 1989a. A new approach to the noninvasive measurement of cardiac output using an annular array Doppler technique. II: Practical implementation and results. *Ultrasound in Medicine and Biology, 15*, in press.

Evans, J. M., Skidmore, R., Luckman, N. P. & Wells, P. N. T., 1989b. A new approach to the noninvasive measurement of cardiac output using an annular array Doppler technique. I: Theoretical considerations and ultrasonic fields. *Ultrasound in Medicine and Biology, 15*, in press.

Evans, J. M., Skidmore, R. & Wells, P. N. T., 1986. A new technique to measure blood flow using Doppler ultrasound. In *Physics in Medical Ultrasound*, ed. by J. A. Evans (Institute of Physical Sciences in Medicine, London), pp. 141–144.

Evers, M. K., Brandestini, M., Phillips, D. J. & Baker, D. W., 1981. Color digital echo/Doppler image presentation. *Ultrasound in Medicine and Biology, 7*, 21–31.

Fish, P. J., 1981. A method of transcutaneous blood flow measurement—accuracy considerations. In *Recent Advances in Ultrasound Diagnosis 3*, ed. by A. Kurjak & A. Kratochwil (Exerpta Medica, Amsterdam), pp. 110–115.

FitzGerald, D. E. & Drumm, J. E., 1977. Non-invasive measurement of the fetal circulation using ultrasound: a new method. *British Journal of Obstetrics and Gynaecology, 2*, 1450–1451.

Flynn, A. M. & Kelly, J., 1977. Evaluation of fetal well-being by antepartum fetal monitoring. *British Medical Journal, i*, 936.

Fu, C.-C. & Gerzberg, L., 1983. Annular arrays for quantitative pulsed Doppler ultrasonic flowmeters. *Ultrasonic Imaging, 5*, 1–16.

Gardin, J. M., Dabestani, A., Glasgow, G. A., Butman, S., Burn, C. S. & Henry, W. L., 1985. Echocardiographic and Doppler flow observations in obstructed and nonobstructed hypertrophic cardiomyopathy. *American Journal of Cardiology*, 56, 614–621.

Gill, R. W., 1979. Pulsed Doppler with B-mode imaging for quantitative blood flow measurements. *Ultrasound in Medicine and Biology, 5*, 223–235.

——— 1985. Measurement of blood flow by ultrasound: accuracy and sources of error. *Ultrasound in Medicine and Biology, 11*, 625–641.

Gill, R. W., Kossoff, G., Warren, P. S. & Garrett, W. J., 1984. Umbilical venous flow in normal and complicated pregnancies. *Ultrasound in Medicine and Biology, 10*, 349–364.

Gosling, R. G. & King, D. H., 1975. Ultrasound angiology. In *Arteries and Veins*, ed. by A. W. Marcus & L. Adamson (Churchill Livingstone, Edinburgh), pp. 61–98.

Griffin, D., Teague, M. J., Tallet, P., Willson, K., Bilard, K., Massini, L. & Campbell, S., 1985. A combined ultrasonic linear array scanner and pulsed Doppler velocimeter for the estimation of blood flow in the foetus and adult abdomen. II: Clinical evaluation. *Ultrasound in Medicine and Biology, 11*, 37–42.

Hackett, G. A., Campbell, S., Gamsu, H., Cohen-Overbeck, T. & Pearce, M. J. F., 1987. Doppler studies in growth retarded fetus and prediction of neonatal necrotising enterocolitis haemorrhage, and neonatal morbidity. *British Medical Journal, 294*, 13–16.

Hames, T. K., Humphries, K. N., Ratliff, D. A., Birch, S. J., Gazzard, V. M. & Chant, A. D. B., 1985. The validation of duplex scanning and conventional angiography. *Ultrasound in Medicine and Biology, 11*, 827–834.

Handsoe, R. & Demaria, A. N., 1985. Doppler assessment of intracardiac pressures. *Echocardiography, 2*, 127–139.

Hanretty, K. P., Whittle, M. J. & Rubin, P. C., 1988. Doppler uteroplacental waveforms in pregnancy-induced hypertension: a re-appraisal. *Lancet, i*, 850–852.

Hatle, L., Brubakk, A., Tromsdal, A. & Angelsen, B., 1978. Non-invasive assessment of pressure drop in mitral stenosis by Doppler ultrasound. *British Heart Journal, 40*, 131–140.

Hill, A. & Volpe, J. J., 1982. Decrease in pulsatile flow in the anterior cerebral arteries in infantile hydrocephalus. *Pediatrics, 69*, 4–7.

Hoeks, A. P. G., Reneman, R. S. & Peronneau, P. A., 1981. A multigate pulsed Doppler system with serial data processing. *IEEE Transactions on Sonics and Ultrasonics, SU-28*, 242–247.

Holen, J., Aaslid, R., Landmark, K., Simonsen, S. & Ostrem, T., 1977. Determination of effective orifice area in mitral stenosis from noninvasive Doppler data and mitral flow rate. *Acta Medica Scandinavica, 201*, 83–88.

Hricak, H., Taylor, K. J. W., Marich, K., Lue, T. F. & Burns, P. N., 1986. Doppler in urology. In *Genitourinary Ultrasound*, ed. by H. Hricak (Churchill Livingstone, New York), pp. 241–270.

Kaluzynsk, K., 1987. Analysis of application possibilities of autoregressive modelling to Doppler blood flow signal spectral analysis. *Medical and Biological Engineering and Computing, 25*, 373–376.

Kaneko, Z., Kotani, H., Komuta, K. & Satomura, S., 1961. Studies on peripheral circulation by "ultrasonic blood-rheograph". *Japanese Circulation Journal, 25*, 203–213.

Kasai, C., Namekawa, K., Koyano, A. & Omoto, R., 1985. Real-time two-dimensional blood flow imaging using an autocorrelation technique. *IEEE Transactions on Sonics and Ultrasonics, SU-32*, 460–463.

Kurjak, A., Alfirevic, Z. & Miljan, M., 1988. Conventional and color Doppler in the assessment of fetal and maternal circulation. *Ultrasound in Medicine and Biology, 14*, 337–354.

Libanoff, J. & Rodbard, S., 1968. Atrioventricular pressure half-time. Measure of mitral valve orifice area. *Circulation, 38*, 144–150.

Light, L. H. & Cross, G., 1972. Cardiovascular data by transcutaneous aortovelography. In *Blood Flow Measurement*, ed. by C. Roberts (Sector Publishing, London), pp. 60–63.

Loperfido, F., Laurenzi, F., Gimigliano, F., Pennestri, F., Briasucc, L. M., Vigna, C., de Santis, F., Favuzzi, A., Rossi, I. & Manzoli, U., 1987. A comparison of the assessment of mitral valve area by continuous wave Doppler and by cross sectional echocardiography. *British Heart Journal, 57*, 348–355.

Luckman, N. P., Evans, J. M., Skidmore, R., Baker, J. D. & Wells, P. N. T., 1987. Backscattered power in Doppler signals. *Ultrasound in Medicine and Biology, 13*, 669–670.

Lusby, R. J., Woodcock, J. P., Skidmore, R., Jeans, W. D., Hope, D. T. & Baird, R. N., 1981. Carotid artery disease: a prospective evaluation of pulsed Doppler imaging. *Ultrasound in Medicine and Biology, 7*, 365–370.

Maklad, N. F., 1986. Ultrasound of the neonatal brain. In *Ultrasound in Perinatology*, ed. by N. F. Maklad (Churchill Livingstone, New York), pp. 129–156.

Malat, J., Taylor, K. J. W. & Morse, S., 1986. Noninvasive carotid artery evaluation by duplex Doppler. *Connecticut Medicine, 50*, 653–657.

Martin, T. R. P., Barber, D. C., Sherriff, S. B. & Pritchard, D. R., 1980. Objective feature extraction applied to the diagnosis of carotid artery disease using a Doppler ultrasound technique. *Clinical Physics and Physiological Measurement, 1*, 71–81.

Masuyama, T., Kodama, K., Kitabatake, A., Sato, H., Nanto, S. & Inoue, M., 1986. Continuous wave Doppler echocardiographic detection of pulmonary regurgitation and its application to noninvasive estimation of pulmonary artery pressure. *Circulation, 74*, 484–492.

Matsumura, T., Kobayashi, H., Kanzaki, T., Utsu M. & Chiba, Y., 1987. Studies on intracardiac blood flow of human fetus and antenatal diagnosis of congenital heart disease by real-time two-dimensional Doppler flow imaging system. *Japanese Journal of Medical Ultrasonics, 14,* 571–579.

Miszalok, V., Fritzsch, T. & Schartl, M., 1986. Myocardial perfusion defects in contrast echocardiography: spectral and temporal localisation. *Ultrasound in Medicine and Biology, 12,* 581–586.

Mitchell, D. G., Merton, D., Desai, H., Needleman, L., Kurtz, A. B., Goldberg, B. B., Graziani, L. & Wolfson, P., 1988a. Neonatal brain: color Doppler imaging. Part II. Altered flow patterns from extracorporeal membrane oxygenation. *Radiology, 167,* 307–310.

Mitchell, D. G., Merton, D., Needleman, L., Kurtz, A. B., Goldberg, B. B., Levy, D., Rifkin, M. D., Pennell, R. G., Vilaro, M., Baltarowich, O., Dahnert, W., Graziani, L. & Desai, H., 1988b. Neonatal brain: color Doppler imaging. Part I. Technique and vascular anatomy. *Radiology, 167,* 303–306.

Morin, J. F., Johnston, K. W. & Law, Y. F., 1988. Factors affecting the continuous wave Doppler spectrum for the diagnosis of carotid arterial disease. *Ultrasound in Medicine and Biology, 14,* 175–189.

Moriyasu, F., Ban, N., Nishida, O., Nakamura, T., Miyake, T., Uchino, H., Kanematsu, Y. & Koizumi, S., 1986. Clinical application of an ultrasonic duplex system in the quantitative measurement of portal blood flow. *Journal of Clinical Ultrasound, 14,* 579–588.

Nowicki, A. & Reid, J. M., 1981. An infinite gate pulsed Doppler. *Ultrasound in Medicine and Biology, 7,* 41–50.

O'Leary, D. H. & Kane, R. A., 1988. Venous ultrasonography of the lower extremities. In *Clinical Applications of Doppler Ultrasound,* ed. by K. J. W. Taylor, P. N. Burns & P. N. T. Wells (Raven Press, New York), pp. 338–353.

Omoto, R., Yokote, Y., Takamoto, S., Kyo, S., Ueda, K., Asano, H., Namekawa, K., Kasai, C., Kondo, Y. & Koyano, A., 1984. The development of real-time two-dimensional Doppler echocardiography and its clinical significance in acquired valvular diseases. *Japanese Heart Journal, 25,* 325–340.

Otto, C. M. & Pearlman, A. S., 1985. Measurement of high velocities using pulsed Doppler echocardiography. *Echocardiography, 2,* 141–152.

Padayachee, T. S., Kirkham, F. J., Lewis, R. R., Gillard, J., Hutchinson, M. C. E. & Gosling, R. G., 1986. Transcranial measurement of blood velocities in the basal cerebral arteries using pulsed Doppler ultrasound: a method of assessing the circle of Willis. *Ultrasound in Medicine and Biology, 12,* 5–14.

Panidis, I. P., Mintz, G. S. & McAllister, M., 1986. Hemodynamic consequences of left atrial myxomas assessed by Doppler ultrasound. *American Heart Journal, 111,* 927–931.

Pearce, J. M. & McParland, P., 1988. Doppler uteroplacental waveforms. *Lancet, i,* 1287.

Perlman, J. M., Hill, A. & Volpe, J. J., 1981. The effect of patent ductus arteriosus on flow velocity in the anterior cerebral arteries: ductal steal in the premature newborn infant. *Journal of Pediatrics, 99,* 767–771.

Piccirillo, M., Taylor, K. J. W., Flye, M. W., Burns, P. N., True, L. D. & Weltin, G., 1988. Investigation of Doppler waveforms in porcine renal allografts: Doppler-pathologic correlation. *Ultrasound in Medicine and Biology, 14,* 111–115.

Pourcelot, L., 1974. Applications cliniques de l'examen Doppler transcutane. In *Velocimetre Ultrasonore Doppler,* ed. by P. Peronneau (Seminaire INSERM, Paris), Vol. 34, pp. 213–240.

Qamar, M. I. & Read, A. E., 1985. Intestinal blood flow. *Quarterly Journal of Medicine, 56,* 417–419.

Qamar, M. I., Read, A. E., Skidmore, R., Evans, J. M. & Wells, P. N. T., 1986a. Transcutaneous Doppler ultrasound measurement of superior mesenteric artery blood flow in man. *Gut, 27,* 100–105.

——— 1986b. Pulsatility index of superior mesenteric artery blood velocity waveforms. *Ultrasound in Medicine and Biology, 12,* 773–776.

Qamar, M. I., Read, A. E., Skidmore, R., Evans, J. M. & Williamson, R. C. N., 1985. Transcutaneous Doppler ultrasound measurement of coeliac axis blood flow in man. *British Journal of Surgery, 72,* 391–393.

Raby, N. & Meire, H. B., 1988. Duplex Doppler ultrasound in the diagnosis of cavernous transformation of the portal vein. *British Journal of Radiology, 61,* 586–588.

Reid, J. M. & Spencer, M. P., 1972. Ultrasonic Doppler technique for imaging blood vessels. *Science, 176,* 1235–1236.

Rigsby, C. M., Burns, P. N. & Taylor, K. J. W., 1988. Renal duplex sonography. In *Clinical Applications of Doppler Ultrasound,* ed. by K. J. W. Taylor, P. N. Burns & P. N. T. Wells (Raven Press, New York), pp. 201–245.

Rigsby, C. M., Burns, P. N., Weltin, G., Chen, B., Bia, M. & Taylor, K. J. W., 1982. Doppler signal quantitation in renal allografts: comparison in normal and rejecting transplants with pathologic correlation. *Radiology, 162,* 39–42.

Roelandt, J. R. T. C. & Sutherland, G. R., 1988. Oesophageal echocardiography. *British Heart Journal, 60,* 1–3.

Rubin, J. M., Carson, P. L., Zlotecki, R. A. & Ensminger, W. D., 1987. Visualization of tumor vascularity in a rabbit VX2 carcinoma by Doppler flow mapping. *Journal of Ultrasound in Medicine, 6,* 113–120.

Sambrook, M., Bamber, J. C., Minasian, H. & Hill, C. R., 1987. Ultrasonic Doppler study of the hormonal response of blood flow in the normal human breast. *Ultrasound in Medicine and Biology, 13,* 121–129.

Sampson, D., 1969. Ultrasonic method for detecting rejection of human renal allotransplants. *Lancet, ii,* 976–978.

Satomura, S., 1957. Ultrasonic Doppler method for the inspection of cardiac functions. *Journal of the Acoustical Society of America, 29,* 1181–1185.

Shattock, D. P., Weinshenker, M. D., Smith, S. W. & von Ramm, O. T., 1984. Explososcan: a parallel processing technique for high speed ultrasonic imaging with linear phased arrays. *Journal of the Acoustical Society of America, 75,* 1273–1282.

Sheldon, C. D., Murie, J. A. & Quin, R. O., 1983. Ultrasonic Doppler spectral broadening in the diagnosis of internal carotid artery stenosis. *Ultrasound in Medicine and Biology, 9,* 575–580.

Shimamoto, K., Sakuma, S., Ishigaki, T. & Makino, N., 1987. Intratumoral blood flow: evaluation with color Doppler echography. *Radiology, 165,* 683–685.

Sillesen, H., Schroeder, T., Steenberg, H. J. & Hansen, H. J. B., 1987. Doppler examination of the periorbital arteries adds valuable hemodynamic information in carotid artery disease. *Ultrasound in Medicine and Biology, 13,* 177–181.

Simpson, I. A., Houston, A. B., Sheldon, D. C., Hutton, I. & Lawne, T. D. V., 1985. Clinical value of Doppler echocardiography in the assessment of adults with aortic stenosis. *British Heart Journal, 53,* 636–639.

Skidmore, R. & Woodcock, J. P., 1980. Physiological interpretation of Doppler-shift waveforms. I. Theoretical considerations. *Ultrasound in Medicine and Biology, 6,* 7–10.

Spencer, M. P. & Reid, J. M., 1979. Quantitation of carotid stenosis with continuous wave (c-w) Doppler ultrasound. *Stroke, 10,* 326–330.

Stuart, B., Drumm, J., FitzGerald, D. E. & Duignan, N.

M., 1980. Fetal blood flow waveforms in normal pregnancy. *British Journal of Obstetrics and Gynaecology*, *87*, 780–785.

Sumner, D. S., 1979. Diagnosis of venous thrombosis by Doppler ultrasound. In *Venous Problems*, ed. by J. J. Bergan & S. T. Yao (Year Book Medical, Chicago), pp. 159–186.

Taylor, G. A., Short, B. L., Glass, P. & Ichord, R., 1988a. Cerebral hemodynamics in infants undergoing extracorporeal membrane oxygenation: further observations. *Radiology*, *168*, 163–167.

Taylor, K. J. W., 1987. A prudent approach to Doppler US. *Radiology*, *165*, 283–284.

——— 1988. Pulsed Doppler ultrasound of the pelvis and the first trimester of pregnancy. In *Clinical Applications of Doppler Ultrasound*, ed. by K. J. W. Taylor, P. N. Burns & P. N. T. Wells (Raven Press, New York), pp. 246–262.

Taylor, K. J. W., Burns, P. N., Wells, P. N. T., Conway, D. I. & Hull, M. G. R., 1985. Ultrasound Doppler flow studies for the ovarian and uterine arteries. *British Journal of Obstetrics and Gynaecology*, *92*, 240–246.

Taylor, K. J. W., Morse, S. S., Rigsby, C. M., Bia, M. & Schiff, M., 1987a. Vascular complications in renal allografts: detection with duplex Doppler US. *Radiology*, *162*, 31–38.

Taylor, K. J. W., Morse, S. M., Weltin, G. G., Riely, C. A. & Flye, M. W., 1986. Liver transplant recipients: portable duplex US with correlative angiography. *Radiology*, *159*, 357–363.

Taylor, K. J. W., Ramos, I., Carter, D., Morse, S. M., Snower, D. & Fortune, K., 1988b. Correlation of Doppler US tumor signals with neovascular morphologic features. *Radiology*, *166*, 57–62.

Taylor, K. J. W., Schwarz, P. E. & Kohorn, E. I., 1987b. Gestational trophoblastic neoplasia: diagnosis with Doppler US. *Radiology*, *165*, 445–448.

Trudinger, B. J., Cook, C. M., Giles, W. B., Connelly, A. & Thompson, R. S., 1987. Umbilical artery flow velocity waveforms in high-risk pregnancy. *Lancet*, *i*, 188–190.

Trudinger, B. J., Cook, C. M., Jones, L. & Giles, W. B., 1986. A comparison of fetal heart rate monitoring and umbilical artery waveforms in the recognition of fetal compromise. *British Journal of Obstetrics and Gynaecology*, *93*, 171–175.

Veyrat, C., Abitol, G., Bas, S., Manin, J. P. & Kalmanson, D., 1984. Quantitative assessment of valvular regurgitation using the pulsed Doppler technique. Approach to the regurgitant lesion. *Ultrasound in Medicine and Biology*, *10*, 201–213.

Veyrat, C., Gourtchiglouian, C., Dumora, P., Abitol, G., Beuve, D. S. & Kalmanson, D., 1987. A new non-invasive estimation of the stenotic aortic valve area by pulsed Doppler mapping. *British Heart Journal*, *57*, 44–50.

Veyrat, C., Witchitz, S., Lessana, A., Ameur, A., Abitol, G. & Kalmanson, D., 1985. Valvular prosthetic dysfunction. *British Heart Journal*, *54*, 273–284.

Wells, P. N. T., 1977. *Biomedical Ultrasonics* (Academic Press, London).

——— 1980. Ultrasonic Doppler equipment. In *Medical Physics of CT and Ultrasound*, ed. by G. D. Fullerton & J. A. Zagzebski (American Institute of Physics, New York), pp. 343–366.

——— 1986. The prudent use of diagnostic ultrasound. *British Journal of Radiology*, *59*, 1143–1151.

——— (Ed.), 1987. *The Safety of Diagnostic Ultrasound*, *British Journal of Radiology*, Supplement 20 (British Institute of Radiology, London).

Wells, P. N. T., Halliwell, M., Skidmore, R., Webb, A. J. & Woodcock, J. P., 1977. Tumour detection by ultrasonic Doppler blood flow signals. *Ultrasonics*, *15*, 231–236.

White, D. N., Ketellaars, C. E. J. & Cledgett, P. R., 1980. Non-invasive techniques for recording of vertebral artery flow and their limitations. *Ultrasound in Medicine and Biology*, *6*, 315 327.

Wilde, P., 1989. *Doppler Echocardiography* (Churchill Livingstone, Edinburgh).

Wladimiroff, J. W., Tonge, H. M. & Stewart, P. A., 1986. Doppler ultrasound assessment of cerebral blood flow in the human fetus. *British Journal of Obstetrics and Gynaecology*, *93*, 471–475.

Woodcock, J. P., 1970. The significance of changes in the blood velocity/time waveform in occlusive arterial disease in the leg. In *Ultrasonics in Biology and Medicine*, ed. by L. Filipczynski (Polish Scientific Publishers, Warsaw), pp. 243–250.

Woodcock, J. P., Owen, G. M., Shedden, E. J., Hodgson, K. J., Macgregor, A. & Srivastava, A., 1985. Duplex scanning of the thyroid. *Ultrasound in Medicine and Biology*, *11*, 659–663.

Zierler, R. E., Phillips, D. J., Beach, K. W., Primozich, J. F. & Strandness, D. E., 1987. Noninvasive assessment of normal carotid bifurcation hemodynamics with color-flow ultrasound imaging. *Ultrasound in Medicine and Biology*, *13*, 471–476.

Zoli, M., Marchesini, G., Cordiani, M. R., Pisi, P., Brunori, A., Trono, A. & Pisi, E., 1986. Echo-Doppler measurement of splanchic blood flow in control and cirrhotic subjects. *Journal of Clinical Ultrasound*, *14*, 429–435.

1989, *The British Journal of Radiology*, 62, 421–432

Nuclear medicine in the 1990s: a quantitative physiological approach*

By R. J. Ott, BSc, PhD, CPhys

Department of Physics, Institute of Cancer Research and the Royal Marsden Hospital, Sutton, Surrey

(*Received July 1988 and in final form January 1989*)

Technological developments in X-ray computed tomography (CT), ultrasound and magnetic resonance imaging (MRI) in the last 10 years have provided radically improved qualitative diagnostic information relevant to a wide range of human diseases. The impact of these advanced technological processes is difficult to quantify in absolute terms but diagnosis is certainly greatly aided by the wealth of precise morphological information now available. However, human disease often presents with no specific anatomical changes and those seen may be late effects of earlier biochemical processes, which have remained undetected until the patient presents with advanced symptoms. Radionuclide imaging techniques can show physiological changes that are a direct consequence of these biochemical mechanisms, but, so far, nuclear medicine has disappointingly made only a limited impact on both the aetiology and diagnosis of disease. This paper examines the limitations of nuclear medicine in the context of the need for basic information relating to biochemical function of the human body and proposes that positron emission tomography (PET) could become more widely available and could radically increase the clinical impact of imaging with radionuclides.

It will be useful to examine some aspects of the morphological imaging techniques that make CT, ultrasound and MRI successful diagnostic modalities, prior to considering the value and limitations of radionuclide imaging. This will lead on to a discussion of possible ways in which PET may contribute to clinical nuclear medicine with the aim of presenting a possible scenario for the coming decade.

Morphological imaging techniques

Some of the most obvious attributes of the morphological imaging techniques that help to account for their success as diagnostic techniques are described. It is necessary only to look at the basic properties of the physics behind each to understand the success and failures.

The use of X rays has, for historical reasons, dominated the field of diagnostic imaging throughout the 60 years prior to this decade. The intrinsic high spatial resolution obtained in a conventional radiograph of the human anatomy has obviously been of enormous value in diagnosis. This is particularly true in cases where the absorption of X rays in adjacent tissues enables sufficient contrast to allow differentiation between tissues (such as between skeletal and soft tissue). This quality has been complemented in recent years by the vast improvement in the use of the dynamic range available in a conventional X-ray, which can provide high-contrast images of soft tissue using X-ray CT and of the vascular system using digital subtraction radiography (DSR). Hence in the 1980s, X-ray imaging provides excellent discrimination between types of structural pathology which, with skill, can be interpreted into useful and sometimes specific diagnostic information. Additionally, the use of CT numbers can provide some quantification, allowing changes in sequential images to be evaluated and related to treatment efficacy. Further invaluable diagnostic features can be extracted using DSR that lead to precise morphological detail of the vasculature.

The limitations of X-ray imaging lie essentially in the dependence on a single variable (tissue electron density). Even with the enhancement obtained by the use of contrast media, images with limited diagnostic value are often produced in cases where differences in electron density values between tissues are small. X-ray imaging remains the most valuable and flexible of diagnostic techniques being widely available in its conventional form. Both CT and DSR can now be found at a large number of General Hospitals and will continue to have a major impact in the diagnosis of a wide range of human diseases.

The rapid growth of ultrasound imaging as a diagnostic tool can be related to the technological improvements in spatial resolution, the development of real-time imaging to provide *in vivo* contrast not available on a single frame image, the relative low cost and of course the fact that no ionizing radiation is involved. The quantification of echo patterns is still an enticing feature, which may yet lead to increased specificity, and the recent combination of Doppler ultrasound with imaging to provide "flow images" may allow this non-ionizing technique to encroach on the vascular field presently in the X-ray domain. However, the imaging process is heavily operator-intensive and the basic physical processes involved in the production of ultrasound images are extremely complex. This latter feature makes the relationship between the echogenic structure of such images and the physiology and morphology of tissues difficult to interpret. Ultrasound imaging requires much skill, and optimal results can only be obtained when the radiologist reports on his own hard-won images.

---

*The 1988 Mayneord Lecture, sponsored by 3M UK PLC, which was delivered at the BJR 1988 Annual Congress, in Glasgow on 23 May.

The last few years have seen the exciting development of MRI, which, like CT, provides us with high-resolution images of the human anatomy but without the use of ionizing radiation. The technique employs multiple parameters such as proton density and proton relaxation times, which can be used to characterize tissues *in vivo*. This may allow a greater flexibility in obtaining high contrast between different tissues than can be achieved with X rays. However, the very nature of this multiparameter technique implies complexity and the search for specific quantitative diagnostic features may be difficult and certainly time-consuming. At present, the relationships between the proton signals and the biochemical nature of the tissues under study are not well understood. Spectroscopic applications using elements other than hydrogen (phosphorous, fluorine, etc), which could throw light on this aspect, contain limited spatial information because of low signal levels. It is this question of sensitivity and available signal in MRI and magnetic resonance spectroscopy that may be the ultimate limitation of the technique, although the overall cost of MRI facilities is prohibitive at present and the technique is unlikely to be widely available in the near future.

From this brief discussion of the major morphological imaging techniques, it can be seen that none show immediate potential to measure, at a basic level, the biochemical changes in the body tissues that lead to much of human disease. Hence, the continued interest in nuclear medicine.

Nuclear medicine in the 1980s

The basic principles of nuclear medicine have been known for some time (Wagner, 1968). The use of radionuclide-labelled tracers to measure *in vivo* function of tissues should provide sensitive early markers of disease by measuring biochemical changes either directly, using the basic chemical agents involved in the body processes, or indirectly, using labelled metabolites, flow agents, etc. The transient nature of many of the biochemical functions could be monitored using temporal measurements and the quantification of function from images stored on a computer could lead to a definitive discrimination between normal and abnormal function long before morphological changes are measurable. Crucially, the very high sensitivity of the technique means that the tracer quantities used are so small as to leave the body systems quite unperturbed, so that the measurements reflect an accurate estimate of function—a feature relatively unique in this range of imaging techiques.

However, at an early stage in the development of imaging with radionuclides, there came a clear division between the use of tracers labelled with radionuclides decaying via positron emission and others decaying via β emission, electron capture, etc. The development of the Anger or gamma camera in the 1950s and 1960s (Hine, 1967), and continued apace until now, favours the use of imaging with single γ photons emitted per disintegration rather than positron-emitting radionuclides. This division has been furthered by the development of the ^{99}Tc^{m} generator in the 1960s, which provided a radionuclide "on tap" to any hospital and a range of imaging agents (Subramanian et al, 1975) for which the gamma camera was ideally suited. Before this time a wide range of radionuclides were used for imaging, but in the 1980s, typically 90–95% of nuclear medicine studies are performed using ^{99}Tc^{m}-labelled agents and imaging with a gamma camera. The modern gamma camera has been optimized for imaging the 140 keV photons emitted from ^{99}Tc^{m} and nuclear medicine has now become almost totally committed to the use of a single radionuclide to the detriment, in many cases, of useful clinical investigations.

However, because both the imaging detector and the radionuclide are relatively cheap and readily available to hospital diagnostic departments, radionuclide imaging has often been seen as a low-cost screening alternative to morphological imaging. This is, on the whole, a poor use of the technique caused by a general misunderstanding, outside specialized nuclear medicine departments, of the clinical potential of functional imaging. There is no doubt that skeletal imaging, as shown in Fig. 1, appears anatomical in nature, is simpler and in many cases more sensitive to skeletal disease than X-ray imaging. However, this image shows the function of the skeleton in terms of the metabolism of the radiopharmaceutical (in this case methylene diphosphonate) and does not replace a radiograph in any way. Indeed, the radionuclide bone scan is very non-specific and may require a follow-up radiograph to specify the actual disease.

Seen from an anatomical viewpoint, even these images show the result of poor sensitivity and very modest spatial resolution available when using the gamma camera–^{99}Tc^{m} combination, and the physiological information in the image is difficult to interpret. Although revolutionary in the 1960s, single photon imaging with a gamma camera has basic limitations that are difficult to overcome. The sensitivity to the injected dose is low, as only ~0.1% of photons within the solid angle of the camera are detected. This is because of the need for collimation of the incident photon flux. Unfortunately, the use of lead collimators limits the spatial resolution of the system to ~6 mm at the very best (close to the collimator surface) and, more generally, to 15–20 mm depth when tomographic imaging (Ott, 1986) is carried out (Fig. 2).

The use of ^{99}Tc^{m} has allowed a large number of studies to be performed with relatively simple, easy-to-make tracers such as metal chelates (Harbert & da Rocha, 1984). These agents allow studies of, for instance, cardiac and kidney function to be performed, but the information provided gives little insight into the

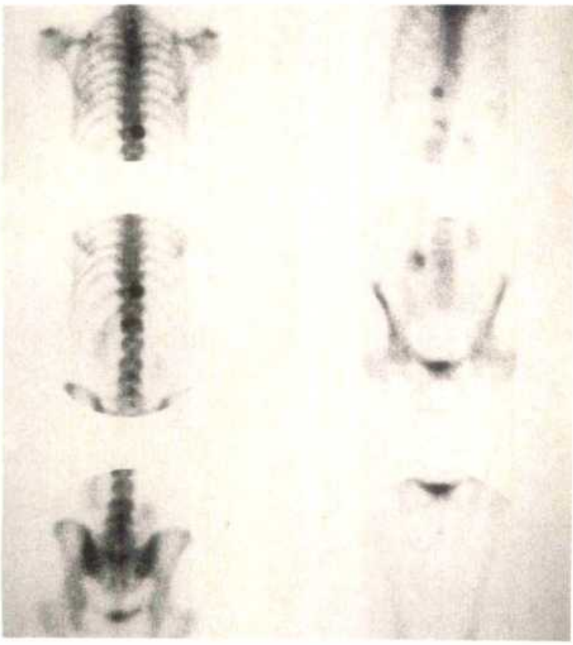

Figure 1. Six planar scintigrams of the human skeleton produced by a gamma camera imaging the distribution of ^{99}Tc^{m}-methylene diphosphonate showing abnormal metabolism in the spine.

biochemical nature of the tissue function and measures only the end product of this function. Tracers that could be used to measure the basic processes involved, such as amino acids, fatty acids, glucose, etc., cannot as yet be complexed to ^{99}Tc^{m}. Hence, it can be seen that single photon imaging, as described here, falls far short of providing the measurements desired from a physiological imaging technique.

The use of positron-emitting radionuclides has been limited to research centres with cyclotron facilities to produce the short-lived radionuclides and having the radiochemistry and radiopharmacy support to provide the agents required. In addition, positron cameras have developed quite separately and differently from single photon imagers, as would be expected by the very nature of the imaging problem. In a very limited way, positron emission tomography (PET) has succeeded where single photon imaging has failed. The technique, as we know it, is based on the use of short-lived radionuclides such as ^{15}O and ^{11}C, which can only be produced by a cyclotron and which, because of their very short half-life, can only be used close to that cyclotron. These nuclides together with ^{13}N and ^{18}F have been used to label a great number of metabolic and physiological agents. Some of the most commonly used are shown in Table I. These agents may be used to study the basic biochemistry of the body processes (Phelps et al, 1986) such as the manufacture of proteins or the generation of energy via metabolism. Positron emission tomography can provide physiological imaging based

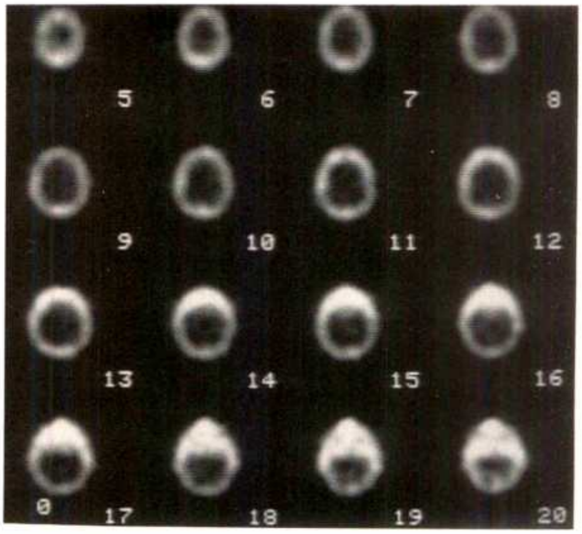

Figure 2. Transaxial 6 mm-thick sections of the brain produced by a rotating gamma camera imaging the distribution of ^{99}Tc^{m}-glucoheptonate. The distribution appears normal showing no activity within the brain tissue.

Table I. Some examples of PET radiopharmaceuticals labelled with short-lived radionuclides produced by a cyclotron

Radio-nuclide	Half-life (min)	Radiopharma-ceutical	Use
^{18}F	110	Fluorodeoxyglucose	Glucose metabolism
		Fluorotyrosine	Amino acid metabolism
		Fluoro-DOPA	Receptor/transmitter studies
		5-Fluorouracil	Anticancer drug kinetics
		Fluoromethane	Tissue perfusion
^{15}O	2	Molecular oxygen	Oxygen metabolism
		Carbon dioxide/water	Tissue perfusion
		Carbon monoxide	Blood volume
^{13}N	10	Ammonia	Tissue perfusion
		Leucine/alanine	Amino acid metabolism
		BCNU	Anticancer drug kinetics
^{11}C	20	Carbon monoxide	Blood volume
		Carbon dioxide	Tissue pH
		Glucose	Glucose metabolism
		L-methionine	Amino acid metabolism
		Palmitic acid	Fatty acid metabolism
		Methylspiperone	Receptor/transmitter studies
		BCNU/CCNU	Anticancer drug kinetics

For more complete list of labelled compounds see Phelps et al (1986).

on these tracers and could supply diagnostic information extending to the aetiology of the disease.

However, the installation of a cyclotron with its associated chemistry have, until now, been prohibited by price and the heavy manpower and space requirements. In addition, the much increased volume of data acquired from these studies has brought about the development of an entirely separate kind of detector system, which is more sophisticated and more expensive then a gamma camera. Based on annihilation coincidence detection techniques, positron cameras include little physical collimation, have a sensitivity approaching 100 times that of a gamma camera and can provide images with a spatial resolution of 4–6 mm throughout the imaging volume. Both these factors are important because the high data rates allow multiple high-count tomographic images to be taken over a period of a few minutes and the resolution provides improved quantitative physiological information in small regions of the anatomy. These data provide the input to the understanding of physiological processes, allowing the extraction of basic parameters relating to tissue function such as flow (in ml/min/g) and metabolism (in, for instance, mg of glucose/g of tissue).

Unfortunately, the expense of the technology has put it beyond the reach of clinical centres in the UK, and PET has, until recently, been exclusively carried out in a single large medical research centre at the MRC Cyclotron Unit at Hammersmith. This has seemed to have been accepted as the *status quo* generally in the UK, although there are two new "PET centres" in the making at Aberdeen University and the Institute of Cancer Research at Sutton, albeit with strictly limited financial support. There has been a much faster growing interest in the potential clinical application of PET elsewhere in Europe (Heiss, 1987).

Recently, commercial radiopharmaceutical manufacturers have spent large sums of money in the development of "equivalent" agents to those used in PET for the measurement of perfusion in the brain and heart. These agents labelled with ^{99}Tc^{m} are complex, and have an unproven relationship to the simple PET agents and, because of the limitations of the gamma camera system, may have only modest clinical applications. Perhaps a more rational approach is a re-examination of the case for the widespread availability of PET for seeking answers to physiological and pathophysiological problems, and to probe the aetiology of disease. We may then have access to a more precise tool to determine treatment efficacy and the prognosis for patients with a wide range of diseases. Before presenting a possible scenario for the use of PET technology at a large number of centres throughout the UK, some of the potential that PET now provides and clinical use that might be made of PET in the next decade should be examined.

Applications of positron emission tomography

The applications of PET to the study of human disease have so far been mainly limited to the brain and to a lesser extent the heart. This has been dictated mainly by the relatively greater understanding of these two systems and by the limited volume that can be imaged using state-of-the-art PET cameras. However, many of the measurements that have been made in the brain and heart are immediately applicable to other organs. In particular, measurements of blood flow in the form of tissue perfusion, oxygen extraction and metabolism, and the metabolism of glucose, amino acids and fatty acids can provide information about the function of many of the body's physiological systems. There is a growing interest in the role of transmitter and receptor ligands in body function and in the kinetics and *in vivo* pharmacology of drugs. Quantitative measurements of regional utilization of a wide range of drugs and agents must surely lead to a greater understanding and control of treatment of disease and it is here that the future power of PET may be realized most effectively.

Examples of the clinical potential of PET can be obtained by looking at some of the applications recently reported (Heiss, 1987). These applications cover the clinical areas of neurology and psychiatry, cardiology, oncology and paediatrics. Obvious future applications are the use of targetted drugs with, for instance, monoclonal antibodies, and studies of other complex physiological systems of the body, such as the endocrine and hepatobilary systems.

Applications in the brain

The role of PET in a wide range of cerebral diseases is now under study at a growing number of centres in Europe, North America and Japan. In particular, studies are in progress to determine the role of physiological imaging in cerebral vascular disease (CVD), senile dementia of the Alzheimer type, multi-infarct dementia, Huntington's chorea, epilepsy, schizophrenia, Parkinson's disease, cerebral palsy and cerebral neoplasm. It would take far too long to describe these applications in detail, so a few examples are given here to illustrate the potential of the technique in the brain.

In CVD, conventional radionuclide imaging with its inherent poor spatial resolution and sensitivity shows unspecific focal damage, whereas X-ray CT and MRI can indicate lesion location and size and may discriminate between tumour, infarct, etc. Positron emission tomography can reveal focal functional disturbances when no morphological damage is visible and, additionally, can show the effect of focal disease on the whole brain (Frackowiak, 1987a). By the use of multiple studies to obtain regional measurements of oxygen extraction and metabolism and blood flow (Baron, 1987), it is possible to delineate between viable and necrotic areas in the brain. These studies (Fig. 3) show that the metabolism of oxygen in the brain can be preserved even when the blood flow is reduced to 55% of normal, that ischaemia sets in when the flow is reduced to 45–55% of normal and infarction takes place when flow is less than 45%. Hence, quantitative

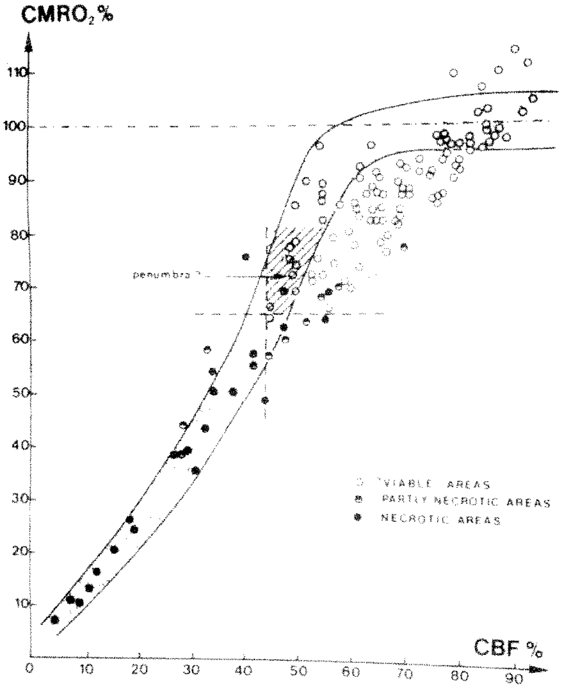

Figure 3. A plot of cerebral oxygen metabolism rates (CMRO$_2$) and cerebral blood flow (CBF) in selected regions of the brain of a patient after an ischaemic attack. The hatched area shows the region of maximal oxygen extraction from the blood supply. (From Heiss, 1987.)

measurements of regional brain perfusion can be predictive and indicative of the efficacy of treatment. Furthermore, measurements of glucose metabolism and blood flow in the brain (Pawlik et al, 1987) suggest variable coupling of the two at different stages in ischaemic stroke (Table II). In the acute stage, uncoupling is the norm, whereas at the chronic stage the two measurements are closely coupled. At the post-acute stage, "luxury perfusion" is prominent. It is possible to make some prognosis from these studies, which indicate that if glucose metabolism is high and perfusion low at the acute stage, a long-term defect is likely, whereas the opposite condition can indicate a favourable clinical outcome. From this we can see that already there appear to be some immediate clinical applications of PET in CVD.

Table II. The relationship between local glucose consumption rates (LCMRGlc) and local blood flow (LCBF) in ischaemic brain lesions. Numbers of patients in the study are shown with percentage of total in parentheses. (From Heiss, 1987.)

	Days after onset of symptoms			
	1–3	4–14	> 14	All
LCMRglc < LCBF	4 (50%)	6 (75%)	5 (20.8%)	15 (37.5%)
LCMRglc ≈ LCBF	1 (12.5%)	2 (25%)	13 (54.2%)	16 (40%)
LCMRglc > LCBF	3 (37.5%)	0 (0%)	6 (25%)	9 (22.5%)
$\sum$	8 (100%)	8 (100%)	24 (100%)	40 (100%)

Dementia, particularly related to senility, is a growing problem in the western world as the average age of the population increases with improved diet and medical care. Alzheimer's dementia has been studied using the available cerebral blood flow, oxygen and glucose metabolism techniques and more recently with ^{11}C-labelled amino acids and ^{18}F-labelled DOPA (dihydroxyphenylalanine) (Frackowiak, 1987b). Glucose studies show that metabolic changes in the brain are often visible before atrophy is seen using CT or MRI. ^{11}C-methionine metabolism has shown specific differences in the utilization of this amino acid between normal subjects and those with borderline and advanced dementia (Bustany & Moulin, 1987). Receptor studies to localize and monitor the effects of drug therapy may play an important role in future in the treatment of a disease of growing importance in our society and for which there is presently no recognized cure. Similarly, the application of blood flow and oxygen metabolism measurements to multi-infarct dementia are likely to show details of impairments and may allow monitoring of treatment of this potentially controllable vascular disease. In particular, these studies may be of importance in cases of mixed dementia (Mazziotta & Phelps, 1986).

In Parkinson's disease and cerebral palsy, studies are being carried out to determine the metabolic changes during on–off syndromes (Schuier, 1987; Chugani & Phelps, 1988), and the measurement of neurotransmitter dysfunction may allow a better characterization of these diseases, perhaps leading to improvement in control and therapy. Here again the use of labelled drugs is likely to be of great importance in the attempts to improve treatment.

Such factors are also important in epilepsy where the relevance of receptor binding sites to this condition may be a major factor for future diagnosis and treatment. Already, measurements of protein synthesis, pH and water content and blood–brain-barrier disruptions can be used to identify disturbances at epileptic foci (Herholz et al, 1987). Indeed, abnormal metabolic patterns in the brain have been seen where morphological lesions are unresolvable.

In schizophrenia there are clear variations in regional metabolism between normal and abnormal subjects and the role of receptors and radionuclide-labelled anti-psychotic drugs can be monitored using ^{18}F-DOPA (Cambon et al, 1987; Farde et al, 1987; Wiesel et al, 1987).

Glucose metabolism in the caudate nucleus of patients with Huntington's chorea is often impaired before atrophy is seen on CT and there appears to be some predictive power in the levels of caudate hypometabolism (Schuier, 1987).

Finally, in the brain, ^{18}F-fluorodeoxyglucose (FDG), and ^{11}C-methionine metabolism together with measurements of regional blood flow and oxygen extraction and metabolism have been used to study primary neoplasms (Mazziotta & Phelps, 1986) and to monitor the effects of therapy (Ogawa et al, 1988). There are indications that there may be some accuracy in tumour grading, particularly for tumours with mixed tissue differentiation where biopsy may be misleading. There are also examples where tumour boundaries are more accurately delineated than with morphological imaging, where there is extensive oedema and where the tumour is invading apparently normal cerebral tissue. These data indicate that there is an immediate application for PET in monitoring the efficacy of treatment of cerebral tumours, which may extend to providing some control over individual treatments.

We can see from this brief review of the use of PET in the study of diseases of the brain that there are already some well documented procedures that could have immediate clinical applications, and that many more will be forthcoming as the technique becomes more accurate and more widely available.

Applications in oncology

An area of growing clinical interest is the applications of PET to a wide range of oncological problems outside the brain. The potential of the techniques used in PET to study the pathophysiological behaviour of tumours in individual patients and the possibility of obtaining information that could differentiate between benign and malignant tissues is now being investigated in several centres in the USA and Europe. The biochemical basis of many of these procedures is ideally suited to the study of degrees of malignancy and tissue growth patterns, and already there are attempts to use specific measurements of tumour metabolism to guide a rational approach to treatment. Once again there is a growing body of evidence that physiological imaging, as discussed here, can, in some cases, show tumour extensions beyond that visualized by morphological imaging and this is particularly aided by the ability to use more than a single agent to examine a tumour system.

Specific studies now being performed with a clinical end-point in view include measurements of perfusion and metabolism to indicate therapeutic response (Fig. 4) and also as a guide to treatment regimes including radiotherapy, chemotherapy and hyperthermia (Beaney & Lammertsma, 1985; Beaney, 1987; Schelstraete, 1987). In addition, follow-up studies show that it is possible to differentiate between tumour recurrence and radiation necrosis and between tumour and surrounding oedema (Ericson et al, 1987).

A likely important application involving PET will be the use of labelled monoclonal antibodies to take dual advantage from the suggested increased specificity of the agent to the disease and the increase in sensitivity and spatial resolution of PET camera systems. Furthermore, the use of anticancer drugs labelled with appropriate radionuclides will allow *in vivo* dosimetry for the first time (Beaney & Lammertsma, 1985; Yamamoto & Diksic, 1985; Mazziotta & Phelps, 1986). Both these applications may have great importance in the treatment of diffuse disease, an area where other techniques have little to contribute at present.

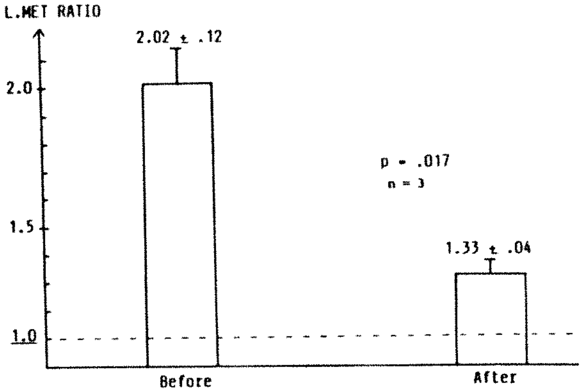

Figure 4. The effect of radiotherapy on the metabolism of ^{11}C-L-methionine in glioblastomas. The L.MET ratio is the ratio of metabolism in tumour compared with normal tissue control values. (From Heiss, 1987.)

Myocardial applications

Studies of the applications of PET to myocardial disease have, until recently, been limited by poor spatial and temporal resolution. With current positron camera systems, it is now possible to apply the familiar techniques to heart disease, particularly to determine the physiological changes in the heart muscle that give rise to heart malfunction. Clearly, the vascular supply to the myocardium is of great importance and DSR studies have been extremely helpful in the diagnosis of heart–vessel disease. However, the relationship between occlusion or stenosis of myocardial vessels and the physiological and biochemical processes taking place subsequently in the muscle is clearly a subject ideally suited for PET. It has been shown by measurements of regional flow and metabolism that the reduction in oxygen supply to the myocardium leads to a reduction in the oxidation of free fatty acids in the tissue and an enhancement of glucose consumption (and increased anaerobic glycolysis) (Schelbert & Schwaiger, 1986; Taegtmeyer, 1986). Using a few selected agents it is possible to examine the changes taking place in the metabolism of the heart in cases of both transient, reversible ischaemia (angina pectoris) (Camici & Araujo, 1987) and prolonged, irreversible ischaemia (myocardial infarction) (Landsheere et al, 1987; Ambrecht et al, 1988).

Figure 5 shows the use of measurements of regional perfusion and glucose metabolism to differentiate between reversible and non-reversible damage to the myocardium, findings that are clearly important if surgical intervention is contemplated. Indeed, these two tests carried out together could indicate whether a bypass operation is sufficient to provide renewed myocardial function or whether a complete transplant is

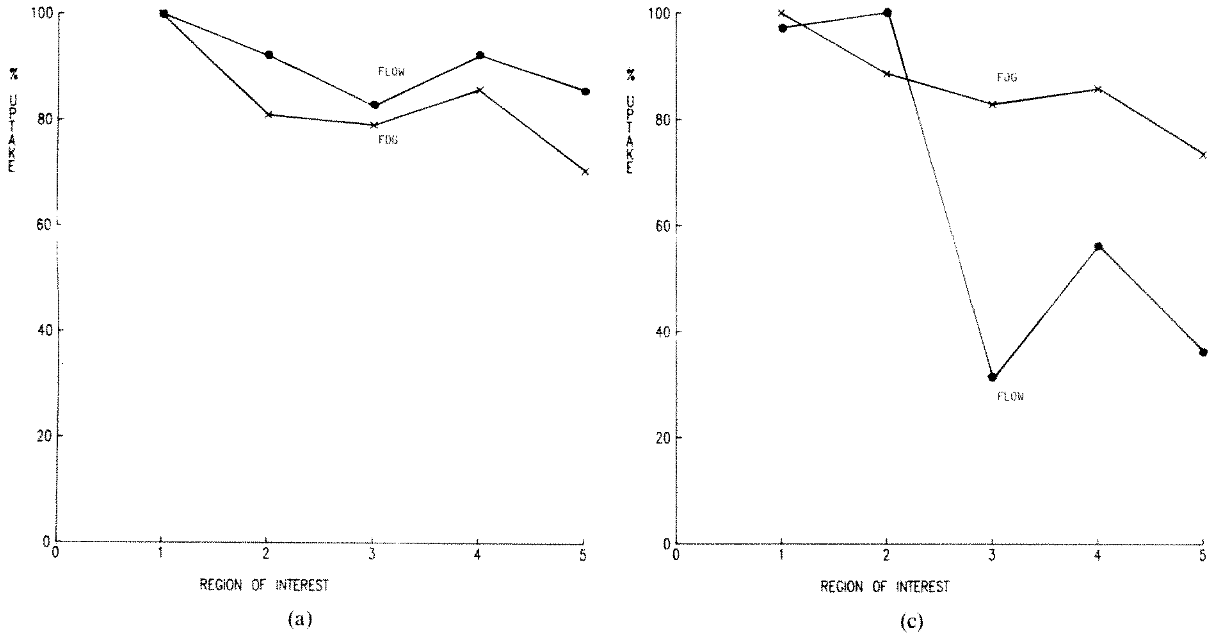

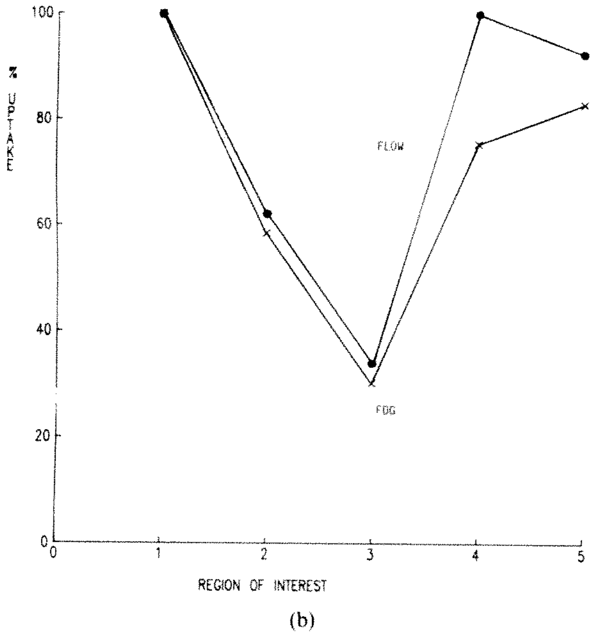

Figure 5. Normalized uptake of ^{38}K (indicating perfusion) and ^{18}F-FDG in the left myocardium. The five regions of interest are: 1, posterior part of the free wall; 2, anterior part of the free wall; 3, anterior wall; 4, anterior part of the septum; and 5, posterior part of the septum. (a) A normal patient; (b) a patient with infarcted regions in the myocardium and (c) a patient with ischaemic regions in the myocardium but with remnant viable tissue. (From Heiss, 1987.)

necessary. At present, the simple perfusion measurements made in nuclear medicine are often inadequate and possibly even misleading.

Another important feature is the ability to repeat measurements over a relatively short time period to study the functional changes brought about by exercise, liquid or food consumption, etc. Clearly, these findings may correlate with prognosis and present an immediate clinical application of PET.

For the near future, two major studies could make a radical contribution to the diagnosis and treatment of heart disease. First, the role of receptors (Syrota, 1987) on the myocardial tissue may lead to a detailed picture of the aetiology of some forms of myocardial disease and perhaps could be predictive of susceptibility. Secondly, the use of labelled drugs such as propanolol may quantify the effects of drug control and perhaps therapy in a manner at present unattainable.

The present development of positron emission tomography

A brief examination of how PET is being viewed by countries other than the UK immediately shows that there is a marked increase in the installation of both research and clinically orientated facilities. In Europe this increase is still slow but steady, and is progressing along classical lines with the provision of a cyclotron, a full radiochemistry/radiopharmacy suite and scanning facilities at large medical research centres. Nevertheless, in Belgium there are now four specialist PET centres and two in Sweden, all now looking to a clinical application of their techniques.

In the USA and Canada the growth of the technique is far greater, partly because of the increased interest in clinical applications (Burns, 1987; Kessler et al, 1987) and the possibility of reimbursement for such studies

Table III. Some examples of ^{18}F-labelled agents that could be available to a user at a distance from a cyclotron

Compound	Classification	Function	Application
NaF	Inorganic salt	Skeletal metabolism	Trauma, neoplasm
Fluoromethane	Inert gas	Freely diffusable tracer	Tissue perfusion
Deoxyglucose	Sugar	Tissue glucose metabolism	Wide range of cerebral and myocardial disease
Deoxyuridine	DNA/RNA base	DNA/RNA synthesis	Tumour growth
Phenyl analine or tyrosine	Amino acid	Uptake and protein synthesis	Tumour growth
DOPA	Amino acid, neurotransmitter ligand	Dopaminergic function	Parkinsons disease
Spiperone	Neurotransmitter/receptor ligand	Dopaminergic function	Schizophrenia

through medical insurance schemes (Hawkins & Phelps, 1986; Berman & Schelbert, 1988). The first centres are now being installed with purely clinical applications in mind and there is evidence that regional cyclotron facilities are about to become available in areas where several medical centres can take advantage of the radiopharmaceuticals provided.

In Japan, there has been a decision at high level to install a large number (~30) of PET centres at teaching and research institutes and progress is now very rapid. Again, the installations follow classical lines and a large financial investment is involved.

By contrast, the UK has the large and excellent PET centre at the MRC Cyclotron Unit, Hammersmith, where a recent sizeable financial investment in upgraded facilities has provided the UK with a front-line medical research centre. In addition, there are the two relatively small-scale new developments in Aberdeen and Sutton. However, as discussed above, these centres will make only a limited contribution to the clinical applications of PET given the extended temporal nature of these studies. In any case, it is the remit of each of these centres to commit much of their time to basic clinical research and there will be precious little time and effort available for widespread clinical applications. Against this background it is possible to present a scenario by which PET may become as widespread in its use as X-ray CT is now.

A scenario for the 1990s

Radiopharmaceuticals

Any examination of the potential availability of PET to a larger number of users must first look at the problem of how to provide a number of useful radiopharmaceuticals for the studies discussed above. Even a brief examination of the plausibility of obtaining short-lived radionuclides at a distance from the producing cyclotron indicates that ^{15}O and probably ^{13}N will be difficult to obtain off-site. However, Table III shows that there are already several ^{18}F-labelled agents that could be made available to users up to 2 h transportation time from the producing site. Similarly, it should be possible to provide ^{11}C-labelled compounds of modest complexity to users within an hour of this site. The feasibility of having several regional cyclotron facilities in the UK should be carefully examined in the light of the radical changes in cyclotron technology now underway. Already, there is one manufacturer of minicyclotrons (Hendry, 1987) producing a negative-ion 11 MeV microprocessor-controlled system with simple protocols to produce the radionuclides of interest. This system can produce enough of the ^{11}C and ^{18}F radiopharmaceuticals to supply perhaps four to eight centres with clinically useful compounds and requires a single operator and minimal space. Table IV gives an example of the yields of the agents available. Furthermore, the development of superconducting magnets for MRI in the UK has inspired the manufacture of a superconducting 12 MeV cyclotron for radionuclide production (Griffiths, 1987)—the first of these is nearing completion and will be installed in Japan!

Table IV. Typical yields of ^{18}F, ^{15}O, ^{13}N and ^{11}C from a state-of-the art 11 MeV negative-ion cyclotron

Radionuclide	Beam current (μa)	Irradiation time (min)	Yield (GBq)
^{11}C	30	40	64
^{13}N	20	20	15
^{15}O	20	10	27
^{18}F	20	30	90

In addition, there have been several important developments in Europe, the USA and Japan in the production of "black box" facilities*, which can provide quite complex radiopharmaceuticals such as ^{18}F-FDG without the need for large-scale radiochemistry intervention, but still, of course, needing the appropriate quality control provided by a radiopharmacist.

Hence we might envisage the installation of six

---

*Data taken from commercial brochures of Japan Steel Works, Tokyo, Scanditronics, Uppsala and Sumitoms Heavy Industries Ltd, Tokyo.

Table V. Long-lived positron-emitting radionuclides readily available from off-site cyclotrons in the UK

Nuclide	Half-life	Use
^{124}I	4 days	Protein labelling, drug targetting
^{55}Co	18 h	Protein label, drug label
^{66}Ga	9.5 h	Protein label, tumour localization
^{52}Fe	8 h	Haematological studies
^{81}Rb	4 h	Cardiac, kidney, tumour perfusion

regional cyclotron centres throughout the UK, which could provide those centres with all the short-lived agents discussed above and, in addition, provide an increasing number of ^{18}F-and ^{11}C-labelled agents to many other nearby institutions. This is precisely the plan now in advanced discussion stages in the USA. Of course, in the UK with its relatively dense population and large urban areas close together, such a plan would be worth much consideration.

Additionally, there are many more longer-lived radionuclides that could be made available from already existing cyclotrons and which could have a significant contribution to make to studies particularly involving the labelling of monoclonal antibodies. ^{124}I, ^{55}Co and ^{66}Ga all fall into this category (Table V), all of these having been produced at the Nuffield cyclotron in Birmingham and used at the new prototype PET installation at the Royal Marsden Hospital in Surrey.

Finally, we must include the invaluable radionuclides that can be produced in-house from radionuclide generators in a similar fashion to ^{99}Tc^{m}. The ^{68}Ge/^{68}Ga generator can provide ^{68}Ga (half-life 68 min) in useful quantities (Robinson, 1985) for the best part of 1 year at a similar price to ^{99}Tc^{m} and this nuclide can be used to label many compounds now in common use in nuclear medicine. The most important of the generators that can produce positron-emitting radionuclides are shown in Table VI.

Hence we may conclude that there would be no shortage of useful agents available for PET imaging at a large number of centres, and access to the "metabolic agents" is possible if regional facilities can be provided.

Positron cameras

Perhaps the most challenging area of technological development required for PET to become more generally available is that associated with positron cameras. Present commercially available systems are based on multiple rings of many scintillation crystals surrounding the patient (Siemens Gammasonics, 1986). The crystals are viewed by a large number of photomultipliers connected to a complex electronics system and interfaced to powerful minicomputer/array processor data-handling facilities. The largest of these detectors has an axial field of view of ~10 cm, which restricts its general use to the brain and the heart. These detectors have a very high detection efficiency and a spatial resolution of 4–6 mm *in vivo*, and collect data at rates of up to 100 000 events per second. Developments to increase the size and improve performance further involve the search for better scintillation crystals, the production of multianode photomultipliers and/or the use of silicon diodes, which may ultimately lead to a reduction in cost. For the present, however, these cameras are typically 10 times more expensive than a tomographic gamma camera and seem unlikely to become cheaper by more than a factor of 2.

Alternative methods for the detection of annihilation γ rays have been tried using large-area scintillation crystals such as pairs of gamma cameras, but such systems have failed to cope with the high count-rates involved and in particular with the accidental coincidence rates produced.

Greater success has been achieved with large-area multiwire proportional chamber cameras as described in Bateman et al (1984) and Ott et al (1988). These detectors employ gas-filled ionization chambers, which include lead γ-ray convertors to produce ionization in the gas from the detected photon. The intrinsic positional information obtained from these detectors is excellent and a spatial resolution of 2 mm (Jeavons et al, 1980) has been achieved. However, as yet, their sensitivity is only 10% of that of the scintillation PET cameras although 10 times greater than the gamma camera. Equally important, the count-rate capacity is still poor and these detectors accept a high fraction of scattered events compared with the more heavily shielded scintillation PET camera. Recent improvements to this technology (Marsden et al, 1986) indicate that the performance gap between the wire chamber and scintillation PET cameras is closing.

Table VII shows the measured performance of the camera at the Royal Marsden Hospital (MUP-PET II) (Fig. 6) and predictions for the future development (MUP-PET III), which will include a new convertor consisting of a lead waffle structure and greatly improved electronics. Developments of this next stage of the MUP-PET camera will take 2 years. Also shown is the predicted performance of a hybrid scintillation detector/wire chamber camera, which uses barium fluoride as the γ-ray detector and a multiwire chamber

Table VI. Examples of positron-emitting radionuclides readily available from in-house generators

Parent	Half-life	Daughter	Half-life	Use
^{68}Ge	280 days	^{68}Ga	68 min	Labelling a wide range of chelates (^{99}Tc^{m} equiv.)
^{82}Sr	25 days	^{82}Rb	75 s	Cardiac, kidney, tumour perfusion
^{62}Zn	9.3 h	^{62}Cu	9.9 min	Label for perfusion agent

Table VII. The performance characteristics of existing and future multiwire positron cameras and a comparison with a state-of-the-art commercial system

	MUP-PET II	MUP-PET III	MUP-PET IV	MRMC
Photon convertor	Lead foil	Lead waffle	Barium fluoride	BGO
Spatial resolution (mm)	6	3–4	5–6	5–6
Sensitivity (Gamma camera = 1)	10	50	100–200	100–200
Maximum (kcps) count-rate	3–4	20	50–100	50–100
Cost in US$ $(\times 10^3)$	200	400	400	2000

to replace the photomultipliers (Mine et al, 1988; Schotanus et al, 1988). A similar system is now under development at the Royal Marsden Hospital and the Rutherford-Appleton Laboratory and has the potential to compete with the conventional positron camera, whose performance is also shown in Table VII (MRMC). The manufacture of a large-scale detector based on this hybrid construction is expected to take 3–4 years. The readers' attention is directed to the last line of Table VII, which shows that the cost of the systems discussed here are very dependent on the technology involved. The intrinsic low cost of wire chambers in comparison with the more conventional positron camera makes the development of wire chamber detectors crucial to the wider availability of PET. At present, the prototype multiwire camera is under evaluation to determine its clinical applications to oncology and is beginning to provide useful clinical images (Fig. 7) and quantitative physiological information (Fig. 8).

Associated requirements

None of the developments discussed above will be viable without much additional effort in two important

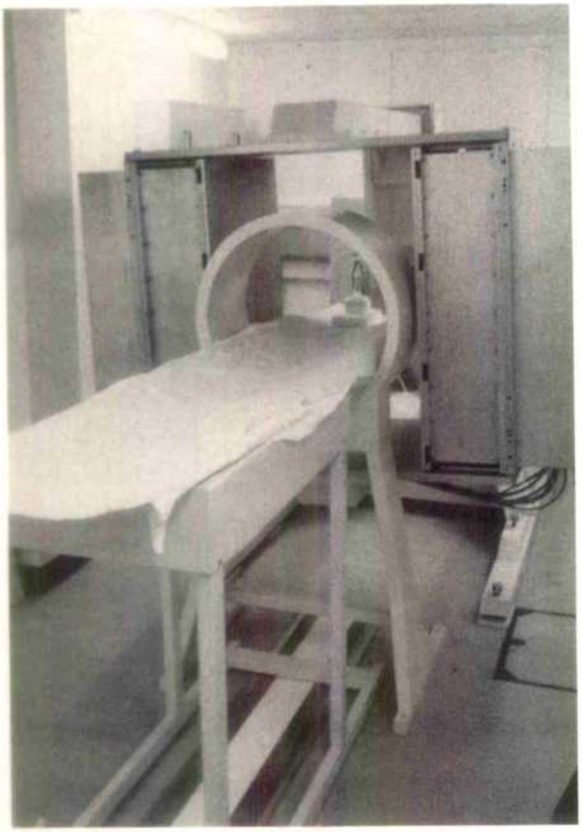

Figure 6. The prototype clinical positron camera MUP-PET.

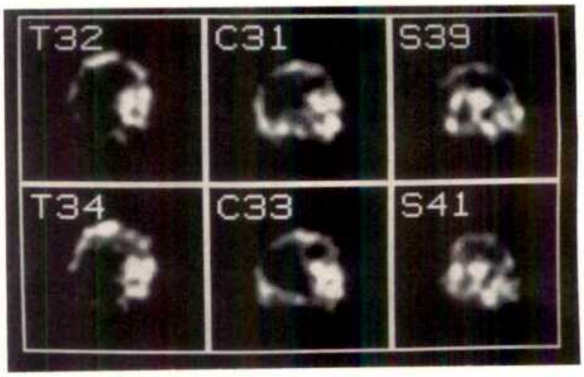

Figure 7. Six-millimetre transaxial, sagittal and coronal sections through the brain of a patient with extensive blood-brain-barrier damage due to a primary cerebral tumour. The images were produced as part of a dynamic scanning sequence using the MUP-PET camera and ^{68}Ga-EDTA.

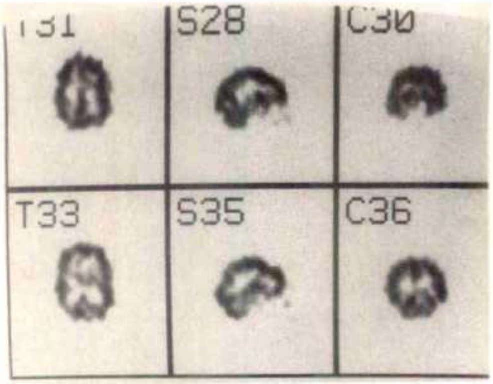

Figure 8. Six-millimetre transaxial, sagittal and coronal sections through the brain of a normal volunteer showing the distribution of ^{18}F-FDG 45 min after injection. These scans took 30 min using the MUP-PET camera.

areas. The first is the improvements needed in computerized data processing, particularly for the wire chamber systems where real-time image reconstruction will need to be performed at high count-rates. For this, some form of advanced parallel processing is needed, based perhaps, on either the development of hardware algorithms in silicon or on the use of multitransputer systems. A single transputer has the ability to reconstruct a three-dimensional image into 128 × 128 × 64 volume elements at a rate comparable with a small array processor, and a multitransputer system may cope with the high data rates required in future.

Secondly, much of the data provided by PET must be related to the body's biochemical function using physiological modelling techniques. The development of computer algorithms for these models is still limited and there is a need for considerable input from research studies to provide the necessary tools for clinical use. However, there are existing models (Huang & Phelps, 1986) for the metabolic processes involving glucose and amino acid utilization in the brain and for the description of perfusion within a range of physiological systems (Solokoff, 1986). Clearly, these models represent a start in the process of converting the image obtained from PET into a metabolic or perfusion map of the body system under study.

Summary

This paper describes the potential advantages to medical diagnosis and treatment that might be obtained from the wider application of positron emission tomography as a clinical tool. Developments along the lines suggested here will require a radical change in thinking from both clinicians and the medically related scientific community in the UK and some enlightened and resourceful funding from a mixture of charitable, industrial and government sources. If these ideas are to be pursued sucessfully, then the work must start now on a much wider scale than is presently perceived in the UK, and close collaboration between physicists, engineers, chemists, biochemists, clinicians and industrialists is needed.

Furthermore, it is imperative that the scientific developments now underway in silicon technology, parallel data processors, biochemical and pharmacological processes and even high-temperature superconductors be kept under close and constant review by those associated with the technological advancements of medicine, so that the value of such developments is rapidly transferred to applications to medicine. This must include closer relationships between academic medicine and science than is the general rule in the UK at present.

In conclusion, the scenario presented here includes the installation of regional cyclotron facilities to provide a large number of institutions in the UK with positron-emitter labelled radiopharmaceuticals. Additionally, agents labelled with radionuclides from in-house generators and other already existing higher-energy cyclotrons will provide a versatile and valuable range of radiopharmaceuticals for the study of human disease.

These developments must be supported by the manufacture of lower-cost positron camera systems, as suggested here, connected to high-data-rate parallel processors to provide images of body function and to determine the effects brought about by disease. These images may then be processed using algorithms based on kinetic models of the body systems to provide information about the basic biochemical and physiological processes of the body. Such a development could have a profound effect on our knowledge of human disease and on our ability to control and treat it successfully.

References

Ambrecht, J. J., Brunken, R. C. & Schelbert, H. R., 1988. Identifying viable myocardium with PET. Reprint from *Cardio, 5(3)* (Miller Freeman, San Francisco).

Baron, J. C., 1987. Ischaemic stroke studied by 0-15-labelled compounds: misery perfusion and luxioury perfusion. In Heiss. W.-D., 1987, pp. 15–23.

Bateman, J. E., Connolly, J. F., Stephenson, R., Tappern, G. J. & Flesher, A. C., 1984. The Rutherford-Appleton Labortory's Mark I, multiwire proportional counter positron camera. *Nuclear Instruments amd Methods in Physics Research*, *225*, 209–231.

Beaney, R. P., 1987. Some biological aspects of soft tissue tumours as studied by PET. In Heiss, W.-D, 1987, pp. 361–370.

Beaney, R. P. & Lammertsma, A. A., 1985. Use of PET in oncology. In *Positron Emission Tomography*, by M. Reivich & A. Alavi (Alan R. Liss, New York), pp. 425–450.

Berman, D. S. & Schelbert, H. R., 1988. Scanning the future of PET. Reprint from *Cardiology Management, II(1) (Macmillan Professional Journals, Santa Monica), pp. 21, 24, 25, 49.*

Bustany, P. & Moulin, M., 1987. PET in dementias and gliomas. In Heiss, W.-D., 1987, pp. 175–192.

Burns, M., 1987. *Positron Emission Tomography: Progress and Opportunities*, American Hospital Association Guideline Report 5(8) (AHA, Chicago).

Cambon, H., Baron, J. C., Boulenger, J. P., Loc'h, C., Zarifian, E. & Maziere, B., 1987. Striatal dopamine receptors: dose-dependent occupation by, and rapid washout of orally given neuroleptics in humans. In Heiss, W.-D., 1987, pp. 221–232.

Camici, P. & Araujo, L., 1987. PET in the study of angina pectoris. In Heiss, W.-D., 1987, pp. 243–252.

Chugani, H. T. & Phelps, M. E., 1988. PET in children with seisures. *Applied Radiology*, May 1988.

Ericson, K., Lilja, A. & Bergstrom, M., 1987. Positron emission tomography with C-11-methionine in brain tumours: methionine kinetics, tumour delineation, and follow-up studies after therapy. In Heiss, W.-D., 1987, pp. 381–390.

Farde, L., Wiesel, F.-A., Halldin, C. & Sedvall, G., 1987. PET determination of central D1-and D2-dopamine receptor occupancy in neuroleptic treated schizophrenics In Heiss W.-D., 1987, pp. 213–220.

Frackowiak, R. S. J., 1987a. Ischaemic disease studied with 0-15-labelled compounds: metabolic and haemodynamic disparities. In Heiss, W.-D., 1987, pp. 25–36.

——1987b. Energy metabolism and neurotransmitter function in ageing and the dementias. In Heiss, W.-D., 1987, pp. 159–174.

Griffiths, R., 1987. *A Mobile Superconducting Cyclotron for PET and Neutron Radiography*. Presented at the 18th Japan Conference on Radiation and Radioisotopes, Tokyo, November 1987.

Harbert, J. & da Rocha, A. F. G. (eds), 1984. *Textbook of Nuclear Medicine*, Volume I: *Basic Applications*, Volume II: *Clinical Applications* (Lea and Febiger, Philadephia).

Hawkins, R. A., & Phelps, M. E., 1986. Clinical PET: operational & cost considerations. *Administrative Radiology*, April 20–26.

Heiss, W.-D. (ed.), 1987. *Clinical Efficacy of Positron Emission Tomography* (Martinus Nijhoff, Dordrecht).

Hendry, G. O., Straatman, M. G., Carroll, L. R., Ramsey, F. A., Wieland, B. W., Padgett, H. C., Bida, G. T., Schmidt, D. G. & Ruth, T. J., 1987. *Design and Performance of a Compact Radioisotope Delivery System*. Reprint from Computer Technology and Imaging Inc., Berkeley, California.

Herholz, K., Pawlik, G., Staffen, W., Ziffling, P., Hebold, I. & Heiss, W.-D., 1987. Localizing epileptic foci by PET. In Heiss, W.-D., 1987, pp. 127–136.

Hine, G. J. (ed.), 1967, 1974. *Instrumentation in Nuclear Medicine* (Academic Press, New York), Vols 1 & 2.

Huang, S. & Phelps, M. E., 1986. Principles of tracer kinetic modelling in positron emission tomography and autoradiography. In Phelps, M. E. et al, 1986, pp. 287-346.

Jeavons, A. P., Kull, K. & Lindberg, B., 1980. A proportional chamber positron camera for medical imaging. *Nuclear Instruments and Methods in Physics Research, 176*, 89–97.

Kessler, R. M., Partain, C. L., Price, R. R. & James, A. E., 1987. Positron emission tomography: prospects for clinical utility. *Investigative Radiology, 22*, 529–537.

Landsheere, C. de, Raets, D., Pierard, L., Lemaire, C., Berthe, C., del Fiore, G., Lamotte, D., Kulbertus, H. E. & Rigo, P., 1987. Investigation of myocardial viability after an acute myocardial infarction using positron emission tomography. In Heiss, W.-D., 1987, pp. 279–290.

Marsden, P. K., Bateman, J. E., Ott, R. J. & Leach, M. O., 1986. The development of high efficiency cathode convertors for a multiwire proportional chamber positron camera. *Medical Physics, 13*, 703–706.

Mazziota, J. C. & Phelps, M. E., 1986. Positron emission tomography studies of the brain. In Phelps, M. E. et al, 1986, pp. 493–580.

Mine, P., Charpak, G., Santiard, J.-C., Scigocki, D., Suffert, M. & Tavernier, S., 1988. Test of a BaF2-MWPC detector for positron emission tomography. *Nuclear Instruments and Methods in Physics Research, A269*, 385–391.

Ogawa, T., Uemura, K., Shishido, F., Yamaguchi, T., Murakami, M., Inugami, A., Kanno, I., Sasaki, H., Kato, T., Hirata, K., Kowado, M., Mineura, K. & Yasuda, T., 1988. Changes of cerebral blood flow, and oxygen and glucose metabolism following radiochemotherapy of gliomas: a PET study. *Journal of Computer Assisted Tomography, 12*, 290–297.

Ott, R. J., 1986. Emission computed tomography. *Journal of Medical Engineering & Technology, 10*, 105–114.

Ott, R. J., Marsden, P. K., Flower, M. A., Webb, S., Cherry, S., McReady, V. R. & Bateman, J. E., 1988. Clinical PET with a large area multiwire proportional chamber PET camera. *Nuclear Instruments and Methods in Physics Research, A269*, 436–442.

Pawlik, G., Heiss, W.-D., Wienard, K., Hebold, I. R., Ziffling, P., Staffen, W., Herholz, K. & Wagner, R., 1987. Brain glucose metabolism and blood flow in ischaemic stroke. In Heiss, W.-D., 1987, pp. 37–54.

Phelps, M. E., Mazziotta, J. C. & Schelbert, H. R. (Eds), 1986. *Positron Emission Tomography and Autoradiography Priniciples and Applications to the Brain and Heart* (Raven Press, New York).

Robinson, G. D., 1985. Generator systems for positron emitters. In *Positron Emission Tomography*, by M. Reivich & A. Alavi (Alan R. Liss, New York), pp. 81–102.

Schelbert, H. R. & Schwaiger, M., 1986. PET studies of the Heart. In Phelps, M. E. et al, 1986, pp. 581–662.

Schelstraete, K., 1987. Circulatory and metabolic studies in extracranial malignant tumours. In Heiss, W.-D., 1987, pp. 345–360.

Schotanus, P., van Eijk, C. W. E. & Hollander, R. W., 1988. A BaF2-MWPC gamma camera for positron emission tomography. *Nuclear Instruments and Methods in Physics Research, A269*, 377-384.

Schuier, F. J., 1987. Changes of cerebral glucose metabolism in movement disorders. In Heiss, W.-D, 1987, pp. 93–100.

Siemens Gammasonics, 1986. *Three-Dimensional Positron Emission Tomography (PET) ECAT Scanner* (Siemens gammasonics, Uithoorn, The Netherlands).

Sokolov, L., 1986. Cerebral circulation, energy metabolism, and protein synthesis: general characteristics and principles of measurement. In Phelps, M. E. et al, 1986, pp. 1–72.

Subramanian, G., Rhodes, B. A., Cooper, J. F. & Sodd, V. J. (eds), 1975. *Radiopharmaceuticals* (Society of Nuclear Medicine, New York).

Syrota, A., 1987. Investigation of myocardial receptors by PET in heart diseases. In Heiss, W.-D, 1987, pp. 253–266.

Taegtmeyer, H., 1986. Myocardial Metabolism. In Phelps, M. E. et al, 1986, pp. 149–196.

Wagner, H. N., 1968. *Principles of Nuclear Medicine* (Saunders, Philadelphia).

Wiesel, F.-A., Wik, G., Sjogren, I., Blomquist, G., Greitz, T. & Stone-Elander, S., 1987. Regional brain metabolism in drug-free schizophrenic patients as measured by positron emission tomography. In Heiss, W.-D., 1987, pp. 203–212.

Yamamoto, Y. L. & Diksic, M., 1985. Positron emission tomography studies of pharmakinetics. In *Positron Emission Tomography*, by M. Reivich & A. Alavi (Alan R. Liss, New York), pp. 413–424.

1989, *The British Journal of Radiology*, 62, 433–437

Relative proton density and relaxation times in liver metastases during interferon treatment

By T. Andersson, MD, A. Ericsson, PhD, *B. Eriksson, MD, A. Hemmingsson, MD, †E. Lindh, MD, R. Nyman, MD and *K. Oberg, MD

Departments of Diagnostic Radiology and †Internal Medicine and *Ludwig Institute for Cancer Research, University Hospital, University of Uppsala, S-751 85 Uppsala, Sweden

(*Received February 1988 and in revised form December 1988*)

Abstract. Relaxation times and relative proton densities were calculated from magnetic resonance examinations of the liver in eight patients with liver metastases from neuroendocrine tumours. Single, spin–echo sequences with eight different repetition times and a four-echo sequence were used to calculate T_1 and T_2 in tumour and normal liver, and the proton density tumour–liver quotient, before and during treatment with interferon. Changes over time of these parameters were compared with variations in tumour marker levels and changes in size and number of the metastases. During therapy, six out of eight cases showed a decrease in tumour T_1, five responding to therapy and one with stationary disease, while the two patients with progressive disease showed unchanged tumour T_1. The proton density quotient also decreased in a corresponding way, indicating a change in water content in tumours responding to interferon therapy. No significant change in liver T_1, tumour T_2 or liver T_2 occurred in any patient. It is thus possible to perform reliable measurements of relaxation parameters over time, which may be valuable in follow-up of tumour treatment.

The possibility of tissue characterization with magnetic resonance imaging (MRI), in terms of relaxation parameters and spin densities (rho), is generally regarded with scepticism as most clinical results indicate a large spread in T_1, T_2 and rho values for both normal and pathological tissues (Bottomley et al, 1985). The reason for this may, to some extent, be technical artefacts or errors in the calculation procedures rather than dissimilarities in the magnetic resonance parameters of different tissues (Smith & Taylor, 1986). However, if relaxation measurements are performed over a period of time and on the same patient, more useful results may be achieved; some studies have indicated a correlation between therapy response and relaxation times (Benson et al, 1987; Nyman et al, 1987; Andersson et al, 1988), based on data from double-echo spin–echo (SE) sequences.

The aim of this investigation was to find out if the results indicating a decrease in T_1 in liver metastases from neuroendocrine tumours during interferon therapy (Andersson et al, 1988) could be verified by using multiple data-point recordings.

Materials and methods

Eight consecutive patients (four men and four women; mean age 61.1 years; median age 61.4 years; range 40–75 years) with biopsy-proven liver metastases from neuroendocrine neoplasms (seven carcinoids and one endocrine pancreatic tumour) were examined with MRI of the liver before and during treatment with interferon. Magnetic resonance imaging was performed before treatment and repeated 4 days after the start of interferon therapy, with further examinations in some patients (Table I). A total of 28 examinations was performed. Analysis of levels of biochemical tumour markers in blood and urine was performed at the same time intervals. These were urinary 5-HIAA and tachykinins, pancreatic polypeptide (PP), human chorionic gonadotrophin (HCG)-α and -β in carcinoid patients and vasoactive intestinal polypeptide (VIP) in the patient with an endocrine pancreatic tumour. Treatment with α-interferon was given as subcutaneous injections of human leucocyte interferon (Oberg et al, 1983) or recombinant interferon (Intron A, Schering AG). Two patients received additional therapy with a long-acting somatostatin analogue, SMS 201-995 (Eriksson et al, 1988), after 4 and 6 months of interferon therapy, respectively.

Magnetic resonance imaging was performed with a superconductive system (Magnetom, Siemens) operating at 0.5 T. Transverse multislice recordings (spin–echo; time to repetition (TR) 250 ms; time to echo (TE) 22 ms;

Table I. Number of MRI examinations performed

Case	Total no. of examinations	Days after start of therapy	
		First examination	Last examination
1	8	4	180
2	6	4	200
3	2	4	4
4	2	4	4
5	4	4	60
6	2	4	4
7	2	4	4
8	2	4	4

Case numbers refer to those in Fig. 2.

Address reprint requests to: Dr T. Andersson.

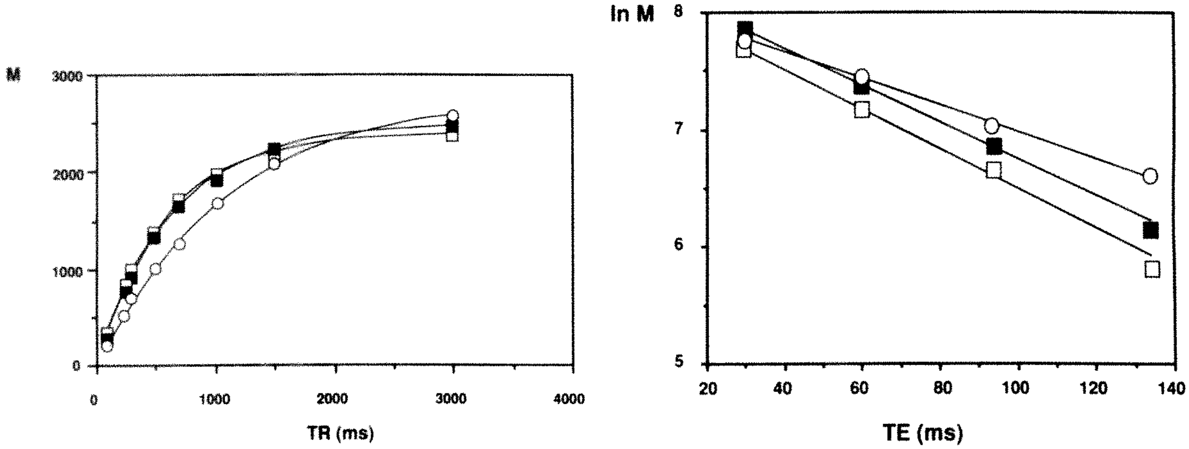

(a)

(b)

Figure 1. (a) Signal intensity (M) as a function of repetition time (TR) for tumour and two liver regions of interest (ROIs). The line curve is the resulting mono-exponential curve from the fitting procedure; (○) measured values for tumour; (■), (□) measured values for liver ROI 1 and 2, respectively, T_1 tumour = 1059 ms; T_1 liver 1 = 623 ms; T_1 liver 2 = 535 ms. (b) Shows ln M as a function of echo time (TE) for the same ROIs as in (a). Symbols as in (a). T_2 tumour = 88 ms; T_2 liver 1 = 64 ms; T_2 liver 2 = 59 ms.

four data acquisitions) covering the liver region were used to select one scan level for both normal liver parenchyma and tumour tissue for further investigations in single-slice mode using the pulse sequences listed in Table II.

The eight single-echo sequences for T_1 determinations used a frequency-selective 90° pulse and a non-selective 180° pulse. The four-echo sequence for T_2 measurements (Carr-Purcell-Meiboom-Gill scheme) used selective 90° and 180° pulses with the nominal width of the latter being about 2.4 times that of the former. The acquisition matrix was 256 × 256 and the total examination time 90 min. Respiratory gating was not used. Regions of interest (ROIs), with a size of 75 to 275 pixels, were placed in tumour and normal liver tissue and T_1 and T_2 relaxation times were calculated by fitting ROI intensities to analytical expressions (Sperber et al, 1986) utilizing the MINUIT function-minimizing package (James & Roos, 1976). From the T_1 fitting, a measure of proton density (rho) was also obtained and tumour rho values were normalized to those of normal liver tissue. In each patient, the same metastasis and the same scan level was used for all measurements. In one case, no normal liver parenchyma was available for measurement and an area of tumour necrosis was used as a control. The change in T_1, T_2 and relative rho over time was analysed with paired Student's t-test. The results from the MRI examinations were compared with objective and subjective signs of therapy response; an objective response was considered present when tumour markers were reduced by 50% or more, and progressive disease when tumour markers and/or tumour size increased by 25% or more or new metastases developed (Norheim et al, 1986). Clinical change was subjectively judged from reduction or increase of symptoms such as diarrhoea and flushing.

Table II. Pulse sequences used for single-slice investigations for T_1 and T_2 measurements

TR (ms)	TE (ms)	Number of acquisitions
100	20	4
250	20	4
300	20	4
500	20	2
700	20	2
1000	20	1
1500	20	1
3000	20	1
2000	30, 60, 94, 134	1

Results

The measured signal intensities from liver and tumour correlated very well with the fitted function for mono-exponential relaxations. Examples of longitudinal (a) and transverse (b) relaxation in a tumour ROI and two liver ROIs are given in Fig. 1.

Before the start of interferon therapy, tumour T_1 and T_2 were substantially longer than corresponding values

Table III. Mean T_1 and T_2 relaxation times (ms) of tumour and liver before interferon therapy

	Mean	Range	SEM
T_1			
Tumour	1156	1006–1468	56.6
Liver	488	409–623	29.7
T_2			
Tumour	78	57–98	4.5
Liver	51	44–67	3.4

SEM = standard error of the mean.

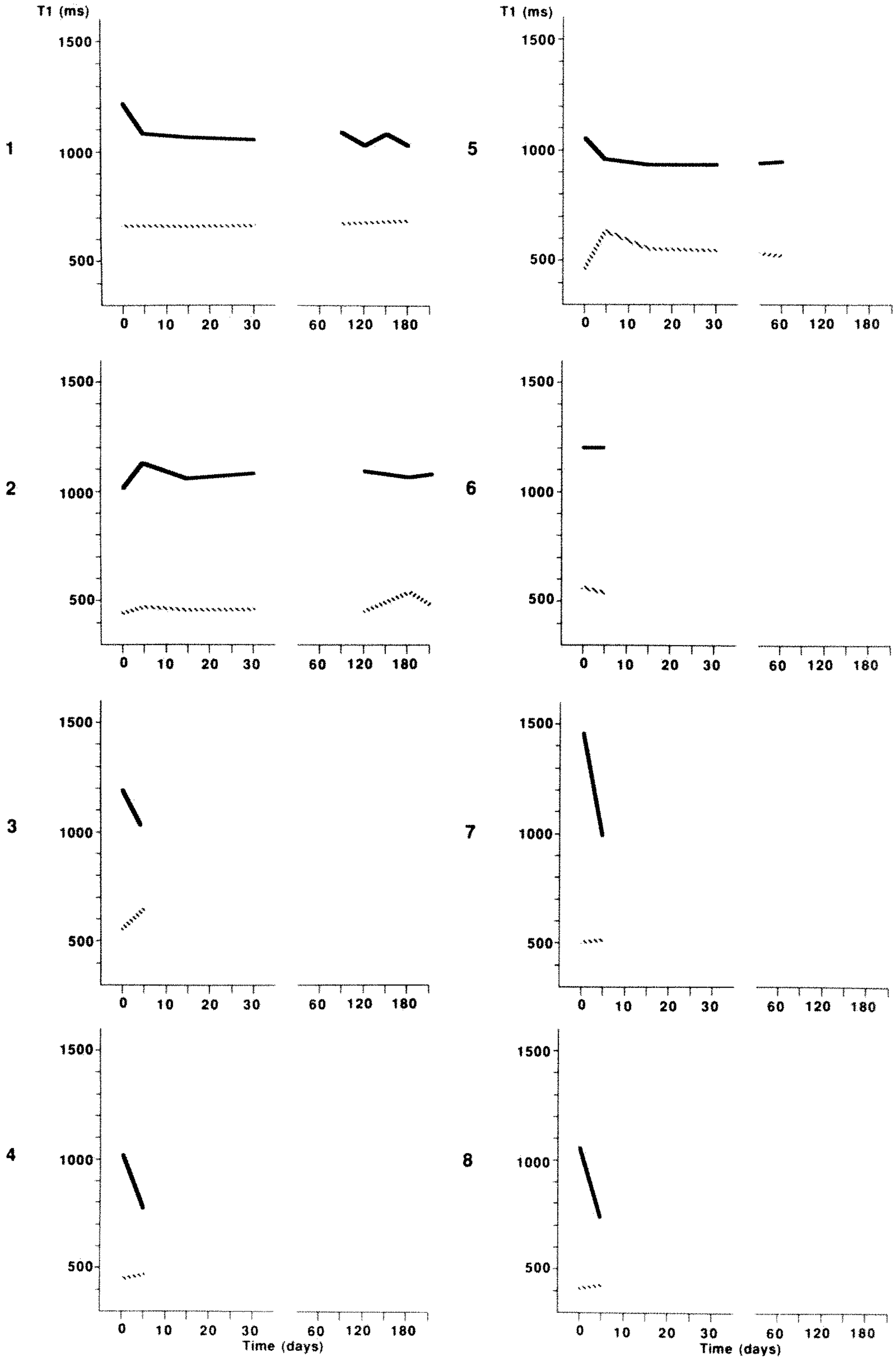

Figure 2. T_1 relaxation times of tumour (straight line) and liver (dotted line) as a function of time of interferon therapy in eight patients. In Case 3 the dotted line indicates T_1 of tumour necrosis. Day 0 = examination before start of therapy.

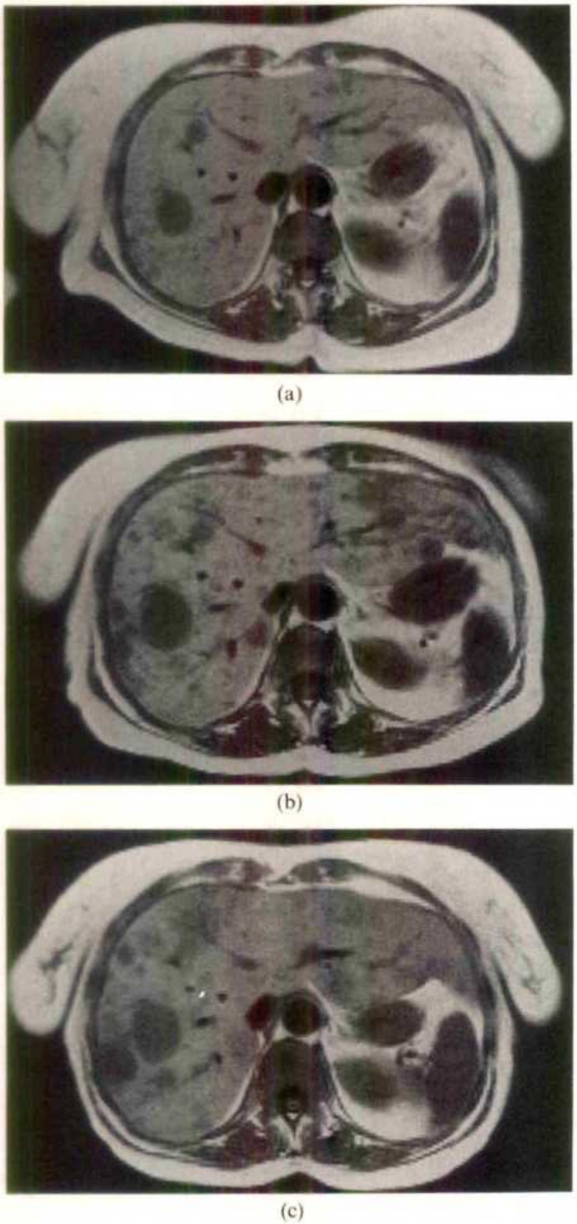
(a)
(b)
(c)

Figure 3. Magnetic resonance scans of the liver in a patient not responding to therapy (Case 2 in Figs 2 and 3). Spin–echo; TR 250 ms; TE 22 ms; four data acquisitions; (a) before, (b) 30 days and (c) 120 days after start of therapy. An increase in tumour size after 30 days with further progression at 120 days is shown.

in liver parenchyma (Table III). The spread in values was rather small compared with an earlier investigation using double-echo technique (Andersson et al, 1988).

After initiation of interferon therapy, a significant decrease ($p = 0.005$) in tumour T_1 occurred in six out of eight patients examined (Fig. 2) and was already obvious on the first post-therapy examination at Day 4. After this initial decrease, tumour T_1 did not significantly change in patients who had follow-up examinations. A similar decrease in relative rho values ($p = 0.002$) were noted in all six patients. No significant change occurred in liver T_1 (Fig. 2), tumour T_2 or liver T_2. Five of these six patients had subjective and objective response to therapy, while one patient without subjective symptoms, receiving therapy for increasing 5-HIAA urinary output, showed stationary disease objectively. All six patients had unchanged tumour size on MRI and none of them developed new metastases.

Two patients (Cases 2 and 6, Fig. 2) had progressive disease and both showed unchanged tumour T_1 and relative rho values during interferon therapy. One of them was a 69-year-old woman with a caecal carcinoid and multiple liver metastases on admission to hospital. She had not received any treatment prior to the start of interferon therapy and the primary tumour was not resected. No clinical improvement was noted, subjectively or objectively, and an increase in tumour markers occurred. On ultrasonography, computed tomography and MRI, an increase in tumour size and number was noted on examination after 30 days, with further progression after 120 days (Fig. 3). Because of this, additional therapy with SMS 201-995 was started after 6 months of interferon therapy, but without positive response. The other patient not responding to therapy died 2 weeks after the first post-therapy MRI examination, showing signs of progressive disease.

Discussion

Our measurements indicate that it is possible to characterize relaxation processes in living tissue with high precision using a mono-exponential model. The combination of multiple data recordings and the use of spin–echo sequences with non-selective or spatially wide refocusing pulses should minimize problems of system instabilities and pulse imperfections (Loeffler et al, 1983; Frahm & Hänicke, 1984) and thus be preferable when quantification of relaxation parameters is the main objective.

The present investigation further shows that tumour tissue in liver metastases from neuroendocrine tumours may undergo relatively rapid internal changes, reflected by a decrease in T_1 relaxation time and relative rho values, after initiation of interferon therapy. These findings confirm the results from our previous study (Andersson et al, 1988), in which a different technique for relaxation time measurements was used on another group of patients with the same type of tumour disease. In the present study, the patients with signs of progressive disease did not show a change in tumour T_1 or relative rho. Although the material is small, it indicates that tumour T_1 measurements may be useful together with tumour marker analysis to evaluate objectively the effect of therapy in patients receiving α-interferon.

The antitumoral mechanisms of action of α-interferon are not yet fully understood, although several effects are possible. Known effects like inhibition of oncogen expression, DNA replication and protein synthesis

(Gresser, 1985; Balkwill, 1986; Kimchi et al, 1986) and blocking of tumour cell division (Taylor-Papadimitriou et al, 1981) may cause changes in hormone content and tumour cell number, which could occur very early, *e.g.* within a few days. A direct cytotoxic effect on tumour cells may also produce rapid changes such as the release of stored hormones (Lörelius et al, 1984). Intra-arterial infusion of α-interferon has demonstrated such effects (Oberg et al, 1987), which may be one of several explanations of the decrease in T_1, since a release of stored hormones and decreased *de novo* synthesis may change the water content of the cells. Although this hypothesis is supported by the decrease in proton density, the mechanisms of interferon activity must be investigated further before it is possible to explain fully the decrease in tumour T_1 that occurred in those patients with good therapy response.

Acknowledgment

This work was supported by grants from the Swedish Medical Research Council (Project No. 6676).

References

Andersson, T., Eriksson, B., Hemmingsson, A., Jung, B., Lindh, E., Thuomas, K. & Oberg, K., 1988. Effect of interferon on T_1 relaxation times of liver metastases from endocrine gastrointestinal tumours. *Acta Radiologica, 29*, 21–25.

Balkwill, F. R., 1986. Interferons: from molecular biology to man. Part I, genetics and molecular biology of the interferon system. *Microbiological Science, 3*, 212–215.

Benson, L., Hemmingsson, A., Ericsson, A., Jung, B., Sperber, G., Thuomas, K. & Westermark, P., 1987. Magnetic resonance imaging in primary amyloidosis. *Acta Radiologica, 28*, 13–15.

Bottomley, P. A., Hardy, C. J., Argersinger, R. E. & Allen, G. R., 1985. Relaxation in pathology: Are T_1's and T_2's diagnostic? *Book of Abstracts* (Society of Magnetic Resonance in Medicine, Berkeley, California) pp. 28–29.

Eriksson, B., Oberg, K., Andersson, T., Lundquist, G., Wide, L. & Wilander, E., 1988. Treatment of malignant endocrine pancreatic tumours with a new long-acting somatostatin analogue, SMS 201–995. *Scandinavian Journal of Gastroenterology, 23*, 508–512.

Frahm, J. & Hänicke, W., 1984. Comparative study of pulse sequences for selective excitation in NMR imaging. *Journal of Magnetic Resonance, 60*, 320–332.

Gresser, I., 1985. How does interferon inhibit tumour growth. *Interferon, 6*, 93–126.

James, F. & Roos, M., 1976. MINUIT. *A System for Function Minimization and Analysis of the Parameter Errors and Correlations* (CERN Computer Centre Program Library, Geneva).

Kimchi, A., Einat, M., Resnitsky, D., Yarden, A. & Gat, G., 1986. Inhibition of C-myc expression and cellular proliferation by endogenous interferons. *Journal of Cell Biochemistry*, Suppl. 10c, M 29 (abstr).

Loeffler, W., Oppelt, A. & Faul, D., 1983. Computer simulations of slice selection in NMR imaging. *Book of Abstracts* (Society of Magnetic Resonance in Medicine), pp. 219–220.

Lörelius, L. E., Jonsdottir, B., Lundquist, G. & Oberg, K., 1984. Malignant endocrine tumours of the pancreas. Response to intra-arterial treatment with streptozotocin. *Uppsala Journal of Medical Sciences*, Suppl. 39, 191–196.

Norheim, I., Theodorsson-Norheim, E., Bordin, E. & Oberg, K., 1986. Carcinoid flush. A possible role of multiple tachykinins. *Journal of Clinical Endocrinology and Metabolism, 63*, 605–612.

Nyman, R., Rehn, S., Glimelius, B., Hagberg, H., Hemmingsson, A. & Jung, B., 1987. Magnetic resonance imaging for assessment of treatment effects in mediastinal Hodgkin's disease. *Acta Radiologica, 28*, 145–151.

Oberg, K., Funa, K. & Alm, G., 1983. Effects of leucocyte interferon on clinical symptoms and hormone levels in patients with mid-gut carcinoid tumors and carcinoid syndrome. *New England Journal of Medicine, 309*, 129–133.

Oberg, K., Lörelius, L. E. & Theodorsson, E., 1987. Does alpha-IFN exert cytotoxic effects in carcinoid tumours? *Journal of Interferon Research, 7*, 737 (abstr).

Smith, M. A. & Taylor, D. G., 1986. The absence of tissue specificity in MRI using *in vivo* T_1 or T_2 determination: true biological variation or technical artefact? *British Journal of Radiology, 59*, 82–83.

Sperber, G. O., Ericsson, A., Hemmingsson, A., Jung, B. & Thuomas, K., 1986. Improved formulae for signal amplitudes in repeated NMR sequences: applications in NMR imaging. *Journal of Magnetic Resonance in Medicine, 3*, 685–698.

Taylor-Papadimitriou, J., Shearer, M. & Rozengurt, E., 1981. Inhibitory effects of interferon on cellular DNA synthesis: modulation by mitogenic factors. *Journal of Interferon Research, 1*, 401–409.

1989, *The British Journal of Radiology*, 62, 438–442

^{51}Cr-EDTA/^{99}Tc^{m}-MDP ratio: a simple non-invasive method for assessing renal osteodystrophy

By A. P. Nisbet, MSc, MRCP, FRCR, *P. Shaw, MRCP, FRCR, †D. Taube, MRCP, S. Edwards, BSc, M. N. Maisey, MD, FRCR, FRCP and G. Mashiter

Departments of Radiology, Nuclear Medicine and Radiological Sciences and Renal Unit, Guy's Hospital, London SE1 9RT

(*Received October 1987 and in revised form November 1988*)

Abstract. We have used ^{99}Tc^{m}-MDP to develop a measure of overall skeletal activity for use in renal disease. The method utilizes the relative clearances of ^{99}Tc^{m}-MDP and ^{51}Cr-EDTA from the blood after simultaneous injection. This is expressed as a ratio and the upper limit in normals is 1.4. This ratio has been evaluated in 42 patients with chronic renal failure and compared with appearances of left-hand radiographs. The ratio was elevated in these patients and the level corresponded to the degree of severity of the subperiosteal resorption. Similarly, there was a close correlation between the ratio values and the serum alkaline phosphatase measurements and parathyroid hormone values. Thirty-three patients had sequential studies performed at intervals of up to 2 years. Twenty-one patients showed no change on clinical, biochemical or bone scan evaluation. Of these, only one patient showed a change in ratio value of greater than 20%. Twelve patients showed evidence of change based either on clinical, biochemical or bone scan alteration and all 12 patients showed changes in ratio values greater than 20%. The ^{51}Cr-EDTA/^{99}Tc^{m}-MDP ratio appears to offer not only a single plasma sample method for the detection and evaluation of renal bone disease, but our results also suggest that it may be valuable in the follow-up of these patients.

Renal bone disease is common. It occurs in 80–90% of patients with chronic renal failure, but assessment is difficult since clinical signs appear in only about 10% of patients (Katz et al, 1969). Radiological change is seen in only a minority of patients (38% in Katz's series) and bone biopsy is invasive.

We have evaluated a plasma sampling method to measure total skeletal activity in renal disease during routine bone scans (Nisbet et al, 1984).

Patients and methods

The method involves the simultaneous injection of technetium-99m methylene diphosphonate (Amersham) (^{99}Tc^{m}-MDP) and chromium-51 ethylene-diamine-tetra-acetate (^{51}Cr-EDTA) at the time of the bone scan. The mixture is made up as 550 MBq ^{99}Tc^{m}-MDP to 2–3 MBq ^{51}Cr-EDTA, providing the standard bone scan dose of ^{99}Tc^{m}-MDP. Standards are made up from the residue after injection. A 10 ml plasma sample is obtained 3–4 h after injection at the time of imaging. Samples and standards are measured for ^{99}Tc^{m} and ^{51}Cr activity after 24 h, and for ^{51}Cr activity after 5 days when the ^{99}Tc^{m} has decayed. Appropriate correction for decay and background is made and a ratio of ^{51}Cr to ^{99}Tc^{m} injected activity/ml is obtained. This indirectly measures the skeletal uptake of ^{99}Tc^{m}-MDP since the ^{51}Cr-EDTA is used to correct for the extracellular and renal handling of ^{99}Tc^{m}-MDP.

The ratio is determined as follows:

$$\text{Ratio of } {}^{51}\text{Cr}/{}^{99}\text{Tc}^{m} = \frac{Cc}{Ct} \times \frac{St \times Dt}{Sc \times Dc}$$

where Cc = sample counts/ml for ^{51}Cr; Ct = sample counts/ml for ^{99}Tc^{m}; St = standard counts/ml for ^{99}Tc^{m}; Sc = standard counts/ml for ^{51}Cr; Dt = dilution of standard for ^{99}Tc^{m}; and Dc = dilution of standard for ^{51}Cr.

The ratio has been evaluated in 360 patients undergoing routine bone scans without bone or renal disease. An upper limit of normal of 1.4 (mean + 2SD) was found. Reproducibility in 30 patients showed a mean of 8% with a range of up to 20% (mean + 2SD).

Forty-two patients in chronic renal failure had radiographs of the left hand and ratio measurements performed. The hand radiographs were evaluated for subperiosteal resorption and graded 1–3 using a modification of Ritz's method (Ritz et al, 1978). The assessment is based on the degree of subperiosteal resorption seen in the middle phalanx of the middle finger of the left hand. Radiographs were examined under magnification (×8 magnifying lens) without knowledge of the ratio measure or the patients' clinical status. Patients were graded as follows.

1. Grade I (Fig. 1a)
   Normal or small cortical cysts without cortical breaks.
2. Grade II (Fig. 1b)
   Cortical breaks involving less than one-third of the diaphyseal shaft.
3. Grade III (Fig. 1c)
   Cortical breaks involving more than one-third of the diaphyseal shaft.

Thirty-five randomly selected patients of this group had alkaline phosphatase measurements performed on the same day using an automated multichannel analyzer. A further 62 patients had parathyroid hormone (PTH)

Present address: *Department of Radiology, University College Hospital, London and †King's College Hospital, London.

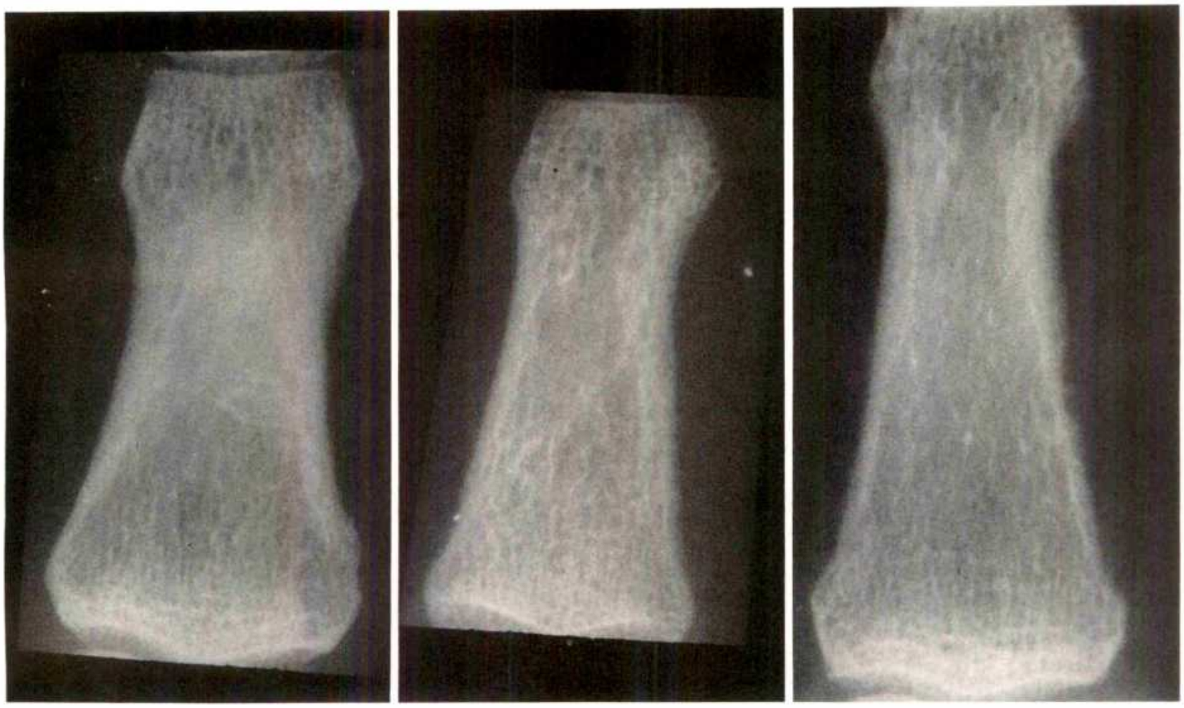

(a) (b) (c)

Figure 1. Radiographs of middle phalanx of middle finger of left hand showing (a) normal/small cortical cysts, (b) cortical breaks less than one-third of the diaphyseal shaft and (c) cortical breaks more than one-third of the diaphyseal shaft.

measurements performed on the same day using a C-terminal assay. Repeated measurements were performed on 33 randomly selected patients at intervals of up to 2 years.

Patients were assessed independently for evidence of change either on clinical, biochemical or bone scan criteria and graded into two groups: (1) no change, (2) change.

Assessment of change was based purely on clinical judgement by a single observer (D.T.) for clinical and biochemical change in comparison with all previous clinical and biochemical assessments, to determine whether a greater than normal change had occurred. Assessment was performed without knowing the ratio change.

Bone scan change was similarly assessed by a single observer (M.N.M.) in comparison with all previous radiographs to assess abnormality in terms of focal lesions or generalized increase in overall uptake into bone relative to soft tissue.

Statistics were assessed by the Wilcoxon Rank Sum test.

Results

When radiographic changes were compared with the ratio results in the three grades, a significant correlation was shown (Fig. 2).

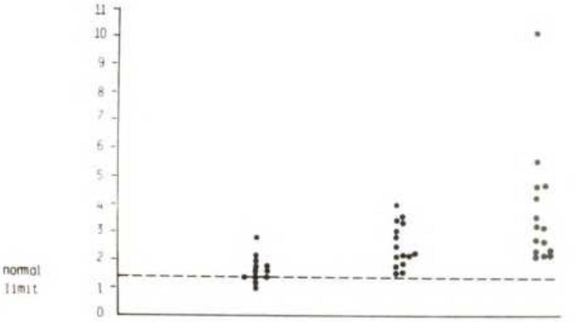

Figure 2. The correlation between radiological grade and the ^{51}Cr-EDTA/^{99}Tc^{m}-MDP ratio.

Grade I

Patients (normal to mild radiographic change) had mean ratio values of 1.67 (range 1.0–2.8).

Grade II

Patients (moderate radiographic change) had mean ratio values of 2.59 (range 1.55–4.06).

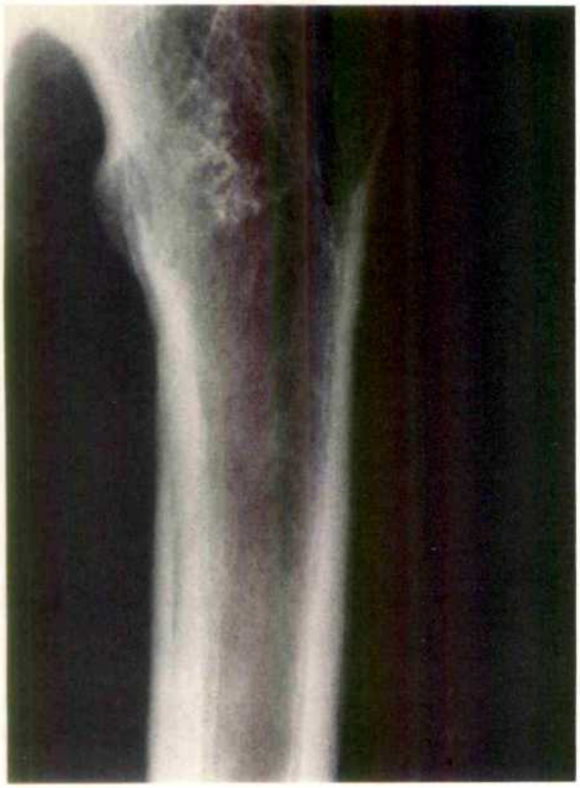

Figure 3. Radiograph of upper femur showing severe periosteal neostosis.

Grade III

Patients (severe radiographic change) had mean ratio values of 3.78 (range 2.24–10.15).

Grade I and Grade II patients showed significant differences ($p=0.001$), similarly Grade I and Grade III ($p=0.001$) and Grade II and Grade III ($p=0.005$) patients.

Three patients showed severe periosteal neostosis, two in the pelvis and upper femora (Fig. 3) and one in the metacarpals. Ratio values were 10.15, 5.19 and 3.61. All three values were markedly elevated at above the 90th percentile for patients in chronic renal failure.

Three patients showed cystic changes in the carpal bones (Fig. 4). These patients had ratios of 10.15 (same patient as in the periosteal neostosis group), 3.50 and 2.53.

When the 37 alkaline phosphatase levels were compared with the ratio values, there was a correlation ($r=0.694$, $p=0.001$) (Fig. 5). However, four out of 14 patients with severe subperiosteal resorption (Grade III)

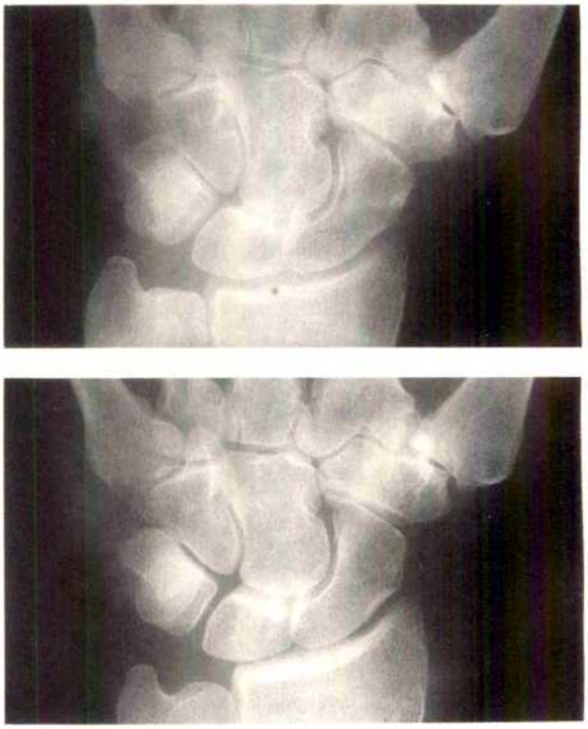

(a)

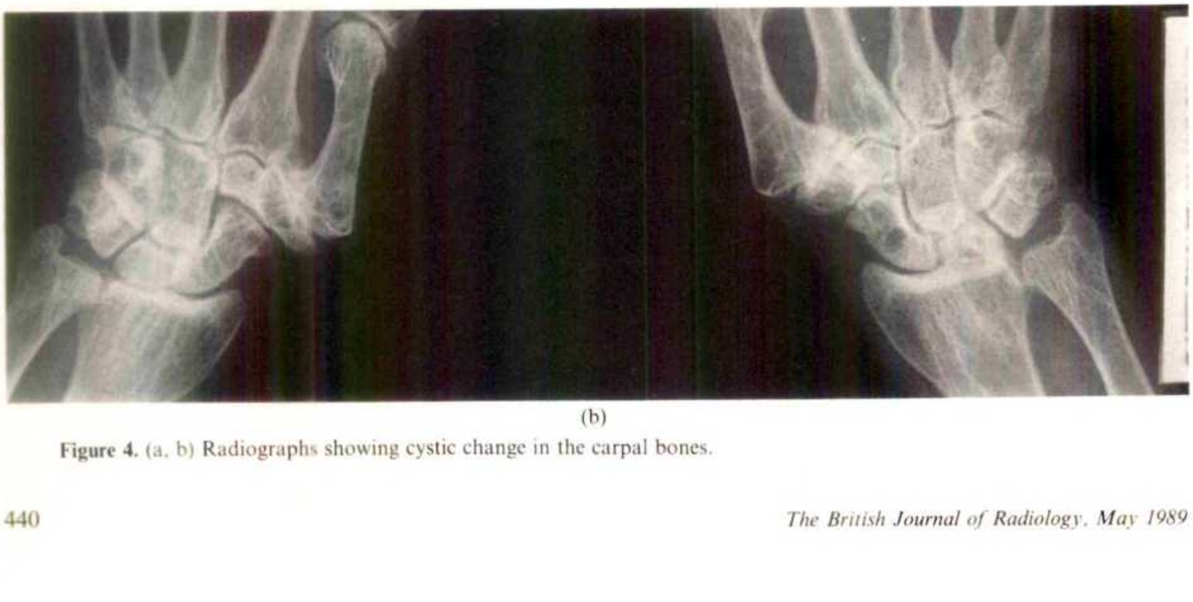

(b)

Figure 4. (a, b) Radiographs showing cystic change in the carpal bones.

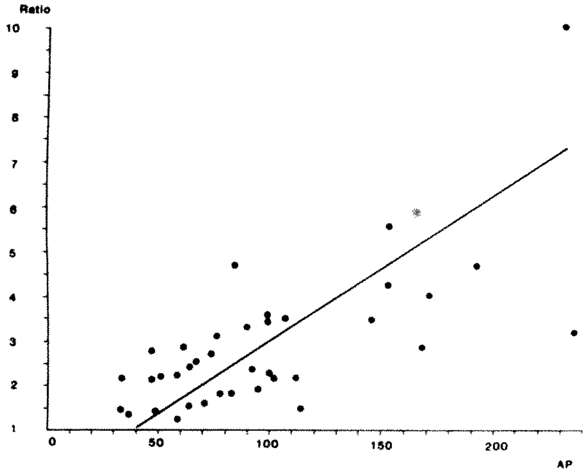

Figure 5. The correlation between alkaline phosphatase levels and the ^{51}Cr-EDTA/^{99}Tc^{m}-MDP ratio.

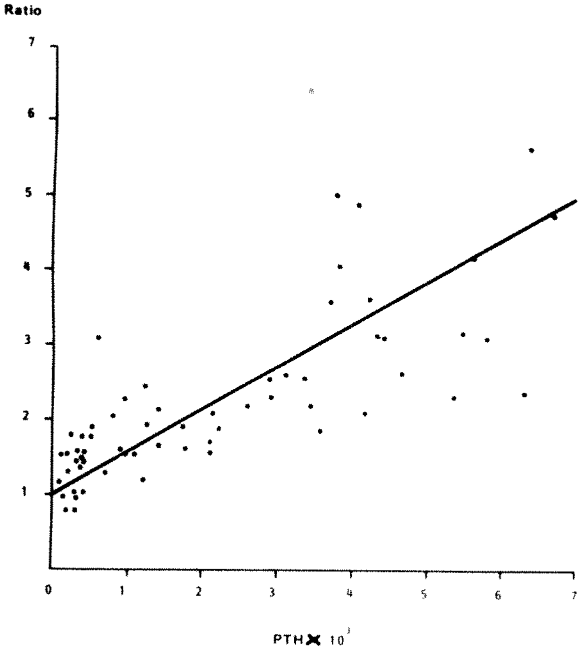

Figure 6. The correlation between PTH levels and the ^{51}Cr-EDTA/^{99}Tc^{m}-MDP ratio.

showed normal alkaline phosphatase levels. When the 62 PTH results were compared with ratio measurements, correlation was also significant ($r=0.779$, $p=0.001$) (Fig. 6).

Of the 33 patients who had sequential studies performed, 21 had no change in bone scan appearances, no clinical change and no biochemical change. Ratio values showed small changes varying from 1.5 to 25% (mean 10%). Only one patient showed a ratio change greater than 20%, which is the upper limit of the range of reproducibility (qv).

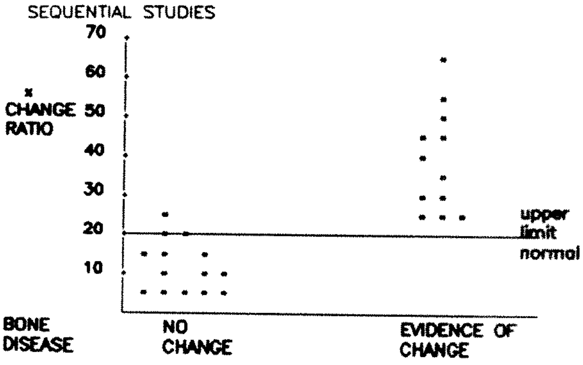

Figure 7. The correlation between patients with evidence of change in bone disease and patients without change and the ^{51}Cr-EDTA/^{99}Tc^{m}-MDP ratio.

Twelve patients showed evidence of change, based on either clinical or bone scan change. Eleven showed improvement and this was associated with a marked decrease in ratio values (percentage change ranging from 21 to 66%, mean 39%). One patient showed progression of disease with elevation of the ratio value (21% change) (Fig. 7).

Discussion

The results show highly significant correlation of the ^{51}Cr-EDTA/^{99}Tc^{m}-MDP plasma ratio values with radiological and biochemical measurements of renal bone disease. When radiological change occurs, it is highly specific (Katz et al, 1969), but may be insensitive. Alkaline phosphatase is a useful measure, but may be inaccurate in individuals. This is confirmed in our study in four patients (29%) who had severe bone disease radiologically, but normal alkaline phosphatase levels. Similarly, the assay of parathyroid hormone levels may be inaccurate because of the long half-life of circulating fragments in chronic renal failure.

The value of periosteal neostosis as a sign of intense secondary hyperparathyroidism (Ritz et al, 1978) is confirmed with all three cases showing severe (Grade III) subperiosteal resorption. These three cases also showed markedly elevated ratio levels.

The three cases with cystic change in the carpals showed high ratio values and Grade III subperiosteal resorption in two cases; however, one case showed a moderate ratio value (2.53) and Grade I subperiosteal resorption. This is in keeping with the findings of Resnick (1974) and Sundaram et al (1981) that cystic change and erosive arthritis may occur in the absence of subperiosteal resorption. The significance of cystic change seems unclear.

The follow-up studies show significant correlation between ratio changes and changes in clinical, biochemical or bone scan status, providing a quantitative measure of disease activity.

The results suggest that the ratio measure is an accurate index of renal bone disease activity and may be useful to assess initial disease activity and also in grading the progression or response to therapy of renal bone disease.

Acknowledgments

We would like to thank the physicians of Guy's Renal Unit for referring their patients, the nurses of Guy's Nuclear Medicine Department and Mrs S. J. Homan for typing this manuscript.

References

KATZ, A., HAMPERS, C. & MERRILL, J., 1969. Secondary hyperparathyroidism and renal osteodystrophy in chronic renal failure. *Medicine (Baltimore)*, *48*, 333–347.

NISBET, A. P., EDWARDS, S., LAZARUS, C. R., MALAMITSI, J., MAISEY, M. N., MASHITER, G. & WINN, P., 1984. ^{51}Cr-EDTA/^{99}Tc^{m}-MDP plasma ratio to measure total skeletal function. *British Journal of Radiology*, *57*, 677–680.

RESNICK, D., 1974. Erosive arthritis of the hand and wrist in hyperparathyroidism. *Radiology*, *110*, 263–269.

RITZ, E., PRAGER, P. & KREMPIEN, B., 1978. Skeletal x-ray findings and bone histology in patients on haemodialysis. *Kidney International*, *13*, 316–323.

SUNDARAM, M., WOLVERSON, M. K., HEIBERG, E. & GRIDER, R. D., 1981. Erosive azotemic osteodystrophy. *American Journal of Roentgenology*, *136*, 363–367.

1989, *The British Journal of Radiology*, 62, 443–446

Endoscopic correction of vesico-ureteric reflux by subureteric Teflon injection: follow-up ultrasound and voiding cystography

By *N. S. Blake, FRCR, FFRRCSI and †E. O'Connell, FRCR, FFRRCSI

Children's Research Centre, Our Lady's Hospital for Sick Children, Crumlin, Dublin 12, Eire

(*Received October 1988 and in revised form November 1988*)

Abstract. The technique of subureteric Teflon injection for the correction of vesico-ureteric reflux was first described by Puri and O'Donnell in 1984. The Teflon granuloma that occurs after the injection anchors the submucosal ureter, thereby preventing reflux. This paper reviews the ultrasound and cystographic findings in 88 patients with 115 refluxing ureters followed-up for periods ranging from 3 months to 3 years. Reflux disappeared in 91 ureters (79.1%) and the degree of reflux improved in 22 ureters (19.1%). In this follow-up study, the size of the granuloma on ultrasound was assessed in relation to the number of injections, the total volume of Polytef paste used and the outcome of the procedure. A well circumscribed granuloma was seen at the orifices of 92 ureters. There was no ureteric granuloma evident in 23 ureters and Teflon plaques were found at the trigone in six patients. Complications were rare. One large granuloma caused severe obstruction requiring re-implantation. The size of the granuloma appears to depend on individual tissue reaction rather than on the other factors. The presence or the size of the granuloma bears no direct relationship to the success of the procedure.

Primary vesico-ureteric reflux is common and has been reported in 30–50% of children presenting with urinary tract infection by Hodson and Cotran (1982). Ureteric re-implantation is quite a formidable operative procedure but the success rate should now exceed 90%.

The technique of endoscopic subureteric Teflon injection (STING) for correction of vesico-ureteric reflux was first described by Puri and O'Donnell (1984) after experimental work on piglets. Teflon paste is a suspension of biologically inert polytetrafluorethylene particles in glycerine. When this paste is injected behind the intravesical ureter, the Teflon particles elicit a foreign-body giant cell granulomatous reaction, which becomes encapsulated with fibrous tissue (Fig. 1).

This granuloma anchors the submucosal ureter and thereby prevents reflux (Puri & O'Donnell, 1984). This technique has been practised in Our Lady's Hospital since March 1984. Success rates of 84–88% for all grades of primary vesico-ureteric reflux have been reported (O'Donnell & Puri, 1986a, b; Puri & O'Donnell, 1987).

We review the findings on ultrasound and voiding cystography in 88 children treated by this procedure, who were followed-up for periods ranging from 3 months to 3 years.

Patients and methods

The series includes 88 patients with primary vesico-ureteric reflux of Grades III to V, according to the international classification (International Reflux Study Committee (IRSC), 1981). There were 67 female and 21 male patients. The age range was 6 months to 14 years with a mean of 7 years. There were 11 patients (12.5%) aged 2 years and younger.

Vesico-ureteric reflux was unilateral in 65 patients (73.8%) and bilateral in 23 patients (26.1%) giving 115 refluxing ureters, including four refluxing duplex systems. Table I shows the grades of reflux in all patients. The STING procedure was carried out according to the technique of Puri and O'Donnell (1984).

Follow-up ultrasound and voiding cystography were performed at 3-monthly, yearly and 3-yearly intervals after the procedure. Recurrence or persistence of vesico-ureteric reflux was assessed and the maximum diameter of the Teflon granuloma at each ureteric orifice seen on ultrasound was measured. The size of the granuloma was then correlated with the total volume of Teflon injected and with the number of injections at each site. Spearman's rank-order correlation coefficient (Rho) was used to assess statistical significance.

Results

Table II shows the results of the STING procedure in 115 ureters. Reflux ceased in 91 ureters (79.1%) and the grade of reflux improved in 22 ureters (19.1%). The reflux increased in two patients with duplex systems. The success rate with duplex systems excluded was 82.2%.

Table I. Grades or reflux (international classification)

	Reflux grade			
	III	IV	V	Total
No. of ureters	68	40	7	115

---

*Author for correspondence.

†Fuji Research Fellow.

Presented at the European Society of Paediatric Radiology, Montreux, Switzerland, April 14, 1988.

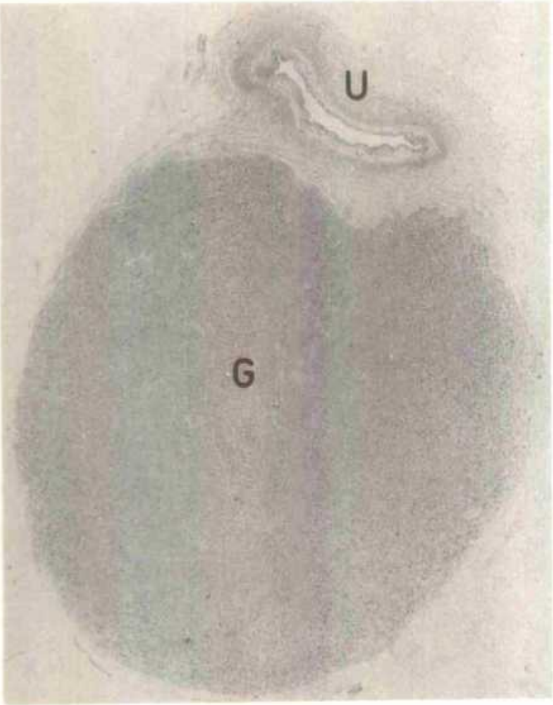

Figure 1. Histology section of guinea pig ureter (U) and Teflon granuloma (G) following subureteric injection of Teflon paste.

Bladder filling defects corresponding to the Teflon granulomas were observed on the post-micturition radiographs of 10 patients at voiding cystography. On ultrasound, a well defined, soft-tissue mass with bright echoes and acoustic shadowing was seen at the ureteric orifices of 92 ureters, corresponding to the Teflon implants (Fig. 2). The absence of a granuloma at the orifices of 23 ureters is worth stressing. In six of these cases there were soft-tissue masses with bright echoes and acoustic shadowing at the trigone, consistent with migrating Teflon (Fig. 3).

The maximum diameter of the granulomas ranged from 0.5 to 2.9 cm with a mean of 1.1 cm. Large, lobulated granulomas were found in four patients and two patients had extensive shallow granulomas.

The total volume of Teflon injected at each ureteric orifice ranged from 0.1 to 2.1 ml with a mean of 0.7 ml. Using Spearman's rank-order correlation coefficient, the critical value for $p = 0.05$ was Rho = 0.186. There was no significant correlation between the size of the granuloma and the total volume of Teflon injected (Rho = 0.137). There was also no significant correlation between the size of the granuloma and the number of Teflon injections (Rho = 0.164).

Complications were rare. Severe obstruction requiring re-implantation of the ureter occurred in only one case. This was a 4-year-old boy who had bilateral Grade V reflux. He had three bilateral, subureteric injections. At follow-up ultrasound, there was marked left hydronephrosis and hydroureter secondary to a large 2.5 cm × 2.9 cm granuloma (Fig. 4a). The total volume of Teflon injected at this ureteric orifice was 1.5 ml. A large filling defect was seen in the left side of the bladder at voiding cystography (Fig. 4b) and a walnut-sized mass was palpable on rectal examination.

The remaining three large, lobulated granulomas were not associated with obstruction or recurrence of reflux.

Table II. Results of subureteric Teflon injection in 115 ureters

	Reflux		
	Cured	Decreased	Increased
No. of ureters	91 (79%)	22 (19%)	2 (1.7%)

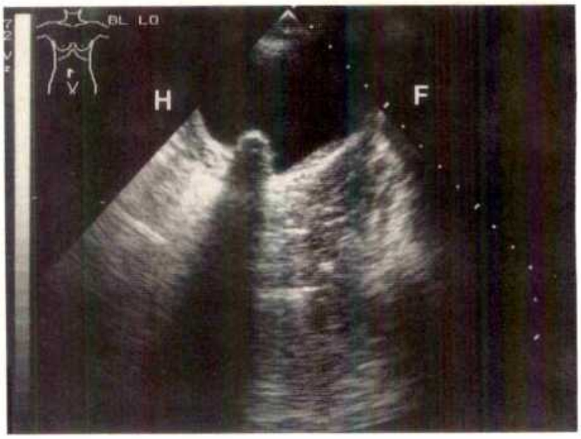

Figure 2. Longitudinal ultrasound section of the bladder showing Teflon granuloma with acoustic shadowing. (H = direction of head; F = direction of foot).

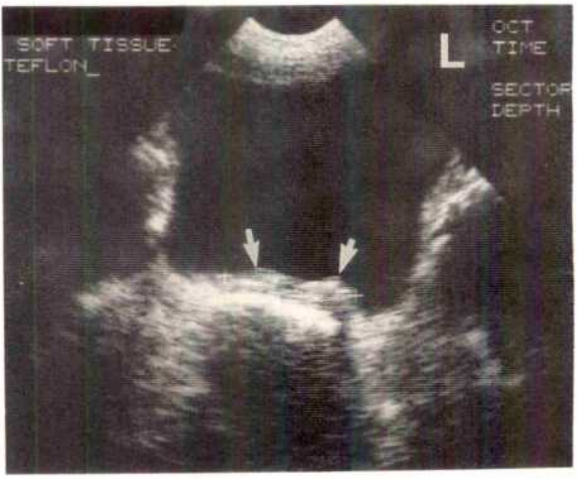

Figure 3. Transverse ultrasound scan of the bladder demonstrating diffuse, soft-tissue swelling in the region of the trigone (arrows). Scattered bright echoes in the swelling suggest migration of Teflon particles.

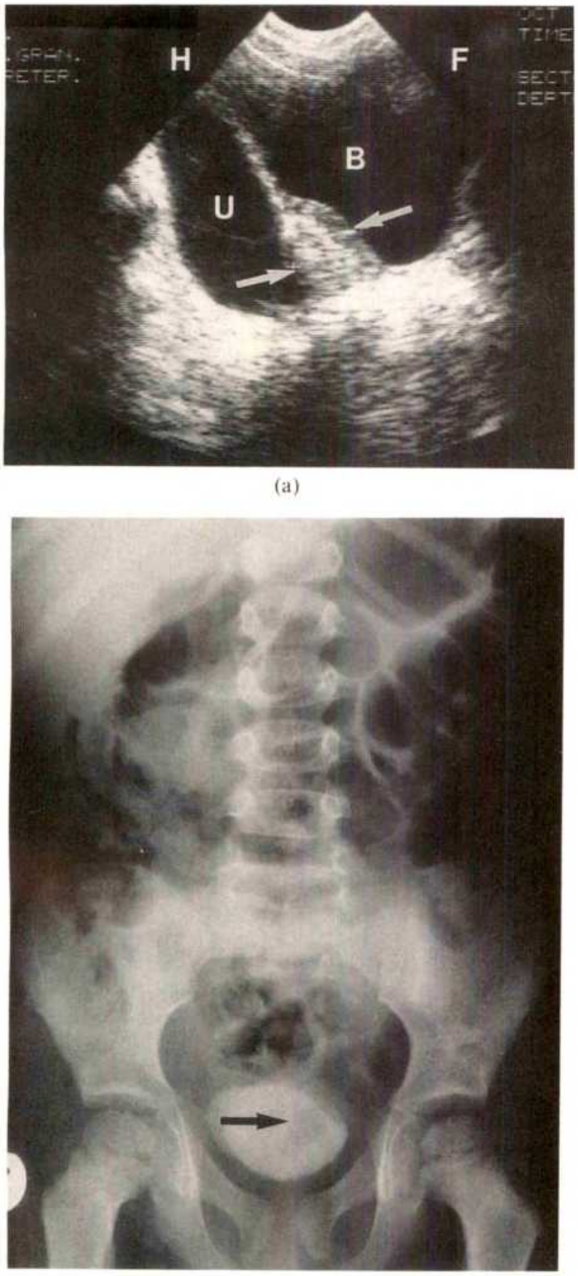

(a)

(b)

Figure 4. Large Teflon granuloma obstructing the left ureter. (a) Longitudinal ultrasound scan outlining the granuloma (arrows). (b) Post-voiding radiograph of the same patient revealing the granuloma (arrow) as a substantial filling defect in the bladder.

There was no recurrent reflux in four of the six patients who had Teflon plaques at the trigone, another developed reflux in the opposite ureter and the degree of reflux improved in the sixth patient. Remarkably, reflux recurred in only one of the remaining ureters not associated with granuloma formation. This raises the possibility of soft-tissue distortion or transient swelling modifying the ureteric orifice sufficiently to prevent reflux.

Discussion

Since it was first introduced in 1984, the STING procedure to correct vesico-ureteric reflux has been used in hundreds of cases worldwide. The follow-up in our series is still relatively short, but complications are rare and are surgically correctable. The success rate of this revolutionary technique in our experience is 80–90% and it has been found to be simple and cost-effective as a day care procedure.

Teflon paste injection has been used since 1963 for enlargement of displaced or deformed vocal cords (Arnold, 1963) and since 1974 periurethrally to treat urinary incontinence (Politano, 1982; Schulman et al, 1984). No untoward side-effects from these uses of the paste in humans have been reported.

Malizia et al (1984) reported distant migration and granuloma formation in animals after periurethral injection of Teflon paste containing radioactive strontium microspheres. The authors expressed concern regarding the safety of its use, particularly in children and young adults. However, Politano, who pioneered the use of Teflon paste for urinary incontinence, did not document a single case of embolization after injection of 10–12 ml periurethrally in over 300 cases since 1964 (Vorstman et al, 1985). Vorstman et al found that Teflon particles had migrated to regional lymph nodes in an autopsy case. However, the death was unrelated to the Teflon injection.

Since the volume of Teflon paste used to treat vesico-ureteric reflux is small, appreciable migration seems unlikely, but long-term follow-up is advisable. The spectrum of appearances following the STING procedure should become familiar to radiologists. Voiding cystography is indicated in follow-up of patients who have had the STING procedure to exclude persisting or recurrent ureteric reflux.

Ultrasound is ideal to exclude obstruction and to assess the injection site. The granuloma at the ureteric orifice could be demonstrated using computed tomography or magnetic resonance but such imaging would be very expensive or impractical, of doubtful advantage and involve unnecessary radiation in the former.

Acknowledgments

We wish to thank Professor Barry O'Donnell and Mr Prem Puri on whose patients these studies were carried out, and also Mr Des Kenny for statistical advice.

References

Arnold, G. E., 1963. Alleviation of aphonia or dysphonia through intrachordal injection of Teflon paste. *Annals of Otology, Rhinology and Laryngology*, *70*, 384–395.

Hodson, C. J. & Cotran, R. S., 1982. Reflux nephropathy. *Hospital Practice*, *17*, 133–156.

IRSC, 1981. International Reflux Study Committee. Medical versus surgical treatment of primary vesico-ureteric reflux. *Paediatrics, 67,* 392–400.

MALIZIA, A. A., REIMAN, H. M., MYERS, R. P., SANDE, J. R., BARHAM, S. S., BENSON, R. C., DEWANJEE, M. K. & UTZ, W. J., 1984. Migration and granulomatous reaction after periurethral injection of Polytef (Teflon). *Journal of the American Medical Association, 251,* 3277–3281.

O'DONNELL, B. & PURI, P., 1986a. Endoscopic correction of primary vesico-ureteric reflux: results in 94 ureters. *British Medical Journal, 293,* 1404–1406.

—— 1986b. Endoscopic correction of primary vesico-ureteric reflux. *British Journal of Urology, 58,* 601–604.

POLITANO, V. A., 1982. Periurethral polytetrafluorethylene injection for urinary incontinence. *Journal of Urology, 127,* 439–442.

PURI, P. & O'DONNELL, B., 1984. Correction of experimentally produced vesico-ureteric reflux in the piglet by intravesical injection of Teflon. *British Medical Journal, 289,* 5–7.

—— 1987. Endoscopic correction of Grades IV and V primary vesicoureteric reflux: 6–30-month follow-up in 42 ureters. *Journal of Paediatric Surgery, 22,* 1087–1091.

SCHULMAN, C. C., SIMON, J., WESPES, E. & GERMEAU, F., 1984. Injections of Teflon to treat urinary incontinence in women. *British Medical Journal, 288,* 192.

1989, *The British Journal of Radiology*, *62*, 447–449

The influence of type of tube and experience of the operator on performance of small bowel enema

By D. A. Nicholson, BM, BS, BMedSci, I. Zammit-Maempel, MRCP, M. Hughes, FRCS, E. Nanda Kumar, MD, FRCR and *D. F. Martin, MRCP, FRCR

Department of Radiology, University Hospital of South Manchester, Nell Lane, Manchester M20 8LR

(*Received November 1988*)

Abstract. Seventy patients underwent small bowel enema (SBE) to assess the influence of experience of the radiologist on the ease of jejunal intubation and the adequacy of SBE using two types of tubes. Comparing intubation time, intubation screening time, total screening time and total room time, we conclude that jejunal intubation is achieved easily, in a reasonable time with both types of tube, by all grades of radiologist, although the experienced operator using the Silk tube achieved intubation in a significantly shorter time. Overall patient acceptability was satisfactory (75%) but was better using the Silk tube, with which entero-gastric reflux and vomiting were less.

Examination of the small bowel by small bowel enema (SBE; enteroclysis) is considered more accurate than the follow-through examination (Sanders & Ho, 1976; Ekberg, 1977; Diner et al, 1984). However, there seems to be reluctance, especially amongst junior radiologists, to perform SBE, possibly because of the time and anticipated difficulty involved in performing jejunal intubation (Nolan & Cadman, 1987; Barloon et al, 1988). We have evaluated the influence of experience of the radiologist on the ease of jejunal intubation and the adequacy of the technique using two SBE tubes.

Materials and methods

Two types of SBE tube were used. The Nolan modification of the Bilbao-Dotter tube (William Cook) is a 12 French "PVC" tube with a closed end and six side holes, 135 cm long, with a Teflon-coated guide wire. The "Silk" tube (Merck) is a 10 French polyurethane tube with a tungsten-weighted tip, 140 cm long, with a single oblique side hole and a braided stainless steel guide wire.

Two groups of radiologists were involved in the study: experienced (those who had performed over 100 SBEs), and inexperienced (less than 10 SBEs). Each radiologist alternated the type of tube on successive occasions. Four groups were thus formed: experienced/Nolan, inexperienced/Nolan, experienced/Silk and inexperienced/Silk.

Patients fasted for 6 h prior to the examination and received one sachet of Picolax the day before. Intubation was performed under pharyngeal anaesthesia using topical lignocaine spray with the patient sitting or standing. The tube was passed through the mouth or nose, depending on the radiologist's and patient's preference. A single-contrast examination was performed using 20% w/v barium (Micropaque, Nicholas Laboratories), infused via a closed bag system. A number of parameters were recorded: total room time, intubation time, screening time for intubation, total screening time, number of films exposed, adequacy of flow of barium, adequacy of examination, entero-gastric reflux, vomiting and the willingness of patients to accept future SBE.

Results

Seventy consecutive patients were included, 28 male and 42 female. The age range was 14–85 years, with a mean of 40.6 years. The commonest indication for referral was Crohn's disease (43), followed by subacute obstruction (eight), abdominal pain, malabsorption, melaena, anaemia and lymphoma.

In two patients, intubation failed as it proved impossible to pass the tube through the pylorus, one by an experienced operator using the Nolan tube and one by an inexperienced operator using Silk tube. In the second patient, intubation was also attempted using the Nolan tube, and by an experienced operator, but failed.

Mean intubation time for the four groups varied from 9.4 to 17.0 min, shorter times being achieved with the Silk tube and by experienced operators (Table I). However, the only statistically significant difference between the groups was that intubation time for the experienced/Silk group (9.4 min) was shorter than for the other groups (*t*-test, $p < 0.05$), but this did not lead to significantly reduced intubation screening time or total

Table I. Comparison of radiologists' experience/tube type for intubation time (IT), screening time for intubation (IST), total screening time (TST) and total room time (RT)

	No. of patients	IT (min)	IST (min)	TST (min)	RT (min)
Ex/Silk	19	9.4	4.7	13.6	38.2
Ex/Nolan	16	13.2	5.3	12.6	38.1
Inex/Silk	17	13.4	4.5	11.3	43.8
Inex/Nolan	16	17.0	5.7	12.9	53.3

---

*Author for correspondence.

Table II. Comparison of radiologist's experience/tube type for the number of patients showing entero-gastric reflux, vomiting, willingness to have the examination repeated and slow flow-rate

	No. of patients	Reflux	Vomiting	Repeat	Slow flow-rate
Ex/Silk	19	4	2	14	7
Ex/Nolan	16	5	3	11	4
Inex/Silk	17	3	1	16	5
Inex/Nolan	16	7	3	10	4

Table III. Comparison of mean number of radiographs (small = 24–30 cm, large = 43–35 cm) per SBE and radiologist's experience

	No. of patients	Number of radiographs	
		Large	Small
Experienced radiologists	35	1.4	3.1
Inexperienced radiologists	33	3.0	5.0

screening time. Total room time was longer ($p < 0.005$) in both the inexperienced groups.

Reflux of barium into the stomach occurred in 12 out of 32 patients with the Nolan tube compared with seven out of 36 for the Silk tube (Table II). The incidence of reflux in all 68 patients was 28%. Vomiting was less common with a total incidence of 13%, although less in the Silk group.

Overall patient acceptability, assessed by willingness to undergo repeat examination, was 51 out of 68 (75%), with 30 out of 36 (83%) in the Silk group and 21 out of 32 (66%) in the Nolan group.

All examinations were of diagnostic quality, despite a slow infusion rate being recorded in 12 out of 36 (33%) using the Silk tube compared with eight out of 32 (25%) using the Nolan tube. This was not reflected in the total screening or room times. The number of radiographs taken per examination by the inexperienced group was almost twice that of the experienced group (Table III).

Discussion

Techniques used to study the small intestine include per oral examination (follow-through), single and double-contrast SBE and retrograde methods. The follow-through remains popular because of its simplicity, but it is said to be "often carried out in a cursory manner" (Gurian et al, 1982; Diner et al, 1984). Small bowel enema is advocated as a more accurate method of detecting focal lesions (Maglinte et al, 1984) and many different techniques have been described (Sellink, 1974; Sellink & Miller, 1982; Nolan & Cadman, 1987). Some radiologists may not adopt SBE because of reluctance to perform jejunal intubation (Nolan & Cadman, 1987), which is time-consuming (Ott et al, 1985), although this may be reduced with experience (Skjennald & Samset, 1980).

This study indicates that the type of tube as well as the experience of the operator is important. The Silk tube was more quickly passed by both inexperienced and experienced radiologists, and experienced operators using Silk tubes achieved intubation in a statistically shorter time compared with the other three groups. The intubation times achieved are comparable to those of previous studies (Nolan & Cadman, 1987). Of the two failed examinations, intubation was attempted with both tubes and by different radiologists. It seems that the failures were attributable to the individual patients and not the tube type or experience of the radiologist.

The mean room time ranged from 38.1 to 53.3 min, being significantly less in the experienced group. This compares with the study by Ott et al (1985), in which a mean room time of 44 min was recorded. These authors also found a mean total screening time of 22 min, whilst in the present study, screening time was less in all groups, ranging from 11.3 to 13.6 min (mean = 12.6 min). Although the inexperienced radiologist may spend more time in the room, in our experience this is not reflected in prolonged screening time or radiation dose. Radiologist's experience does have an influence on the number of films exposed (Table III). Ott et al (1985) recorded nine radiographs per examination, which compares with our inexperienced radiologists, but the number of radiographs was substantially reduced in the experienced group.

Patient acceptability was satisfactory (75%). It seems to be improved by using the smaller-calibre Silk tube (10 F), with which entero-gastric reflux and vomiting are reduced. The apparent slow flow rate of this tube does not appear to be a disadvantage in terms of room time or adequacy of examination.

Jejunal intubation can be achieved easily, in a reasonable time with both types of tube, by all grades of radiologist. This should give both the inexperienced and unwilling confidence when contemplating SBE for the investigation of the small bowel.

References

BARLOON, T. J., LU, C. C., FRANKEN, E. A., HONDA, H. & BERBAUM, K., 1988. Small bowel enteroclysis survey. *Gastrointestinal Radiology, 13*, 203–206.

DINER, W. C., HOSKINS, E. O. & NAVAB, F., 1984. Radiological examination of the small intestine: review of 402 cases and discussion of indications and methods. *South Medical Journal, 77*, 68–74.

EKBERG, O., 1977. Double contrast examination of the small bowel. *Gastrointestinal Radiology, 1*, 349–353.

GURIAN, L., JENDRZEJEWSKI, J., KATON, R., BILBAO, M., COPE, R. & MEINKY, C., 1982. Small bowel enema: an underutilised method of small bowel examination. *Digestive Diseases and Sciences, 27*, 1101–1108.

MAGLINTE, D. D., HALL, R. & MILLER, R. E., 1984. Detection of surgical lesions of the small bowel by enteroclysis. *American Journal of Surgery, 147*, 225–229.

NOLAN, D. J. & CADMAN, P. J., 1987. The small bowel enema made easy. *Clinical Radiology, 38*, 295–301.

OTT, D. J., CHEN, Y. M., GELFAND, D. W., SWEARINGEN, F. V. & MUNITZ, H. A., 1985. Detailed per-oral small bowel examination vs enteroclysis. *Radiology, 155*, 29–34.

SANDERS, D. E. & HO, C. S., 1976. The small bowel enema: experience with 150 examinations. *American Journal of Roentgenology, 127*, 743–751.

SELLINK, J. L., 1974. Radiologic examination of the small intestine by duodenal intubation. *Acta Radiological Diagnosis, 15*, 318–322.

SELLINK, J. L. & MILLER, R. E. 1982. *Radiology of the Small Bowel: Techniques and Atlas* (Martinus Nijhoff, The Hague).

SKJENNALD, A. & SAMSET, J. H., 1980. Duodeno-jejunal intubation in examination of the small intestine. *Clinical Radiology, 31*, 221–224.

1989, *The British Journal of Radiology*, *62*, 450–456

First Interim Progress Report on the second British Institute of Radiology Fractionation study: Short *versus* long overall treatment times for radiotherapy of carcinoma of the laryngo-pharynx*

By G. Wiernik (Chairman), C. J. Alcock, T. D. Bates, R. J. Berry, J. M. Brindle, J. E. Dalby, J. F. Fowler (Joint Honorary Secretary), W. R. Gajek, S. Goodman, J. L. Haybittle (Consultant Statistician), J. M. Henk, J. W. Hopewell (Joint Honorary Secretary), N. Howard (Joint Honorary Secretary), R. Lindup, D. L. Phillips, R. S. Pointon, M. Rezvani (Data Manager/Statistician) and J. S. Tobias

The British Institute of Radiology, 36 Portland Place, London W1N 4AT

(*Received August 1988 and in revised form December 1988*)

Abstract. Preliminary data from a second British Institute of Radiology Fractionation Trial comparing short (≤4 weeks) and long (>4 weeks) overall treatment times are reported. The intake of patients ran from January, 1975 to December, 1985 when 611 patients with carcinoma of the laryngo-pharynx were registered in this prospective, randomized, multicentre clinical trial. No significant differences have, so far, been demonstrated between the two arms of the trial with respect to observed survival rates, tumour-free or laryngectomy-free rates. Further long-term follow-up is continuing.

In 1962 The British Institute of Radiology (BIR) convened a Working Party to look into the effects of dose fractionation in radiotherapy. A clinical trial was set up initially to investigate whether treatment with three fractions per week (3F/wk), instead of with the standard treatment of five fractions per week (5F/wk), would be safe for patients and would give rise to as good or better survival rates at the expense of no greater normal-tissue damage. The Final Report on the general clinical results of this trial (BIR Working Party, 1989) has shown that curtailed fractionation gave similar results when compared with standard treatment, with several possible advantages: first, for patients, because of fewer treatment visits, and secondly, for treatment centres, because of related financial and other savings.

In the light of the successful running of the first trial, the Working Party set up a second trial in order to investigate whether radiation treatment with a "short overall time", 3–4 weeks, gave as good results as a standard treatment, designated "long overall time", given in >4 weeks, which in the majority of centres was, in the event, ≥6 weeks. The second clinical trial had an entry from January, 1975 to December, 1985, during which time a total of 611 patients were registered.

Materials and methods

The second clinical trial, though asking a new question, was run on exactly the same basis as the first trial, the methodology for which has been reported in full in a Preliminary Report (BIR Working Party, 1963), seven Interim Progress Reports (BIR Working Party, 1964, 1968, 1970, 1971, 1972, 1978, 1982) and a Final Report (BIR Working Party, 1989). The second trial was a prospective, randomized, multicentre trial and was planned to produce no significant difference in the radiation reactions seen in the normal tissues of patients whether they were treated with the short or the long overall time regime.

Sealed, randomly numbered envelopes, which had to be opened in order, were supplied to individual centres through the BIR, which also acted as "Post Box" for the return of all forms and histological slides. The allocation envelope contained duplicate primary registration cards, which carried the specific trial number for the prospective patient as well as the direction for a "short" or a "long" overall treatment time that had to be adopted. The individual centre was free to choose its own fractionation pattern of either three or five fractions per week and they were given the appropriate doses for each fractionation pattern. These were based on the dose and fractionation scheme that was standard practice in that particular centre.

The envelope also contained a letter addressed to the local pathologist requesting him to submit to the BIR a

---

Patients were entered into the trial from the following centres: Bristol (J. Bullimore and S. Goodman), Liverpool (J. E. Dalby), London: Charing Cross (B. M. Southcott and N. Howard), Middlesex Hospital (N. M. Bleehen and R. J. Berry), Royal Marsden Hospital (J. M. Henk), St. Thomas' Hospital (T. D. Bates), and University College Hospital (J. S. Tobias), Manchester (R. S. Pointon), Oxford (C. J. Alcock, K. R. Durrant, A. H. Laing, C. H. Paine and G. Wiernik), Plymouth (J. M. Brindle), Southend (D. L. Phillips), Stoke on Trent (R. Lindup), and Swansea (W. R. Gajek).

*Reprints are available from The British Institute of Radiology, Publications Office, 36 Portland Place, London W1N 4AT at £2 per copy or $ equivalent (remittance with order please).

stained histological section of the tumour biopsy on which the diagnosis had been made. One of the duplicate registration cards was returned to the BIR with the initial completed pre-circulated trial form that carried all the clinical data for entry of the patient. The other duplicate registration card was retained at the local centre for reference.

Each centre also held a second block of trial forms on which the acute radiation reactions for each patient were recorded for a period of 12 weeks from the start of radiation treatment. Thereafter, the trial office sent out personalized follow-up forms to the centres, carefully timed so as to reach the centre 2 weeks before the appointment date for the 6-monthly check-up. This form was returned to the centre in relation to the annual check-ups, which were requested to be as near as possible to the anniversary of the start of radiation treatment. "Chase-up" letters were sent to the centres if forms were not returned promptly. For this long-term follow-up the same form was shuttled backwards and forwards so that the clinician completing the form knew what had been reported previously. Each time the form came back to the trials office the new data were transcribed onto a coding form so that no data should be lost if, for any reason, the original form went astray. To date, it has not been possible to obtain full data for 36 out of the 611 patients entered into the trial. The present analysis is based on the remaining 575 patients. Attempts are being made to trace the missing details for these 36 patients.

The numbers of patients entered by individual centres, for whom follow-up information for 12 or more weeks after the start of treatment has been obtained, are listed in Table I. The analyses throughout this report are based on the prospective random allocation of an individual patient to either the short or the long overall time regime. No alteration has been made to the resulting subdivision to allow for minor time variations, which occurred in a few patients, because of Bank Holidays, machine failures, etc.

The original data for each patient have been used to determine their TNM classification so that meaningful comparisons could be undertaken. It was possible to use the latest revision (UICC, 1987) of the TNM system for both the T category and the S stage grouping, but a previous classification (UICC, 1978) has had to be adopted for the N category of the patients as data were only available for the fixity of nodes. Details of the dimension of nodes, required for classification by the latest revision of the TNM system, were not available. This has resulted in a slightly hybrid basis for the S stage grouping but, as stated (BIR Working Party, 1989), this does not detract from the scientific validity of the analyses as all patients with stage groupings S2, S3 and S4 were treated as a single group.

All patients with evidence of distant spread of their disease that would have fallen into the M1 category were excluded from entry into the trial by the protocol specifications.

Patients were allocated into one of three sub-groups according to the anatomical site of their primary tumour. The first sub-group comprised only patients with tumours confined to a laryngeal subsite; there was sufficient data for these patients to allow segregation into the T1, T2 and T3 categories. The second sub-group

Table I. Numbers of patients allocated to different treatment regimes for whom there is follow-up information for ⩾ 12 weeks after the start of treatment

Treatment regime	Centre number	Overall treatment time						Dose reduction (%)
		Short (⩽4 weeks)			Long (>4 weeks)			
		Number of patients	Planned number of fractions	Modal dose (cGy)	Number of patients	Planned number of fractions	Modal dose (cGy)	
5F/wk								
	30	42	16	5457	46	30	6493	16
	32	19	16	4663	18	30	6048	23
	33	3	21	5250	3	31	6510	19
	35	13	16	4909	14	32	6500	24
	38	2	15	5250	3	25	6159	15
	40	1	21	5250	—	—	—	—
	41	54	16	4640	55	30	6000	23
	46	17	16	4800	13	32	6500	26
	50	35	16	5000	36	31	6265	20
	52	—	—	—	1	30	6000	—
3F/wk								
	33	1	13	4750	3	19	5795	18
	34	75	13	4729	70	19	5780	18
	39	8	12	5433	10	19	6253	13
	40	—	—	—	1	19	6000	—
	44	15	10	4200	17	18	5563	24

Table II. Numbers of patients distributed by randomization into short (S) and long (L) overall treatment time groups showing their categorization according to the TNM classification and anatomical site

	TNM classification																							
	T1		T2		T3		T4		N0		N1		N2		N3		S1		S2		S3		S4	
Overall treatment times	S	L	S	L	S	L	S	L	S	L	S	L	S	L	S	L	S	L	S	L	S	L	S	L
Site																								
Larynx	111	117	60	56	67	60	0	0	236	227	2	3	0	2	0	1	111	116	59	54	68	60	0	3
Pharynx	2	3	5	3	0	0	0	0	4	5	2	0	1	0	0	1	1	3	3	2	2	0	1	1
Dual	0	2	5	11	30	33	5	5	32	34	2	6	3	2	3	9	0	1	5	6	28	30	7	14
Total number of patients	113	122	70	70	97	93	5	5	272	266	6	9	4	4	3	11	112	120	67	62	98	90	8	18

contained those patients with primary tumours confined to a pharyngeal subsite; for these patients it was only possible to use the T1 and T2 categories as there were no data on the fixity of the tumours. Thus in the pharyngeal sub-group the category T2 includes all patients who might have fallen into the T2, T3 and T4 categories. The third sub-group has been termed "dual tumours" and contains those patients with either early tumours that occurred in anatomical positions that can be classified as either larynx or pharynx, such as the aryepiglottic fold, or who had advanced tumours that had spread into both laryngeal and pharyngeal structures.

The details concerning the fractionation schedule and dosage chosen by individual centres are also given in Table I. When centres that entered $\geqslant 10$ patients into the trial are considered, three centres opted for treatment schedules involving 3F/wk compared with six centres who chose 5F/wk. Taking into account the inherent reduction in the total number of fractions, the three centres using 3F/wk applied an average 18% dose reduction for their short overall time when compared with the dose used for their long overall time regime, whereas the average dose reduction was 22% for those centres that employed 5F/wk regimes. This difference was not statistically significant ($p > 0.10$).

The treatment protocol specified that the short treatment regime should be $\leqslant 4$ weeks and that the long overall time should be >4 weeks. In any individual centre the difference in overall treatment time between their treatment regimes was always a minimum of 2 weeks.

Results

Distribution of patients

A nearly equal distribution of patients was achieved by the process of randomization into the various groups that were associated with the major prognostic factors, such as the TNM classification and the anatomical site. This is shown in Table II. Of the 575 assessable patients, 285 were treated in a short overall time ($\leqslant 4$ weeks) and 290 were treated in a long overall time (>4 weeks).

Tumour responses

Observed survival rates

It must be stressed, as in the report on the first BIR trial of dose fraction in radiotherapy (BIR Working Party, 1989), that the data and analyses now presented relating to the second trial comparing short and long overall time, are in the nature of an interim progress account and can only provide a guide. A final assessment cannot be undertaken until the necessary long-term follow-up data are available.

The observed survival rates for all patients in the trial for whom adequate data are available, when they are split into the two groups of short and long overall treatment times, are shown in Fig. 1a. These data show that there are no discernible differences between the short and long overall treatment time groups.

When the patients were subdivided according to their TNM stage grouping, to allow a comparison between early and more advanced disease at presentation, in both the short and the long overall treatment time groups no significant differences between the two treatment groups of patients for early, S1 stage (Fig. 1b) and the more advanced stage groupings, S2, S3 and S4 (Fig. 1c) were found.

Tumour-free rates

The classification of "tumour-free" has been used in this report rather than that of "recurrence-free", which was used for the progress reports of the first trial (BIR Working Party, 1982). The use of the word "recurrence" created a problem in the allocation of patients who had persistent disease (BIR Working Party, 1989). There was no apparent difference between the two arms of the trial, short *versus* long overall treatment times, when all patients who had neither persistent nor recurrent tumour at the primary site were compared (Fig. 2a).

Breakdown of the data into sub-groups of early lesions, Stage S1 (Fig. 2b), and more advanced tumours, Stages S2, S3 and S4 (Fig. 2c), showed that there was no significant difference in either case between the two arms of the trial. However, as expected, the method of classification helped to identify the significant difference in prognosis between early and more advanced lesions ($\chi^2 = 21.76$, $p = <0.0001$).

Laryngectomy-free rates

Laryngectomy has been shown to be curative in the treatment of persistent or recurrent squamous cell carcinoma of the larynx and pharynx after radical

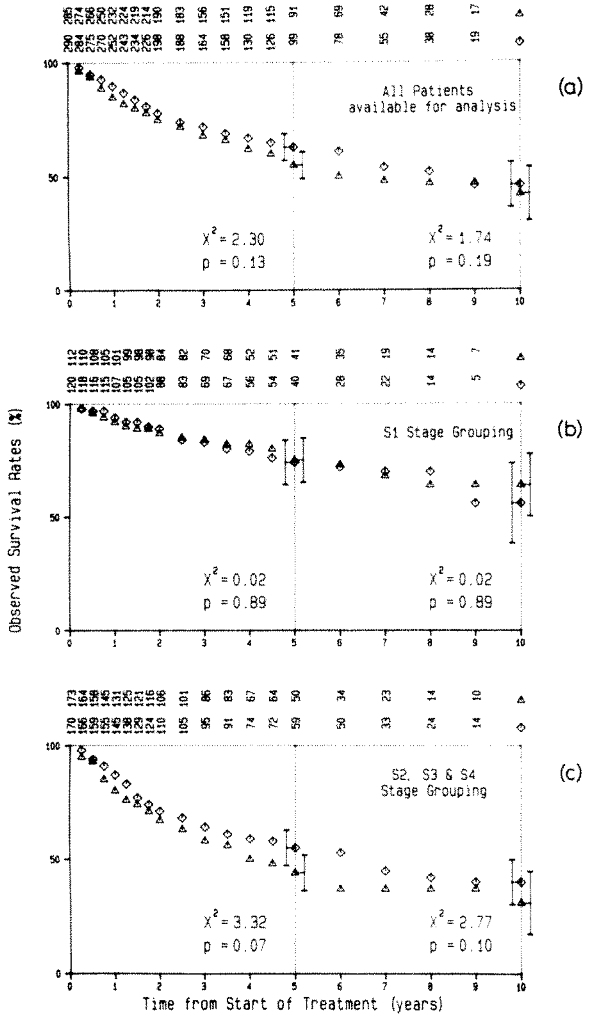

Figure 1. Observed (*i.e.* crude) survival rates. (a) For the 575 patients entered into the trial for whom adequate records are available at present *versus* time after the start of radiation treatment. No correction for age of the patients or mortality of patients without cancer has been made. The numbers of patients surviving at each anniversary are shown across the top of the figure. Triangles represent short overall time and diamonds represent long overall time. The values of χ^2 are calculated by the method described by Mantel (1966) for the periods 0–5 and 0–10 years. $p < 0.05$ would normally indicate a statistically significant difference when all data are included in the analysis but for two sub-groups $p < 0.025$ is more appropriate. The error bars shown at 5 and 10 years represent 95% confidence limits for the probability of the survival. (b) Confined to patients in the S1 stage grouping. (c) For patients in the S2, S3 and S4 stage grouping.

irradiation (Kirchner & Owen, 1977). Thus it was necessary to assess the effectiveness of the irradiation treatment by looking at the laryngectomy-free rates so that the curative effect of the radiation was not blurred by salvage surgery. The percentages of patients who did not require a laryngectomy are compared for the short and long overall treatment times in Fig. 3a. There was no significant difference between the two treatment modalities. This was also true when the sub-groups S1 (Fig. 3b) and S2, S3 and S4 (Fig. 3c) were assessed.

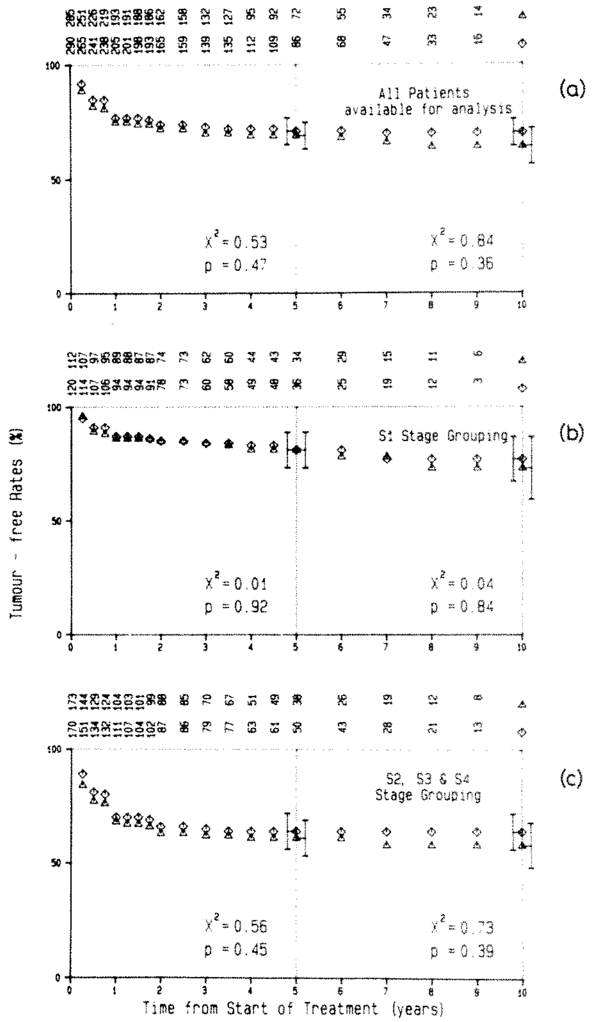

Figure 2. Tumour-free rates. (a) Percentage of all patients available for analysis who were without persistent or recurrent tumour versus time from start of treatment. Short compared with long overall treatment time. (b) Confined to patients in the S1 stage grouping. (c) For patients in the S2, S3 and S4 stage grouping. Symbols as in Fig. 1.

Normal-tissue reactions

Acute reactions

For each patient, acute radiation reactions, both symptoms and signs, were recorded regularly both during and after the course of treatment for a period of 12 weeks from the start of fractionated irradiation. To obtain figures for analysis, only the first record of the incidence of any particular acute radiation reaction was used (Table III). Individual patients could exhibit

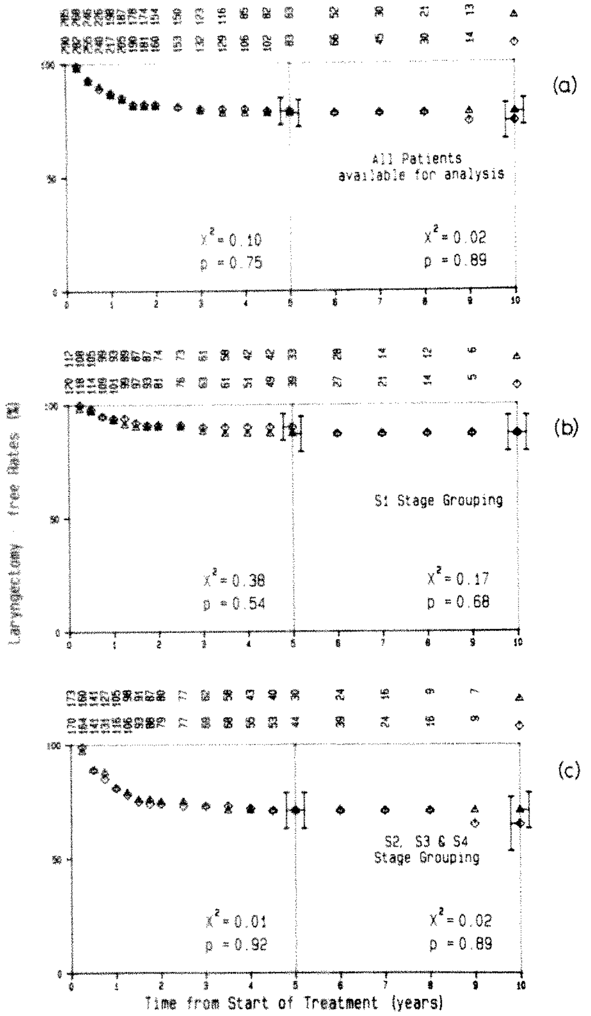

Figure 3. Laryngectomy-free rates. (a) Percentage of all patients available for analysis without having had a laryngectomy *versus* time from start of treatment. (b) Confined to patients in the S1 stage grouping. (c) For patients in the S2, S3 and S4 stage grouping. Symbols as in Fig. 1.

multiple degrees and types of radiation reaction and so these patients could appear under each appropriate heading. For this reason, in order to avoid problems associated with multiplicity, statistical evaluation of any comparison between the short and long overall time results has had to be confined to a single form of assessment, namely the number of patients who had a record of any symptom or sign of an acute radiation reaction. No significant difference was found between the two methods of treatment being compared for acute normal tissue reactions.

Another, and possibly more reliable, method of assessing acute radiation reactions is to include the duration as well as the incidence of a specific reaction. When this was done (Table IV) no significant difference was found between the two groups being compared.

Table III. First incidence of acute radiation reactions at any time within 12 weeks from the start of treatment

Acute radiation reactions	Short ($\leqslant$4 weeks) (285 patients)		Long (>4 weeks) (290 patients)	
Mucous membrane reactions				
Any kind	262	(92%)	268	(92%)
Erythema	216	(76%)	227	(78%)
Fibrinous reaction	155	(54%)	151	(52%)
Ulceration	6	(2%)	5	(2%)
Oedema	152	(53%)	159	(55%)
Skin reactions				
Any kind	220	(77%)	244	(84%)
Erythema	209	(73%)	233	(80%)
Moist desquamation	16	(6%)	34	(12%)
Ulceration	4	(1%)	3	(1%)
Dyspigmentation	94	(33%)	112	(39%)
Perichondritis	6	(2%)	10	(3%)
Dysphagia	151	(53%)	166	(57%)
Any kind of early reaction	266	(93%)[a]	274	(94%)[a]

[a] Statistical comparison: $\chi^2 = 0.02$, $p = 0.89$.

Late radiation effects

The results available so far for late radiation effects (Table V) show no significant difference between the short and long overall treatment time groups. However, because entry into the trial was only completed in December, 1985, the data available for comparison are limited. Some types of late radiation effects have been recorded in more than half the treated patients.

Necrotic ulceration has been reported on five occasions. In three patients, two having been treated with a long and one with a short overall time regime, the necrosis was associated with active recurrent tumour; two of these patients had previously received a second full course of irradiation to the originally treated tissues. The necroses, in these circumstances, are considered to be attributable to tumour necrosis with no evidence to suggest excessive radiation damage to normal tissues from the primary course of irradiation. In one patient, treated with a short overall time regime, a transient necrosis occurred between 6 months and 1 year and had already healed spontaneously at the first annual review and remained healed for the subsequent 9 years. In only a single patient, treated with a short overall time regime, did an unequivocal normal-tissue necrosis occur, at 4 months after the start of the irradiation treatment, for which a laryngectomy had to be performed. The histological report showed massive necrosis, post-radiation changes and no evidence of tumour. As all the normal-tissue necroses reported in the first BIR fractionation trial (BIR Working Party, 1989) occurred within 1 year of the start of the irradiation treatment, it is not anticipated that further cases are likely to occur in the patients treated in this trial.

Table IV. Incidence of acute radiation reactions lasting >4 weeks

Acute radiation reactions	Short (≤4 weeks) (285 patients)		Long (>4 weeks) (290 patients)	
Mucous membrane reactions				
Any kind	192	(67%)	214	(74%)
Erythema	100	(35%)	118	(41%)
Fibrinous reaction	30	(11%)	41	(14%)
Ulceration	0	0	0	0
Oedema	85	(30%)	86	(30%)
Skin reaction				
Any kind	90	(32%)	126	(43%)
Erythema	63	(22%)	97	(33%)
Moist desquamation	1	(0.4%)	1	(0.3%)
Ulceration	0	0	0	0
Dyspigmentation	33	(12%)	43	(15%)
Perichondritis	0	0	0	0
Dysphagia	44	(15%)	64	(22%)
Any kind of early reaction	214	(75%)[a]	233	(80%)[a]

[a] Statistical comparison: $\chi^2 = 0.51$, $p = 0.48$.

Table V. Incidence of late radiation effects

Acute radiation reactions	Short (≤4 weeks) (285 patients)		Long (>4 weeks) (290 patients)	
Skin reaction				
Any kind	40	(14%)	50	(17%)
Oedema	0	0	0	0
Telangiectasia	12	(4%)	17	(6%)
Fibrosis	10	(4%)	11	(4%)
Atrophy	3	(1%)	8	(3%)
Dyspigmentation	28	(10%)	33	(11%)
Mucous membrane reaction				
Any kind	110	(39%)	127	(44%)
Oedema	73	(26%)	100	(34%)
Telangiectasia	46	(16%)	37	(13%)
Atrophy	7	(2%)	6	(2%)
Pain	21	(7%)	20	(7%)
Dysphagia	22	(8%)	12	(4%)
Probable myelitis	0	0	0	0
Laryngeal cartilage reactions				
Any kind	9	(3%)	3	(1%)
Any kind of late effect	148	(52%)[a]	182	(63%)[a]

[a] Statistical comparison: $\chi^2 = 2.93$, $p = 0.08$.

Discussion

An improvement in the radiotherapy treatment of patients would result if the present standard form of treatment could be curtailed by reducing the total number of treatment sessions and consequently shorten the overall treatment time without diminishing the effectiveness of the therapy. The first BIR fractionation trial addressed the question of reducing the number of attendances by giving treatment on alternate days; the results from this trial provided evidence that treatment with three fractions per week, using a suitably diminished dose, gave rise to survival rates that were not significantly different from those that were achieved by the standard daily treatment method (BIR Working Party, 1989). The second BIR fractionation trial, the subject of this report, addressed the question as to whether the current, standard, overall treatment time of 6 weeks could be shortened to, perhaps, half this time. A comparison between two such regimes must be evaluated in terms of both tumour responses and normal-tissue effects and the inter-relationship between these two.

The results showed that there was no significant difference in the observed survival rates between the two groups being compared, whether this was assessed using all patients entered into the trial (Fig. 1a) or as separate sub-groups of patients with early lesions (Fig. 1b) or in patients presenting with more advanced tumours (Fig. 1c). These survival data were supported by further analyses based on tumour-free rates (Fig. 2) and laryngectomy-free rates (Fig. 3), neither of which showed a significant difference.

A measure of how close the present regimes are to the optimum tumour ablation rate that is attainable is to be found in the levels of acute and late normal-tissue damage that were reported. With the fractionation regimes adopted in this trial, it is the acute radiation reactions that are dose-limiting and so an incidence of fibrinous mucous membrane reaction of 54% (Table III) is probably as high as will be found tolerable when this results in up to 63% of the patients having developed evidence of late radiation effects (Table V). The level of normal-tissue radiation damage that is acceptable to patients and individual radiotherapists varies. Since each centre used its own standard form of treatment regime for one of the arms of the trial it would appear that, as there was no significant difference in either the comparisons of acute or late radiation effects between the two arms of the trial (Table III, IV and V), this trial was conducted at dose levels that approximated closely to the maximum dose acceptable to the participants. More detailed analyses, such as those that were used in the first BIR Trial (BIR Working Party, 1989), must await the accumulation of more late radiation effect follow-up data.

Conclusions

The conclusions that may justifiably be drawn from the present preliminary data are limited. Further follow-up data must be awaited before more definitive analyses should be performed but, within these restrictions, it would appear that radiation treatment given in a short overall time may be as effective as treatment given in a long overall time.

Acknowledgments

The authors wish to thank the Council of the British Institute of Radiology for their help and encouragement and the Medical Research Council for continued project grant support, without which this work could not have been brought to completion. We wish to acknowledge our indebtedness to Dr Frank Ellis, who was responsible for initiating the BIR Fractionation Working Party, and to thank especially Mrs Eileen Marriott, who has continued to send out follow-up forms and encode them on their return ready for entry into the computer data file. Finally, we express our thanks to the very many colleagues who have contributed to this work from Departments of Radiotherapy and Oncology, Otolaryngology and Pathology in the multiple centres that co-operated to allow this work to be achieved.

References

BIR WORKING PARTY, 1963. Preliminary Report of the Working Party of the British Institute of Radiology on the effects of dose fractionation in radiotherapy. *British Journal of Radiology*, *36*, 382–383.

—— 1964. Progress Report of the Working Party of the British Institute of Radiology: the effect of dose fractionation in radiotherapy. *British Journal of Radiology*, *37*, 562.

—— 1968. Second Progress Report of the British Institute of Radiology Fractionation Working Party. *British Journal of Radiology*, *41*, 723–724.

—— 1970. Third Progress Report on the British Institute of Radiology fractionation study on 3F/week or 5F/week treatment of larynx and pharynx. *British Journal of Radiology*, *43*, 558–560.

—— 1971. Fourth Progress Report on the British Institute of Radiology fractionation study on 3F/week or 5F/week treatment of larynx and pharynx. *British Journal of Radiology*, *44*, 211–213.

—— 1972. Fifth Progress Report on the British Institute of Radiology fractionation trial of 3F/week or 5F/week treatment of larynx and pharynx. *British Journal of Radiology*, *45*, 754–756.

—— 1978. Sixth Interim Progress Report of the British Institute of Radiology fractionation study of 3F/week versus 5F/week in radiotherapy of the laryngo-pharynx. *British Journal of Radiology*, *51*, 241–250.

—— 1982. Seventh Interim Progress Report of the British Institute of Radiology fractionation study of 3F/week versus 5F/week in radiotherapy of the laryngo-pharynx. *British Journal of Radiology*, *55*, 505–510.

—— 1989. Final Report of the general clinical results of the British Institute of Radiology fractionation study of 3F/week versus 5F/week in radiotherapy of carcinoma of the laryngo-pharynx. *British Journal of Radiology*, in press.

KIRCHNER, J. A. & OWEN, J. R., 1977. Five hundred cancers of the larynx and pyriform sinus. Results of treatment by radiation and surgery. *The Laryngoscope*, *87*, 1288–1303.

MANTEL, N., 1966. Evaluation of survival data and two new rank order statistics arising in its consideration. *Cancer Chemotherapy Reports*, *5*, 163–170.

UICC, 1978. *TNM Classification of Malignant Tumours*, 3rd edn (International Union Against Cancer, Geneva).

UICC, 1987. *TNM Classification of Malignant Tumours*, 4th edn (International Union Against Cancer, Springer-Verlag, London).

1989, *The British Journal of Radiology*, 62, 457–462

Platinum chemotherapy, radiotherapy and the inner ear: implications for "standard" radiation portals

By P. Kirkbride, MRCP and *P. N. Plowman, MD, FRCR

Department of Radiotherapy, St Bartholomew's Hospital, West Smithfield, London EC1A 7BE

(*Received November 1988 and in revised form January 1989*)

Abstract. In this centre, platinum chemotherapy precedes radiotherapy in several primary malignancies arising in structures adjacent to the mastoid bone. The augmented ototoxicity of platinum and radiotherapy to fields encompassing the inner ear is exemplified by a case report. The order of administration may not be critical. This important toxicity, particularly for young patients, may be reduced by careful shielding considerations during planning of radiation portals, as exemplified in two further cases, and by carboplatin chemotherapy.

Although *cis*-platinum has been shown to be a radiosensitizer in the laboratory (Douple et al, 1979a, b; Dewit, 1987), this phenomenon was not appreciated to be of clinical significance until recently. Earlier clinical observations have been extended to demonstrate the severe sensory neuronal hearing loss that may follow concomitant/simultaneous *cis*-platinum administration and external-beam radiotherapy encompassing the inner ear (Walker et al, 1989).

This paper examines two conditions (nasopharyngeal carcinoma and pineal germ cell tumour) in which both platinum chemotherapy and external-beam radiation to volumes abutting the inner ear are now routinely delivered to young patients at this centre. The augmented cochlear damage described previously is demonstrated, and then in a further two cases, ways in which this recently appreciated radiation morbidity may be minimized are illustrated. In the discussion, these observations are extended to the recent proposals for initial chemotherapy in medulloblastoma of young children.

Case reports

Case 1

An 11-year-old boy presented with a 3-month history of upper left cervical lymphadenopathy. At examination under anaesthesia he was found to have an extensive nasopharyngeal carcinoma and a large, fixed left cervical node. There were also nodes palpable in the right side of the neck (TNM stage T_2N_2). He was initially treated with three courses of chemotherapy (*cis*-platinum, etoposide and bleomycin) with a total dose of 300 mg m^{-2} of *cis*-platinum over 90 days. He then received megavoltage radiotherapy to the nasopharynx and neck. Using parallel opposed lateral 6 MV X-ray portals, the base of skull, nasopharynx and neck nodes down to the thyroid cartilage received a tumour dose of 4000 cGy in 23 fractions over 36 days (Fig. 1a). The lower neck nodes received the same dose prescription as an applied dose from an anterior field simultaneously. In a consecutive second phase of treatment, the nasopharynx was boosted by a three-field 6 MV X-ray technique (lateral portal shown, Fig. 1b), to a total dose of 5440 cGy in 31 fractions over 54 days. The neck nodes were taken to a total applied dose of 5000 cGy in 28 fractions before an electron boost to the left node of a further 600 cGy in three fractions was delivered.

The patient responded well to both chemotherapy and radiotherapy and remains in clinical remission at 41 months, but by 1 year later had developed bilateral high-tone deafness (Fig. 2) without any evidence of a conductive defect. This has persisted.

Case 2

A 10-year-old-boy presented with an enlarged left upper deep cervical node and was found to have a primary nasopharyngeal carcinoma in the region of the left eustachian tube. There was no base of skull invasion. He was originally treated at another centre with three cycles of chemotherapy with carboplatin and 5-fluorouracil. Using a similar technique as in Case 1 but with more attention paid to cochlear shielding, the base of skull, nasopharynx and neck nodes received a tumour dose of 4000 cGy in 23 fractions over 32 days (Fig. 3). Following this, the nasopharynx was boosted to a total dose of 5566 cGy in 32 fractions over 44 days and the anterior neck to 5044 cGy in 29 fractions over 40 days. An electron boost was then given to the nodes in the left side of the neck of a further 900 cGy in four fractions.

Case 3

A 22-year-old West Indian man presented to the Casualty Department with a 3-month history of weight loss, anorexia, gynaecomastia, increasing lethargy and polydipsia. He was found to have Parinaud's syndrome and a pregnancy test was positive. A computed tomographic (CT) scan of the brain confirmed a pineal tumour but also a separate midline mass in the anterior recess of the third ventricle. The serum β-HCG was grossly raised at 6000 U ml^{-1}, and matched plasma and

---

*Author for reprints.

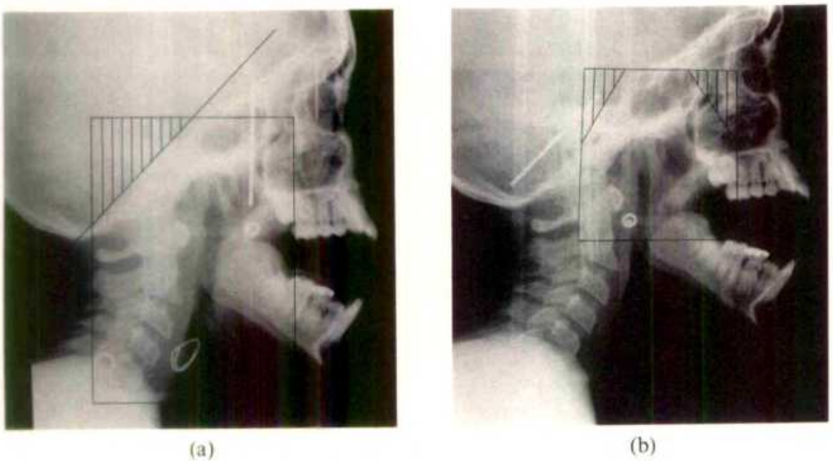

(a) (b)

Figure 1. *Case 1.* Lateral cranial portals of nasopharyngeal carcinoma treatment. (a) The first phase of treatment of 40 Gy and (b) the second phase. Note the lead screening of the super-posterior corner, which partially screens the petrous temporal bone.

serum osmolarities indicated diabetes insipidus. Because of his rapidly deteriorating condition he was commenced on steroids and given two fractions of 160 cGy to his whole brain (megavoltage photons). There was some immediate response. Eight days after the radiotherapy a further CT scan was performed (Fig. 4a). He was then commenced on chemotherapy with etoposide, *cis*-platinum, vincristine, methotrexate and bleomycin (EP/OMB) (Rustin et al, 1986). The total dose of *cis*-platinum received was 240 mg m^{-2}. After receiving two courses of this combination, his condition was much improved and the CT scan showed good response (Fig. 4b). He then proceeded to craniospinal radiation, receiving 3000 cGy in 17 fractions over 24 days to his whole neuraxis, using parallel opposed lateral 6 MV portals to his cranium (Fig. 5a) and two direct posterior 6 MV fields to his whole spine. Following this he received a boost of 1430 cGy in eight daily fractions to the region of the primary tumours, via two opposed lateral 6 MV fields. The inner ears and mastoid region were shielded by a lead block for this part of the treatment (Fig. 5b). At the end of treatment his serum (and CSF) β-HCG had returned to normal and his CT scan showed only pineal calcification; however, his diabetes insipidus persists.

Discussion

In 1983, McHaney et al demonstrated a marked increase in the ototoxicity of *cis*-platinum when administered to young children, with 21 of 24 children who received *cis*-platinum at doses >270 mg m^{-2} developing bilateral high-frequency hearing loss with increasingly severe loss as the dose increased to a peak at 450 mg m^{-2}. Regardless of dosages, younger children showed greater hearing loss. These results show that the prevalence of platinum-induced toxicity is much greater in young children (and at lower doses) than was previously appreciated.

In 1983, Granowetter et al noted enhanced ototoxicity in six children who received *cis*-platinum chemotherapy following radiotherapy for brain tumours. Five of the six had significant audiographic abnormalities after doses of only 110–120 mg m^{-2} of *cis*-platinum. In 1986, Goebel et al also reported two children who developed bilateral deafness within 14 weeks of receiving single doses of *cis*-platinum (100 and 120 mg m^{-2}) after cranial irradiation as treatment for a brain tumour. They suggested that capillary hyperaemia due to the radiation could enhance the ototoxicity of *cis*-platinum.

Recently, Walker et al (1989) have described four

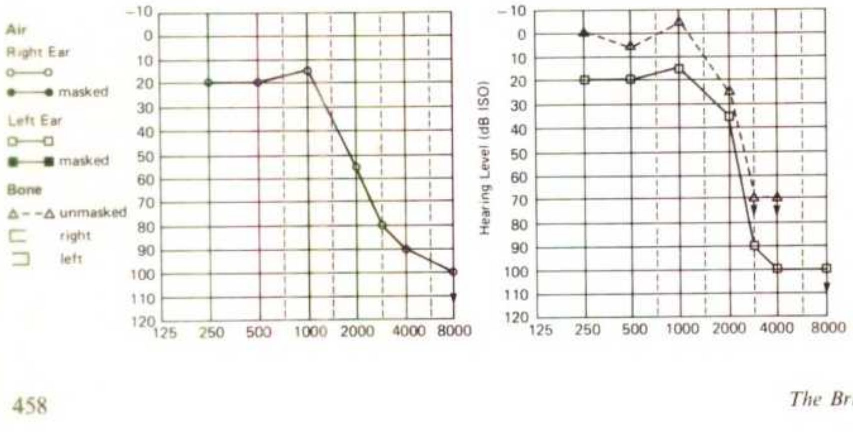

Figure 2. *Case 1.* Audiogram 16 months after *cis*-platinum chemotherapy (300 mg m^{-2}) and radiotherapy, showing bilateral high-tone hearing loss.

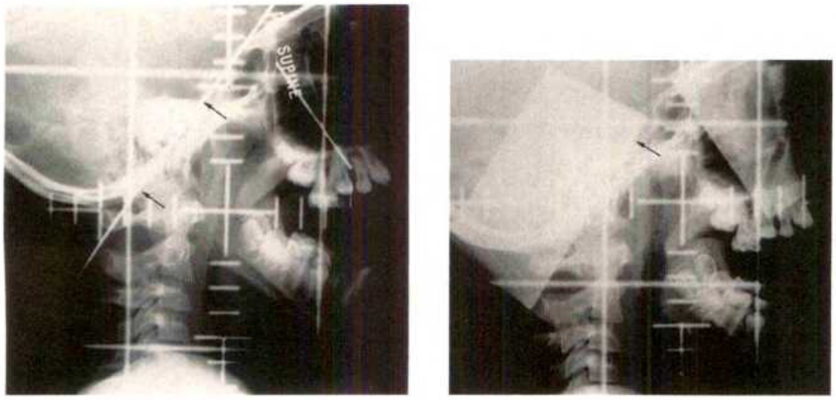

(a)

(b)

Figure 3. *Case 2.* Lateral cranial portals of nasopharyngeal carcinoma treatment. (a) The first phase of treatment to 40 Gy and (b) the second phase. Note the lead screening of the supero-posterior corner (arrowed), which is more generously screening the petrous temporal bone (*c.f.* Fig. 1).

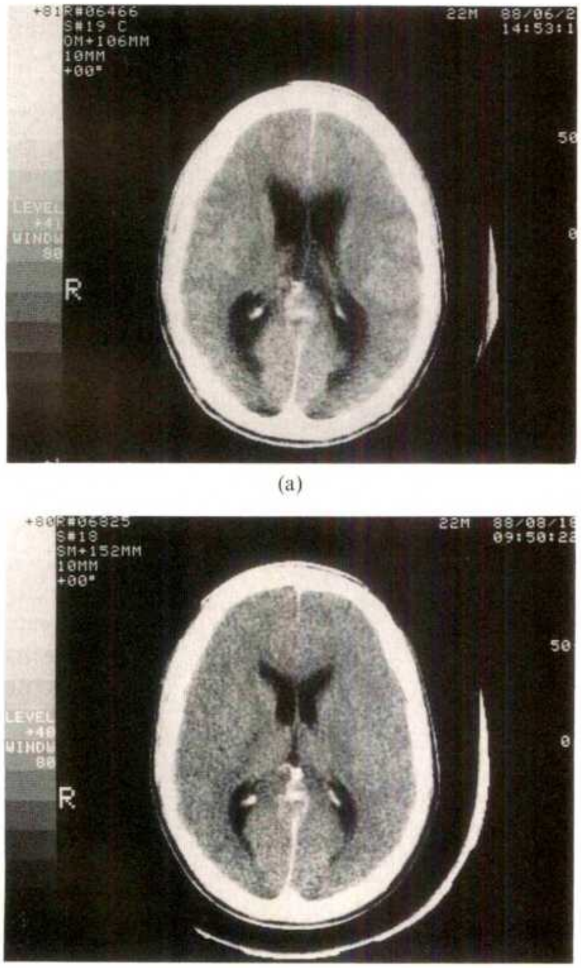

(a)

(b)

Figure 4. *Case 3.* Computed tomographic scans demonstrating response of pineal germ cell tumour to chemotherapy. (a) The tumour prior to chemotherapy (and 1 week after other specific therapy) and (b) after two cycles of chemotherapy.

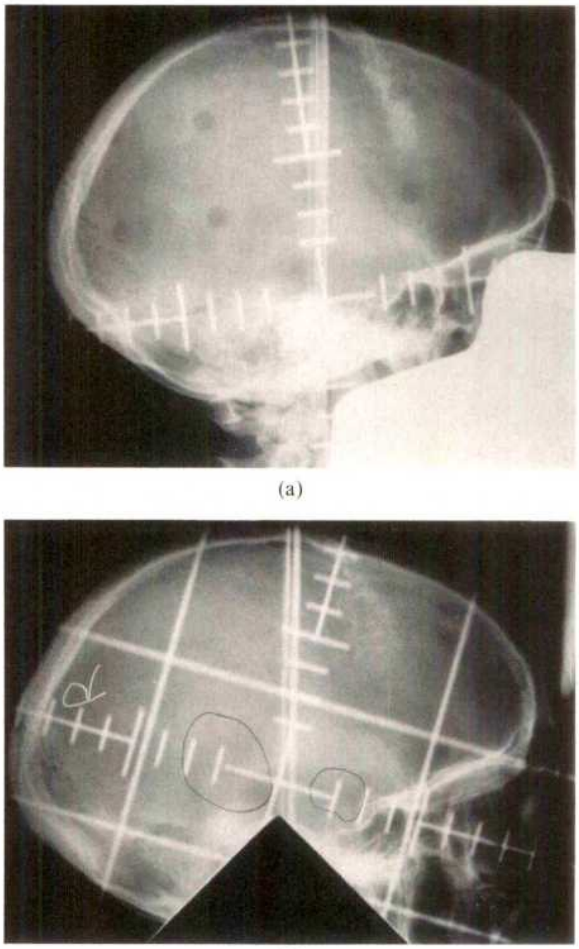

(a)

(b)

Figure 5. *Case 3.* Lateral cranial radiation portals. (a) The cranial portal during whole neuraxis radiotherapy (note that the inner ear is encompassed) and (b) the boost portal (which in this case was not our usual three-field technique but lateral portals to also encompass the entire third ventricle; note the protection to the cochlea).

cases with severe sensory neuronal deafness after simultaneous *cis*-platinum and radiation (three cases) or *cis*-platinum after radiation (one case). When compared with a control population of patients who had received comparable doses of *cis*-platinum only, there was unquestionably augmented deafness in the irradiated group. Walker et al state that this deafness was throughout the auditory range of frequencies although scrutiny of the audiograms suggests it to be most severe in the high-frequency range, as one would expect from previous data on *cis*-platinum VIIIth nerve morbidity (von Hoff et al, 1979).

Case 1 reported here is of interest because following a relatively low total dose of *cis*-platinum (300 mg m^{-2}) and radiotherapy [in that order, *c.f.* Walker et al (1989) and Goebel et al (1986)], there has been severe high-tone deafness (Fig. 2), to a degree that we have never encountered following similar doses of *cis*-platinum alone. Although radiotherapists are now used to the concept of greater CNS methotrexate toxicity when methotrexate is delivered "after" rather than "before" cranial radiation (Bleyer, 1980), and although Walker et al (1989) may be correct in that simultaneous *cis*-platinum and radiation or *cis*-platinum after radiation are particularly toxic, the data presented here in Case 1 argue that the order of administration of the two modalities is not all important.

The previous literature on radiation toxicity to the ear has indicated that the inner ear was the most radioresistant part of the hearing apparatus and that ototoxicity was mainly confined to serous otitis media and late necrosis of the ossicles (Rubin & Casaret, 1968). However, some authors have shown evidence of late injury to the inner ear with subsequent delayed sensory neuronal deafness occurring up to 6 years post-radiotherapy (Leach, 1965; Moretti, 1976).

Although platinum is known to be a radiosensitizer, there have been few studies that have convincingly demonstrated the clinical importance of this phenomenon (Dewit, 1987). In particular, any enhancement of toxicity has usually been observed to be in the form of increased nausea, vomiting and myelosuppression, which could perhaps be predicted from the known effects of each modality. However, it has only recently been appreciated in organs and tissues that have previously been thought to be radioresistant, such as the inner ear (Granowetter et al, 1983).

There are certain cancers in which it is highly likely that both platinum-based chemotherapy and external radiation therapy portals abutting the inner ear will find a routine place in management.

Although the role of pre-radiation chemotherapy for advanced squamous head and neck cancer is not established in large studies, there are data supporting this practice, particularly for advanced disease presenting in the oral cavity or nasopharynx in young people (Mead, 1982; Decker, 1983). Indeed it is the policy of this unit to initiate therapy of $T_{2\text{-}4}$ oral cavity or nasopharyngeal squamous carcinomas with two cycles of *cis*-platinum and bleomycin chemotherapy, prior to radical radiotherapy in young patients. For childhood nasopharyngeal squamous cancer, which so often presents with N_+ disease (Plowman & Pritchard, 1987), our treatment protocol is for all patients to receive such primary chemotherapy. Cases 1 and 2 reported here are just such cases, although the different induction chemotherapy regimens used reflect the different paediatric oncology centres that referred the two patients. Of interest, however, is the use of carboplatin instead of *cis*-platinum in Case 2. Carboplatin appears to be less ototoxic than *cis*-platinum (Evans et al, 1985) and if it is as effective, then this may be one way to reduce the incidence of late deafness.

Another primary tumour to be considered is the pineal germ cell tumour for which we predict induction platinum-based chemotherapy will precede radiotherapy in standard treatment regimens. Rustin et al (1986) and our own unpublished observations on three primary CNS germinomas lead us to conclude that these tumours are highly chemosensitive to platinum-based chemotherapy. Although primary radiotherapy for CNS germinomas cures the majority of cases (Sung et al, 1978; Bloom, 1983), the cure rate may be further improved by induction chemotherapy followed by radiation. Walker et al (1989) would extend these observations further in their childhood practice to other brain tumours. Indeed, there has recently been an interest in the use of radiotherapy and chemotherapy in an attempted to improve the prognosis in children with medulloblastoma and other CNS tumours. The drugs used may include platinum-containing regimes (Bleyer, 1983; Kretschmar, 1988) given prior to "standard" radiation therapy such as craniospinal irradiation.

These observations have implications for the standard radiation portals in such patients.

Consideration of the upper borders of the fields used for nasopharyngeal carcinoma (Lederman et al, 1967; Ho, 1982) demonstrate that all authorities consider the skull base must be generously encompassed, which has usually led to high radiation doses to the mastoid and inner ear. Whilst we would not disagree with this viewpoint for $T_{3\text{-}4}$ lesions, it may well be that for $T_{1\text{-}2}$ nasopharyngeal primaries, the "margin of safety" of the radiation portal above the skull base may be safely reduced. This may be particularly true with modern shelling and treatment set-up sophistication, which has led to much greater reliability of day-to-day treatment accuracy. The child described as Case 2 in this paper illustrates this point. He presented with cervical lymphadenopathy and a small primary in the region of the eustachian tubal orifice. The superior radiation portal border was considered carefully (with the deafness of Case 1 in mind at that time). As Fig. 3 demonstrates, the skull base is encompassed but not as generously as in "standard" teaching, and the inner ear is screened.

Noteworthy also in Case 2 is the lower dose to the hypothalamus. We have recently reported on the damage to the hypothalamus following radical

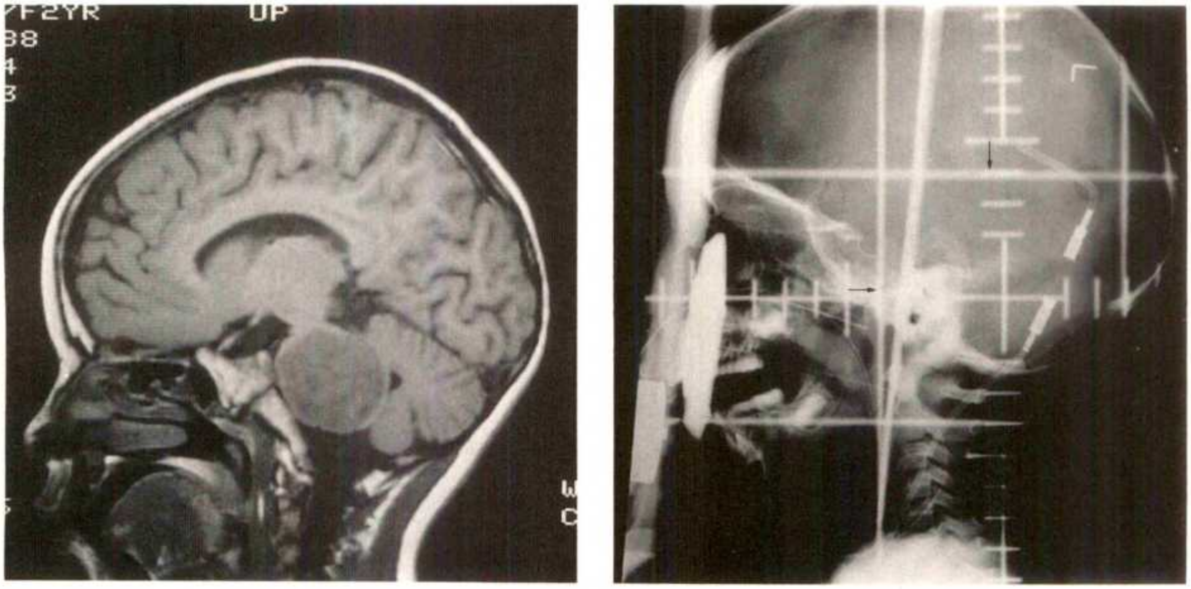

(a) (b)

Figure 6. (a) Pre-treatment magnetic resonance imaging scan of a child with histologically proven medulloblastoma demonstrating the tumour extending into the brain stem. (b) The boost portal to the posterior fossa of this child. The anterior field border is determined by the brain stem invasion but, as a consequence, the inner ear is encompassed in the radiation portal.

radiotherapy for nasopharyngeal carcinoma (Blacklay et al, 1986), and these remarks on the upper radiation portal border are relevant to this late morbidity also.

Case 3 was treated by standard whole neuraxis radiotherapy followed by a third ventricular boost. Mindful of the potential for augmented sensory neuronal deafness, care was taken to ensure the portals minimized the mastoid dose by a lead screen (Fig. 5a).

Thus from Cases 2 and 3 it appears possible to reduce the radiation dose to the cochlea in selected patients with nasopharyngeal or third ventricular germ cell tumours who are also receiving platinum chemotherapy. The use of carboplatin (Case 2) may be a further means of reducing morbidity.

These observations may have further relevance as medulloblastoma in young children in particular is now regarded as a research area for drug treatment prior to radiotherapy (Kretschmar et al, 1988) and *cis*-platinum is one active agent.

Figure 6 illustrates a 2½-year-old girl who presented with anorexia, vomiting and a left strabismus and was found to have a large posterior fossa tumour extending anteriorly into the brain stem. Histologically this was a medulloblastoma, and as is our current practice with young children she received primary chemotherapy with carboplatin, etoposide and vincristine. Owing to the anterior extent of this tumour (Fig. 6), complete shielding of the inner ear and mastoids was not possible, and she will require careful audiological follow-up.

In conclusion, there is evidence that the combination of *cis*-platinum chemotherapy and irradiation of the inner ear may rapidly produce profound high-tone deafness, especially in young children. As this treatment combination is being investigated and adapted for use in several head and neck and central nervous system tumours of children and young adults, it is important to bear this in mind when planning radiotherapy portals in patients receiving such combinations and to protect the inner ear as much as possible. The use of the less ototoxic carboplatin in these settings warrants further investigation.

The mechanism for this potentiation of ototoxicity is unknown, although as it appears to occur not only when radiation is given before platinum chemotherapy but also following it, it is unlikely to be due to radiation-induced increased blood flow to the inner ear. Thus these precautions in planning radiotherapy treatment should be observed in all cases that receive chemotherapy containing platinum.

Acknowledgments

It is with great pleasure that we acknowledge the assistance of Drs Kingston, Kosmidis and Pritchard and the Radiography and Physics staff of St Bartholomew's Hospital in the treatment of these patients. Miss T. Cocks kindly typed the manuscript.

References

BLACKLAY, A., GROSSMAN, A., SAVAGE, M., PLOWMAN, P. N., COY, D. H. & BESSER, G. M., 1986. Cranial irradiation in children with cerebral tumours—evidence for a hypothalamic defect in growth hormone release. *Journal of Endocrinology*, *108*, 25–29.

BLEYER, W. A. & GRIFFIN, T. W., 1980. White matter necrosis, mineralizing microangiopathy and intellectual abilities in survivors of childhood leukaemia: associations with central nervous system irradiation and methotrexate therapy. In *Radiation Damage to the Nervous System*, ed. by H. A. Gilbert & A. R. Kagan (Raven Press, New York), pp. 155–179.

Bleyer, W. A., Milstein, J., Balis, F., Prendergass, T. U., Chard, R. & Hartmann, J., 1983. 8 drugs in 1 day chemotherapy for brain tumours: a new approach and rationale for pre-radiation chemotherapy. *Medical and Paediatric Oncology*, *11*, 213.

Bloom, H. J. G., 1983. Primary intracranial germ cell tumours. *Clinics in Oncology*, *2*, 233–257.

Decker, D. A., Drelichman, A., Al-Sarrot, M., Crissman, J. & Read, M. L., 1983. Chemotherapy for nasopharyngeal carcinoma: a ten year experience. *Cancer*, *52*, 602–605.

Dewit, L., 1987. Combined treatment of radiation and *cis*-diamminedichloroplatinum (II): a review of experimental and clinical data. *International Journal of Radiation Oncology, Biology, Physics*, *13*, 403–426.

Douple, E. B. & Richmond, R. C., 1979a. A review of platinum complex biochemistry suggests a rationale for combined platinum-radiotherapy. *International Journal of Radiation Oncology, Biology, Physics*, *5*, 1335–1339.

—— 1979b. Radiosensitization of hypoxic tumor cells by *cis*- and *trans*-dichlorodiammineplatinum. *International Journal of Radiation Oncology, Biology, Physics*, *5*, 1369–1372.

Evans, B., Raju, K., Calvert, A., Harland, S. & Wiltshaw, E., 1983. A phase II study of JM8, a new platinum analog in advanced ovarian carcinoma. *Cancer Treatment Reports*, *67*, 997–1000.

Goebel, U., Lamprecht, A. & Beron, B., 1986. Akuter Hoverlust bei Kindern mit vorbestrahtlen intrakraniellen Tumoren nach einmaliger hochdosierter Cis-Platinum-Gabe. *Klinical Paediatrics*, *198*, 277–280.

Granowetter, L., Rosenstock, J. G. & Packer, R. J., 1983. Enhanced cis-platinum neurotoxicity in paediatric patients with brain tumours. *Journal of Neuro-oncology*, *1*, 293–297.

Ho, J. L., 1982. Nasopharynx. In *Treatment of Cancer*, ed. by K. E. Halnan (Chapman and Hall, London), pp. 254–264.

von Hoff, D., Schilsky, R., Reichart, C., Reddick, R., Rozencweig, M., Young, R., & Muggia, F., 1979. Toxic effects of *cis*-dichlorodiammineplatinum in man. *Cancer Treatment Reports*, *63*, 1527–1531.

Kretschmar, C., Loeffler, J., Lavally, B., Tarbell, N. & Sallan, S., 1988. Response to chemotherapy before radiation in children with medulloblastoma. *Proceedings of the American Society of Clinical Oncology*, *7*, Abstract 311.

Leach, W., 1965. Irradiation of the ear. *Journal of Laryngology and Otology*, *79*, 870–880.

Lederman, M., & Mould, R. F., 1968. Radiation treatment of the pharynx with special reference to telecobalt therapy. *British Journal of Radiology*, *41*, 251–274.

McHaney, V. A., Hammond, B., Champion, J., Thompson, E., Hayes, A. & Green, A., 1983. Severe hearing loss due to cisplatin (DDP) administered after irradiation to the inner ears. *Proceedings of the American Society of Clinical Oncology*, Abstract C-285.

Mead, G. & Jacobi, C., 1982. Changing role of chemotherapy in the treatment of head and neck cancer. *American Journal of Medicine*, *73*, 582–595.

Moretti, J., 1976. Sensori-neural hearing loss following radiotherapy to the nasopharynx. *Laryngoscope*, *86*, 598–602.

Plowman, P. N. & Pritchard, J., 1987. Tumours of the head and neck in childhood. In *Paediatric Otolaryngology* (Butterworth Scientific Ltd, Guildford), pp. 364–341.

Roth, B. J., Griest, A., Kubilis, P. S., Williams, S. P. & Einhorn, L. H., 1988. Cisplatin-based combination chemotherapy for disseminated germ cell tumours: long term follow up. *Journal of Clinical Oncology*, 1239–1247.

Rubin, P., & Casaret, G. W., 1968. Organs of special sense: the ear. In *Clinical Radiation Pathology* (W.B. Saunders, Philadelphia), pp. 702–720.

Rustin, G. J. S., Newlands, E., Bagshawe, K. D., Begent, R. H. J. & Crawford, S. M., 1986. Successful management of metastatic and primary germ cell tumours in the brain. *Cancer*, *57*, 2108–2113.

Sung, D., Harisiadis, L. & Chang, C. H., 1976. Midline pineal tumours and suprasellar germinomas: highly curable by irradiation. *Radiology*, *128*, 745–751.

Walker, D., Pillow, J., Waters, K. & Keir, E., 1989. Enhanced cis-platinum ototoxicity in children with brain tumours who have received simultaneous or prior cranial irradiation. *Medical and Paediatric Oncology*, *17*, 48–52.

1989, *The British Journal of Radiology*, *62*, 463–467

In vivo viability of ^{111}In-labelled granulocytes demonstrated in a sham-dialysis model

By W. Becker, MD, *R. M. Schaefer, MD and W. Börner, MD

Clinic of Nuclear Medicine and *Department of Nephrology of the University of Würzburg, Federal Republic of Germany

(*Received July 1988 and in revised form November 1988*)

Abstract. In seven febrile patients undergoing regular dialysis treatment, sham-dialysis with a dialyzer equipped with a cuprophane membrane was performed during a routine ^{111}In-oxine white blood cell scan with "pure" granulocytes isolated on a discontinuous gradient (Percoll/plasma: $n = 5$; Metrizamide/plasma: $n = 2$). The patients were in contact with the cuprophane membrane over 45 or 90 min. Twenty-five (±5) minutes after the start of the dialysis, the peripheral leucocyte count (59±22%) and the ^{111}In activity in the peripheral blood decreased to a minimum of their initial range (64±21%) because of leucocyte activation. The activity over both lungs increased symmetrically (29±15%), the spleen activity decreased (14.8±8%) and the liver activity remained constant. At the end of the dialysis (45–90 min post-injection), the number of circulating neutrophils, peripheral ^{111}In activity and activity distribution in the organs regained their initial level. In conclusion, these data confirm previously described data concerning the sequestration of neutrophils into the lung during dialysis treatment. The data demonstrate the origin of the activated neutrophils in the circulation and the spleen. The identical behaviour of ^{111}In-oxine-labelled and unlabelled granulocytes is demonstrated. Additionally, the accumulation of activity in the spleen is due not to opsonized cells but to sequestrated neutrophils, which are able to migrate from the spleen after adequate activation. The migration of activated cells into the lung explains the diagnostic difficulties posed by diffuse lung uptake in leucocyte scans in patients with leucocyte-activating diseases.

A pathogenic role for the intravascular aggregation of granulocytes has been postulated as a mechanism for tissue injury in several clinical syndromes, such as haemodialysis, cardiopulmonary by-pass, nylon filter leucophoresis, endotoxic shock and adult respiratory distress syndrome (Craddock et al, 1977a, b, c; Hammerschmidt et al, 1978). An increased ^{111}In-labelled leucocyte activity in the lung was reported for most of these cases, for example respiratory distress syndrome (McAfee & Samin, 1985), endotoxic or septic shock and haemodialysis (McAfee & Samin, 1985).

This aggregation of leucocytes and pulmonary sequestration of microaggregates in the lung is believed to constitute a possible mechanism for haemodialysis-induced leucopenia (Craddock et al, 1977a; Hakim & Lowrie, 1982; de Backer et al, 1983). Because this pulmonary sequestration of leucocytes could be experimentally reproduced in animal models (Craddock et al, 1977b), because acute leucopenia occurs in all patients during the first hour of haemodialysis with cuprophane dialyzer membranes (Craddock et al, 1977c) and because, during haemodialysis, an increased lung activity was described in leucocyte scans (McAfee & Samin, 1985), a sham-dialysis seemed to be a promising model to compare the kinetic changes of ^{111}In-labelled and unlabelled granulocytes *in vivo*.

Materials and methods

Patients

Seven patients (Table I) with chronic renal failure, who underwent regular dialysis (mean time of dialysis treatment: 5.2±0.4 years) were examined with a ^{111}In-oxine-labelled granulocyte scan. The patients were admitted to our department because of fever of unknown origin or leucocytosis.

After informed consent, a sham-dialysis was performed during the first hours after re-injection of the labelled cells. The study was not submitted to the ethical committee, because all the patients underwent regular dialysis treatment exclusively with cuprophane membranes during fever and leucocytosis, *i.e.* the use of the cuprophane membrane was not an experiment.

Cell separation and labelling

A pure population of granulocytes was isolated by discontinuous gradient centrifugation (Percoll/plasma gradient; $n = 5$; Metrizamide/plasma gradient; $n = 2$) and labelled with 8–10 MBq ^{111}In-oxine. The different isolation and labelling procedures have been described previously (Becker et al, 1986, 1987).

Sham-dialysis and data collection

The labelled granulocytes were injected with the patient supine. For this procedure, two needles were placed into the arterio-venous fistula and a bolus injection of heparin (2000 i.u.) was given. The extracorporeal circuit consisted of one blood pump and a capillary dialyzer. The dialyzer was equipped with a cellophane membrane (Cuprophan) and the blood

---

Address correspondence to: Prof. Dr W. Becker, Clinic and Policlinic of Nuclear Medicine, University of Erlangen-Nürnberg, Krankenhausstraße 12, D-8520 Erlangen, Federal Republic of Germany.

This work is supported by the Deutsche Forschungsgemeinschaft (BE 1054/1-2).

Table I. Patients studied and results of neutrophil activation during sham-dialysis

Case	Age (years)	Sex	Time of dialysis (min)	Decrease in unlabelled neutrophils (%)	Decrease in ^{111}In activity (%)	Increase in total lung activity (%)	Decrease in spleen activity (%)
1	60	M	90	87	65	31	11
2	52	F	75	78	92	35	15
3	53	F	45	16	62	33	16
4	44	F	45	62	82	50	31
5	56	F	45	43	64	40	19
6	64	F	45	62	63	15	7
7	49	F	45	36	25	4	5
Mean ±SD				59±22	64±21	29±15	14.8±8

passed through the dialyzer without dialysate flow or ultrafiltration.

The patients were examined supine by a gamma camera, which was fitted with a parallel-hole, high-resolution, low-energy collimator (GE Maxi 400) connected on-line to a computer system (DEC Gamma 11). The granulocyte kinetics were imaged over both lungs, the heart, the spleen and the liver, 45 or 90 min post-injection (matrix: 64 × 64; one frame/30 s). Time/activity curves were generated by the region of interest (ROI) technique.

Sham-dialysis was started 25 min after the injection of the ^{111}In-oxine-labelled white blood cells because previous studies (Becker et al, 1988) have demonstrated a steady state of activity over the lungs at this time; dialysis was stopped 45 or 90 min later.

The decrease of the ROI curves over the spleen and the increase of the lung curves was calculated from the difference between the minimum or maximum of the curves during dialysis and the value of the curve during the plateau phase before the start of the dialysis.

Blood sampling

Five millilitres of venous blood for leucocyte counts and measurement of ^{111}In activity was taken 5 min prior to the start of sham-dialysis, immediately after injection of the labelled cells and in 5-min intervals thereafter. The peripheral leucocyte concentration was counted by a routine laboratory procedure and the ^{111}In activity in the same samples was measured in a gamma counter. The decrease in the peripheral leucocyte count or peripheral ^{111}In activity was calculated from the difference between the initial leucocyte count or peripheral ^{111}In activity in the blood before the start of dialysis and the minimal concentration or minimal ^{111}In activity during dialysis, expressed as a percentage.

Results

Peripheral leucocyte count and ^{111}In activity

The leucocyte count in all seven patients decreased rapidly after the start of the sham-dialysis (10±5 min). The minimum peripheral neutrophil concentration was reached at 25±5 min after starting dialysis. At the end of dialysis, 83±5% of the initial neutrophil count was reached (Table I). The maximal decrease in the neutrophil count under dialysis was 87% of the initial concentration (from 10 100/ml to 1400/ml of blood). The decrease ranged between 16 and 87% (mean 60±25%) of the initial concentration.

The ^{111}In activity in the peripheral blood samples decreased 10±5 min after starting sham-dialysis. The decrease in activity ranged between 25 and 92% of the initial activity (mean 66±21%) (Table I, Fig. 1).

On the basis of these data, the amount of cells migrating out of the circulation into the lung (presuming 5000 ml of blood volume) was calculated as 2×10^7 leucocytes.

In vivo *kinetics of ^{111}In-labelled neutrophils*

After a plateau phase of lung activity, the count rate over the lungs (Fig. 1) and the granulocyte content of the lungs (Fig. 2) increased 10 min after the start of haemodialysis in all patients and reached a maximum at 25±5 min. The increase in activity was symmetrical over both lungs (Fig. 3). The increase in activity ranged between 8 and 100% of the initial lung activity (mean 60±25%) (Table I).

The spleen activity decreased during sham-dialysis varying between 5 and 31% (mean 14.8±8%). At the end of the dialysis the initial organ distribution patterns were restored.

Discussion

The ^{111}In-labelled granulocyte scan has proved to be a highly sensitive and specific method in routine nuclear medicine for the localization of abscesses and inflammatory diseases and the study of granulocyte kinetics in different diseases, such as chronic inflammatory bowel disease (Becker et al, 1988). It was felt to show promise in the study of granulocyte kinetics in humans undergoing dialysis treatment, especially in patients with neutropenia. The idea for such a study was not new. Dodd et al (1983) have already published their data on neutrophil accumulation in the lung measured with ^{111}In-labelled neutrophils. The outstanding difference between this and our own study consists of our use of a gamma camera, with the possibility of exact localization

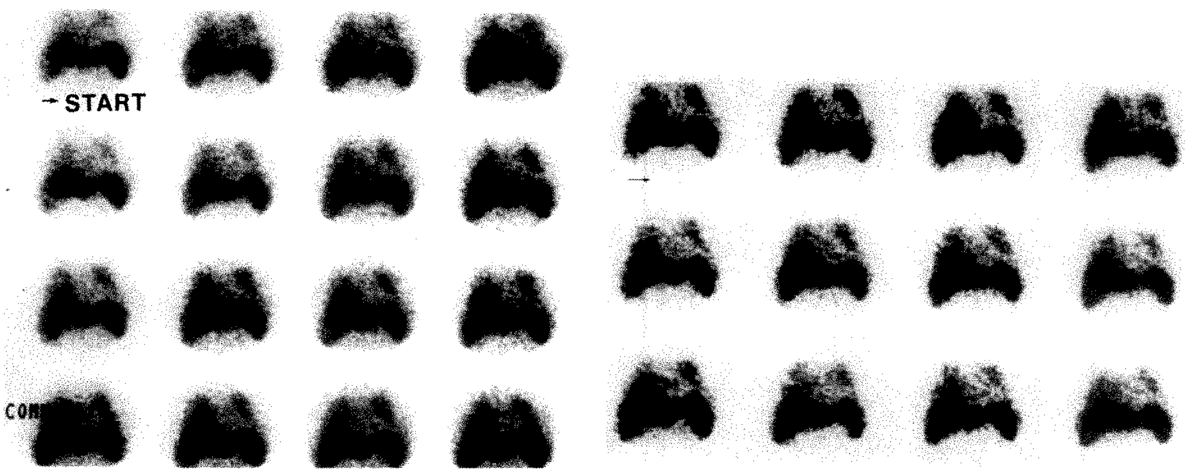

(a) (b)

Figure 1. Dynamic lung scan (1 frame/60 s) in a 55-year-old man (Case 3) demonstrating (a) increase and (b) decrease in lung activity during sham dialysis.

of the liver, spleen, lungs and heart and consequent accurate assessment of the granulocyte kinetics in these organs.

The basic mechanism of granulocyte sequestration seems to be an increased expression of an adhesion-promoting, surface glycoprotein in the granulocytopenia of haemodialysis (Arnaout et al, 1985). Also observed was a five-fold increase in the mean cell surface expression of a granulocyte-adhesion promoting surface glycoprotein (Mo1) within 15 min after the start of dialysis with a cuprophane membrane. The peak increase in the surface Mo1 coincided with the maximal drop in neutrophil count and the peak rise in the plasma levels of the complement-activation products C5a and C3a.

Granulocyte sequestration was studied using different acquisition times of 45 or 90 min after re-injection of the labelled cells and different time intervals (10–25 min) between re-injection and the start of the dialysis. This difference in the acquisition time was due to our increasing experience of the lung kinetics of ^{111}In-labelled and sequestrated cells and knowledge of the time of the plateau phase of blood activity after re-injection of the cells (Becker et al, 1988). The estimation of the neutrophil migration to the lungs was 2×10^7 cells, which leave the peripheral blood after the start of the sham-dialysis. This amounts to ~60 ± 25% of all circulating cells.

The calculation of the total cell number entering the lungs from the blood is only a rough estimation of the migrating cell number. Moreover, this calculation does not take into account those granulocytes that bypass the lung and go to the marginating pools elsewhere, nor those that replenish the blood from the spleen. Our data (Table I) suggest that not all granulocytes leaving the blood during dialysis end up in the lungs, since the increase in the lung activity was only 29% compared with a decrease in blood activity of 64%. Our data do not explain whether the cells go elsewhere or whether the lung marginating pool is much bigger than was originally thought. The difference in the numbers of granulocytes leaving the circulation in individual patients was not due to the presence or absence of an infection and did not correlate with the initial leucocyte count of the patients before the start of the dialysis. It is more likely that the amount of the decrease is related to other factors such as the number of preceding dialysis treatments (Arnaout et al, 1985). The latter also demonstrated that a five-fold re-use of the same membrane induced no more Mo1 expression during complement activation. However, in the small number of patients examined, no close correlation could be found between the level of the leucocyte decrease and the number of preceding treatments.

These data demonstrate that the sudden increase in spleen activity after re-injection of ^{111}In-oxine or ^{99}Tc^{m}-HMPAO labelled cells (Saverymuttu et al, 1983; Becker et al, 1988) is not due to mere granulocyte opsonization and destruction, but to sequestration of viable cells in an

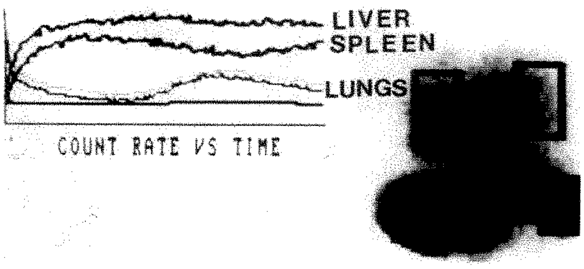

Figure 2. Activity curves over both lungs, the liver and the spleen in a 44-year-old woman (Case 4) demonstrating symmetrical lung uptake after the start of sham-dialysis. The liver curve remains stable and the spleen activity is decreased.

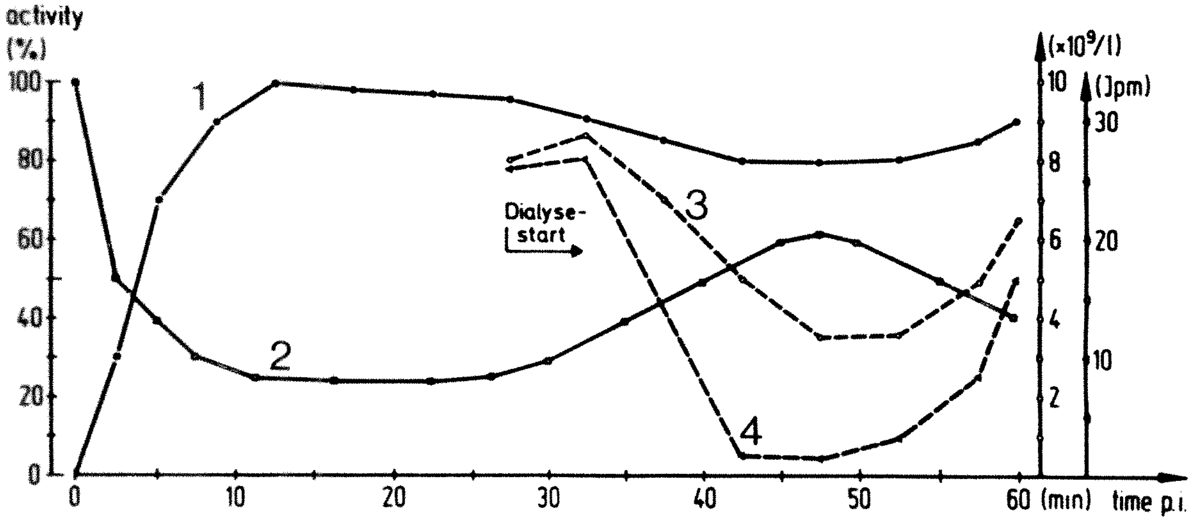

Figure 3. Graph showing sham-dialysis-induced changes. Curve 1, spleen activity; Curve 2, lung activity; Curve 3, peripheral neutrophil count (× 10^9/l); Curve 4, ^{111}In activity in peripheral blood (I pm).

immediately available reservoir of neutrophils, which can migrate into the circulation after adequate cell activation. It is important to note that liver activity did not change during dialysis, implying that the activity in the liver is due much more to cell destruction than sequestration (Saverymuttu et al, 1983). The data additionally demonstrate that the decrease in splenic activity is smaller than one might expect if the splenic activity represents labelled granulocytes that are in dynamic equilibrium with blood granulocytes. Perhaps this difference may be explained by destruction of cells that have been altered during the labelling procedure and that the other cells migrating into the lungs come from other marginating cell pools. The parallel decrease in the ^{111}In-labelled and the unlabelled granulocytes indicated identical behaviour in both groups.

These results explain at least the problems of interpretation of a diffuse lung uptake in ^{111}In white cell scan (Hammerschmidt et al, 1978), which is not due to pneumonia (Saverymuttu et al, 1985) but dependent on activation of neutrophils, and can be observed in patients undergoing regular dialysis treatment, in patients with sepsis or respiratory distress syndrome (Hammerschmidt et al, 1980).

In conclusion, our data confirm previously described data concerning the sequestration of neutrophils into the lung during dialysis treatment. The data demonstrate that the origin of the cells that migrate into the lungs is from the circulation and the spleen. The identical comparable behaviour of ^{111}In-oxine-labelled and unlabelled granulocytes in the blood pool seems to demonstrate normal behaviour of ^{111}In-labelled cells in the circulation. Additionally, the accumulation of activity in the spleen is due not to opsonization of non-viable cells but to sequestration of neutrophils, which are able to migrate from the spleen after complement activation. The migration of activated cells into the lung explains the diagnostic difficulty resulting from diffuse lung uptake in leucocyte scans in patients with endotoxic and septic shock (McAfee & Samin, 1985).

References

ARNAOUT, M. A., HAKIM, R. M., TODD, R. F., DANA, N. & COLTEN, H. R., 1985. Increased expression of an adhesion-promoting surface glycoprotein in the granulocytopenia of haemodialysis. *New England Journal of Medicine, 312*, 457–462.

DE BACKER, W. A., VERPOOTEN, W. A., BORGONJON, D. J., VERMEIRE, P. A., LINS, R. R. & DE BROE, M. E., 1983. Hypoxemia during haemodialysis: effects of different membranes and dialysate compositions. *Kidney International, 23*, 738–743.

BECKER, W., BORST, U., MAISCH, B., EPPING, J., BÖRNER, W. & KOCHSIEK, K., 1987. In-111-labelled granulocytes in inflammatory heart diseases. *European Heart Journal, 8* (Suppl.), 307–310.

BECKER, W., FISCHBACH, W., REINERS CHR. & BÖRNER, W., 1988. Three-phase white blood cell scan: diagnostic validity in abdominal inflammatory diseases. *Journal of Nuclear Medicine, 27*, 1109–1115.

BECKER, W., SCHOMANN, E., FISCHBACH, W. & BÖRNER, W., 1988. Comparison of Tc-99m-HMPAO and In-111-oxine-labelled granulocytes in man: first clinical results. *Nuclear Medicine Communications, 9*, 435–447.

CRADDOCK, P. R., FEHR, J., BRIGHAM, K. L., KRONENBERG, R. S. & JACOB, H. S., 1977a. Complement and leukocyte-mediated pulmonary dysfunction in haemodialysis. *New England Journal of Medicine, 296*, 769–774.

CRADDOCK, P. R., HAMMERSCHMIDT, D. E., WHITE, J. G. DALMASSO, A. F. & JACOB, H. S., 1977b. Complement (C5a)-induced granulocyte aggregation *in vitro*: a possible mechanism for complement-mediated leucostasis and leucopenia. *Journal of Clinical Investigation, 60*, 260–264.

CRADDOCK, P. R., FEHR, J., DALMASSO, A. P., BRIGHAM, K. L. & JACOB, H. S., 1977c. Haemodialysis leucopenia: pulmonary vascular leucostasis resulting from complement activation by dialyzer cellophane membranes. *Journal of Clinical Investigation, 59,* 879–888.

DODD, N. J., GORDGE, M. P., TARRANT, J., PARSONS, V. & WESTON, M. J., 1983. A demonstration of neutrophil accumulation in the pulmonary vasculature during haemodialysis. *Proceedings of EDTA, 20,* 186–189.

HAKIM, R. M. & LOWRIE, E. G., 1982. Haemodialysis-associated neutropenia and hypoxemia: the effect of dialyzer membrane materials. *Nephron, 32,* 32–39.

HAMMERSCHMIDT, D. E., CRADDOCK, P. R., MCCULLOUGH, J., KRONENBERG, R. S., DALMASSO, A. P. & JACOB, H. S., 1978. Complement activation and pulmonary leucostasis during nylon fibre filtration leucapheresis. *Blood, 51,* 721–730.

HAMMERSCHMIDT, D. E., WEAVER, L. J., WHITE, J. G., DALMASSO, A. P. & JACOB, H. S., 1980. Association of complement activation and elevated plasma-C5a with adult respiratory distress syndrome: pathophysiological relevance and possible prognostic value. *Lancet, i,* 947–949.

MCAFEE, J. G. & SAMIN, A., 1985. In-111-labelled leucocytes: a review of problems in image interpretation. *Radiology, 155,* 221–229.

SAVERYMUTTU, S., PETERS, A., DANPURE, H., REAVY, H. & OSMAN, S., 1983. Lung transit of indium-111-labelled granulocytes. *Scandinavian Journal of Haematology, 30,* 151–160.

SAVERYMUTTU, S. H., PHILLIPS, G., PETERS, A. M. & LAVENDER, J. P., 1985. Indium-111 autologous leucocyte scanning in lobar pneumonia and lung abscesses. *Thorax, 40,* 925–930.

1989, *The British Journal of Radiology*, 62, 468–472

Radiation toxicity of indium-111-2-mercaptopyridine-N-oxide on HeLa S-3 cells

By Seong Su Hong, MD, PhD, Edith H. Ford, MD and Bennet Greenspan, MD

Department of Radiology, University of Medicine and Dentistry of New Jersey, 100 Bergen Street, Newark, NJ 07103, USA

(*Received August 1988 and in revised form December 1988*)

Abstract. As one of a series of systematic studies to determine the cytotoxicity of radiopharmaceuticals, indium-111-2-mercaptopyridine-N-oxide (^{111}In-merc) was studied using a monolayer of HeLa S-3 cells. Exponentially growing cells were incubated with up to 2.96 MBq/ml (80 μCi/ml) of ^{111}In-merc (molecular ratio of In/Cd to merc was 1:1000) in phosphate buffered saline for up to 240 min at room temperature. Surviving fractions were assayed by the colony-forming method. The cell uptake curve was upward concave with increasing activity and was saturated after an incubation time of 60 min. A clonogenic assay resulted in an exponential dose–survival curve with a shoulder (D_0 of 0.44 MBq/ml (12 μCi/ml); $n=5$), and an upward concave time–survival relationship. Merc alone and decayed In-merc were non-toxic at the equivalent range, substantiating radiation-induced cytotoxicity of ^{111}In-merc.

During the past few years, the use of indium-111 labelled leucocytes has become an indispensable technique in the diagnosis of inflammatory disorders. For these studies, it is important that labelled cells remain viable and functionally normal.

Since indium-111-8-hydroxyquinoline (^{111}In-oxine), the first compound for labelling blood cells with a γ-emitting radionuclide, was established (McAfee & Thakur, 1976), several newer agents, such as ^{111}In-acetylacetone (Sinn & Silvester, 1979), ^{111}In-tropolone (Danpure et al, 1982) and ^{111}In-2-mercaptopyridine-N-oxide (^{111}In-merc) (Thakur et al, 1985) have been developed for reduced toxicity. ^{111}In-merc is a unique agent because of the possibility of a kit procedure of labelling and the possibility of labelling in serum (Thakur et al, 1985). However, a full evaluation, including cytotoxicity and diagnostic efficacy of these agents, has not been carried out.

There has been controversy over the cause of the cytotoxicity of blood-cell-labelling radiopharmaceuticals. Cell damage could be due to chemical toxicity and/or radiation effects. With regard to ^{111}In-oxine, Chisholm et al (1979) reported that the cytotoxicity was due to irradiation. Conversely, Kassis and Adelstein (1985) concluded that the cytotoxicity was due to the chemical. More studies are required to solve this problem.

As part of a systematic study to evaluate the cytotoxicity of radiopharmaceuticals, the effects of ^{111}In-merc on cultured HeLa S-3 cells were determined using the clonogenic assay system.

Materials and methods

Preparation of ^{111}In-merc

Preparation of ^{111}In-merc was performed following the method of Thakur et al (1985). Briefly, a known amount of ^{111}In-chloride in 0.005 M hydrogen chloride (not more than 200 µl in volume) was mixed with a defined amount of merc (sodium salt) in 1 M citrate buffer (pH 6.5) in a polystyrene tube. The solution was diluted to the desired concentration with Dulbecco's phosphate-buffered saline (PBS). In order to determine the contribution of radiation, the chemical (merc) and/or the metals (indium and its decay product, cadmium) on cell damage, the molecular ratio of In/Cd to merc was fixed at 1:1000. This provides a specific activity of 2220–2960 MBq (60–80 mCi)/mg merc according to the time after which ^{111}In was prepared.

Cell culture, labelling and survival assay

Experiments were carried out with HeLa S-3 cells grown in Eagle's minimal essential medium supplemented with 10% fetal bovine serum. Details of the cell culture procedures, including maintenance, trypsinization and the test for contamination of cultures with mycoplasma, are described elsewhere (Kim et al, 1978). Exponentially growing cells in 25 cm^2 plastic culture flasks were rinsed with PBS twice, labelled with ^{111}In-merc in PBS at room temperature for 15 to 240 min, and then the radioactive solution was removed at specified time intervals. The cells were rinsed with PBS three times and then removed with 0.25% trypsin containing no EDTA. Trypsin was neutralized with medium containing 10% fetal bovine serum, the cells counted using a haemocytometer and appropriate dilutions were plated. Radioactivity in the cell suspensions was then counted with a well-type gamma scintillation counter (Canberra Model 10).

Nine to eleven days after plating, the petri dishes were fixed, stained and the number of colonies counted. Cells treated with PBS alone for 1 min were used as controls; these demonstrated a plating efficiency of 50 to 60% throughout the experiments.

Merc alone and decayed ^{111}In-merc, which originated

Reprint requests to: Seong Su Hong, Department of Radiology, Dokkyo University School of Medicine, Mibu, Tichigi 321-02, Japan.

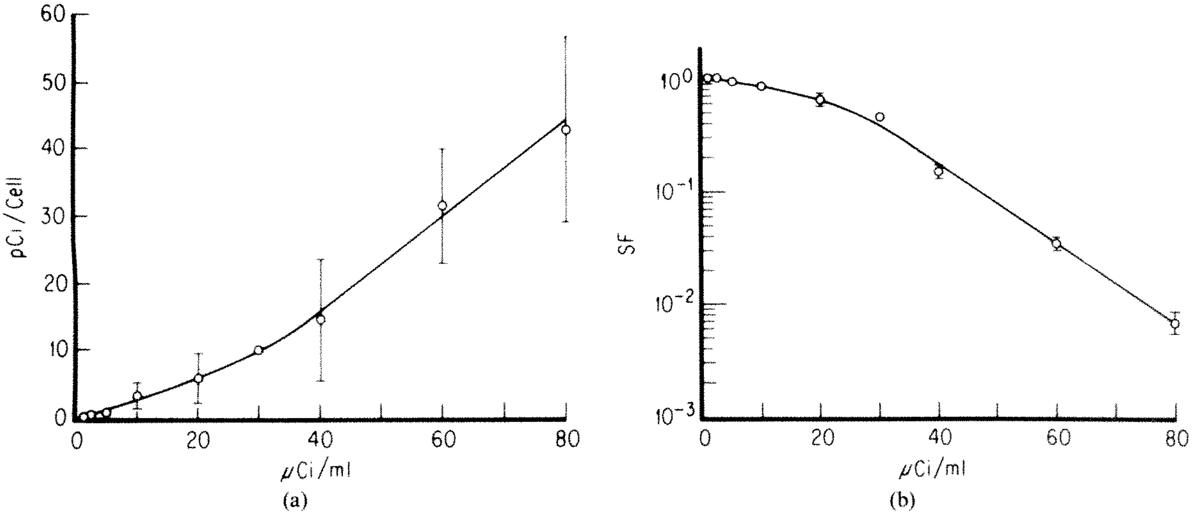

(a) (b)

Figure 1. (a) Initial cellular uptake of ^{111}In-merc and (b) surviving fraction of HeLa S-3 cells as a function of ^{111}In-merc concentration in the incubation solution. The cells were incubated at room temperature for 15 min. Each data point represents the average (±SD) of three different experiments.

from the same batch of ^{111}In used for the radioactive experiments and which had been left to decay for 3 weeks (7.5 half-lives of ^{111}In, radioactivity decrease to 0.55%), were also examined by the same procedure.

Change in radioactivity of the cells

In order to determine the loss of radioactivity from the cells, 5×10^4 cells were plated after the treatment described above and radioactivity of the cells was counted for 10 days. The cell numbers were counted by the method described above.

Results

Cell labelling

Cellular uptake of radioactivity increased as the concentration of ^{111}In-merc in the incubation solution increased (Fig. 1a). The cellular uptake of ^{111}In at concentrations of 0.74 and 1.48 MBq/ml (20 and 40 μCi/ml) began to saturate after 60 min of incubation (Fig. 2a).

Cell survival

Cell survival analysis as a function of dosage up to 2.96 MBq/ml (80 μCi/ml) of ^{111}In-merc for 15 min

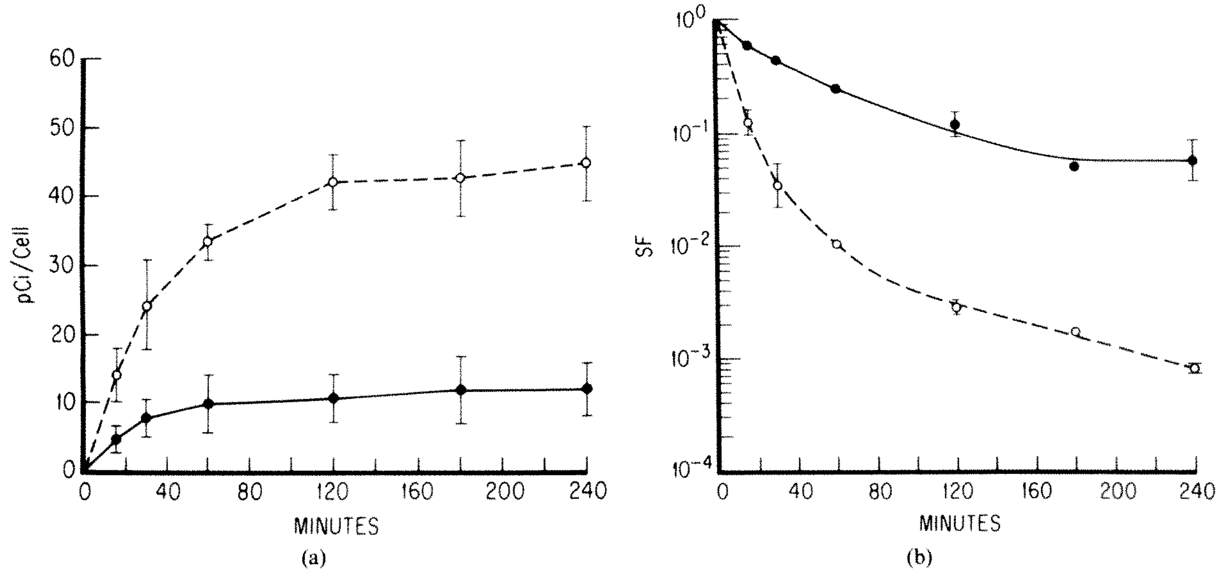

(a) (b)

Figure 2. (a) Initial cellular uptake of ^{111}In-merc and (b) surviving fraction of HeLa S-3 cells as a function of incubation time. (●) 0.74 MBq/ml (20 μCi/ml); (○) 1.48 MBq/ml (40 μCi/ml). Each data point is the average (±SD) of three different experiments.

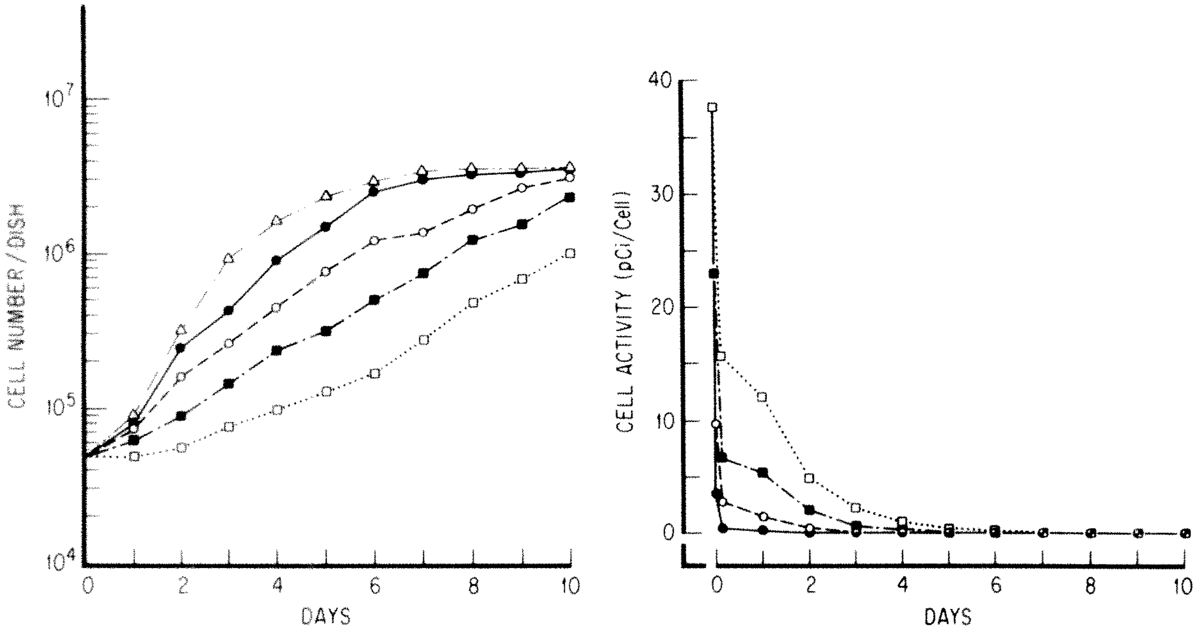

(a) (b)

Figure 3. (a) Cell multiplication and (b) changes of radioactivity per cell during the colony-forming period. The cells were treated with 0.74 (●), 1.48 (○), 2.22 (■) and 2.96 (□) MBq/ml (20, 40, 60 and 80 μCi/ml, respectively) of ^{111}In-merc at room temperature for 15 min prior to plating; (△) control.

incubation showed an exponential reduction in cell survival with a shoulder. The D_0 was determined as 0.44 MBq/ml (12 μCi/ml) ($n = 5$) (Fig. 1b).

The effect of incubation time on cell survival at the two different concentrations was an upward concave decrease of survival followed by a continuous slow decrease until 240 min (Fig. 2b). This was different from the cell uptake pattern, which demonstrated no saturation in cell killing.

The treatment with PBS alone for up to 240 min was non-toxic (surviving fraction greater than 0.9). Decreased survival of the cells incubated with decayed ^{111}In-merc and with merc alone was not detected within the dose- and time-range equivalent to those of the radioactive experiments (highest merc concentration, 1.3 μg/ml).

Change of radioactivity of the cells during colony formation

The cell numbers in the dish (Fig. 3a) and radioactivity in the cells (Fig. 3b) were counted during colony formation. Figure 3b shows a typical radioactivity curve per cell as a function of days after plating, which demonstrates that the cells were irradiated during the initial phase of incubation; greater than 95% of irradiation was within the first doubling time.

The survival fraction as a function of initial cellular uptake was reconstructed from Fig. 1a and 1b (Fig. 4a). A single exponential line (D_0 of 9 pCi/cell) without a significant shoulder can be demonstrated. Figure 4b shows the survival fraction as a function of disintegrations per cell (calculated from Fig. 3b). A downward concave dose–survival relationship with no shoulder was generated.

Discussion

Radiation toxicity of ^{111}In-merc on a monolayer of HeLa S-3 cells was demonstrated using a clonogenic assay system. The differences that were seen, *e.g.* Figs 1b and 4a, are related to initial cellular uptake. Cellular incorporation of ^{111}In is not so effective at lower concentrations compared with the higher concentrations (Fig. 1a), resulting in relatively low cell killing at lower concentrations.

The survival curves shown in Fig. 4 have no shoulder, suggesting that the cytocidal effect of ^{111}In-merc is related to the Auger electrons released from electron capture of ^{111}In decay. These electrons have high-linear energy transfer (LET)-type biological effects once localized in the cell nucleus (Hofer et al, 1977). Additional studies are needed to determine the effects of Auger electrons and the subcellular distribution of ^{111}In.

As for radiation toxicity, DNA is the most important target (Okada, 1970). In the case of chemical toxicity, however, there could be significant damage to organelles or membranes resulting in functional inactivation rather than reproductive damage. These results may not necessarily be seen as a loss of viability. These kinds of chemical toxicity should be studied using other experimental systems.

Another consideration that should be made in determining cytotoxicity of radiopharmaceuticals using the clonogenic assay is that cells were continuously

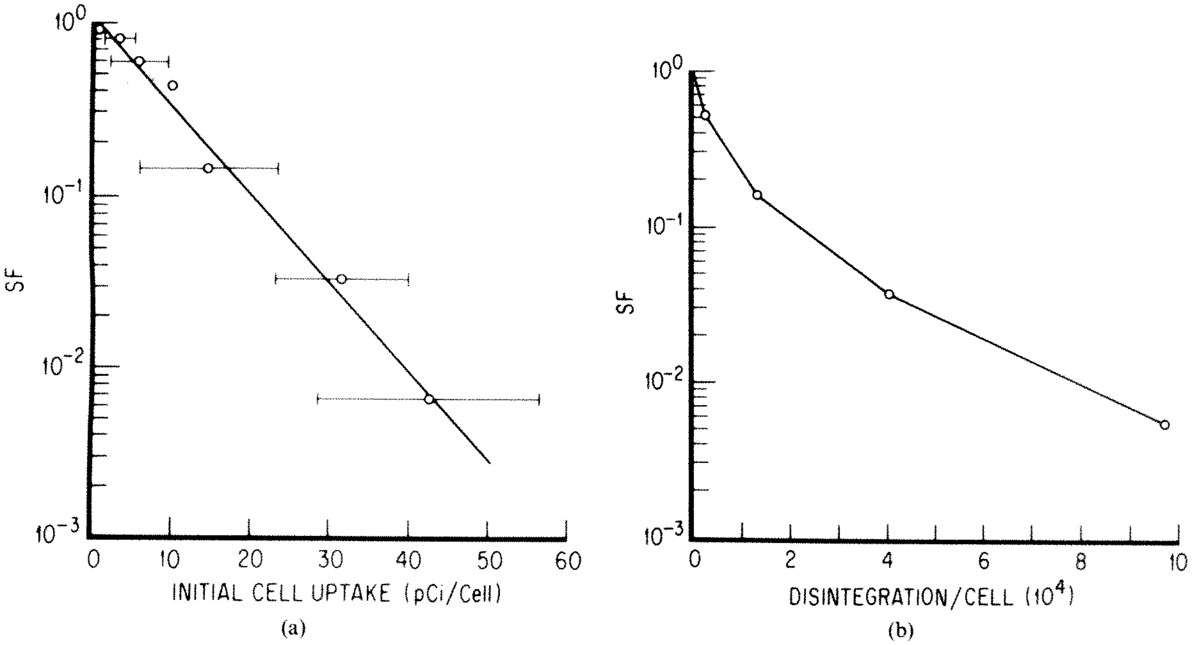

Figure 4. (a) Surviving fraction as a function of initial cellular radioactivity reconstructed from the data of Fig. 1. (b) Surviving fraction as a function of average disintegrations per cell, calculated from Fig. 3b).

irradiated during the colony-forming period. The effects of radiation after the first cell division might be underestimated because the cells were no longer single cells. In these experiments the cells were predominantly irradiated within the first cell doubling. If dose-rate effects are taken into account, the low dose-rate decreases the radiation cell-killing effect (Hall, 1972), so that the contribution after the first division should be negligible. The dose–survival curve calculated from growth delay (Fig. 3a) demonstrated a similar curve (data not shown).

There are several reports using the clonogenic assay system for determining the cytotoxicity of blood-cell-labelling radiopharmaceuticals. Chisholm et al (1979) and Danpure and Osman (1981) reported radiation-induced cytotoxicity of ^{111}In-oxine and ^{111}In-acetylacetone, respectively, on HeLa S-3 cells. They found lower cell survival than we did. This might suggest that ^{111}In-merc is less radiotoxic than ^{111}In-oxine or ^{111}In-acetylacetone. However, they treated trypsinized cells. The effect of trypsin on the cell survival might be taken into account, considering the mechanism of action of these indium chelators on transport of ^{111}In through the cell membrane (Choi & Hwang, 1987).

Table 1. Average radiation dose to the cells during the colony-forming period

Treatment (μCi/ml)	Initial cellular uptake (pCi/cell)	Cumulative activity (pCi h/cell)	Disintegration /cell (× 10³)	Dose (cGy)
20	3.49	18.8	2.5	130
40	9.75	98.9	13.2	690
60	23.0	301.9	40.2	2110
80	37.6	730.0	97.2	5090

Kassis and Adelstein (1985) reported chemical toxicity of ^{111}In-oxine on V79 cells. Their conclusion was that the toxicity of ^{111}In-oxine was induced by the chemical and not by radiation. Three possibilities might be considered: (1) the specific activity might not be high enough to detect radiation toxicity; (2) V79 cells might not be radiosensitive enough; and (3) incubation times of as long as 2 and 18 h in their experiment might be too long. Binding of ^{111}In to the cells begins to saturate after 30 min of incubation according to their data. Unnecessarily long incubation could result in the manifestation of the chemotoxicity.

Lockshin et al (1985) reported that 1 μCi of ^{111}In-oxine per 1 000 000 cells did not show any cytotoxicity on several cultured human cells. This is in accordance with our results for ^{111}In-merc.

Regarding desirable labelling time and concentration in relation to radiation toxicity, it is clear that an incubation time of more than 60 min should be avoided, because after this time cellular uptake saturates (Fig. 2a) while cell survival continues to decrease (Fig. 2b). This is probably related to changes of subcellular distribution of ^{111}In; in the case of ^{111}In-oxine, there is more accumulation in the cell nucleus with longer incubation time (Thakur et al, 1982). Accumulation of ^{111}In in the nucleus results in more cell killing via targeting of short-range Auger electrons to DNA.

Appendix

Radiation dose (cGy) was calculated based on the average energy of Auger electrons from single disintegration of ^{111}In of 0.0070 MeV (Silvester, 1979), and assuming that (a) all the cells are 16 μm diameter spheres and do not change their size and shape, (b) radiation from the other cells and medium can be ignored and (c) distribution of ^{111}In in the cell is even (Table I).

Table I. Average radiation dose to the cells during the colony-forming period

Treatment (μCi/ml)	Initial cellular uptake (pCi/cell)	Cumulative activity (pCi h/cell)	Disintegration /cell ($\times 10^3$)	Dose (cGy)
20	3.49	18.8	2.5	130
40	9.75	98.9	13.2	690
60	23.0	301.9	40.2	2110
80	37.6	730.0	97.2	5090

References

Chisholm, P. M., Danpure, H. J., Healey, G. & Osman, S., 1979. Cell damage resulting from the labelling of rat lymphocytes and HeLa S3 cells with In-111 oxine. *Journal of Nuclear Medicine, 20,* 1308–1311.

Choi, H. & Hwang, K. J., 1987. Mechanism of ionophoric transport of indium-111 cations through a lipid bilayer membrane. *Journal of Nuclear Medicine, 28,* 91–96.

Danpure, H. J. & Osman, S., 1981. Cell labelling and cell damage with indium-111 acetylacetone—an alternative to indium-111 oxine. *British Journal of Radiology, 54,* 597–601.

Danpure, H. J., Osman, S. & Brady, F., 1982. The labelling of blood cells in plasma with In-111-tropolonate. *British Journal of Radiology, 55,* 247–249.

Hall, E. J., 1972. Radiation dose-rate: a factor of importance in radiobiology and radiotherapy. *British Journal of Radiology, 45,* 81–97.

Hofer, K. G., Keough, G. & Marshall Smith, J., 1977. Biological toxicity of Auger emitters: molecular fragmentation versus electron irradiation. *Current Topics in Radiation Research, 12,* 335–354.

Kassis, A. I. & Adelstein, S. J., 1985. Chemotoxicity of indium-111 oxine in mammalian cells. *Journal of Nuclear Medicine, 26,* 187–190.

Kim, S. H., Kim, J. H. & Hahn, E. W., 1978. Selective potentiation of hyperthermic killing of hypoxic cells by 5-thio-D-glucose. *Cancer Research, 38,* 2935–2938.

Lockshin, A., Mendoza, J. T., Giovanella, B. C. & Stehlin, J. S. Jr, 1985. Indium-111 labelling of cultured human tumour cells. *Oncology, 42,* 322–327.

McAfee, J. G. & Thakur, M. L., 1976. Survey of radioactive agents for *in vitro* labelling of phagocytic leukocytes. I. Soluble agents. *Journal of Nuclear Medicine, 17,* 480–487.

Okada, S., 1970. Are there other target molecules? In *Radiation Biochemistry, Vol. I: Cells,* ed. by S. Okada (Academic Press, New York), pp. 148–155.

Silvester, D. J., 1979. Consequences of indium-111 decay *in vivo.* Calculated absorbed radiation dose to cells labelled by indium-111 oxine. *Journal of Labelled Compounds and Radiopharmaceuticals, 16,* 193–194.

Sinn, H. & Silvester, D. J., 1979. Simplified cell labelling with indium-111 acetylacetone. *British Journal of Radiology, 52,* 758–759.

Thakur, M. L., McKenney, S. L. & Park, C. H., 1985. Simplified and efficient labelling of human platelets in plasma using indium-111-2-mercaptopyridine-n-oxide: preparation and evaluation. *Journal of Nuclear Medicine, 26,* 510–517.

Thakur, M. L., Segal, A. W., Louis, L., Welch, M. J., Hopkins, J. & Peters, T. J., 1977. Indium-111-labelled cellular blood components: mechanism of labelling and intracellular location in human neutrophils. *Journal of Nuclear Medicine, 18,* 1020–1024.

1989, *The British Journal of Radiology*, *62*, 473–481

The quality of high-energy X-ray beams

By *Philip D. LaRiviere
Varian Associates, Inc., 611 Hansen Way, Palo Alto, California 94303, USA

(*Received January 1988 and in revised form September 1988*)

Abstract. Supplement 17 of the *British Journal of Radiology* is a survey of central-axis depth doses for radiotherapy machines, patterned largely on *BJR* Supplement 11 published some 11 years earlier. Inspection of the high-energy X-ray depth doses for a 10 × 10 cm field at an SSD of 100 cm disclosed large differences between the two sets of data, especially for qualities above 8 MV. For example, a depth dose of 80% at 10 cm is rated at about 19 MV according to *BJR* Supplement 11, and 23 MV according to *BJR* Supplement 17. It was found that the Supplement 17 depth–dose data above 8 MV were erratic, but that the Supplement 11 data could be represented by an analytical expression, providing a unique means of assigning MV quality. It was also found that the dose-weighted average energy of the filtered beam plotted smoothly against depth dose. For dosimetric purposes, it is suggested that this parameter be used as a true measure of beam quality, removing the discrepancies introduced by the use of nominal MV for this purpose.

Supplement No. 11 of the *British Journal of Radiology* (*BJR*, 1972) established itself to a large extent as a standard reference for central-axis depth–dose data, widely used by both the accelerator manufacturing and radiotherapy communities. The high-energy X-ray depth–dose data published more recently in *BJR* Supplement No. 17, however, is in gross disagreement with Supplement 11 above 8 MV (*BJR*, 1983). As a consequence, there is no longer a standard reference for correlating depth–dose performance with beam quality. Confusion is also introduced into the marketplace, since, for example, a machine producing an 80% depth dose at 10 cm depth for a 10 cm × 10 cm field at 100 cm source–surface distance (SSD) might be assigned a nominal quality of 18 MV by one manufacturer, based on *BJR* Supplement 11, while identical performance by a competing machine could be claimed to produce 23 MV X rays, based on *BJR* Supplement 17.

At the time *BJR* Supplement 11 was written, only betatrons were available above 15 MV, so the data in this region were sparse and scattered. In spite of this, there was remarkably little disagreement between published reports and the manufacturers' literature on how to rate their machines. More machines were available for *BJR* Supplement 17, but, unfortunately, there was so much variation in the data obtained above 8 MV that averaging was deemed meaningless and resort was made to selecting "typical" results.

In *BJR* Supplement 11 it was recognized that in the 20–24 MV region, filtration by the beam flattener played an important part in the depth–dose values reported. This idea was discussed briefly in *BJR* Supplement 17, but no analytical investigation was made. Filter materials and thicknesses were not identified and no steps were taken to see if the machines were being operated at the designated energy. It was acknowledged that a very poor correlation was found between depth–dose values and nominal MV, and that above 8 MV a check of individual machine performance was essential for each user.

The scope of this study is restricted to central-axis X-ray depth doses in water for a square field 10 cm on a side at an SSD of 100 cm. Field sizes of this magnitude are of clinical importance and accelerator manufacturers have historically specified the depth of dose maximum (D_{max}) and the 10 cm depth dose for this field size to describe X-ray penetrating power. In this paper the concept of X-ray "quality" is examined. The dose-weighted average energy of the target bremsstrahlung is related to the electron energy; the target spectrum is folded into the attenuation curve of the filter to obtain the output spectrum, as was thoroughly discussed years ago (Johns et al, 1949); the dose-weighted average energy of the flattened beam is obtained, and a general curve is developed relating it to depth dose.

X-ray quality

Quality is defined in *BJR* Supplement 17 in the special sense of the ability of a beam to penetrate water; however, in a more general sense, it is used with X rays to represent the energy spectral distribution (Attix, 1986). In the latter case, electrons of energy E (MeV) on target are said to produce an X-ray quality of Q, measured in millions of volts (MV), where Q is numerically equal to E. Quality has also been expressed in terms of mm of Al or Cu, or, in the case of a radionuclide, simply as the name of the nuclide (International Commission on Radiation Units and Measurements (ICRU), 1976). Supplement 17 of the *BJR* and the International Electrotechnical Commission (IEC, 1985) have advanced yet another index of quality, d_{80}, the depth at which the absorbed dose is 80% of the dose maximum, in which case the unit of quality is a length.

The concept of quality appears to go back many years to X rays in the keV range, expressed in terms of percentage depth dose for specified field areas and SSD, factors of direct meaning to the clinician (ICRU, 1964). This consideration seems to have dropped by the wayside for higher energy machines. In 1970, for example, it was recommended that for X rays above 2 MV it was sufficient to state "the MV" only (Massey, 1970). In the light of data from today's high-energy machines, it is easy to demonstrate that quality can better be expressed in terms of some measurable physical parameter of the output X-ray spectrum.

---

*Address for correspondence: 453 Tennessee Lane, Palo Alto, California 94306, USA.

Depth–dose relationships

The depth–dose data of *BJR* Supplements 11 and 17 are plotted against stated quality in MV in Fig. 1. It was found empirically that the *BJR* Supplement 11 data could be represented by a straight line on semilog paper. The equation of the least-squares line, excluding the scattered betatron values above 30 MV[*] is:

$$d = 26.09 \log Q + 46.78 \quad (\text{for } 4 \leqslant Q \leqslant 45) \qquad (1)$$

or, solving explicitly for the other variable:

$$Q = 10^{(d-46.78)/26.09} \qquad (2)$$

where d is the percentage depth dose at 10 cm for a 10-cm square field and an SSD of 100 cm, and Q is the quality in megavolts. The value of the reduced χ^2 goodness-of-fit test is $\chi^2_\nu = 0.14$. A value greater than 1 indicates that the fitting function is not appropriate for describing the data, whereas a value less than 1 indicates the existence of an uncertainty in the variance from experiment to experiment (Bevington, 1969).

It can be seen in Fig. 1 that the line, which is a smooth representation of *BJR* Supplement 11 data, reflects rather well the various manufacturers' published specifications of 62–63% for 4 MV, 67% for 6 MV, 73% for 10 MV, 77% for 15 MV, approximately 79% for 18 MV, and 83% for 24 MV. It also is within 0.5 percentage points of the Nordic Association of Clinical Physics (NACP) values at 4, 6, 8, 10, 12 and 15 MV, where 15 MV was the highest quality reported (Johansson, 1982).

On the other hand, the *BJR* Supplement 17 points in Fig. 1 are initially higher than the *BJR* Supplement 11 line, but cross over it at about 15 MV, and terminate in a large uncertainty box wherein a range of betatron depth doses from 83–92% was found for Q between 30 and 43 MV.

The 10 MV point at the extremely high value of 75.3% is attributed in *BJR* Supplement 17 to differences in target and filter materials; it is also one of the points "selected as typical". The analysis described below leads to a value of 74.4% with 10 MeV electrons, for a conventional linear accelerator equipped with a thick high-Z target and an Al filter, which provides about the maximum beam hardening possible. The work of Podgorsak et al (1975) bears this out, since 74% was the maximum performance they obtained with an experimental Pb target and an Al flattening filter, for 10 MeV electrons on target. It would appear that the "typical" 10 MV machine sampled in *BJR* Supplement 17 was actually operating with an electron energy in the vicinity of 12 MeV.

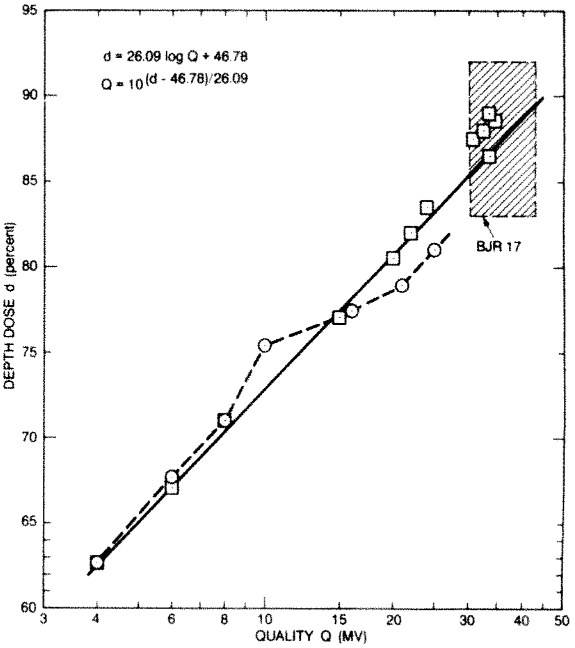

Figure 1. Percentage depth dose at 10 cm for a 10-cm square field and an SSD of 100 cm. □, *BJR* Supplement 11 data; ○, *BJR* Supplement 17 data.

This off-energy situation is not uncommon. Boyer et al (1987) found in a recent analysis of a dual-energy machine that the nominal 18 MV beam was actually generated by 18.8 MeV electrons, and the nominal 6 MV beam by 7.6 MeV electrons, the latter being more than 25% above nominal! The reported depth doses were 80% and 69%, respectively, which according to the smooth *BJR* Supplement 11 curve of Fig. 1 would correspond to 18.8 and 7.1 MV, in good agreement with Boyer's determinations.

Conversely, the *BJR* Supplement 17 assignment of 81% to a 25 MV machine is very low. Good machine design will produce a depth dose in the neighborhood of 84% with this energy. It should be noted that it is not an easy design problem to achieve the depth doses indicated by the straight line in Fig. 1. Beyond about 8 MV, the geometry of the treatment head and the choice of beam forming, flattening and limiting materials becomes more and more critical with increasing energy.

While it is important that the electron energy on target be known, it should not be supposed that beam quality in MV (as defined by the straight line in Fig. 1) is always numerically equal to the electron energy in MeV. The reason is that the target spectrum is modified by the characteristic attenuation curve of the flattening filter material. Figure 2, calculated by methods to be

---

[*] See section on "Relationship of output E_d to depth dose" for a discussion of the betatron data.

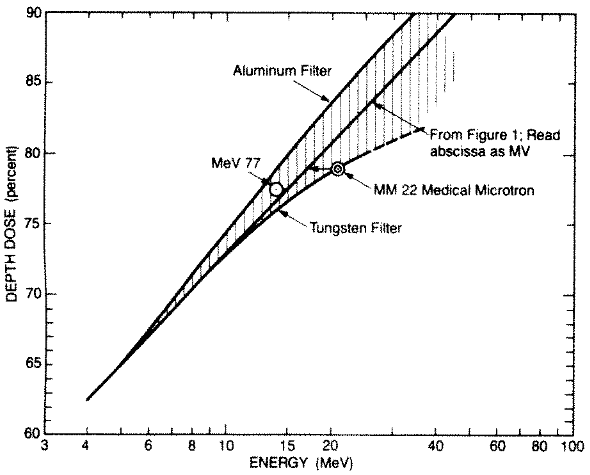

Figure 2. Envelope of all possible percentage depth doses at 10 cm attainable with flattening filters with atomic numbers between 13 (aluminium) and 74 (tungsten). Field size 10 cm square, SSD = 100 cm.

described below, shows the envelope enclosing all possible depth doses attainable with filters whose atomic numbers are between 13 (Al) and 74 (W), in thicknesses sufficient to flatten a square field 35 cm on a side.

Two experimental points are shown in Fig. 2, illustrating this effect. One is for a Siemens 15 MV machine, achieved with an electron energy of 13.9 MeV hardened with a steel ($Z = 26$) filter (Taumann, 1979). The quality was described as 15 MV by the manufacturer because the measured depth dose was 77.5%, which checks exactly with the straight-line 15 MV value of Fig. 1 (superimposed on Fig. 2). The other point in Fig. 2 is for a Scanditronix MM 22 Medical Microtron with a lead filter, in which 21 MeV electrons on target produced a depth dose of 78.9% and an acceleration potential (NACP, 1980) of 17.7 MV (George & Hartson-Eaton, 1985). Referring to Fig. 2, it can be seen that the point falls just on the tungsten line (which is very close to lead in performance) and the quality is 17 MV, in reasonable agreement with the acceleration potential.

Comparison of Figs 1 and 2 also shows that (i) the combination of 10 MeV and 75.3%, discussed above, falls outside the envelope, which is inconsistent with theory (unless the beam was hardened by a lower-Z material than Al) and (ii) the remainder of the *BJR* Supplement 17 curve falls within the envelope. Thus we see that the straight-line *BJR* Supplement 11 relationship shown in Fig. 1 is fortuitous. That depth doses from many machines fall along this particular line is probably a consequence of the fact that only a limited number of flattening filter materials meet all of the requirements imposed at the higher energies on this component. It is believed that designers have in many cases converged to essentially the best practical hardening materials available, so that it is difficult to obtain performance better than indicated by the straight-line relationship shown in Fig. 1.

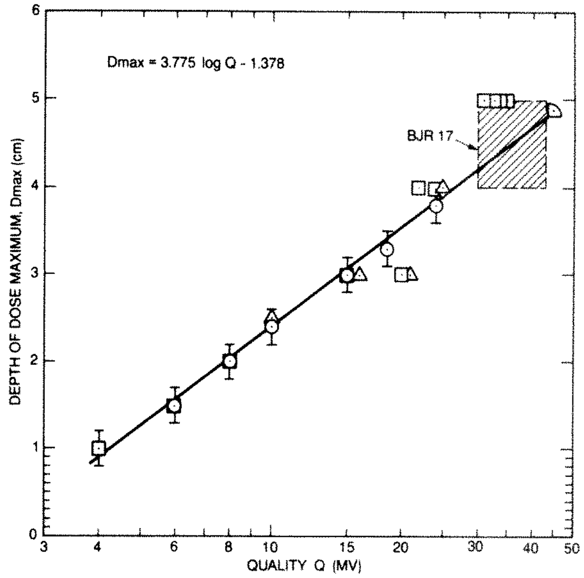

Figure 3. D_{max} for a 10-cm square field and an SSD of 100 cm. □, *BJR* Supplement 11; △, *BJR* Supplement 17; ○, Varian published specifications; ◺, Suntharalingam and Steben (1977); ◇, Aldrich and Andrew (1985).

It is easy to fall short of this performance, but sometimes this is done deliberately with a two-component filter, as in the case of the MM 22, in order to improve some other parameter, such as beam flatness over a wide range of depths and field sizes. In this case, the photon spectrum on axis is softened, in order to reduce the disparity in energy between axial and peripheral rays.

It is not known why the *BJR* Supplement 17 points above 8 MV in Fig. 1 are at odds with earlier results. It would appear that the least-squares representation of the *BJR* Supplement 11 data in Fig. 1 is more reliable than the Supplement 17 data, because it predicts depth doses that are in good agreement with manufacturers' traditional specifications and with results published in the literature over the years.

Depth of dose maximum (D_{max})

Manufacturers usually specify both D_{max} and the 10-cm depth dose to characterize the penetrative quality of their X-ray beams. Figure 3, in combination with Fig. 1, provides compatible pairs of these values for conventional machines, *i.e.* those which employ no special means of suppressing electron contamination in the X-ray beam.

Figure 3 shows that D_{max} against quality also can be represented adequately by a straight line on semilog paper, with a maximum departure of about 0.2 cm for most of the points and $\chi_v^2 = 0.05$. There is obvious trouble with the *BJR* Supplement 11 points that jump from 3 cm to 4 cm between 20 and 22 MV. These were omitted from the least-squares fit, as was the *BJR* Supplement 11 betatron group at 5 cm. Data introduced in Fig. 3 include the 45 MV AECL Brown-Boveri betatron (Suntharalingam & Steben, 1977), the 25 MV Therac 25 (Aldrich et al, 1985) and the Varian specifications with tolerances published in marketing brochures. The equation of the line is:

$$D_{\max} = 3.775 \log Q - 1.378 \text{ (for } 4 \leqslant Q \leqslant 45) \quad (3)$$

where $D_{\max}$ is the depth of dose maximum in centimetres for a 10-cm square field and an SSD of 100 cm, and Q is the stated quality of the beam in megavolts. The NACP data (Johansson, 1982) are slightly shallower above 8 MV, with considerable scatter, but in general the agreement is good to within 1–2 mm.

The least-squares lines shown in Figs 1 and 3 represent good state-of-the-art performance for any type of accelerator. Although in principal $D_{\max}$ could be used to estimate beam quality, depth dose provides a more reliable determination because it can be measured more precisely than $D_{\max}$ and is less influenced by variations in electron contamination.

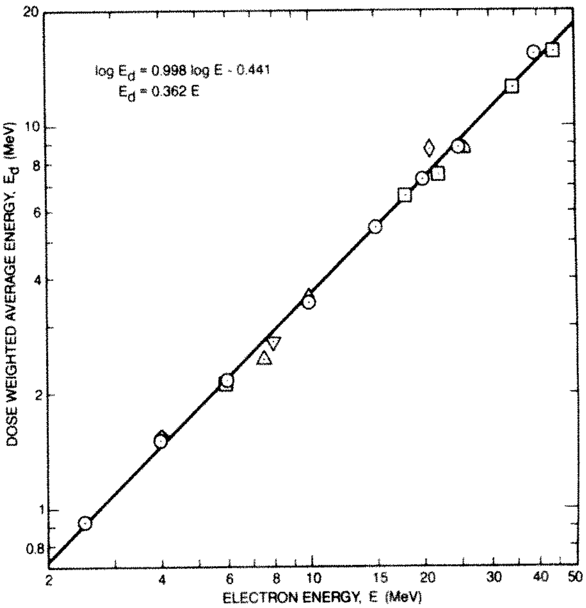

Figure 4. Dose-weighted average energy for target X rays (no beam flattener) on the central axis. △, Boyer et al (1987); ○, Brynjolfsson and Martin (1971); ◊, Ford et al (1976); ◇, Hansen et al (1972); ▽, Levy et al (1976); □, McCall (1978).

Target bremsstrahlung spectra

Only those targets whose thickness is about equal to the range of the electrons are considered here. For such targets, the atomic number Z plays a relatively minor role in the energy distribution of the axial X rays produced compared with that of the flattening filter, especially above 10 MeV or so (McCall et al, 1978). This is also clearly discernible in Podgorsak et al's (1975) experimental work. In addition, in-house Monte Carlo target analyses using the EGS program of Ford and Nelson (1978) have verified the weak effect of target Z on energy, as have in-house experiments at 15 MeV on practical targets of equivalent thickness in Cu, W and in optimum thickness (for yield) of W backed with Cu.

The forward (0–2°) spectra calculated by Brynjolfsson and Martin (1971) for thick targets were used, because they comprised a coherent set covering electron energies ranging from 1 to 40 MeV. These were augmented by other calculated and experimental spectra (Hansen et al, 1972; Sherman et al, 1974; Ford et al, 1976; Levy et al, 1976; McCall, 1978; Boyer et al, 1987).

The above spectra were presented either as fluence distributions, *i.e.* the relative number of photons in each energy interval, or as energy fluences, *i.e.* the relative number of photons in each interval weighted (multiplied) by their energy. The relative *dose* in each interval was obtained by weighting the number of photons with a function proportional to dose per photon cm^{-2} (Patterson & Thomas, 1973). Below 1 MeV, it is proportional to the intensity; above 1 MeV however, the dose function weights the higher energies about one-half as much as energy weighting. The result is that energy fluences and dose distributions are similar, but markedly different from fluence distributions.

The average of the interval doses, *i.e.* the dose-weighted average energy, is given by:

$$E_{\mathrm{d}} = \frac{\int_0^{E_{\max}} E R(E)(\mathrm{d}N/\mathrm{d}E)\mathrm{d}E}{\int_0^{E_{\max}} R(E)(\mathrm{d}N/\mathrm{d}E)\,\mathrm{d}E} \quad (4)$$

where E is the electron energy, $R(E)$ is the fluence-to-dose conversion factor (not shown) and $\mathrm{d}N/\mathrm{d}E$ is the number of photons in an energy interval $\mathrm{d}E$ (McCall et al, 1978).

The dose-weighted average energy in the direction of the electron beam is of fundamental importance. Since filter transmissions and depth–dose measurements are made with dose-measuring devices, we require something proportional to the dose content in each energy interval, and hence, the dose-weighted distribution. The results of these computations are shown in Fig. 4, where E_d is plotted on log–log paper against the electron energy. The equation of the least-squares straight-line fit to the points ($\chi_v^2 = 0.01$) is:

$$\log E_d = 0.998 \log E - 0.441 \text{ (for } 2.5 \leqslant E \leqslant 45) \quad (5)$$

where E_d is the dose-weighted average energy of the unflattened bremsstrahlung and E is the electron energy, both in MeV. It can be shown easily that Equation 5 reduces to:

$$E_d = 0.362\, E \quad (6)$$

with negligible error, since the coefficient of log E is approximately unity. Equation 6 can be identified with the long-standing rule of thumb that the average energy is about one-third of the maximum photon energy. The average energies of fluence spectra are considerably lower (McCall et al, 1978; Mohan & Chui, 1985).

Dose-weighted average energy of filtered beams

The method employed to calculate output spectra and associated parameters is illustrated in Table I for a lead filter. The first three columns describe the energy interval and its midpoint E_{mid}. The unfiltered target dose spectrum, obtained as described above, is listed next, followed by the mass attenuation coefficient (in $\text{cm}^2\ \text{g}^{-1}$) of lead for each value for E_{mid} (Radiological Health Handbook (RHH), 1970). The transmitted dose in the filtered beam is obtained for each interval by multiplying the unfiltered spectral value by the narrow beam attenuation factor:

$$e^{-\mu/\rho(\rho t)} \tag{7}$$

where the thickness ρt in the Table I example was chosen as $40\ \text{g cm}^{-2}$. Calculations for the filter transmission and the resulting depth dose are illustrated at the foot of Table I.

Figure 5, based on the spectra of Brynjolfsson and Martin (1971), shows the results of such calculations for a number of filter materials distributed in atomic number between Al and W. As can be seen in Table I, E_d depends not only on the Z of the filter, but on its thickness as well, which in turn is set by the electron energy and the maximum field size to be covered by the filter. In Fig. 5, the filter transmissions used are indicated along the abscissa. They closely approximate those required to flatten a square field 35 cm on a side at 100 cm SSD. The figure discloses clearly that at the lower electron energies all filter materials are very much alike, as far as average X-ray energy is concerned. By 10 MeV, however, the effects of the different atomic numbers (with their differently-shaped absorption curves) begin to show, and at 25 MeV they are pronounced.

The inset to Fig. 5 represents the degree of beam hardening as the ratio of the dose-weighted average energy of the filtered beam to that of the unfiltered beam. It can be seen in the insert that tungsten and tin become degrading elements between 15 and 20 MeV, while iron, vanadium and aluminium remain as hardening elements beyond 25 MeV, because their pair production cross-section are smaller.

Relationship of output E_d to depth dose

Figure 6 brings together the output dose-weighted average energies developed in the preceding section with their measured depth doses. Additional data included in Fig. 6 were taken from Varian internal measurements, Aldrich et al (1985), George and Hartson-Eaton (1984), McCall et al (1978) and Patterson and Shragge (1981). The labels accompanying each point identify the electron energy and the filter material.

It is evident that the least-squares straight line shown in Fig. 6 provides a good fit to the data, with a

Table I. Output spectra for 0–2° bremsstrahlung produced by 35 MeV electrons on a thick target, as modified by a $40\ \text{g cm}^{-2}$ thick lead flattening filter.

Energy interval (MeV)			Unfiltered spectrum	μ/ρ (cm^2g^{-1})	Filtered spectrum
	E_{mid}				
0.10 —	0.18 —	0.25	0	1.2	0
0.25	0.38	0.50	0.024	0.25	0
0.5	0.75	1	0.102	0.095	0.002
1	1.5	2	0.210	0.0517	0.027
2	2.5	3	0.196	0.0435	0.033
3	3.5	4	0.144	0.0415	0.027
4	5	6	0.275	0.0424	0.050
6	7	8	0.208	0.0460	0.033
8	9	10	0.207	0.0475	0.031
10	12.5	15	0.419	0.0520	0.052
15	17.5	20	0.362	0.0580	0.036
20	21.2	22.5	0.138	0.0620	0.012
22.5	23.8	25	0.121	0.0640	0.009
25	27.5	30	0.203	0.0710	0.012
30	32.5	35	0.186	0.0750	0.009
$\Sigma E_{\text{mid}}D(E)$			35.094		3.350
$\Sigma D(E)$ = relative dose			2.795		0.334
$E_d = \Sigma E_{\text{mid}}D(E)/\Sigma D(E)$			12.56 MeV		10.03 MeV
$\dfrac{\Sigma D(E)\ \text{filtered}}{\Sigma D(E)\ \text{unfiltered}}$ = transmission			1		0.119
Percentage depth dose (Enter Fig. 6 with E_d)			—		84.1

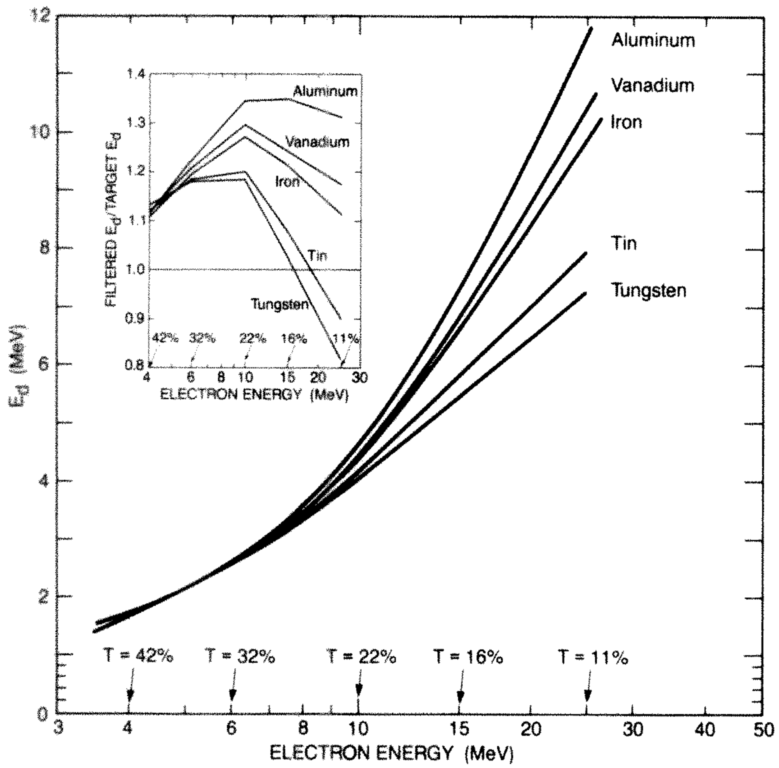

Figure 5. Calculated dose-weighted average energy for X rays filtered by the beam flattener to the transmissions indicated, which approximate those required to flatten a 35-cm square field at an SSD of 100 cm.

maximum departure at any energy of about one percentage point in depth dose ($\chi_v^2 = 0.40$). The equation of the line is:

$$d = 28.68 \log E_d + 55.37 \; (1.7 \leqslant E_d \leqslant 12) \qquad (8)$$

or, solving explicitly for the other variable:

$$E_d = 10^{(d-55.37)/28.68} \qquad (9)$$

where d and E_d are as defined in Equations 1 and 5, respectively. Besides accurately predicting depth doses for various energies, Fig. 6 also demonstrates, in the case of the 24 MeV Varian Clinac 2500, how the depth dose can be made to vary by as much as six percentage points simply by the substitution of W or Al experimental flattening filters for the standard steel filter supplied with this machine. Other interesting examples can be found in the plot, such as 18 MeV filtered with Fe + Ta outperforming a 24 MeV beam filtered with W.

Figure 6 can also be used in conjunction with Fig. 5 to predict the depth–dose performance of any desired combination of electron energy and filter material covered. As an example, Mantel et al (1979) reported a depth dose of 76% for a 14 MeV Toshiba LMR-16 accelerator equipped with a Pb filter. Turning to its near-equivalent, W, it is found in Fig. 5 that $E_d = 5.25$ MeV for 14 MeV electrons. In Fig. 6, a depth dose of 76% is found opposite 5.25 MeV, in agreement with measurement.

A final point of interest in Fig. 6 is that the spectra computed by Mohan and Chui (1985) for five Varian machines included the flattening filter, so that these spectra could be utilized directly without the necessity of folding the target spectrum into the filter attenuation curve. It can be seen that three of the five energies covered fall directly on the line, and the remaining two are within one percentage point of it. It appears that Fig. 6 is a universal curve, along which all combinations of electron energy and filter material lie, although there is no *a priori* reason known to us for the dose-weighted average energy to control depth dose in water, as it appears to do.

In the section on "Depth–dose relationships", discussion of the betatron points shown in Fig. 1 was deferred. It can now be appreciated just how strongly the flattening filter can affect depth dose, especially at the higher energies. It was shown in the 35 MeV example of Table I how a lead filter about 40 g cm^{-2} thick will produce a depth dose of 84%, close to the bottom of the hatched box in Fig. 1. It can be shown similarly how a 100 g cm^{-2} aluminium filter would increase the depth dose to 90%, close to the top of the box.

Both of these materials are used for betatron filters, and in several thicknesses. The above analysis is approximate only, because no account has been taken of the smaller maximum field size produced by betatrons and the possibility that targets in these machines may produce more energetic bremsstrahlung than calculated here for thick linear-accelerator targets. It is believed that a more detailed study is not

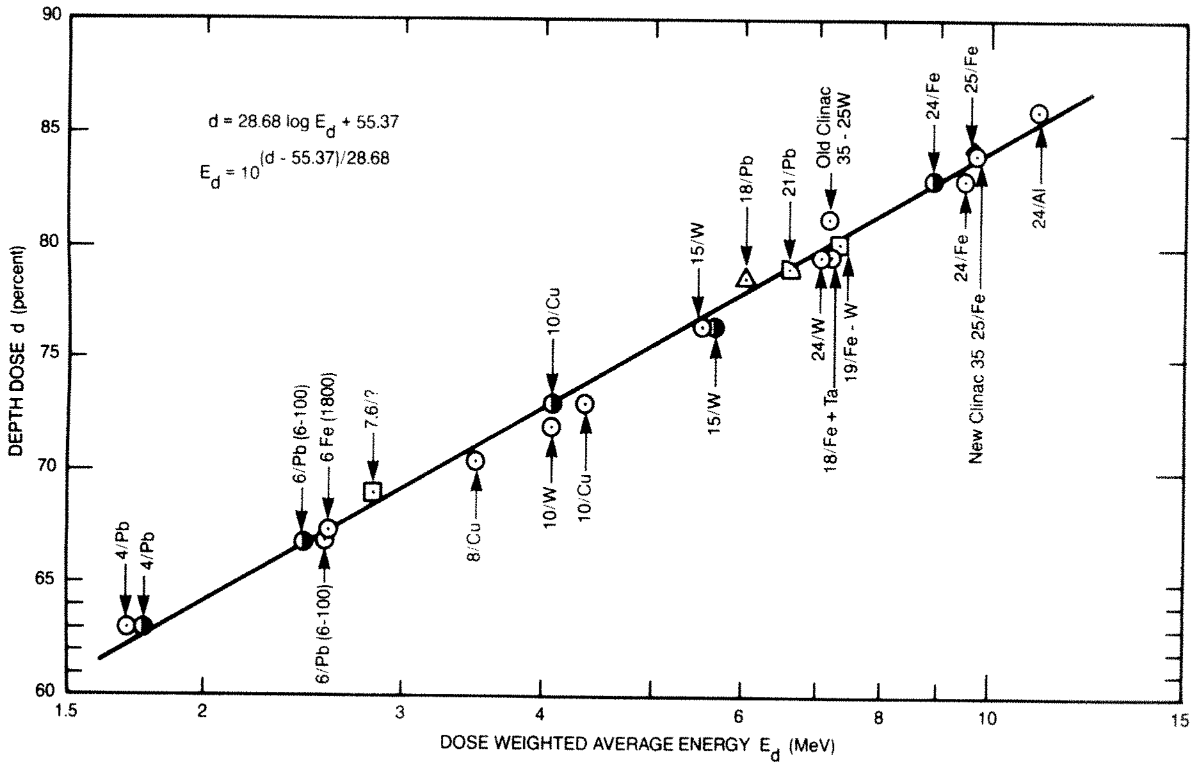

Figure 6. Dependence of 10-cm depth dose on the dose-weighted average energy of the output X-ray beam. Field size 10-cm square, SSD = 100 cm. ○, Varian machines, spectra from Brynjolfsson and Martin (1971); ◑, Varian machines, spectra from Mohan and Chui (1985); □, Siemens machines, spectra from Boyer et al (1987); △, Therac 20, Patterson and Shragge (1981); ◳, MM 22 Microtron, George and Hartson-Eaton (1985); ◇, AECL 25, Aldrich et al (1985). The labels accompanying the points include the nominal beam quality for identification, the filter material and the machine identity, when necessary for clarity.

warranted since, as stated in *BJR* Supplement 17, there was so much overlap in depth doses over the entire 32–43 MV range that it was necessary to choose "typical" data and state the range of variation.

Dosimetric considerations

The acceleration potential (NACP, 1980) is based on the *BJR* Supplement 11 depth–dose curves. It does not provide a good way to compare beams for relative penetrating power because the ratio of the ionization at a depth of 10 cm to that at 20 cm becomes very flat and insensitive beyond about 15 MeV. Nizin and Kase (1986) have calculated that each dose in the ratio must be measured with a precision of better than ±0.4% in order to detect changes in a 10 MV beam with an uncertainty of ±5%.

As pointed out by Nahum et al (1988), Andreo and Brahme (1986) demonstrated by Monte Carlo simulation, including the spectrum-altering effects of the flattening filter, that the water/air stopping power ratio is closely correlated to TPR_{10}^{20}, the ratio of the dose under 20 cm of water to that at 10 cm, measured with a constant source–detector distance. However, they noted that this dose ratio was poorly correlated with nominal MV. Attix (1984) has also noted discrepancies between Figs 2 and 3 in the American Association of Physicists' in Medicine (AAPM, 1983) protocol involving the nominal accelerating potential. It seems clear that any quality descriptor that does not include the effects of the flattening filter on the output spectrum is not useful for dosimetric purposes.

Conclusions and recommendations

With regard to central-axis high-energy X-ray depth doses at 10 cm depth for square fields 10 cm on a side, at an SSD of 100 cm:

(1) *BJR* Supplement 17 data above 8 MV are in poor agreement with those in *BJR* Supplement 11. For example, a depth dose of 80% is rated at 19 MV in Supplement 11 and 23 MV in Supplement 17. As a consequence, there is no longer a standard reference for correlating depth–dose performance with beam quality. To resolve this difficulty and to provide a unique, sensitive assessment of relative penetrating power, it is believed that the measured depth dose at 10 cm should be retained and the quality Q calculated therefrom, using Equation 2:

$$Q = 10^{(d-46.78)/26.09}$$

where Q is in megavolts and d is depth dose in per cent.

Conversely, the depth dose can be calculated and assigned an appropriate tolerance for a given quality. The above equation describes the least-squares fit to the *BJR* Supplement 11 data shown in Fig. 1. Preference was given to the older data because they plot smoothly, are in agreement with manufacturers' calibrations and with reports in the open literature, and have stood the test of time since 1972.

(2) It is concluded that megavolt quality, which is taken in both *BJR* Supplements 11 and 17 to be numerically equal to the electron energy on target, is not a meaningful descriptor for dosimetric purposes because the true quality of a beam cannot be assessed without taking into account the filtration of the flattening filter.

(3) It has been shown that depth dose can be predicted accurately from the dose-weighted average energy. It is therefore suggested that the dose-weighted average energy of the filtered output beam, a physical quantity that can be measured and calculated, might correlate well with TPR^{20}_{10}, and thereby remove the uncertainty in efforts to date to correlate *BJR* Supplement 17 megavolt quality with this ratio.

Acknowledgment

The author wishes to thank Dr Stanley W. Johnsen for performing the least-squares and goodness-of-fit calculations.

References

Aldrich, J. E., Andrew, J. W., Michaels, H. B. & O'Brien, P. F., 1985. Characteristics of the photon beam from a new 25-MV linear accelerator. *Medical Physics, 12*, 619–624.

AAPM, 1983. A protocol for the determination of absorbed dose from high-energy photon and electron beams. Task Group 21, Radiation Therapy Committee. *Medical Physics, 10*, 741–771.

Andreo, P. & Brahme, A., 1986. Stopping power data for high-energy photon beams. *Physics in Medicine and Biology, 31*, 839–858.

Attix, F. H., 1984. Presentation of nominal accelerating potential as a function of the ionization ratio in the new AAPM protocol. *Medical Physics, 11*, 565–566.

——1986. *Introduction to Radiological Physics and Radiation Dosimetry*, 1st edn (John Wiley, New York).

Bevington, P. R., 1969. *Data Reduction and Error Analysis for the Physical Sciences* (McGraw-Hill, New York).

BJR, 1972. *Central Axis Depth Dose Data for Use in Radiotherapy, British Journal of Radiology*, Suppl. 11 (British Institute of Radiology, London).

——1983. *Central Axis Depth Dose Data for Use in Radiotherapy, British Journal of Radiology*, Suppl. 17 (British Institute of Radiology, London).

Boyer, A. L., Cassady, A. E. & Wange, L. L., 1987. Monte Carlo calculation of the photon beam spectra of a dual energy linac. Paper presented at the AAPM annual meeting, Chicago.

Brynjolfsson, A. & Martin, T. G., 1971. Bremsstrahlung production and shielding of static and linear electron accelerators below 50 MeV. Toxic gas production, required exhaust rates, and radiation protection instructions. *International Journal of Applied Radiation and Isotopes, 22*, 29–40.

Ford, R. L. & Nelson, W. R., 1978. *The EGS Code System: Computer Programs for the Monte Carlo Simulation of Electromagnetic Cascade Showers (Version 3)*, Report No. SLAC-210 (Stanford Linear Accelerator Center, Stanford, California).

Ford, R. L., Nelson, W. R. & McCall, R. C., 1976. Calculation of depth–dose curves in water due to thick target bremsstrahlung. Read to Summer Meeting of AAPM, Houston, Texas.

George, R. E. & Hartson-Eaton, M., 1984. Characteristics of an MM 22 medical microtron 21 MV photon beam. Undated preprint received November 1984.

——1985. Characteristics of an MM 22 medical microtron 21 MV photon beam. *International Journal of Radiation Oncology, Biology, Physics, 11*, 1221–1224.

Hansen, H. H., Connor, W. G., Doppke, K. & Boone, M. L., 1972. A new field flattening filter for the Clinac 4. *Radiology, 103*, 443–446.

ICRU, 1964. *Physical Aspects of Irradiation*, ICRU Report 10b (International Commission on Radiation Units and Measurements, Washington DC). Also published as *National Bureau of Standards Handbook 85* (US Government Printing Office, Washington DC).

——1976. *Determination of Absorbed Dose in a Patient Irradiated by Beams of X or Gamma Rays in Radiotherapy Procedures*, ICRU Report 24 (ICRU, Washington DC).

IEC, 1985. *Electrical Equipment in Medical Practice, Subcommittee 62C: High-energy Radiation Equipment and Equipment for Nuclear Medicine* (International Electrotechnical Commission, Geneva).

Johansson, K.-A., 1982. Dosimetric intercomparison at the Nordic Radiation Therapy Centres. Part III. Absorbed dose distributions. In *Studies of Different Methods of Absorbed Dose Determination and a Dosimetric Intercomparison at the Nordic Radiotherapy Centres* (Radiation Physics Department, University of Gothenburg, Gothenburg, Sweden).

Johns, H. E., Darby, E. K., Haslam, R. N. H., Katz, L. & Harrington, E. L., 1949. Depth dose data and isodose distributions for radiation from a 22 MeV betatron. *American Journal of Roentgenology, 62*, 257.

Levy, L. B., Waggener, R. G. & Wright, A. E., 1976. Measurement of primary bremsstrahlung spectrum from an 8 MeV linear accelerator. *Medical Physics, 3*, 173–175.

Mantel, J., Perry, H. & Weinkam, J. J., 1979. X-ray depth-dose characteristics of the Toshiba LMR-16. *Medical Physics, 6*, 95–99.

Massey, J. B., 1970. *Manual of Dosimetry in Radiotherapy*, IAEA Technical Reports Series No. 110 (International Atomic Energy Agency, Vienna).

McCall, R. C., 1978. *Unpublished Target Spectra at 6, 18, 22, and 35 MeV* (Radiation Physics, Stanford Linear Accelerator Center, Stanford, California).

McCall, R. C., McIntyre, R. D. & Turnbull, W. G., 1978. Improvement of linear accelerator depth-dose curves. *Medical Physics, 5*, 518–524.

Mohan, R. & Chui, C., 1985. Energy and angular distributions of photons from medical linear accelerators. *Medical Physics, 12*, 592–597.

NACP, 1980. Procedures in external radiation therapy dosimetry with electron and photon beams with maximum energies between 1 and 50 MeV. Recommendations by the Nordic Association of Clinical Physics, Stockholm. *Acta Radiologica, 19*, 55.

Nahum, A. E., Thwaites, D. I. & Andreo, P., 1988. An analysis of the revised HPA dosimetry protocols. *Physics in Medicine and Biology, 33*, 923–938.

Nizin, P. & Kase, K., 1986. Determination of nominal accelerating potential. *Medical Physics, 13*, 961–962.

PATTERSON, H. W. & THOMAS, R. H., 1973. *Accelerator Health Physics* (Academic Press, New York).

PATTERSON, M. S. & SHRAGGE, P. C., 1981. Characteristics of an 18 MV photon beam from a Therac 20 medical linear accelerator. *Medical Physics, 8*, 312–318.

PODGORSAK, E. B., RAWLINSON, J. A. & JOHNS, H. E., 1975. X-ray depth doses from linear accelerators in the energy range from 10 to 32 MeV. *American Journal of Roentgenology, 121*, 182–191.

RHH, 1970. *Radiological Health Handbook*, US Department of Health Education and Welfare (US Government Printing Office, Washington DC).

SHERMAN, N. K., LOKAN, K. H., HUTCHEON, R. M., FUNK, L. W., BROWN, W. R. & BROWN, P., 1974. Bremsstrahlung radiators and beam filters for 25-MeV cancer therapy. *Medical Physics, 1*, 185–192.

SUNTHARALINGAM, N. & STEBEN, J. D., 1977. Physical characterization of 45-MV photon beams for use in treatment planning. *Medical Physics, 4*, 134–140.

TAUMANN, L., 1979. Design criteria for photon beam exits on high energy medical accelerators to minimize neutron production. In *Proceedings of a Conference on Neutrons from Electron Medical Accelerators, Gaithersburg, MD, April 9–10, 1979*, ed. by H. T. Heaton II & R. Jacobs, NBS Special Publication 554 (US Government Printing Office, Washington DC).

1989, *The British Journal of Radiology*, *62*, 482–483

Memorandum from the British Committee on Radiation Units and Measurements

Quantities for Environmental Monitoring

(*Received November 1988*)

The British Committee on Radiation Units and Measurements (BCRU) *Guide to the Measurement of Environmental Gamma-ray Dose Rate* (Spiers et al, 1981) recommended the use of the quantity "absorbed dose to air free-in-air (*i.e.* scatter-free except for air scatter) and that the measuring device has a wall thick enough to give electron equilibrium. Air kerma, which uses the same unit, gray, as absorbed dose, can be taken to have the same numerical value as absorbed dose to air under conditions of electron equilibrium". Conversion factors from exposure, air kerma and absorbed dose to air effective dose equivalent were included as Chapter 7 in this BCRU guide.

The authors of the Guide noted that the International Commission on Radiation Units and Measurements (ICRU) had set up a working party to put forward proposals on the most appropriate quantity to use for measuring ambient radiation for routine protection purposes and suggested that their recommendations could influence the choice of quantities used in future. The International Commission on Radiation Units and Measurements has now published its recommendations (ICRU, 1985) and has proposed various quantities of which ambient dose equivalent is recommended for the measurement of penetrating environmental γ radiation. The National Radiological Protection Board (NRPB, 1986) and the BCRU (BCRU, 1986) have endorsed the ICRU recommendations (ICRU, 1985) for use in assessing the exposure of people. Various organizations have written to BCRU to ask for advice on which quantity should be used for environmental monitoring around installations producing ionizing radiations, and they have advocated one of two alternatives, *viz.* air kerma and ambient dose equivalent, each interpreted in terms of effective dose equivalent where necessary. This memorandum examines both alternatives and makes recommendations.

The conversion factor between air kerma and ambient dose equivalent will depend on the γ-ray spectrum in the environment as shown in Table I. Variations in the natural background spectrum arise from differences from place to place in the relative abundance of ^{40}K, ^{232}Th + daughters and ^{238}U + daughters as well as the contribution due to cosmic rays. The introduction of man-made radioactivity into the environment from nuclear weapon tests, nuclear accidents and the disposal of radioactive wastes from medical and industrial applications produce other changes in the environmental radiation spectrum.

The objective in environmental monitoring is either to monitor the stability of the radiation environment or to assess the exposure of people within that environment; the appropriateness of the quantities air kerma and ambient dose equivalent in realizing these objectives is discussed below. However, with existing instruments and radiation environments, either quantity may be measured and interconversion made satisfactorily within acceptable uncertainties.

The definition of air kerma is well established and is unlikely to be affected by changes of view by ICRU [or the International Commission on Radiological Protection (ICRP)]. Ambient dose equivalent has been defined more recently by ICRU and adopted by ICRP (ICRP, 1987) but its numerical value may be more subject to change if, for instance, the quality factor Q was revised. Thus where the measurements are made over long time periods in order to demonstrate whether changes in the radiation environment have occurred, then air kerma is the most appropriate quantity and the unit is the gray (Gy).

Many measurements of environmental γ radiation are made for comparison with limits designed to restrict to acceptable levels the radiation risks to people not occupationally exposed or exposed in medical practice. Acceptability is often judged not only in relation to legal limits but also in relation to natural background levels of radiation. The quantity recommended by ICRP for control and limitation of doses to people is effective dose equivalent. The operational quantity recommended for the control and limitation of doses to people from external sources by both the ICRU and NRPB is ambient dose equivalent (or in some circumstances directional dose equivalent) and the unit is the sievert (Sv).

If either air kerma or ambient dose equivalent is selected for monitoring, the detector should normally have an isotropic response. From Fig. 1 of ICRU Report 39 (1985), we can obtain the required conversion coefficient from ambient dose equivalent to effective dose equivalent. For isotropic radiation and typical natural terrestrial radiation, conversion factors of about 0·7 Sv/Gy for the quotient of effective dose equivalent to air kerma (Taylor & Webb, 1978) or about 0·6 for the ratio of effective dose equivalent to

Address for reprints and correspondence: M. J. Rossiter, Secretary, BCRU, National Physical Laboratory, Teddington, Middlesex TW11 0LW.

Table I. Ratio of ambient dose equivalent to air kerma as a function of γ-ray energy

γ-ray energy (keV)	$\frac{\text{Ambient dose equivalent}}{\text{Air kerma}}$ (Sv Gy^{-1})
20	0.60
25	0.86
30	1.10
40	1.47
50	1.67
60	1.74
70	1.75
80	1.72
90	1.68
100	1.65
125	1.56
150	1.49
200	1.40
250	1.35
300	1.31
500	1.23
662	1.20
1000	1.17
1250	1.16
3000	1.13
5000	1.11
10000	1.10

ambient dose equivalent are obtained. Thus a measurement of the ambient dose equivalent will overestimate the effective dose equivalent by a factor of about 1.7. This has been recognized by ICRU in Report 39 (1985): "If the overestimation of H_E by $H^*(10)$ is unacceptable for photons at low energies, or for near isotropic radiation fields, more complex measurements will be needed."

Neutrons are rarely measured in the environment but when they are, then ambient dose equivalent is the appropriate quantity for monitoring both the stability of the environment and exposure of people.

In conclusion, it is recommended that:

1. If measurements are made with the objective of monitoring radiation levels in the environment to elucidate long-term changes in these levels, then air kerma should be used.
2. If the objective is to give an indication that levels from man-made sources are acceptable within specified limits for the exposure of people, then ambient dose equivalent should be used. It should be noted that radiation risks to individuals are best expressed by the quantity effective dose equivalent. If this latter quantity is to be accurately assessed, it may be necessary to obtain details of the quality of the environmental radiation that cannot be described adequately by simple measurements of either air kerma or ambient dose equivalent.
3. If the above objectives pertain, the measurements should record both air kerma and ambient dose equivalent.
4. If neutrons are measured in the environment then ambient dose equivalent is the appropriate quantity for both the above objectives.

This paper was prepared by J. A. B. Gibson, J. A. Dennis and J. R. Harvey and endorsed by BCRU for publication in this journal.

References

BCRU, 1986. New quantities in radiation protection and conversion coefficients. *British Journal of Radiology*, *59*, 946–950.

ICRP, 1987. *Data for use in Protection Against External Radiation*, ICRP Publication 51 (Pergamon Press, Oxford).

ICRU, 1985. *Determination of Dose Equivalents Resulting from External Radiation Sources*, ICRU Report 39 (International Commission on Radiation Units and Measurements, Washington).

NRPB, 1986. *New Radiation Quantities Recommended by ICRU for Practical use in Radiological Protection: Their Implementation in the United Kingdom*, Guidance Standard NRPB GS5 (Her Majesty's Stationery Office, London).

SPIERS, F. W., GIBSON, J. A. B. & THOMPSON, I. M. G., 1981. *A Guide to the Measurement of Environmental Gamma-ray Dose Rate*, BCRU Report (BCRU, National Physical Laboratory, Teddington).

TAYLOR, F. E. & WEBB, G. A. M., 1978. *Radiation Exposure of the UK Population*, NRPB Report R77 (Her Majesty's Stationery Office, London).

1989, *The British Journal of Radiology*, 62, 484–486

Technical note

An alignment test jig for measuring the effective focal-spot size of mammographic X-ray tubes

By M. L. Ramsdale, MSc, P. A. Hiles, MSc and *C. P. Lawinski, MPhil

Department of Medical Physics, St Luke's Hospital, Guildford GU1 3NT and *Department of Medical Physics, King's College Hospital, London SE5 9RS

(*Received September 1988 and in revised form January 1989*)

Following publication of the Forrest Report (Department of Health and Social Security (DHSS), 1986) and with the implementation of a breast cancer screening programme in the UK, there is considerable interest in the technical aspects of mammographic systems. The equipment requirements for mammographic X-ray screening units have been identified (DHSS, 1987) and guidance on the commissioning and routine testing of mammographic X-ray equipment is also expected (Institute of Physical Sciences in Medicine (IPSM), 1989). These documents relate to all aspects of the mammographic X-ray set including the specification and measurement of the size of the X-ray tube focal spot.

Design criteria

It is recommended (DHSS, 1987) that effective focal-spot sizes are measured using a pair of slit radiograms in the manner described in BS 6530 (British Standards Institution (BSI), 1985). This standard provides details on the construction of the slit diaphragm and the geometry to be employed when performing focal-spot measurements. In particular, the method requires that the centre of the slit diaphragm and its axis of symmetry are aligned with the reference axis, which is defined as the line through the centre of the radiation source and parallel to the reference direction or that specified direction to which the characteristics such as target angle are referenced. The manufacturer should specify the reference axis when providing data on anode target angle and size of focal spot. With conventional X-ray equipment the reference axis is usually coincident with a vertical central ray at right angles to the long axis of an X-ray tube aligned horizontally. However, since the design of mammographic X-ray equipment generally includes a fixed geometry with the X-ray tube angled a few degrees from the horizontal, the reference axis may not be vertical and it may be necessary to conduct focal-spot-size measurements along an inclined plane.

A simple test jig has therefore been designed, constructed and used during the measurement of focal-spot sizes on a number of different mammographic X-ray units. The primary design requirements were to provide the necessary angulation and support of the slit diaphragm, aligned correctly with the reference axis of the X-ray tube and with the film maintained parallel to the diaphragm plane. It was also considered essential to provide a means of checking the alignment prior to the measurement of focal-spot size. A certain degree of versatility was incorporated into the design to allow for differences in mammographic equipment geometry and the need to provide suitable magnification of the slit diaphragm.

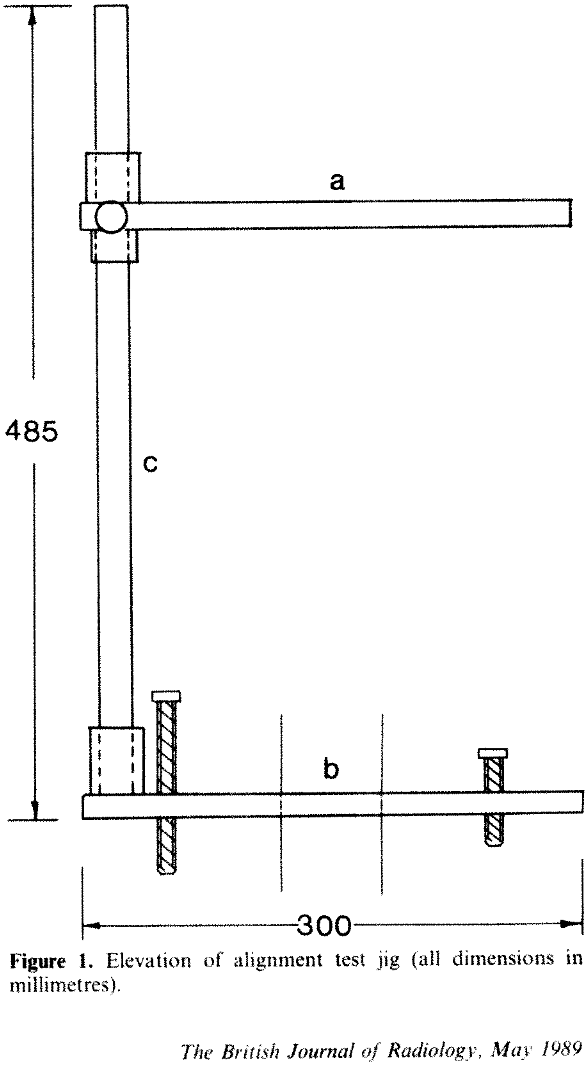

Figure 1. Elevation of alignment test jig (all dimensions in millimetres).

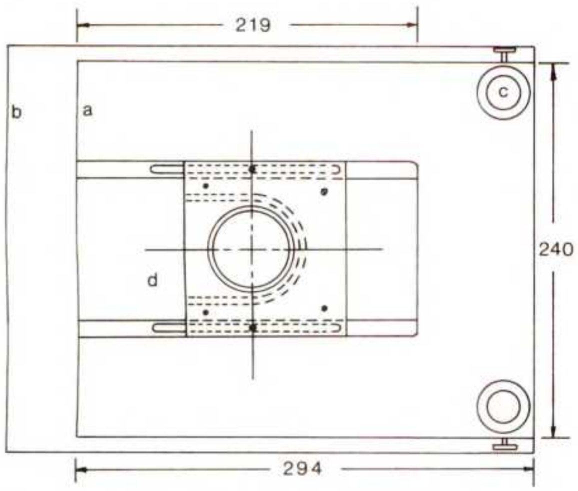

Figure 2. Plan view of the apparatus showing the top plate and sliding circular aperture.

Equipment

The apparatus in use (including approximate dimensions) is shown in Fig. 1. It consists of two Perspex plates (a and b) which support the slit diaphragm and radiographic film, maintained parallel by steel tubing (c). Separation of the plates can be varied and smooth movement has been achieved with the use of PTFE sleeves. The top or object plate (a) has a circular aperture (d) (Fig. 2) designed to support either a slit diaphragm or a star resolution test pattern. The ideal centre of this aperture from the front of the object plate depends on the geometry of the mammographic machine under investigation. A moveable aperture like the one shown (which can be locked into position) may be required if machines of very different geometry are to be examined (Fig. 2). A slot in the object plate allows a commercially available alignment test tool (e) consisting of two 1 mm diameter ball bearings of known separation to be located exactly below the slit diaphragm aperture (Fig. 3). Aluminium screws of two different lengths located in the base plate provide for any angulation and balancing of the jig that may be required to align the object plane normal to the reference axis.

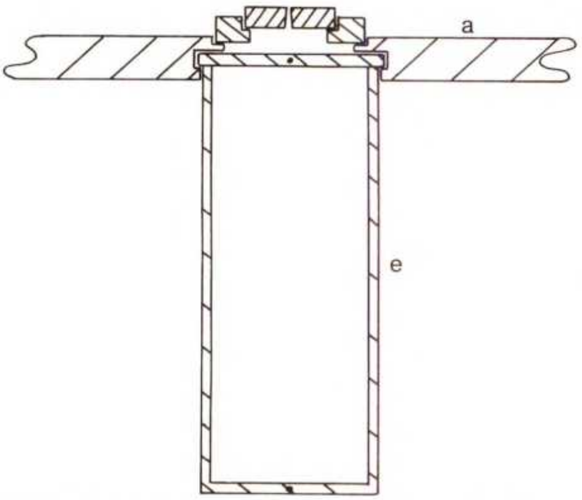

Figure 3. A cross-section of the top plate with the slit diaphragm and alignment test tool in place.

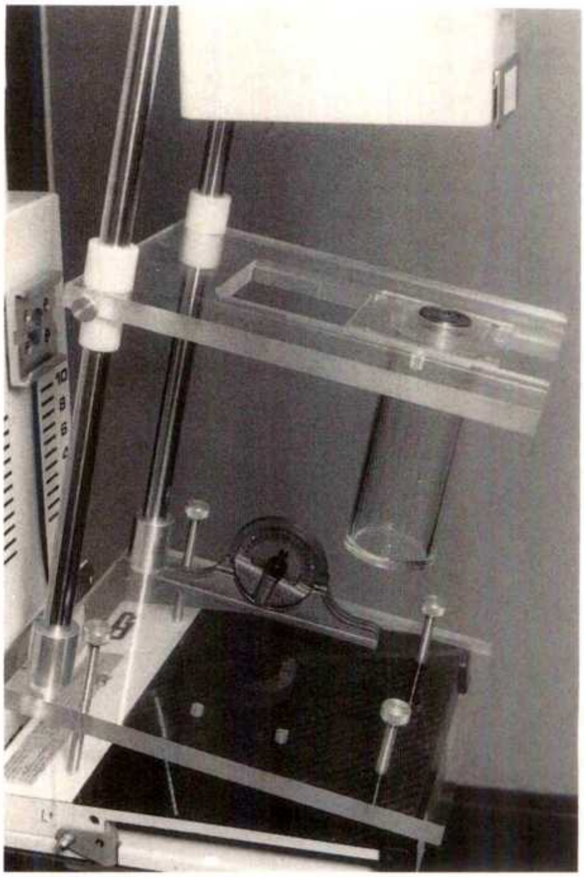

Figure 4. The focal spot alignment jig in use.

Experience of use

The jig is placed on the film cassette platform of the mammographic X-ray machine with the uprights passing either side of the X-ray tube housing and located close to the main column of the unit. The arrangement is angled and balanced as necessary in order to align the test jig correctly with the known reference axis of the X-ray tube (Fig. 4). Angulation can be measured using a graduated compass. The alignment is verified by imaging the test tool using either a fluorescent screen or X-ray film. The alignment tool can then be replaced by the slit diaphragm or star pattern and focal-spot images obtained under exactly the same geometry.

The jig is lightweight, relatively simple to use and is sufficiently versatile to enable suitable magnifications to be obtained. Effective focal-spot-size measurements using the alignment test jig have been made on a variety of different machines with satisfactory results. Further uses of the jig have arisen from regular quality-assurance work carried out in mammography, the most useful of which is the provision of a suitable platform for supporting the thin aluminium filters used in half-value layer measurements.

Conclusion

One important parameter to be measured when acceptance or routine testing the mammographic X-ray set is the effective focal-spot size. Care must be exercised when conducting such measurements to ensure the correct alignment of the object and image planes to the reference axis of the X-ray tube. The test jig described enables the necessary alignment to be obtained easily and accurately.

Acknowledgment

We thank Mr S. J. Hester for his artistry in producing the line drawings.

References

BSI, 1984. *British Standard Methods for Determining the Characteristics of Focal Spots in Diagnostic X-ray Tube Assemblies for Medical Use*, BS 6530 (BSI, London).

DHSS, 1986. *Breast Cancer Screening*. Report of a Working Group chaired by Professor Sir Patrick Forrest (HMSO, London).

——1987. *Guidance Notes for Health Authorities on Mammographic Equipment Requirements for Breast Cancer Screening*, STD/87/34 (DHSS, London).

IPSM, 1989. *The Commissioning and Routine Testing of Mammographic X-ray Systems* (IPSM, York), in press.

1989, *The British Journal of Radiology*, *62*, 487–488

Case reports

An isolated capitate fracture in a 9-year-old boy

By *W. W. Gibbon, MB, BS, FRCS and *A. Jackson, PhD, MRCP

Department of Diagnostic Radiology, Hope Hospital, Eccles Old Road, Salford M6 8HD

(*Received September 1988 and in revised form December 1988*)

Fracture of the capitate in children is rare but probably underdiagnosed. Diagnosis may require delayed radiographs or, if clinical suspicion is high, alternative investigations such as tomography or radionuclide bone scanning may be helpful. The presence of scaphoid tenderness should not reduce suspicion of a possible capitate fracture. The relatively high incidence of quite serious complications in both scaphoid and capitate fractures should alert one to the possibility of carpal bone fractures even in children.

Case report

A 9-year-old boy presented to the accident and emergency department after falling onto his outstretched right hand whilst running. On physical examination, there was tenderness and swelling over the dorsum of his right wrist with mild tenderness in the anatomical snuff box. The standard four projections used in our department (postero-anterior, lateral and two oblique views) showed no evidence of fracture. A provisional diagnosis of scaphoid fracture was made on clinical grounds and a plaster of Paris wrist cast was applied. A further series of radiographs was performed 10 days later, again with no evidence of bone injury, but in view of persisting discomfort the plaster cast was re-applied.

Radiographs performed some 24 days after injury demonstrated a fracture of the capitate, which could be seen as a band of sclerosis across the waist of the bone (Fig. 1).

Retrospective examination of the previous radiographs revealed a constant small break in the posterior cortex of the capitate on the lateral projections of both series (Fig. 2). No other associated fracture was seen in any other carpal bone.

Discussion

Review of the literature suggests that this is the youngest recorded capitate fracture, an injury which is uncommon at any age. Rand et al (1982) identified an incidence of 1.3% in 978 patients with carpal fractures treated at the Mayo clinic between 1966 and 1979. Snodgrass (1937) described 1.2% in his series of 170 cases and Bizarro (1922) 4.9% in a series of 123 carpal fractures.

Carpal bone fractures in children are even rarer than in adults and in this age group the scaphoid is the most commonly fractured carpal bone. Vahvanen and Westerlund (1980) found scaphoid fractures in 1.7% of all childhood fractures of the upper limb, whilst Mussbichler (1961) found scaphoid fractures in only 100 of 3406 children undergoing radiographic examination of the hand or wrist following trauma.

There are very few recorded cases of capitate fracture in children. Gouldesbrough (1916) described a case of fractured scaphoid and capitate in a 10-year-old boy, which was probably the first reported fracture of the capitate in a child. Anderson (1987) described an 11-year-old boy and Minami et al (1987) a 13-year-old girl

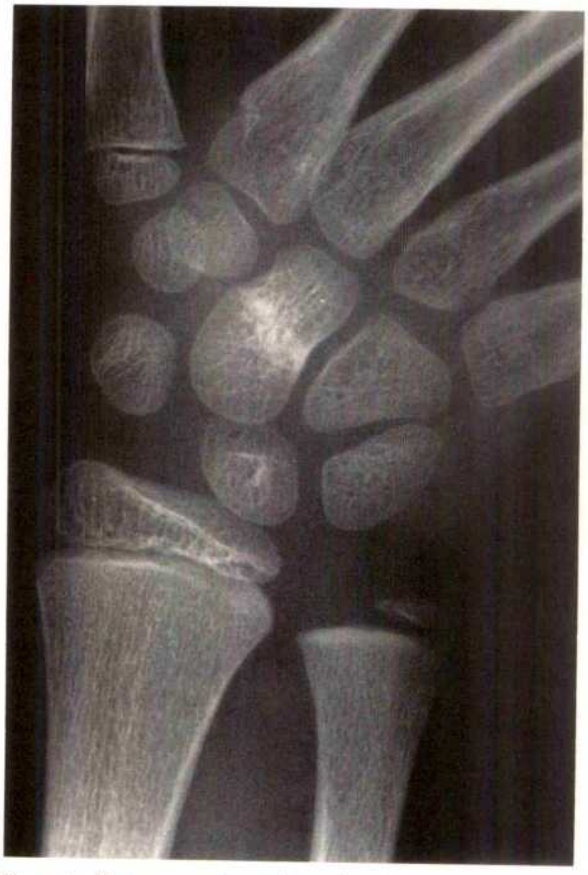

Figure 1. Postero-anterior radiograph of the carpus 24 days after initial injury showing sclerosis at the site of capitate fracture.

---

*Present address: Department of Diagnostic Radiology, North Manchester General Hospital, Delauneys Road, Crumpsall, Manchester M8 6RB.

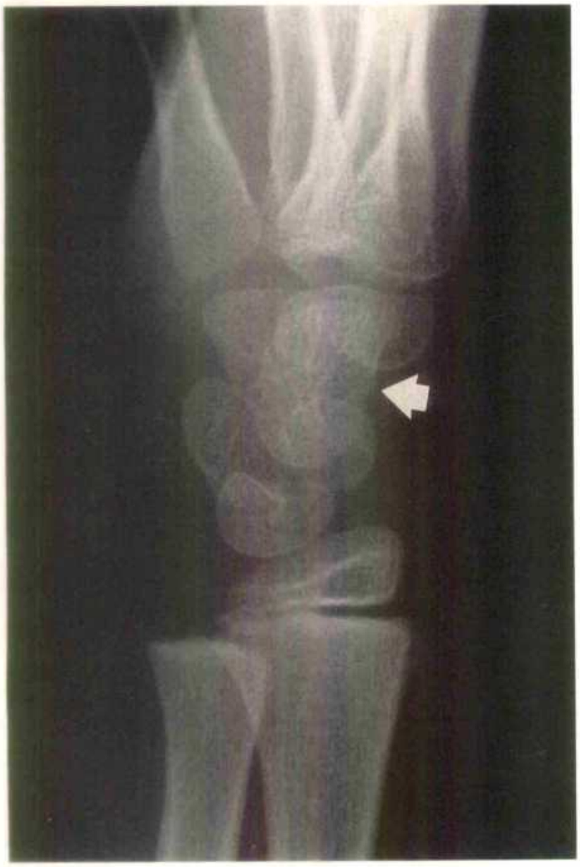

Figure 2. Oblique radiograph of the carpus at presentation showing a small cortical break in the waist of the capitate (arrowed). This was not originally diagnosed.

with scapho-capitate fracture syndrome. Young (1986) reported a 10-year-old boy with an isolated fracture of the capitate and Rand et al (1982) included a child of 11 years in his 13 adult cases.

Capitate fractures are usually divided into isolated fractures and those with associated scaphoid fracture. The fact that our patient had localized scaphoid tenderness without scaphoid fracture in combination with a fracture of the capitate implies a possible common mechanism for both patterns of injury. Capitate fractures are probably underdiagnosed and in the present case the diagnosis was not made until sclerosis started to appear at the fracture site 3½ weeks after injury. In their nine cases, Adler and Shaftan (1962) reported two fractures that were demonstrated only on re-examination and a third in which diagnosis required tomography. According to these same authors, Cave was able to demonstrate a fracture line in one case, only by radiographs made during distraction. Radionuclide bone scanning using ^{99}Tc^{m} has also been used to aid the diagnosis of carpal fractures, including fractures of the capitate, and may be helpful in suspicious circumstances (Rolfe et al, 1981).

The complication rate for capitate fractures is relatively high and the consequences serious. Non-union has been described by a number of authors, in addition to avascular necrosis, dorsi-flexion instability and capito-lunate fusion. Lowry and Cord (1981) reported a case of avascular necrosis in a 19-year-old patient with a capitate fracture, in whom the diagnosis had been missed at the time of injury 8 months previously. Rand et al (1982) presented two old and two recent non-unions in their series of 13 capitate fractures. The young are not exempt from complications and Minami et al (1987) reported a case of a 13-year-old girl with non-union of the capitate diagnosed 6 months after an initial injury, which had been treated as a sprain.

Acknowledgments

The authors are grateful to Mr S. G. W. Gough for permission to report this case.

References

Adler, J. B. & Shaftan, G. W., 1962. Fractures of the capitate. *Journal of Bone and Joint Surgery, 44A*, 1537–1547.

Anderson, W. J., 1987. Simultaneous fracture of scaphoid and capitate in a child. *Journal of Hand Surgery, 12A*, 271–273.

Bizarro, A. H., 1922. Traumatology of the carpus. *Surgery, Gynaecology & Obstetrics, 34*, 574–588.

Gouldesborough, C., 1916. A case of fractured carpal navicular and os magnum in a boy 10 years old. *Lancet, ii*, 792.

Lowry, W. E. & Cord, S. A., 1981. Traumatic avascular necrosis of the capitate bone—case report. *Journal of Hand Surgery, 6*, 245.

Minami, M., Yamazaki, J., Chisaka, N., Kato, S., Ogino, T. & Minami, A., 1987. Non-union of the capitate. *Journal of Hand Surgery, 12A*, 1089–1091.

Mussbichler, H., 1961. Injuries of the carpal scaphoid in children. *Acta Radiologica, 56*, 361–368.

Rand, J. A., Linscheid, R. L. & Dobyns, J. H., 1982. Capitate fractures. A long-term follow up. *Clinical Orthopaedics, 165*, 209–216.

Rolfe, E. B., Garvie, N. W., Khan, M. A. & Ackery, D. M., 1981. Isotope bone imaging in suspected scaphoid trauma. *British Journal of Radiology, 54*, 762–767.

Snodgrass, L. E., 1937. Fractures of the carpal bones. *American Journal of Surgery, 38*, 539–548.

Vahvanen, V. & Westerlund, M., 1980. Fracture of the carpal scaphoid in children: clinical and roentgenological study of 108 cases. *Acta Orthopaedia Scandanavia, 51*, 909–913.

Young, T. B., 1986. Isolated fracture of the capitate in a 10-year-old boy. *Injury, 17*, 133–134.

1989, *The British Journal of Radiology*, *62*, 489–490

Case reports

Distal bowel infarction following angioplasty of the internal iliac artery

By I. C. Bennett, MB, BS, FRACS, *†M. O. Downes, MB, BS, FRCR and R. E. C. Collins, MB, BS, FRCS, FACS

Departments of Surgery and *Radiology, Kent and Canterbury Hospital, Canterbury, Kent CT1 3NG

(*Received October 1988*)

Percutaneous transluminal angioplasty is becoming more widely used, finding clinical application not only in peripheral vascular occlusion (Zeitler et al, 1983; Doubilet & Abrams, 1984), but also in renovascular hypertension (Levin, 1984) and coronary artery disease (Levin et al, 1985).

While success rates, particularly for peripheral vascular disease, are in the order of 90% (Katzen, 1984; Gardiner et al, 1986), there is a definite morbidity with complications occurring in about 2–5% of cases (Gardiner et al, 1985, 1986). We report a case in which angioplasty of the internal iliac artery was complicated by infarction of the distal bowel, as a consequence of previously impaired mesenteric blood flow due to radiotherapy.

Case report

A 70-year-old man presented with a history of increasing left buttock claudication over a 2-year period. He had a past history of a transitional cell carcinoma of the bladder, which had been treated 4 years previously by partial cystectomy and pelvic irradiation. He gave a precise history of left buttock pain brought on by walking 300 yards, which was relieved by rest. He admitted to being a heavy smoker for most of his life.

No tenderness or mass was evident on abdominal palpation or rectal examination. Both femoral pulses were present; in the right leg pulses were palpable to the level of the ankle, but in the left leg no distal pulses could be felt. The left buttock pain, therefore, appeared ischaemic in nature, but in view of the past history of bladder cancer, pelvic computed tomography (CT) was performed, which revealed no evidence of pelvic malignancy. A right transfemoral aorto-bifemoral arteriogram confirmed the presence of stenosis at the origin of the left internal iliac artery (Fig. 1). This was considered to be the most likely cause of his buttock pain, and it was felt that balloon dilatation angioplasty was the most appropriate method of dealing with it.

The catheter was introduced via the right femoral artery and the origin of the left internal artery was dilated to 8 mm (Fig. 2). No difficulty was encountered in performing the procedure. On the following day, the patient felt nauseated and generally unwell, but by the second day he was comfortable and pain-free. He was discharged home and had no further buttock pain even on exercise.

Nine days following the angioplasty the patient was re-admitted with vomiting and lower abdominal pain. On examination he was tender with guarding across the hypogastric area. He was afebrile and the white cell count was $10 \times 10^9/1$, but a plain abdominal radiograph showed free intraperitoneal gas. At laparotomy, the lower sigmoid colon and upper rectum were found to be infarcted and perforated and adherent to the pelvis. A sigmoid colectomy and Hartmann's procedure was performed with formation of an end-colostomy and oversewing of the rectal stump. His post-operative course was uneventful and he was discharged 8 days following surgery. Histology of the resected specimen confirmed the presence of necrotic large bowel, with no evidence of malignancy. At follow-up 1 month later, he was well, his colostomy was healthy and he remained free of his former buttock pain.

Discussion

The mechanism of infarction of the rectosigmoid colon in this patient probably resulted from a thrombo-embolic event occurring in the middle rectal arterial system, in the presence of an already tenuous inferior mesenteric arterial tree compromised by previous irradiation. A better understanding is achieved on reviewing the arterial anatomy of the region (Last, 1978).

The blood supply to the lower sigmoid colon and rectum essentially comes from two sources: the inferior mesenteric artery, which arises from the lower abdominal aorta, and the middle rectal arteries, which arise bilaterally from the internal iliac arteries. The inferior mesenteric artery supplies sigmoid branches to the distal colon and then continues on as the superior rectal artery, which supplies the mucous membrane of the rectum, continuing as far down as the

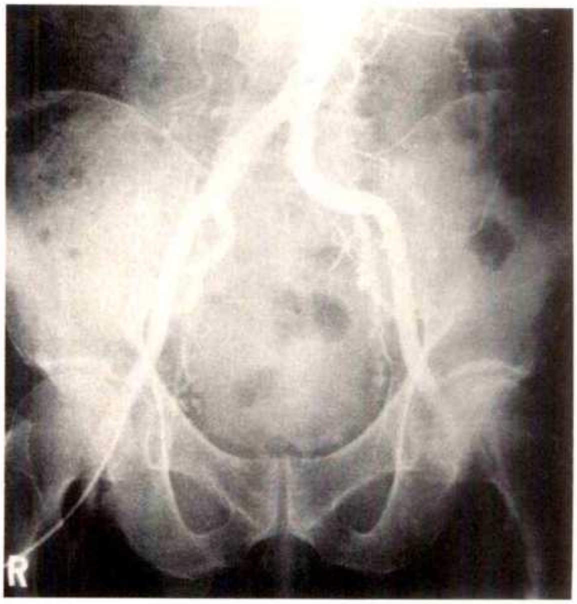

Figure 1. Aortogram showing left internal iliac artery origin stenosis and small inferior mesenteric artery branches.

---

†Author for correspondence.

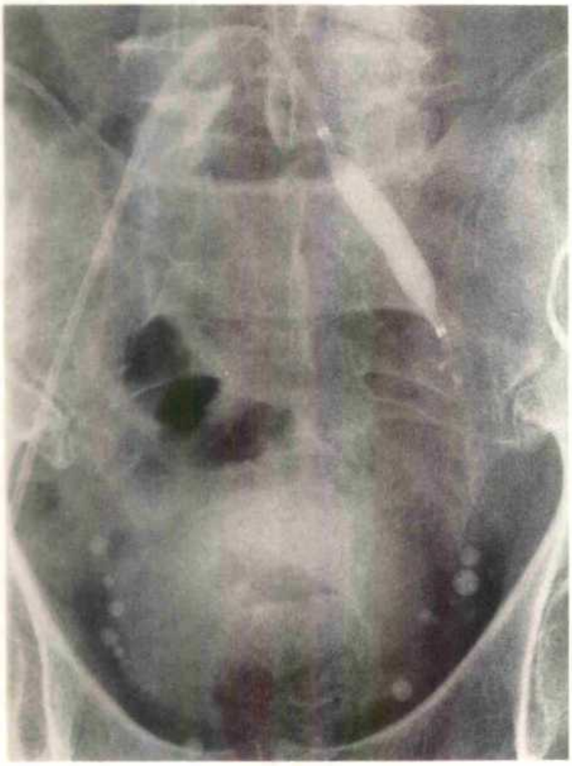

Figure 2. An 8 mm balloon is inflated in the proximal internal iliac artery from a contralateral approach.

mucocutaneous junction of the anal canal. The internal iliac artery divides in the pelvis into a small posterior division, one of whose branches is the superior gluteal artery, and a larger anterior division that has both parietal branches (including inferior gluteal artery) and visceral branches (including the middle rectal arteries). The middle rectal arteries provide blood supply to the muscular coat of the rectum. There is usually considerable overlap and intercommunication between the branches of the superior rectal system and the middle rectal vessels within this distal segment of gut.

In this patient, however, the arterial supply to the distal bowel had obviously been greatly compromised by the previously administered radiotherapy, and in particular, the inferior mesenteric artery had been severely narrowed, as seen on review of the arteriogram (Fig. 1). Blood supply to the rectosigmoid junction was therefore precariously balanced between the compromised flow from the inferior mesenteric artery and the supportive collateral flow from the middle rectal arteries. The angioplastic procedure to the internal iliac artery, while successfully improving gluteal blood flow, was complicated by a vascular event, either thrombotic or embolic, which resulted in occlusion of the left middle rectal artery. This produced a decompensation in the blood flow to the rectosigmoid junction as the blood supply from the inferior mesenteric artery was insufficient to maintain viability of the bowel. It is unlikely that a similar event occurred in the inferior mesenteric artery as the angioplasty catheter did not venture near its origin during the procedure.

Percutaneous transluminal angioplasty of stenotic or occluded arteries is becoming an increasingly successful method of treating patients with peripheral vascular disease (Zeitler et al, 1983; Doubilet & Abrams, 1984) and is gaining acceptance as the treatment of choice in many clinical situations as complication rates decrease and results improve. The primary angiographic success rate for angioplasty is now in the order of 92–97% for the iliac arteries and 80–85% for the femoral and popliteal arteries (Katzen, 1984; Gardiner et al, 1985, 1986). Apart from the more common puncture site complications (usually haematomas), serious complications include thrombosis, embolism, arterial dissection, false aneurysm formation, arterio-venous fistula and arterial spasm (Gardiner et al, 1985, 1986). The incidence of thrombo-embolic complications is approximately 2% overall.

While infarction of bowel following angioplastic procedures at or near the origin of mesenteric arteries is not unfamiliar (Perry, 1985), bowel ischaemia following dilatation of a pelvic vessel is certainly unexpected, but is obviously a complication that must be borne in mind in the presence of previous irradiation. We know of no other similar cases previously reported.

References

Doubilet, P. & Abrams, H. L., 1984. The cost of underutilization: percutaneous transluminal angioplasty for peripheral vascular disease. *New England Journal of Medicine*, *310*, 95–101.

Gardiner, G. A., Meyerovitz, M. F. & Harrington, D. P., 1985. Dissection complicating angioplasty. *American Journal of Roentgenology*, *145*, 627–631.

Gardiner, G. A., Meyerovitz, M. F., Stokes, K. R., Clouse, M. E., Harrington, D. P. & Bettmann, M. A., 1986. Complications of transluminal angioplasty. *Radiology*, *159*, 201–208.

Katzen, B. T., 1984. Percutaneous transluminal angioplasty for arterial disease of the lower extremities. *American Journal of Roentgenology*, *142*, 23–25.

Last, R. J., 1978. *Anatomy: Regional and Applied*, 6th edn (Churchill Livingstone, Edinburgh).

Levin, D. C., 1984. Percutaneous transluminal angioplasty of the renal arteries. *Journal of the American Medical Association*, *251*, 759–763.

Levin, D. C., Boxt, L. M., Abben, R., Garnic, J. D., Kirschenbaum, J. D., Adler, D., Shook, T., Friedman, P. & Ganz, P. 1985. Segmental balloon technique in angioplasty of severe coronary obstruction. *American Journal of Cardiology*, *56*, 789–791.

Perry, M. O., 1985. Intramural dissection of superior mesenteric artery: a complication of attempted renal artery balloon dilatation. *Journal of Vascular Surgery*, *2*, 480–484.

Zeitler, E., Richter, E., Roth, F. J. & Schoop, W., 1983. Results of percutaneous transluminal angioplasty. *Radiology*, *146*, 57–60.

1989. *The British Journal of Radiology*, 62, 491–494

Case reports

Atypical radiological features of β-glucuronidase deficiency (mucopolysaccharidosis VII) occurring in an elderly patient from an inbred kindred

By S. Chapman, MRCP, FRCR, *R. G. F. Gray, BSc, MSc, PhD, †T. J. Constable, FRCP(Ed) and ‡S. Bundey, FRCP

Departments of Radiology and *Clinical Chemistry, The Children's Hospital, Birmingham, †Department of Medicine, The Manor Hospital, Walsall and ‡Clinical Genetics Unit, Birmingham Maternity Hospital

(*Received October 1988*)

Sly et al (1973) described the first patient with mucopolysaccharidosis VII and concluded that the condition was autosomal recessive in view of the profound deficiency of β-glucuronidase in the affected patient and intermediate levels in his parents. The classical clinical picture consists of mental retardation, failure to thrive, hepatosplenomegaly, macrocephaly, dysostosis multiplex and inconstant corneal clouding. However, this can vary as shown by the further 20 patients (Bernsen et al, 1987) described since 1973. For example, two patients have died in the neonatal period with hydrops, while three adult patients have been asymptomatic. In addition, one sister, clinically affected like her two siblings, had a level of β-glucuronidase that was in the heterozygote range (Bernsen et al, 1987) so that even the enzyme levels do not correlate with the clinical picture.

Case report

This patient, now 37 years old, was born in Pakistan, and came to this country in 1984. Deformed feet were noticed at birth and he did not walk until the age of 7 years. His height was normal as a child, but as he aged, short stature became apparent and the joints of his hands became swollen. He has had two herniorrhaphies; he is not deaf nor has he had attacks of rhinitis.

On examination, he is severely mentally retarded, is very short (height 144 cm) and has a large head (90th centile) and coarse facial features (Fig. 1a). His short stature is associated with a short trunk, (upper/lower segment ratio 0.75) and the arm span is equal to height. He has a lumbar kyphosis, slight scoliosis and a small pectus excavatum. His hands are short (19 cm) and metacarpals and proximal interphalangeal joints are swollen (Fig. 1b); however, the joints of his wrists and hands are fully mobile. There is limited elevation of shoulders and extension of knees but full movement of neck, elbows and hips. The feet are short (19 cm) and very wide (13 cm) with varus deformity (Fig. 1c). There is no oedema; the skin is soft and the liver is palpable for two finger breadths. There are no abnormal neurological signs. He has recently developed a cataract in the right eye but the corneae are clear.

There are no similarly affected relatives. He has three younger siblings who are healthy. His parents are first cousins and both sets of grandparents are consanguineous, giving an inbreeding coefficient between 0.0781 and 0.0937.

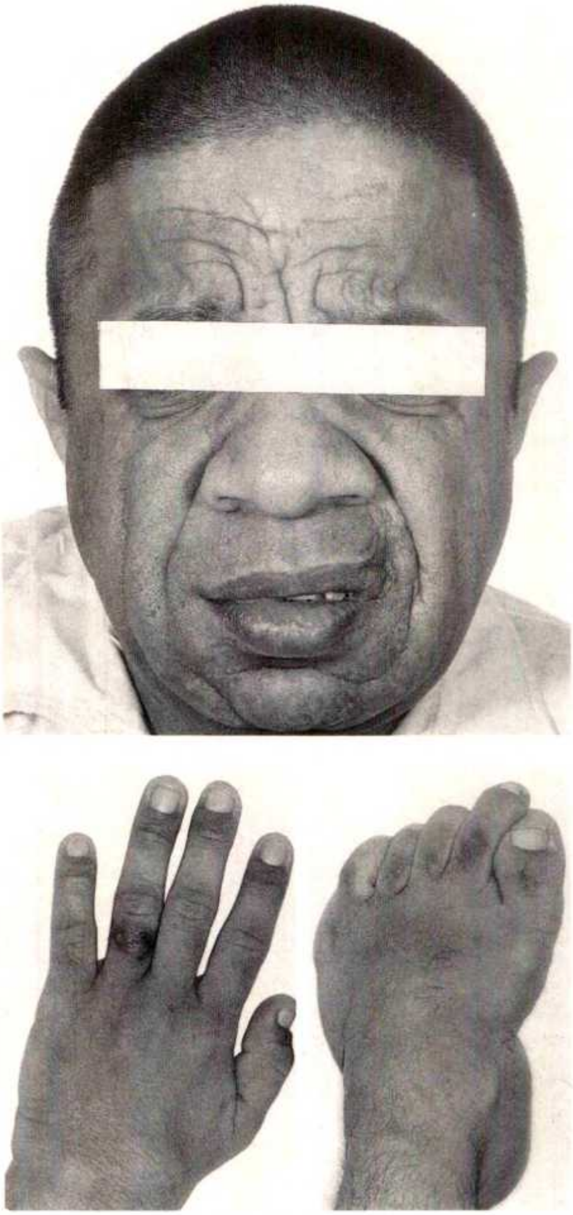

Figure 1. Photographs of the face, left hand and left foot of the patient.

Address correspondence and reprint requests to Dr S. Chapman, Department of Radiology, The Children's Hospital, Ladywood Middleway, Birmingham B16 8ET.

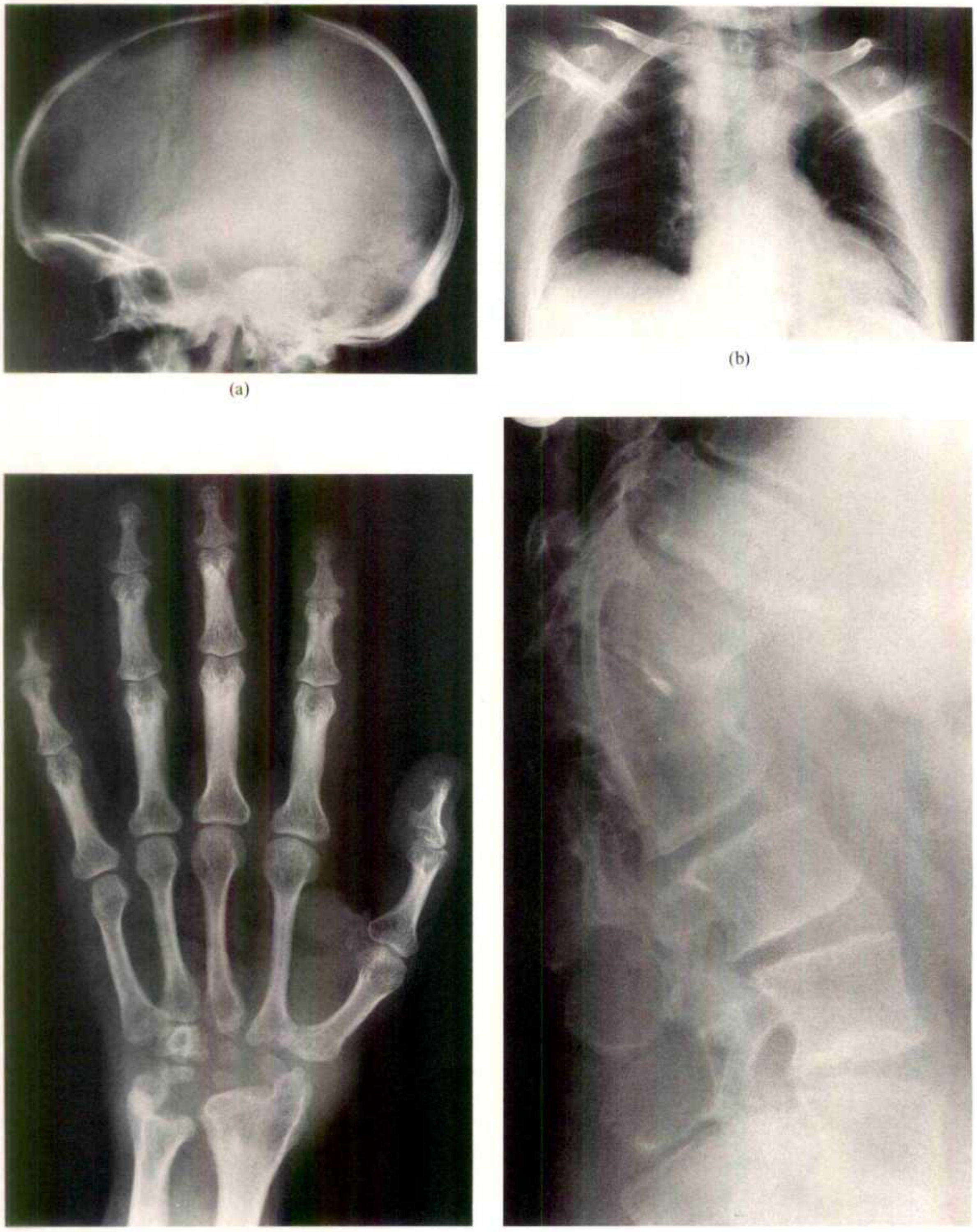

(a)

(b)

(c)

(d)

Figure 2. Radiographs of (a) the skull, showing a ballooned pituitary fossa and open sutures; (b) chest and shoulder girdles (note shallow glenoid fossae); (c) hand, showing short metacarpals and small irregular carpal bones; (d) spine; (e) pelvis (there is contrast medium in the bladder); and (f) foot. (g) A CT slice through the head at the level of the pituitary fossa.

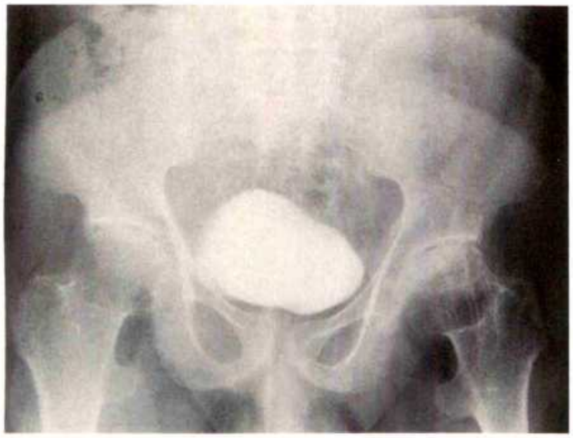

(e)

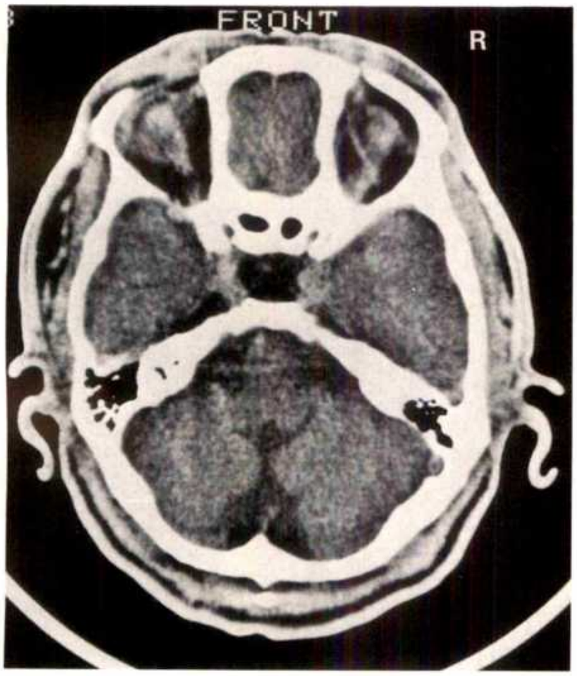

(g)

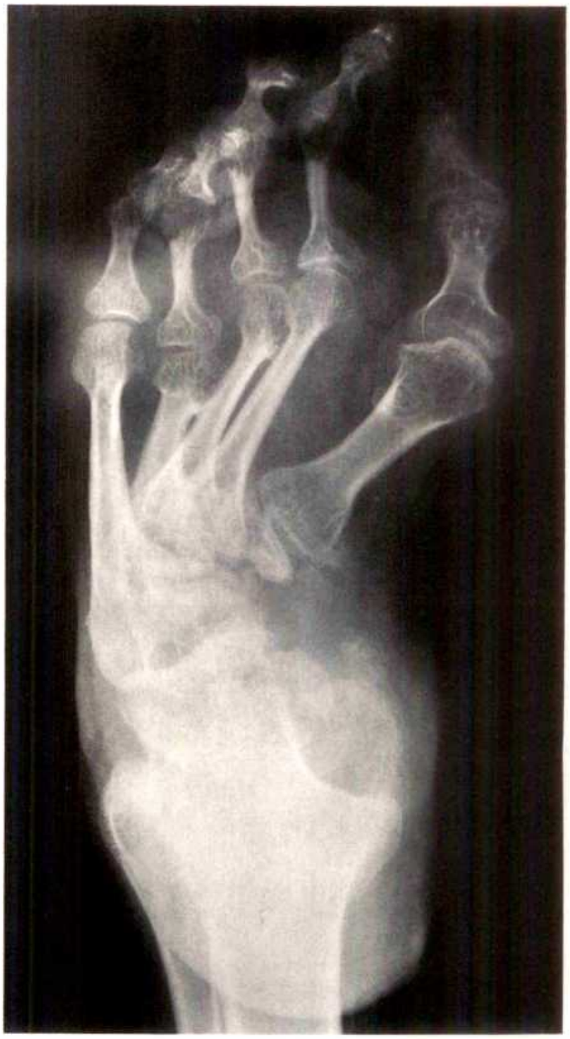

(f)

Biochemical investigations

Thyroid function tests revealed normal values for serum T4, T3-binding and free-T4 index. Serum testosterone, follicle stimulating hormone and testosterone stimulating hormone concentrations were also normal.

Two-dimensional cellulose acetate membrane electrophoresis of alcian blue precipitated urinary glycosaminoglycans revealed an abnormal spot partially co-migrating with chondroitin sulphate. This may have been the partially degraded dermatan sulphate reported to be excreted in this disorder (Pfeiffer et al, 1977). Urinary uronic acid concentrations were normal for age.

Assay of β-glucuronidase using 4-methylumbelliferyl-β-D-glucuronide revealed a gross deficiency of activity in leukocytes (patient 2.6; normal range 177–811 mU/U hexosaminidase) and cultured fibroblasts (patient 0.4; normal range 12–38 mU/U hexosaminidase).

Radiological features (Fig. 2)

Skull. The pituitary fossa is ballooned and the lamina dura eroded. The sutures remain open.

Spine. The body of D12 is hypoplastic anteriorly producing a gibbus and is associated with a mild scoliosis. There is posterior scalloping of the lumbar vertebral bodies but no anterior beaking or end-plate irregularity. There is no odontoid hypoplasia.

Chest. The ribs are not abnormally wide. The glenoid fossae are rather shallow.

Pelvis. The proximal left femur is osteoporotic and the femoral head is flattened, although the hip joint space is preserved, suggestive of a previous inflammatory arthropathy.

Limbs. The long bones and metacarpals show overtubulation but the hand phalanges are normally tubulated. The metacarpals are not pointed proximally. Metacarpophalangeal pattern profile analyis (Fig. 3) reveals shortening of the metacarpals and thumb distal phalanx. The carpal and tarsal bones are small and irregular. The 4th metatarsals are short.

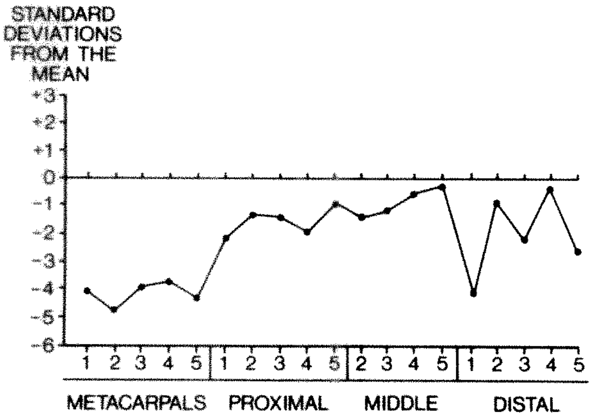

Figure 3. Metacarpophalangeal pattern profile of the left hand showing relative shortening of the metacarpals and thumb distal phalanx.

Computed tomography of the head. This shows the enlarged pituitary fossa to be due to an empty sella with only a small amount of pituitary tissue identifiable. There is mild dilatation of the entire ventricular system. The skin and subcutaneous tissues show marked thickening.

Discussion

This patient differs from others with β-glucuronidase deficiency in that his severe mental retardation, short stature and abnormal appearance indicate severe affection, yet he has no corneal clouding and the radiological changes are unusual. Dysostosis multiplex, the spectrum of radiological signs that characterize the mucopolysaccharidoses, has been recorded in 17 of the 21 previous cases, but this case does not fulfill all the appropriate criteria. Indeed, the initial radiological diagnosis was that of untreated cretinism, until the finding of normal thyroid function. He has some features of dysostosis multiplex (posterior scalloping of vertebral bodies, shallow glenoid fossae and small, irregular carpal bones) but his overall appearance is most atypical. The metacarpophalangeal pattern profile does resemble that seen in other mucopolysaccharidoses where there is relatively greater shortening of metacarpals and, occasionally, of the thumb distal phalanx (Poznanski, 1984) demonstrating the value of this means of assessment.

The great variation in clinical manifestation makes it likely that some patients are heterozygous for different allelic mutations of the structural locus for β-glucuronidase deficiency on chromsome 7 (Francke, 1976), a situation akin to that found with Hurler-Scheie disease. This suggestion of multiallelism would explain why there have only been two previous reports of parental consanguinity, in contrast to the high level of parental consanguinity expected with a rare homozygous recessive disease. However, the patient reported here must represent a homozygous condition, since he comes from an inbred family. It will be interesting to see whether further similar patients are found among British Pakistanis.

Alternatively, the clinical variability may reflect variations in the residual activity of the deficient enzyme. Since assays are often performed with artificial substrates, these residual activities may not reflect the true *in vivo* activity of the enzyme. A further complication is that regulatory loci for this enzyme have been identified in mice (Paigen et al, 1979) and mutations here could well influence clinical and biochemical manifestations.

Acknowledgments

We are grateful to Dr I. M. Sardharwalla of the Willink Biochemical Genetics Unit at the Royal Manchester Children's Hospital for help in confirming the biochemical diagnosis and to Miss Kathleen Snow and the Department of Medical Illustration, Birmingham Children's Hospital.

References

Bernsen, P. L. J. A., Wevers, R. A., Gabreels, F. J. M., Lamers, K. J. B., Sonnen, A. E. H. & Stekhaven, J. H. S., 1987. Phenotypic expression in mucopolysaccharidosis VII. *Journal of Neurology, Neurosurgery and Psychiatry, 50,* 699–703.

Francke, U., 1976. The human gene for β-glucuronidase is on chromosome 7. *American Journal of Human Genetics, 28,* 357–362.

Paigen, K., Labarca, C. & Watson, G., 1979. A regulatory locus for mouse β-glucuronidase induction, Gur, controls messenger RNA activity. *Science, 203,* 554–556.

Pfeiffer, R. A., Kresse, H., Baumer, N. & Sattinger, E., 1977. Beta-glucuronidase deficiency in a girl with unusual clinical features. *European Journal of Pediatrics, 126,* 155–161.

Poznanski, A. K., 1984. *The Hand in Radiologic Diagnosis,* 2nd edn (W. B. Saunders, Philadelphia), pp. 496–505.

Sly, W. S., Quinton, B. A., McAllister, W. H. & Rimoin, D., 1973. Beta glucuronidase deficiency: report of clinical, radiologic and biochemical features of a new mucopolysaccharidosis. *Journal of Pediatrics, 82,* 249–257.

1989, *The British Journal of Radiology*, *62*, 495–496

Case of the month

The warm and tender hip

By Stephen H. Lee, MB, FRCS, FRCR

Department of Imaging, The Middlesex Hospital, Mortimer Street, London W1

(*Received March 1988 and in revised form May 1988*)

An 18-year-old white woman presented with left-sided low back pain of 9 months duration. Physical examination revealed a warm, tender area over the left sacro-iliac joint. There was wasting of the ipsilateral quadriceps femoris muscle and limitation of hip movements because of pain. The patient was apyrexial. Investigations revealed a haemoglobin of $12.4\,g\,dl^{-1}$, a white cell count of $7.9 \times 10^9\,l^{-1}$, an erythrocyte sedimentation rate (ESR) of $33\,mm\,h^{-1}$ and an alkaline phosphatase of $341\,i.u.\,l^{-1}$. A radiograph of the pelvis (Fig. 1) and computed tomography (CT) (Fig. 2) were performed.

What is the abnormality and the differential diagnosis? How would one proceed with further management?

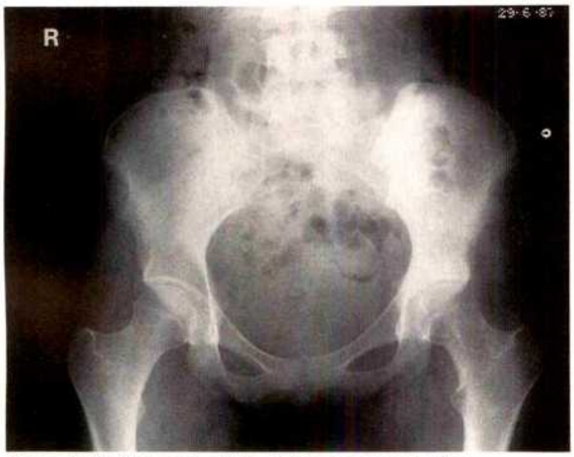

Figure 1. Radiograph of the pelvis on presentation.

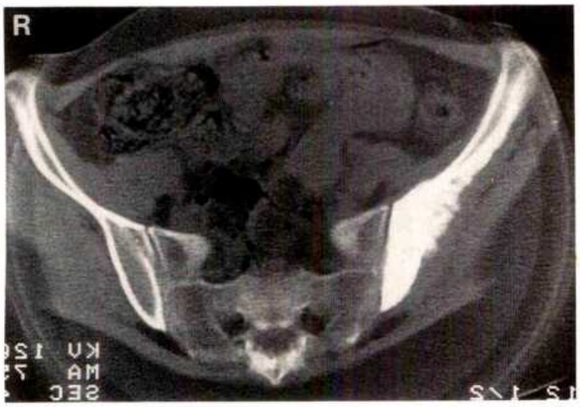

Figure 2. A CT scan of the upper pelvis on presentation.

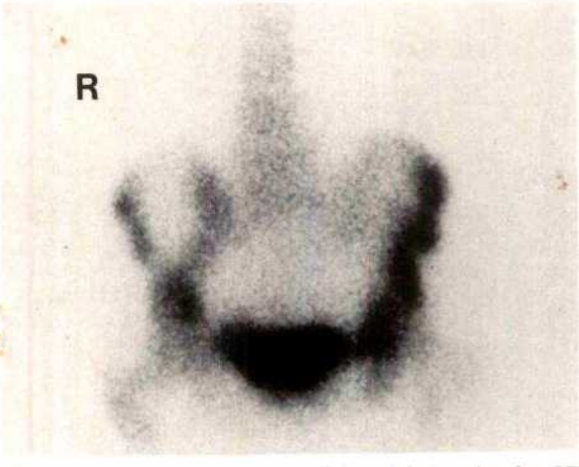

Figure 3. Radionuclide bone scan of the pelvis 8 weeks after CT scan. Supine view showing increased uptake over left anterior iliac bone.

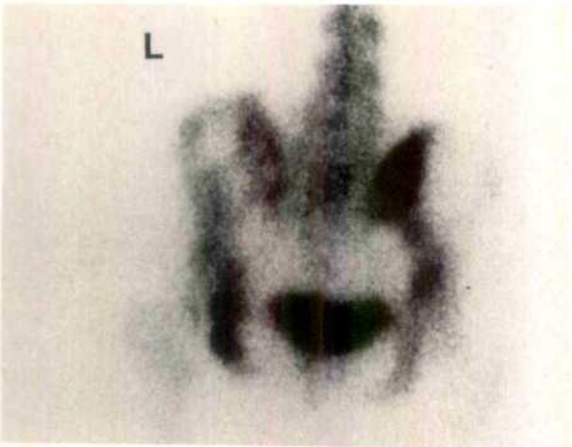

Figure 4. Prone view showing increased uptake in the metastasis over the right posterior sacro-iliac joint.

The plain radiograph shows diffuse sclerosis adjacent to the left sacro-iliac joint and the CT scan also shows widespread sclerosis, a spiculated periosteal reaction and wasting of the left iliopsoas and gluteal muscles. These appearances could be caused by a Brodie's abscess, primary bone tumour or a lymphoma. There was no evidence elsewhere of lymphadenopathy, and the patient was apyrexial, so that a primary bone tumour seemed most likely. An open bone biopsy was performed, and it was noted that there was new bone completely replacing the medullary cavity and extensive periosteal new bone. Bacteriology showed no growth of organisms.

Histological examination with haematoxylin and eosin stain showed marrow replacement with malignant round cells, the majority of which had undergone necrosis. Glycogen granules positive to periodic acid–Schiff stain were present in some cells, which helped confirm the diagnosis of Ewing's sarcoma. Lymphoma markers were not detectable.

A radionuclide bone scan was done to look for other lesions or metastases and a chest radiograph should also be done with CT of the chest if no metastases are seen. The bone scan was performed 8 weeks following the initial CT and showed an increased uptake of ^{99}Tc^{m} on the left side of the pelvis on the supine view (Fig. 3), and the postero-inferior aspect of the right ilium on the prone view (Fig. 4). A further radiograph of the pelvis at that time showed a sclerotic area in the right side of the pelvis conforming to the area of increased uptake on the bone scan. There were no other abnormalities present. Magnetic resonance imaging confirmed the bilateral iliac bone involvement and soft-tissue extension on the left side, but added no other useful information.

Discussion

Ewing's sarcoma represents 10% of all primary malignant bone tumours and is seen in patients aged 3 to 25 years. It typically presents with an area of permeative destruction and a variable amount of surrounding reactive sclerosis. The appearances may be similar to those of osteomyelitis. The pelvis is the second commonest site after the femur where it tends to occur in the diaphysis. In the upper age range, as in this patient, there is an increase in the incidence of Ewing's tumour occurring in flat bones because of the relative increase in red marrow in these sites. A periosteal reaction is present in most cases. In the series of 372 cases in the Intergroup Ewing's Sarcoma Study (IESS), 56.6% had a laminated periosteal reaction and 27.7% had a spiculated periosteal reaction, the latter being vertically orientated and unlike the "sunburst" appearance typical of osteosarcoma (Reinus & Gilula, 1984).

Diffuse sclerosis in Ewing's sarcoma is an increasingly recognized feature. It was found in 10% of cases in an early series (Sherman & Soong, 1956). In a later series it was seen in 27% of cases (Lombardi et al, 1979). More recently, the incidence of diffuse sclerosis in the large series collected by the IESS was 37.6%, with 57% of pelvic tumours showing this feature. Sclerosis alone was seen in only two cases out of a total of 210.

Systemic symptoms occur as a result of necrosis within the tumour, resulting in general malaise and raised ESR. There may be fever, normochromic anaemia and raised white cell count. Computed tomography of the primary lesion shows the extent of periosteal new-bone formation, tumoral reactive sclerosis, cortical invasion and tumour infiltration into soft tissues (Vanel et al, 1982). Magnetic resonance imaging is superior to CT for showing marrow infiltration and soft-tissue extension and has replaced CT in many centres in the United States for the assessment of operability (Boyko et al, 1987). However, unlike CT, MRI cannot show cortical destruction, and both periosteal new bone and reactive sclerosis are more difficult to assess with this technique.

Acknowledgments

I would like to thank Dr A. Jelliffe for his permission to report this case and Dr A. Coral for his help and advice.

References

BOYKO, O. B., CORY, D. A., COHEN, M. D., PROVISOR, A., MIRKIN, D. & DE ROSA, G. P., 1987. MR imaging of osteogenic and Ewing's sarcoma. *American Journal of Roentgenology*, *148*, 317–322.

LOMBARDI, F., GASPARINI, M., GIANNI, C., PETRILLO, R., TESORO-TESS, J. D., VOLTERRANI, F. & MUSUMERI, R., 1979. Ewing's sarcoma: an approach to radiologic diagnosis. *Tumori*, *65*, 389–399.

REINUS, W. R. & GILULA, K. A., 1984. Radiology of Ewing's sarcoma: Intergroup Ewing's Sarcoma Study (IESS). *Radiographics*, *6*, 929–944.

SHERMAN, R. S. & SOONG, K. W., 1956. Ewing's sarcoma: its roentgen classification and diagnosis. *Radiology*, *66*, 529–539.

VANEL, D., CONTESSO, G., COUANET, D., PIEKARSKI, J. D., SARAZIN, D. & MASSELOT, J., 1982. Computed tomography in the evaluation of 41 cases of Ewing's sarcoma. *Skeletal Radiology*, *9*, 8–13.

1989. *The British Journal of Radiology*, *62*, 497–498

Correspondence

(The Editors do not hold themselves responsible for opinions expressed by correspondents)

Splenic accumulation of ^{99}Tc^{m}-methylene diphosphonate

THE EDITOR—SIR,
The case reported by McHugh et al (1988) refers to their interesting observation that in a patient with chronic lymphocytic leukaemia, complicated by a Coombs-positive haemolytic anaemia, 99Tcm-MDP (methylene disphosphonate), a bone scanning agent, was selectively concentrated in the spleen.

This selective concentration was attributed to a large deposition of predominantly extracellular iron in the spleen, as shown at autopsy. It occurred to us that it would be of interest to add that we have observed a case of transient splenic uptake of 99Tcm-MDP had disappeared. Therefore, it Hodgkin's disease and haemolytic anaemia (Alevizaki et al, 1982).

In our case, the ^{99}Tc^{m}-MDP accumulation in the spleen was associated with the haemolysis, as a repeat bone scan 3 months later, when the Coombs test was negative, showed that the splenic uptake of ^{99}Tc^{m}-MDP had disappeared. Therefore, it seem possible that newly liberated iron from red cell destruction has a higher affinity for ^{99}Tc^{m}-MDP than other forms of iron. The accumulation of diphosphonates in haemosiderosis, although not unknown, is not common (Brill, 1981). It is of course probable that other factors, except for the active haemolysis and/or the iron load of the spleen, might contribute to the splenic affinity for accumulation of disphosphonates, such as ^{99}Tc^{m}-MDP.

Yours, etc.,
C. ALEVIZAKI
E. GEORGIOU
E. NIKIFORAKIS
C. PROUKAKIS

Department of Medical Physics,
School of Medicine,
Athens University,
Goudi, Athens,
Greece 11527

(*Received November 1988*)

References

ALEVIZAKI, C. C., GEORGIOU, E., NIKIFORAKIS, E. & PROUKAKIS, C., 1982. Transient splenic uptake associated with haemolysis. *European Journal of Nuclear Medicine*, *7*, 510–512.

BRILL, A., 1981. Radionuclide imaging of non-neoplastic soft tissue disorders. *Seminars in Nuclear Medicine*, *11*, 277–288.

MCHUGH, K., LEE, D. M. & BATTY, V. B., 1988. Splenic acculation of technetium 99m in chronic lymphocytic leukaemia. *British Journal of Radiology*, *61*, 957–959.

A pressure valve for pneumatic reduction of intussusception

THE EDITOR—SIR,
The pneumatic reduction of ileocolic intussusception in childhood has been attracting increasing attention of late (Miles, 1988; Paes et al, 1988). The problem of finding a system to limit and monitor safely the air pressure used has been solved in as many ways as there are radiologists doing the procedure.

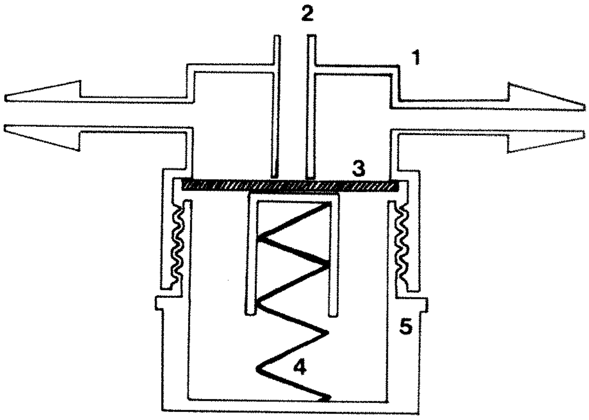

Figure 1. Diagramatic representation of the pressure valve. 1, main air chamber; 2, central vent port; 3, rubber diaphragm; 4, spring; 5, spring housing.

Your readers may be interested in the system we use in the Royal Alexandra Hospital for Sick Children, Brighton. This is a small valve (2.5 inches in length) designed for dialysis equipment (Fig. 1). It comprises a cylindrical main air chamber with two main ports and a central vent port. The base of the chamber is a rubber diaphragm, which is held against the vent port by a spring. When pressure in the main chamber exceeds that exerted on the diaphragm by the spring, the diaphragm is pushed outwards allowing air to escape through the vent port until the pressure equalizes, when the diaphragm again occludes the vent port. The spring supplied is stronger than required, but by replacing it, or by a little judicious clipping down, the valve can be made to vent at around 100 mmHg. The spring housing is screwed to the main housing and thus some adjustment of spring tension and therefore the vent pressure can be achieved by tightening or loosening as required.

A simple puffer as used in double-contrast enemas is attached to one main port and a sphygmomanometer pressure gauge attached to the other. The valve is calibrated at each use. The pressure gauge is subsequently replaced by tubing/catheter to the patient and reduction commenced. Continuous pressure monitoring during reduction is possible via a T-junction on the outlet side.

We find this system safe, reliable and extremely simple to use. It costs approximately £14.00 and is re-usable since it should remain uncontaminated by body fluids. We would be happy to supply full details to anyone interested.

Yours, etc.,
IAN J. KENNEY
*JOHN E. LUTKIN

X-ray Department,
Royal Alexandra Hospital,
Dyke Road,

Brighton,
East Sussex, BN1 3JN and
*Department of Medical Physics,
Royal Sussex County Hospital,
Brighton, East Sussex, BN2 1HA
(*Received December 1988*)

References

MILES, S. G., 1988. Pneumatic reduction of ileocolic intussusception in children. *Paediatric Radiology, 18*, 3–5.
PAES, R. A., HYDE, I. & GRIFFITHS, D. M., 1988. The management of intussusception. *British Journal of Radiology, 61*, 187–189.

"Out-of-hours" radiography

THE EDITOR—SIR

I agree fully with the statements of Clarke and Adams (1988) in their recent paper. However, the cause of so-called unnecessary X-ray examinations being requested, especially those performed "out-of-hours", is not only due to lack of consideration and the craze for completeness, but also stimulated by the fear that if a necessary investigation is omitted because of lack of clinical experience on the part of the doctor making the request, there may be fear of litigation following a mistaken diagnosis. This difficulty can only be avoided if a consultant and/or very experienced senior registrar is responsible for the clinical service, especially in an Accident & Emergency Department.

Finally, the excessive and sometimes unnecessary use of X-ray examinations reported by Clarke and Adams is an international "disease" debated around the world. However, all this discussion seems to have had no obvious effect on resolving the problems.

Yours, etc.,
H-J. MAURER

Im Wiesental 3, D-8990 Lindau,
Federal Republic of Germany
(*Received December 1988*)

Reference

CLARKE, J. A. & ADAMS, J. E., 1988. A critical appraisal of "out-of-hours" radiography in a major teaching hospital. *British Journal of Radiology, 61*, 1100–1105.

The cost of imaging procedures

THE EDITOR—SIR

Dr Jeans (1989) is of course quite right to draw attention to the benefits as well as the possible harm resulting from diagnostic radiology. But why bring in money? Before anything can be priced it must first be defined and if possible measured, *e.g.* how often does radiology enable the correct treatment to be given, how many operations are avoided, what proportion of lives are prolonged by correct diagnosis and how is their quality enhanced? These questions are difficult enough to answer but at least there is sufficient progress to believe that, at least in principle, answers do exist. Such questions present a permanent challenge to radiology and surely it is the job of professional radiological scientists to attempt to answer them.

Only after having estimated the benefit can one begin to think about the financial value to be attached to it. This, however, is a task for society as a whole, not just for professionals. We know that in some societies life is relatively cheap, in others expensive, even sacrosanct. Despite such uncertainties, if we would provide the best measures we can of both benefit and detriment, that would at least lay a rational basis upon which society could set its priorities.

I might add that these observations apply equally to both the diagnostic and the therapeutic branches of radiology.

Yours, etc.,
M. J. DAY

Claremont Cottage, Claremont Street,
Newcastle upon Tyne NE2 4AJ
(*Received February 1989*)

Reference

JEANS, W. D., 1989. The cost of imaging procedures. *British Journal of Radiology, 62*, 194.

1989. *The British Journal of Radiology*, *62*, 499–503

Proceedings of The British Institute of Radiology

Paediatric nuclear medicine

Abstracts of papers presented at the above meeting held at The British Institute of Radiology, 36 Portland Place, London W1N 4AT on Wednesday, November 23, 1988

Session 1

Chairman: Dr A. M. Peters

The value of nuclear medicine in renal disease, by T. M. Barratt
Dynamic renal scintigraphy, by A. Piepsz
Dimercaptosuccinic acid static renal scintigraphy in children, by S. T. Meller
Radionuclide cystography, by M. N. Maisey and S. J. Chapman
Transitional nephrology: the role of radionuclide scanning, by I. Gordon
Ante-natal hydronephrosis: is there an obstruction?, by P. G. Ransley. Abstract not received
The role of ^{99}Tc^{m}-DTPA scans: a prospective study, by A. Piepsz

The value of nuclear medicine in renal disease

T. M. Barratt
Department of Paediatric Nephrology, Institute of Child Health, London

The forte of nuclear medicine is quantitation: it is the numbers, not the images, that count. Radioisotopic techniques are particularly well suited to the estimation of renal function. Glomerular filtration rate (GFR) can be easily estimated from the plasma clearance of solutes such as ^{51}Cr-EDTA that are rapidly distributed in the extracellular fluid (ECF) and cleared by glomerular filtration. Single exponential analysis carries a systematic error (the Chantler "fudge factor"), but is very reproducible in the same individual. Individual kidney GFR (IKGFR), estimated from the absolute uptake of ^{99}Tc^{m}-DTPA, correlates very well with ^{51}Cr-EDTA plasma clearance GFR in children with a solitary kidney. Estimates of renal function must be related to body size. Traditionally, body surface area (SA) has been used, but there is a case for ECF volume instead. The ratio GFR/ECF is a measure of the rate of turnoer of an ECF solute, and is related to the half-time ($T_{\frac{1}{2}}$) of excretion of ^{51}Cr-EDTA:

$$\mathrm{GFR/ECF} = \ln 2/T_{\frac{1}{2}}$$

$T_{\frac{1}{2}}$ values have greater physiological significance than GFR/SA. $T_{\frac{1}{2}}$ in neonates is three to four times longer than in in adults, accounting for the poor excretion and high background in the ^{99}Tc^{m}-DTPA scan as well as the "babygram" and poor visualization in the intravenous urogram. Mean parenchymal transit time (MPTT) of ^{99}Tc^{m}-DTPA can be derived by deconvolutional analysis. It is affected by renal tubular reabsorption of sodium and water, and the ^{99}Tc^{m}-DTPA scan is best carried out under the controlled physiological conditions of hypotonic volume expansion (HVE). During HVE the fractional excretion of filtered water (V/GFR) inversely reflects proximal renal tubular sodium reabsorption. V/GFR is low and MPTT prolonged in acute urinary tract obstruction, and the two correlate well in children with solitary, questionably obstructed kidneys. Evaluation of methods for diagnosing urinary tract obstruction are hampered by the lack of robust independent means for confirming significant obstruction. The clearest functional evidence of urinary obstruction is improvement in GFR following surgical intervention, and there is a significant inverse correlation between the percentage increase in IKGFR and MPTT measured pre-operatively in children with unilateral pelvi-ureteric junction obstruction. These considerations are of particular importance in infants with simple hydronephrosis diagnosed ante-natally. In addition the ^{99}Tc^{m}-DTPA scan detects the presence of vesico-ureteric reflux with accuracy. The ^{99}Tc^{m}-DMSA scan is the most sensitive technique for demonstrating renal scarring, and can also detect renal ischaemia, particularly with captopril enhancement. The precise route of uptake of DMSA is not resolved, but the decreased renal uptake and increased urinary excretion of ^{99}Tc^{m}-DMSA in patients with the Fanconi syndrome point to filtration and re-absorption. Hyperfiltration states are difficult to assess, but perhaps in the future might be evaluated by combining data from the DTPA and DMSA scans.

Dynamic renal scintigraphy

A. Piepsz
Akademisch Ziekenhuis, Free University of Brussels, Belgium

DTPA is a chelator that is filtered exclusively by the glomerulus. It is bound to the technetium radionuclide (^{99}Tc^{m}) so that several functional parameters of the kidney can be determined using a gamma camera connected to a minicomputer. After intravenous injection of the tracer, a 20 min acquisition is started, using 20 s frames. Regions of interest are drawn over the two kidneys and the heart region, and time-activity curves are generated. The heart curve is calibrated by means of a 20 min blood sample and gives an estimate of the plasma disappearance curve. The first parameter is the separate glomerular filtration rate (SGFR) obtained from the ascending slope of the background—corrected renal curve and the corresponding plasma activity. The normal values in older children and adults are around 56 ml/min/1.73 m^2/kidney and this corresponds well to a glomerular clearance. Separate glomerular filtration rate is well correlated with separate creatinine clearance obtained by means of urine diversion and is only poorly correlated with the degree of dilatation of the renal cavities or the cortical thickness on intravenous urography, and constitutes a useful instrument in the evaluation of the parenchymal impairment in the follow-up of patients with hydronephrosis. The second parameter is the whole-kidney transit time, which is defined as the time necessary for a molecule of DTPA to pass through the entire nephron, from the glomerulus to the ureter. It is obtained by the deconvolution of the renal time–activity curve by the heart curve. In well hydrated patients, the normal mean transit time is about 3.5 min. It exceeds 8 min in the case of renal obstruction. However, although it is a very sensitive parameter, it does not appear as a specific parameter of obstruction, since simple dilatation of the cavities, because of a reservoir effect, can produce the same increase in the transit time. For that reason, several authors have proposed the use of a third parameter, namely the cortical transit time, in order to avoid the effect of the dilated cavities. We have constructed a functional image in which each colour provides a given value of the regional transit. It is therefore possible to delineate a cortical area with a cortical transit that may be different from the whole kidney transit, simply by inspecting the functional image. We can expect that, in the case of obstruction, the cortical transit will be significantly prolonged, whereas in simple dilatation of the cavities the cortical transit will remain normal. In children, however, the interpretation of these functional images is not easy, because of the huge overlap between the dilated cavities and the cortex. The fourth parameter is the response to a furosemide injection. In renal stasis, a dose of furosemide is injected at the end of the first acquisition and a second acquisition is started. Images and curves can be obtained that will provide useful information on the ability of the kidney to empty under urine flow stimulation. Care should be taken not to end the procedure without emptying the bladder; dramatic emptying of the dilated kidney may occur a few minutes after voiding. In conclusion, ^{99}Tc^{m}-DTPA dynamic scintigraphy allows the quantification of several parameters of renal function. It is, however, important to be aware of the pitfalls and limitations of this technique. In no way can valuable morphological information be obtained on the basis of this test.

Dimercaptosuccinic acid static renal scintigraphy in children

S. T. Meller
Royal Marsden Hospital, Sutton, Surrey

Dimercaptosuccinic acid (DMSA) scintigraphy is a relatively simple method of renal imaging in children, but attention must be paid to technique to obtain high-resolution images without movement artefacts. Posterior and posterior oblique views should be obtained 2 to 3 h after injection of 2 MBq/kg (max. 150 MBq) ^{99}Tc^{m}-DMSA, with the child lying directly on the face of the collimator, using sand bags for support. Analogue images should be acquired for 500 kcounts and the acquisition terminated in the event of patient movement. Digital images can be manipulated to accentuate focal parenchymal defects and relative percentage renal function can be calculated using region of interest analysis with background subtraction. Absolute quantitation of uptake can be employed to provide additional functional information for serial study of renal recovery and hypertrophy following infection, trauma and renal surgery in childhood. The resulting image is a map of functioning proximal renal tubules and is a sensitive method of detecting parenchymal abnormalities due to infection, vascular disturbances or space-occupying lesions. In paediatric urology, the DMSA scan is particularly helpful, together with ultrasound, in the evaluation of duplex kidneys and kidneys that do not excrete on intravenous urography.

Radionuclide cystography

M. N. Maisey and S. J. Chapman
Division of Radiological Sciences, UMDS, Guy's Hospital, London

Several radiopharmaceuticals may be used for the assessment of patients with vesico-ureteric reflux; these include ^{99}Tc^{m}-DMSA for the assessment of local scarring and individual renal function and ^{99}Tc^{m}-DTPA for the functional evaluation of individual renal function, excretion and drainage together with indirect radionuclide cystography. The advantages of indirect radionuclide cystography compared with MCU include lower radiation doses, the lack of bladder catheterization and the measurement of individual renal function. Features of vesico-ureteric reflux using intravenous ^{99}Tc^{m}-DTPA and cystography include renal scarring, decreased renal function, dilatation of the collecting system and spikes of reflux in the third phase of the renogram. The cystogram phase of the study may show reflux occurring at rest and/or during bladder emptying. Detailed attention to the performance of the study and the interpretation and presentation of the results with careful quality control is essential if accurate and reliable results are to be achieved. Potential sources of error include failure to fully empty the upper tracts before bladder emptying, the use of diuretics, patient movement, inadequate bladder emptying and the failure to correlate time–activity curves and images obtained during bladder emptying. From a series of 47 children, 85 renal units were evaluated. Positive reflux for all grades of reflux was seen in 30 "units"; in 17 it was demonstrated by radionuclide cystography only, in 16 by micturating cystogram only and no reflux in 27 units. Severe reflux was detected in nine units by radionuclide cystography and in only one case was reflux detected by micturating cystourethrography. The results indicate a potential for increased sensitivity using the radionuclide technique.

Transitional nephrology: the role of radionuclide scanning

I. Gordon
Department of Radiology, Hospital for Sick Children, London WC1

The neonate shows a natural maturation of the kidney, which is most marked in the early neonatal period but continues throughout childhood. This transitional nephrology is based on both anatomical and physiological changes. At 36 weeks gestation there is the full complement of glomeruli, but with a small surface area. The tubules at birth are relatively short with poor re-absorbtion of the glomerular filtrate. The circulatory change is mainly decreased resistance of the efferent arteriole; there is a relatively large extracellular fluid space (ECV). Both of these result in an increased effective filtration pressure with a low glomerular filtration rate (GFR). The large ECV results in a prolonged half-life, which has important bearing when DTPA is injected, since it is distributed in both the intravascular and extravascular space. The GFR increases with age; the mean in the 1st week of life is 38, from 2 to 4 weeks of life it is 48, up to the 3rd month of life it is 58 and up to the 6th month of life it equals 77 ml/min/1.73 m^2. From 6 to 12 months the mean is 103 ml/min/1.73 m^2. The adult GFR is reached around puberty. The DTPA scan is characterized by difficulty in visualization of the renal outlines owing to both a high background reflecting the large ECV and to the low GFR, which makes the region-of-interest delineation difficult. There is a short transit time with rapid transit of radionuclide into the bladder, as a result of the tubular immaturity. The combined effects result in non-renal-type curves even in the normal kidney. Improvement in function in the pathological kidney during the 1st month of life may simply reflect renal maturation rather than the effects of treatment. Dimercaptosuccinic acid scans are characterized by a high background, indistinct renal outlines and a high bladder activity, which makes identification of focal defects within the renal parenchyme difficult during the neonatal period.

The role of ^{99}Tc^{m}-DTPA scans: a prospective study

A. Piepsz
Akademisch Ziekenhuis, Free University of Brussels, Belgium

In the strategy of management of pelvi–ureteric junction (PUJ) stenosis, two assumptions are regularly found. The first one is that non-operated PUJ will progressively lead to the destruction of the kidney. However, this assumption relies essentially on the observations of total obstruction. The second one is that surgical relief of the obstruction will improve the renal function. This is true for the drainage function, whereas the parenchymal function will improve in a percentage of cases, which is variable from one author to another. An experimental study was first undertaken in order to evaluate on a long-term basis the progression of the separate glomerular filtration rate (SGFR) in a series of young rats submitted to a partial obstruction of the left ureter. We observed, like other authors, an initial variable post-operative SGFR decrease, depending on the degree of provoked obstruction. However, after this initial period, the SGFR remained stable until the natural death of the animal. The second study was a clinical prospective study on 14 asymptomatic neonates with PUJ obstruction detected on prenatal ultrasound. When the SGFR was abnormal, with very asymmetrical left and right function, the patients underwent pyeloplasty, in the hope of improving renal function. When the SGFR was normal, a conservative attitude was chosen, despite the other radionuclide parameters (furosemide test or cortical transit). In patients who had surgery, despite a slight increase in the SGFR probably related to the normal renal maturation during the first year of life, the SGFR generally remained below the normal range. In the non-operated hydronephrotic kidneys with initial normal function, the SGFR constantly remained in the normal range over a follow-up period of 1 to 6 years. We observed a significant decrease in SGFR in only one patient after 1 year and the patient was placed in the surgical group. This patient was the only one with a persistent non-response to furosemide. It was therefore decided to modify slightly the protocol and to operate on patients with a persistent absence of response to furosemide after the age of 6 months. This protocol should be constantly modulated by the appearance of clinical symptoms or by a sudden increase of hydronephrosis on ultrasound.

Session 2

Chairman: Dr I. Gordon

Radionuclide scanning in bone disease in paediatrics, by H. Carty
Oesophageal studies using radionuclides, by A. Piepsz
Neuroblastoma: role of MIBG, by A. M. Peters
The role of krypton-81m ventilation/technetium-99m MAA perfusion lung scanning in children, by H. Davies
Results of pyeloplasty for pelvi–ureteric junction obstruction in children, by K. McHugh, A. Najmaldin, V. Batty, D. M. Ackery, J. D. Atwell, D. M. Burge and I. Gollow
Technetium-99m dimercaptosuccinic acid scans in acute *E. coli* urinary tract infection, by J. R. MacKenzie, D. Tappin, R. Shaw, T. J. Beattie and A. V. Murphy
Technetium-99m mercaptoacetyltriglycerine for paediatric renal function studies in a district and general hospital, by G. C. Vivian and D. H. Kelling

Radionuclide scanning in bone disease in paediatrics

Helen Carty
Royal Liverpool Children's Hospitals, Alder Hey Branch, Liverpool

The main indications for radionuclide scanning in children with bone disease are trauma, infection, occult pain and arthritic disease. The role of radionuclides in bone tumours in children is identical to that in adults. It is important when interpreting scans not to misinterpret normal hot spots, due to normal structures in children, as metastases. The role in trauma is to identify occult trauma, particularly in sports-related injuries and in non-accidental injury, together with identification of the causes of occult pain, particularly in the back. Attention is drawn to ensuring that good views of the sacrio-iliac joints are obtained in all children, as this is a source of pain. The essential role of radionuclides in the investigation of the painful hip in children is emphasized, as is the non-specificity of the appearances in distinguishing infection from synovitis. Classical changes of Perthes' disease are demonstrated. Bone scintigraphy plays an important role in distinguishing foci of infection in the bone from septic arthritis and cellulitis, but again it is emphasized that a negative scan hAs to be interpreted with caution, particularly in the very young child. Its role in the identification of areas of involvement in juvenile chronic arthritis and in identifying areas suitable for injections is emphasized. The importance of obtaining two views at right angles to each other cannot be overstressed in localizing a lesion on radionuclide scanning.

Oesophageal studies using radionuclides

A. Piepsz
Akademisch Ziekenhuis, Free University of Brussels, Belgium

Radionuclide methods using technetium 99m have been developed in the last few years for the assessment of oesophageal transit. The method is physiological, easy to perform and gives interesting information concerning the severity of the disease as well as the effect of the applied treatment. In children, however, one is limited by radiation protection considerations, and the results are often of poor quality because of the low count-rate. Furthermore, the risk of external contamination and the impossibility of repeating the test constitute significant disadvantages, particularly in young children. These problems are avoided by using a tracer with an ultrashort half-life, namely krypton 81m, diluted in a glucose solution. A few millilitres are taken by the patient in one single swallow and 60 1-s frames are recorded. Several parameters of oesophageal transit can be extracted in a few minutes using time–activity curves and parametric images. The test is very sensitive in detecting minor regional-transit alterations. The reproducibility of the test is good and phenomena such as intercurrent gastro-oesophageal reflux or asynergic peristaltic waves can easily be detected. The test has provided helpful information concerning the localization and the importance of transit abnormalities in caustic and peptic oesophagitis, post-operative cases (atresia or fundoplication) and in patients with neuromuscular disorders.

Neuroblastoma: role of MIBG

A. M. Peters
Hospital for Sick Children, Great Ormond Street and Hammersmith Hospital, London

Radioiodinated meta-iodo benzyl guanidine (MIBG), which localizes in neural crest tumours, is showing promise for diagnosing and staging neuroblastoma. Indeed, the suggestion has been made that it should replace ^{99}Tc^{m}-MDP bone scanning for diagnosing Stage IV disease. We therefore prospectively compared ^{123}I-MIBG and ^{99}Tc^{m}-MDP for the detection of skeletal disease in 28 patients with neuroblastoma at presentation ($n = 22$) and at follow-up ($n = 18$) between 3 and 64 months after diagnosis (mean = 9 months). At presentation, 19 of the 22 patients had histological evidence of bone marrow involvement. All these had positive MDP scans, but five patients had negative MIBG scans. All three children with negative marrows had extensively abnormal MDP scans, which, with the clinical data, were thought to indicate Stage IV disease. One of these, three patients had a negative MIBG scan. There was, therefore, significant false-negative rate for MIBG at presentation. The results at follow-up were less clear: there was poor correlation between MDP and MIBG, and all of 10 marrow examinations performed were normal, yet seven of the 18 patients died soon afterwards. MDP scans are less specific for skeletal disease at follow-up because of continuing increased bone turnover associated with healing. New, or more strikingly abnormal lesions, therefore, carry more significance. There were three such children at follow-up; two of these died from disseminated disease, yet had normal MIBG scans. We conclude that these data do not justify the replacement of MDP by MIBG for the diagnosis of skeletal disease in neuroblastoma.

The role of krypton-81m ventilation/technetium-99m MAA perfusion lung scanning in children

H. Davies
St Mary's Hospital, London

Ventilation/perfusion (V/Q) lung scanning has well established clinical and physiological applications in paediatric practice, but with the different spectrum of disease seen in childhood, imaging of regional lung function has a more important function. Many authors have reported the value of radionuclide techniques in the differential diagnosis of congenital lung disease (Godfrey & McKenzie, 1977; Gordon et al, 1981; Gordon & Helms, 1982) and recent work has suggested that V/Q imaging may also be useful in assessing lung damage after long-term neonatal ventilation (Wong & Silverman, 1982). In older children a different group of diseases is seen: foreign body inhalation, asthma, cystic fibrosis and consequences of thoracic cage deformation such as kypho-scoliosis. Knowledge of lung function may help diagnosis, clinical decision making or monitoring therapy. The physiological applications of V/Q lung scanning have been examined in detail in adults but there is very little information in children. Pulmonary mechanics, however, are very different in children and regional lung function might be expected to differ. This will obviously have important clinical consequences. Recent work (Davies et al, 1985) has demonstrated that while perfusion is similarly distributed in children and adults, the pattern of regional ventilation is the reverse. In children, ventilation is preferentially distributed to uppermost rather than dependent lung regions, a difference that has clinical consequences for the management of critically ill children with lung disease. Further work is necessary to establish at what age children adopt the adult pattern. In clinical practice, regional lung ventilation is usually assessed using the steady-state image. If, however, activity is acquired in short-timed frames, the tidal fluctuation of breathing can be clearly seen. This technique has been validated and can offer the possibility of non-invasive regional broncho-spirometry. It could be used in children with a variety of conditions to assess the pathophysiological consequences of lung disease. In conclusion, V/Q lung scanning is well established in paediatric practice and has important clinical and physiological applications. It is well tolerated by children and the radiation doses are well within acceptable limits for secondary radiological investigation. It provides a useful tool for the investigation of pulmonary physiology in children, thus helping clinical management.

References

Davies, H., Kitchman, R., Helius, P. & Gordon, I., 1985. Regional ventilation in infants and very young children: reversal of adult pattern. *New England Journal of Medicine*, 1626–1628.

Godfrey, S. & McKenzie, S., 1977. Place of radioisotope lung function studies in paediatrics. *Archives of Disease in Childhood, 71*, 71–78.

Gordon, I. & Helms, P., 1982. Imaging the small lung. *Archives of Disease in Childhood, 57*, 696–701.

Gordon, I., Helms, P. & Fazio, F., 1981. Clinical applications of radionuclide scanning in infants and children. *British Journal of Radiology, 54*, 576–585.

Wong, Y.-C. & Silverman, M., 1982. Kr81m ventilation lung scans in the assessment of lung function during infancy. *Modern Problems in Paediatrics, 21*, 230–236.

Results of pyeloplasty for pelvi–ureteric junction obstruction in children

K. McHugh, *A. Najmaldin, V. Batty, D. M. Ackery, *J. D. Atwell, *D. M. Burge and *I. Gollow
*Departments of Nuclear Medicine and *Paediatric Surgery, General Hospital, Southampton*

Forty-one children, age range 2 weeks to 15 years, were shown to have pelvi–ureteric junction (PUJ) obstruction by diuresis renography. All were treated by Anderson–Hynes pyeloplasty. Three to 6 months post-operatively, the renograms were repeated and the findings correlated with the clinical outcome. Renographic improvement was defined as improved washout of tracer as judged on the analogue images, correction of the renogram curves to a normal pattern and normalization of the parenchymal mean transit times. Thirty-six children (87%) showed unequivocal renographic improvement and all these were clinically well. Three had a significant increase (>5%) in divided renal function post-pyeloplasty and five (13%) had unchanged or equivocal post-operative studies. One patient had continued loin pain and necessitated repeat pyeloplasty. The other four patients were clinically well. Their renograms were technically inadequate because of excess motion (3) and poor function (1). Interpretative problems encountered included grossly dilated renal pelves and thin renal cortices, which make assessment of parenchymal regions of interest in the estimation of parenchymal mean transit times difficult. The vast majority of children who have a pyeloplasty for PUJ obstruction have a favourable outcome. However, there is a potential risk of progression of the hydronephrosis with deterioration in renal function. Hence the need for objective evaluation of the post-operative result. An awareness of the pitfalls of diuresis renography is necessary to allow accurate assessment of post-pyeloplasty function. Our experience indicates that renography provides accurate and reliable post-operative information that has proven clinical usefulness.

^{99}Tc^{m}-dimercaptosuccinic acid scans in acute *E. coli* urinary tract infection

J. R. MacKenzie, D. Tappin, R. Shaw, T. J. Beattie and A. V. Murphy
Departments of Radiology, Microbiology and Nephrology, Royal Hospital for Sick Children, Glasgow

Escherichia coli is the commonest organism causing urinary tract infections and some workers believe that P-fimbriae +ve *E. coli* are responsible for greater upper renal tract damage than P-fimbriae −ve. In a prospective study commencing April 1985, children presenting with a first documented *E. coli* infection had a DMSA scan within 4 weeks of the infection. One hundred and two children were studied (35 P-fimbriae +ve and 67 P-fimbriae −ve). The two groups show no significant difference in the abnormalities detected on the DMSA scan, namely scarring, photon deficient areas and abnormal divided function. The photon deficient areas correlate with elevated peripheral white blood cell count, length of symptoms, systemic upset and pyrexia, and are commoner in the under 2 year olds. Reflux was assessed by MCU or DTPA scan and occurred in 28 children, three of whom had scarring and eight photon deficient areas. There was a significantly increased incidence of reflux in children with P-fimbriae +ve *E. coli.*

P-fimbriae status	Scarring	Photon-deficient area	Reflux
+ve 35	3	7	15
−ve 67	6	15	13
102	9	22	28

The DMSA scan is felt to localize infection to the renal parenchyma and is recommended in children with acute urinary tract infection.

Technetium-99m mercaptoacetyltriglycine for paediatric renal function studies in a district and general hospital

G. C. Vivian and D. H. Keeling
Nuclear Medicine Department, Plymouth General Hospital and Royal Cornwall Hospital, Treliske

^{99}Tc^{m}-mercaptoacetyltriglycine (MAG 3) is a hippuran analogue that may be substituted for ^{99}Tc^{m}-DTPA in many clinical studies. The physiological handling of the tracer is predictable and quantitative techniques may be applied to dynamic studies. Early summed images give parenchymal definitions that are superior to DPTA and hippuran and may be comparable to DMSA. Computer-assisted dynamic renal scintigraphy is now generating estimates of renal blood flow, tracer clearance and parenchymal function. The bladder and ureter are being assessed by scintigraphy and "urodynamics" with the possibility of studies of bladder-emptying patterns and urine flow rate. The potential now is for a full assessment of renal tract function at one attendance, minimal intervention and acceptable radiation dosimetry. From January to July 1988 we studied 30 children with a variety of indications with this protocol and present the results.

1989, *The British Journal of Radiology*, 62, 504–506

Book reviews

Atlas of Hysterosalpingography. By Stephen Karasick and David Karasick, pp. xx + 192, 1987 (Charles C. Thomas, Springfield, Ill.), $46.75.
ISBN 0-398-05379-0

At first sight it may seem an anachronism to have a new book devoted to a single radiographic technique. There is certainly little new to say on hysterosalpingography. Nevertheless, it is still a commonly performed procedure and one which remains a first-line investigation in female infertility. Hysterosalpingography is a technique which may be performed by a gynaecologist, a radiologist or both in collaboration, so there has to be a mutual understanding between specialties.

This book is rather more than an atlas, clinical and pathological aspects being covered in the text. Its eight chapters encompass technical considerations as well as the usual range of conditions in which there are findings on hysterosalpingography; these include the increasingly important assessment of tubal surgery. A list of references accompanies each chapter. There are 124 illustrations.

Although the illustrations are generally of a high standard, there are some questionable practices and a number of omissions. Although oblique views in addition to two radiographs during the filling phase are recommended, the authors do not suggest a routine delayed radiograph. The advantages and shortcomings of the various means of uterine cannulation could have been described, especially in regard to the increasingly popular balloon catheter technique. The description of normal variations in endometrial outline is incomplete. While the uterine changes due to diethylstilboestral exposure are well described, there is no mention of the other appearances of uterine hypoplasia. There is no mention of the crucial lateral view in the evaluation of a caesarian section scar. The alleged small polyp in the left cornual region, on the side of tubal occlusion, in Fig. 54 looks suspiciously like an air bubble. Despite the shortcomings, the illustration and description of a wide range of conditions in a compact atlas is likely to make this a useful reference for those involved in hysterosalpingography.

G. H. WHITEHOUSE

International Strategies for the Eradication of Carcinoma of the Cervix in Developing Areas: Proceedings of the International Working Party Meeting in India 1987. Ed. by R. F. Mould and Arabinda Rose, pp. xxvii + 293, 1987 (Adam Hilger, Bristol), £50.00.
ISBN 0-85274-473-0

This meeting dealt with carcinoma of the cervix in developing countries. Amongst other aspects, the book considers the relationship between the different cultures of the respective countries, the high incidence of the condition, the difficulty in screening and why most women present in the late stages. This leads to discussion of the treatment of advanced stages of carcinoma of the cervix, in comparison with the experience of the developed countries. Towards the end of the book there is a summary of the working party meetings, and précis of the guest lectures and panel discussion at the end of the conference. The final report at the end reviews the topics covered and their relationship to developing countries.

The book represents the contributions of many authors and inevitably there are overlaps in some of the topics discussed and the style and print throughout the book is not uniform. Nevertheless, it is still easy to read. Obviously it will interest all those involved in the management of cancer of the cervix and help in understanding the problems faced by developing countries as well as in appreciating how advanced stages of the disease are treated in different centres.

This book is likely to be more suitable for libraries than for individual possession.

V. R. TINDALL

A Textbook of Radiological Diagnosis, Vol. 4. The Alimentary Tract: the Hollow Organs and Salivary Glands. Ed. by K. C. Simpkins, pp. x + 754, 1988 (H. K. Lewis, London), £85.00.
ISBN 0-7186-0463-6

It was to be expected that the advent and use of the newer methods of imaging would alter the content and format of the new edition of what was formerly known as *A Textbook of X-ray Diagnosis*.

The changes are major and reflect clearly the beliefs and clinical practice of the editor and the numerous contributors from both Britain and North America. This is now an exceptionally well produced and printed textbook with a modern format, easily read type and good, pertinent illustrations, which are supplemented where necessary by labelled diagrams — this is particularly valuable in chapters such as Bartram's on the anatomy of the pelvic floor.

This is a large book covering all sections of the alimentary tract from the salivary glands to a final chapter on paediatric gastroenterology. Each section has an initial discussion on normal anatomy and motility, included also is a wealth of practical advice on technical aspects of equipment — contrast media and suggested methods of performing radiological procedures. It is pleasing to see how clever the radiological, endoscopic and pathological findings have been correlated and to find in a radiological textbook, a section on the practical aspects of endoscopy. The chapter titles give a clear indication of the clinical approach of the contributors, such as Stevenson and Beckly's "The Differential Diagnosis and Management of Oesophageal Strictures" and Herlinger's "Malabsorption and Immune Deficiency".

In a book of this size with many authors, one looks for repetition and overlap, and variation in style and presentation. No criticism on these counts can be made, the references are eclectic and up-to-date, and include recent material on AIDS and its related diseases.

One can recommend this volume not only as a reference book to be used in the diagnosis of the rare and difficult case but a book well worth reading by both senior and junior staff, who are interested in gut radiology.

J. A. GLEESON

Gamuts in Nuclear Medicine, 2nd edn. By Frederick L. Datz, pp. xxii + 390, 1987 (Appleton & Lange, Norwalk, Conn.), £37.50.
ISBN 0-8385-3076-1

This is a shopping list for nuclear medicine in its most supermarket form. There is a catalogue of brands to choose from for each item on the imaging shelf, designed for the MCQ mentality. To help to identify the best buy the choices are listed as common, uncommon and rare, and the content of each carton is helpfully documented with a reference, although the particular condition is not related to the list of references numerically. Asthma is given as an "uncommon" cause of a perfusion defect on lung imaging. This highlights the real problem of this approach. In asthma, perfusion defects are common, but as lung perfusion imaging is not commonly performed in asthmatics, then is the finding uncommon? No basis is given for the categorization. Again, neuroblastoma is listed as a "rare" cause of MIBG uptake, yet it is the commonest cause in children.

The absence of any illustrations or even any descriptions makes, for example, sections on the "fish eye" and "oval eye" signs in thyroid imaging unhelpful. In some sections the absence of any statement on the radiopharmaceutical used may also cause a problem, so a "rare" cause of decreased uptake in the thyroid image is given as "entire liquid dose not ingested", presuming oral ^{131}I for thyroid imaging which should have been superseded by ^{99}Tc^{m} or ^{123}I by injection. Neither surgery, tumour, infarction, nor rotation of a pelvic kidney are included in the causes of a unilateral decrease in renal size. While a recent contrast angiogram is given as a cause of a "flattened renogram", drug causes (penicillin and its derivatives, probenecid, etc.) and renal biopsy are not included. In adrenal cortical imaging, Barter's syndrome is not included as a cause of symmetrical visualization and dexamethasone escape is not included in the causes of bilateral visualization of the adrenals on dexamethasone suppression. Oncology is not given as a section and radioimmunoscintigraphy, which has a wealth of possibilities for this approach, is not included.

I visualize the MCQ: "Which of the following give multiple sites of uptake on bone imaging? 1. Unilateral pulmonary hypovascularity 2. Chester-Erdheim disease 3. Migrating osteoporosis 4. Polycythaemia vera 5. Sinus disease." The answer, apparently, is all of them. Did you know that and did you want to know that? If you did, then this is the book for you.

Incidentally, a "gamut", according to the Shorter Oxford Dictionary, is the "first and lowest note in the medieval scale of music".

K. E. Britton

Clinical Radioimmunoimaging. By Zachary D. Grossman and Scott F. Rosebrough, pp. xviii + 138, 1988 (Grune & Stratton, Orlando, Florida), $27.50.
ISBN 0-8089-1894-X

This is a fun book, and as the preface states, "This slim volume could have been titled 'A Quick and Dirty Guide to Radioimmunoimaging'." The authors aim to target readers over 40, as radioimmunoscintigraphy postdated their training period. They attempt to provide "a simplified clearly written explanation" and largely succeed.

The "major emphasis is placed upon the most clinically relevant work" so the text is selective by intention. The sections on general considerations and relevant techniques are the most useful to the uninitiated, as they give deft explanations of the language and of abbreviations such as ELISA, SDS-PAGE, and Protein A. The growth of non-tumour radioimmunoimaging of the heart, the blood clot (antibody-labelled platelets, antifibrin) and the abscess (antibody-labelled leukocytes) is well documented.

The tumour section provides the majority of the text and includes neuroblastoma, colorectal cancer, melanoma (including the important Italian work), ovarian cancer, prostatic cancer and T-cell lymphoma, which are critically reviewed. Immunolymphoscintigraphy is mentioned but the section on radioimmunotherapy is disappointingly brief. Nevertheless a suitable caveat on over-enthusiasm is included.

In spite of the rapid growth in this field, the references are relatively recent and the balance of the text is modern. The final chapter on the problems of the technique is good, for example: "Indium-111 labelled antibodies have not proved consistently superior to those labelled with ^{123}I. If a stable ^{99}Tc^{m} label were devised it would probably be superior". Reliable ^{99}Tc^{m} labelling of antibodies and their fragments is now with us.

This book is strongly recommended not only to the imagers (both sceptics and converts will benefit) but to oncologists, general physicians and surgeons as well.

K. E. Britton

Microneurosurgery, Vol IIIA. By M. G. Yasargil, with P. J. Teddy and A. Valavanis, pp. x + 408, 1987 (Thieme, Stuttgart/New York), DM360.
ISBN 3-13-645001-9 (Stuttgart)
0-86577-258-4 (New York)

This is the first of two volumes devoted to the surgical aspects of intracranial arteriovenous malformation, which together comprise the third volume of a series of four on microneurosurgery. Five of its nine chapters are contributed by authors other than Yasergil and his immediate collaborators, and deal with embryology, Doppler ultrasound, neuroradiology, anatomy of the cortical blood vessels and anatomy of the calcarine sulcus. The main authors are responsible for the history of diagnosis and treatment, pathology, haemodynamics and microsurgical anatomy of the brain relevant to AVM. In each chapter the literature is reviewed, but the text is essentially based on the wealth of clinical experience accumulated in Zürich over the last 20 years, and presents the authors' experience and analysis of the management of 414 patients undergoing operation for intracranial AVM, and of 86 patients who were managed conservatively.

Initial chapters on the history of diagnosis and management of AVMs and embryology of CNS vasculature precede a detailed account of their pathology, in which all conceivable variations of size, site, shape, feeding and draining vessels are described in detail and illustrated with clear diagrams and radiological examples. Unfortunately the authors do not seem to have drawn from their own series to ascribe the incidence of the various features; for example, there is no indication of the incidence of AVM at various sites. This and other apparent deficiencies may, of course, be dealt with in the second part of Volume III. The radiographs, although numerous, do vary in quality and presumably in age, as some are printed as positives, some reversals and some subtractions.

A useful chapter on the haemodynamic aspects follows, although in some parts clarity could be improved. It is perhaps surprising that a chapter is devoted to the use of extracranial Doppler ultrasound in the diagnosis of intracranial AVM, even though the author reports a diagnostic accuracy of only 89%. Although providing information on flow in different vessels, this technique clearly does not replace the need for CT or angiography, a detailed account of the use of which is presented in the chapter on neuroradiology, although there is only brief discussion of NMR imaging. There is no mention of the role of CT scanning in localizing vascular malformation in patients with negative angiography.

The last three chapters concentrate on anatomy. The first provides valuable information on the sulci, fissures, cisterns and vascular supply of the brain. Again, the illustrations excel in their clarity. The second chapter describes the micro-circulation within the cerebral and cerebellar cortex in the smallest detail. Although this completes the anatomical description, such detail is of little clinical value. Similarly, the last chapter describes every possible variation in the size and shape of the calcarine sulcus, but with such variability in structure, this information would appear to have negligible practical value. For some reason the second author of this chapter is not included in the list of contributors in the title page, nor is his address given.

The book is full of references, but the long lists in the text, covering many pages, tend to interrupt the flow of reading. The index is not comprehensive; for example, the pages on which the terms "cryptic" and "occult" are defined are not listed.

The present reviewers, a surgeon and a radiologist, concede that the availability of only half of a two-part volume may limit their ability to assess this publication fully, but it is clear that even this first part, which includes diagnostic imaging methods, has much more appeal to neurosurgeons than to radiologists. Superselective angiographic techniques are not described, nor is there any attempt to describe or assess the value of interventional radiology. As one of a series of four volumes on microneurosurgery, there is no doubt this book will attract major interest and provide a valuable source of reference. Its individual purchase by even the most diligent and affluent radiologist is unlikely, but libraries, and those neurosurgeons particularly interested in AVM, will consider its purchase essential.

K. W. Lindsay and A. R. Valentine

Neuroradiology, 2nd edn. By Ruth G. Ramsey, pp. viii + 852, 1987 (W. B. Saunders, Philadelphia), £75.00.
ISBN 0-7216-1827-8

Neuroradiology is a discipline in which the ground rules have changed more radically and in a shorter time than in almost any other single area in radiology. In 1973 relatively small numbers of patients were being investigated by angiography and air encephalography, and the interpretation of the images required considerable skill, clinical neurological expertise and more than a little art. Computed tomography then appeared and within 5 years relatively untrained general radiologists were able to make more accurate neuroradiological diagnoses than the experts had been able to before the advent of CT.

Professor Ramsey published the first edition of her book in 1981, when the title was *Neuroradiology with Computed Tomography*. The new edition assumes that CT is an implicit part of neuroradiology, brings in magnetic resonance, and has a short section on digital angiography.

It must be difficult when writing a textbook of this type to decide on the balance of techniques, anatomical areas, and pathology. This book has initial sections on choosing the right investigation, the plain skull radiograph, and good explanations of CT, MRI and angiographic techniques, together with normal anatomy. The major part of the book covering pathology then starts with techniques — angiography in brain tumours and vascular abnormalities, where many illustrations are of CT scans accompanied by angiograms. It then proceeds to degenerative, metabolic and inflammatory lesions, where almost all the illustrations are of scans, and has specific chapters on meningiomas, hydrocephaly, metastases, trauma and atheroma. The other chapters are anatomically based, dealing with deep hemisphere and midline lesions, the orbit, posterior fossa, and in the longest chapter, the spine and myelography.

There is no mention of ultrasound and Doppler and little of paediatric neuroradiology. Each section commences with text, followed by the figures, so that finding a relevant illustration always means turning over the pages — more than 80% of the book is made up of illustrations, and many CT scans are from older machines. Occasional errors appear — Fig. 2.12B is wrongly labelled and has the illustrations in the wrong order. On p.133 it is stated that "angiography at first used Thorotrast" — hardly the first agent used. However, in general the binding, print, layout and illustrations are good.

Professor Ramsey is obviously a good teacher and her material is well presented. The sections on normal anatomy using each technique are ideal for first year registrars, and there is some text and an illustration concerning almost all the pathological conditions one can think of. The crux of the problem is stated on p. 548: "It is becoming apparent that in some cases a definitive operative procedure can be performed on certain posterior fossa lesions without using any invasive studies after evaluation by CT scanning." After reading the book I am left with a strong feeling that it represents a historical watershed, and that almost half of the material is now or soon will be of little daily use even for neuroradiologists. Perhaps the next edition will say "neuroradiologists at one time used angiography to localize masses . . ."

W. D. Jeans

Radiology for Anaesthesia and Critical Care. Ed. by C. H. Murphy and M. R. Murphy, pp. xii + 273, 1987 (Churchill Livingstone, Edinburgh), £37.50.
ISBN 0-443-08306-1

The subjects covered within this book will be of particular value to anaesthetists as indicated by the title, although the approach may also be of interest to radiologists. There is certainly a need for a text dealing with the interpretation of radiographs encountered during intensive care and the peri-operative period of relevance to anaesthesia.

Numerous illustrations are included, covering a wide spectrum of disorders encountered in both adult and paediatric practice. Unfortunately the overall presentation lacks cohesion and is unbalanced in terms of conditions which are encountered most commonly. This is probably a result of the number of contributors — 15 — covering a relatively specialized area. A smaller book dealing purely with the subject material suggested by the title would have been more successful. Chapters are included on special imaging modalities, radiation safety and anaesthesia for radiological procedures. The latter two chapters seemed particularly out of place given the approach adopted throughout the rest of the book. Over a third of the remaining pages cover paediatric radiology, which is excessive. Much emphasis is placed on chest radiographs, yet very little is said about radiology of the spine, where a description of the recognition of cervical subluxation, etc. would be helpful. The place of radiology imaging of relevance to the anaesthetist during various invasive procedures, for example insertion of catheters, placement of cannulae for regional analgesia or chronic pain relief, is barely discussed.

Some readers on this side of the Atlantic may object to the style of writing, but the layout of the text is clear and the quality of the radiographic material is remarkably good.

As a textbook occupying a unique niche, it offers good value for money, although mainly as a reference text for departmental and intensive care libraries.

S. L. Snowdon

BIR Bulletin

Honorary Editor, BIR Bulletin: D. Rickards, LRCP, MRCS, FFR(D)SA, FRCR
Please address all correspondence to: Honorary Editor, BIR Bulletin, The British Institute of Radiology,
36 Portland Place, London W1N 4AT

The British Institute of Radiology is not responsible for opinions expressed in the BIR Bulletin

In order to keep BIR members informed of what is happening at the BIR, the BIR Bulletin will publish a report, written by the Honorary Secretaries, of the meetings of Council. In each session, running from 1 October to 30 September, four Council meetings are held. The following is a report of the meeting held on 15 December 1988.

Report from Council

Mrs M. J. Harvey and Dr M. Gowland
Honorary Secretaries

THE PRESIDENT welcomed the new members of Council to the first meeting of the 1988/89 session, which was held on Thursday 15th December 1988.

Institute Membership

As well as the usual business of approving applications and noting resignations, retirements and defaulting members, Council was presented with a profile of membership by date elected, which suggested that the majority of members are under 50 years of age. Some Council members felt that it was the members in the upper age bracket (*i.e.* over 50) who are more actively involved in the work of the Institute and that the profile therefore showed that there is a wealth of younger expertise available, on which the BIR could draw. It was decided to produce a multiple-choice questionnaire for circulation to all members. The information obtained would be used to identify sources of expertise for use as and when required by the BIR.

Committees

The Chairmen and Secretaries were noted, as shown in Table I.

Table I: Chairmen and Secretaries of BIR Committees

Committee/Sub-cttee	*Chairmen*	*Secretary*
Radiation Oncology	Prof. C. A. Joslin	Mr. J. M. Wilkinson
Radiobiology	Dr I. J. Stratford	Dr M. P. Law
Radiation Protection	Mr D. Gifford	Dr I. Watt
Radiation Dosimetry	Mr D. Gifford	Mr R. B. Richardson
Diagnostic Methods	Prof. B. S. Worthington	Prof. C. R. Hill
Nuclear Medicine	Dr N. Garvie	Dr A. H. Smith
General Programme	Prof. B. S. Worthington/ Prof. C. R. Hill	Ms N. van Helfteren
Industry	Mr J. Twydle	Mr A. Budge
Library	Dr A. B. Ayers	Ms S. Dewhirst
Publications	Dr J. T. Patton & Dr N. J. McNally	Mr R. Smith

Highlights of Reports from Committees

Industry: There is to be an interesting competition for Radiology '89 delegates to encourage attendance at MED X RAY. First prize is two return air tickets to RSNA 1989 plus accommodation costs. Two runners up will each receive a case of champagne. RAD Magazine is the generous sponsor.

Publications: Dr Patton retires as Honorary Editor of the *BJR* in June 1989 and the Medical Committee has approved Dr D. Shaw's nomination as his successor, for confirmation at the AGM.

Finance

The Treasurer reported that the year-end projection for 1988 looked healthy, with the surplus from MED X RAY being an important element. Council approved the budget for 1989, which aimed at a reasonable surplus and allowed for the purchase of a desk-top publishing unit and laser printer, which should soon pay its way with savings on typesetting costs.

In response to the popularity of the Access credit card facility, arrangements are being made for payments to the BIR to be made also by VISA.

Library

Discussions are continuing on the establishment of a National Radiological Library at the BIR.

Table II: BIR representatives on other bodies

Association of Learned & Professional Society Publishers	N.J. McNally
The Biological Council	M. Law
British Medical Association: CCHMS Radiology Subcommittee	I. Watt
British Radiation Protection Association: Council	D. Gifford (1987) M. Fitzgerald (1988)
DHSS Working Group on Safety of MR Equipment	I. Isherwood (1985) I. Young (1986)
Edinburgh Congress Educational Trust	P.N.T. Wells (1988)
L.H. Gray Memorial Trust	R.J. Berry (retiring 1989) V. Barley (until 1991), R.D. James (until 1993)
Professions Supplementary to Medicine Radiographers Board (BIR/IPSM)	D. Gifford (1988–90)
Radiological Research Trust Scientific Panel	I. Isherwood, D.S. McIntosh, P.H.S. Smith (1986–88; 1989–91)
Royal Society National Committee for Biophysics	N.J. McNally (1988–90)
Royal Society National Committee for Physics	C.R. Hill (1988–93)
UK Liaison Committee for Sciences Allied to Medicine and Biology	C.R. Hill (1987)
UK National Committee for Medical Physics	C.R. Hill (1992)
World Federation of Nuclear Medicine & Biology (BIR/BNMS/HPA Delegation)	P.J. Ell (clinician 1987) alt: K.E. Britton, J.G. Hardy (physicist 1987)

Future Venues of the BIR Annual Congress

At the recent meeting of the Congress Committee it was agreed that the choice of London as venue for 1991 be abandoned because of very high costs and the danger of losing conference fellowship in the evenings. The small number of alternative sites that might accommodate both the BIR and COR conferences and MED X RAY are being explored as a matter of urgency for the problem years of 1991 and 1993.

Concern was expressed that the conference should at some stage in the future be held in London as many participants were based there.

Premises

The BIR Surveyor has advised that although there is no need for immediate action, the state of the Library ceiling will require considerable expensive attention in the next year or so to prevent further detachment of the paint and plaster from the surface. Until the work commences this summer, it is not possible to know the extent of the repairs necessary, nor their cost, but he estimates "thousands, rather than hundreds". The possibility of obtaining assistance in the form of a grant is being investigated, in the first instance with English Heritage.

Other Organizations and Societies

Dr Rickards reported on the initial meeting of the British Society of Interventional Radiologists (BSIR). This was highly successful with over 90 attending; the BSIR intend to make this an annual one-day meeting. The BSIR wishes to be an autonomous organization, although it will liaise with the RCR Interventional Steering Group. The head of the organization is Dr E. W. L. Fletcher. The BIR will encourage the BSIR to hold its meetings at the Institute.

Reports were received from various BIR representatives on other organizations and societies. A list of these organizations and the BIR representatives is given in Table II.

Date of Next Meeting

Thursday 23rd March 1989.

RADIOLOGY '89

EASTBOURNE

4-6 May 1989 Eastbourne

TO GIVE A TASTE of what is in store for you at Radiology '89, the organizers have prepared precis of some of the major sessions. These will appear in the *Bulletin* each month from now until May.

Dr Maureen Gowland
Scientific Programme Chairman

Pathophysiology of Disease: Insights from Magnetic Resonance

May 4, 1989

It has become increasingly apparent that magnetic resonance imaging (MRI) and spectroscopy provide a valuable research tool for addressing fundamental questions relating to the pathophysiology and natural history of human disease. There are still many questions remaining to be answered before we have a complete understanding of the pathogenesis of multiple sclerosis (MS), the commonest primary disorder of the nervous system in the UK. The remarkable sensitivity of MRI in demonstrating the areas of demyelination in this condition coupled with the use of gadolinium–DTPA to demonstrate associated breakdown in the blood–brain barrier has revolutionized our ability to study the distribution and activity of the disease. Professor G. Du Boulay will discuss the contribution MRI has made towards extending our understanding of MS and our ability to assess potential treatments.

Several methods are available for the assessment of regional tissue perfusion in the brain and these include single photon emission computed tomography (SPECT) and positron emission tomography, but such studies are additional to a basic imaging study. Professor R. E. Steiner will discuss research directed towards mapping directional capillary flow as an extension of conventional MRI and outline its clinical potential.

Superimposed on the slow net circulation of CSF are cardiac and respiratory fluid movements that can be identified on

MRI studies of the cranium and spinal canal by "time of flight" as well as reversible and irreversible phase effects. Professor B. S. Worthington will discuss the implications of these changes as well as the significance of alterations in their pattern and magnitude in several conditions associated with disordered CSF dynamics.

Magnetic resonance spectroscopy is a unique tool in clinical medicine, being the only one that can provide non-invasive access to tissue chemistry in human disease. Professor D. Gadian will provide a brief overview of how the technique can be a source of new information about the pathophysiology of disease and where the most likely areas are for it to be harnessed in the diagnosis and assessment of therapeutic interventions.

B. S. WORTHINGTON

Teach-in: Pitfalls in Abdominal Computed Tomography
May 5, 1989

This session will begin with a fairly general appraisal as to why the abdomen and pelvis are such difficult areas for CT interpretation. The importance of correct bowel preparation and other features of technique will be discussed. So too will some areas where the anatomy of the axial plane may appear confusing. This will be followed by a more didactic lecture from Dr Reznek on particular problems relating to the upper abdomen. Hepatobiliary, splenic and pancreatic pitfalls will be discussed, as will problems in and around the para-aortic nodes. After open discussion of the problems raised so far, a critical appraisal of errors made in a busy body CT unit will be presented. These errors will be subdivided into those of observation and interpretation and some suggestions will be made as to how these might be reduced.

A. K. DIXON

Interventional Radiology
May 5, 1989

Interventional radiology continues to play an important role in the management of a vast number of patients. This session will concentrate on three important conditions, two common and one less common, which illustrate many different aspects of interventional radiological techniques.

Peripheral vascular disease remains a common cause of significant morbidity and mortality in the UK. Dr Anna-Maria Belli (Senior Lecturer, Sheffield) will be presenting recent advances in peripheral artery recanalization, concentrating not on simple balloon angioplasty but on the newer techniques that may be used alone or in conjunction with balloon PTA. Laser-assisted PTA, atherectomy and intravascular stents will all be discussed.

Pulmonary arteriovenous malformations (PAVMs), although not very common, when they occur can cause serious problems for the patient, ranging from breathlessness to cerebral abscess. Interventional radiology (embolization) is able successfully to treat the vast majority of these patients with minimal loss of normal lung tissue. Dr James Jackson, in association with Professor Allison (RPMS, London), has unique experience with a large number of these patients and will present their combined work on embolization in the management of PAVMs with a fascinating insight into the physiological changes that occur pre- and post-treatment.

The third subject to be discussed is again a very common and disabling condition – gallstones. Dr Alison Keightley (Guy's Hospital, London) will be discussing modern interventional techniques in the biliary tree, including lithotripsy. Are the days of cholecystectomy numbered? After lithotripsy of gallstones, what happens to the sludge? Do the stones recur? We hope to hear the answers to some of these questions in this session.

A. P. HEMINGWAY

Imaging in Organ Transplantation
May 6, 1989

In this session, Drs Dubbins, Karani, Higenbottom and Verney will address the subject of imaging in renal, liver, lung and heart transplantations, respectively. These types of transplant have been chosen because of the importance of imaging techniques, old and new, in their assessment and management. In the UK, renal, liver, cardiac and cardio-pulmonary transplantations have been established for 30, 20, 10 and 5 years, respectively. In each there are distinctive features both in patient selection and in early and late post-operative management, but there are also aspects common to them all. Despite the advances in the 30-year period the problems of rejection, infection and vascular obstruction are continuing challenges, and in particular the benefits brought about by cyclosporin A in the fight against rejection have to be viewed in the knowledge of the complications associated with treatment protocols. The same period has seen enormous developments in imaging techniques such as ultrasound, duplex Doppler, isotope scintigraphy and interventional procedures.

Has intravenous urography or renal arteriography any place in the pre-operative assessment or post-operative management of renal transplants? How far can non-invasive techniques sort out the problems of acute tubular necrosis, rejection and cyclosporin toxicity? Can Doppler studies lead to a confident diagnosis of any of the renal transplant complications? When should isotope studies be performed and which techniques?

Which radiological techniques are the most helpful in patient selection and surgical planning of liver transplants? Can ultrasound deal with the majority of post-operative problems or how far are interventional techniques required?

Heart–lung transplantation is indicated in severe irreversible generalized pulmonary vascular disease and end-stage chronic lung disease. At what stage in these processes should transplantation ideally be performed and does imaging have a significant part in this decision? Post-operatively, what does the abnormal chest radiograph mean? Can it distinguish pulmonary rejection from infection? Does it play an important part in the decision to proceed to transbronchial biopsy? When are isotope studies or pulmonary angiography required?

The basic indication for cardiac transplantation is end-stage heart failure with an acceptable pulmonary vascular resistance. Ten years development of immunosuppression protocols has reduced early mortality from infection and rejection. The problems of late complications now loom larger, and in particular the development of coronary artery disease. What has routine annual or biennial coronary angiography of transplanted heart shown? Does the pattern differ from "ordinary" coronary disease and does it help in management? Is there a prospect that isotope scintigraphy or echocardiography can reduce the need for invasive techniques?

These are some of the questions addressed by radiologists dealing with these problems, and the four speakers in this session are in a position to give an up-to-date assessment of the efficient use of the techniques available. The value of the co-operation between surgeon, physician, pathologist and radiologist will emerge in each of the four presentations.

G. I. VERNEY

Curt Westman Scholarship

Members wishing to visit the clinic in Vällingby, Sweden, of the late Dr Curt Westman, now owned by AB Medicinsk Röntgen, should write to the General Secretary of the BIR. Return air fares and 2 weeks' accommodation are generously provided by AB Medicinsk Röntgen, and the BIR provides a sum towards expenses.

1988 Nycomed Scandinavian Scholarship Report

by A. Gholkar

I WAS SUCCESSFUL in receiving one of the Nycomed Scandinavian Scholarships for 1988, which enabled me to spend September and October working with Professor Paul Svendsen in the Department of Neuroradiology at the Sahlgrenska Hospital, Gothenburg.

Gothenburg is the second largest city in Sweden, with a population of 450 000. The city was founded in 1621 by King Gustaf II Adolf as Sweden's major western port. It has now become the largest trading port in the whole of Scandinavia and is also an important fishing port with an annual catch of 25 000 tons. It is a beautiful city, where the influence of Dutch builders and architects is clearly seen in the low bridges and canals of the old city.

Sahlgrenska hospital, which has 1500 beds, is one of the largest teaching hospitals in Scandinavia. It is a regional centre for neurosciences, cardiothoracic surgery and oncology. The main hospital buildings were built in the late 1950s and are situated in pleasant surroundings, particularly on the south side, where there is a large botanical garden.

The radiology department is located on two floors. Most of the day-to-day work of the department is carried out on the lower floor, where there are conventional radiography rooms, an ultrasound department, four angiography suites and three CT scanners. The top floor houses offices, conference rooms and film stores. The department has two professors and 45 radiologists, 12 of whom are in training. It is a system-orientated department where every radiologist has a special interest. There are two libraries in the department where most of the radiological literature is at easy hand. Attached to the department are two research secretaries and three photographers, who assist in all the research work going through the department. There is also a biomedical engineering section attached to the diagnostic radiology department. This section consists of seven qualified engineers who service and maintain most of the equipment in the department. They not only offer prompt service in cases of technical failure, but also have saved a lot of money on expensive service contracts.

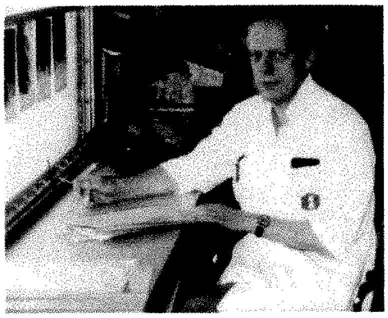

Professor Paul Svendsen, head of neuroradiology at Sahlgrenska Hospital, Gothenburg.

The neuroradiology department consists of four full-time and one trainee neuroradiologist. In addition, a rotation trainee in general radiology is always attached to the department. Most of the head and spine CT scans are performed on two third-generation CT scanners, although an old EMI 10/10 scanner is still operational and is sometimes used in selected clinical situations. All the angiography and myelography procedures are performed in a single room, which is equipped with a Siemens angioscope (C-arm) and has conventional as well as digital imaging facilities. It was obvious that there was need for another angiography room in such a major neuro centre, and I wish them well in their prolonged effort in obtaining such a facility.

Swedish neuroradiology has a reputation for its high standard of examination and I was fortunate to witness this in person. The quality of the routine CT scans was excellent. High-resolution axial and direct coronal scans were routinely performed while examining lesions at the base of skull and reformatted images were frequently available for complete assessment. Diagnostic radiography is always performed using a conventional film changer, except in cases of tumours, when digital imaging was used. I was surprised to see not a single digital intravenous examination performed during my stay. Eleven myelograms and 47 diagnostic angiograms were performed in 2 months and over two-thirds of these examinations were abnormal, which is only possible when you have good clinical colleagues.

The main aim of my visit was to gain experience in interventional neuroradiology. I was able to perform some diagnostic procedures and to participate in most interventional procedures. Professor Svendsen has been offering an interventional neuroradiology service since 1981 and now receives patients from all over Scandinavia and Iceland. Because of the lack of angiography room facilities, only one such procedure can be performed every day and the waiting list for routine embolization is now approximately 4 months.

Every case referred for embolization is discussed in a meeting by the embolization team, which consists of a neuroradiologist, neurosurgeons, neuroanaesthetists and neuroradiography nurses. The patient is then admitted under the neurosurgeons, who temporarily look after the patient's care. Although there is no need for a formal consent in Sweden, all patients are seen by the neuroradiologists on admission and the procedure as well as complications are explained. The interventional procedures are usually carried out under sedation and throughout the procedure the patient is monitored by an anaesthetic nurse. There are three neuroradiography nurses who assist in interventional procedures. These nurses are skilled in using the modern equipment, which is now available for interventional procedures. They are well informed in interventional techniques and frequently attend major international conferences along with the radiologists.

Twenty-nine interventional procedures were performed during my stay. Intracranial arterio-venous (AV) malformations (13) and dural fistulae (four) were embolized using isobutyl 2-cyanoacrylate (IBCA) injected through a flow-guided calibrated leak balloon or a tracker infusion catheter (Target Therapeutics). Spinal arterio-venous malformations (two) and angiofibroma (one) were embolized using PVA particles. Carotid cavernous fistulae (two), internal carotid aneurysm (one) and pulmonary AV malformation (one) were treated using Debrun detachable balloons. Venous malformations (five) were treated by direct percutaneous puncture and injection of absolute alcohol. There were two complications: in one patient the spinal artery was partially dissected by a steerable guide wire without any neurological deterioration. A repeat arteriogram 1 month later demonstrated no permanent injury. In another patient, the balloon catheter was glued in the vessel feeding the AV malformation but the patient remained neurologically stable.

I have no doubt that the success of interventional neuroradiology in Sahlgrenska hospital is mainly due to the concentrated experience they have gained over years, being the only department practising such skills in Scandinavia. Dedication and hard work by members of the embolization team made significant contribution to such success.

In conclusion, I have gained a special experience during my visit to Gothenburg, which would not have been possible without the help of The British Institute of Radiology or the generosity of Nycomed (UK) Ltd. I am most grateful to Professor Svendsen and his staff for their hospitality. I would strongly recommend any young British radiologist to take advantage of this scholarship.

New members of the BIR

Medical

Dr Stuart Bell, MB, BS, MRCP (London), Diagnostic Radiologist

Dr John R. Brown, MB, ChB, DA, DMRT (At present in USA), Radiotherapist Oncologist

Dr Melanie Y. N. Chin, BM (Bristol), Diagnostic Radiologist

Dr Bharatrai Gajjar, MB, ChB, FRCR (Watford), Diagnostic Radiologist

Dr Thomas P. Kane, MB, ChB, FRCR, DMRD (Blackpool), Diagnostic Radiologist

Dr Brendan Morrissey, MB, BCh, BaO, MRCPI (Manchester), Diagnostic Radiologist

Non-medical

Mr James Canning, MRPharm Soc, Dipl Man Studies, FBIM (London), Director Talbex Group

Mrs Harriet E. Crusher, DCR(R), DMU (Haywards Heath, W. Sussex), Radiographer

Mr Christopher M. T. Medley, BSc (Aylesbury, Bucks), Amersham International PLC

Mr Jeremy R. Williams, BA, MSc, FIPSM (Edinburgh), Physicist

BIR ties

BIR ties are available to members at £5 each (£6 including post and packing). They are navy blue or maroon red and carry the rays from the Institute's logo, in gold. Please send a cheque payable to the BIR with the order.

FAX at the BIR

A FAX machine has now been installed at the BIR. The number is: **01-255 3209**. This can be used for urgent business, including library photocopies for which there will be an extra charge.

Key to product areas:

1 Diagnostic X-ray inc. NMR and CT.
2 Interventional radiology.
3 Ultrasound.
4 Nuclear medicine.
5 Radiopharmaceuticals.
6 Radiotherapy and oncology.
7 Radiobiology.
8 Radiation protection.
9 PACS.
10 Image processing.

BIR Company Subscribers

The BIR company subscriber scheme was launched at the end of 1987 and is aimed at all companies who advertise in the *BJR* or exhibit at the MED-X-RAY technical exhibition.

For a subscription of just £250 per annum for an initial period of 3 years, an attractive package of benefits is offered (see March 1988 *Bulletin* for details).

If your company is interested in joining the scheme, please contact: Miss Susan Johnstone, General Secretary, British Institute of Radiology, 36 Portland Place, London W1N 4AT; Tel: 01-580 4085. Companies which have enrolled to date are listed below.

Agfa-Gevaert Ltd
27 Great West Road, Brentford, Middlesex TW8 9AX; tel. 01-560 2131. *Product areas* 1. *Contact* Mr G. Mountford, Director.

Amersham International PLC
Lincoln Place, Green End, Aylesbury, Bucks HP20 2TP; tel. 0296-395222. *Product areas* 4, 5, 6. *Contact* Mr James McLaughlin, Sales and Marketing Manager.

Cardiac Services Ltd
95A Finaghy Road, South Belfast BT10 0BY; tel. 0232-625566. *Product areas* 1, 3, 4, 5, 6. *Contact* Mr R. J. Brown, Managing Director.

Central Electricity Generating Board
15 Newgate Street, London EC1A 7AU; tel. 01-634 6898. *Product areas* 7, 8. *Contact* Mr R. V. Brierley, Office Services Manager.

Elscint (GB) Ltd
Tower Road, Berinsfield, Oxfordshire OX9 8LW; tel. 0865-340900. *Product areas* 1, 3, 4. *Contact* Ms Elizabeth Beckmann, Managing Director.

E-Z-EM Ltd
19 Clarendon Road, London N8 0DD; tel. 01-881 1818. *Product areas* 1, 2, 8. *Contact* Mr D. F. Wills, Sales and Marketing Manager.

Gammex-RMI Ltd
4 Clarendon Chambers, Clarendon Street, Nottingham NG1 5LN; tel. 0602-483807. *Product areas* 1, 3, 4, 5, 6. *Contact* Miss Eileen Parr, Commercial Manager.

IGE Medical Systems Ltd
260 Bath Road, Slough, Berks SL1 4ER; tel. 0753-874000. *Product areas* 1, 3, 4, 5, 6, 8. *Contact* Mr Jack Strange, Sales Administration.

Kodak Ltd
PO Box 66, Station Road, Hemel Hempstead, Herts HP1 1JU; tel. 0442-61122. *Product areas* 1. *Contact* Mr P. E. Blackwell, Manager, Health Sciences Division.

Mallinckrodt Diagnostica (UK) Ltd
11 North Portway Close, Round Spinney, Northampton NN3 4RQ; tel. 0604-46132. *Product areas* 4, 5. *Contact* Mr D. G. L. Wood, Business Manager.

Nodecrest Ltd
Unit A, Sprint Industrial Estate, Chertsey Road, Byfleet, Surrey KT14 7BD; tel. 09323-40555. *Product areas* 4, 5, 6, 9. *Contact* Mr J. C. Nott, Marketing Manager.

Nuclear Associates
100 Voice Road, Carle Place, New York 11514–1593, USA; tel. 516-741 7614. *Product areas* 1, 3, 4, 5, 6, 8. *Contact* Mr H. Glasser, General Manager.

Nycomed (UK) Ltd
Nycomed House, 2111 Coventry Road, Sheldon, Birmingham B26 3EA; tel. 021-742 2444. *Product areas* 1, 3. *Contact* Mr L. Birch Hansen, Managing Director.

Polaroid (UK) Ltd
Ashley Road, St Albans, Herts AL1 5PR; tel. 0727 59191. *Product areas* 1. *Contact* Ms Tina Thompstone, Product Supervisor.

Premise Engineering Ltd
Tibbs Hill Road, Abbots Langley, Watford, Herts WD5 0DR; tel. 09277-67433/63320. *Product areas* 8. *Contact* Mr R. K. Beach, Sales and Marketing Manager.

Quantel Ltd
Administration Centre, Kiln Road, Newbury, Berkshire RG13 2HA; tel. 0635-32222. *Product areas* 2, 10. *Contact* Mr Christopher Trim, Publicity Officer.

Schering Health Care Ltd
The Brow, Burgess Hill, West Sussex RH15 9NE; tel. 04446-6011. *Product areas* 1, 2, 3. *Contact* Mr A. Greaves, Product Manager.

3M UK PLC
3M House, Bracknell, PO Box 1, Berks RG12 1JU; tel. 0344 426726. *Product areas* 1. *Contact* Mr Alan Budge, Marketing Manager.

Toshiba Medical Systems Europe BV
Schieweg 1, 2627 An Delft, The Netherlands; tel: 015 61 0121. *Product areas* 1, 6. *Contact* Mr P. Blonk, Office Manager, X-ray BU.

Wardray Products Ltd
Hampton Court Estate, Summer Road, Thames Ditton, Surrey KT7 0SP; tel. 01-398 9911. *Product areas* 8. *Contact* Mr R. B. Wardley, Managing Director.

Meeting Report

BIR North of England Branch

by D. W. Pilling

THE 115TH MEETING of the North of England Branch of the BIR was held at Doncaster District General Hospital, on Saturday, 15th October, 1988, at the kind invitation of Dr Pamela Martin and her colleagues. During the meeting, seven papers and three case reports were presented.

The first paper, by Dr David Ward, was entitled "Abscess drainage under ultrasound and CT control" and outlined the criteria for abscess drainage in the X-ray department, including the need to avoid traversing bowel. With experience, more complicated masses, including appendix abscesses and pancreatic abscesses, could be attempted. The value of saline irrigation if the pus was particularly thick was emphasized. The failures were analysed and it was clear that whilst perhaps not all the abscess could be drained, with antibiotic therapy satisfactory resolution often occurred in spite of drainage not being ideal. The fact that it is extremely difficult to differentiate between a pancreatic abscess and a necrotic non-infected pancreatic lesion was made.

Mr Peter Howells then presented a paper on "White cell labelling", which described imaging of inflammation using gallium, indium and a new agent, technetium HMPAO. The technetium agent has many advantages, including a lower cost, more suitable energy emissions for cameras, and easier preparation of the radiopharmaceutical. Gallium and indium give bigger absorbed doses, and indium in particular gives a large dose to the leucocytes, which is not a problem with technetium. The experience of normal scans with HMPAO was demonstrated and the need to image as early as 3 h in inflammatory bowel disease was emphasized.

The meeting next heard from Dr Robert Peck, who presented a paper entitled "Aspects of hepato biliary disease, Hong Kong style". Hepatoma is the second commonest tumour in Hong Kong and many patients are symptom free until presenting with large tumours. The need to image the liver accurately and to assess how many lobes are involved was emphasized, and the presence of micro-tumour emboli in the lungs in these tumours was demonstrated and the accuracy of technetium perfusion scanning was shown. Treatment using direct hepatic arterial injection of chemotherapy and lipiodol, which enabled the tumour size to be accurately followed up on CT scan, was also demonstrated. Infection and infestation of the liver is the second most commonest cause of surgical admission in Hong Kong and the treatment using ERCP-introduced naso biliary drainage was shown. Infection of the liver with ascaris and schistosomiasis was also demonstrated, emphasizing the value of barium meal, cholecystograms and ultrasound, depending on the site of infestation, and the use of ultrasound in schistosomiasis.

"The digitized department of the future" was the subject of Mr Gary Cook's paper. As well as the already well recognized uses of MRI, CT and DMSA, this paper addressed the problems of image storage on optical discs, the storage of the records as reports and the long-term storage of images for immediate retrieval onto a VDU system. Mr Cook envisaged a department with very little need for conventional X-ray film and with facilities for rapid retrieval of images from a disc storage system, within a matter of seconds for the recent images and within minutes if a filed disc needed to be retrieved.

The next paper entitled "The CT appearance of vascular complication of pancreatic disease" was presented by Dr Anna Belli, and was based on the premise that splenic and portal venous thrombosis are well described complications of pancreatitis that are almost certainly under-diagnosed. With enhanced dynamic scanning on CT in cases of acute pancreatitis, these complications can be diagnosed early with ring enhancement around the thrombosed vessels, collateral vessels demonstrated or liver ischaemia. Follow-up angiography prior to surgical management is necessary for complete diagnosis.

"Uses and abuses of urodynamics" was the title of Dr Charles Corney's and Dr Martin Taylor's paper. The indications for the use of urodynamics were presented, including stress incontinence, detrusor instability, upper motor neurone neuropathic bladders, lower motor neurone neuropathic bladders and bladder outflow obstruction. The technique of obtaining radiographic images during filling and emptying of the bladder along with pressure monitoring of the bladder and rectum and also monitoring of the flow rate was emphasized. The value of the technique in males under the age of 55 with prostatism or following surgery, or females with urgency and nocturia and also following gynaecological surgery, was shown. The need for very careful clinical assessment and patient selection and the limitation of the technique in unselected children or old people was clearly made.

There then followed a series of case reports. In the first of these, Professor Brian Worthington showed recent advances that Professor Mansfield and his colleagues had made with MRI, particularly the new technique of echo planar imaging in which the whole head can be scanned on a 128 matrix with each slice taking 64 ms. This allows studies of CSF dynamics to be undertaken and a more rapid throughput of patients, although the quality of the images are not as high as those at present obtainable on standard techniques. Dr Michael Collins then showed an abdominal wall mass which was ultimately demonstrated to be an epigastric hernia, and showed how important the plain radiograph with tangential views can be when ultrasound appears normal. Finally, Dr Peter Ward showed a patient from the intensive care unit who had suffered a traumatic fracture dislocation at C5/6 and had a large air collection in the chest. The value of CT in demonstrating the site for insertion of a chest drain in this complicated case was well made.

BIR Calendar

Unless otherwise indicated, enquiries about the following events should be addressed to the Conference Co-ordinator, British Institute of Radiology, 36 Portland Place, London W1N 4AT (Tel. 01-580 4085).

3-D Planning and Confirmation Therapy

April 12, 1989

Joint IPSM/BIR all-day meeting organized by IPSM.

Further details: General Secretary, IPSM, 2 Low Ousegate, York YO1 1QU. Tel: 0904-610821.

Annual General Meeting

The AGM of the BIR, to which all members are invited, will take place at 5.30 pm on Friday, 5 May 1989, in the Congress Theatre, Devonshire Park Centre, Eastbourne.

Clinical Relevance of Radiobiological Models

May 26, 1989

All-day work-in-progress meeting organized by the Radiobiology Sub-committee.

Conversazione

June 8, 1989

Science Museum, London

Lecture by Dr D. Brothwell: "Disease in Antiquity—a Modern Perspective".

RADIOLOGY '89

EASTBOURNE

4-6 May 1989 Eastbourne

British Institute of Radiology
47th Annual Congress

incorporating the joint Spring Provincial meeting with the Royal College of Radiologists and Radiology Section of the Royal Society of Medicine

Radiology '89 follows the annual conference of the College of Radiographers in Eastbourne. The two complementary though separately organized conferences will again be spanned by Britain's biggest radiological technical exhibition, MED-X-RAY.

The exhibition and meetings will be held in the Winter Gardens Complex, Eastbourne—an ideal site. Radiology '89 will cover all aspects of diagnostic radiology and radiotherapy.

Final programme and registration forms are available now from the Conference Office, BIR, 36 Portland Place, London W1N 4AT (Tel: 01-580 4085).

Radiology '89 Competition

The BIR's Industry Committee is organizing a competition to be held at Radiology '89 within the technical exhibition MED X RAY. All registrants at Radiology '89 will be eligible to enter this challenging radiological quiz and have the chance to win one of the fabulous prizes, sponsored by RAD Magazine.

Come to Radiology '89, visit MED X RAY on 4–5 May, enter the competition, and give yourself the chance to win the first prize of two air tickets to Chicago and accommodation at the RSNA in November 1989. The two runners-up will each receive a case of champagne.

See the Radiology '89 advertisement on this page for programme and registration details or contact the Conference Office at the BIR.

Hire of Institute facilities

Readers are reminded of the availability for hire of the Lecture Theatre, Foyer and Library. Affiliated societies are offered a discount.

The Lecture Theatre holds up to 100 people in raked seating and has excellent audio-visual equipment, including VHF video. The Foyer provides space for registration and refreshment breaks for 40 people. The Library, with its beautiful Adam ceiling, can accommodate up to 75 people for refreshment breaks or for an evening reception.

Library News

The BIR Library is open weekdays 9 a.m.–5 p.m. (7 p.m. on Tuesdays).

The Librarian, Mrs Gunnel Ingham, is in attendance Tuesdays 11 a.m.–7 p.m., and Thursdays 11 a.m.–5 p.m. Miss Sheila Dewhirst and Miss Helen Smith will be able to give assistance in the absence of the Librarian. (Tel. 01-580 4085).

The journal stock includes more than 100 titles. Though journals may not be taken out of the library, there is a photocopy service, also available by post or FAX. A list of current journals is available on request and is also published in the March and September issues of the Bulletin. Most books (excepting the historical collection) are available on loan.

Recent additions to the Library

Aird, E. G. A.: Basic physics for medical imaging. 1988

CEC: Beta dosimetry. Fifth information seminar on the radiation protection dosemeter intercomparison programme. 1987

Hoppe, R. (Ed.): Recent advances in the treatment and research in lymphoma and Hodgkin's disease. 1985

L'Annunziata, M. F.: Radionuclide tracers Their detection and measurement. 1987

Sutton, D. (Ed.): A textbook of radiology and imaging. 4th edn. Vols 1–2. 1986

Tannock, I. F. & Hill, R.P. (Eds): The basic science of oncology. 1988

New Professor for Barts

Professor Peter Armstrong, MB, BS, FRCR, DMRD, currently Professor and Vice-Chairman, Department of Radiology, University of Virginia Medical Center, Charlottesville, Virginia, USA, has been appointed to the Mercers' Chair in Diagnostic Radiology at St Bartholomew's Hospital Medical College from 1 June 1989. The Chair is privately funded by the Mercers' Company and The Special Trustees of St Bartholomew's Hospitals.

Whilst in the USA, Professor Armstrong acted as Associate Editor Overseas for the BJR, and we are pleased to announce that he has agreed to continue as an Associate Editor on his return to the UK.

Meetings and courses

The Sumner Trust Conference: Monoclonal Antibodies and Immunoconjugates in Cancer Treatment
April 6–7, 1989
Royal Society of Medicine, London
Further details: Miss Barbara Komoniewska, The Royal Society of Medicine, 1 Wimpole Street, London W1M 8AE. Tel: 01-408 2119.

One-day Symposium on Magnetic Resonance Imaging
April 21, 1989
University College of Swansea
Speakers include: Prof. L. Hall (Cambridge), Dr D. Shaw (Oxford), Dr C. Freer (Cambridge) and Mr D. Longmore (London)
Further details: Mrs Gaynor Demery, School of Postgraduate Studies, Morriston Hospital, Swansea SA6 6NL. Tel: 0792-703578.

Faculty of Radiologists, Royal College of Surgeons in Ireland, Spring Scientific Meeting: Emergency in Radiological Practice
April 21–22, 1989
Kinsale, Co. Cork
Further details: Secretary, Scientific Subcommittee, Faculty of Radiologists, Royal College of Surgeons in Ireland, St Stephen's Green, Dublin 2.

The London/Bart's FRCR Part I Revision Course
April 22–23, 1989
Fee £110
Further details: Dr P. Butler, Department of Neuroradiology, The London Hospital, Whitechapel, London E1 1BB. Tel: 01-377 7164.

Modern Interstitial Implant Therapy Course
April 24–26, 1989
Cookridge Hospital, Leeds
Further details: Dr D. Ash, University Department of Radiotherapy, Cookridge Hospital, Leeds LS16 6QB.

Association of Head and Neck Oncologists of Great Britain Meeting
April 28, 1989
Royal Society of Medicine, London
Further details: Dr M. F. Spittle, Meyerstein Institute of Radiotherapy and Oncology, The Middlesex Hospital, Mortimer Street, London W1N 8AA. Tel: 01-636 8333.

College of Radiographers 43rd Annual Conference
May 1–3, 1989
Eastbourne
Further details: Caroline Aldridge, COR, 14 Upper Wimpole Street, London W1M 8BN.

Non-invasive Vascular Diagnostic Techniques
May 15–17 and October 18–20, 1989
Southampton

Blood Vessel Imaging Using Ultrasound Techniques
May 17–19 and October 16–18, 1989
Southampton

For further details on the above courses, contact: Mr K. N. Humphries, Medical Ultrasound Courses, 10 Swale Drive, Woodland Park, Chandler's Ford, Hampshire.

4th International Symposium of the Society for Radiological Protection
June 4–9, 1989
Venue to be confirmed
Further details: Central Electricity Generating Board, Health and Safety Dept, Nuclear Safety Branch, Courtenay House, 18 Warwick Lane, London EC4P 4EB.

CAR '89: Computer Assisted Radiology
June 25–28, 1989
Berlin
Further details: Heinz U. Lemke, Institute for Technical Computer Science, Technical University Berlin, Sekr. CG/FR 3-3, Franklinstr. 28–29, D-1000 Berlin 10.

17th International Congress of Radiology
July 1–8, 1989
Paris, France
Further details: Convergences-ICR 89, 16 rue J.-J.-Rousseau, 75001 Paris, France.

International Society of Radiographers and Radiological Technicians 9th World Congress
July 3–6, 1989
Paris, France
Further details: 9th World Congress Secretariat, 52 Greenwich Park Street, London SE10 9LT. Tel: 01-853 2150.

The Leeds Gastroenterology Course for Radiologists
July 10–14, 1989
St James' University Hospital, Leeds
Course fee: £160
Further details: Miss Pat Kentley, Level 7, Worsley Medical Building, University of Leeds, Leeds LS2 9JT. Tel: 0532-433144.

5th Symposium Mammographicum
September 6–8, 1989
Imperial College, London
Call for papers
Further details: The Conference Office, The Royal College of Radiologists, 38 Portland Place, London W1N 3DG. Tel: 01-636 4432.

5th Annual London–Paris Fall Ultrasound Symposium
September 16–23, 1989
Vancouver, Canada
Further details: Fall Ultrasound Symposium, c/o Medical Seminars International, Inc., 9800-D Topanga Canyon Boulevard, Suite 232, Chatsworth, California 91311, USA. Tel: 818-700 9821.

New Techniques and Technology in the Treatment of Occlusive Vascular Disease
October 28, 1989
Queens Hotel, Leeds
Abstract deadline: April 30, 1989
Further details: Dr John Fisher, Department of Mechanical Engineering, University of Leeds, Leeds LS2 9JT. Tel: 0532-332128.

International Conference on Gallstones and their Management
February 25–28, 1990
Jerusalem
Further details: Gallstone Conference, Vered Congress, 15 Weizman Street, Nes Ziona 70400, Israel. Tel: 08-400777/8/9.

10th International Conference on the Use of Computers in Radiotherapy
November 11–14, 1990
Lucknow, India
Further details: Dr S. Hukku, Department of Radiotherapy, Sanjay Gandhi PGI, Rai Bareli Road, PO Box 375, Lucknow 226001, India. Tel: 0522-54336.

As a service to our readers, notice of meetings or courses will be inserted free of charge. Please send full details to the Honorary Editor, BIR Bulletin.

BIR Bulletin

Honorary Editor, BIR Bulletin: D. Rickards, LRCP, MRCS, FFR(D)SA, FRCR
Please address all correspondence to: Honorary Editor, BIR Bulletin, The British Institute of Radiology,
36 Portland Place, London W1N 4AT

The British Institute of Radiology is not responsible for opinions expressed in the BIR Bulletin

RADIOLOGY '89

EASTBOURNE

4-6 May 1989 Eastbourne

TO GIVE A TASTE of what is in store for you at Radiology '89, the organizers have prepared precis of some of the major sessions. These will appear in the *Bulletin* each month from now until May.

Dr Maureen Gowland
Scientific Programme Chairman

PACS: Fact or Fantasy

May 4, 1989

For several years, PACS has been a concept in the minds of everyone connected with radiology. There have been many debates about possible projects in this area, but how many people are clear about what is really meant by and involved in PACS, or for that matter what has already been achieved? How many people are aware of what is now possible with existing technology or what will be feasible in the future, given the current trends in technology? How will it affect the operation of a radiology department? What should we be considering today — should we be taking steps to ensure minimum problems when PACS is introduced?

These will be some of the questions under discussion at the session on PACS, to be held on Thursday, 4 May 1989, during the annual BIR Congress. This meeting will also be an opportunity to learn about the technical aspects of PACS and, in addition, the clinical needs and how these can be achieved. It will be an ideal occasion for a discussion on all aspects of PACS and its future application in radiology departments, particularly within UK hospitals.

E. Beckmann

Contemporary Issues in Uroradiology

May 4, 1989

The purpose of this seminar is to highlight topics that reflect recent developments in urological practice, to re-appraise standard imaging techniques within the urinary tract and to explore some aspects of interventional radiology.

The pharmacokinetics and renal handling of urographic contrast agents will be reviewed by Dr Peter Dawson (RPMS, Hammersmith Hospital), in order to clarify factors that dictate image quality in urography. The possible mechanisms underlying nephrotoxic manifestations of contrast agents will be discussed in detail.

The current role of radionuclide imaging will be reviewed by Dr Malcolm Merrick (Western General Hospital, Edinburgh). Nuclear medicine not only provides information about renal function that cannot be obtained by other imaging methods, but is also very useful for detecting pyelonephritic scarring and vesicoureteric reflux in childhood. The role of isotope techniques in the quantification of renal blood flow will be compared with other methods. Another important application is in the assessment of the relative contribution of each kidney to total renal function in chronic renal failure, as well as in the presence of urinary obstruction or non-obstructing calculus.

The role of imaging in the management of renal transplant patients will be described by Dr Colin Evans (Cardiff Royal Infirmary). Apart from nuclear medicine techniques, other non-invasive methods of evaluating graft dysfunction include ultrasound and, more recently, duplex Doppler and magnetic resonance imaging. These techniques will be discussed in terms of their limitations and advantages. Interventional techniques that are appropriate in the management of renal transplantation include renal artery angioplasty, percutaneous nephrostomy, ureteric dilatation and percutaneous stone removal.

While extracorporeal lithotripsy now has a well established role in the treatment of renal calculi, it is clear that percutaneous nephrolithotomy has a complementary role in the follow-up of this method. Furthermore, there is a minority of calculi that cannot be treated by shockwave lithotripsy and where percutaneous nephrolithotomy is the first-line treatment. Dr Michael Kellett (St Peter's Hospitals, London) will summarize the specific roles of shockwave lithotripsy and percutaneous nephrolithotomy, emphasizing which category of stone should be treated by each method. Percutaneous access to the kidney for endoscopic inspection of possible vascular malformations and superficial tumours will be discussed, together with the problem of endoscopy in cases of ureteric obstruction.

Radiology plays an important role in the evaluation of the newer forms of urinary tract reconstruction. Dr Caroline Parks (St Peter's Hospitals, London) will describe the various operative techniques and their radiological manifestations.

G. H. Whitehouse

Dosimetry of Risk Estimates in Systemic Therapy

May 5, 1989

The radioiodine treatment of thyroid disorders has demonstrated the cost effectiveness of systemic radionuclide therapy over more than 40 years. Unlike conventional radiology, much of the prescribing has been done without a real knowledge of the dose–response relationship. With the higher resolution offered by positron emission tomography, radiation doses can be estimated with greater accuracy. Dr M.A. Flower will discuss the Royal Marsden Hospital experience in measuring radiation doses to patients with thyrotoxicosis and thyroid cancer. From this information it should be possible, in future, to tailor the activity to the patient requirement, reducing unnecessary radiation where further therapy will be of no benefit.

More recently, the scope of systemic radiotherapy has widened and many centres are trying to use monoclonal antibodies to target the radionuclide. The results so far have been disappointing when the intravenous route is used for the administration. The intracavitary route shows more promise of achieving the high tumour to normal tissue ratio required for successful therapy. The ideal technique of using the tumour to metabolise the administered radiopharmaceutical has worked well with thyroid pathology and radioiodine. A similar approach in neural crest tumours is also proving to be successful. Dr Diana Tait will outline the clinical use of radioiodine-labelled metaiodobenzylguanidine as well as the other clinical applications of systemic therapy.

Many clinicians have an irrational fear of any technique using radionuclides. In the end it is the risk versus benefit that matters. Dr Jim Malone (Dublin), a well known and entertaining speaker on this subject, will close the symposium with an analysis of the risks of therapeutic and diagnostic radiation and will show that, in general, they are trivial when compared with the benefits.

R. McCready

Meeting Preview

Clinical Relevance of Radiobiological Models

by M. P. Law

THE SHORTER Oxford Dictionary defines a model as "something that accurately resembles something else". Most studies in radiobiology involve some type of laboratory model. *In vitro* models are used to study the radiation response of cells, animal models have been developed to investigate the response of normal tissues and tumours, and mathematical models have been formulated to gain an understanding of the mechanism of radiation damage in cells and to describe the response of normal tissues and tumours *in vivo*. How relevant are these models to radiotherapy? Developments in radiobiology have influenced clinical practice. For example, the concept that there is a dissociation between acute and late responses in tissues, which is now being taught to radiotherapists in training, has come from studies of animal models. Studies of animal tumours have shown that there is a distribution of radiosensitivities within a tumour and are influencing clinical views about the radiosensitivity of human tumours. The current interest in hyperfractionation and accelerated fractionation has developed from mathematical models that describe normal tissue and tumour response in animals. New models are always being developed by radiobiologists.

The meeting on 26 May will consider the clinical relevance of these models. The major part of the day will be devoted to proffered papers on the topic but Dr Tom Wheldon will introduce the meeting by discussing the relevance and limitations of various models and Dr Michele Saunders will sum up by giving a clinician's view. The opportunity to find out how accurately radiobiological models resemble radiotherapy patients should not be missed. ●

Dose Fractionation

May 5, 1989

The BIR has always been a major forum for the discussion of new ideas relating to dose fractionation in radiotherapy, bringing together clinical radiotherapists, physicists and experimental scientists. Modified dose-fractionation regimes in radiotherapy can bring great benefits either by an improvement in the therapeutic ratio or by reducing the burden of the treatment for the patient. Any new idea needs testing, and this can only be done by carefully controlled clinical trials. Thus in 1963, the presidential year of Dr Frank Ellis, the BIR set up a Fractionation Working Party to organize and run multi-centre clinical trials.

To date, two important clinical trials, with a follow-up of up to 10 years, have been run and successfully completed. This has involved, in the first trial, the comparison of 3F/week versus 5F/week and, in the second trial, the comparison of "short" versus "long" overall treatment times. Both have been for the treatment of carcinoma of the laryngopharynx. The final clinical results of these two important trials are now available, and an overview of the findings will be provided by the present Chairman of the BIR Fractionation Working Party, Dr George Wiernik. The findings provide valuable pointers as to how curtailed fractionation may be given safely with no disadvantage to patients. It also provides useful information as to the successful organization of future clinical trials in radiotherapy.

With the completion of the above trials it is important for the BIR to look to the future. In recent years there has been a considerable improvement in the understanding of the biology of human tumours. This will be reviewed by Prof. Klaus Trott, who will present the biological basis for future improvements in dose fractionation in radiotherapy. For rapidly proliferating tumours, an acceleration of the treatment would appear to provide an advantage. This is an area in which there is now considerable clinical interest, treatments involving two or three fractions per day. Prospects for future clinical trials involving the comparison of accelerated fractionation with conventional fractionation will be presented by Dr Stan Dische and Dr Keith Durrant. It is the intention of the BIR to continue its interest in dose fractionation in radiotherapy by organizing a comparative study of accelerated dose fractionation in advanced bladder cancer.

S. Arnott
J. W. Hopewell

FAX at the BIR

A FAX machine has now been installed at the BIR. The number is: **01-255 3209**. This can be used for urgent business, including library photocopies for which there will be an extra charge.

The British Radiation Protection Association (BRadPA)

D. Gifford

MANY MEMBERS of the BIR, and many others who are not so fortunate, frequently express the view that they do not know very much about BRadPA: what it is, what its purpose may be and why it has a structure that is so very different from that of other societies.

The answers to these questions are lengthy and complex (and half as old as time), but this note endeavours to cast a little light on the situation in the hope of encouraging more members of the BIR to express their interest and concern in radiation protection by asking to become members of BRadPA through the BIR, if they are not already members through the Royal College of Radiologists or the Institute of Physical Sciences in Medicine.

The British Radiation Protection Association came into being in order to give the UK access to the international radiation protection forum. The International Radiation Protection Association (IRPA), which was founded in the early '60s, is a federal organization of 27 radiation protection societies representing some 31 countries and more than 12 000 individual members, and will not accept more than one organization representing radiation protection interests from each member country.

The primary purpose of IRPA is to serve as a medium for international communication and co-operation in radiation protection with the goal of advancing sound and effective radiation protection in all parts of the world. It is governed and authorized to function by its members and for its members through conventional democratic processes. The individual member of IRPA is the most important constituent.

The first International Congress was convened in Rome in 1966, although initial organizational efforts took place for several years prior to 1966. Subsequent International Congresses took place in Brighton (1970), Washington, DC (1973), Paris (1977), Jerusalem (1980), West Berlin (1984) and Sydney (1988).

Major programmes and other important matters are discussed and decided at the General Assembly, which is a key part of each International Congress. Delegates are appointed by Associate Societies in a proportional manner and Officers and other members of the Executive Council are elected at the General Assembly for designated terms of office. The Executive Council directs the affairs of the Association on behalf of the membership.

Commencing with the 1973 Congress, each congress has been opened by the Sievert Lecture, which is presented by the winner of the Sievert Award. The Award is in honour of Rolf M. Sievert, a pioneer in radiation physics, and the lecture is published in *Health Physics*. The recipients of the Sievert Award have been:

1973	Prof. B. Lindell	(Sweden)
1977	Prof. W. V. Mayneord	(UK)
1980	Dr L. S. Taylor	(USA)
1984	Sir Edward Pochin	(UK)
1988	Prof. Dr W. Jacobi	(FRG)

Members of IRPA may attend International Congresses at a reduced rate and the proceedings are normally pre-printed and remain a timely source document of international protection activities. The association also supports Regional Congresses, which are sponsored by two or more Associate Societies, and these now take place regularly, being offered annually in recent years. Members of IRPA are also welcomed at a reduced congress fee.

The British Radiation Protection Association adopted limited liability status to protect against any losses incurred in running IRPA '70 in Brighton, and became known as BRPA Ltd. More recently, other organizational changes have taken place and in order clearly to identify the present organization, it was decided that it should be known as BRadPA.

The constituent societies in Britain are the following: the Association of University Radiation Protection Officers (AURPO), the British Institute of Radiology (BIR), the British Nuclear Medicine Society (BNMS), the British Occupational Health Society (BOHS), the College of Radiographers (COR), the Hospital Physicists' Association (HPA), the Royal College of Radiologists (RCR), and the Society for Radiological Protection (SRP).

These organizations represent widely differing areas of interest, and apart from differences that may arise owing to academic or industrial backgrounds, other differences of emphasis arise because of medical and non-medical backgrounds, and particularly in connection with professionalism in the practice of radiation protection, relating as to whether part-time practitioners properly represent UK practice at the international level.

For these reasons, it is important that as many members of the BIR as possible express their interest in radiation protection matters by asking the General Secretary to register their wish to belong to BRadPA through the BIR, which will pay the necessary membership fee. Any increase in the total membership of BRadPA will also be beneficial as it will increase the number of UK delegates representing BRadPA at the next International Congress of IRPA, which is to be held in Montreal in 1992, and to which members of the BIR are warmly invited.

Please write to the BIR General Secretary, Miss Susan Johnstone, at 36 Portland Place, London W1N 4AT, if you wish to join BRadPA via the BIR, citing this article.

Institute Sponsored Visits to Paris

Members should write to the General Secretary of the BIR for application to visit radiotherapy centres in Paris, arranged through the collaboration of Professor M. Tubiana.

Product News

Major breakthrough in spinal research

Alan Breen and a team of researchers at the Anglo-European College of Chiropractic, Bournemouth, have achieved a major breakthrough in the diagnosis of back pain, following a 2-year research programme. The investigation into the mechanics of spinal disorders has produced a revolutionary method of providing fast and accurate diagnosis, using the latest in digital image processing technology.

Mr Breen, Director of Research at the College, explains: "We needed to find a way of measuring movement between vertebrae, and I believe that our research has produced the beginning of a type of technology which will become the state of the art in the next century. We will be able to work out the back's ability to withstand strain and to predict whether a person might suffer recurring problems. The trial, which began its main phase in 1986, is the first of its kind in the world. Detailed objective analysis of the mechanical function of the spine depends on the ability to measure motion between individual segments."

Using the latest computer technology, it will be possible to measure this movement from low radiation X-ray fluoroscopy. The image processing technique makes possible detailed motion studies with minimal X-ray dosage, which enables a greater amount of information to be gleaned from patients. The researchers claim that they are now able to build up a complete pattern of movement for each vertebrae.

For further information, call Nikki Richards on 0272-741198.

Philips Tomoscan CX/S in mobile installation

A mobile CT scanner containing a Philips Tomoscan CX/S was recently handed over to the Health Authorities in the Province of Zeeland, The Netherlands. The scanner is installed in a purpose-built trailer, designed to protect the system, even under the most difficult transit conditions.

A mobile unit bringing a scanner to all the local hospitals in the region on a regular basis is the ideal solution where it is uneconomic for any single hospital to acquire a CT scanner.

The layout of the Tomoscan CX/S is comparable to that of a stationary installation. The walls of the scanner area can be hydraulically extended on site, thus providing a comfortable working space in which patients can be brought into the examination area, even while still in bed, and carefully transferred to the patient table.

The technical equipment housed at the back of the trailer is also accessible from the outside. The trailer is equipped with a camera and automatic developing unit, and a diagnostic console for the radiologist. This allows maximum use of the equipment during the time available and diagnosis can be made on the same day. The unit is complete with all necessary services for patient examinations, including a patient lift and telephone and intercom systems for contact with hospital radiologists and other personnel.

Pictures by telephone

The Photophone is the latest in communications from Cameron Video Systems Ltd. Using digital technology to transmit a black and white image from a television camera by normal telephone link, the system has been demonstrated using a normal land line to a radio communications station, from where the signal was bounced off the stratosphere to a receiving station on an oil rig.

There are some obvious radiographic uses for equipment of this type. For example, the system has been tested in mammography, where it has been shown to have adequate resolution.

The time taken to transmit one image is typically between 10 and 20 seconds and a second opinion can be obtained in as little time as it takes to place a phone call.

For further information, contact Neil Macdonald, Cameron Video Systems, Burnfield Road, Giffnock, Glasgow G46 7TH. Tel: 041-633 0077; or visit stand 64 at MED X RAY, Eastbourne, May 4-5.

Radiology management system

The Princess of Wales Hospital in Bridgend, Wales, recently installed a computerized management system for its Radiology Department. The software, called FOCUS, runs on IN2's Pick-based fault tolerant multi-user system, the IN8000 series.

FOCUS is an integrated radiology management system designed to streamline all administrative procedures throughout the department. It produces Korner statistics and can handle complex tasks such as speciality costing. It features a comprehensive daybook and diary facility, which reduces record search times, a film library management system and a powerful statistical reports package. With the new system in place, reports can be drawn instantaneously from any of 15 IN2 terminals installed at points of use in admin headquarters, in each of the four hospitals and in the WHCSA computer centre.

For further information, contact: Bryan Wrighton, IN2 Ltd, Richmond House, Bath Road, Speen, Newbury, Berkshire RG13 1QY. Tel: 0635-43913.

BIR Company Subscribers

The BIR company subscriber scheme was launched at the end of 1987 and is aimed at all companies who advertise in the *BJR* or exhibit at the MED-X-RAY technical exhibition.

For a subscription of just £250 per annum for an initial period of 3 years, an attractive package of benefits is offered (see March 1988 *Bulletin* for details).

If your company is interested in joining the scheme, please contact: Miss Susan Johnstone, General Secretary, British Institute of Radiology, 36 Portland Place, London W1N 4AT; Tel: 01-580 4085. Companies which have enrolled to date are listed below.

Agfa-Gevaert Ltd
27 Great West Road, Brentford, Middlesex TW8 9AX; tel. 01-560 2131. *Product areas* 1. *Contact* Mr G. Mountford, Director.

Amersham International PLC
Lincoln Place, Green End, Aylesbury, Bucks HP20 2TP; tel. 0296-395222. *Product areas* 4, 5, 6. *Contact* Mr James McLaughlin, Sales and Marketing Manager.

Cardiac Services Ltd
95A Finaghy Road, South Belfast BT10 0BY; tel. 0232-625566. *Product areas* 1, 3, 4, 5, 6. *Contact* Mr R. J. Brown, Managing Director.

Central Electricity Generating Board
15 Newgate Street, London EC1A 7AU; tel. 01-634 6898. *Product areas* 7, 8. *Contact* Mr R. V. Brierley, Office Services Manager.

E. G. & G. Astrophysics Research Ltd
Vale Road, Windsor, Berkshire SL4 5JP; tel. 0753-855611. *Product areas* 1, 6, 7, 8. *Contact* Miss Susan Holgate, Sales Executive (Therapy).

Elscint (GB) Ltd
Tower Road, Berinsfield, Oxfordshire OX9 8LW; tel. 0865-340900. *Product areas* 1, 3, 4. *Contact* Ms Elizabeth Beckmann, Managing Director.

E-Z-EM Ltd
19 Clarendon Road, London N8 0DD; tel. 01-881 1818. *Product areas* 1, 2, 8. *Contact* Mr D. F. Wills, Sales and Marketing Manager.

Gammex-RMI Ltd
4 Clarendon Chambers, Clarendon Street, Nottingham NG1 5LN; tel. 0602-483807. *Product areas* 1, 3, 4, 5, 6. *Contact* Miss Eileen Parr, Commercial Manager.

IGE Medical Systems Ltd
352 Buckingham Ave, Slough, Berks SL1 4ER; tel. 0753-874000. *Product areas* 1, 3, 4, 5, 6, 8. *Contact* Mr Jack Strange, Sales Administration.

Kodak Ltd
PO Box 66, Station Road, Hemel Hempstead, Herts HP1 1JU; tel. 0442-61122. *Product areas* 1. *Contact* Mr P. E. Blackwell, Manager, Health Sciences Division.

Mallinckrodt Diagnostica (UK) Ltd
11 North Portway Close, Round Spinney, Northampton NN3 4RQ; tel. 0604-46132. *Product areas* 4, 5. *Contact* Mr D. G. L. Wood, Business Manager.

Nodecrest Ltd
Unit A, Sprint Industrial Estate, Chertsey Road, Byfleet, Surrey KT14 7BD; tel. 09323-40555. *Product areas* 4, 5, 6, 9. *Contact* Mr J. C. Nott, Marketing Manager.

Nuclear Associates
100 Voice Road, Carle Place, New York 11514–1593, USA; tel. 516-741 7614. *Product areas* 1, 3, 4, 5, 6, 8. *Contact* Mr H. Glasser, General Manager.

Nycomed (UK) Ltd
Nycomed House, 2111 Coventry Road, Sheldon, Birmingham B26 3EA; tel. 021-742 2444. *Product areas* 1, 3. *Contact* Mr L. Birch Hansen, Managing Director.

Polaroid (UK) Ltd
Ashley Road, St Albans, Herts AL1 5PR; tel. 0727 59191. *Product areas* 1. *Contact* Ms Tina Thompstone, Product Supervisor.

Premise Engineering Ltd
Tibbs Hill Road, Abbots Langley, Watford, Herts WD5 0DR; tel. 09277-67433/63320. *Product areas* 8. *Contact* Mr R. K. Beach, Sales and Marketing Manager.

Quantel Ltd
Administration Centre, Kiln Road, Newbury, Berkshire RG13 2HA; tel. 0635-32222. *Product areas* 2, 10. *Contact* Mr Christopher Trim, Publicity Officer.

Schering Health Care Ltd
The Brow, Burgess Hill, West Sussex RH15 9NE; tel. 04446-6011. *Product areas* 1, 2, 3. *Contact* Mr A. Greaves, Product Manager.

3M UK PLC
3M House, Bracknell, PO Box 1, Berks RG12 1JU; tel. 0344 426726. *Product areas* 1. *Contact* Mr Alan Budge, Marketing Manager.

Toshiba Medical Systems Europe BV
Schieweg 1, 2627 An Delft, The Netherlands; tel: 015 61 0121. *Product areas* 1, 6. *Contact* Mr P. Blonk, Office Manager, X-ray BU.

Wardray Products Ltd
Hampton Court Estate, Summer Road, Thames Ditton, Surrey KT7 0SP; tel. 01-398 9911. *Product areas* 8. *Contact* Mr R. B. Wardley, Managing Director.

Key to product areas:

1 Diagnostic X-ray inc. NMR and CT.
2 Interventional radiology.
3 Ultrasound.
4 Nuclear medicine.
5 Radiopharmaceuticals.
6 Radiotherapy and oncology.
7 Radiobiology.
8 Radiation protection.
9 PACS.
10 Image processing.

High-speed processor at MED X RAY

The world's fastest X-ray film processor, the Konica Super-Rapid SRX-501, together with a completely new film, MG-SR, can be seen for the first time in the UK on the Konica stand at MED X RAY in Eastbourne (May 4-6).

The Super-Rapid SRX-501 offers a 45 second processing cycle, with no loss of image quality or increase in running costs. The processor has been completely redesigned and Konica has also developed new films for use with the system. The films, MG-SR and MCH-SR, bear a new, multilayered grain to capture the latent image, permitting higher processing speeds without any significant corresponding increase in the fog level.

Since the release of the system in Japan in May 1988, over 280 systems have been installed in Japanese hospitals.

For further information, contact: Judith Patten, Public Relations, Rowe House, 55/59 Fife Road, Kingston upon Thames, Surrey KT1 1TA. Tel: 01-547 1566.

Use of RSM Library

BIR members might be pleased to know that there is an agreement which allows limited use of the RSM library for reference purposes, including photocopying and searches.

Members should apply to the BIR librarian, Mrs Gunnel Ingham, for a visitors card.

BIR Calendar

Unless otherwise indicated, enquiries about the following events should be addressed to the Conference Co-ordinator, British Institute of Radiology, 36 Portland Place, London W1N 4AT (Tel. 01-580 4085).

Annual General Meeting

The AGM of the BIR, to which all members are invited, will take place at 5.30 pm on Friday, 5 May 1989, in the Congress Theatre, Devonshire Park Centre, Eastbourne.

Clinical Relevance of Radiobiological Models

May 26, 1989
All-day work-in-progress meeting organized by the Radiobiology Sub-committee.
See preview on p. B122 for further details.

Conversazione

June 8, 1989
Science Museum, London
Sherry reception
Lecture by Dr D. Brothwell: "Disease in Antiquity—a Modern Perspective".
Buffet with wine in the Upper Wellcome Gallery.
All BIR members and friends welcome.

Library News

The BIR Library is open weekdays 9 a.m.–5 p.m. (7 p.m. on Tuesdays).

The Librarian, Mrs Gunnel Ingham, is in attendance Tuesdays 11 a.m.–7 p.m., and Thursdays 11 a.m.–5 p.m. Miss Sheila Dewhirst and Miss Helen Smith will be able to give assistance in the absence of the Librarian. (Tel. 01-580 4085).

The journal stock includes more than 100 titles. Though journals may not be taken out of the library, there is a photocopy service, also available by post or FAX. A list of current journals is available on request and is also published in the March and September issues of the Bulletin. Most books (excepting the historical collection) are available on loan.

Recent additions to the Library

AAPM: The physical aspects of total and half body photon irradiation. 1986
Exeter Health Authority: Incident in radiotherapy department. The report of the Committee of Enquiry (the Thwaites report) and the summary report by Prof. Charles Joslin. 1988
Freeman, L. M. & Weissmann, H. S. (Eds): Nuclear medicine annual 1987
Kadir, S.: Diagnostic angiography. 1986
Keats, T. E.: Atlas of normal roentgen variants that may simulate disease. 4th edn. 1988
Margulis, A. R. & Gooding, C. A. (Eds): Diagnostic radiology 1987
Moseley, H.: Non-ionising radiation: microwaves, ultraviolet radiation and laser radiation. 1988
Perry, J. A.: RPL dosimetry. Radiophotoluminescence in health physics. 1987
Vignaud, J., Jardin, C. & Rosen, L. (Eds): The ear: diagnostic imaging. 1986

RADIOLOGY '89

EASTBOURNE

4-6 May 1989 Eastbourne

The exhibition and meetings will be held in the Winter Gardens Complex, Eastbourne—an ideal site. Radiology '89 will cover all aspects of diagnostic radiology and radiotherapy.

Final programme and registration forms are available now from the Conference Office, BIR, 36 Portland Place, London W1N 4AT (Tel: 01-580 4085).

Exciting prizes at Radiology '89

Come to Radiology '89, visit MED X RAY on 4–5 May, enter the competition, and give yourself the chance to win the first prize of two air tickets to Chicago and accommodation at the RSNA in November 1989. The two runners-up will each receive a case of champagne.

See the Radiology '89 advertisement on this page for programme and registration details or contact the Conference Office at the BIR.

Meetings and courses

4th International Symposium of the Society for Radiological Protection

June 4–9, 1989
Malvern, Worcs
Further details: Peter Shrimline, CEGB, Health and Safety Department, Nuclear Safety Branch, Courtenay House, 18 Warwick Lane, London EC4P 4EB. Tel: 01-634 5111 ext 5080.

5th Annual Guy's CT Course with MRI Correlation

June 9–10, 1989
Guy's Hospital, London
Further details: Kim Latimer, Postgraduate Department, Guy's Hospital, London SE1 9RT. Tel: 01-407 7600 ext. 3342.

The Bart's/London FRCR II Revision Course

August 29–31, 1989
St Bartholomew's Hospital, London
Further details: Mrs C. Burrage, Course Secretary, Room 26, Dunn Laboratories, St Bartholomew's Hospital, West Smithfield, London EC1A 7BE. Tel: 01-601 7531.

Paediatric Radiology Course

September 13–15, 1989
Sheffield Children's Hospital, Sheffield
For consultants and registrars
Further details: Dr G. M. Steiner, X-ray Department, Sheffield Children's Hospital, Western Bank, Sheffield S10 2TH. Tel: 0472-761111 ext. 3201.

Human Exposure to Natural Radiation: its Variation, Regulation and Consequences

October 3, 1989
The Commonwealth Institute, London
Further details: Dr D. N. S. Dixon, Programme Committee Secretary, 67 Oatlands Park, Linlithgow, W. Lothian EH49 6AS, Scotland. Tel: 031-244 2253.

New Techniques and Technology in the Treatment of Occlusive Vascular Disease

October 28, 1989
Queens Hotel, Leeds
Abstract deadline: May 31, 1989
Further details: Dr John Fisher, Department of Mechanical Engineering, University of Leeds, Leeds LS2 9JT. Tel: 0532-332128.

As a service to our readers, notice of meetings or courses will be inserted free of charge. Please send full details to the Honorary Editor, BIR Bulletin.